LBNL-41700
CONF-980228

ERNEST ORLANDO LAWRENCE
BERKELEY NATIONAL LABORATORY

# Proceedings of the Workshop on GRETA Physics A Slide Report

**Ernest Orlando Lawrence**
**Berkeley National Laboratory**
**February 5-7, 1998**

Paul Fallon, Editor
**Nuclear Science Division**

REFERENCE COPY
Does Not
Circulate
Bldg. 50 Library - Ref.
Lawrence Berkeley National Laboratory
Copy 1
LBNL-41700

## DISCLAIMER

This document was prepared as an account of work sponsored by the United States Government. While this document is believed to contain correct information, neither the United States Government nor any agency thereof, nor the Regents of the University of California, nor any of their employees, makes any warranty, express or implied, or assumes any legal responsibility for the accuracy, completeness, or usefulness of any information, apparatus, product, or process disclosed, or represents that its use would not infringe privately owned rights. Reference herein to any specific commercial product, process, or service by its trade name, trademark, manufacturer, or otherwise, does not necessarily constitute or imply its endorsement, recommendation, or favoring by the United States Government or any agency thereof, or the Regents of the University of California. The views and opinions of authors expressed herein do not necessarily state or reflect those of the United States Government or any agency thereof or the Regents of the University of California.

# Workshop on GRETA Physics

## A SLIDE REPORT

Paul Fallon, Editor

*Lawrence Berkeley National Laboratory*
*Berkeley, California*

February 5-7, 1998

This work was supported by the Director, Office of Energy Research, Office of High Energy and Nuclear Physics, Division of Nuclear Physics, of the U.S. Department of Energy under Contract No. DE-AC03-76SF00098.

# FOREWORD

This report contains the transparencies from talks presented at the "Workshop on GRETA Physics" held at Lawrence Berkeley National Laboratory on February 5-7, 1998. The goal of this workshop was to develop the scientific case for the next generation of gamma ray detector arrays, such as GRETA. The program included invited talks covering the technical developments related to GRETA and the wide range of physics opportunities made possible with a GRETA type device. The last day was devoted to parallel discussion groups, which provided a more focused discussion on the various topics addressed in the plenary sessions and allowed additional contributions to made by a wider group of participants. More than 100 scientists attended the meeting.

On behalf of the organizing committee I would like to thank all the speakers and discussion leaders for the time and effort that they put into making this a very successful and stimulating meeting. This meeting was sponsored by Lawrence Berkeley National Laboratory.

*Paul Fallon*

Organizing Committee:
*R.M.Clark, M.Cromaz, M.A.Deleplanque, P.Fallon, I.Y.Lee, A.O.Macchiavelli, F.S.Stephens, K.Vetter, D. Ward.*

Workshop On Greta Physics
Lawrence Berkeley National Laboratory
Feb 5 -7, 1998.

*THURSDAY FEB 5, MORNING 9:00AM - 12:30PM (Bldg. 66 Auditorium)*

**Session Leader: D.Sarantites**

| | | |
|---|---|---|
| 09.00 | L.S.Schroeder | Welcome. |
| 09:05 | M.A.Deleplanque | Workshop introduction. |
| 09:15 | I-Y.Lee | Greta overview. |
| 10:00 | K.Vetter | Greta prototype test and simulations. |
| 10:30 | BREAK | |

**Session Leader: R.Lieder**

| | | |
|---|---|---|
| 11:00 | P.J.Nolan | An overview of developments in Europe towards a gamma-ray tracking device. |
| 11:30 | J.Eberth | Segmented encapsulated germanium detectors for the next generation of gamma-ray arrays. |
| 12:00 | D.Bazzacco | Status of the MARS project. |

*THURSDAY FEB 5, AFTERNOON 2:00PM - 5:10PM (Bldg. 66 Auditorium)*

**Session Leader: L.Riedinger**

| | | |
|---|---|---|
| 14:00 | S.Frauendorf | Rotation beyond the standard scenario. |
| 14:40 | W.Satula | The mean field: can it still surprise ? |
| 15:20 | BREAK | |

**Session Leader: D.Fossan**

| | | |
|---|---|---|
| 15:40 | M.Riley | Reaching for the sky with GRETA: how high in spin can nuclei go and what do they do up there ? |
| 16:10 | C.Baktash | Nuclear structure near the N=Z line. |
| 16:40 | I.Ahmad | Structure and stability of the heaviest elements. |
| 17:30 | RECEPTION | *(cafeteria)* |

*FRIDAY FEB 6, MORNING 9:00AM - 12:00PM (Bldg. 66 Auditorium)*

**Session Leader: P.Regan**

| | | |
|---|---|---|
| 09:00 | B.Sherrill | Techniques for mapping halo wavefunctions. |
| 09:30 | M.Thoennessen | Giant resonances. |
| 10:00 | T.Glasmacher | The spectroscopy of neutron-rich nuclei with a gamma-ray tracking device. |
| 10:30 | BREAK | |

**Session Leader: J.Becker**

| | | |
|---|---|---|
| 11:00 | D.Habs | Miniball physics. |
| 11:30 | D.Cline | Spectroscopy of neutron-rich nuclei. |

*FRIDAY FEB 6, AFTERNOON 2:00PM - 5:00PM (Bldg. 66 Auditorium)*

**Session Leader: G.Ball**

| | | |
|---|---|---|
| 14:00 | S.Freedman | Weak interactions. |
| 14:30 | M.Smith | Nuclear astrophysics opportunities with GRETA. |
| 15:00 | BREAK | |

**Session Leader: J.Cizewski**

| | | |
|---|---|---|
| 15:30 | W. Swiatecki | Jacobi shapes, fission barriers, surface diffuseness. |
| 16:00 | B.Herskind | Limit to completeness. |
| 16:30 | T-L.Khoo | Structure of hot nuclei. |

*SATURDAY FEB 7, MORNING 9:30AM - 12:30PM*

Introduction to the parallel discussion sessions *(Bldg. 50 Auditorium).*

| Parallel Groups *(rooms to be announced)* | Discussion Leader |
|---|---|
| 1. Low-spin/High-spin/Far from stability | **M.Carpenter** |
| 2. Chaos/Continuum/Warm nuclei | **S.Åberg** |
| 3. Fundamental/Astrophysics | **G.Savard** |
| 4. Fragmentation/Coulex/Giant resonance | **M.Thoennessen** |
| 5. Detectors/Technical/Analysis/Aux. detectors | **J.Waddington** |

*SATURDAY FEB 7, AFTERNOON 2:00PM - 5:00PM (Bldg. 50 Auditorium).*

| | | |
|---|---|---|
| 14:00 | General discussion and GRETA organization. | **I-Y.Lee** |
| 15:00 | BREAK | |
| 15:30 | Reports from the discussion groups. | **P.Fallon** |

# CONTENTS

GRETA Overview ..... 1
I-Y. Lee

GRETA Prototype: Tests & Simulations ..... 33
K. Vetter

Developments Toward a Tracking Array—A European Overview ..... 61
P.J. Nolan

Segmented Encapsulated Germanium Detectors for the
Next Generation of Gamma-Ray Arrays ..... 89
J. Eberth

Status of MARS Project ..... 113
D. Bazzacco

Rotation Beyond the Standard Scenario ..... 135
S. Frauendorf

The Mean Field: Can It Still Surprise? ..... 165
W. Satula

Reaching for the Sky with GRETA: How High in Spin Can Nuclei Go
and What Do They Do Up There? ..... 195
M. Riley

Nuclear Structure Near the N=Z Line ..... 237
C. Baktash

Structure and Stability of the Heaviest Elements ..... 267
I. Ahmad

Techniques for Mapping Halo Wavefunctions ..... 295
B. Sherrill

Giant Resonances ..... 319
M. Thoennessen

The Spectroscopy of Neutron-Rich Nuclei with a Gamma-Ray
Tracking Device ..... 357
T. Glasmacher

Miniball Physics ..... 383
D. Habs

Spectroscopy of Neutron-Rich Nuclei ..... 409
D. Cline

Weak Interactions ..... 445
S. Freedman

Nuclear Astrophysics Opportunities with GRETA ..... 489
M. Smith

Jacobi Shapes, Fission Barriers, Surface Diffuseness ..... 509
W. Swiatecki

Limit to Completeness ..... 533
B. Herskind

Structure of Hot Nuclei ..... 557
T-L. Khoo

I-Y.Lee
Greta overview.

# GRETA Overview

- Concept
- R/D Status
- Future Plan
- Physics opportunities

**I. Y. Lee**

Lawrence Berkeley National Laboratory

tk/title.iw

## Compton Shielded Ge

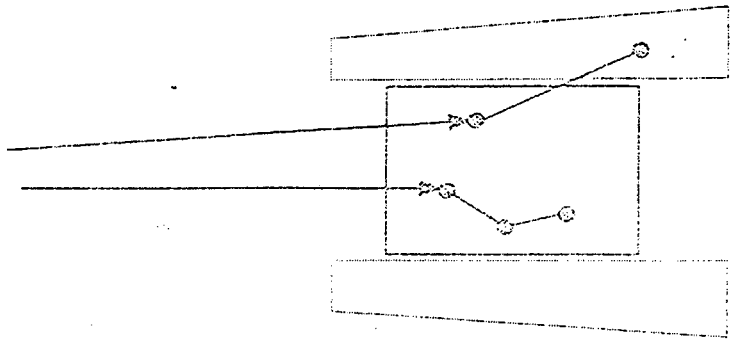

$\varepsilon = 0.15$

Ndet = **100**

## Ge Sphere

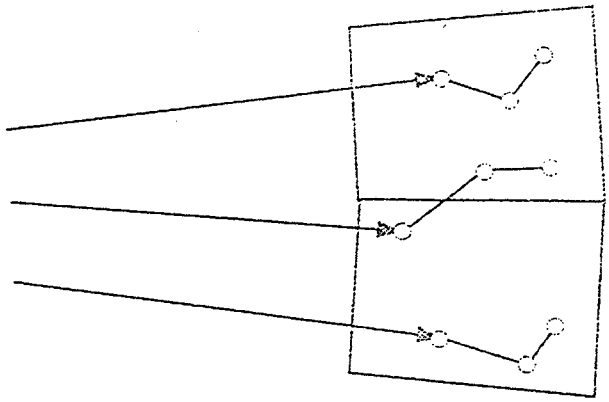

$\varepsilon = 0.6$

Ndet = **1000**
**(summing)**

## GRETA

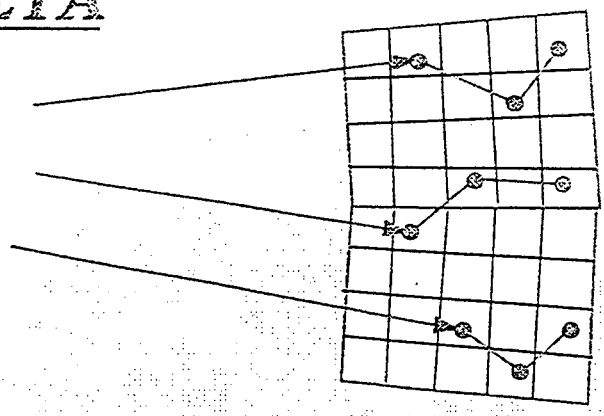

$\varepsilon = 0.6$

Ndet = **100**

# GRETA Concepts

- Detector with 3-D position information.
  - **Segmentation gives angular and longitudinal position.**
  - **Drift time gives radial position.**
- Signals processed by flash ADC's and DSP's.
  - **Energy**
  - **Position interpolation**
  - **Drift time determination**
- Algorithms to identify interaction points belonging to a particular gamma ray.
  - **Cluster recognition**
  - **Tracking -Compton scattering formula**

tk/greta_concept.iw

# Segment Signals

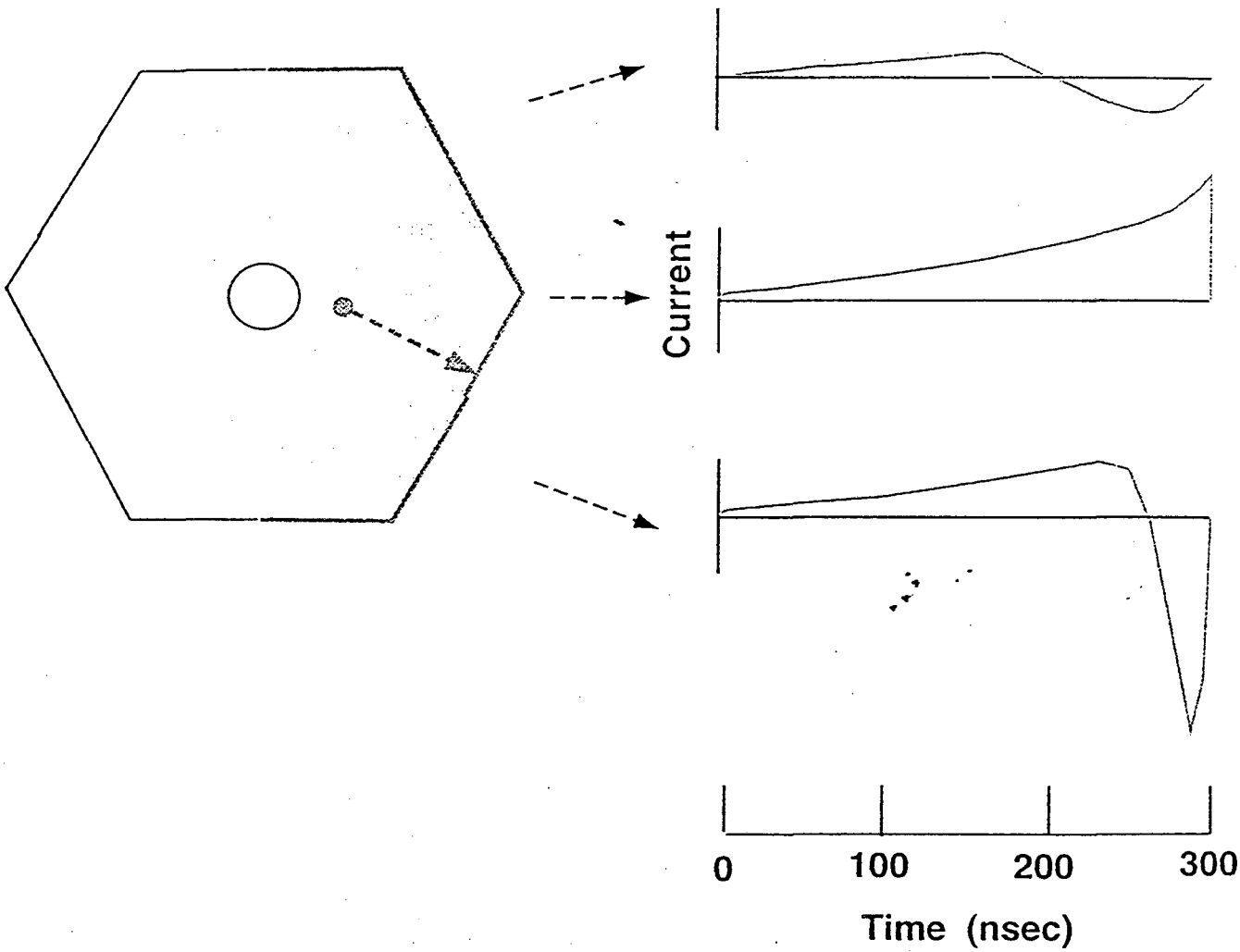

# GRETA R/D status

February 1998

## Detector Prototype

- A 12-fold segmented detector is received.

## Signal Processing (Kai Vetter)

- Measured and analyzed pulse shapes of the 12-fold segmented detector.
- Calculated signals of the 12-fold segmented detector.
- Study position sensitivity of the signals.
- Determine the accuracy of 3-D position measurement.
- Electronics Response are being studied.

## Tracking (Greg Schmid)

- Continue development of algorithm.
- Efficiency and P/T are studied as functions of gamma-ray energy, multiplicity, and position resolution.
- Effects of realistic detector packing and neutron are being studied

# GRETA Prototype

## Segmented tapered hexagonal Ge detector

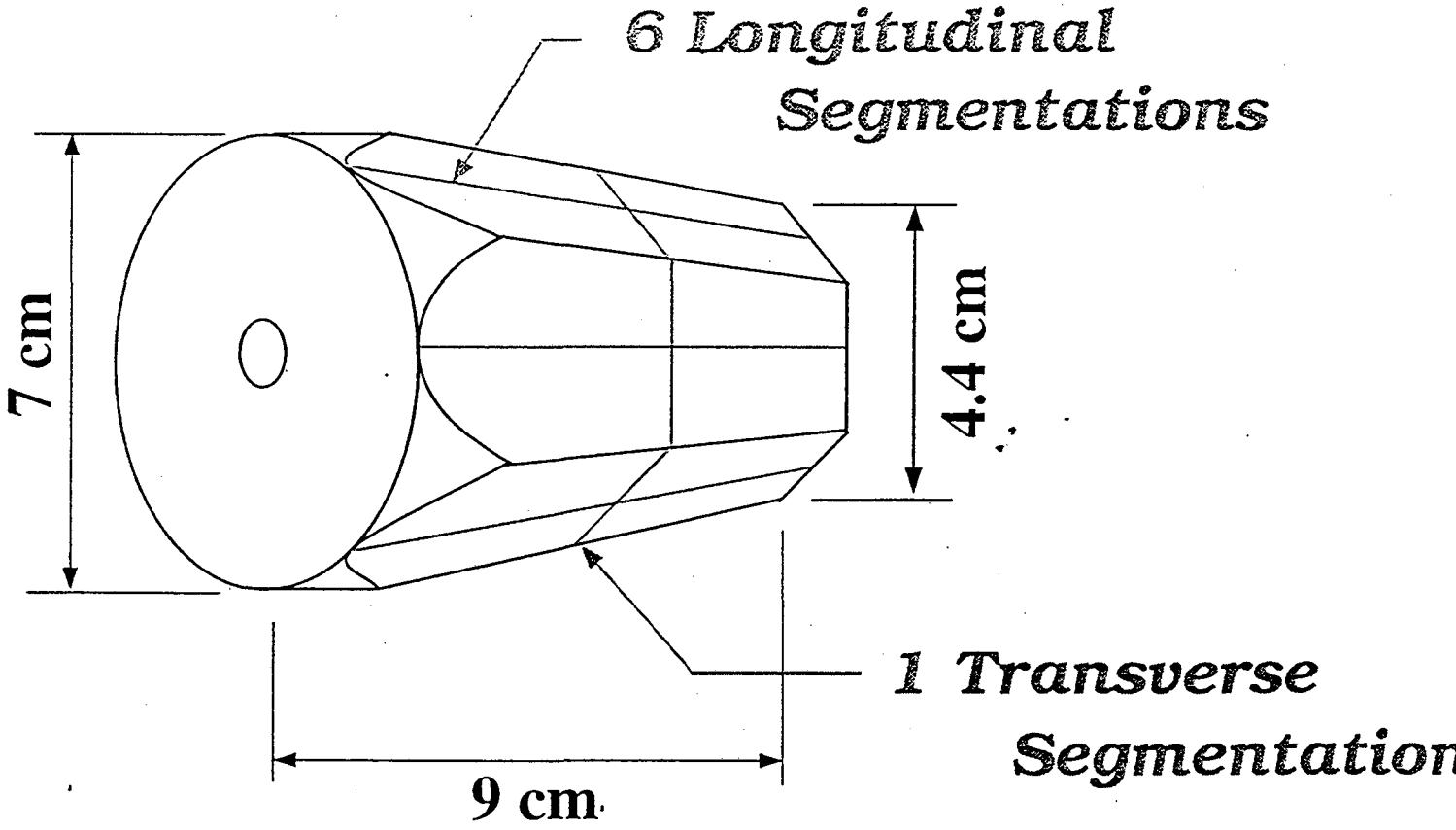

Energy Resolution of GRETA Prototype Detector

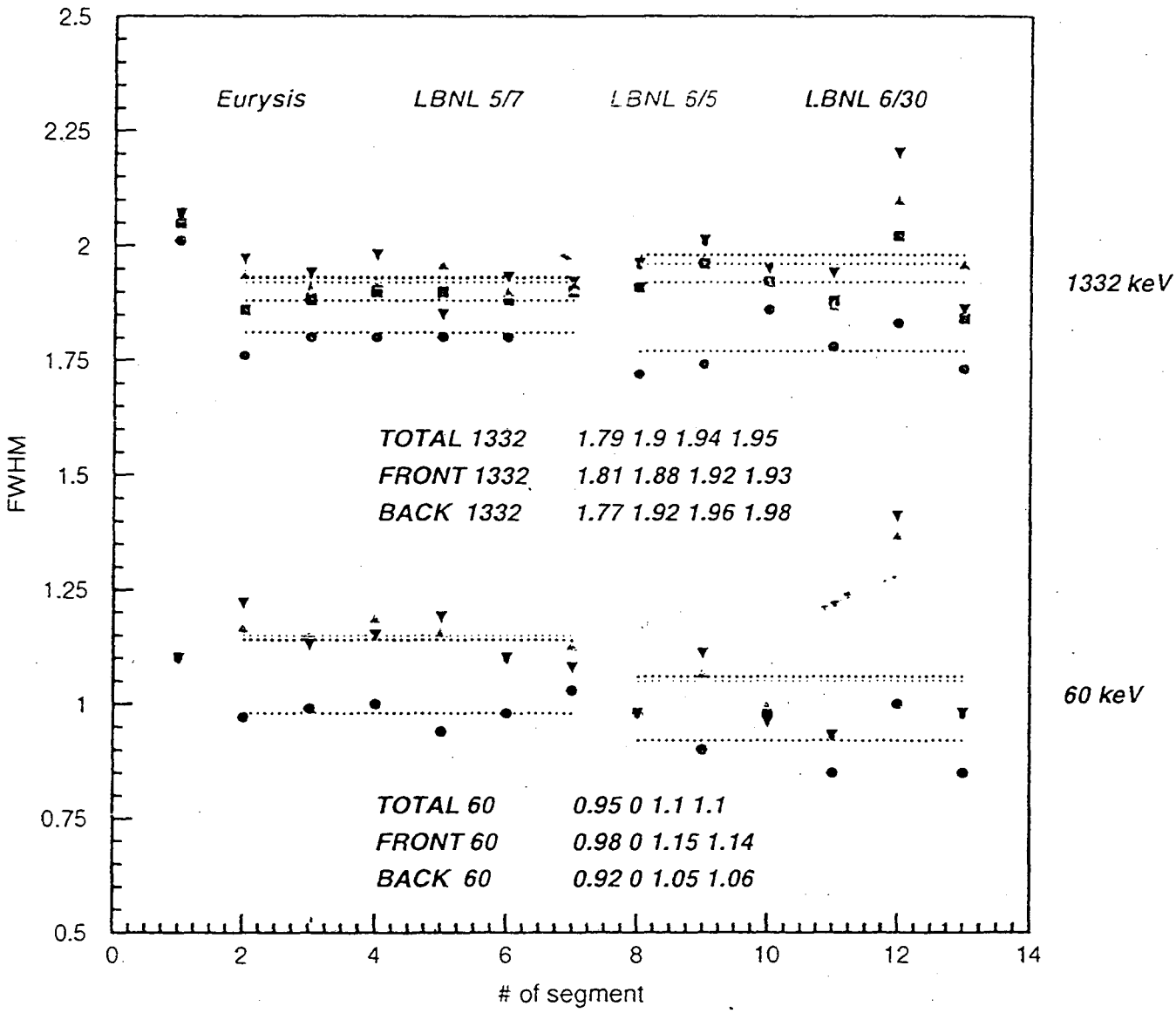

Current Signals in a Segmented Gammashere Detector

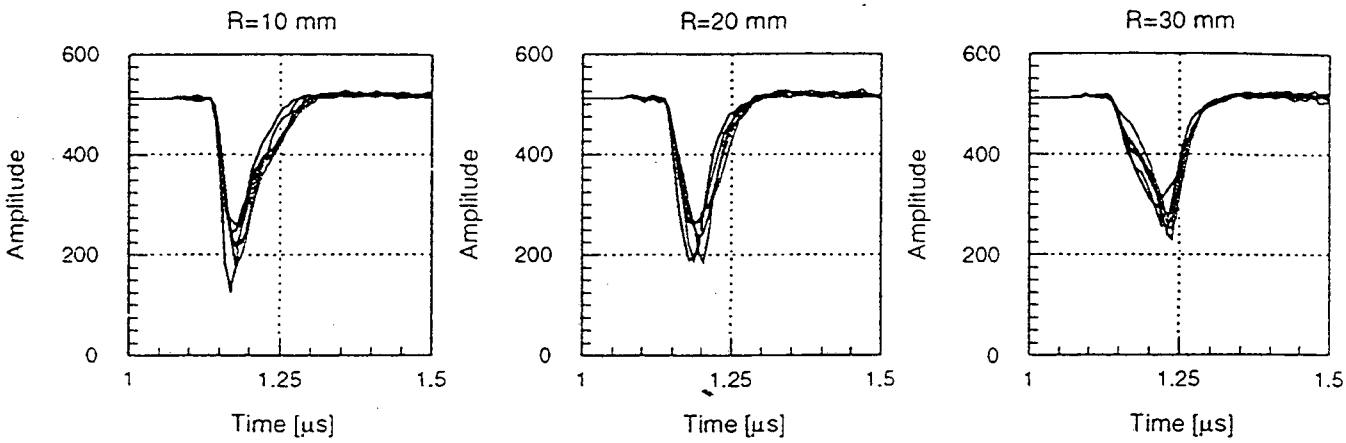

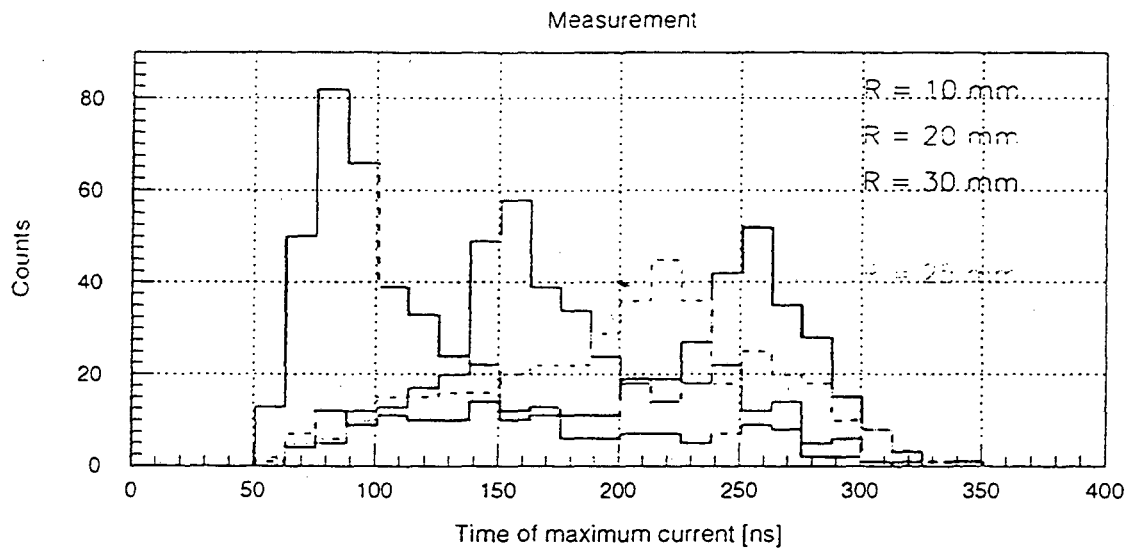
Measurement
R = 10 mm
R = 20 mm
R = 30 mm
Counts
0
20
40
60
80
0
50
100
150
200
250
300
350
400
Time of maximum current [ns]

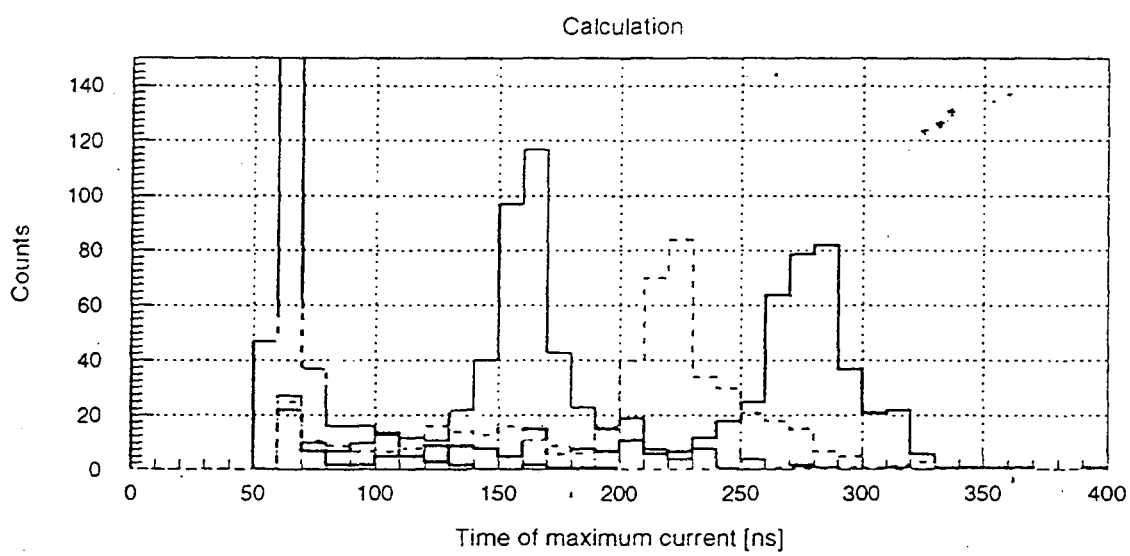
Calculation
Counts
0
20
40
60
80
100
120
140
0
50
100
150
200
250
300
350
400
Time of maximum current [ns]

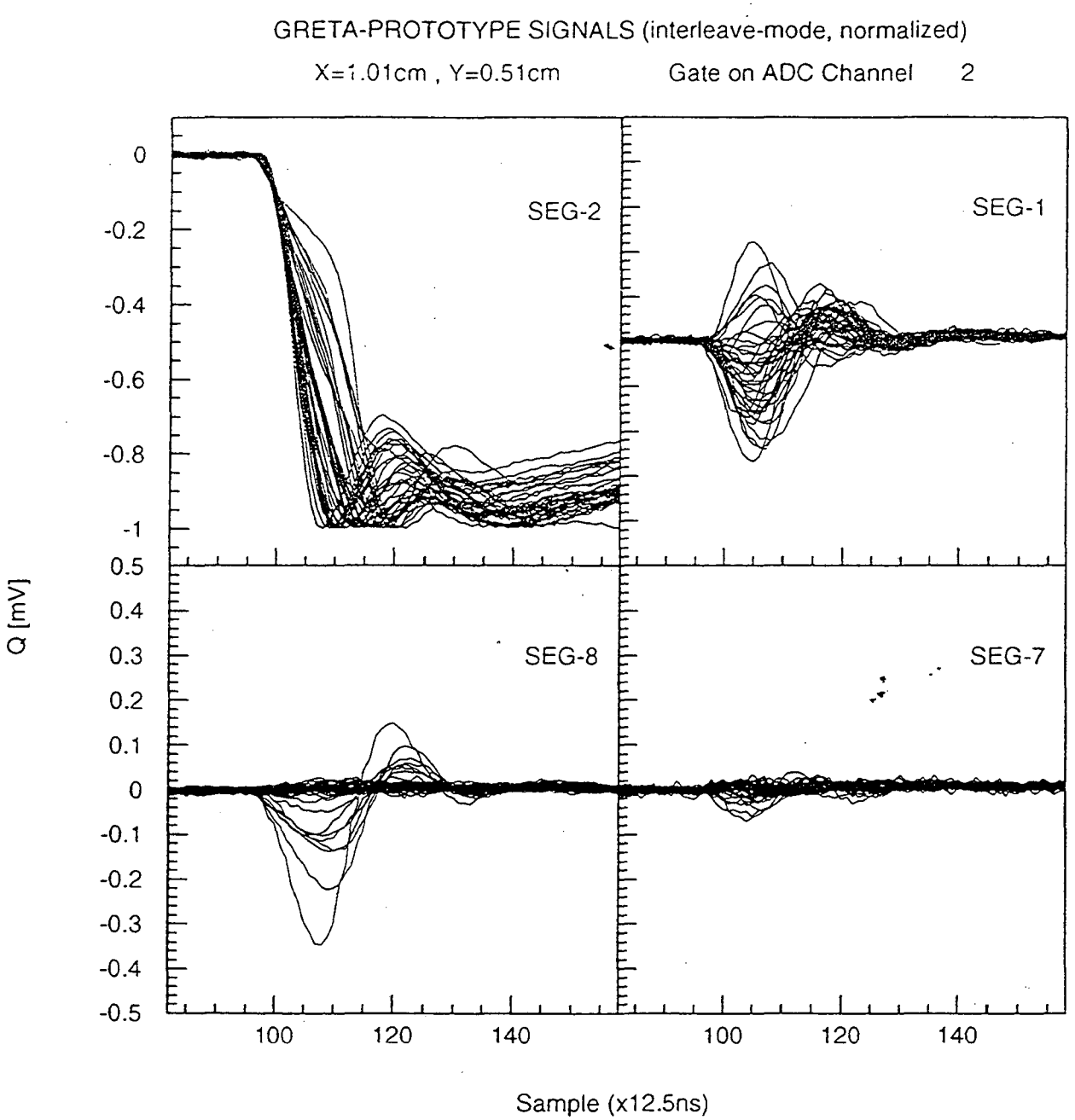
GRETA-PROTOTYPE SIGNALS (interleave-mode, normalized)
X=1.01cm , Y=0.51cm
Gate on ADC Channel 2
SEG-2
SEG-1
SEG-8
SEG-7
Q [mV]
0
-0.2
-0.4
-0.6
-0.8
-1
0.5
0.4
0.3
0.2
0.1
0
-0.1
-0.2
-0.3
-0.4
-0.5
100
120
140
100
120
140
Sample (x12.5ns)

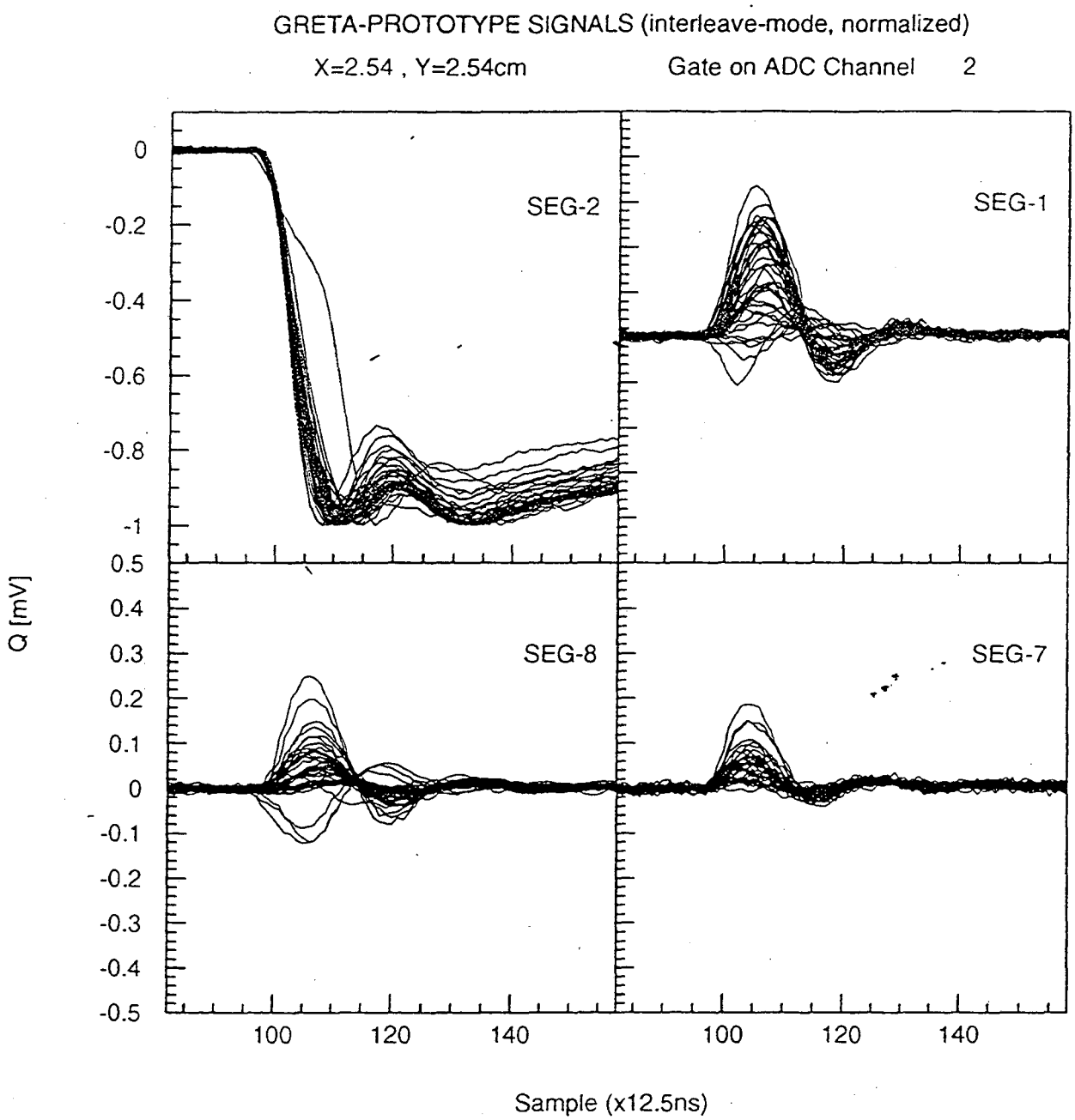
GRETA-PROTOTYPE SIGNALS (interleave-mode, normalized)
X=2.54 , Y=2.54cm
Gate on ADC Channel 2
SEG-2
SEG-1
SEG-8
SEG-7
Q [mV]
0
-0.2
-0.4
-0.6
-0.8
-1
0.5
0.4
0.3
0.2
0.1
0
-0.1
-0.2
-0.3
-0.4
-0.5
100
120
140
100
120
140
Sample (x12.5ns)

Calculated Signals in a Sixfold-Segmented Ge-Detector (Basis Functions)

1mm ≤ Y ≤ 28mm , 6mm ≤ R ≤ 33mm , ΔR = ΔY = 3mm

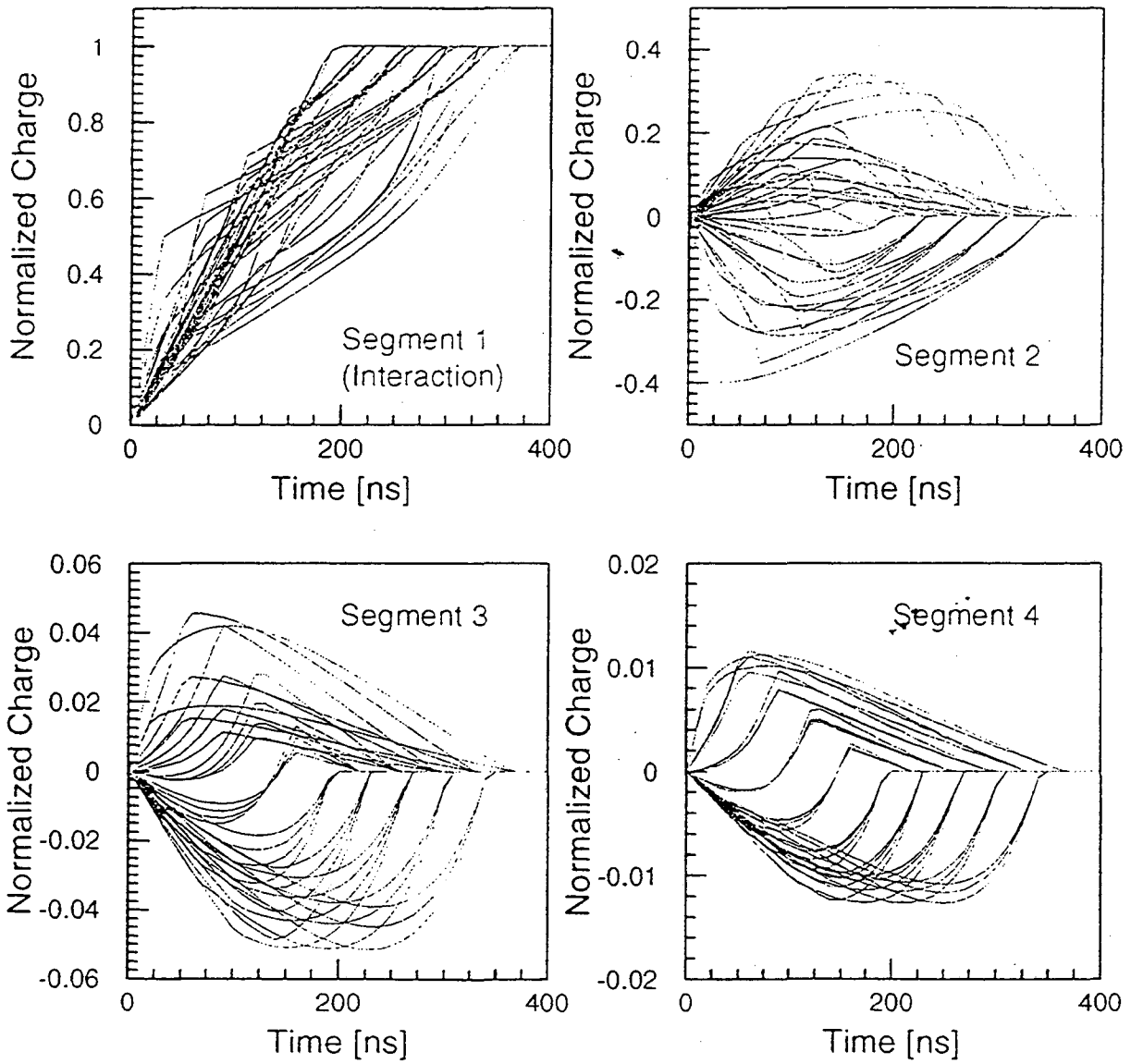

# Maximum Amplitudes in Induced Signals

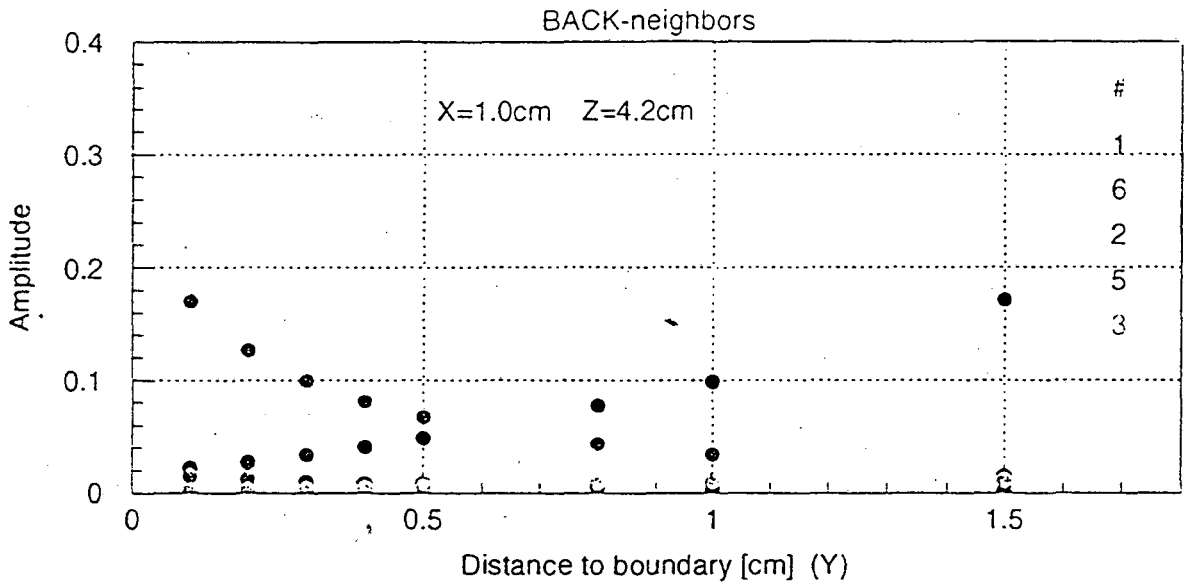


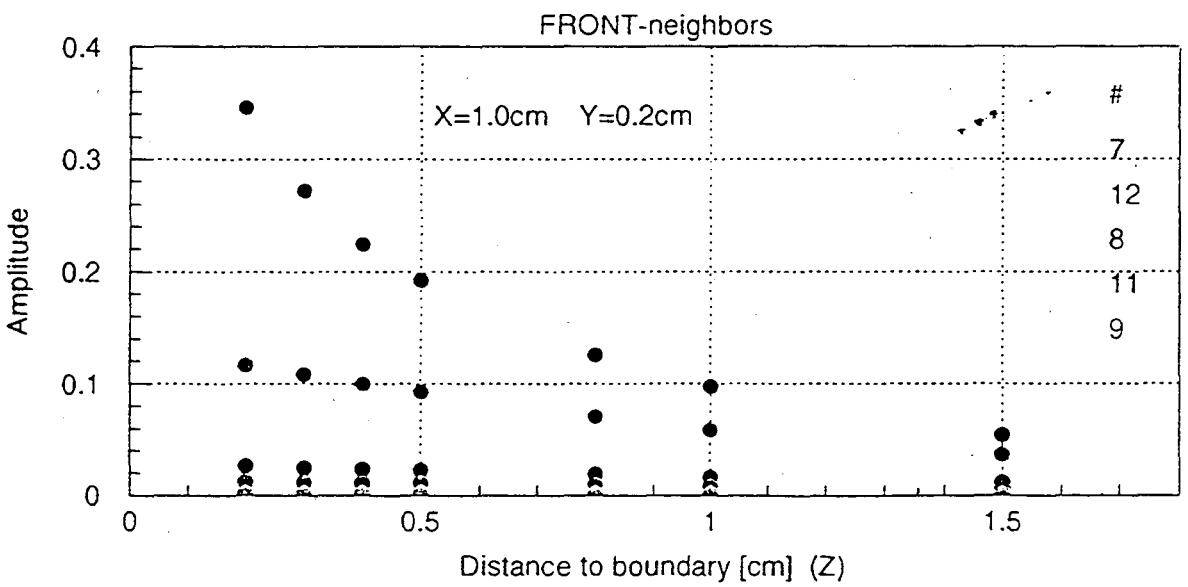

Calculated Signals in Six-Fold Segmented Closed-Ended Ge-Detector (GEANT)

R-ϕ- CORRELATIONS

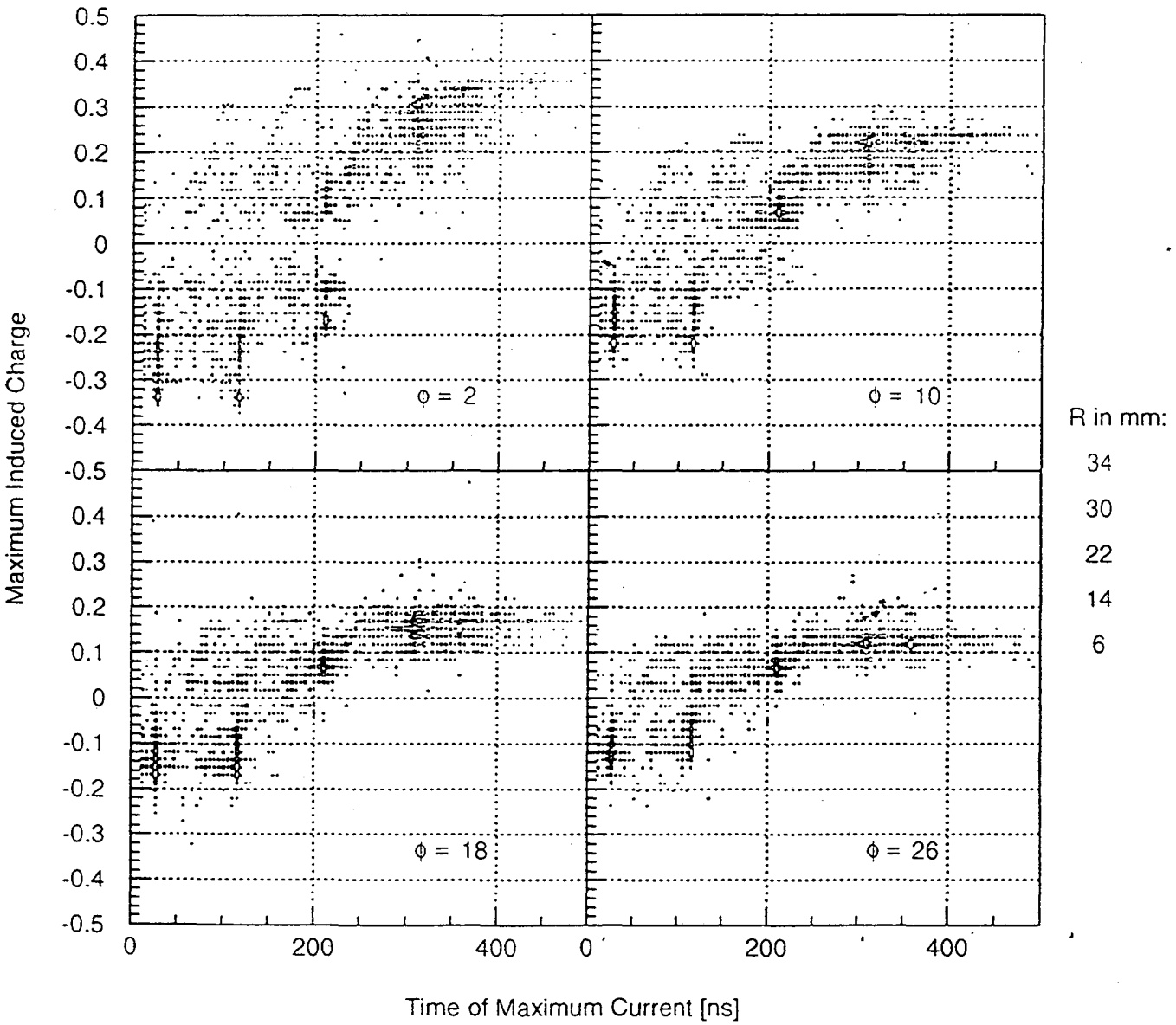

Cluster identification: Use angle parameter to group pts. into clusters.

**"World Map" showing interaction pts. in Ge shell**

(25 coincident γ-rays, E = 1.33 MeV)

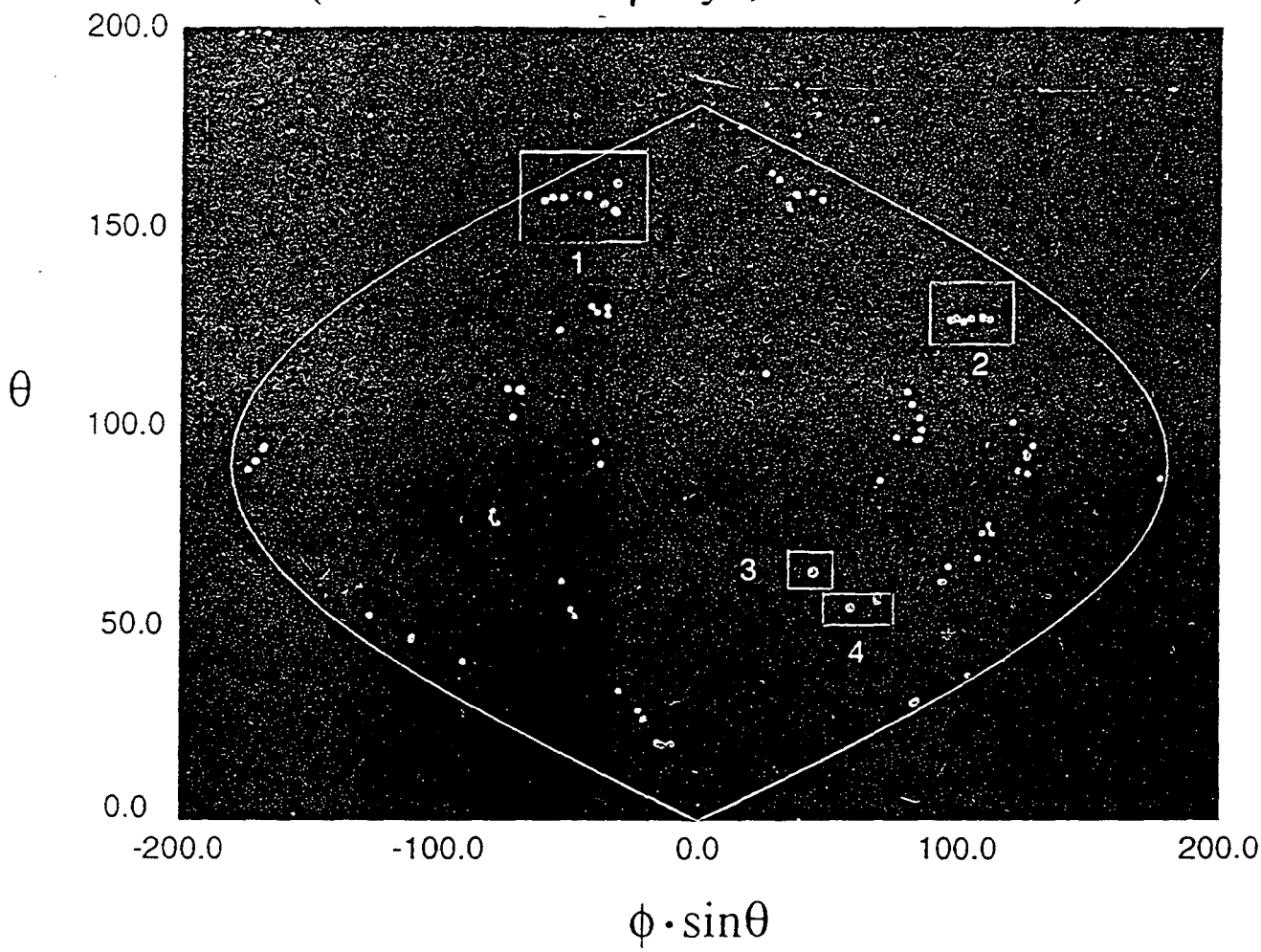


**Any 2 pts. with $\theta_p < 10^\circ$ are grouped into same cluster.**

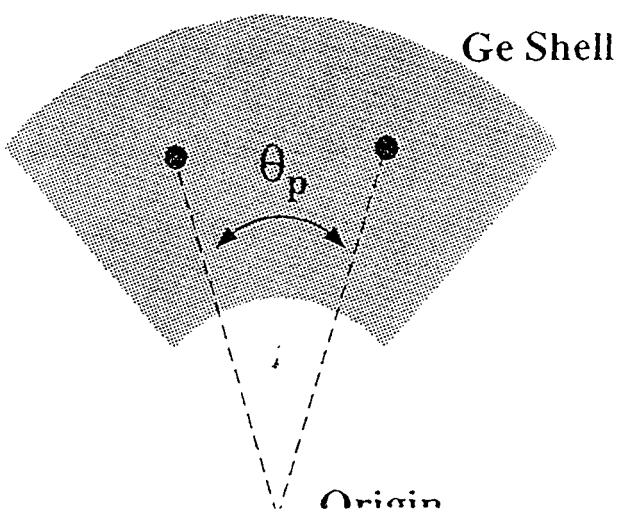

# Flowchart for Current Algorithm

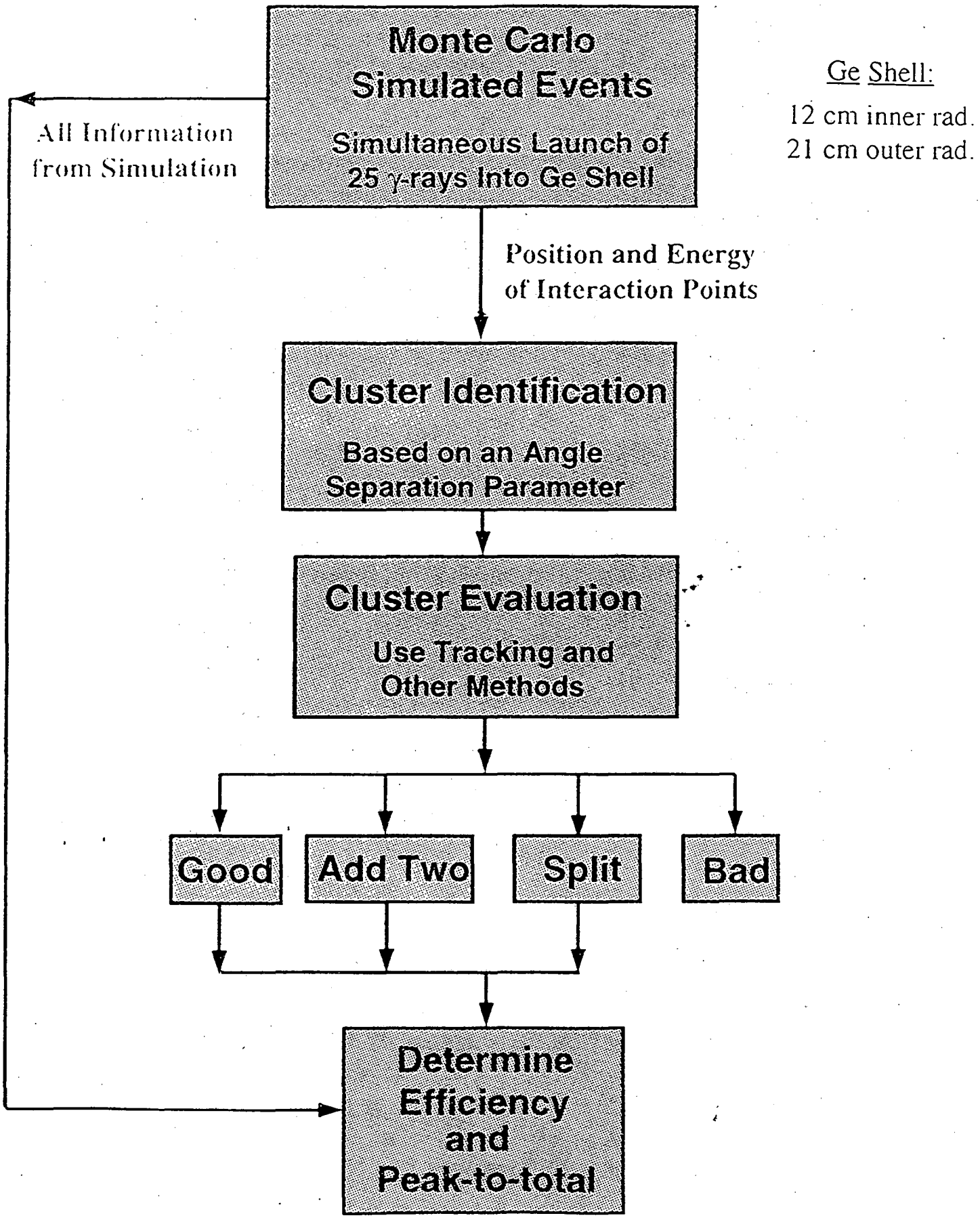

# Algorithm results

## Isotropic launch for GRETA

(25 coincident γ-rays, E=1.33 MeV)

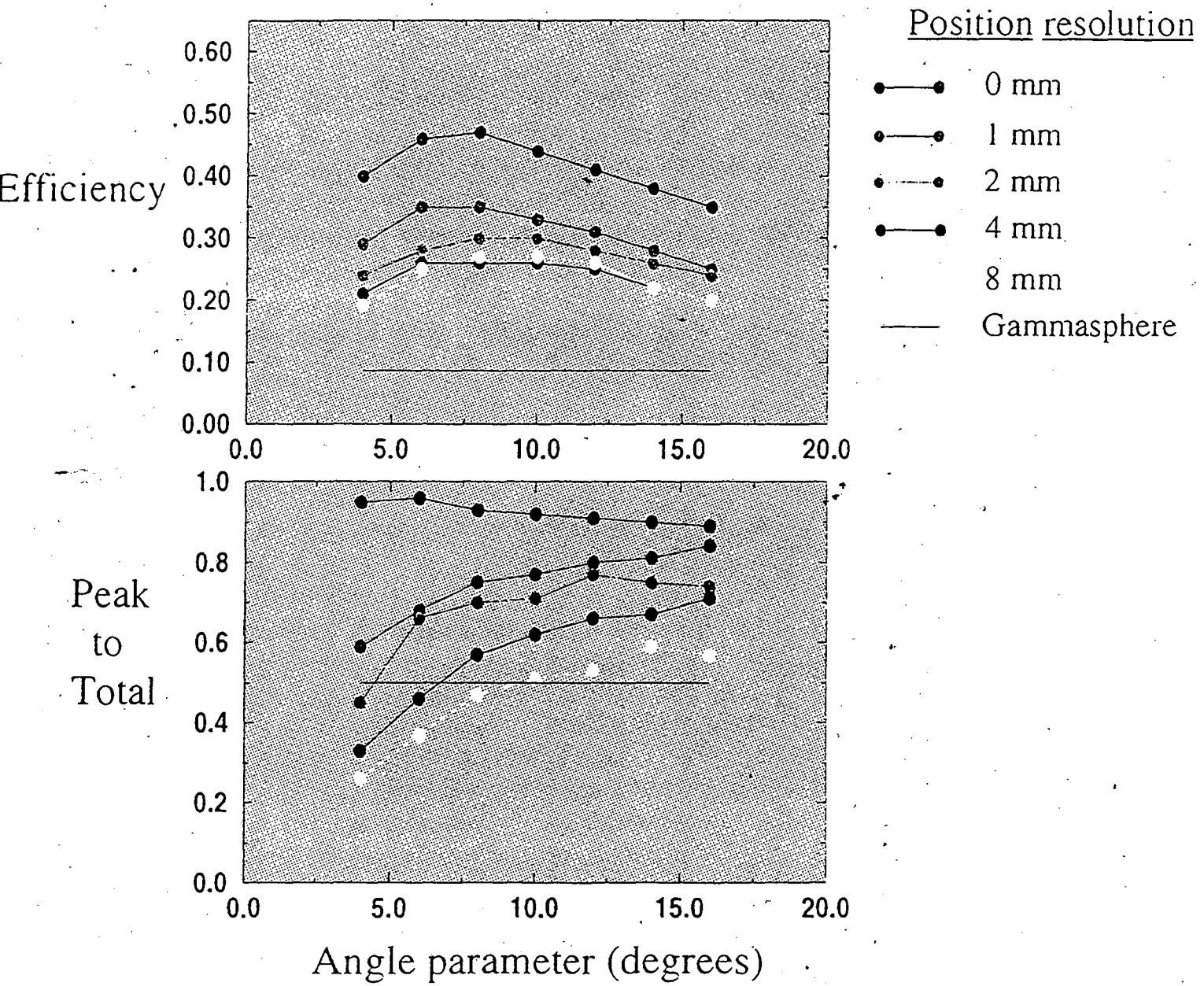

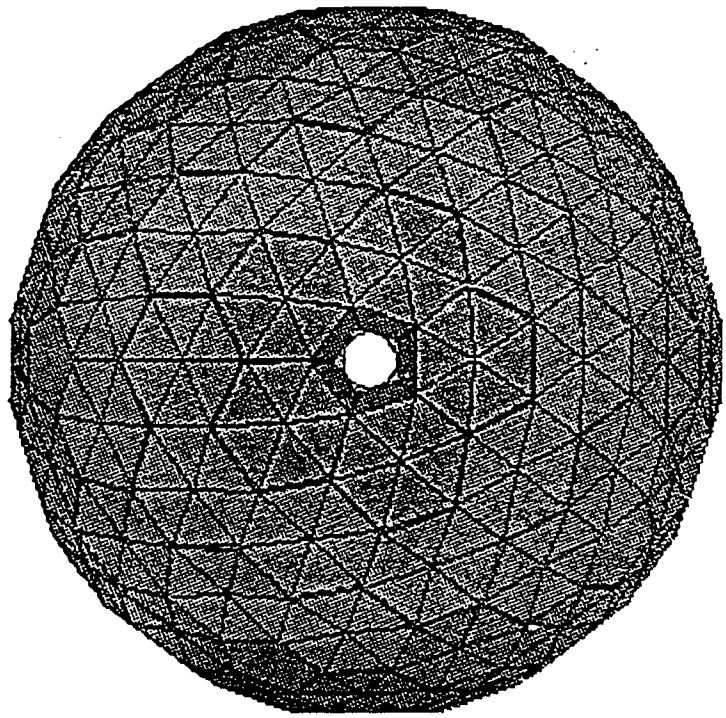

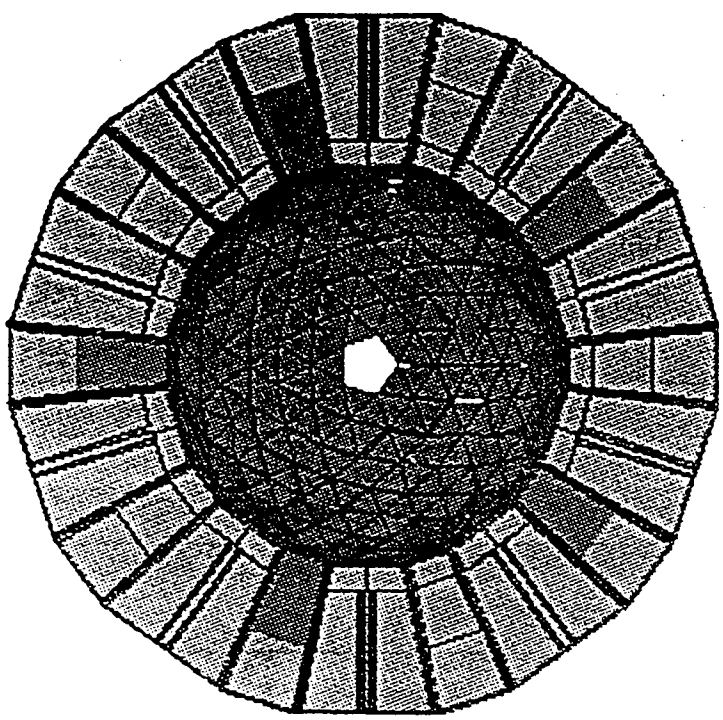

10 cm

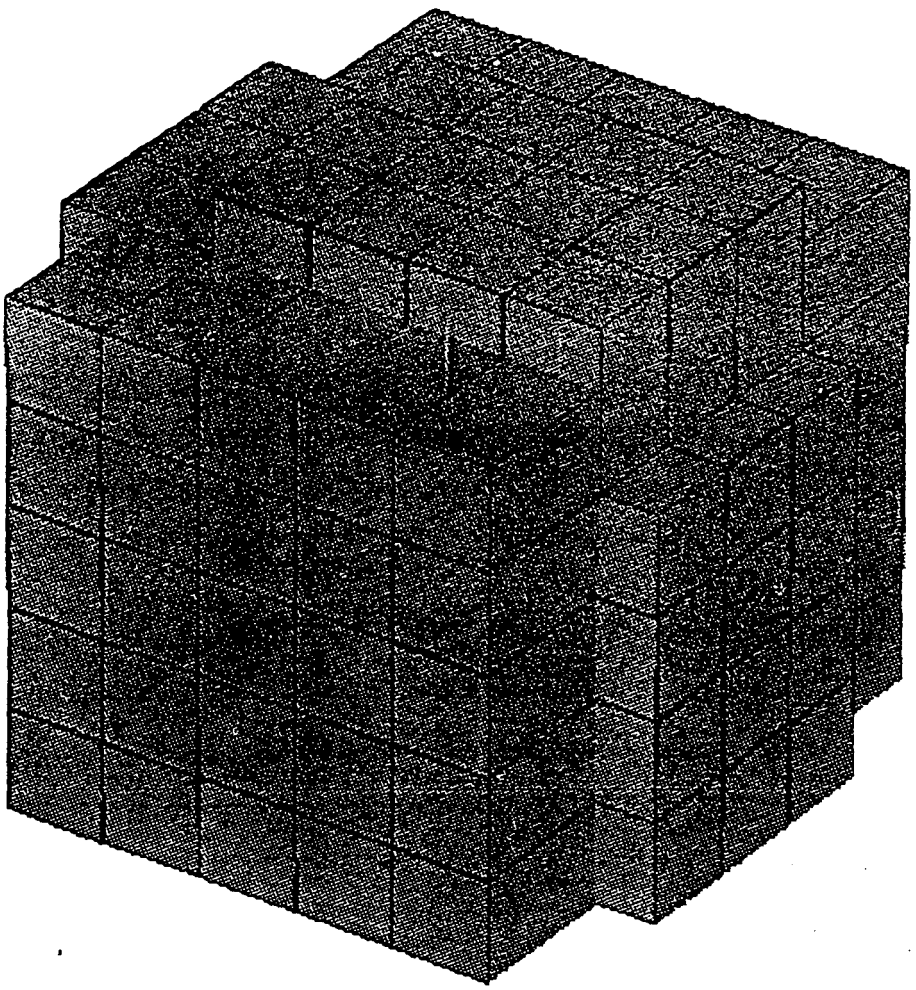

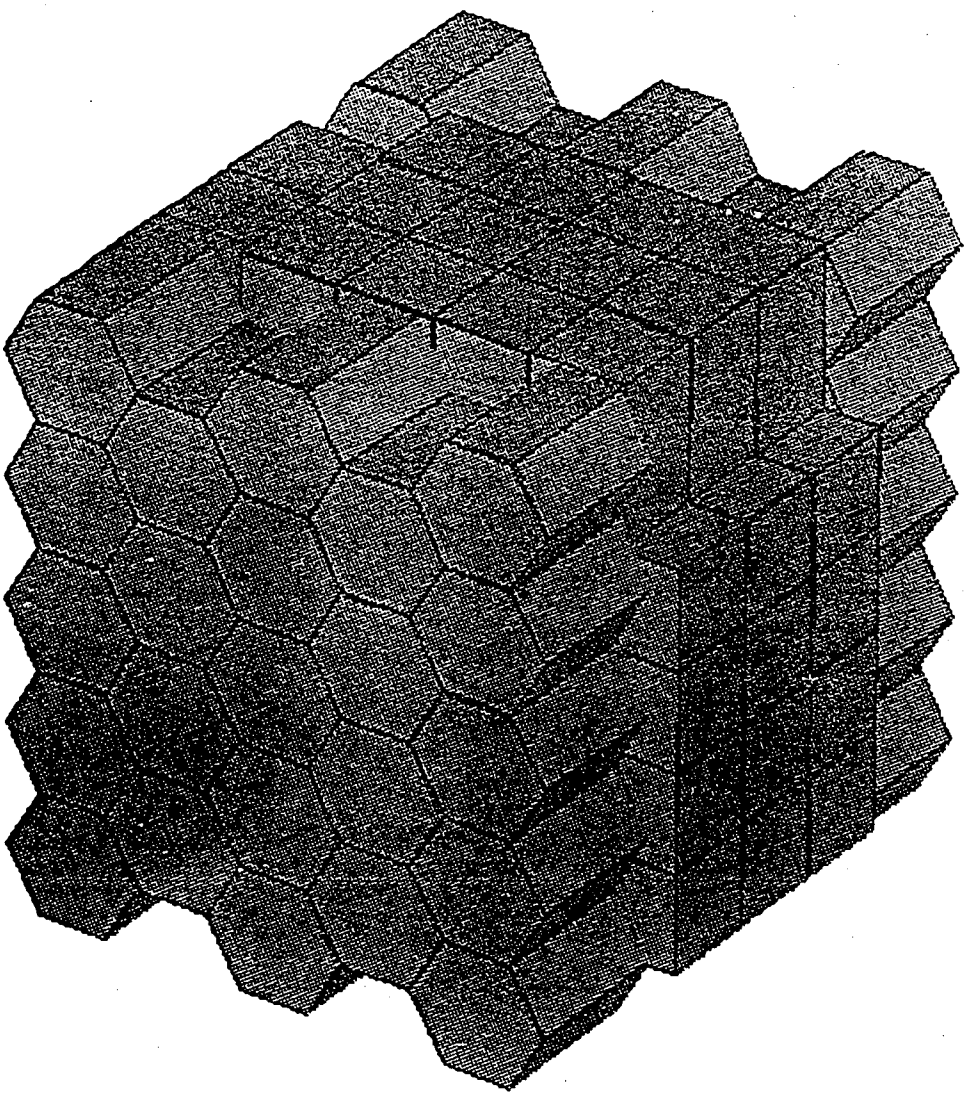

# Effect of Detector Packing

| | tappered hexagon | cube | cube + hexagon |
|---|---|---|---|
| number of detector | 120 | 98 | 94 |
| efficiency no gap | 66.0% | 65.5% | 67.4% |
| efficiency with gap | 54.0% | 55.8% | 57.8% |

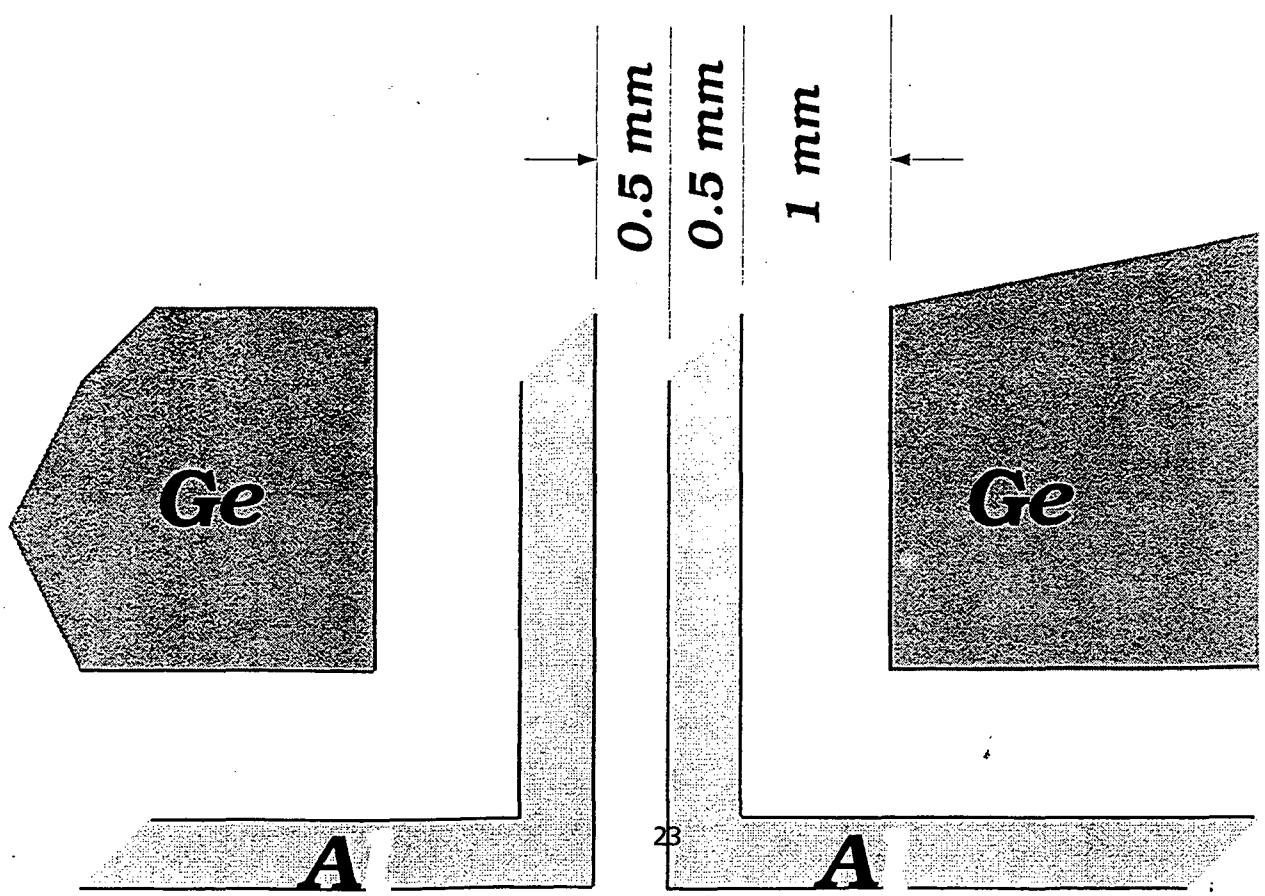

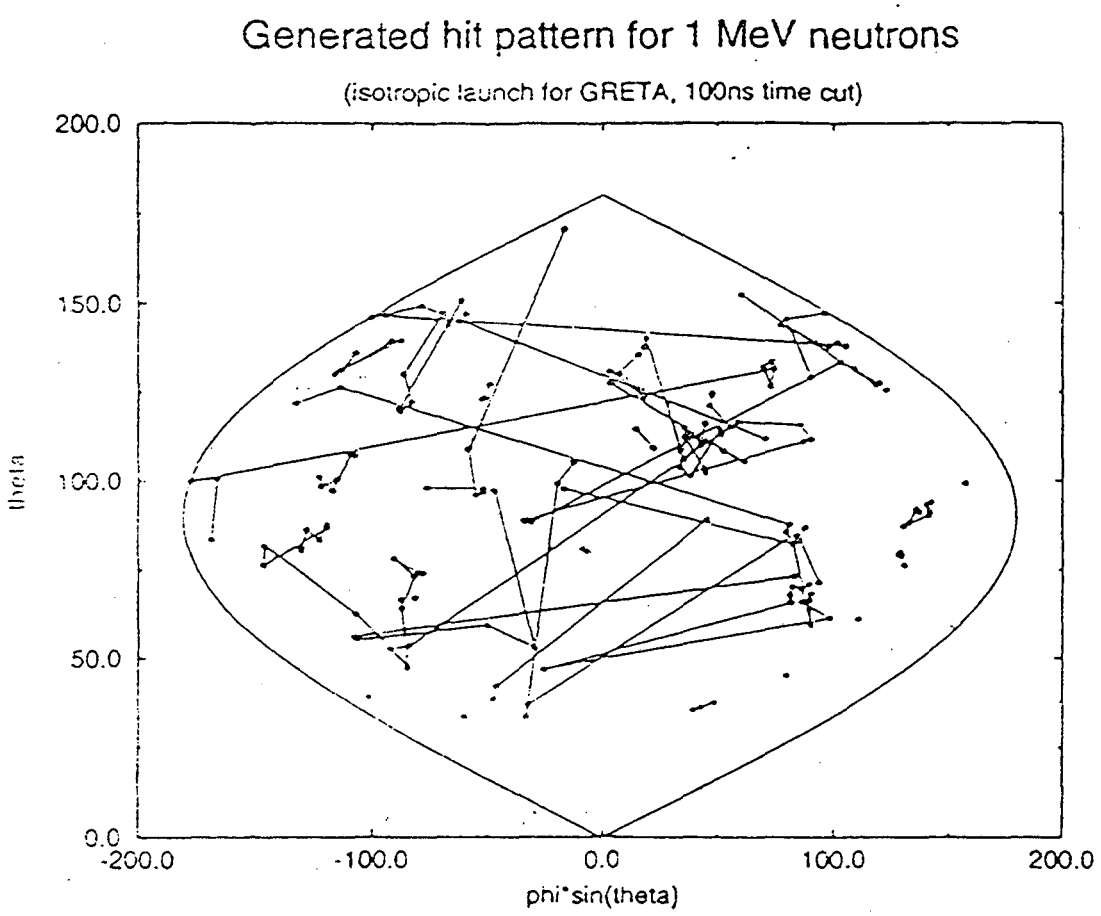
Generated hit pattern for 1 MeV neutrons
(isotropic launch for GRETA, 100ns time cut)
200.0
150.0
100.0
50.0
0.0
theta
-200.0
-100.0
0.0
100.0
200.0
phi*sin(theta)

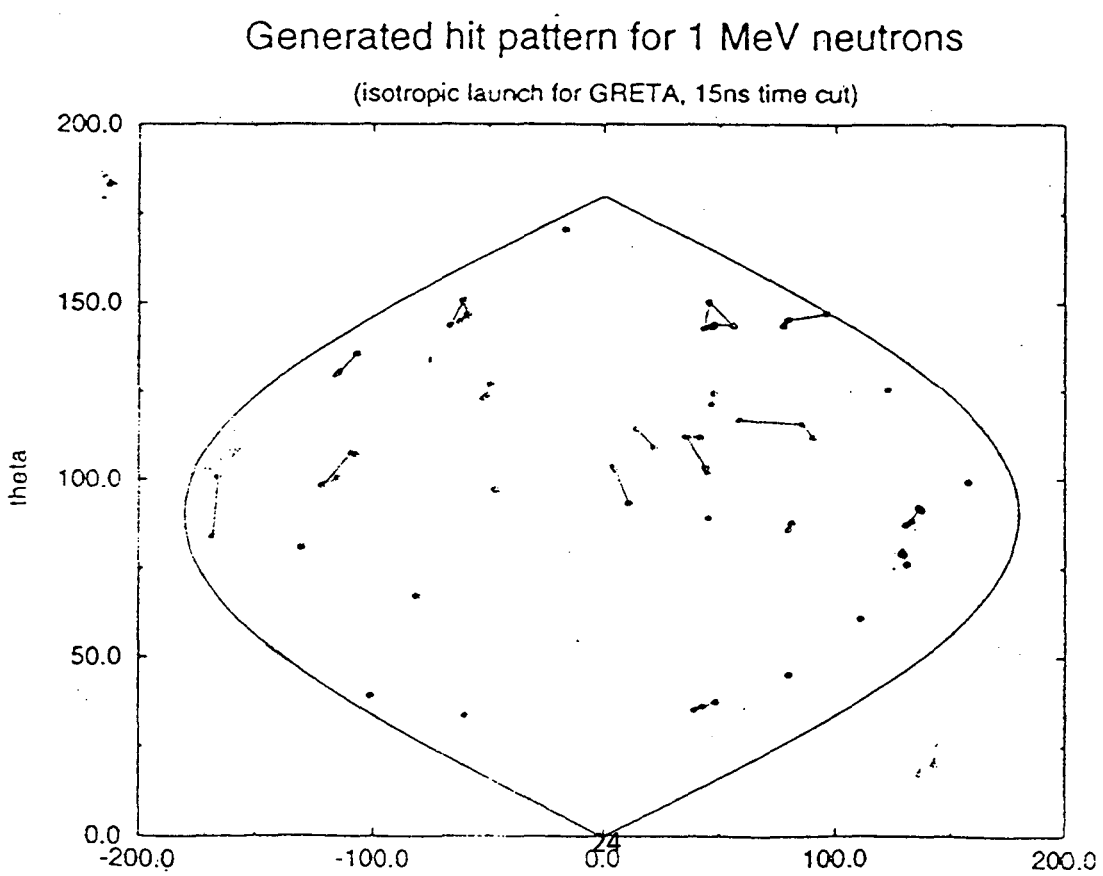
Generated hit pattern for 1 MeV neutrons
(isotropic launch for GRETA, 15ns time cut)
200.0
150.0
100.0
50.0
0.0
theta
-200.0
-100.0
0.0
100.0
200.0

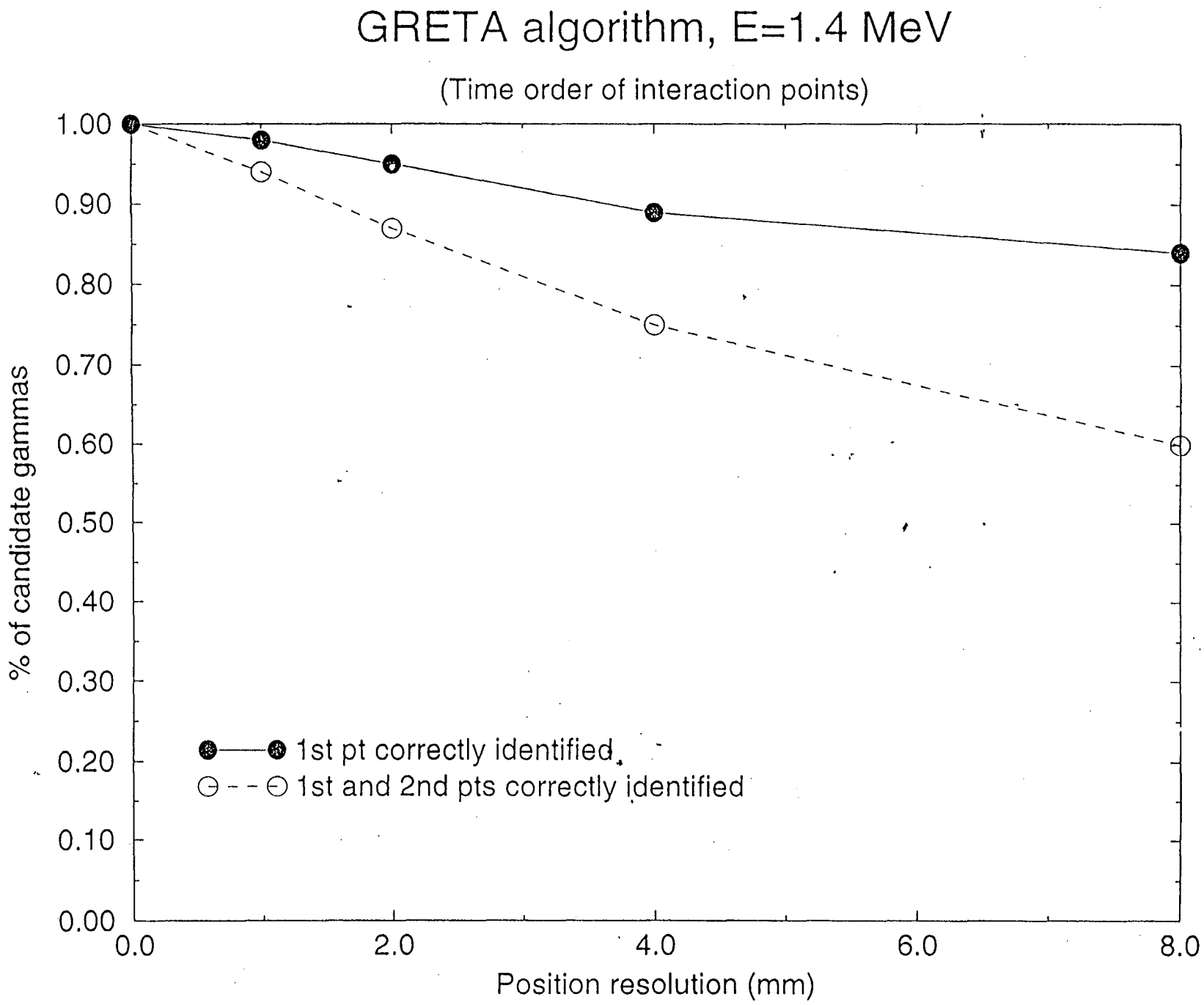
GRETA algorithm, E=1.4 MeV
(Time order of interaction points)
% of candidate gammas
1.00
0.90
0.80
0.70
0.60
0.50
0.40
0.30
0.20
0.10
0.00
0.0
2.0
4.0
6.0
8.0
Position resolution (mm)
1st pt correctly identified
1st and 2nd pts correctly identified

# Polarization sensitivity (Q) for GRETA

(E=400 keV)

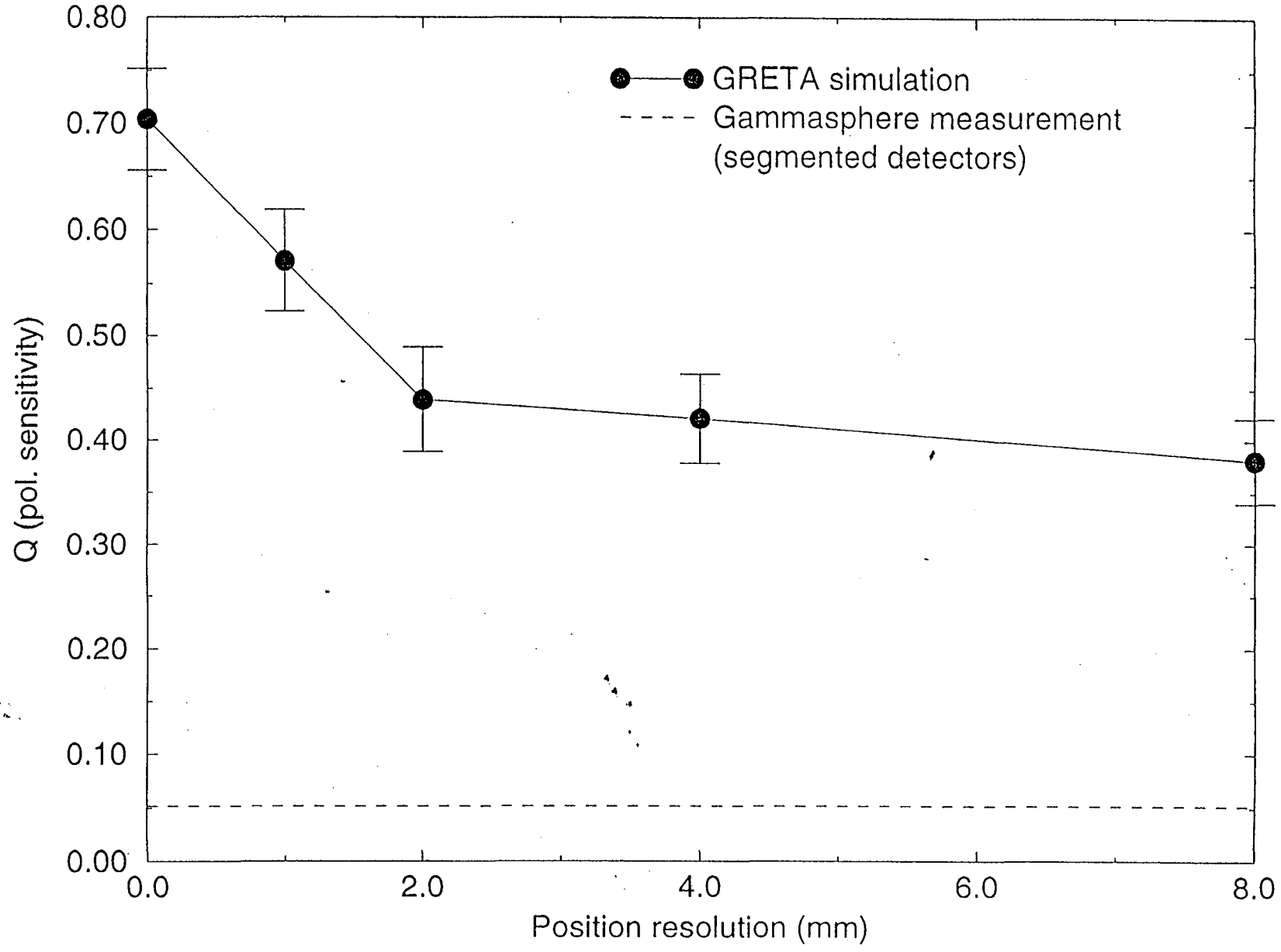

# GRETA R/D Plan

- **Detector Prototype**

  12-fold segmented detector
  36-fold segmented detector
  cluster of 1x7 or 3x3 modules

- **Signal Processing**

  position
  energy
  time

- **Tracking**

  high energy gamma ray
  neutron
  neural network method

- **Electronics**

  preamplifier
  waveform digitizer
  digital signal processor

# GRETA Prototype II

## 36 - fold Segmented Ge detector

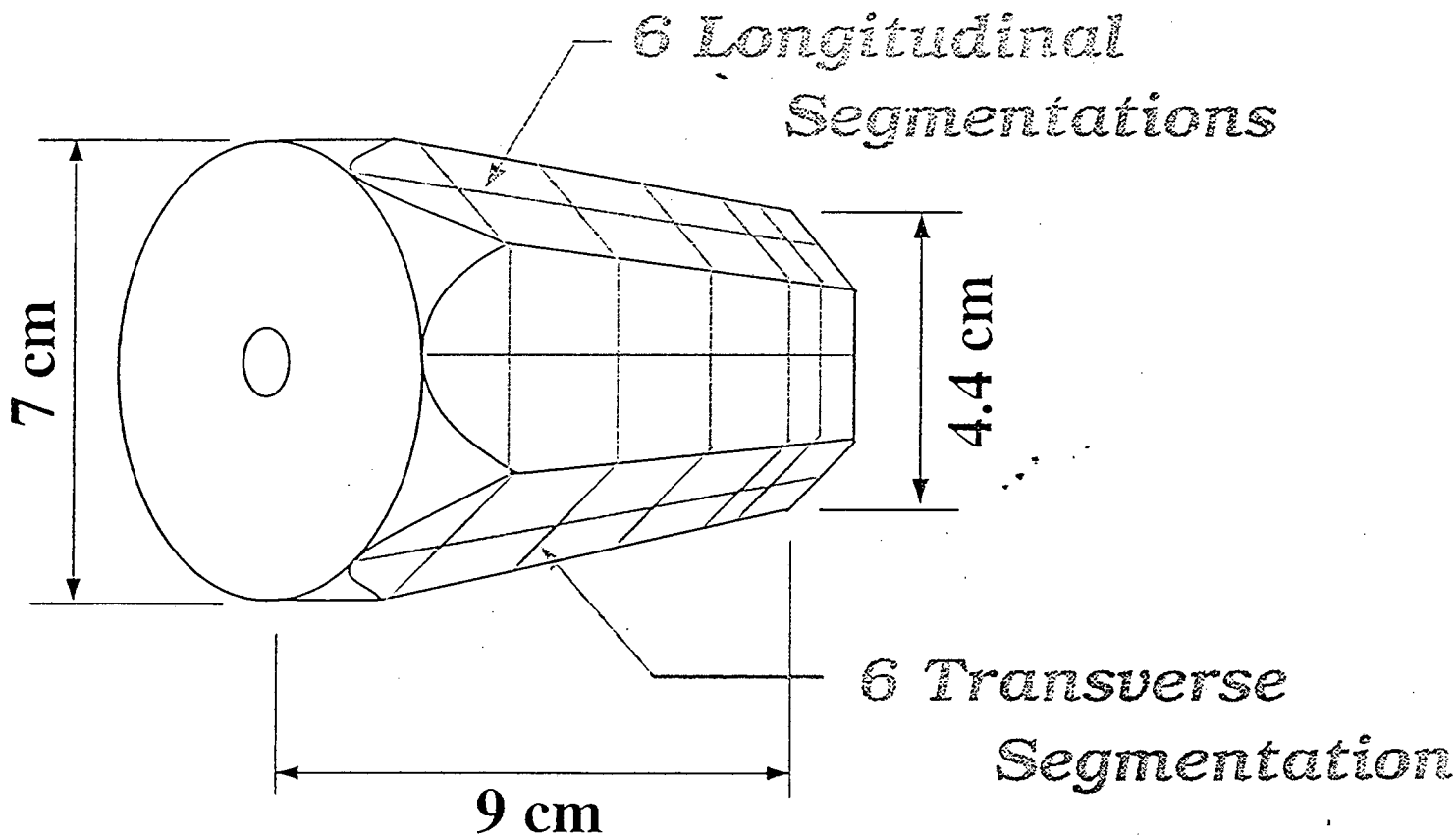


- Push segmentation technology
- Test warm vs. cold FET
- Test new preamp design

# GRETA Prototype III

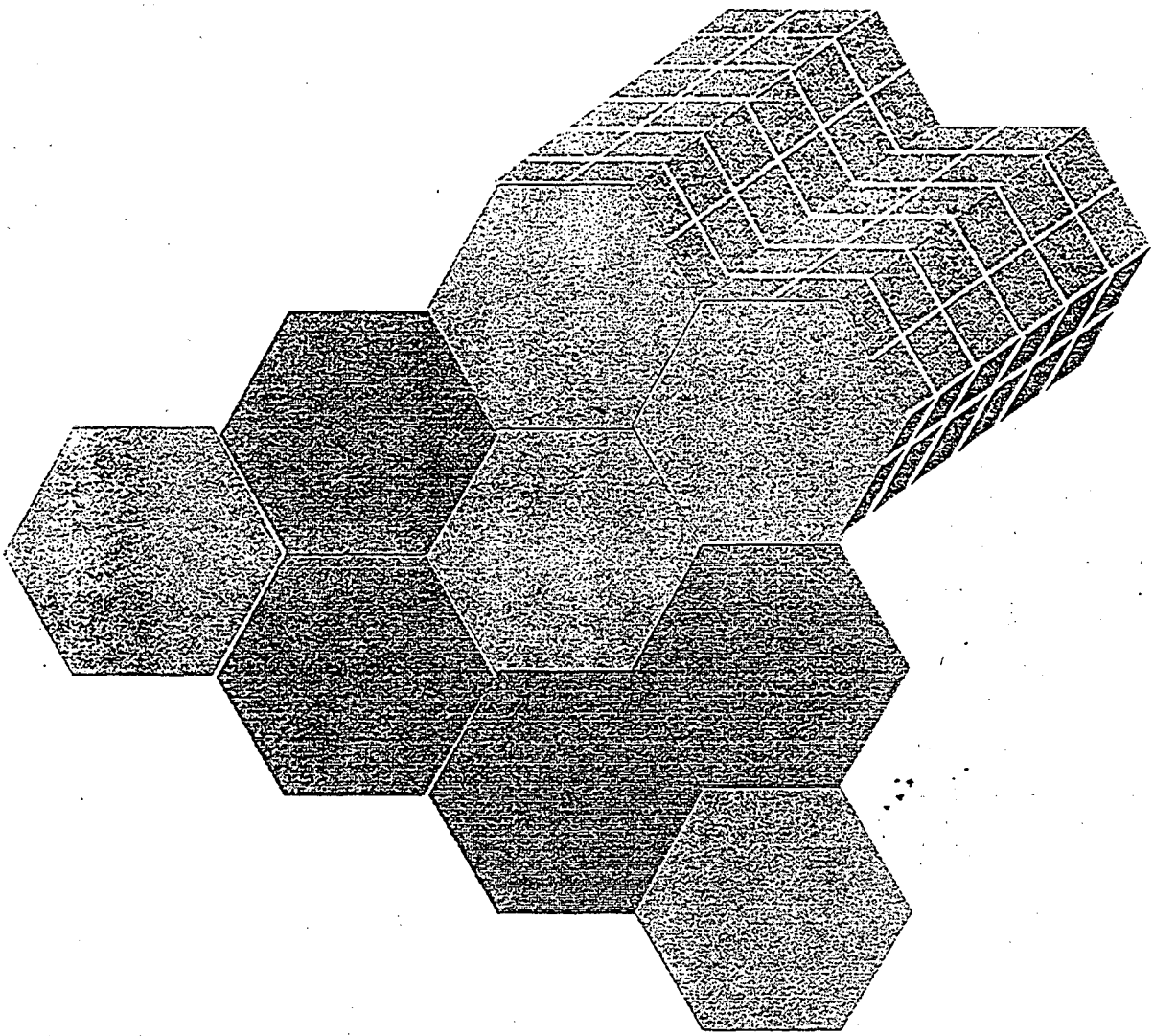

- Detector packaging schemes
- Tracking across detectors
- Physics program

# Detector Efficiency

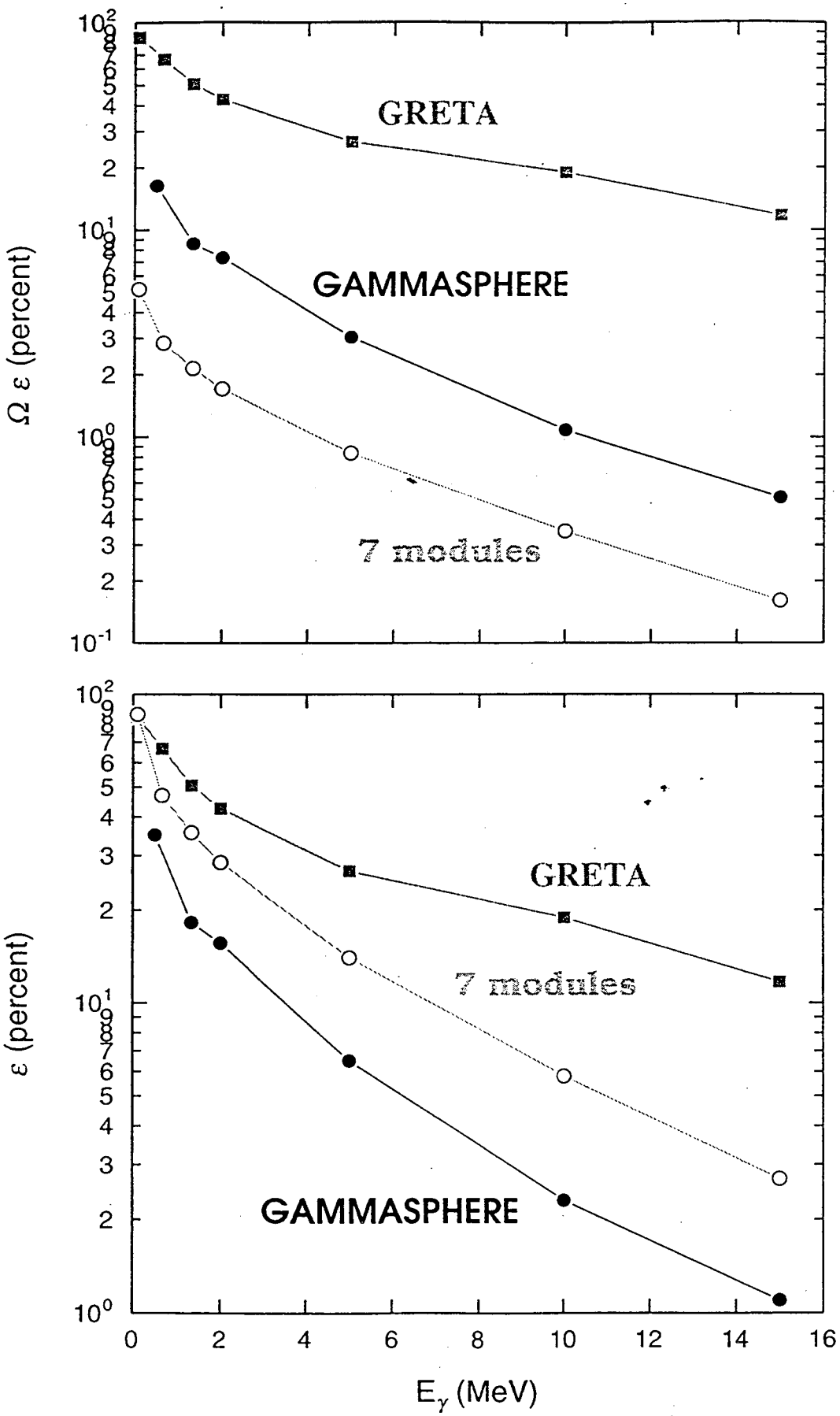




Efficiency.ps

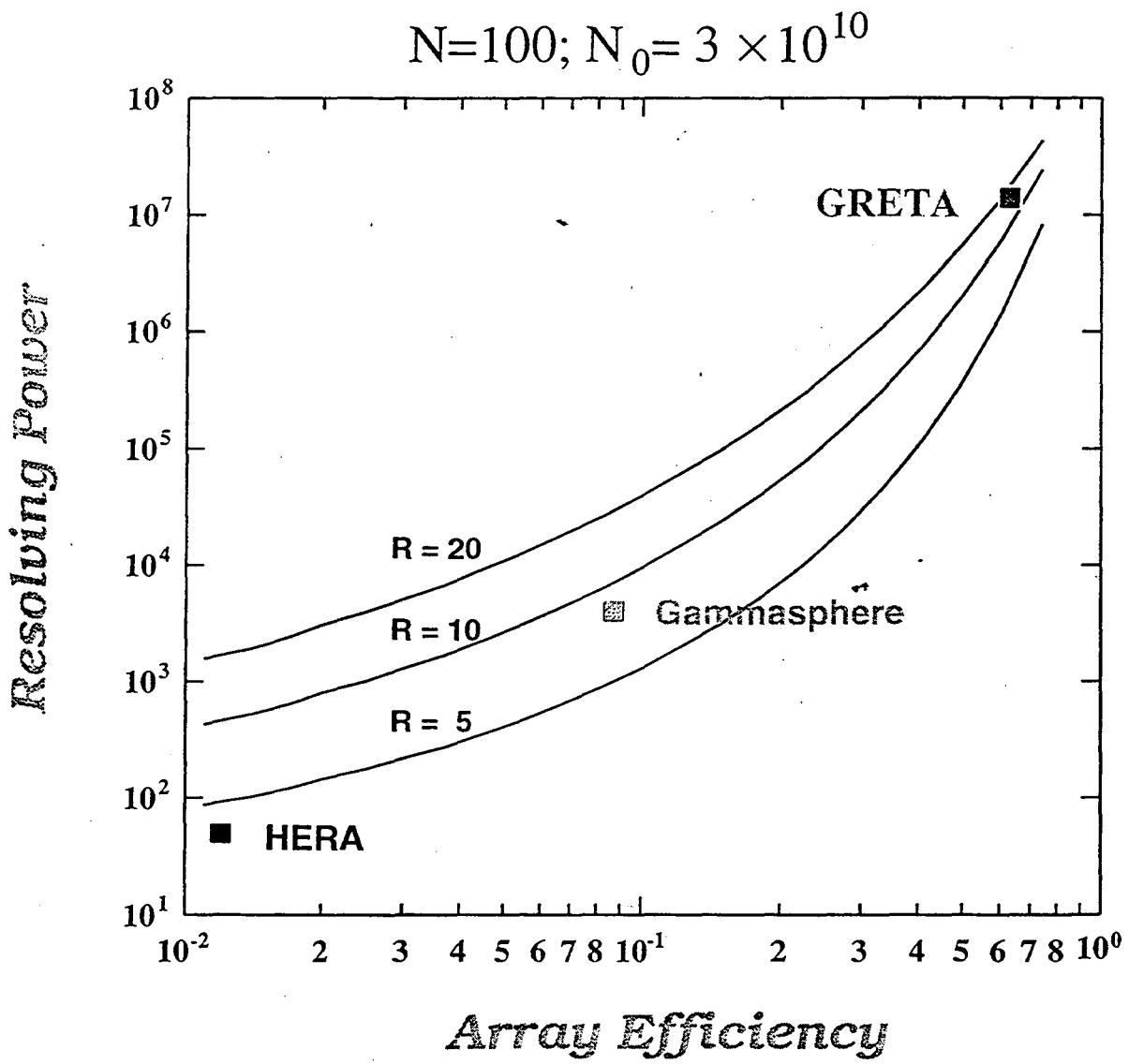


E: plot_r_power.ps
17-Jan-95 16:34:43 NSD, LBL

# GRETA Physics

- Characterization: track every interaction of each $\gamma$ ray
  - o Event-by-event $\gamma$-ray polarization
  - o Branching ratio in $^{10}C$ decay - electroweak coupling constant
  - o Four-$\gamma$ decay of positronium
  - o Second class currents
  - o Parity violation

- Localization: 2-3 mm in 3 dimensions (Doppler correction)
  - o Gamma-ray studies following inverse reactions
  - o Coulomb excitation of exotic RIB nuclei
  - o Nuclear structure following (GDR,n) reactions on RIBs
  - o Gamma rays from bound and unbound states in light nuclei
  - o Gamma rays following reactions on halo nuclei

- Full-energy efficiency: ~90% @ 0.1 MeV; ~20% @ 10 MeV
  - o Studies with exotic beams at an ISOL-type RIB facility
  - o Searches for strange matter
  - o Develop new cosmic-ray chronometers
  - o Studies of hypernuclei
  - o GDR shapes (fn. of temp., spin, and nuclear shape)
  - o Damping in giant resonances (e.g. GDR vs. GQR)

- Sensitivity: resolution, P/T, efficiency, granularity, rate
  - o Observation limit 100 nb (out of ~1b) in typical nuclear reactions
  - o Access to more exotic nuclei (very proton or neutron rich)
  - o Decay out of superdeformed nuclei (links)
  - o Signatures of chaos in nuclei
  - o Study of larger deformations (hyperdeformed or Jacobi shapes)
  - o Nuclear structure studies on nuclei with $Z > 100$

K.Vetter

Greta prototype test and simulations.

# GRETA Prototype :

## Tests & Simulations

GRETA workshop 5-7 Feb. 1998

**Kai Vetter**

**LBNL**

# GRETA Prototype: Test & Simulations

work being done in 2 areas:

| pulse shape analysis | $\gamma$-ray-tracking |
|---|---|
| first level "pre-processing" | second level "post-processing" |
| measures $Q_j(t)$ | takes $E_i$ , $x_i$ , $y_i$ , $z_i$ , $(t_i)$ |
| determines $E_i$ , $x_i$ , $y_i$ , $z_i$ , $(t_i)$ | determines $M_\gamma$ , $E_\gamma$ , $P_\gamma$ , ... |

3 dimensional position resolution ?

Radius ok (GS: drift time (trap. corr.), T30-T90, ...)

But : Z & $\phi$ ?

Already eg for first hit identification complementary $\phi$ required

→ segmentation

segmentation → **induced signal ?**

"physical" cross-talk ↔ "electronical" cross-talk ?

→ Gammasphere : two-fold segmented Ge detector

Induced Signals in a Segmented GAMMASPHERE Detector (#70)

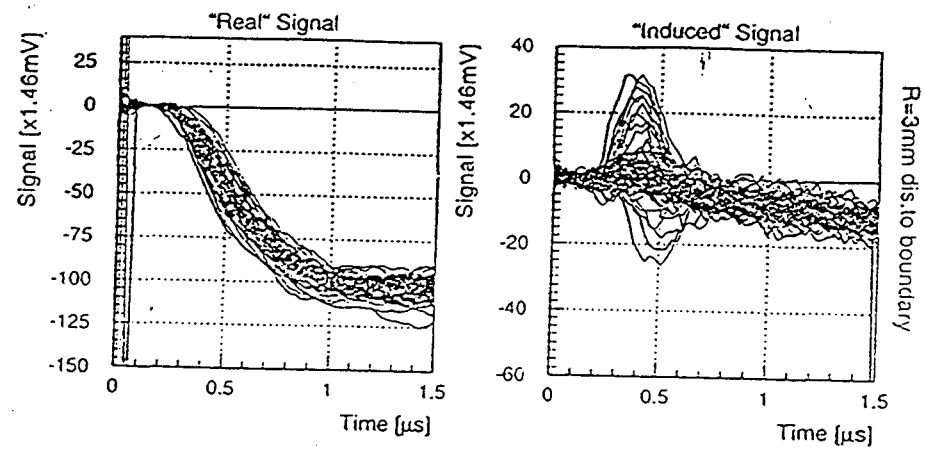


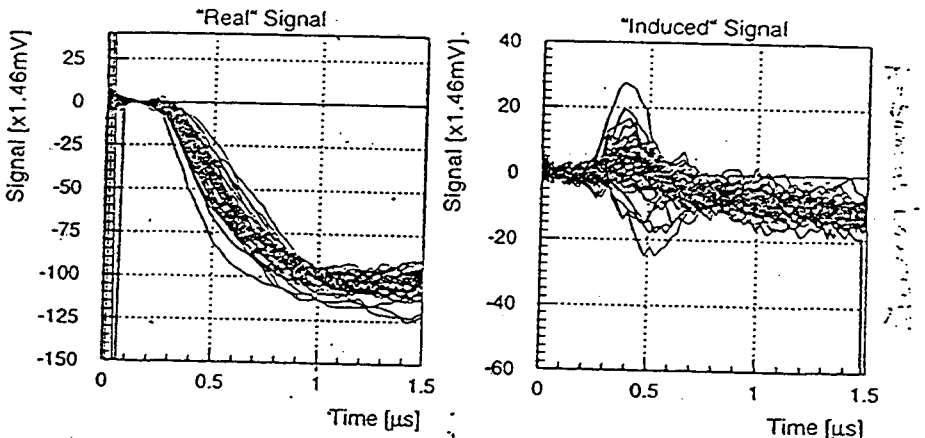


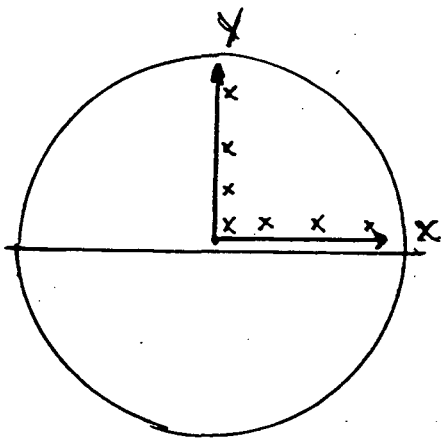


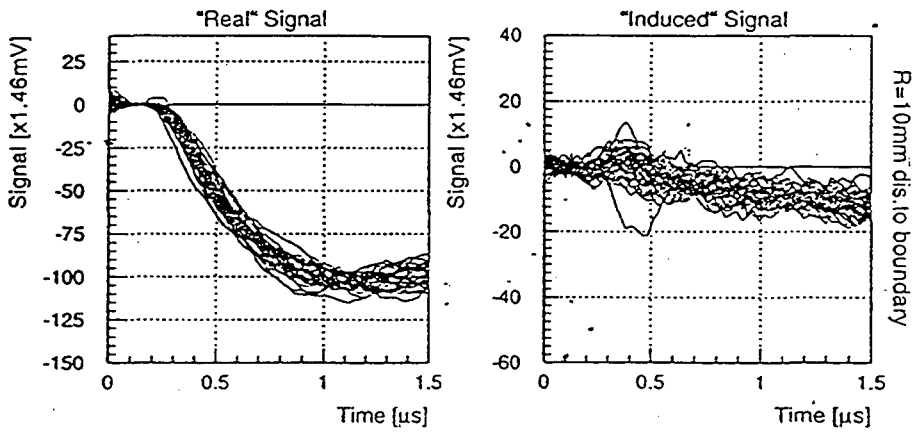


10 mm away from boundary

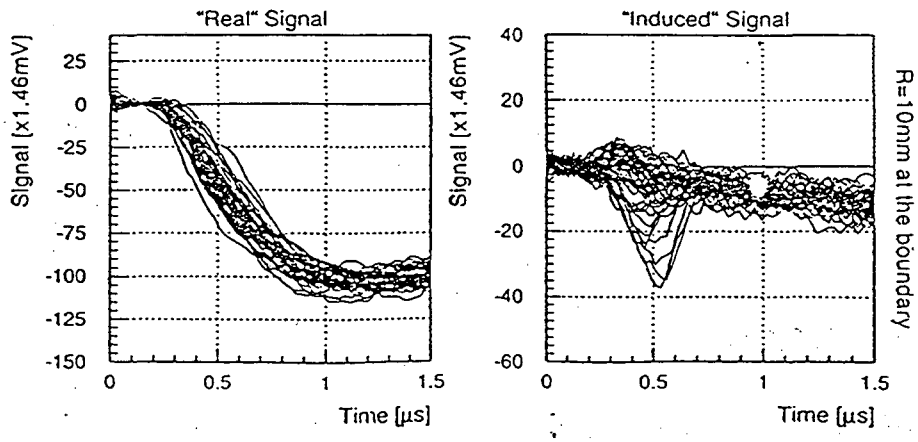


10 mm along boundary

Induced Signals in a Segmented GAMMASPHERE Detector (#70)

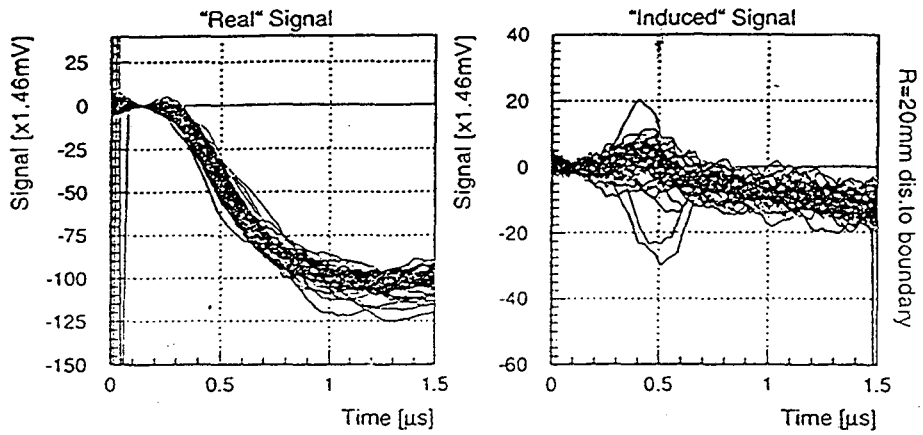


20 mm away from boundary

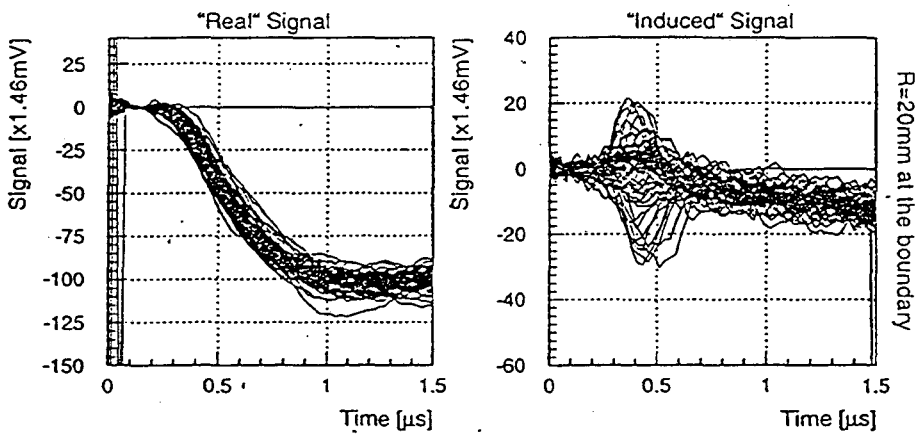


20 mm along boundary

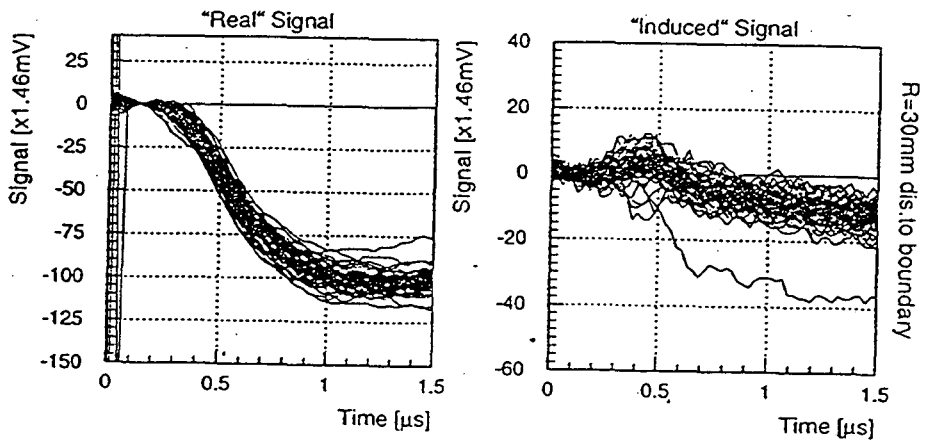


30mm away

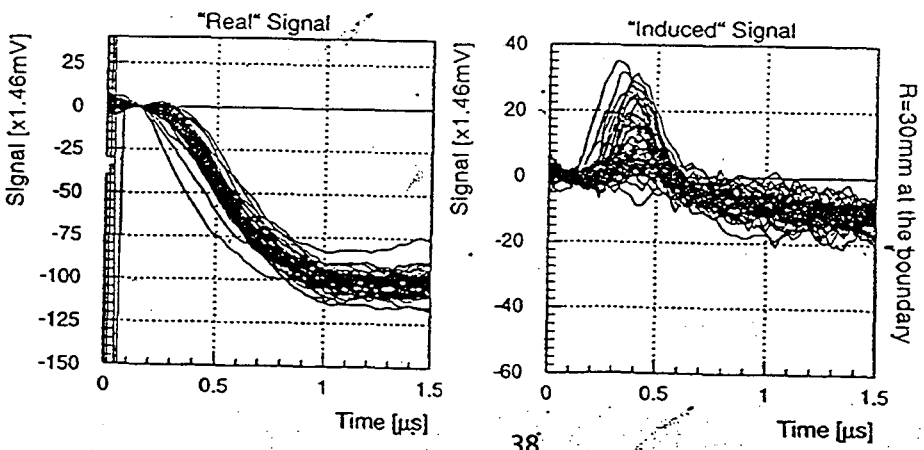


30mm along

Signals in a Segmented GAMMASPHERE Detector

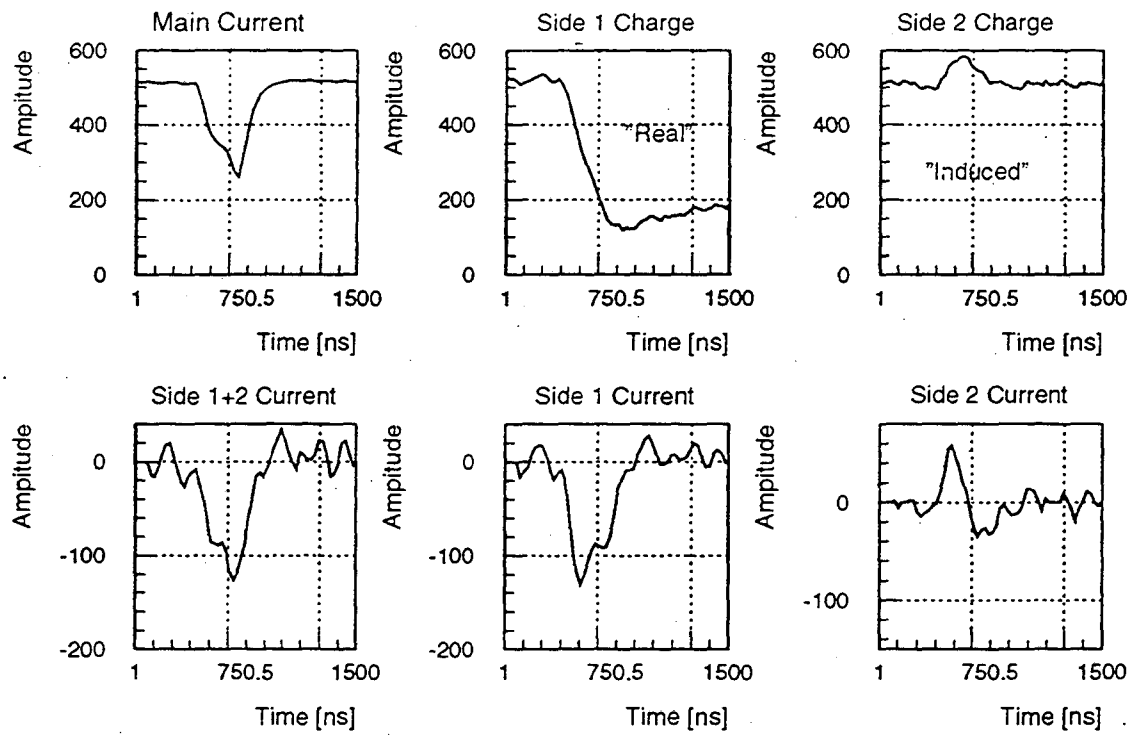

Crystal illuminated from the side

661 keV

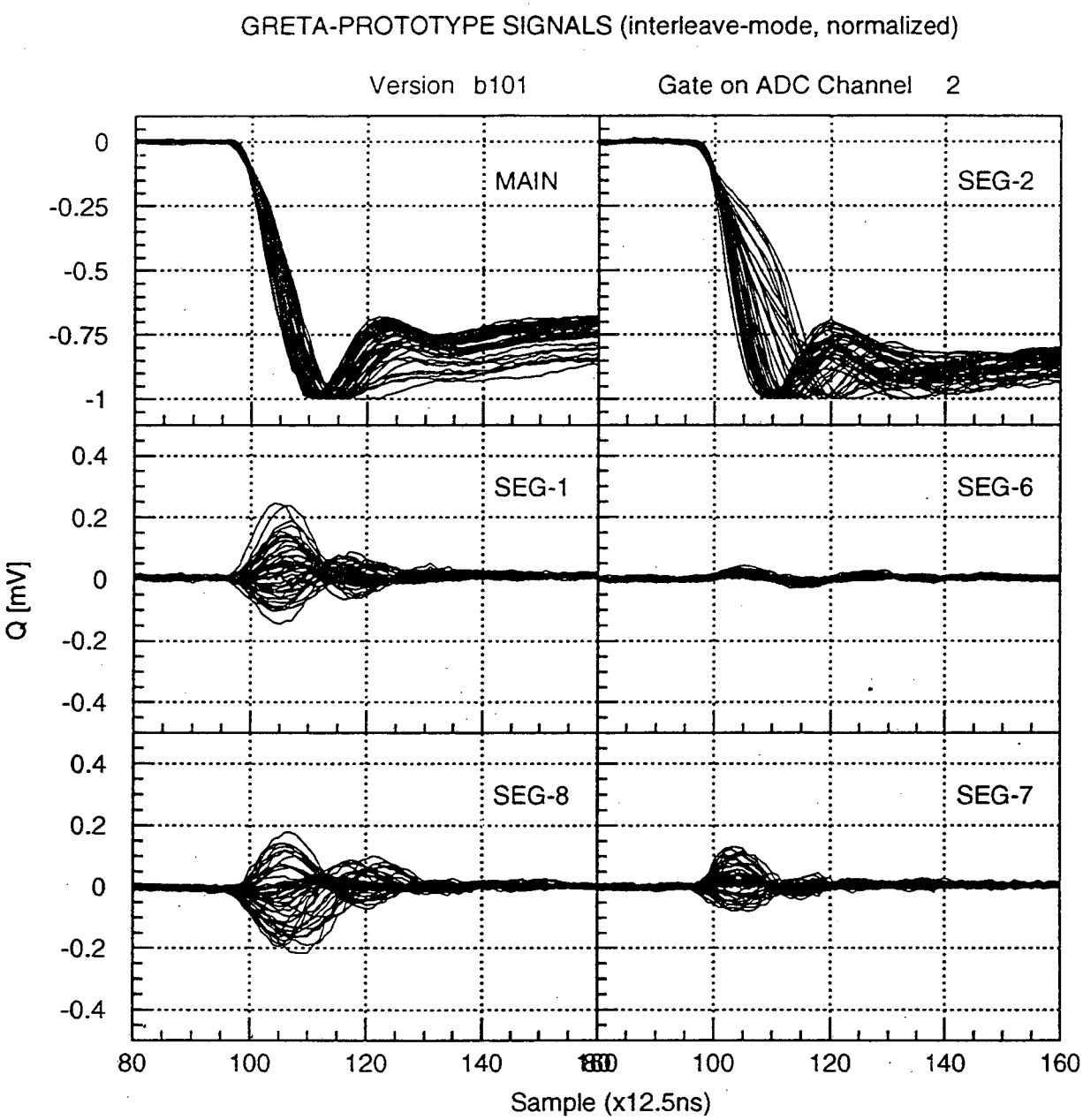

Gammasphere detector (2 segments, AC coupled)

Induced signals can be measured

however, about 50 - 100 keV noise level

no quantitative comparison possible

Greta prototype I. (12 segments, DC coupled)

about 5 - 8 keV noise

---

Data acquisition:

3 Le Croy waveform digitizer modules:

12 channels / 40 MHz / 10bit or

6 channels / 80 MHZ / 10 bit

---

## Calculations of pulse shapes

Some details of calculations:

- numerical solution of Poisson equation
- 3 dimensional grid ( polar / cartesian)
- HV on whole crystal contact (main signal)
- "HV" on segment contact (weighted field, segment signals)
- relaxation method

→ potential → electrical field → pulse (one interaction)

- GEANT → positions and energies of multiple interactions

Charge Signals

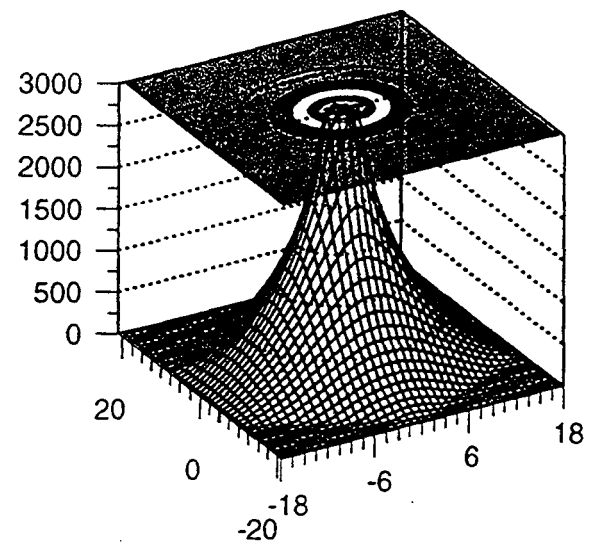


Potential-ZCUT-2

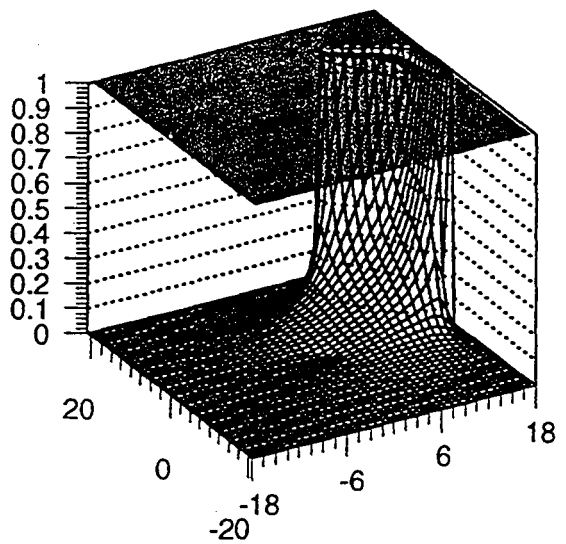


W-Potential-ZCUT-2

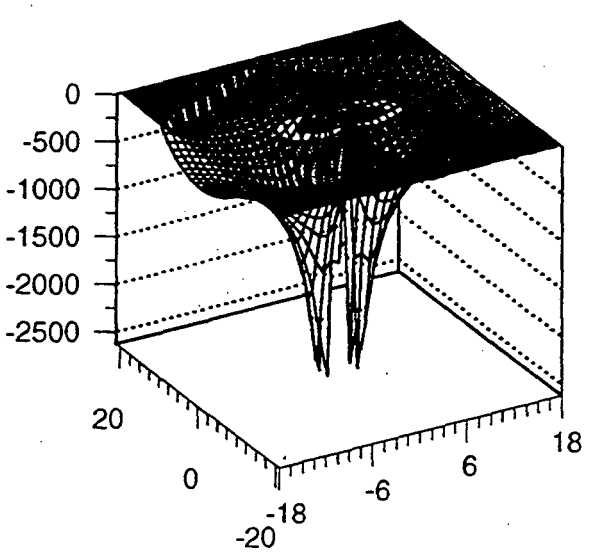


EX-ZCUT-2

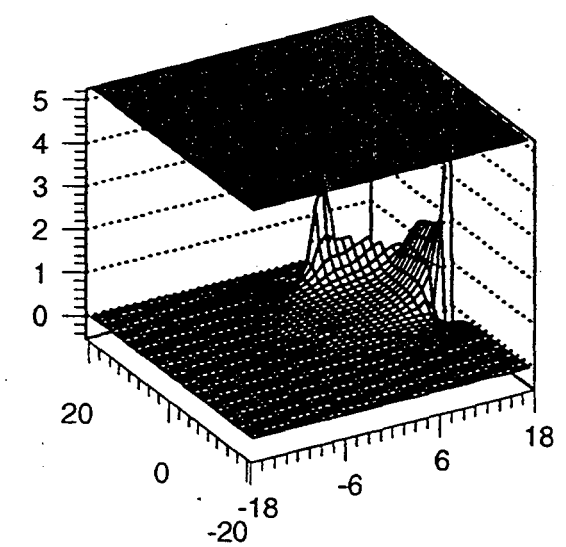


WEX-ZCUT-2

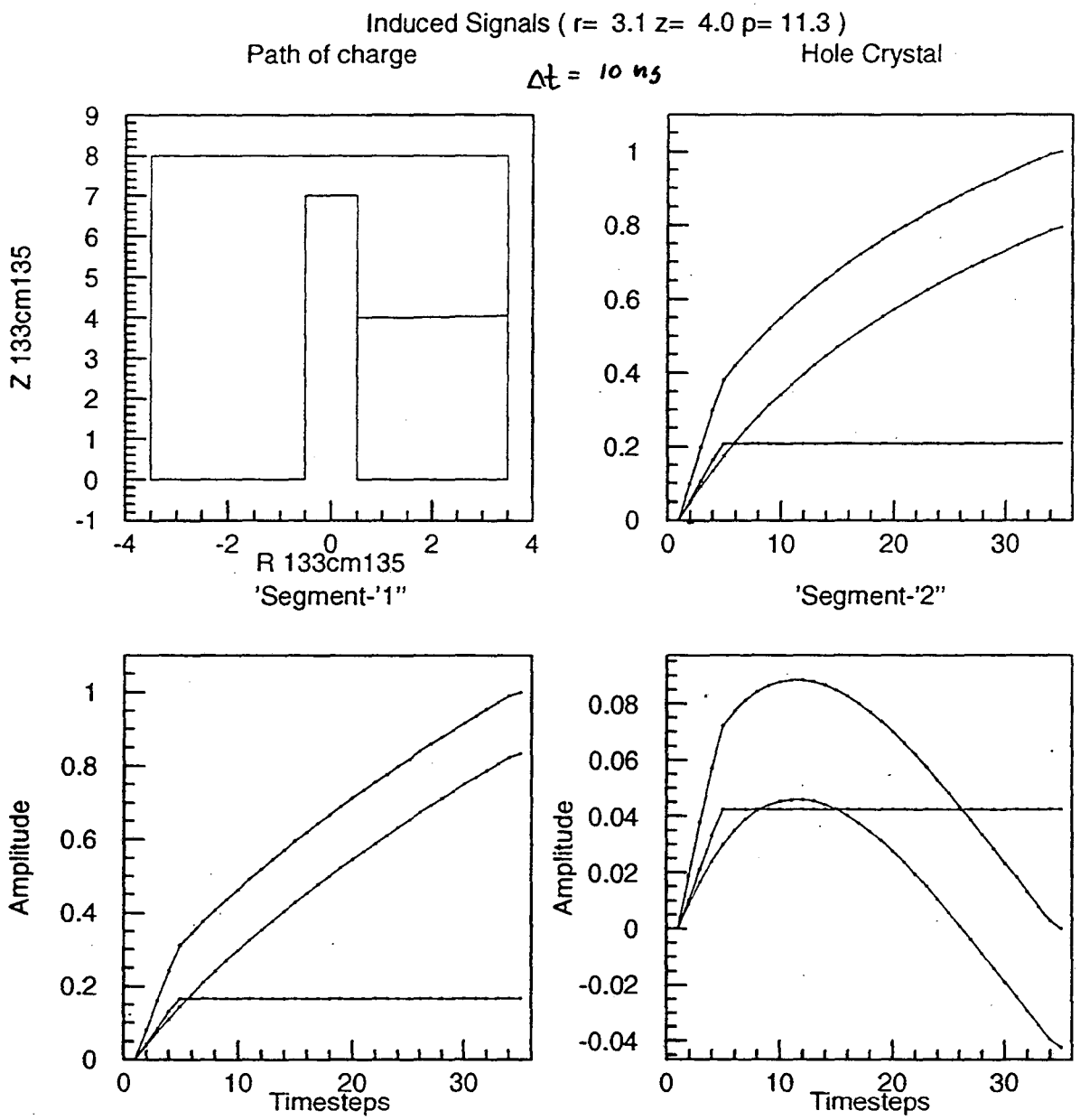
Induced Signals ( r= 3.1 z= 4.0 p= 11.3 )
Path of charge
Hole Crystal
Δt = 10 ns
Z 133cm135
R 133cm135
'Segment-'1"
'Segment-'2"
Amplitude
Timesteps
Amplitude
Timesteps

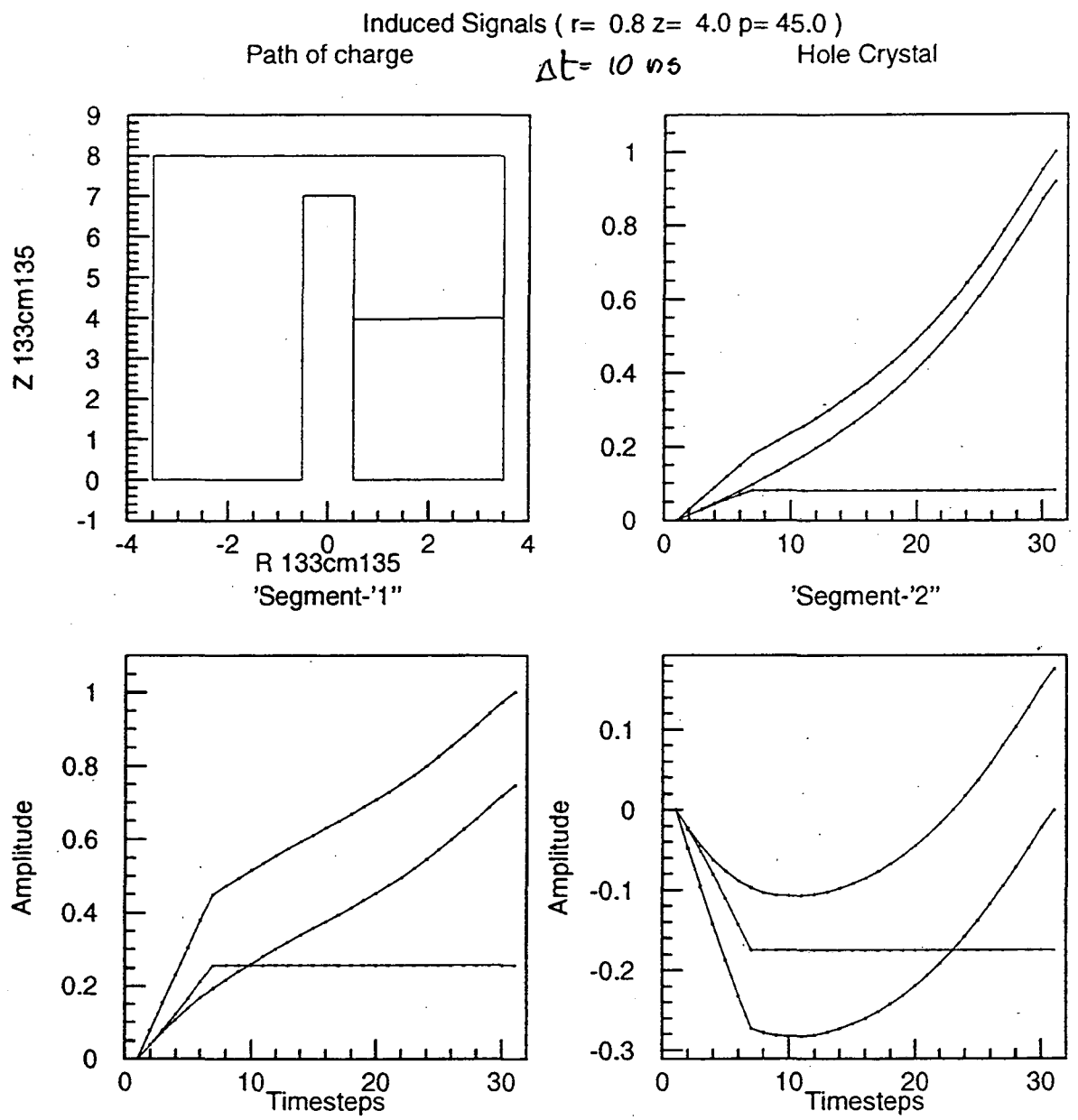
Induced Signals ( r= 0.8 z= 4.0 p= 45.0 )
Path of charge
Δt= 10 ns
Hole Crystal
Z 133cm135
R 133cm135
'Segment-'1"
'Segment-'2"
Amplitude
Timesteps
Amplitude
Timesteps

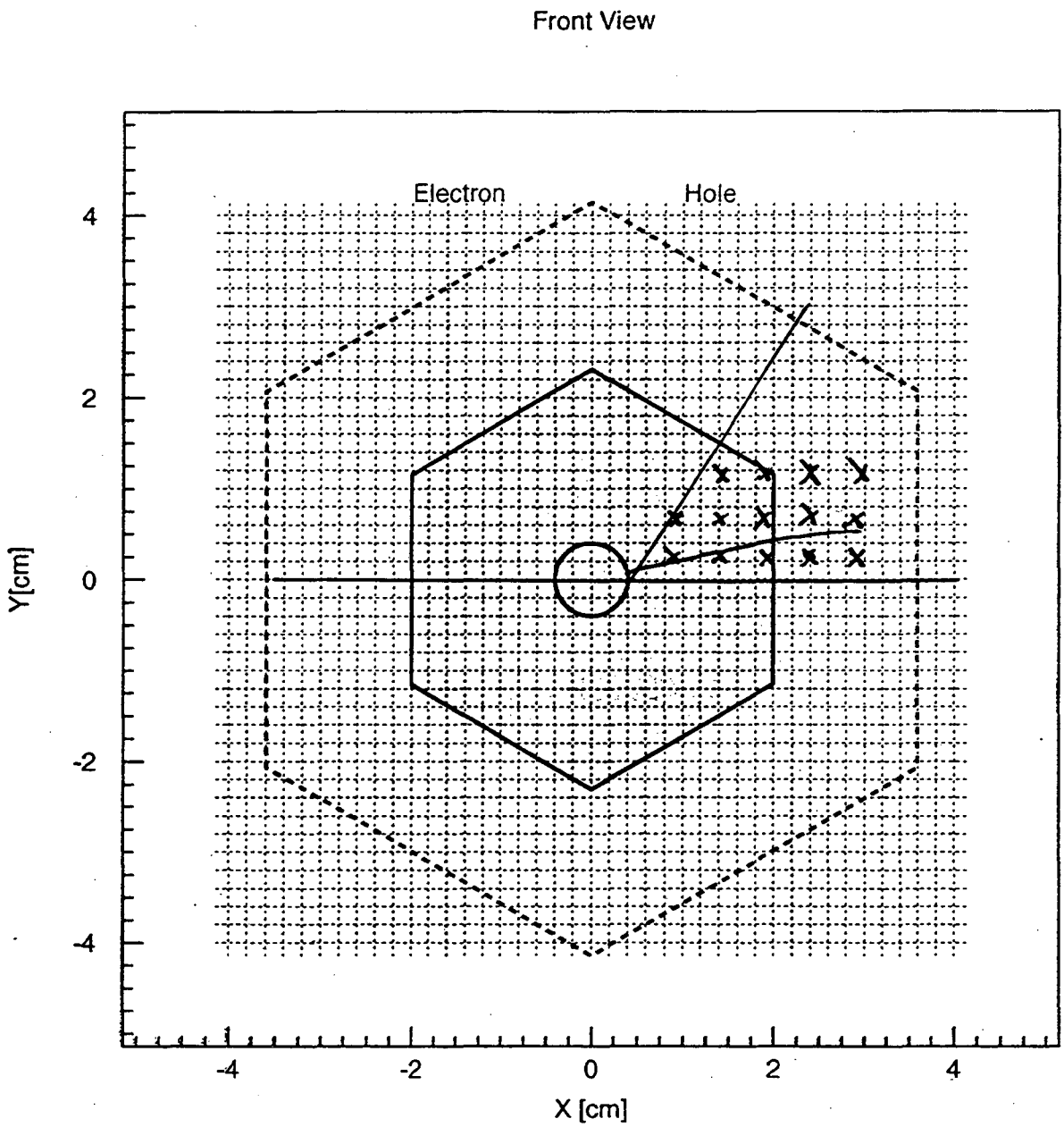
Front View
Electron
Hole
4
2
0
-2
-4
Y[cm]
-4
-2
0
2
4
X [cm]

Side View (min)

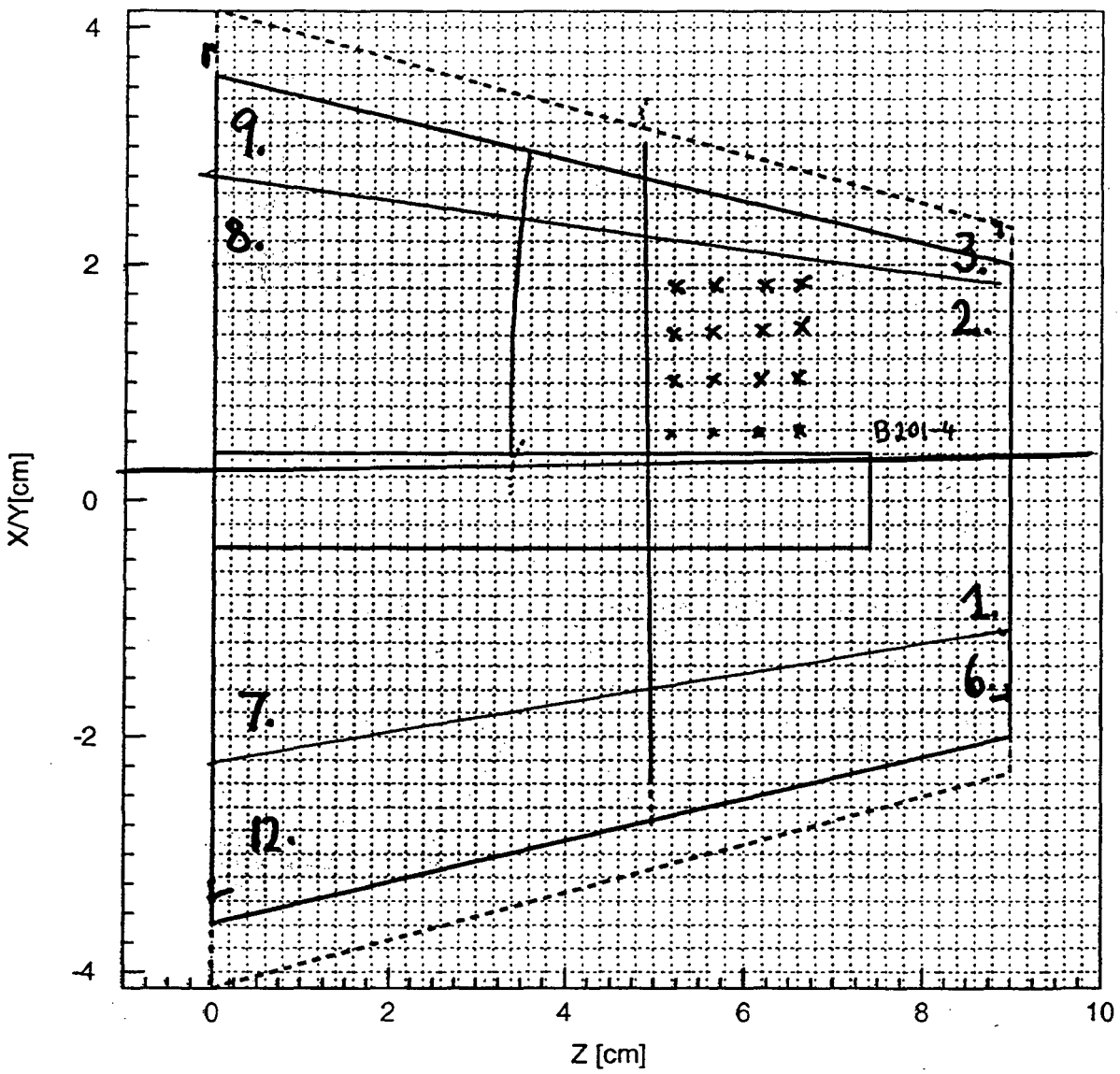

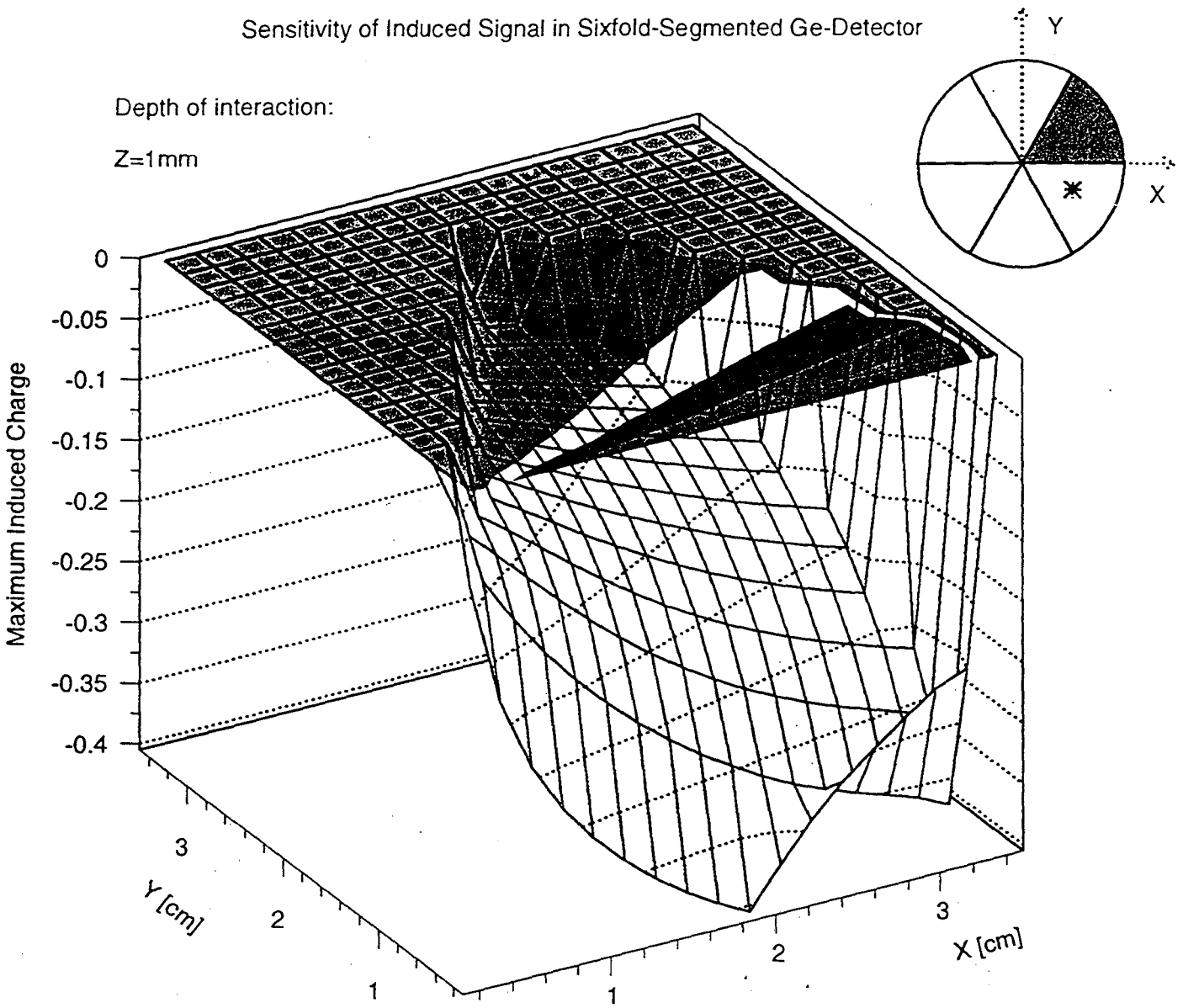
Sensitivity of Induced Signal in Sixfold-Segmented Ge-Detector
Depth of interaction:
Z=1mm
Y
X
Maximum Induced Charge
0
-0.05
-0.1
-0.15
-0.2
-0.25
-0.3
-0.35
-0.4
Y [cm]
1
2
3
X [cm]
1
2
3

Sensitivity of Induced Signal in 6x4 Segmented Ge-Detector

Interaction in next front neighbor...

Z : distance to Z-boundary

Y : distance to ϕ-boundary

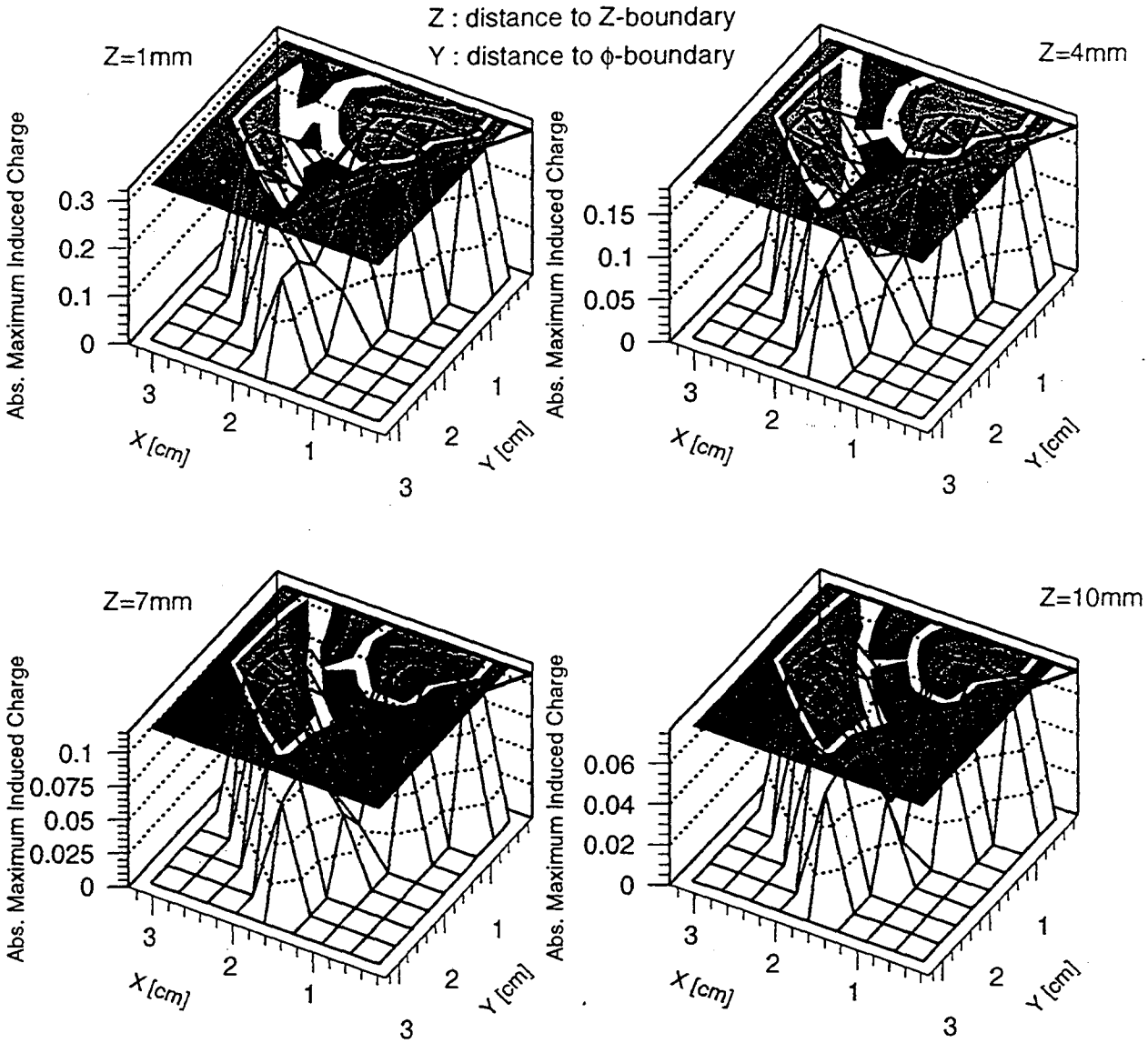

Sensitivitv of Induced Signal in 6x4 Segmented Ge-Detector

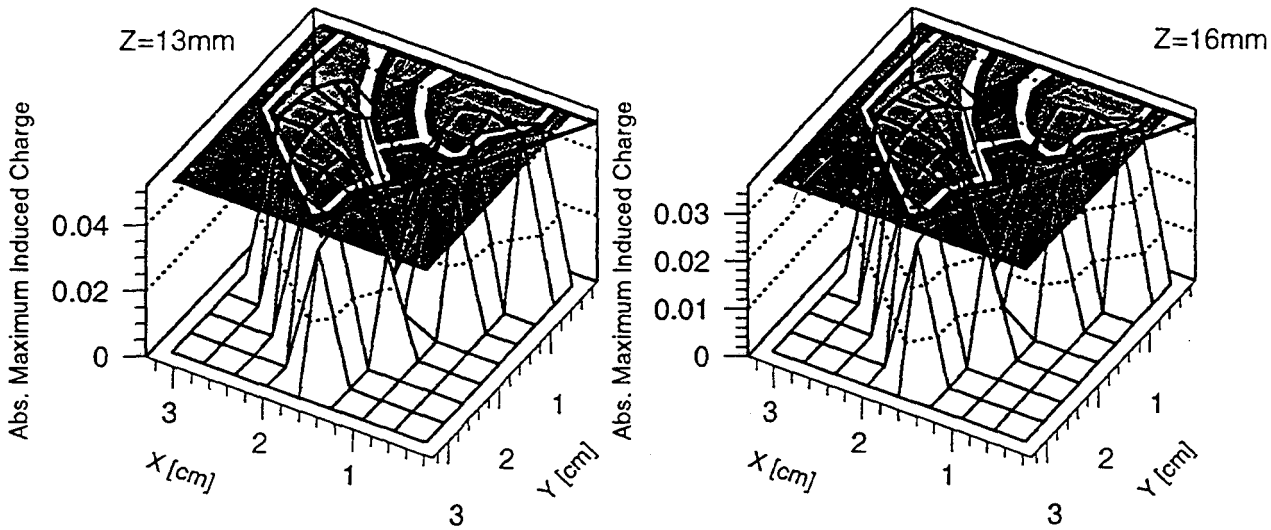

Sensitivity of Induced Signal Segmented Ge-Detector

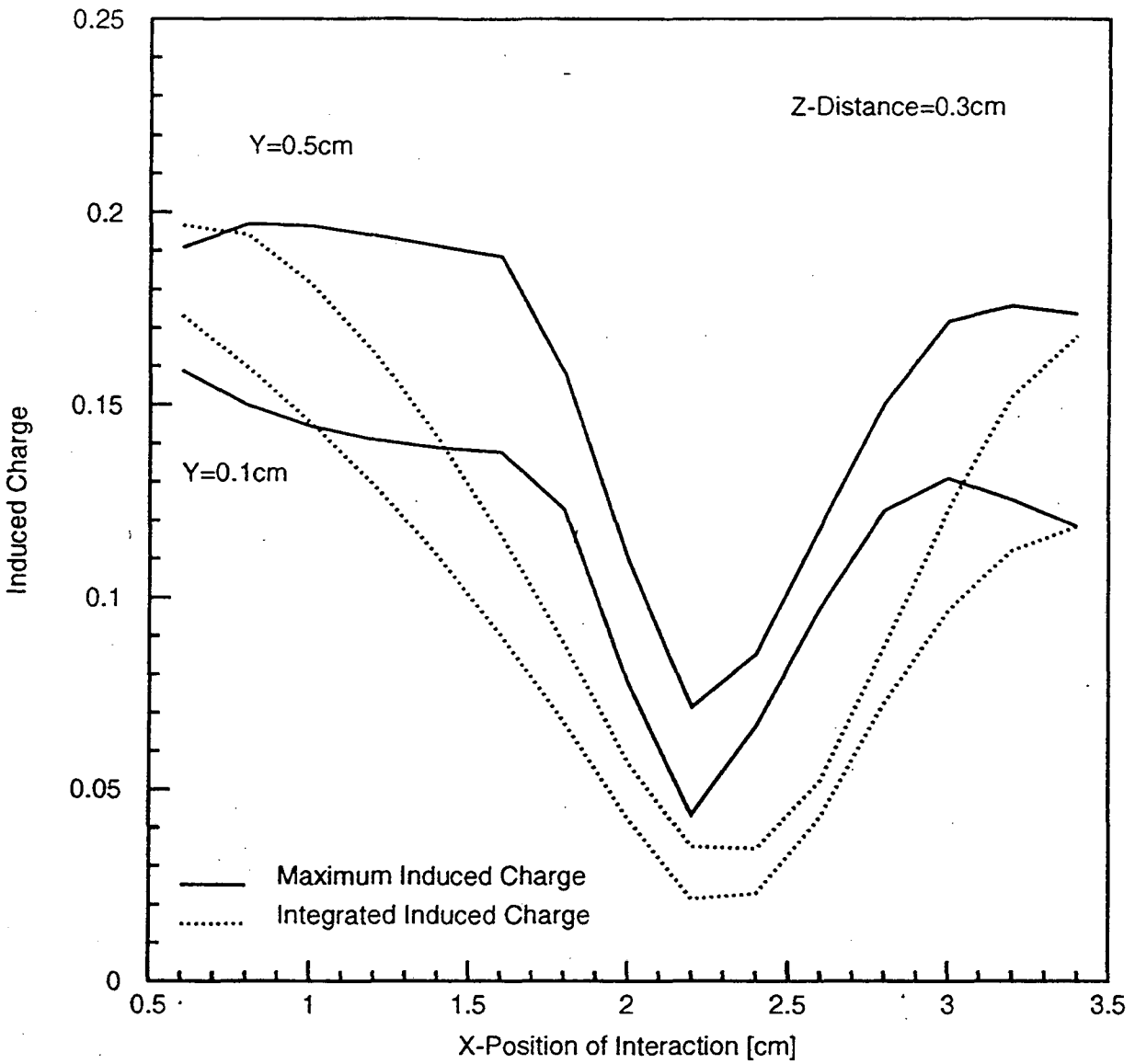

Crystal illuminated from the side

60 keV

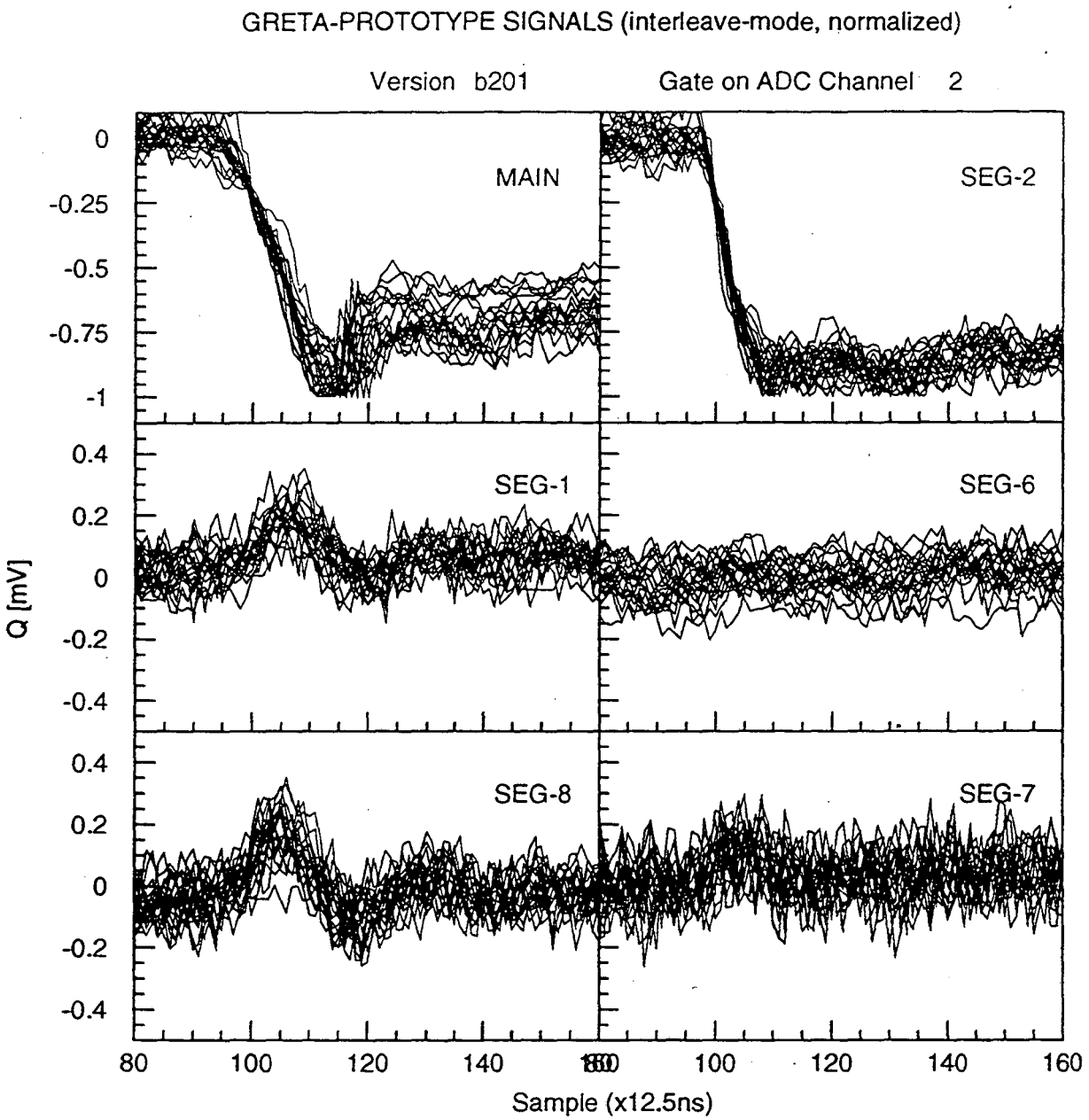

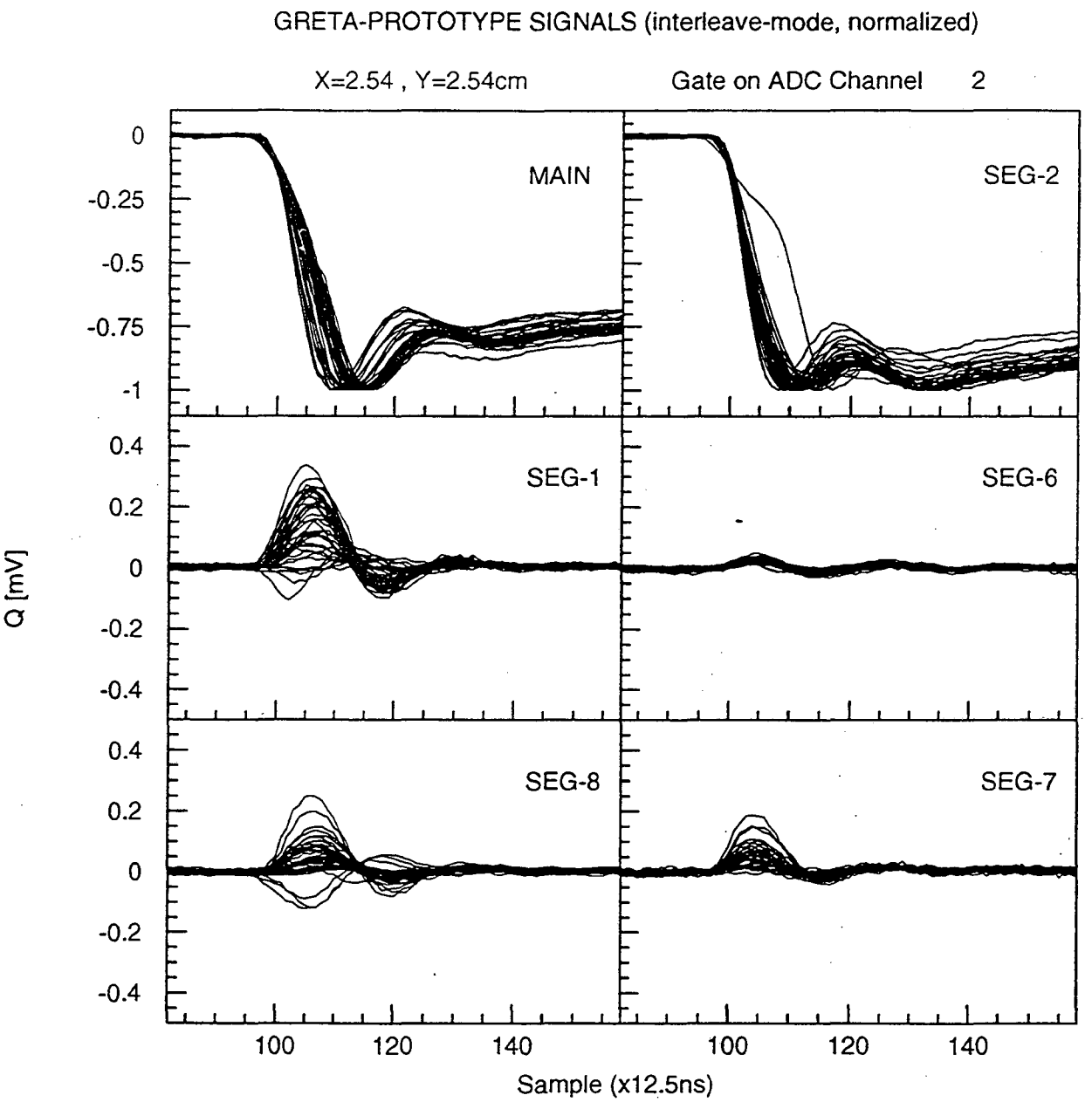
GRETA-PROTOTYPE SIGNALS (interleave-mode, normalized)
X=2.54 , Y=2.54cm
Gate on ADC Channel 2
MAIN
SEG-2
SEG-1
SEG-6
SEG-8
SEG-7
Q [mV]
0
-0.25
-0.5
-0.75
-1
0.4
0.2
0
-0.2
-0.4
100
120
140
Sample (x12.5ns)

Crystal illuminated from the side

60 keV ; average signal (N ~ 100)

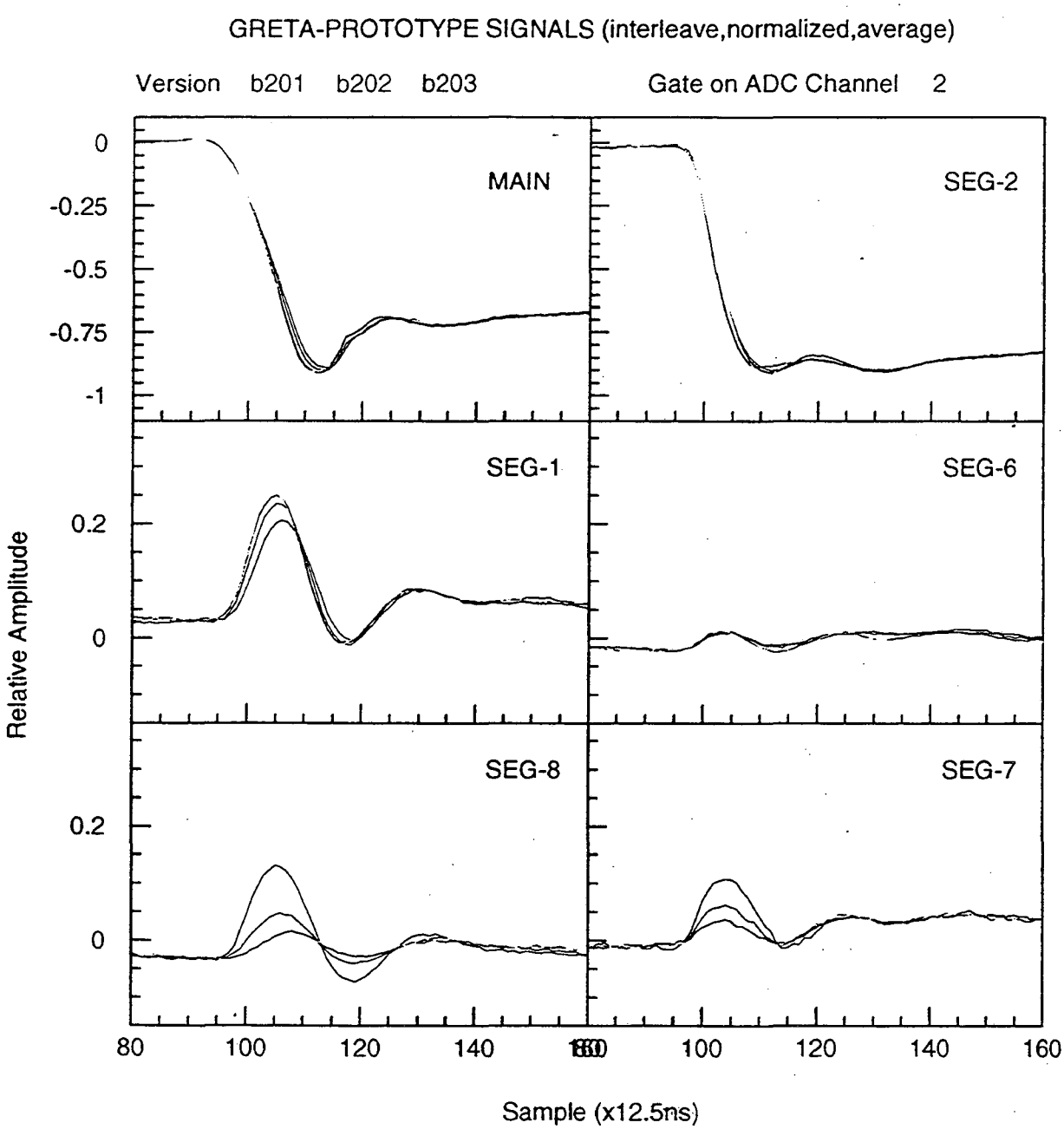

SCAN OF BACK,

GRETA-PROTOTYPE Induced Signal Amplitudes (2mm hole / 60keV)

Full Energy in Segment 2

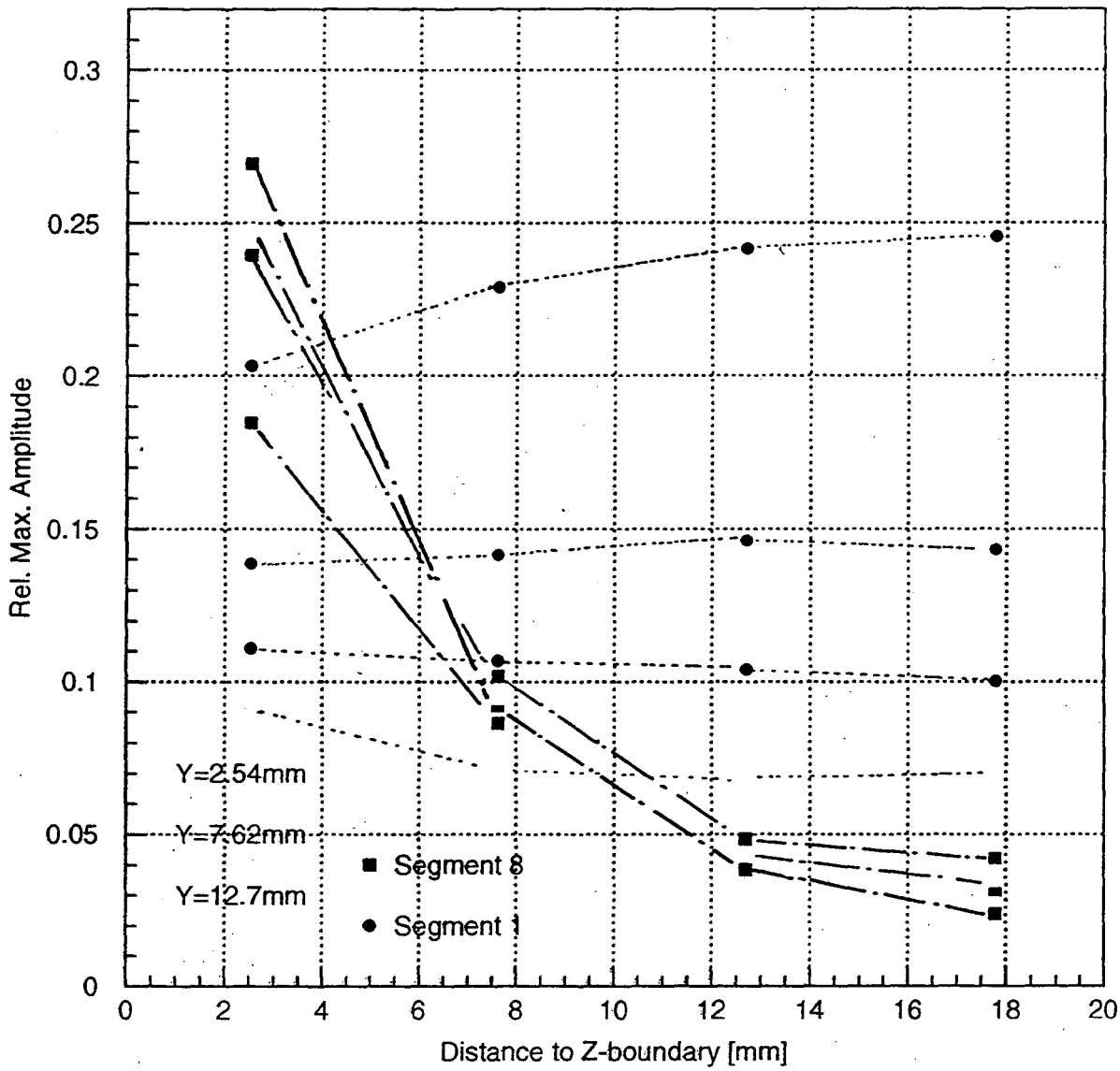

SCAN OF BACK

GRETA-Calculations: Induced Signal Amplitudes

Full Energy in Segment 2

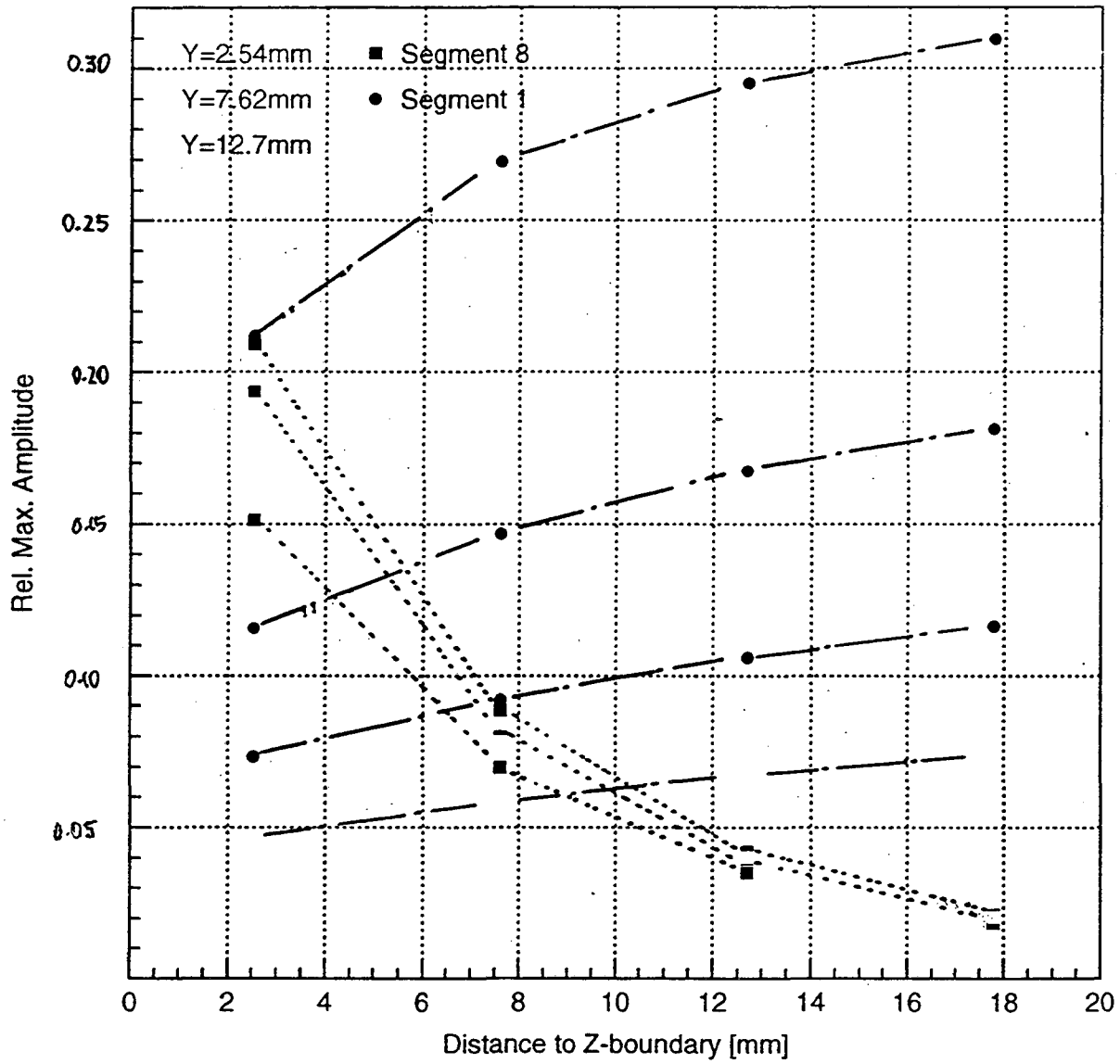

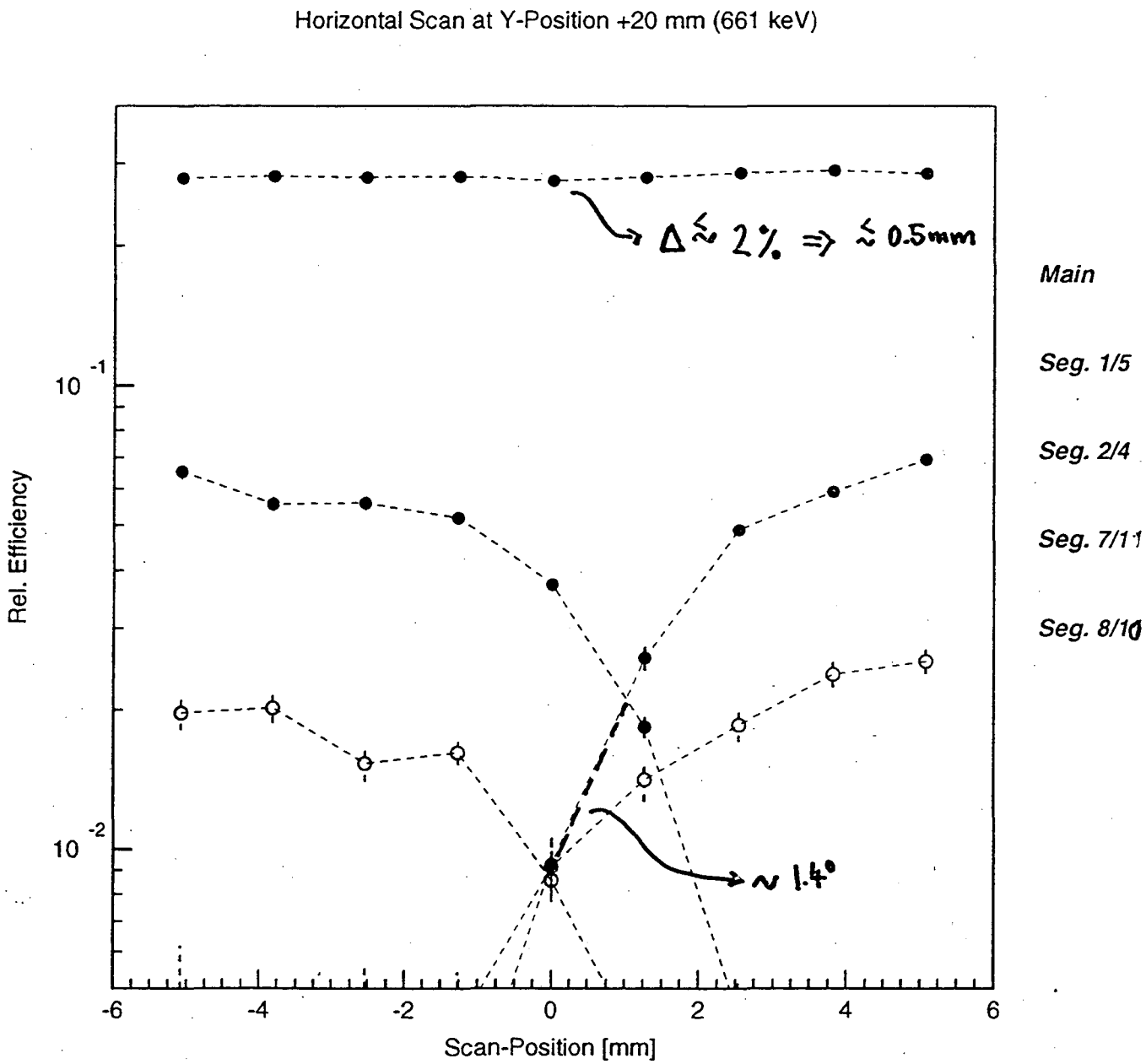
Horizontal Scan at Y-Position +20 mm (661 keV)
Rel. Efficiency
10 -1
10 -2
-6
-4
-2
0
2
4
6
Scan-Position [mm]
Main
Seg. 1/5
Seg. 2/4
Seg. 7/11
Seg. 8/10
Δ ≲ 2% ⇒ ≲ 0.5mm
~ 1.4°

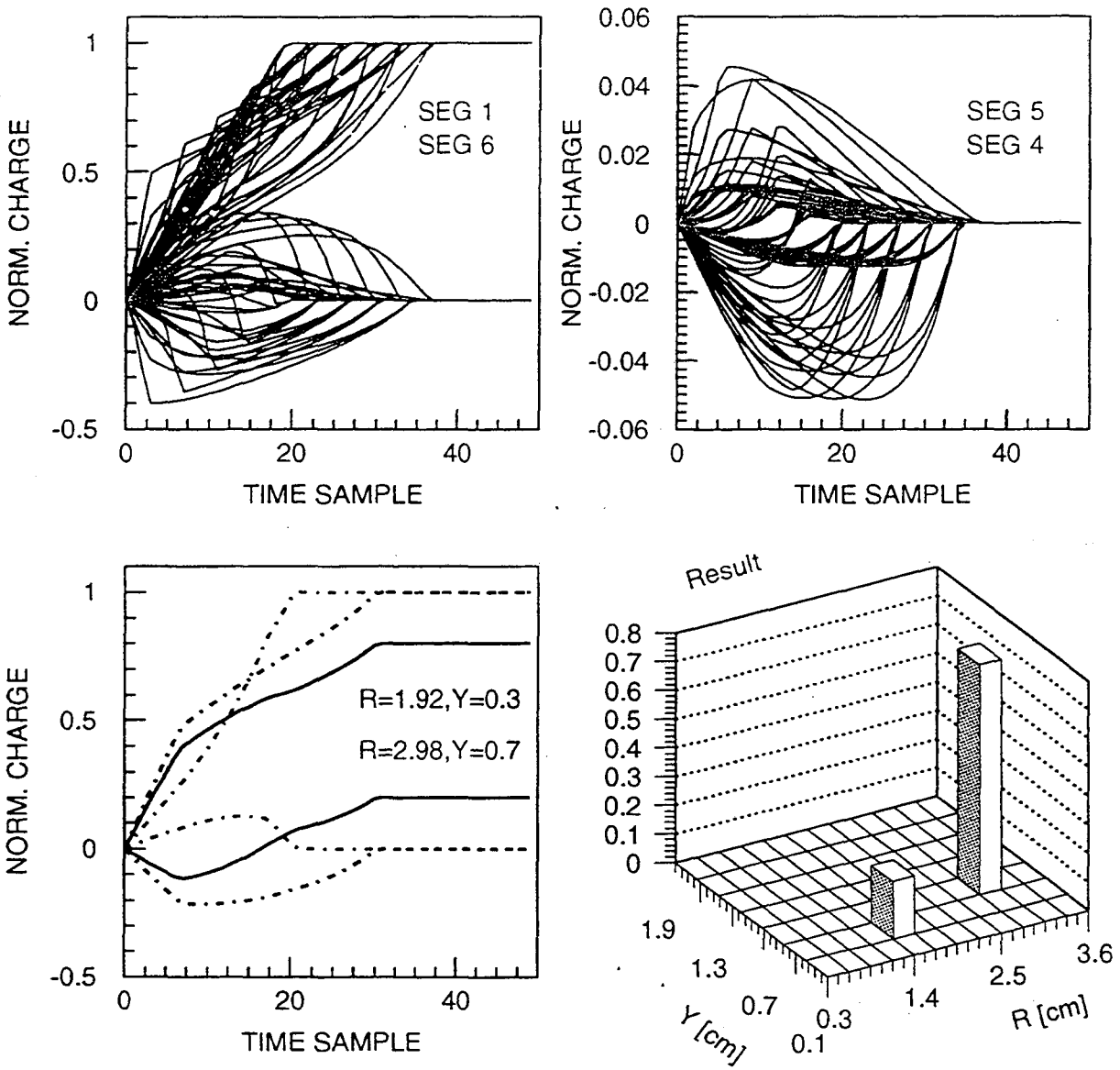
NORM. CHARGE
TIME SAMPLE
SEG 1
SEG 6
SEG 5
SEG 4
R=1.92,Y=0.3
R=2.98,Y=0.7
Result
Y [cm]
R [cm]

Calculated Signals in a Sixfold-Segmented Ge-Detector

1mm ≤ Y ≤ 28mm , 6mm ≤ R ≤ 33mm , ΔR = ΔY = 3mm

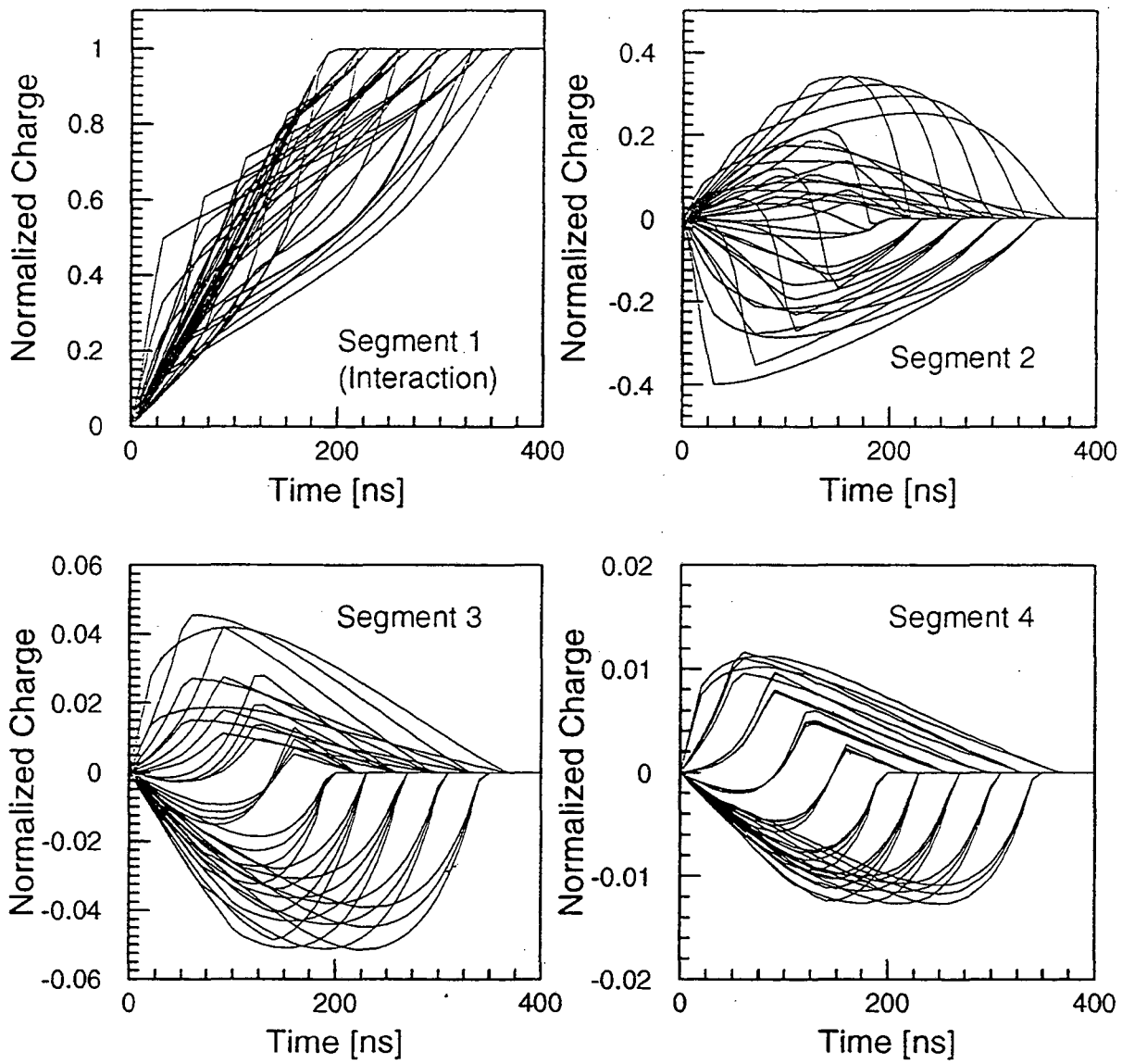

## Summary

- Segmented detector not only useful for alignment of collimator ...

- "Induced" signals are "Real" ...

- Expected sensitivity of induced signal : 1-5 mm
  depending on position and energy of interaction

- Useful range of induced signal : 12 - 15 mm

- Radial position resolution : 4-5 mm limited by preamplifier

## Future

- New preamplifier

- Response and noise analysis

- Decomposition of multiple interactions in multiple segments

- New multi FADC channel data acquisition system

- Determination of energy, drift time and maximum induced
  charge on DSP based system (XIA)

- Artificial neural network algorithm

P.J.Nolan

An overview of developments in Europe towards a gamma-ray tracking device.

# Developments towards a tracking array

## A European Overview

**P J Nolan**

EUROBALL: single crystals
clover detectors
cluster detectors

Developments: segmented clover detectors
segmented cluster detectors
pulse shape analysis
2-dimensional segmentation

# The Clover Detector

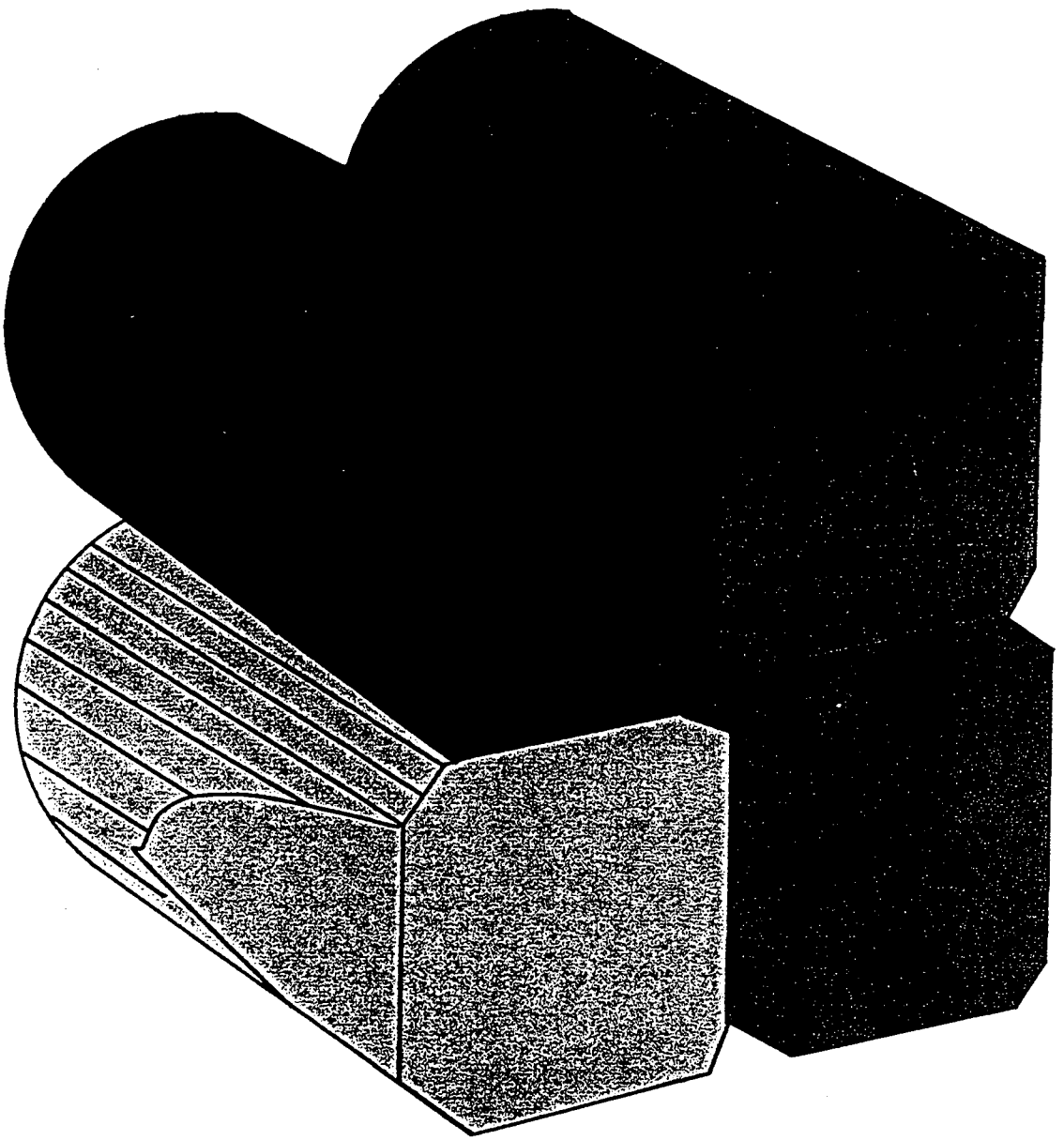

## Clover detectors

Use add back mode to improve efficiency

e.g. at 1.33MeV add back factor is 1.44

Doppler broadening improved as subtended angle is smaller

Linear Polarisation

## Limitations

Isolated hit probability - Multiplicity response

Doppler performance for close geometry and high v/c

☞ **Segmented clovers**

# Fold Distribution of Clover Detector

at 1332 keV

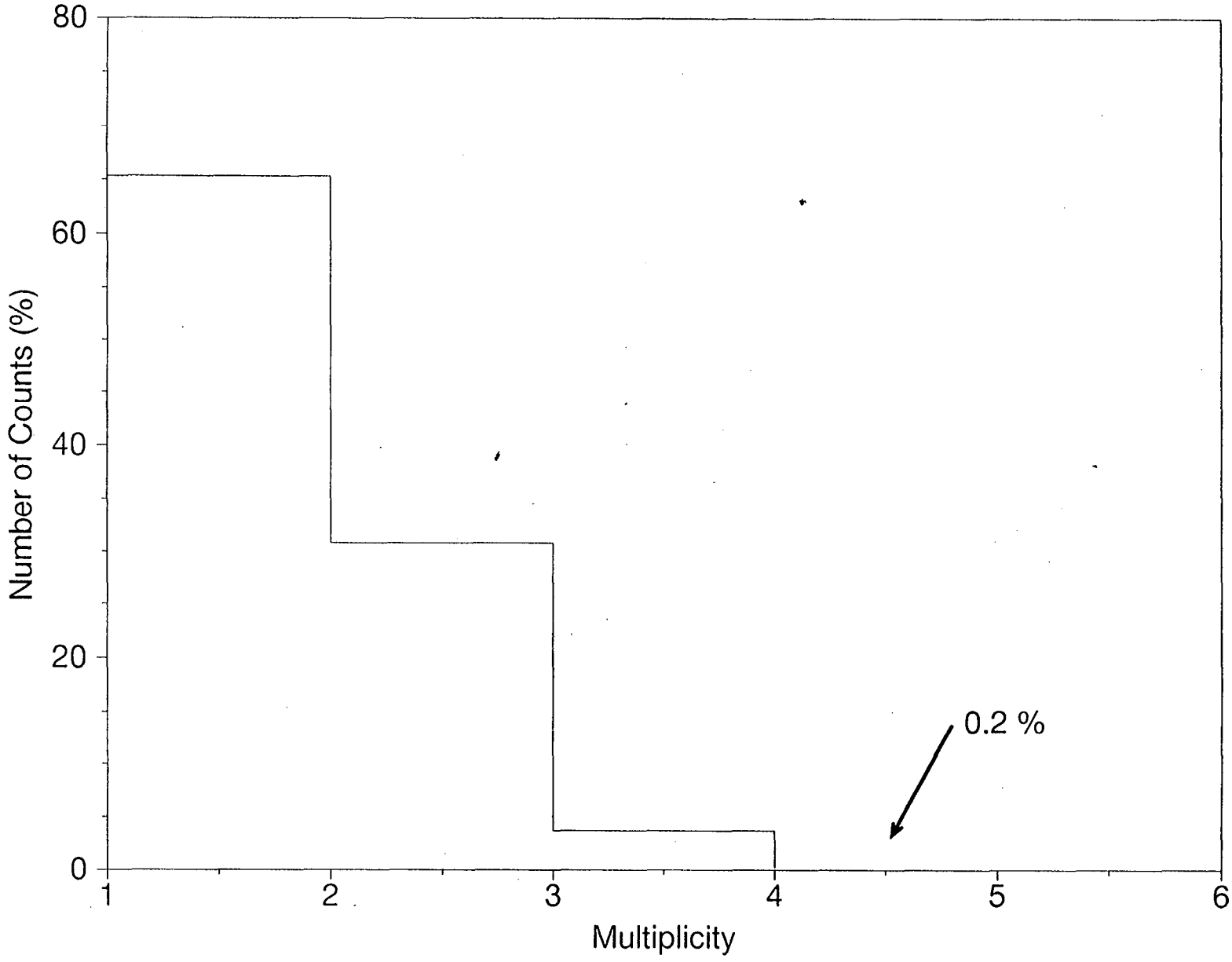

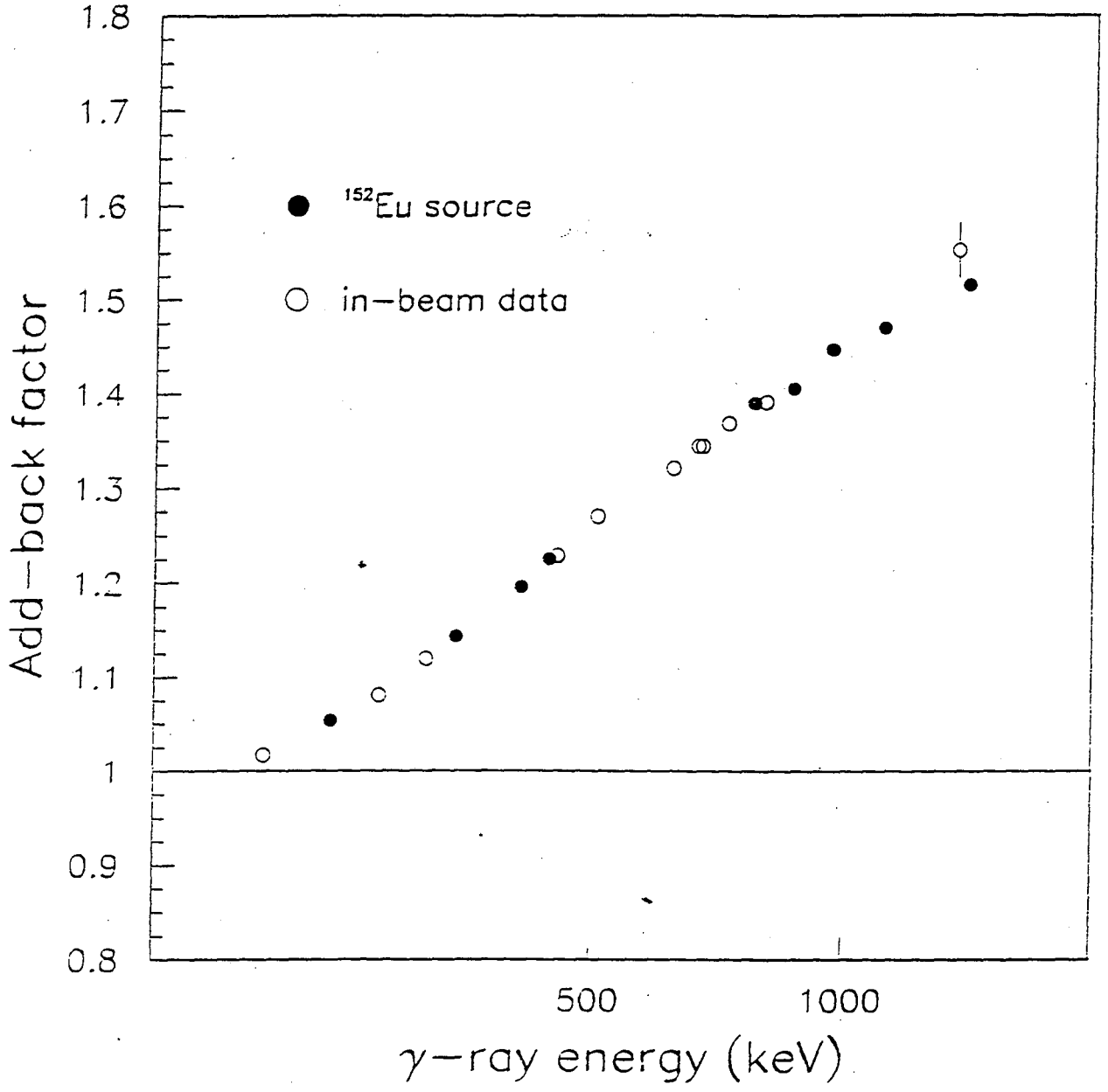
1.8
1.7
1.6
1.5
1.4
1.3
1.2
1.1
1
0.9
0.8
Add−back factor
$^{152}$Eu source
in−beam data
500
1000
γ−ray energy (keV)

# The Segmented Clover Detector

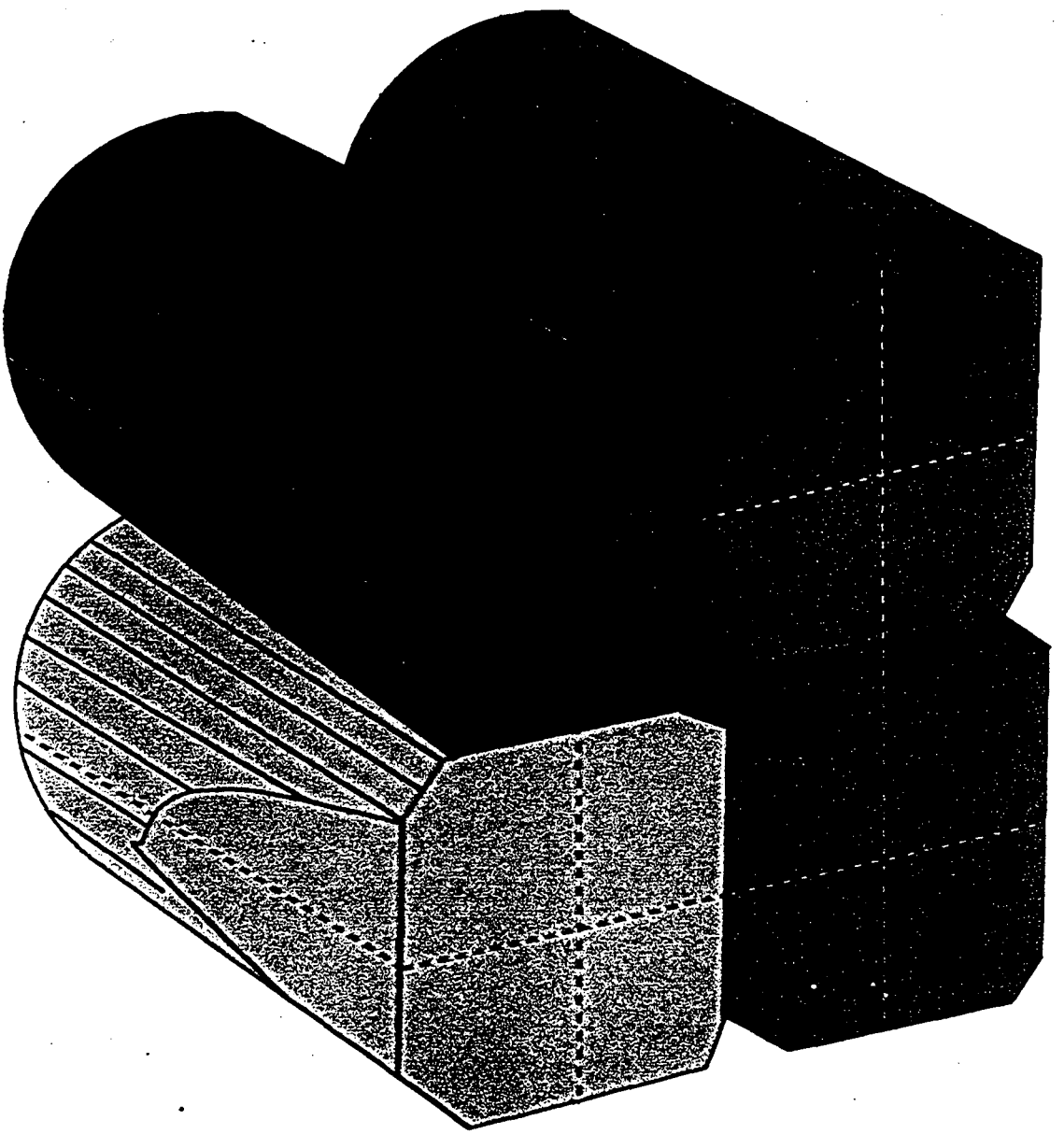

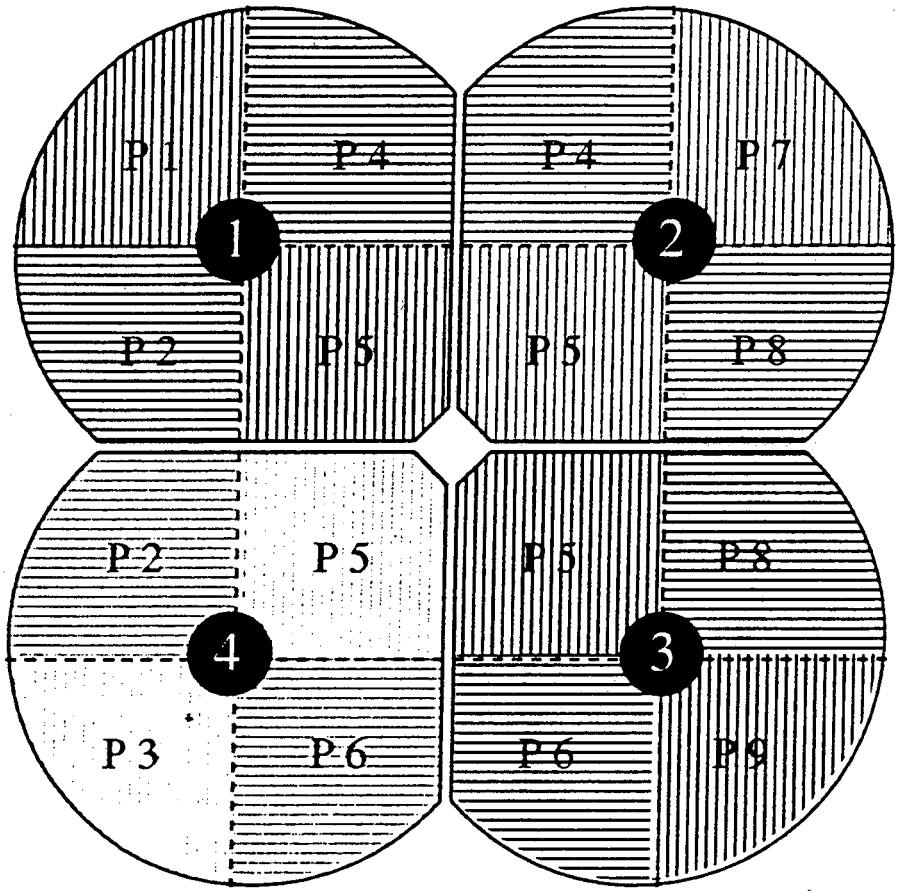


- 4 coaxial n-type Germanium crystals arranged like a four leaf clover.
- Outer p-type contact of each crystal segmented longitudinally, splitting each crystal into four quadrants.
- Energy readouts from 9 crystal zones.

# Clover Results

The following performance characteristics have been measured :

Energy signals (high resolution)

| Crystal | Red | Green | Black | Blue |
|---|---|---|---|---|
| FWHM 1332 keV | 1.81 | 1.81 | 1.85 | 1.89 |
| FWTM/FWHM | 1.88 | 1.85 | 1.82 | 1.81 |
| FWFM/FWHM | 2.52 | 2.50 | 2.38 | 2.38 |
| FWHM 122 keV | 1.02 | 1.10 | 1.06 | 1.06 |
| Rel Effic % | 22.19 | 22.81 | 21.52 | 22.06 |
| Peak/Compton | 53.66 | 56.48 | 53.01 | 52.40 |
| Peak/Total | 0.139 | 0.141 | 0.135 | 0.139 |

Position signals (low resolution)

| Position | P1 | P2 | P3 | P4 | P5 | P6 | P7 | P8 | P9 |
|---|---|---|---|---|---|---|---|---|---|
| FWHM 1332 keV | 3.47 | 6.01 | 3.62 | 5.88 | 8.92 | 6.01 | 3.39 | 6.06 | 3.90 |

# Measurements

In August, the detector was taken to G.S.I, Germany.

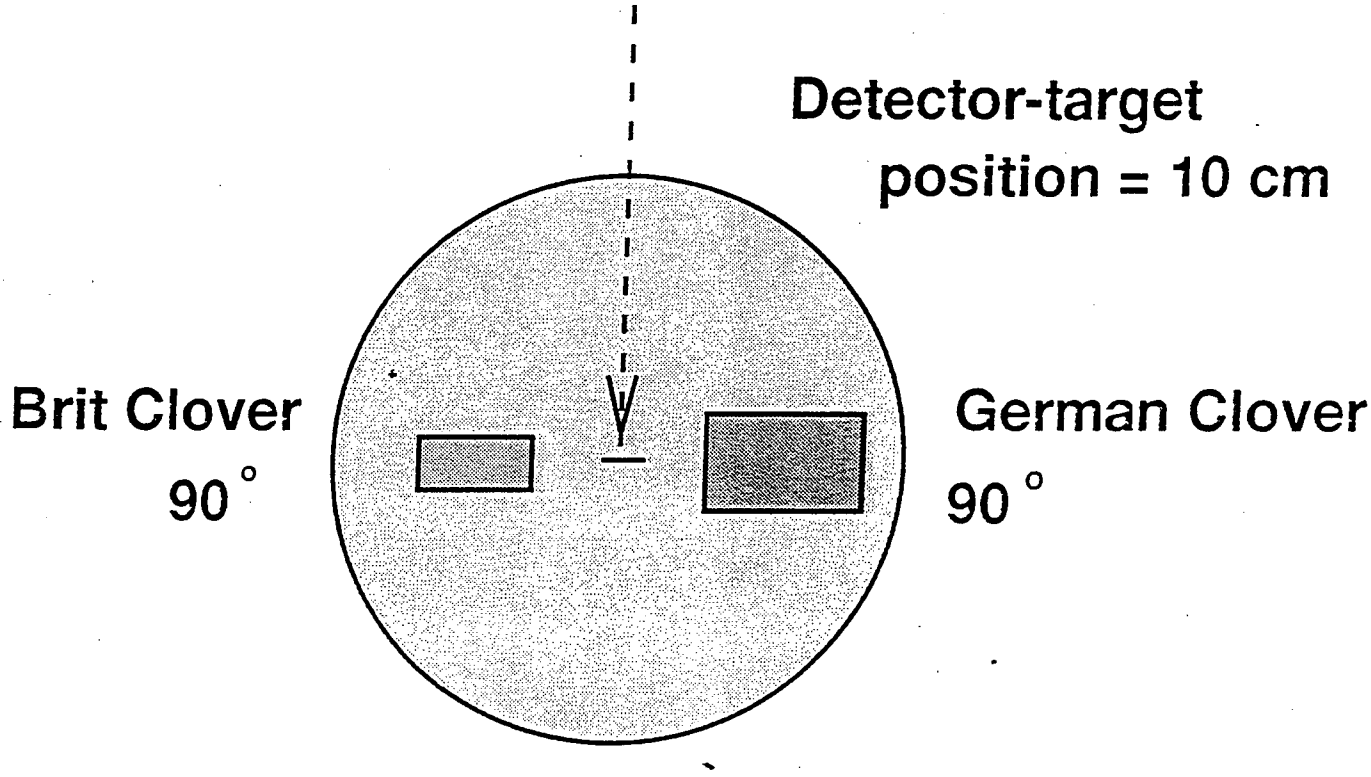


Reaction: Coulex of $^{197}$Au

$^{197}$Au + $^{12}$C @4.3 MeV/u, v/c = 8.5%

During the run we obtained coincident source data for $^{152}$Eu, $^{133}$Ba, $^{226}$Ra, $^{137}$Cs, $^{60}$Co.

We will use this data to examine the scattering between the crystal segments.

# Doppler Broadening of Segmented Clover Detector

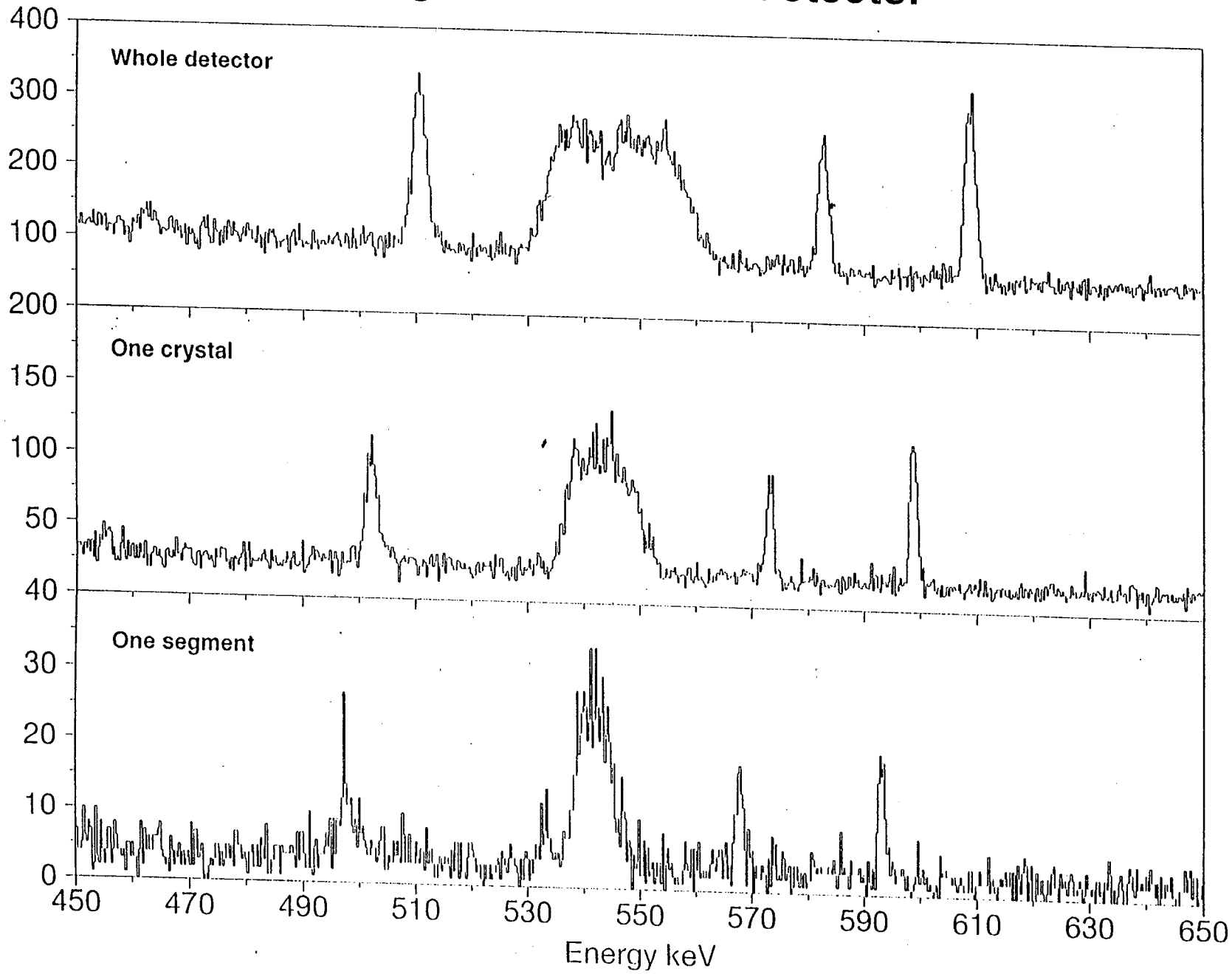

# Doppler Broadening

Several components

| | |
|---|---|
| Detector opening angle and position | $E_\gamma v/c \sin\theta \, \Delta\theta_D$ |
| Variation of recoil velocity | $E_\gamma v/c \cos\theta \, \Delta(v/c)$ |
| Variation of recoil angle | $E_\gamma v/c \sin\theta \, \Delta\theta_R$ |
| Intrinsic resolution | Fixed |

Components add in quadrature, the first depending on the detector opening angle. If the opening angle of each segment is $\Delta\theta_S$ then $\Delta\theta_D$ varies how many segments are coupled together.

| | | |
|---|---|---|
| One segment is | $n \, \Delta\theta_S$ | where $n = 1$ |
| One crystal is | $n \, \Delta\theta_S$ | where $n = 2$ |
| One clover is | $n \, \Delta\theta_S$ | where $n = 4$ |

Plot $(\text{Resolution})^2$ versus $n^2$

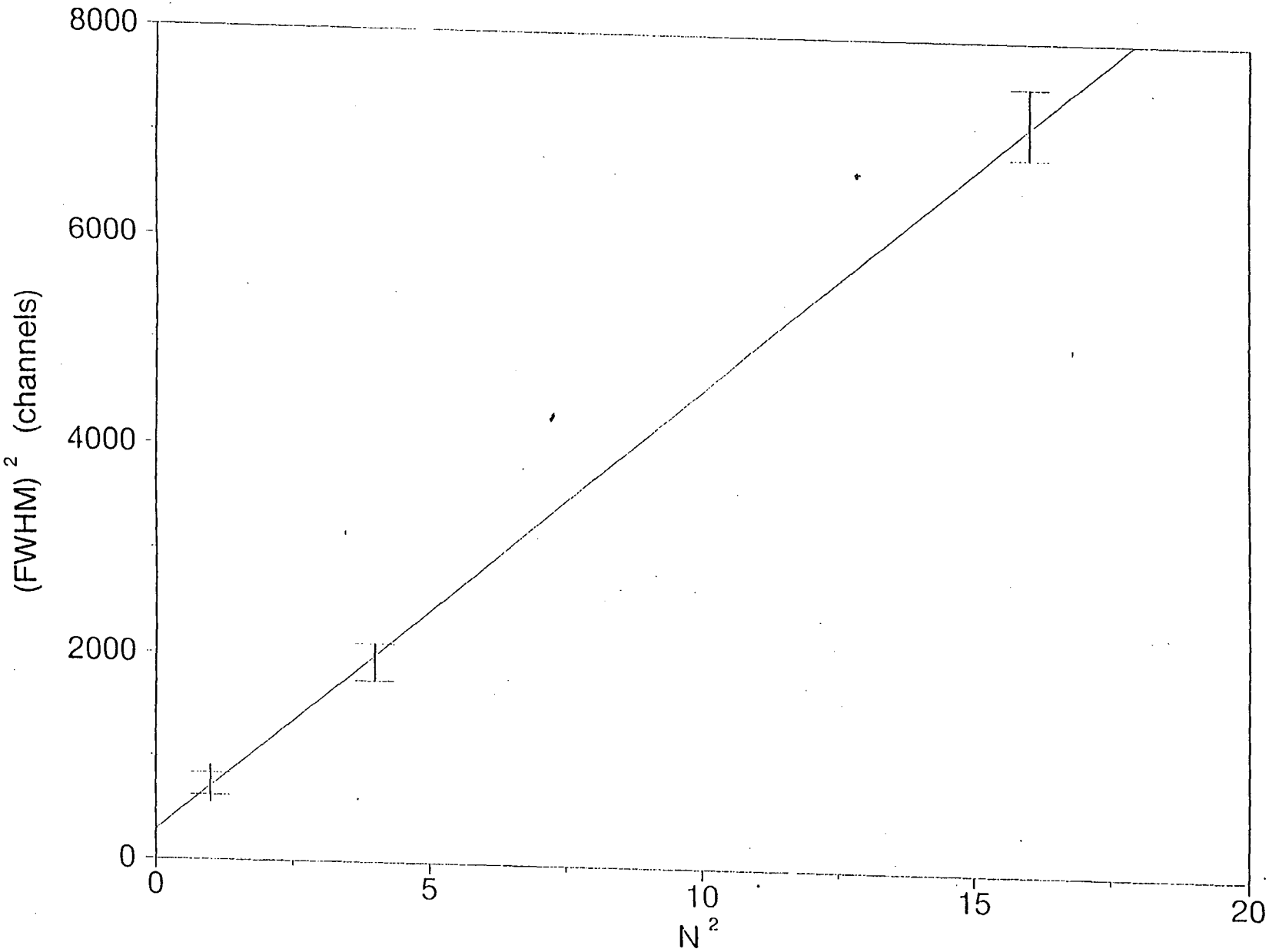
8000
6000
4000
2000
0
(FWHM) 2 (channels)
0
5
10
15
20
N 2

Gives $\Delta\theta_s$ = 0.245 experiment

Compare to 0.21 geometry

# Isolated Hit Probability

This accounts for the possibility of a second $\gamma$ - ray hitting the same detector.

**The original Clover detector could not distinguish between such an event (b), and a $\gamma$-ray Compton scattering between two adjacent crystals (a)**

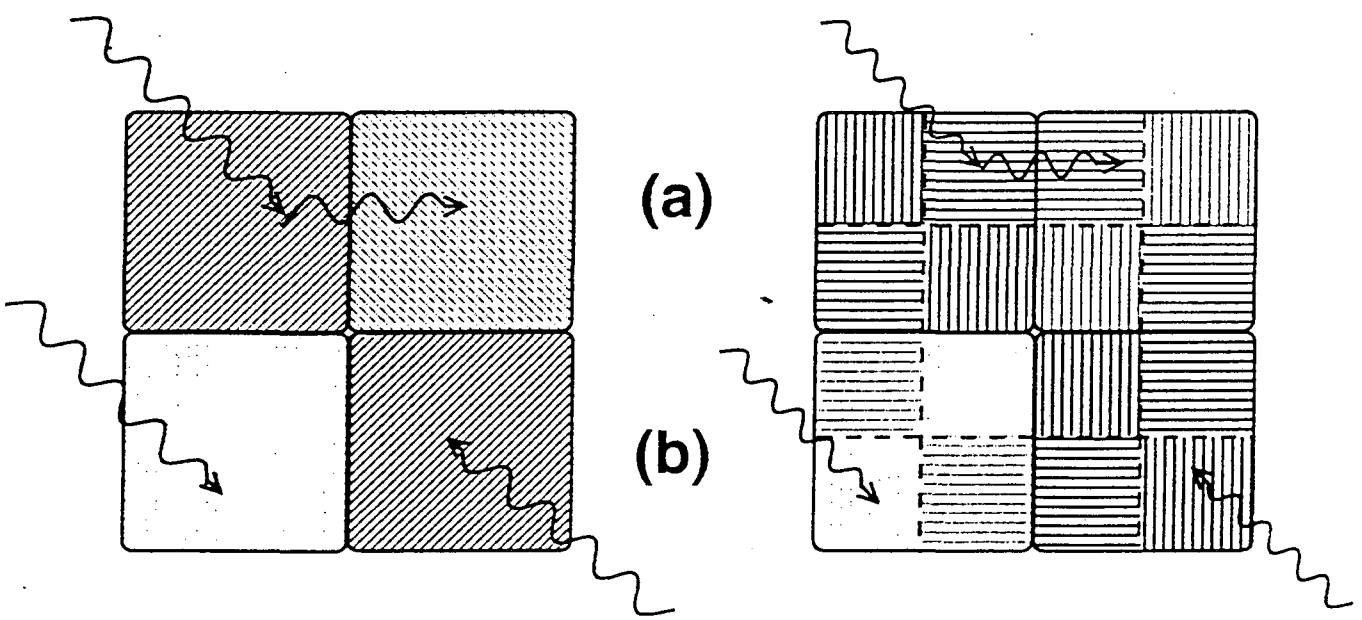


The improved granularity of the segmented Clover reduces this problem.

# Intra crystal scattering

## $^{137}$Cs data

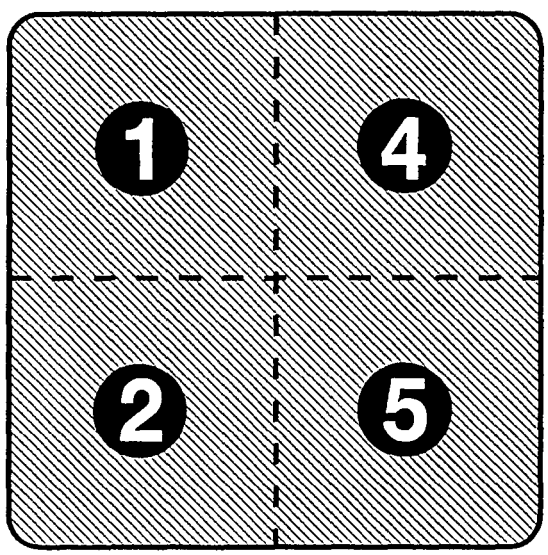


M = 2 events

| scatter | measured | modelled |
|---|---|---|
| 1 ⟷ 2 | 18.84 % | 24.08 % |
| 1 ⟷ 4 | 19.65 % | 23.92 % |
| 1 ⟷ 5 | 7.07% | 6.82 % |
| 4 ⟷ 5 | 23.29% | 19.66% |
| 2 ⟷ 4 | 8.07% | 6.74 % |
| 2 ⟷ 5 | 23.08% | 18.72 % |

# $^{137}$Cs source data

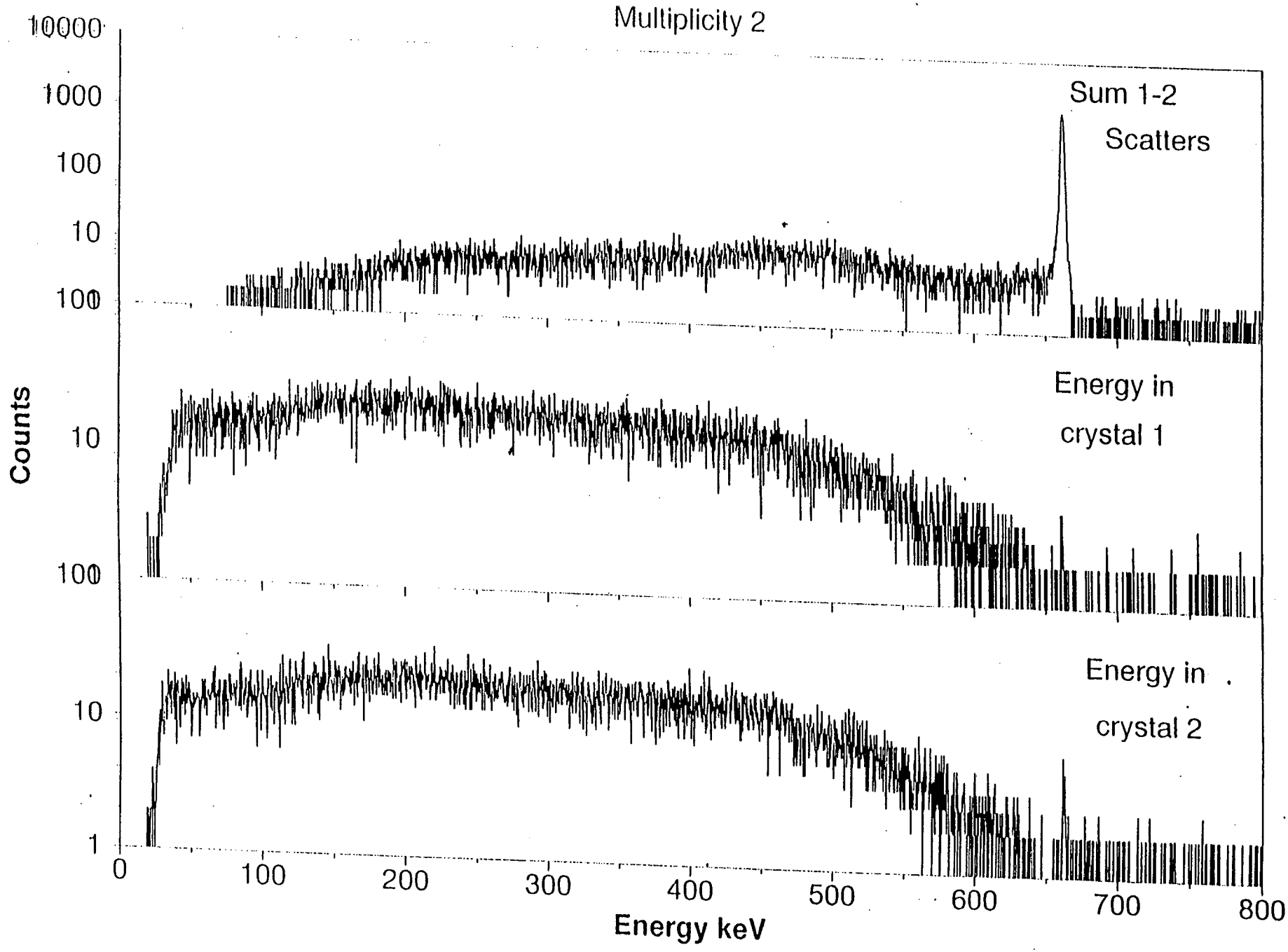

# Scattering Patterns

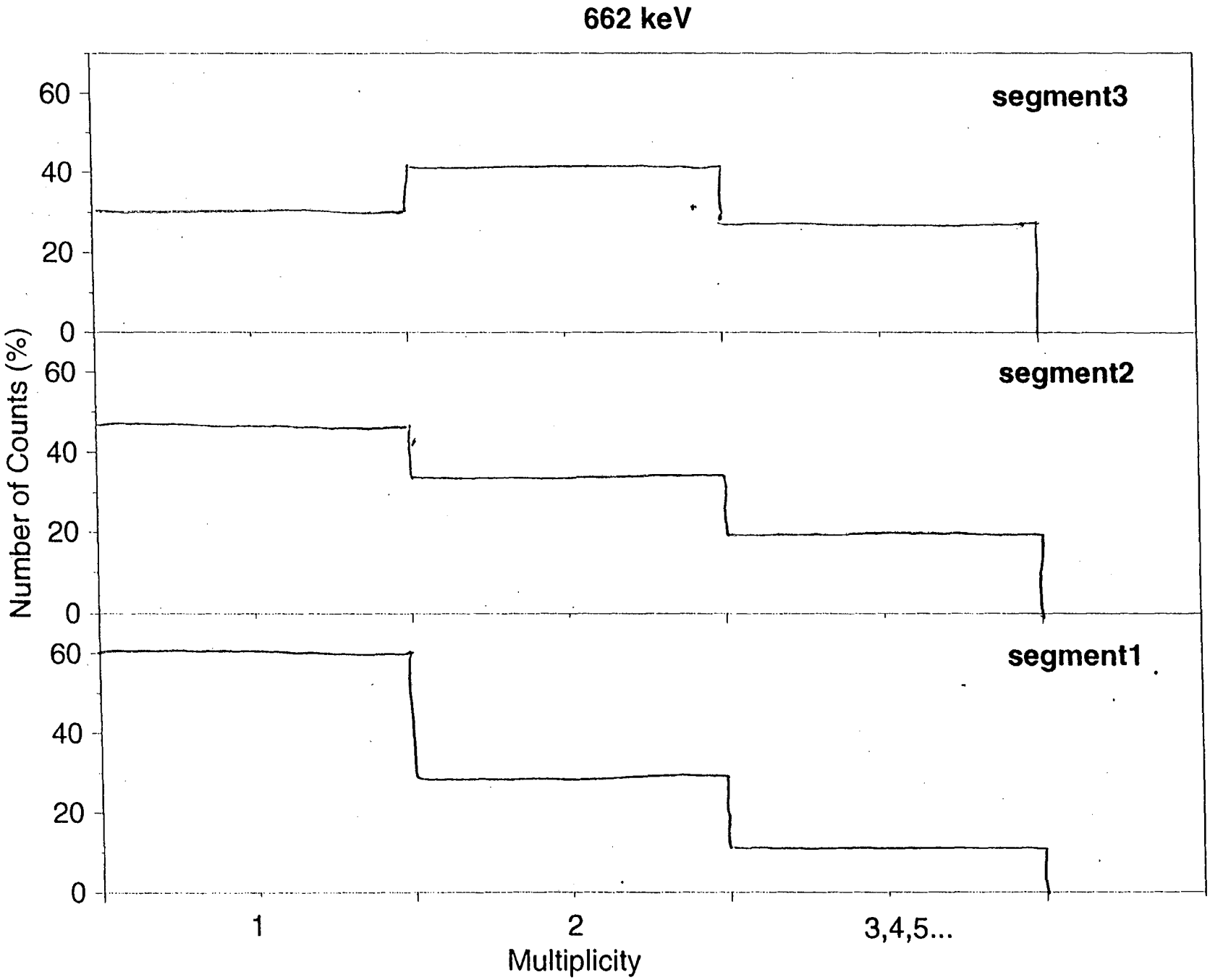

# Scattering Patterns

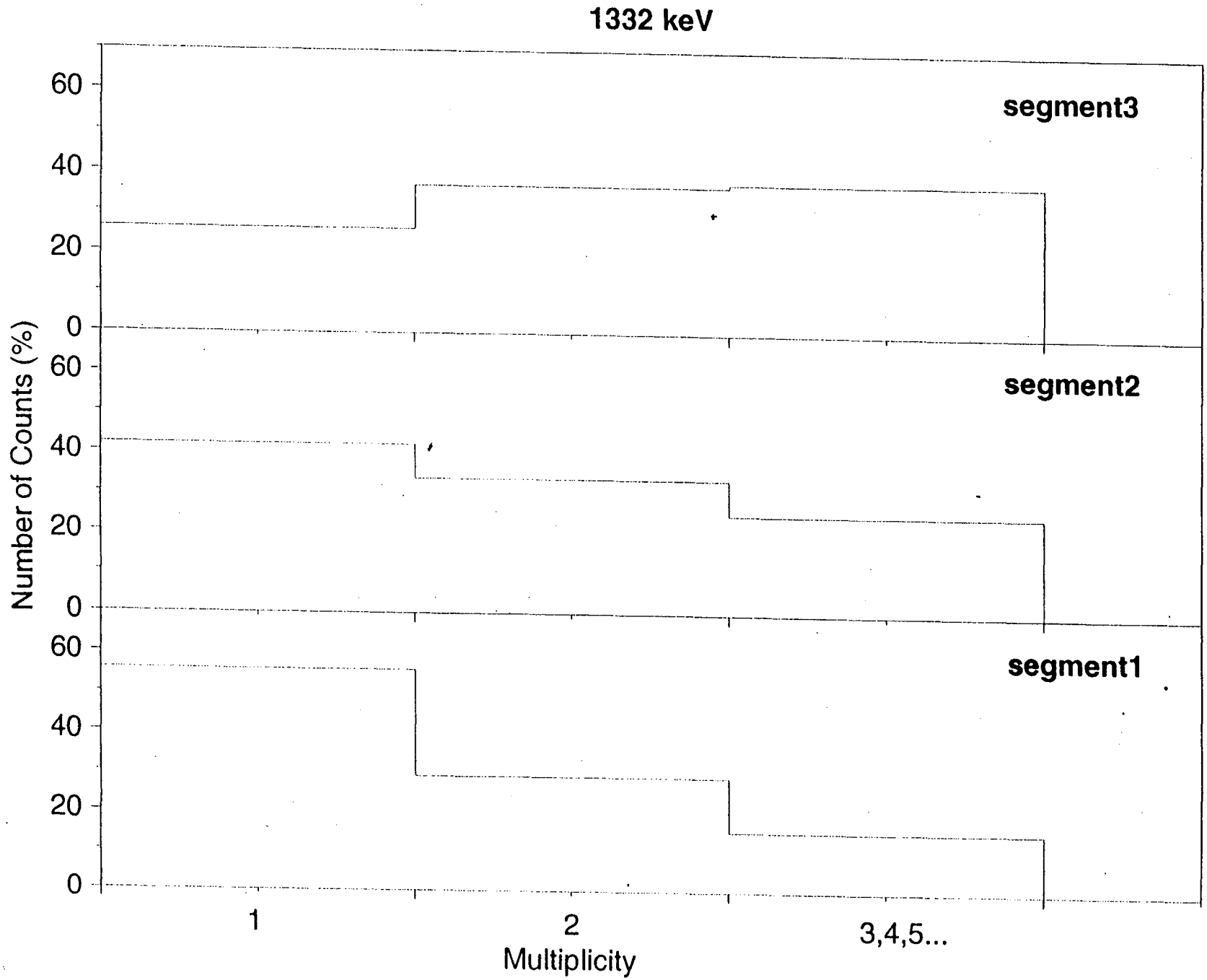

# Pulse shape analysis

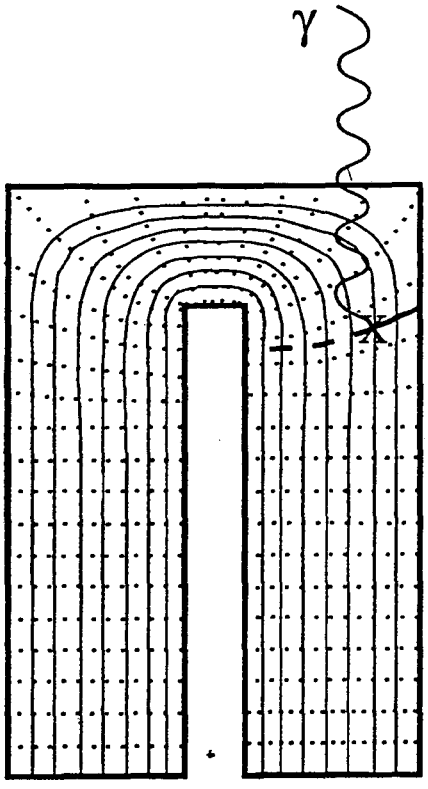


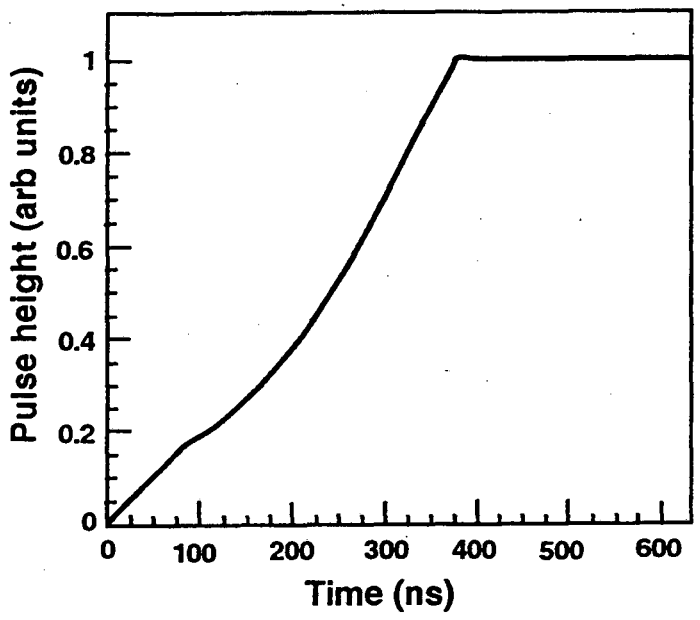


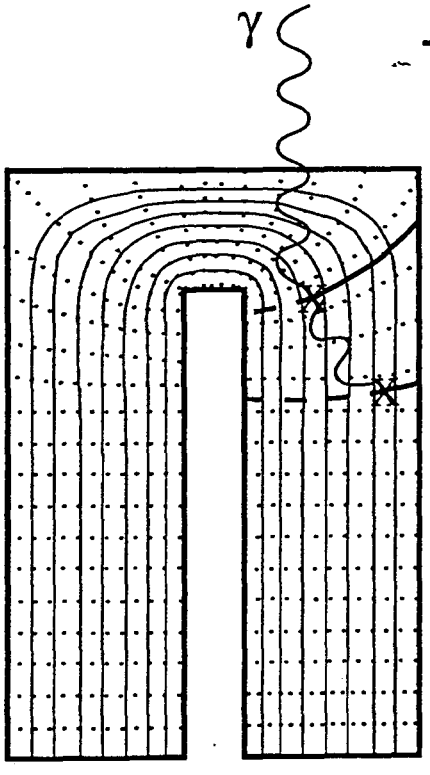


Trajectories — electrons
- - - - holes

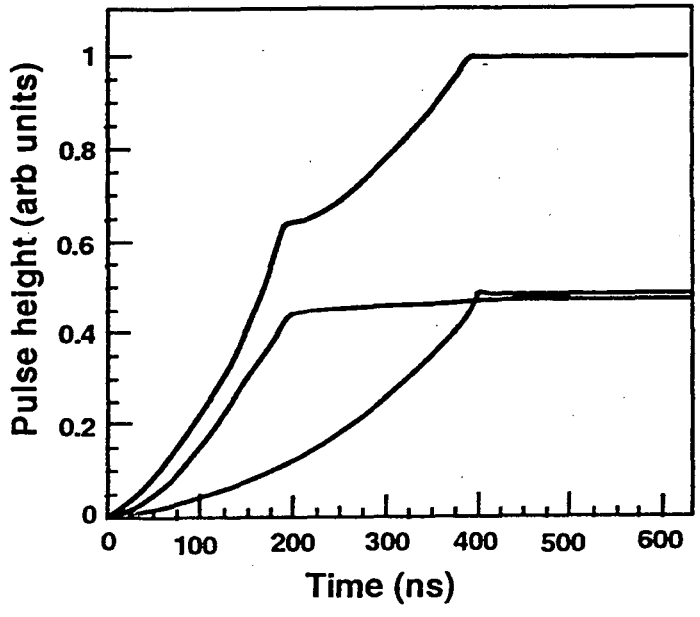

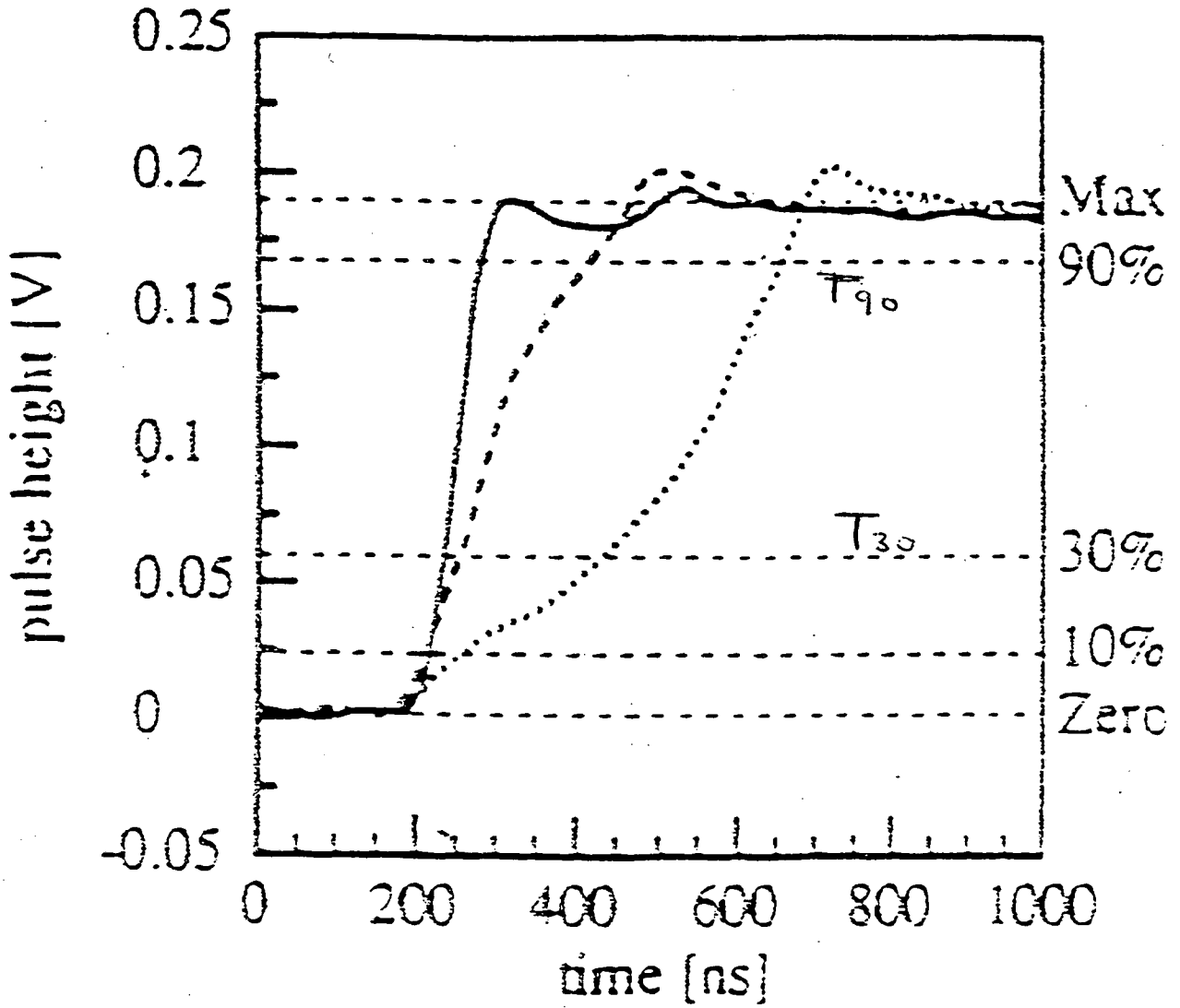
0.25
0.2
0.15
0.1
0.05
0
-0.05
pulse height [V]
0
200
400
600
800
1000
time [ns]
Max
90%
30%
10%
Zero
T90
T30

# GSI SEGMENTED CLOVER (70 mm ϕ, 140 mm long)

Mean T30 distribution at 779 keV

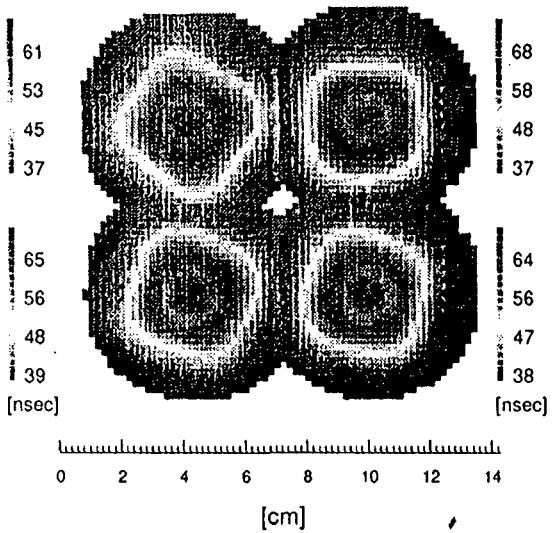


Mean T60 distribution at 779 keV

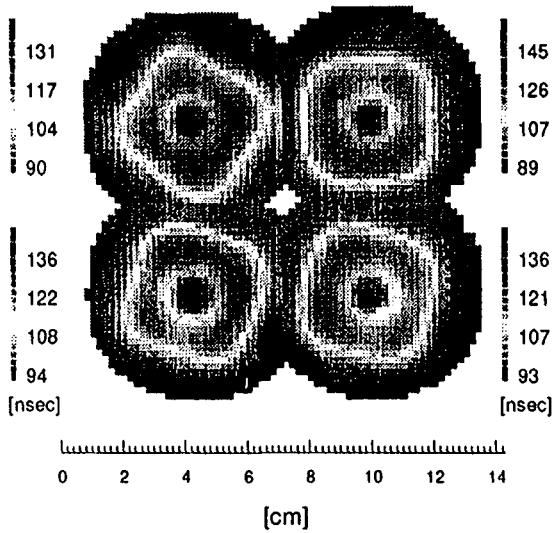


Mean T90 distribution at 779 keV

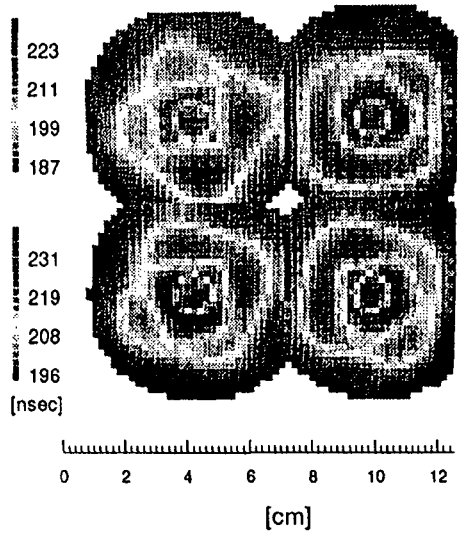


# Small SEGMENTED CLOVER (50 mm ϕ, 70 mm long)

Mean T30 distribution at 779 keV

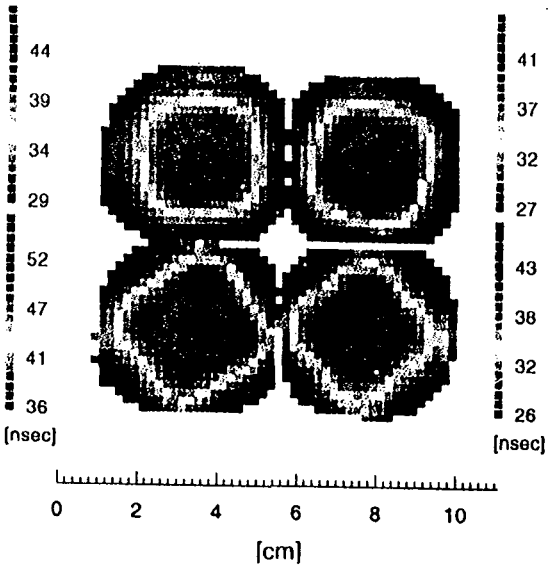


Mean T60 distribution at 779 keV

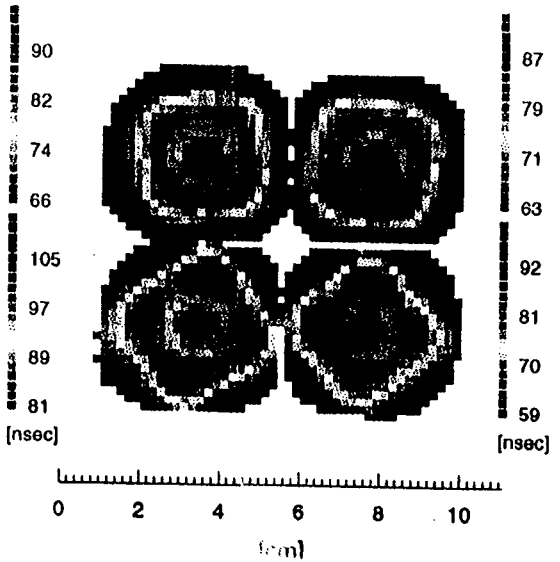


Mean T90 distribution at 779 keV

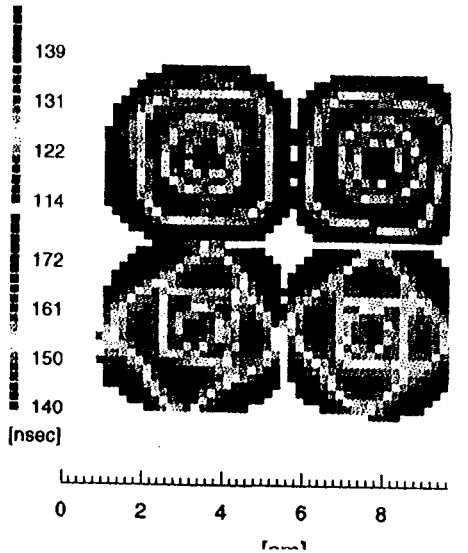

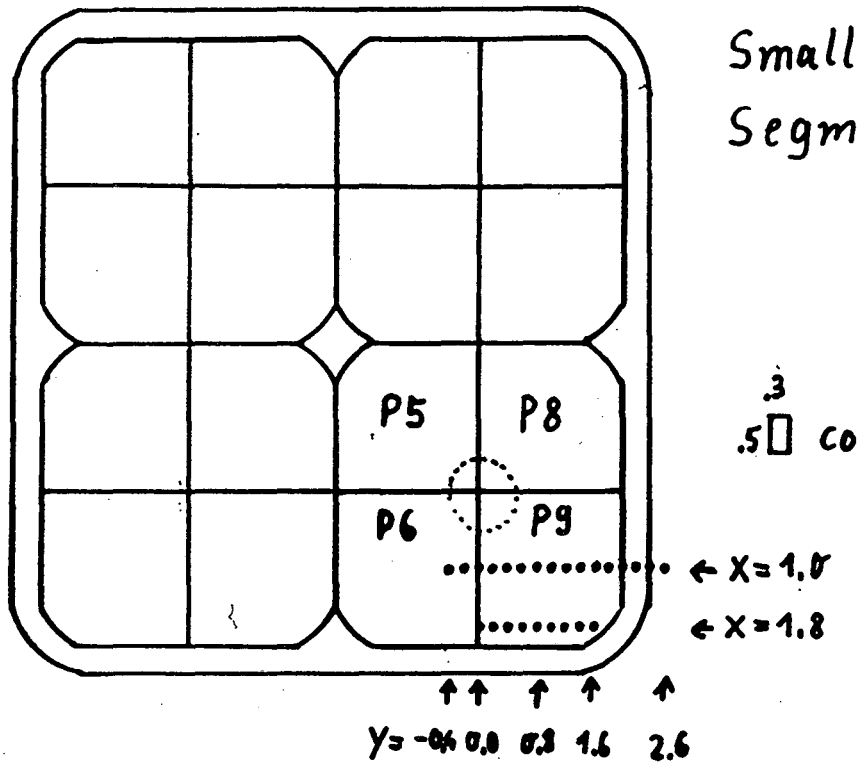


Small
Segmented Clover

.3
.5□ collimator

$^{137}$Cs source

γ-ray aimed at P9

Image charge measured
on P6

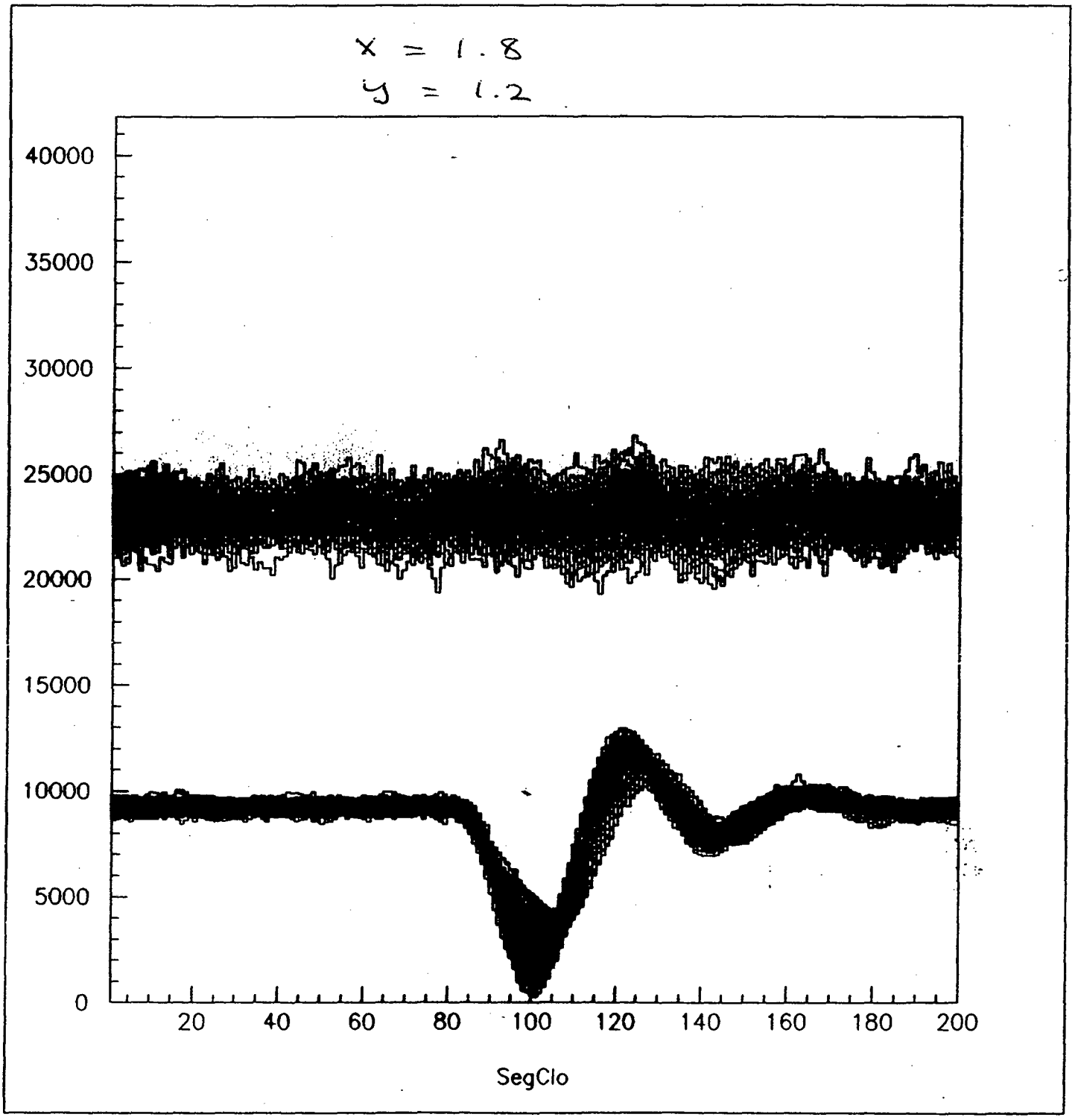
x = 1.8
y = 1.2
40000
35000
30000
25000
20000
15000
10000
5000
0
20
40
60
80
100
120
140
160
180
200
SegClo

$^{137}$Cs source

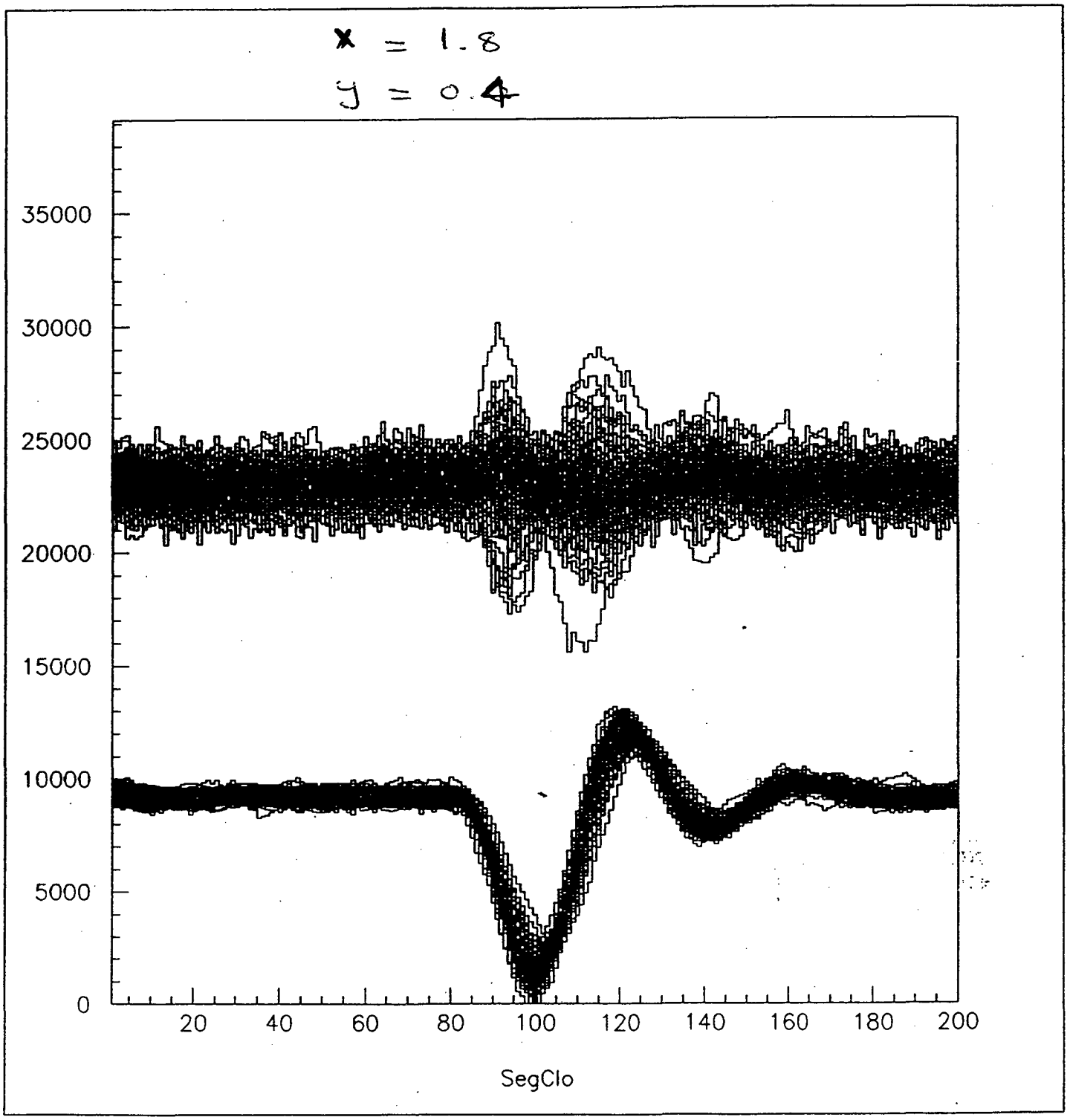

$^{137}Cs$ Source

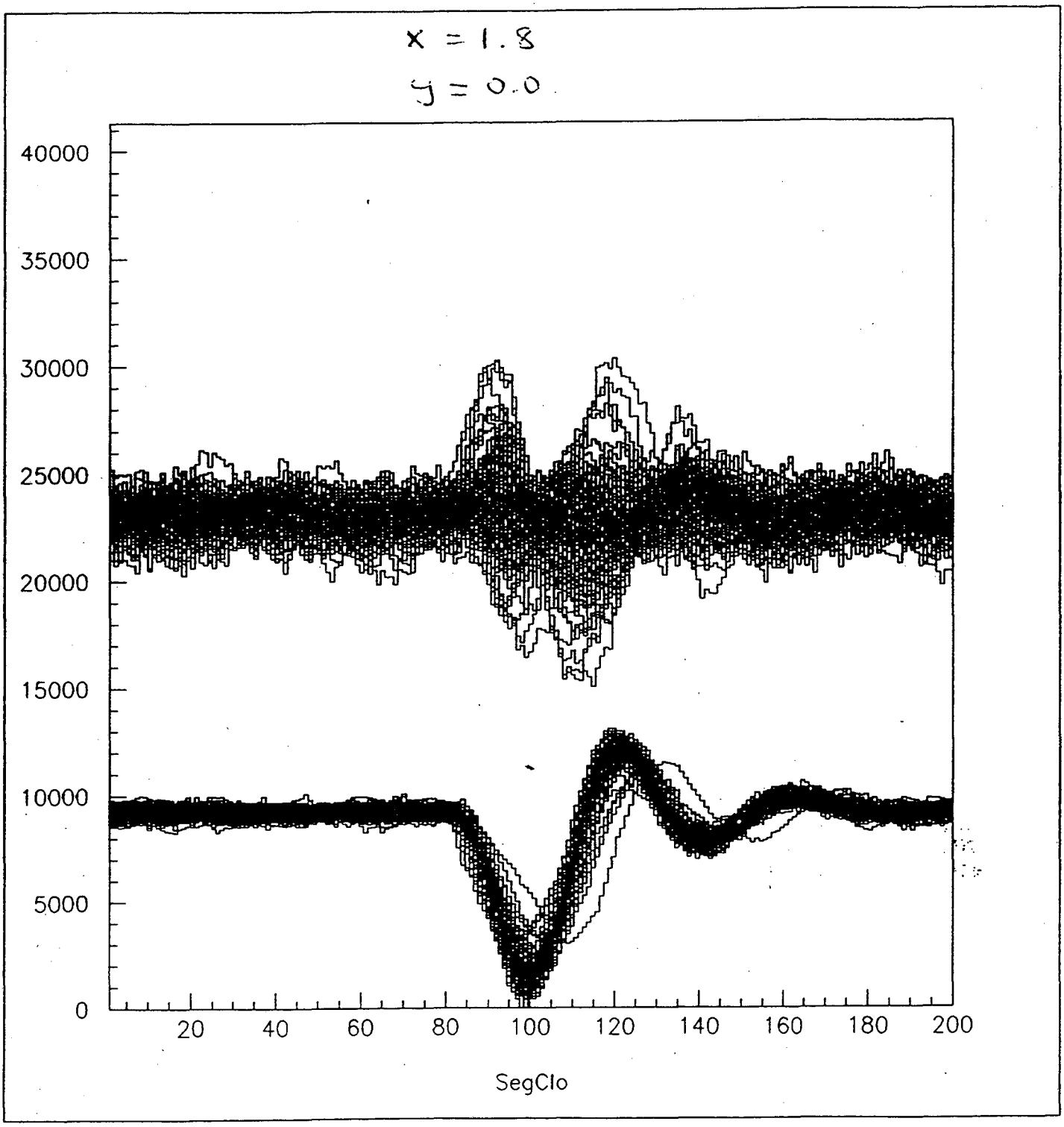

# Acknowledgements

| | |
|---|---|
| G Duchene *et al* | Clover detector |
| G de France | Monte Carlo |
| J Gerl *et al* | Measurements |

Dave Cullen
Duncan Appelby
Sarah Shepherd

J.Eberth

Segmented encapsulated germanium detectors for the next generation of gamma-ray arrays.

# Segmented encapsulated Germanium detectors for the next generation of γ-rays arrays

J. Eberth
University of Köln

- European facilities for γ-ray spectroscopy
- Encapsulated Ge detectors: a status report
- The segmented encapsulated Ge detector as building block for variable arrays
- The Miniball - Array at REX-ISOLDE
- Outlook: Transverse segmentation of encapsulated Ge detectors

This work is performed within the projects EUROBALL and MINIBALL. The work is supported by the EC programme TMR and by the German BMBF under contract No. 06OK862I.

# European facilities for γ-ray spectroscopy

- REX-ISOLDE at CERN : radioactive beam 2 (5) MeV/u
- Accelerated fission fragments from PIAFE at Grenoble and FRM II at Munich ( 6 MeV/U )
- GSI : relativistic radioactive beams from SIS and FRS

  UNILAC: decay studies at the velocity filter SHIP and GSI/ISOL,
  prompt γ-rays in coincidence with separated reaction products at SHIP

- Heidelberg/GSI : Ge detectors combined with the crystal ball (162 NaJ detectors)
- Upgrade of EUROBALL : Replacement of 1 π of tapered Ge detectors

Demands : high total-absorption efficiency
high granularity (large v/c)
flexibility: different geometries with the same set of detectors

Solution: segmented, encapsulated Ge detectors
several types of cryostats

## Prerequisites for Flexible Ge Detector Systems

easy handling of
composition of
→ Ge Detector Units

**but ...**

Ge crystal surfaces very sensitive to contamination !

Individual cryostats for cooling
and for contamination protection !

**Solution:**

Encapsulation Technology for Ge Detectors

hermetically sealed aluminum can, vacuum < $10^{-6}$ mbar maintained by internal getter

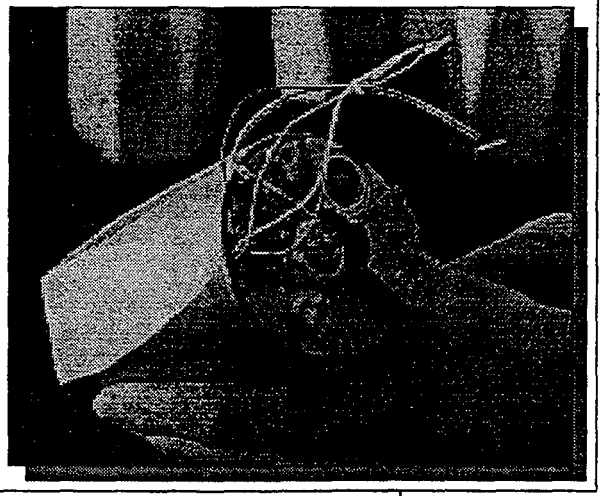

The CLUSTER Detector:
... an example for a flexible spectrometer system !

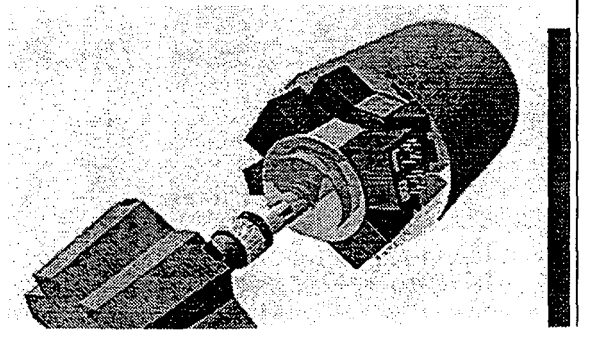

J. Eberth et al. NIM A 369 (1996) 135
Collaboration: Köln, Jülich, Eurisys

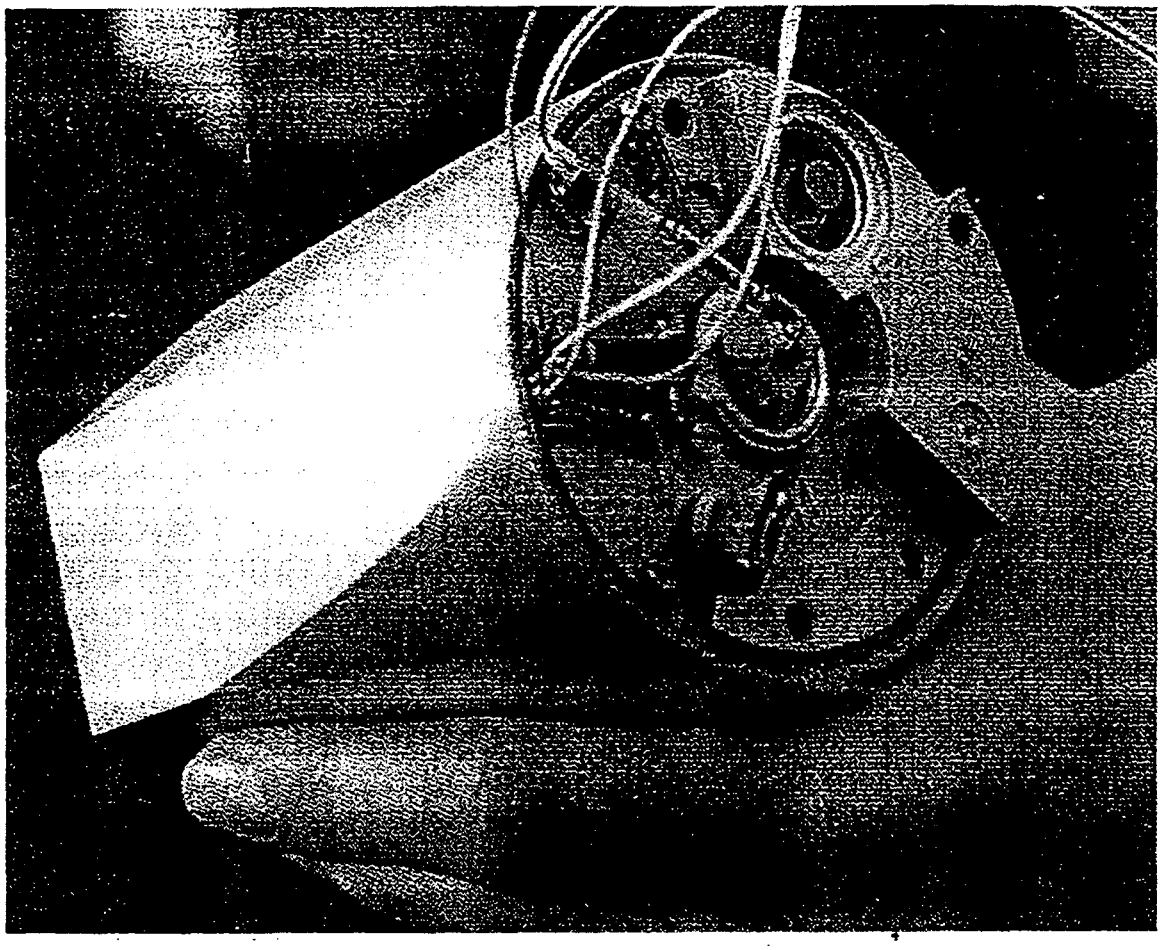

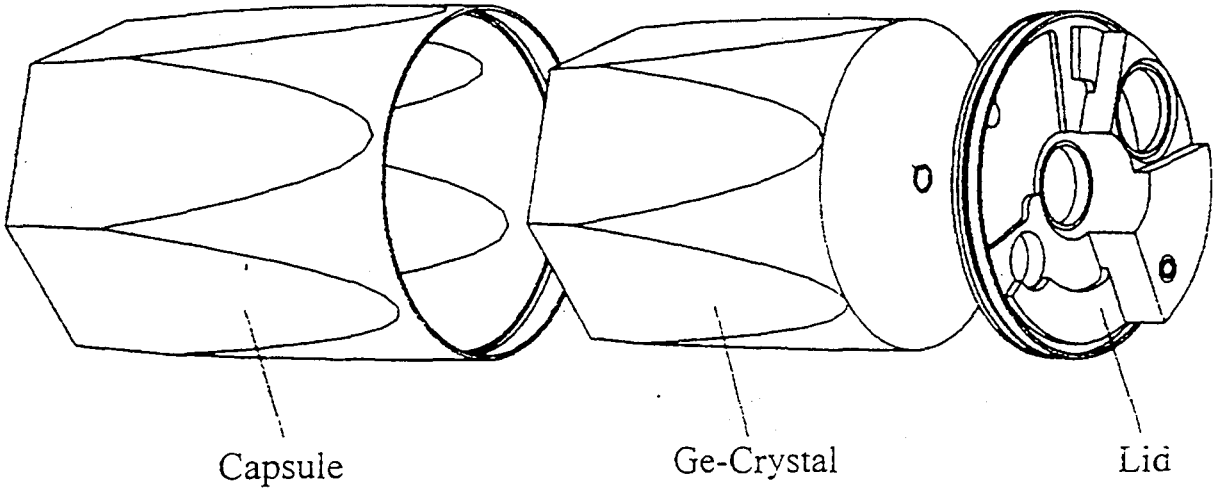


Al 0.7 mm thick

d = 70 mm
l = 78 mm

~ 60 % Eff.



2.5 mm Ge – Ge of adjacent detectors

# Advantage of the Encapsulation Technology

Back Lid of an encapsulated Ge Detector

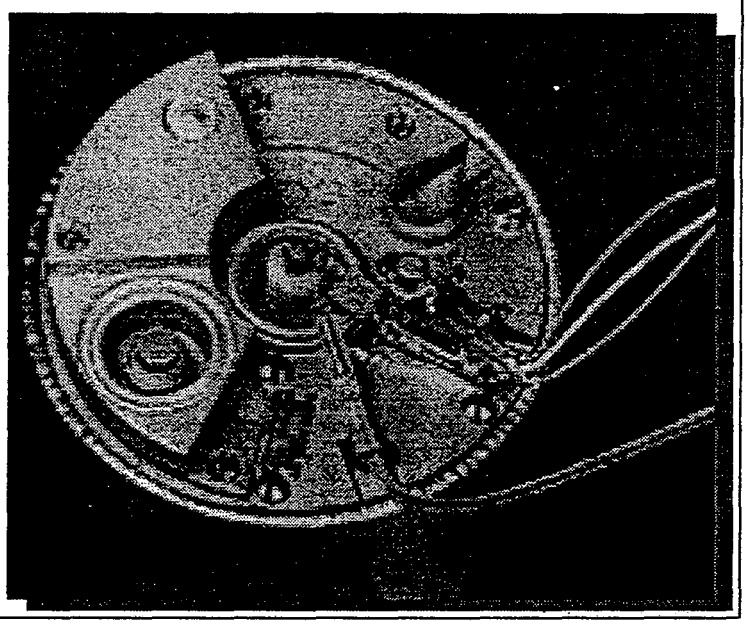

easily accessible
and exchangeable
cold electronics
like FET,
Coupling Capacitor
plugs ...

## Regeneration of Neutron-Induced Radiation Damage of Encapsulated HPGe Detectors:

Neutron Damage Anneal in a Standard Oven:

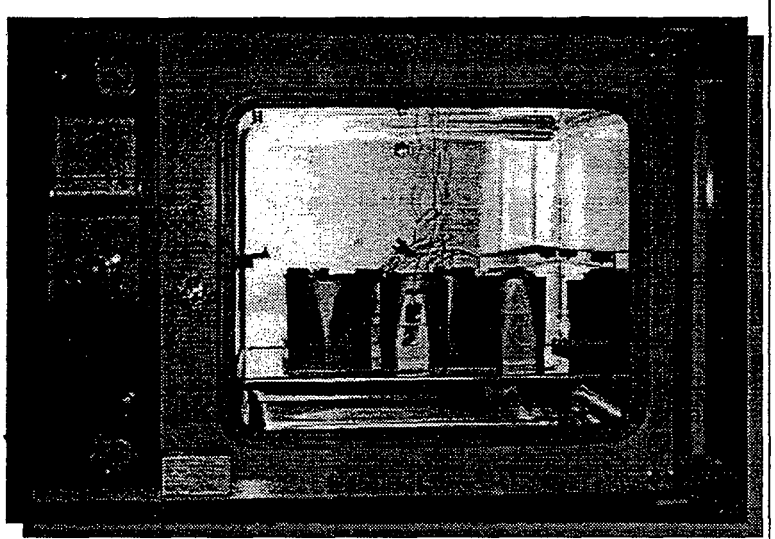

Annealing Temp. [Celsius]

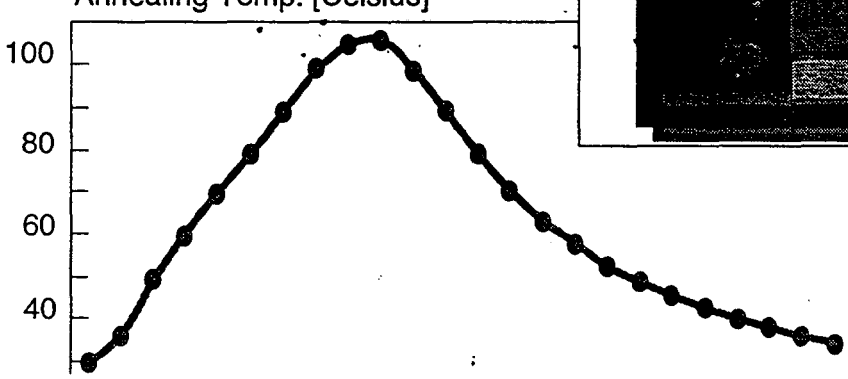


D. Weisshaar, Köln

# Annealing Procedure:

(thanks to D. Weisshaar. IKP Koln)

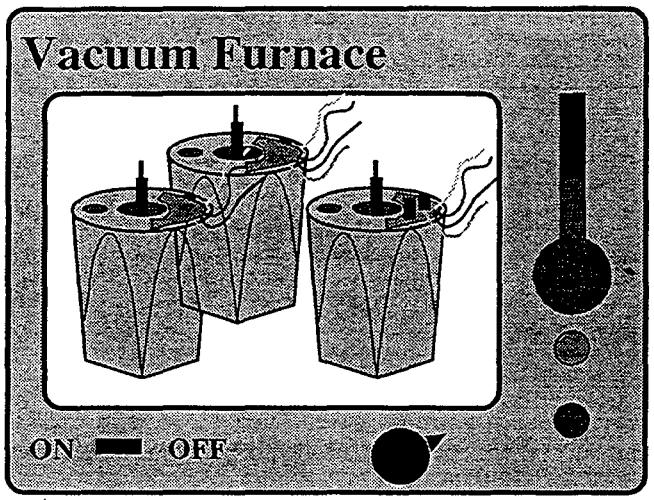


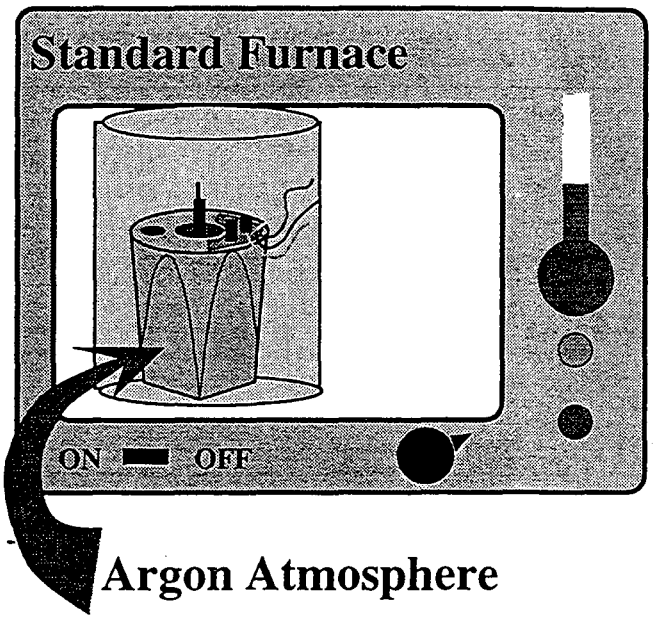


**Annealing Temperature: 105$^0$C for 2 hours**

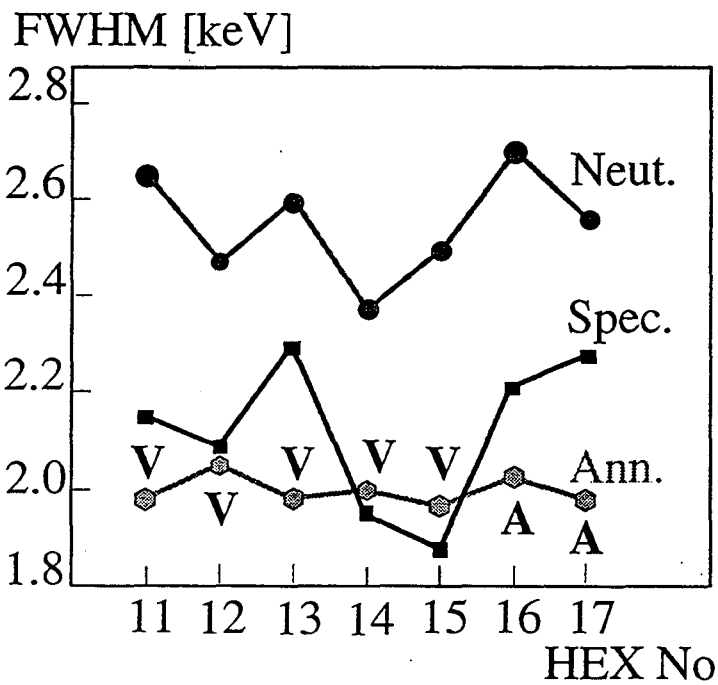


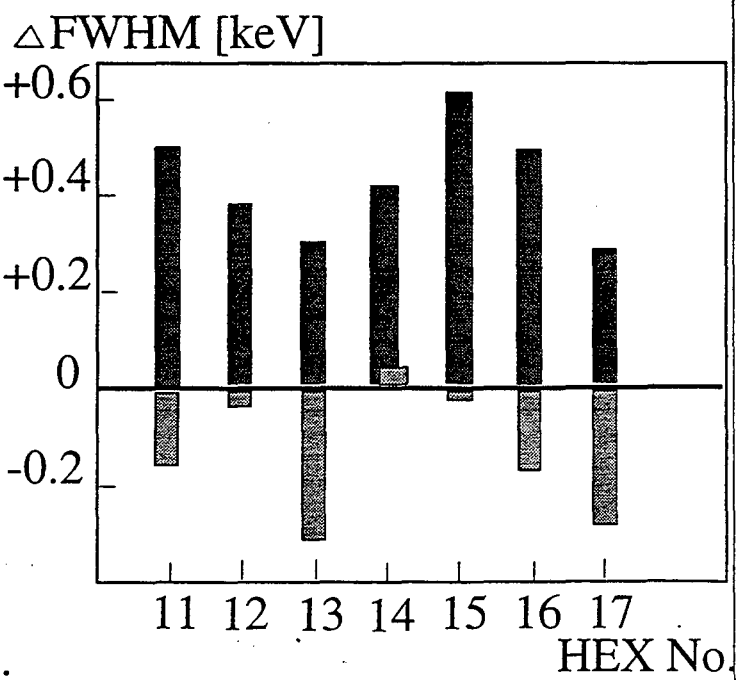

# The EUROBALL CLUSTER Detector:

**a flexible system optimized for high gamma energies**

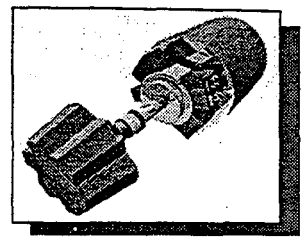

**Specifications:**
(measured at 1.33 MeV)

**Resolution** $\triangle E$ **= 2.3 keV**

**Add-Back Factor = 1.45**

**abs. Efficiency = 29 %**

**rel. Efficiency = 600 %**

**P/T** without BGO **= 39 %**

**P/T** with BGO **= 63 %**

The CLUSTER Arrangement

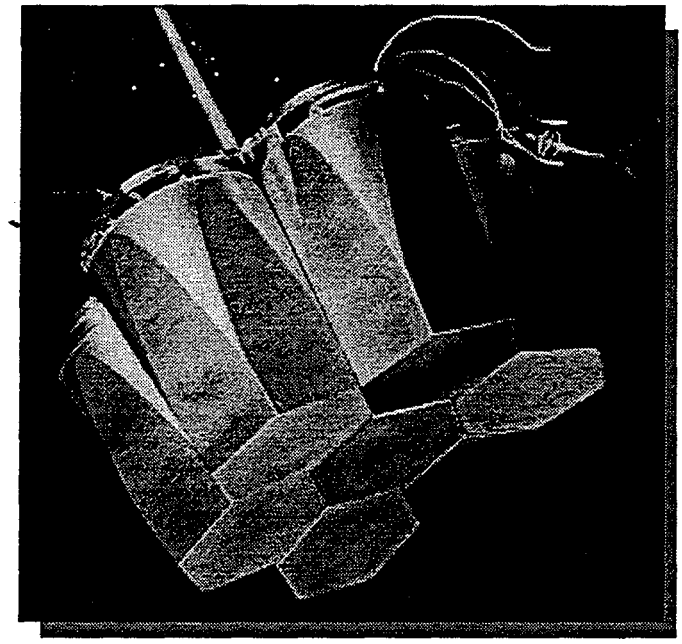

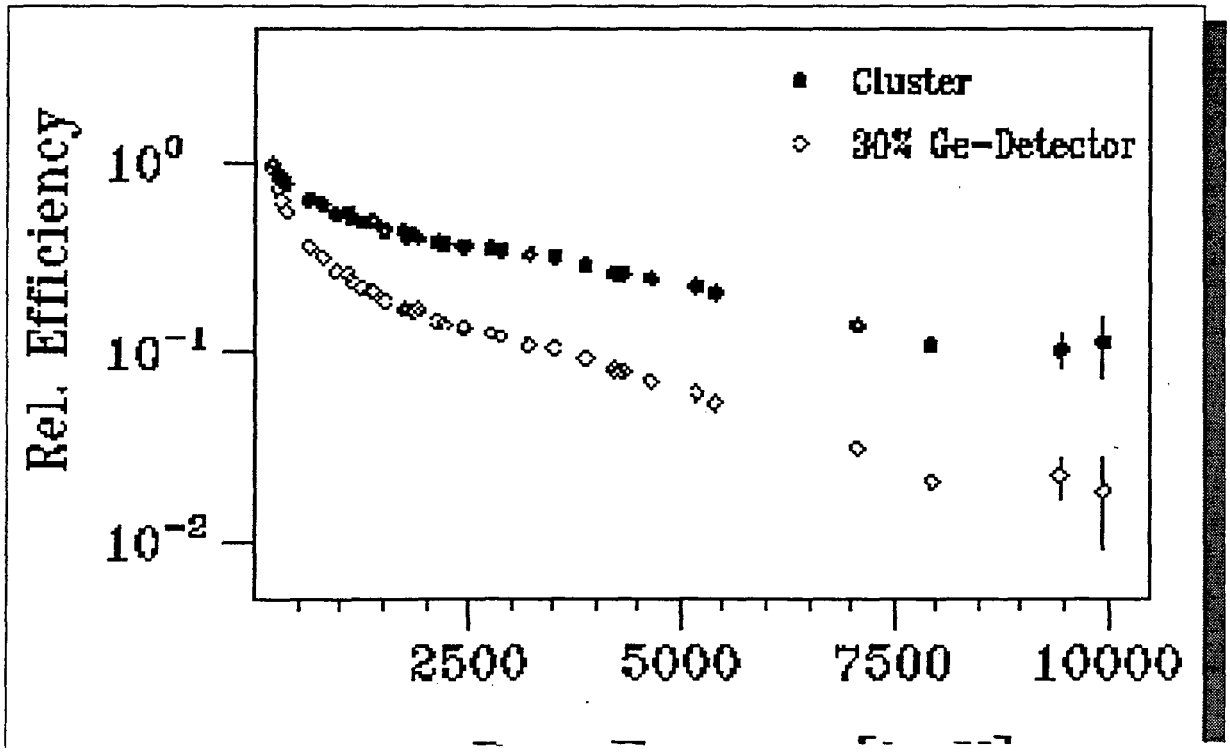

## Reliability and Flexibility of these Systems (-1-):

In 18 months were built up successfully:

more than 10 complex set-ups in various Europeanaccelerator laboratories (e.g.: Univ. Cologne, MPI-K Heidelberg, GSI and TU Darmstadt, NBI Risø and INFN Legnaro)

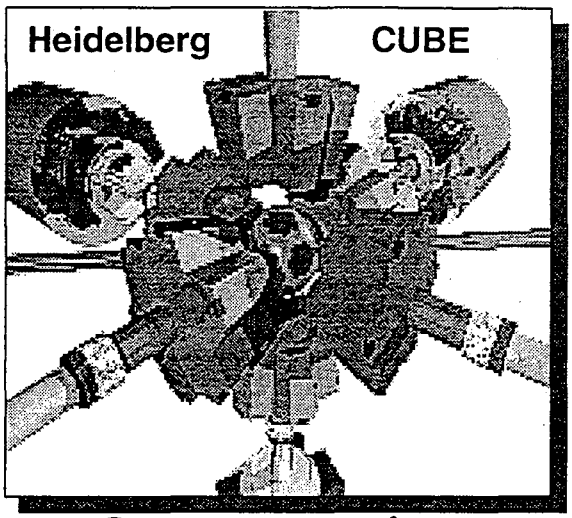


$P_{ph} \approx 19\%$

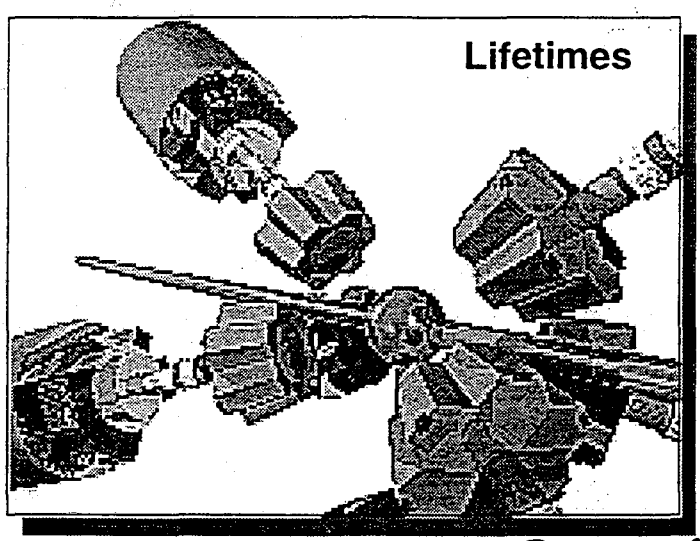


$P_{ph} \approx 6\%$

No CLUSTER and no capsule failed after shipment or rearrangement

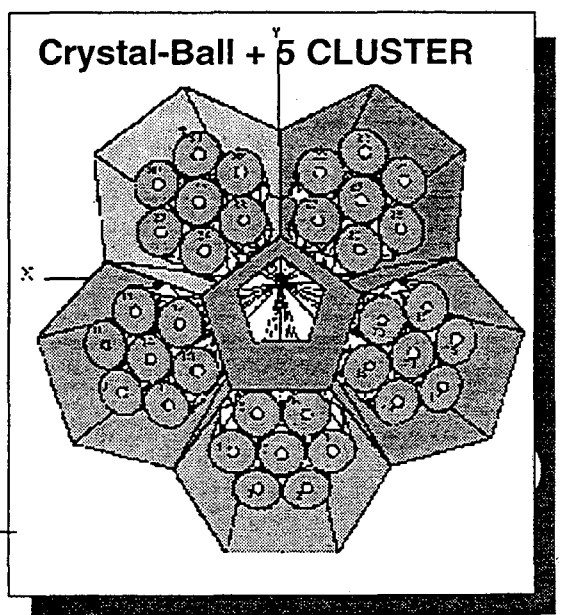


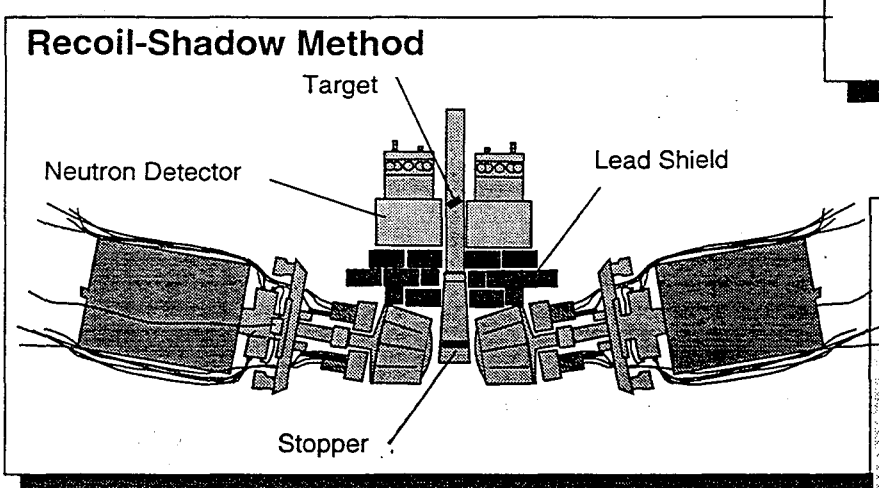

## Reliability and Flexibility of these Systems (-2-):

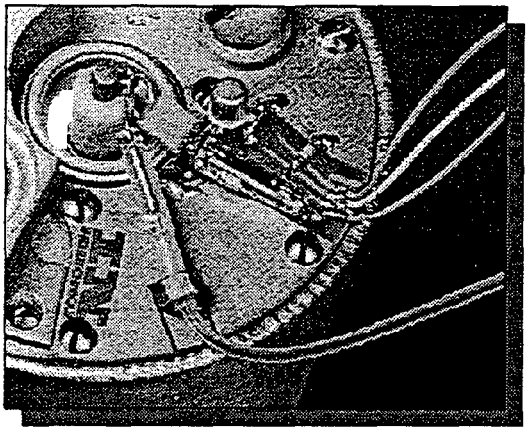

- easy repair of defect cold electronics (like FET ...) within one week in the lab (as warming up, pumping, cooling ...)
- no shipment to the manufacturer !
- high availibility of the expensive detector systems!

---

- ▲ More than 100 encapsulated detectors were annealed so far
- ▲ sets of seven capsules were annealed simultaniously in a standard oven
- ▲ not even one encapsulated Ge detector failed after the annealing
- ▲ the resolutions could be restored to the original values (in average 2.1 keV)

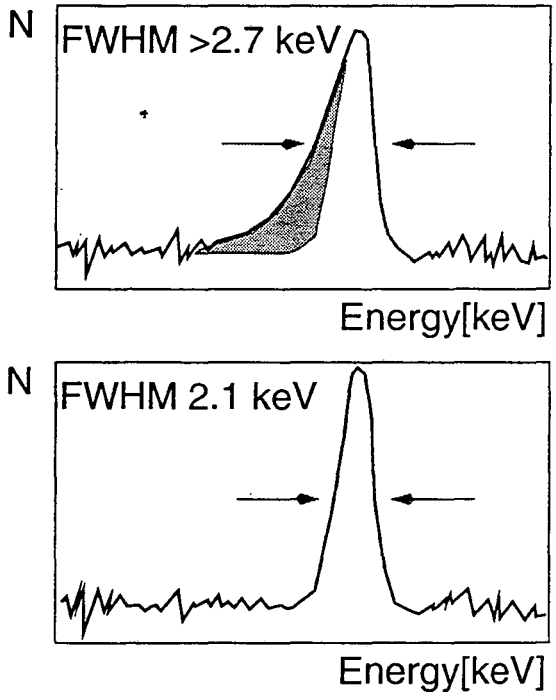


---

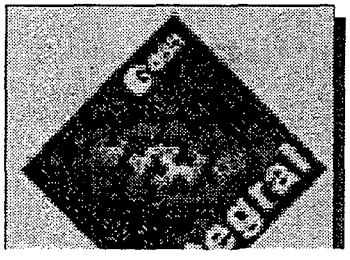

high realibility
suitable for
space applications,
e.g.

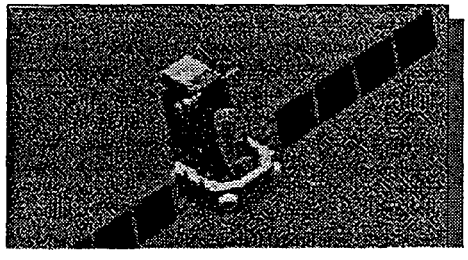

# The CLUSTER Cube

- $P_{ph} = 0.19$ ( $E_\gamma = 1.33$ MeV )
- $\Omega_{Ge} = 0.65$
- $\Delta E_\gamma \approx 13$ keV ( $E_\gamma = 1.33$ MeV, v/c = 0.04 )
- $P_{isol} \approx 0.87$ ( $M_\gamma = 10$ )
- $R_{Ge} \approx 11$ cm

**Outstanding Feature :**

**Large detection efficiency up to $E_\gamma = 10$ MeV**

**for experiments with with small recoil velocities and low gamma multiplicity**

# The Segmented CLUSTER Detector

a possible solution for Miniball

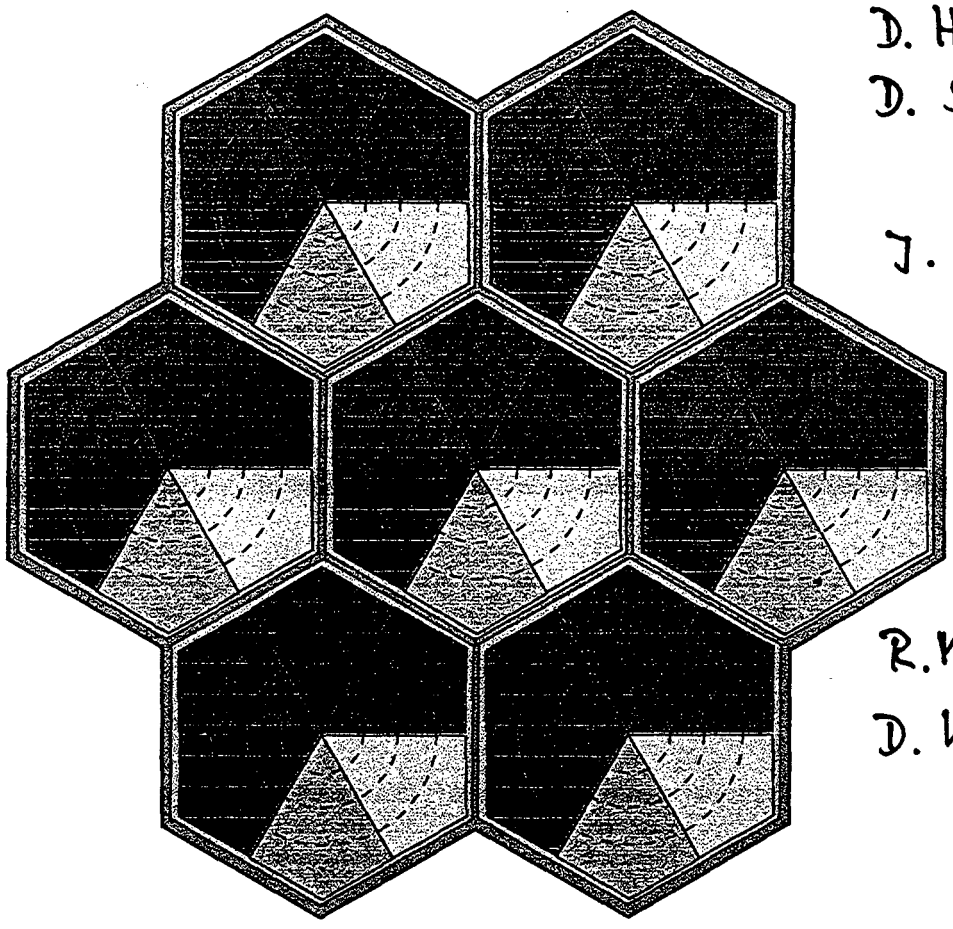

D. Habs, Munich
D. Schwalm, Heidelberg
J. Eberth, Cologne
J. Gerl, GSI
P. van Duppen, Leuven
R.M. Lieder, Jülich
D. Warner, Daresbury

**seven high-resolution sum-energy outputs with additional radial event information, E < 2.4 keV**

**42 segment energy outputs with E < 3.5 keV**

---

# Multi-Segmented CLUSTER for best Doppler-Shift Correction !

# The 6-Fold Segmented and Encapsulated Ge Detector

Sketch of the capsule and the segmented Ge crystal

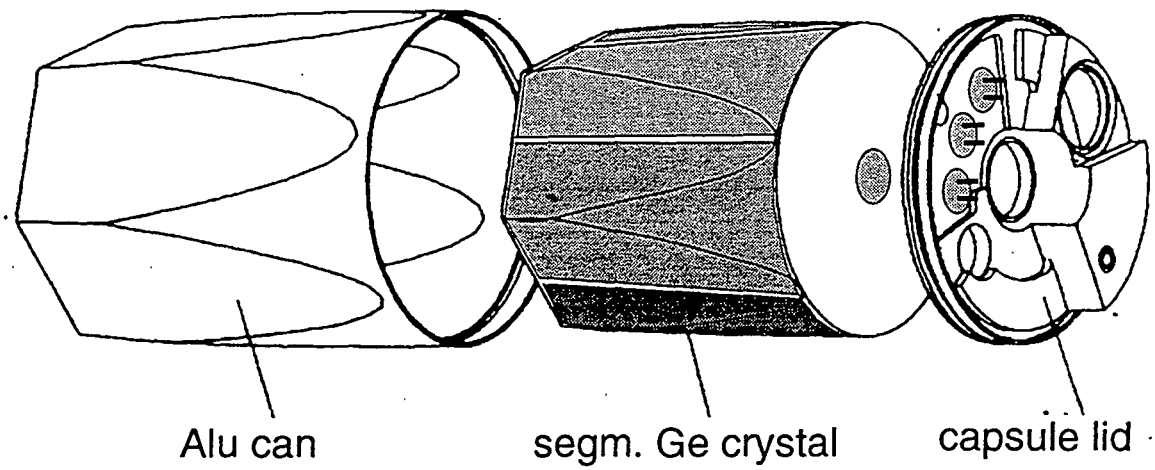


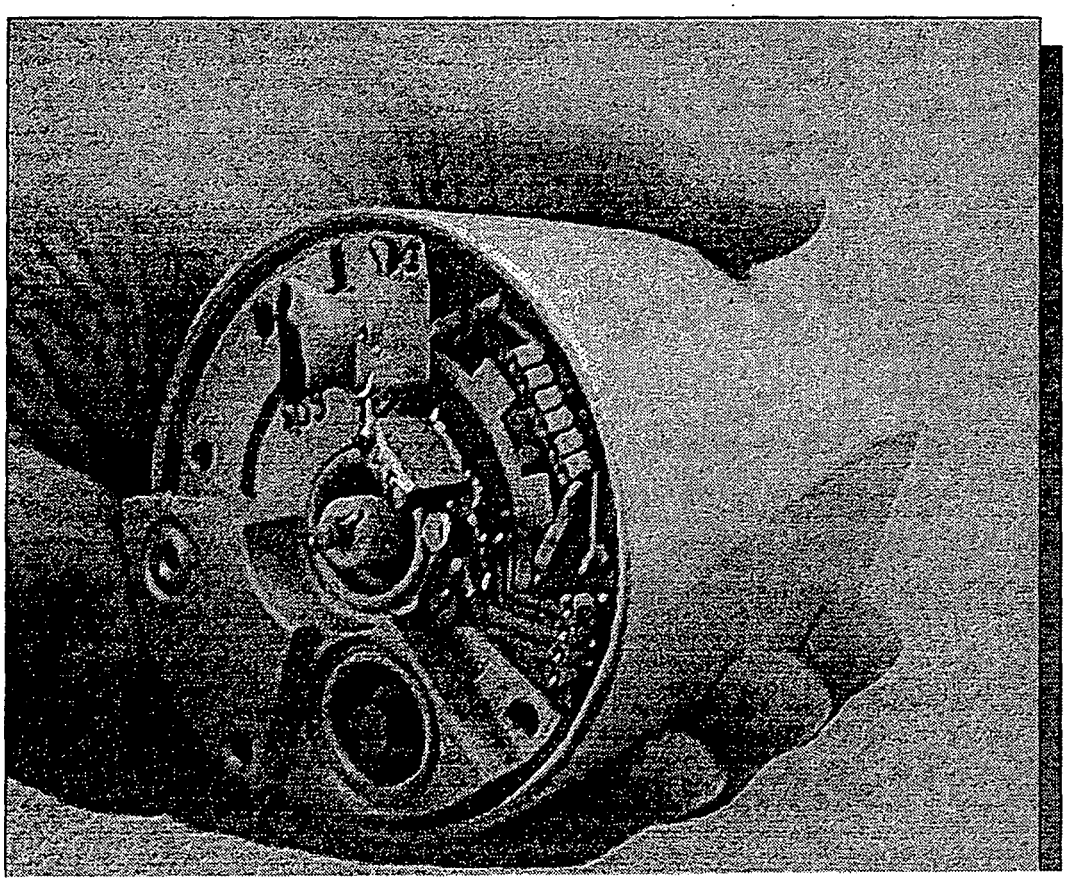

## Data of the Encapsulated 6-Fold Segmented Ge Detector

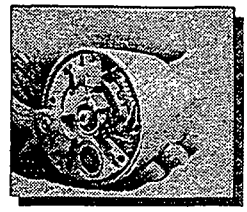

Back lid of an encapsulated
6-fold segmented Ge Detector:

**central HV feed-through**

**cold preamp-board**

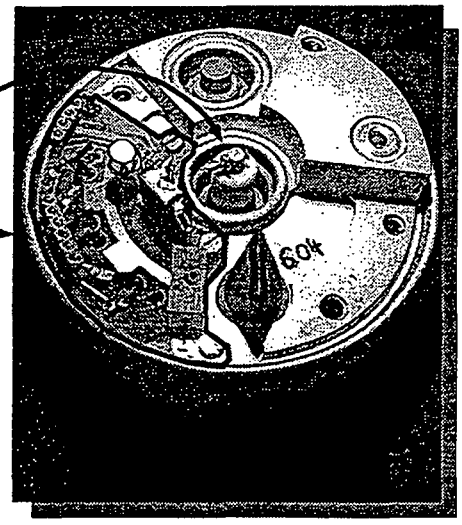

**crystal data of the prototype detector:**

rel. eff. (at 1.33 MeV) : 60.2 %
P/T (200 - 1340 keV): 23.8 %

(identically to those of standard encapsulated EUROBALL moduls)

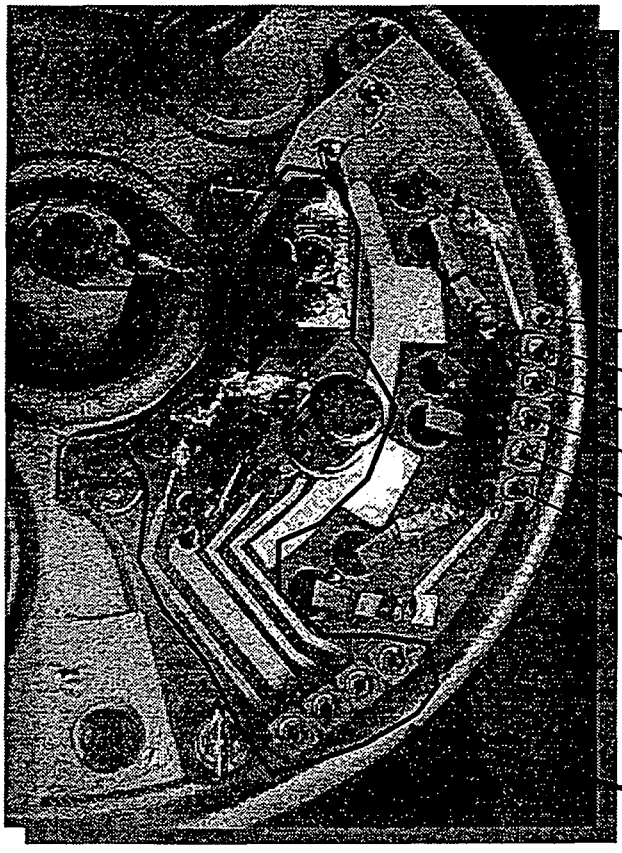

**Segments with warm preamps !**
(capacity ~ 90 pF - 100 pF,
depending on length of cables)

| γ− Energy | 122 / | 1333 keV |
|---|---|---|
| Segm. no.1: | 2.54 / | 3.16 keV |
| Segm. no.2: | 2.44 / | 3.07 keV |
| Segm. no.3: | 2.27 / | 2.99 keV |
| Segm. no.4: | 2.26 / | 3.08 keV |
| Segm. no.5: | 2.13 / | 2.80 keV |
| Segm. no.6: | 2.16 / | 2.90 keV |

**Core with cold FET !**

core (grounded segm.): 1.20 / 2.09 keV

# SM - / J • Kö n

G. Pascovici

**Conversion gain: 175 mV/ MeV**
**(unterminated)**

**ntegral nonlinearity: less than +/- 0.025**
**(for 0 to +/- 9.5V , unterminated**

**Warm FET option:**

**Equivalent input noise: 0.9 keV / 0 pl**
**Slope: 17 eV / pl**

**Rise time: 18ns / 0 pF ;**
**Slope: 0.4 ns / pl**

**Cooled FET option:**

**Equivalent input moise: 0.6 keV / 0 pl**
**Slope: 17 eV / pl**

**Rise time: 15 ns / 0 pF ;**
**Slope: 0.3 ns / pl**

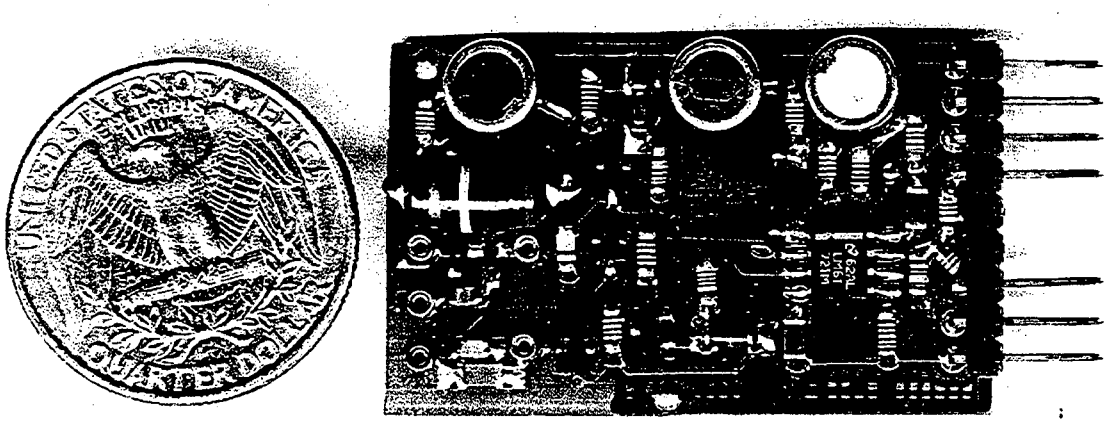

C. Gund, L. Palafox (Heidelberg)

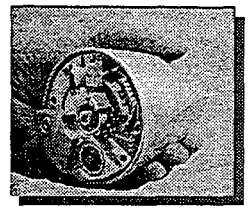

# Data of the Encapsulated 6-Fold Segmented Ge Detector

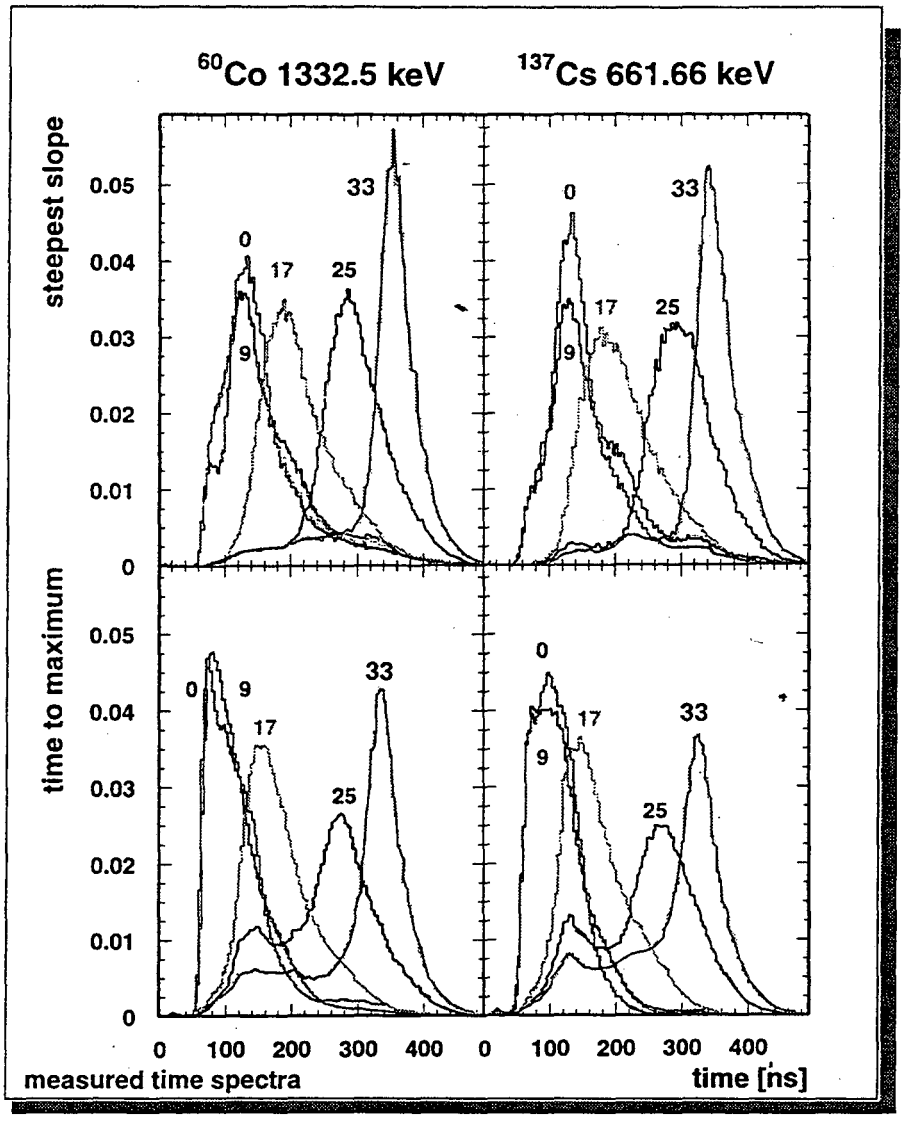


$\Delta r \sim 5-8$ mm

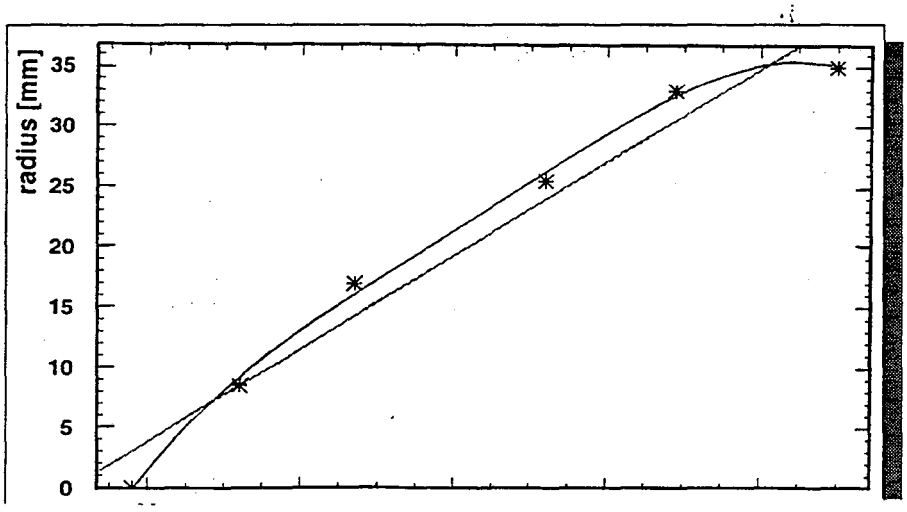

# The MINIBALL-Spectrometer as Segmented CLUSTER-Cube

Distance ~11 cm

$\Omega_{Ge}$ = 65 %

$P_{ph}$ = 13 %

$P_{ph}$ = 19 % in Add-Back Mode

P/T = 40 %

P/T = 50 % with Back Catcher

P/T = 63 % with Back Catcher and Side Shield

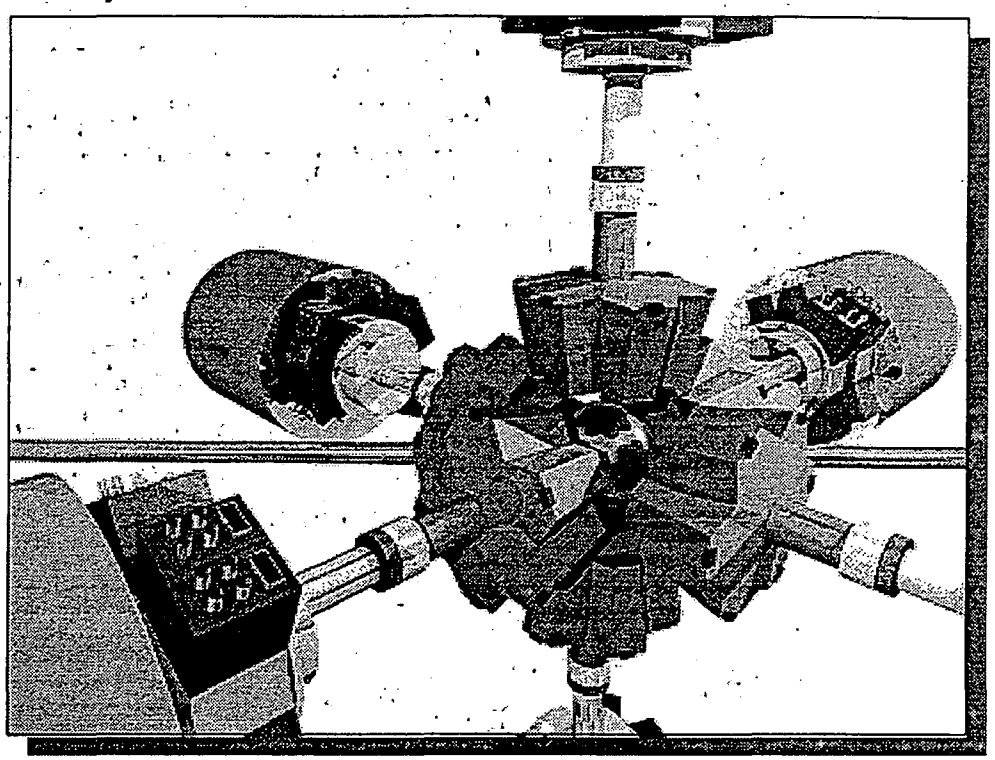

| γ− Energy | β = 2.3 % | β = 4.5 % | β = 7.8 % |
|---|---|---|---|
| 344 keV | 3.3 keV | 4.9 keV | 8 keV |
| | 2.5 keV | 3.1 keV | 5 keV |
| 844 keV | 5.5 keV | 10.1 keV | 23 keV |
| | 3.7 keV | 6.0 keV | 14 kev |
| 1332 keV | 8.1 keV | 16.5 keV | 32 keV |
| | 4.8 keV | 8.5 keV | 14 keV |

unsegmented encapsulated Detectors

# Configurations of Crystals and BGO - Escape Suppression Shields

(H.G. Thomas)

Köln

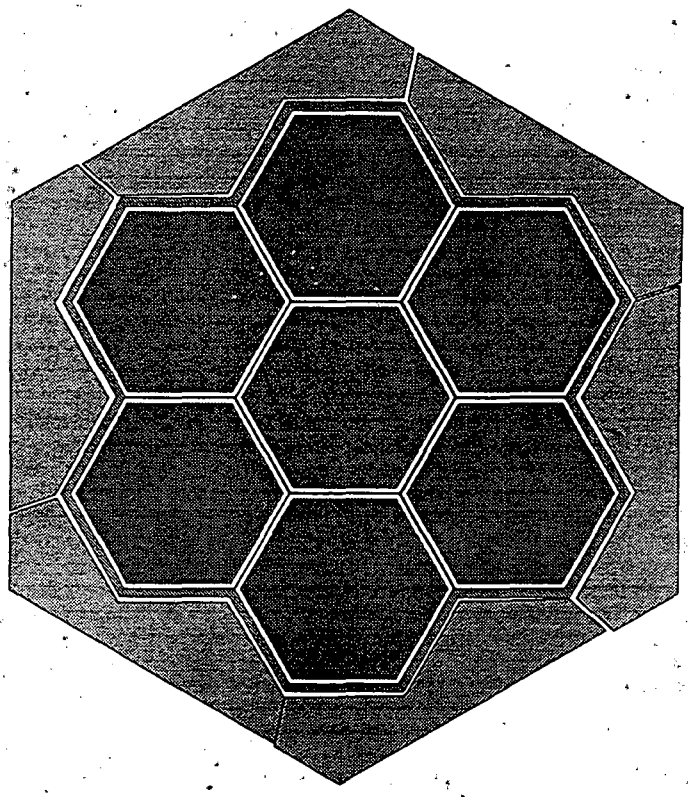

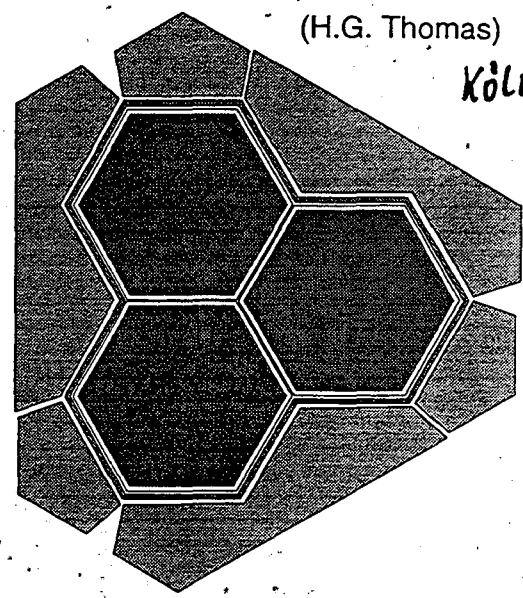

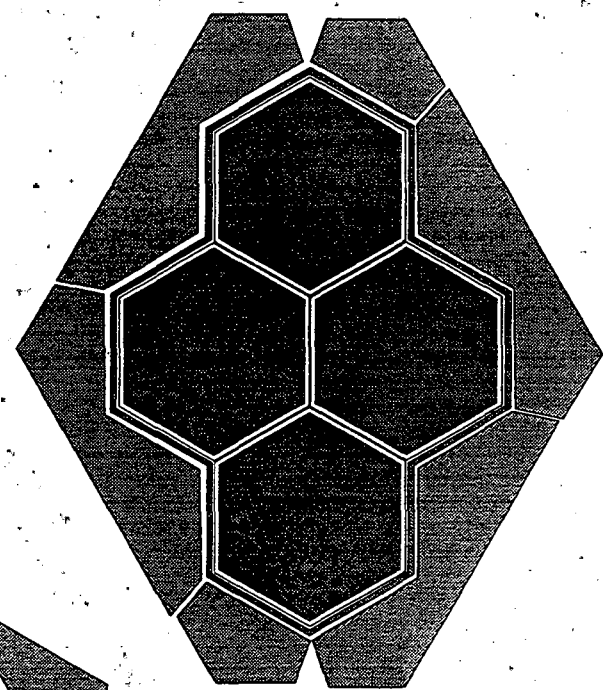

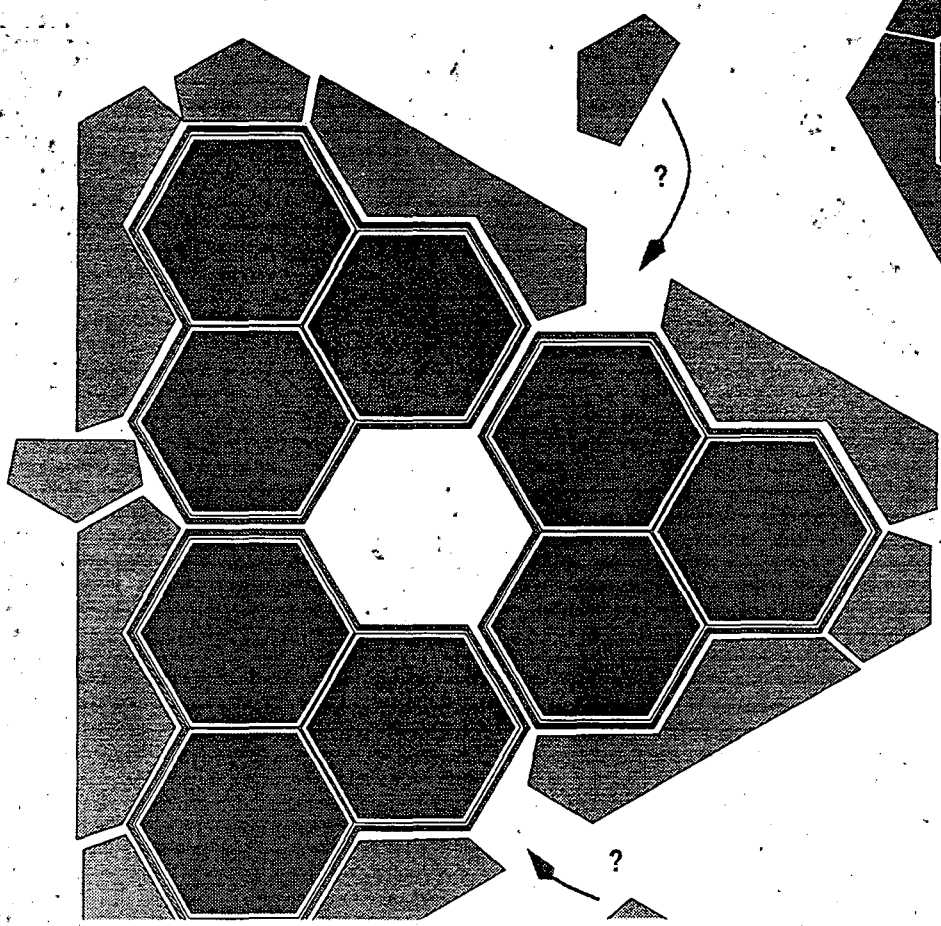


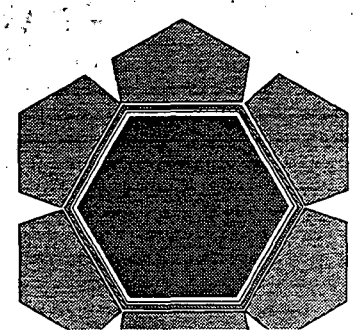

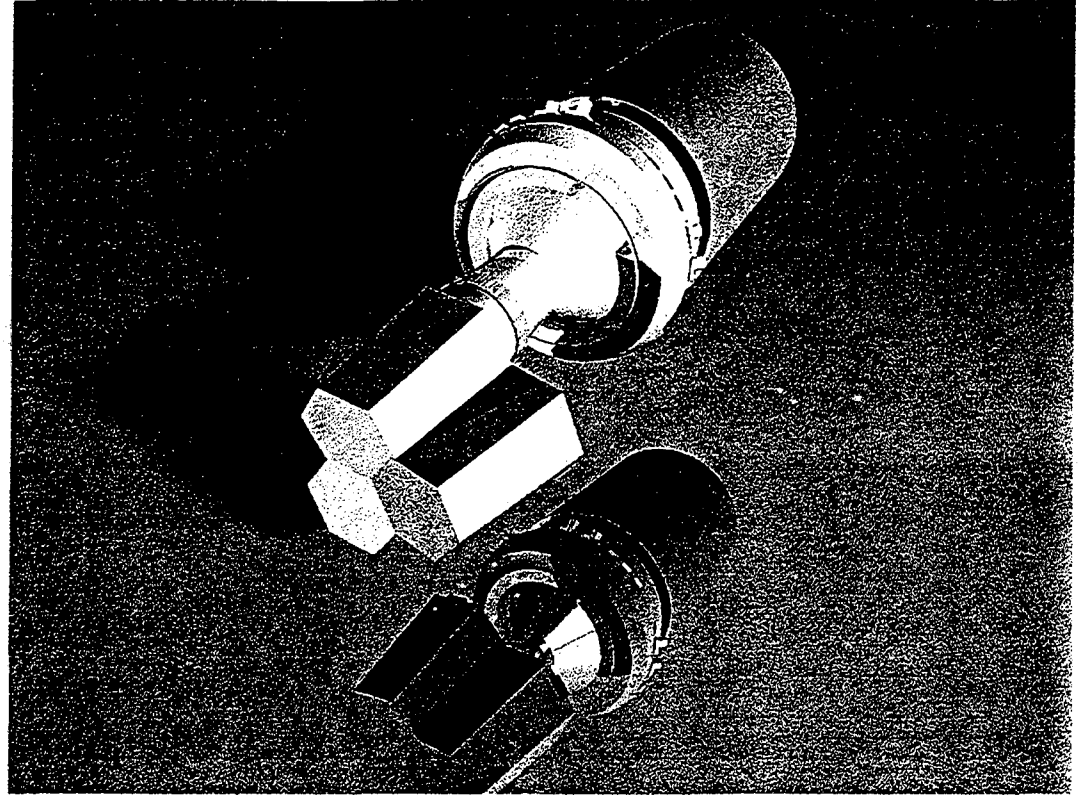

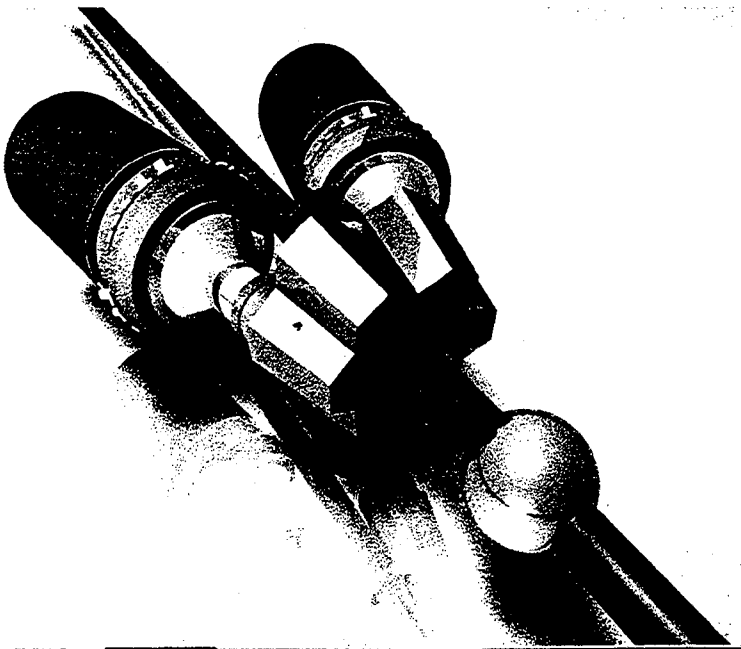

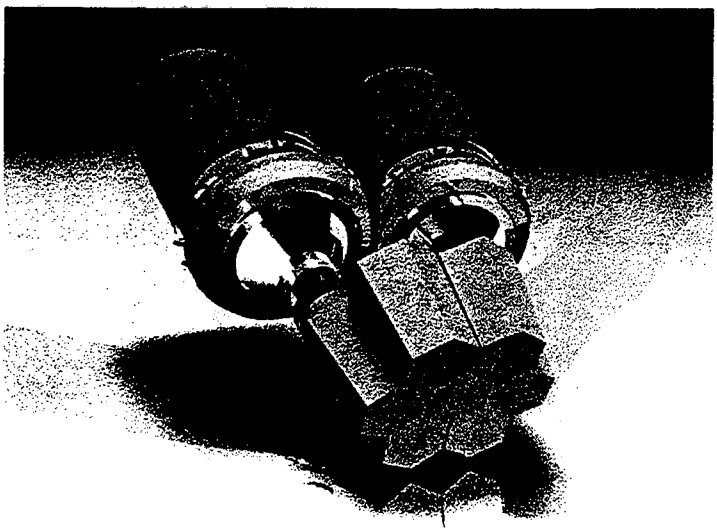

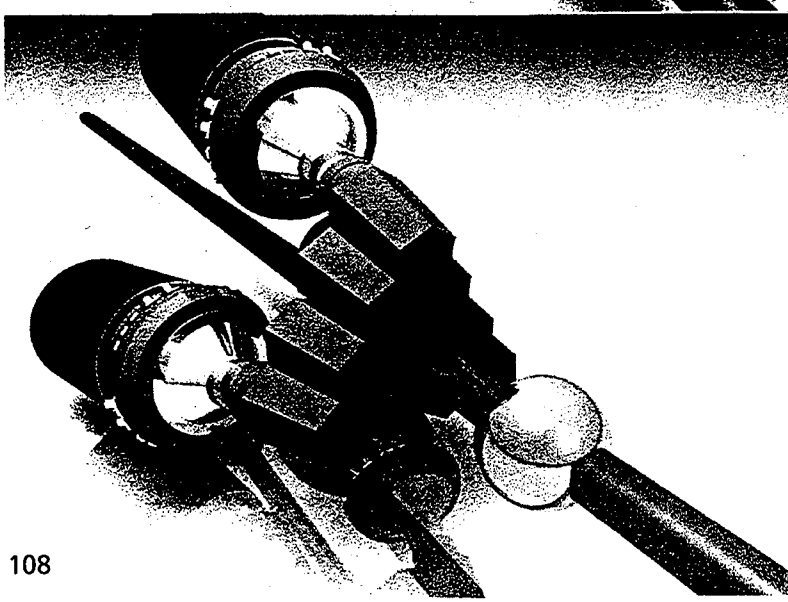

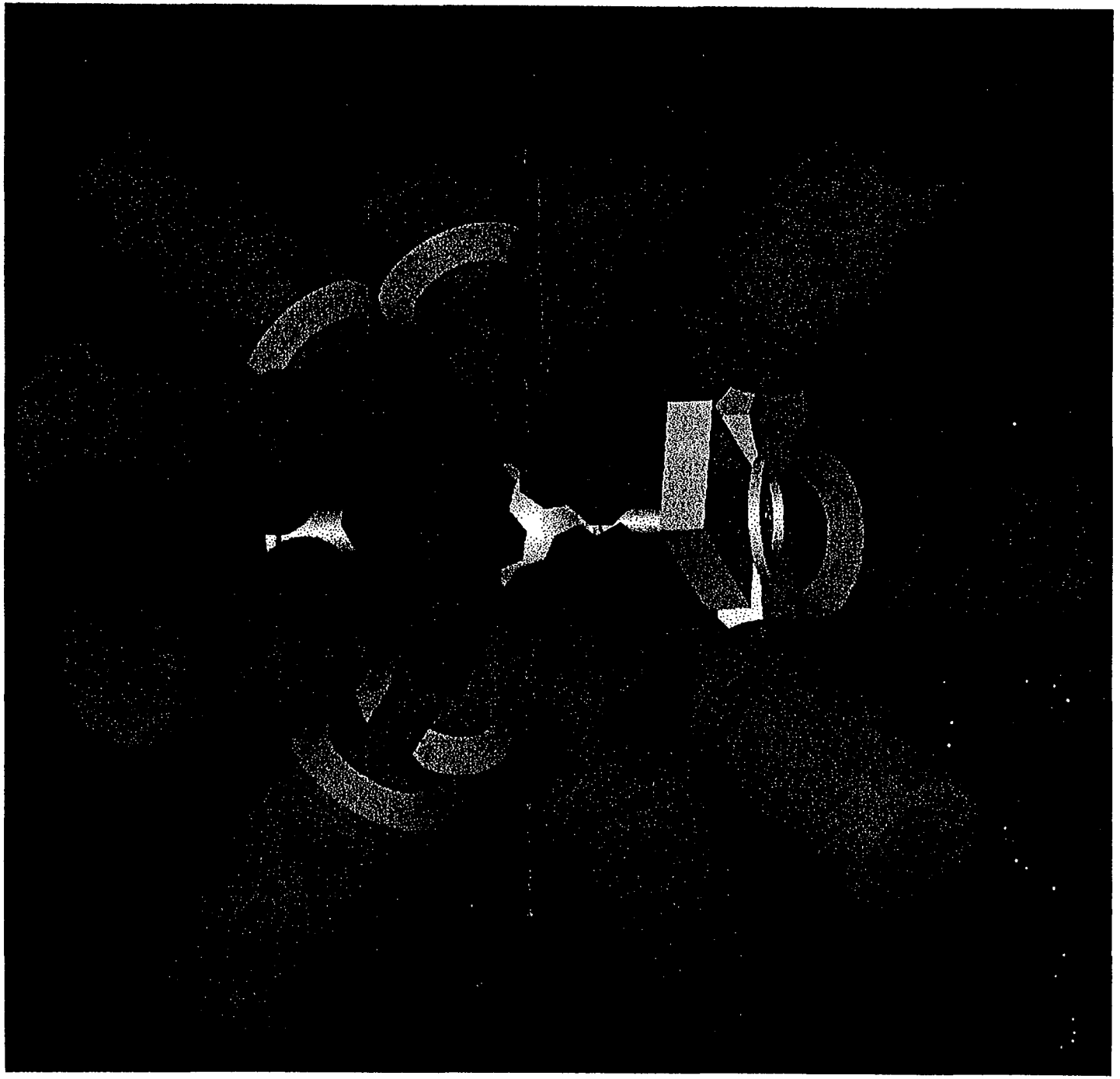

MINIBALL
CLUSTER
CUBE

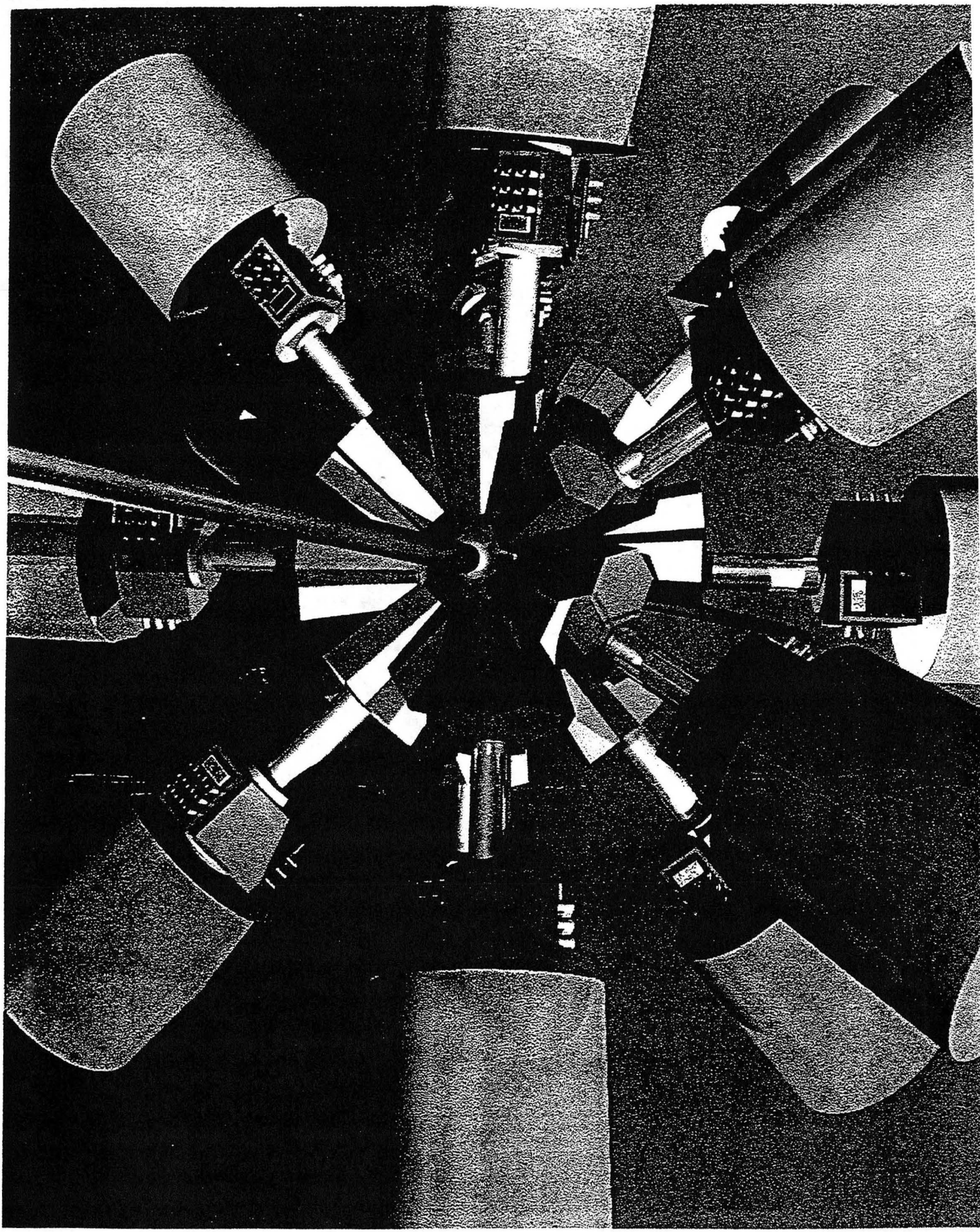

Miniball with 3 segmented detectors in one Cryosh

## Summary

The CLUSTER
an example for
a flexible

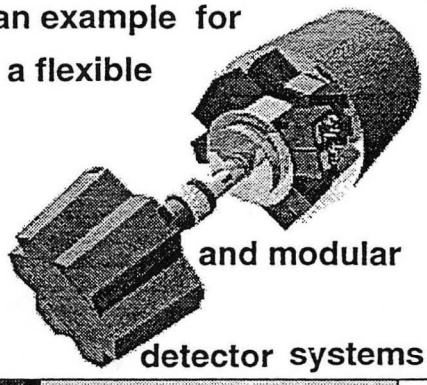

and modular
detector systems

## Outlook

### Encapsulation

new technology
high reliability

EUROBALL

composite
detectors

Segmentation

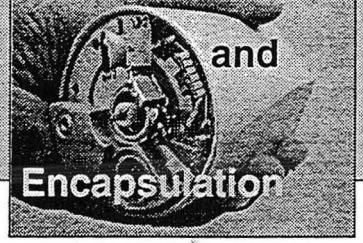

and
Encapsulation

MINIBALL

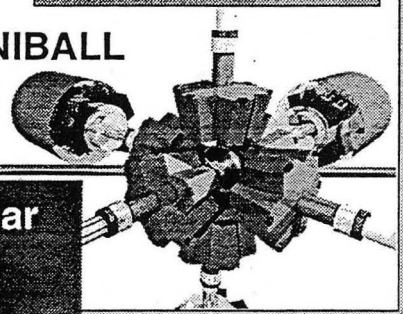

Miniball

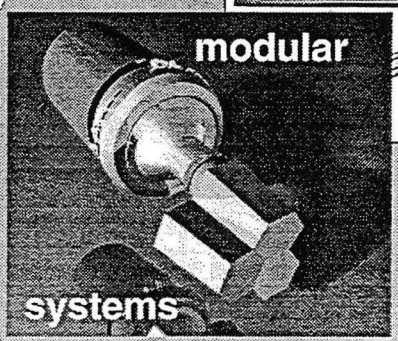

modular
systems

highly segmented Ge detector systems for γ– ray tracking:

high absorption efficiency with less Germanium

Upgrade of EUROBALL

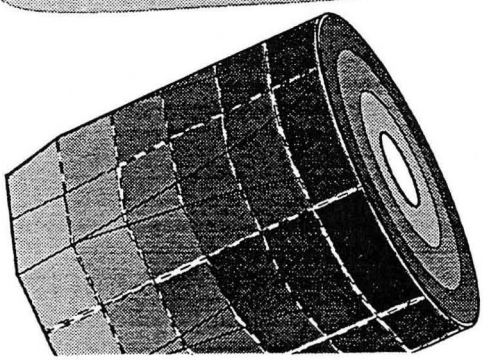

Problems:
amount of
electronics

D.Bazzacco

Status of the MARS project.

Mini
ARray of
Segmented detectors

# The MARS project

Padova - Milano - Legnaro

- Geant Simulations A. GADEA, Z. Podolyak
- Study of Pulse Shapes Th. Kroell
- Electronics and prototype Ge
- Perspectives

D. R. Napoli

G. Ripamonti, M. Bellato

Dino Bazzacco, GRETA workshop, LBL Feb. 5-7,1998

# Ball with 110 hexagonal tapered detectors

same shape for all 110 Detectors ⇒ larger gaps = lower efficiency

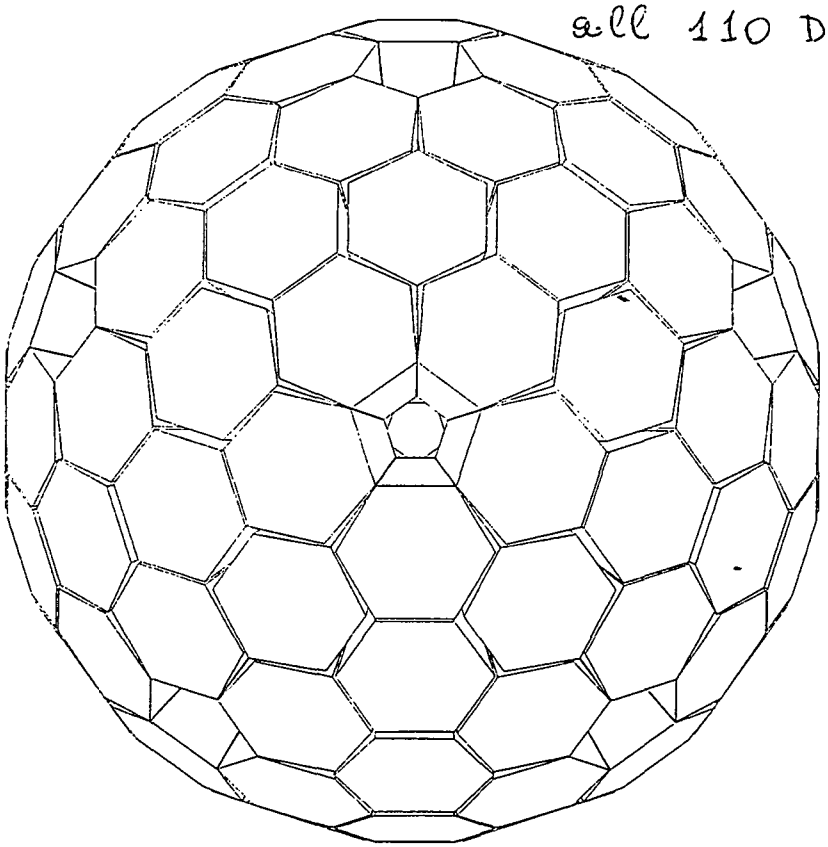

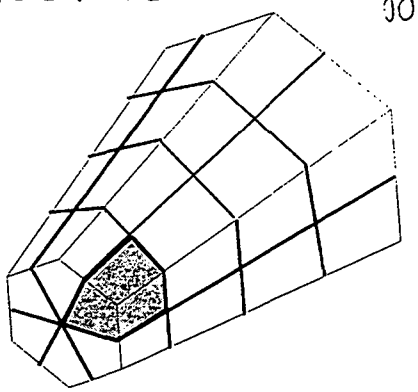

L=9.7 cm

D=7 cm d=3.5 cm

2.5 kg ---> 1.15 kg less than 50 of origin Ge volume after tape

24 segments

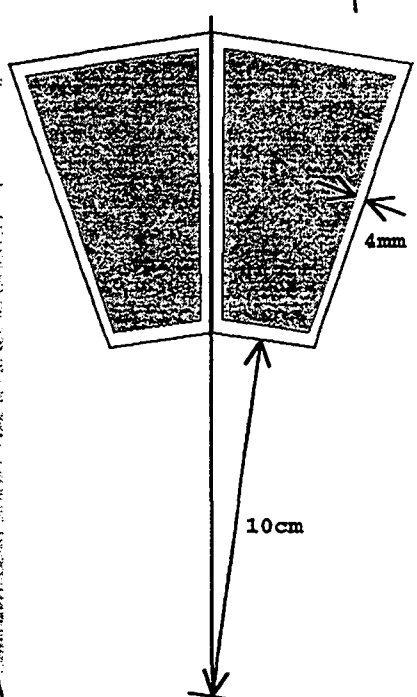


$R_i$ = 10.4 cm

$R_e$ = 20.0 cm

$\Omega$ = 71.3 % (75.8)

$\varepsilon$ = 27.5 % (30.2)

PT = 45.1 % (46.6)

$\Delta E$ = 2.18 (2.6) keV

$E_\gamma$ = 1.33 MeV $M_\gamma$ = 1 v/c = 3%

Summing all detectors

2.18 resolution using center of first hit segment for Doppler

Andres Gadea & Zolt Podolyak

# Some Geodesic Solutions

## (using simple clusters of hexagonal tapered crystals)

number of hexagonal crystals of the ball (+ pentagonal crystals)

$N_I = 20\,n\ (+12)$ Icosahedron 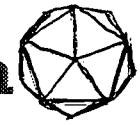

$N_O = 8\,n\ (+\,6)$ Octahedron 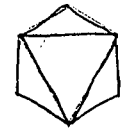

$n = (i^2 + 3j^2 - 4)/8$

$\boxed{i + j = \text{even}}$

number of hexagons of the basic regular triangle

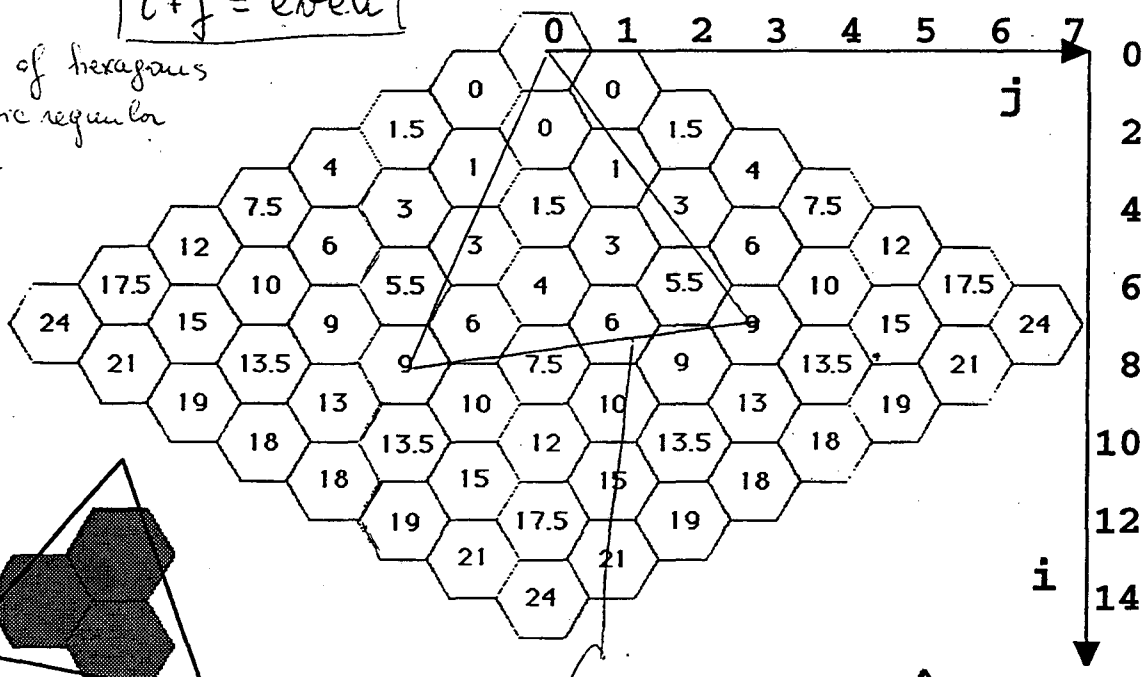


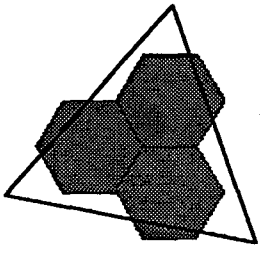

3(60-24)

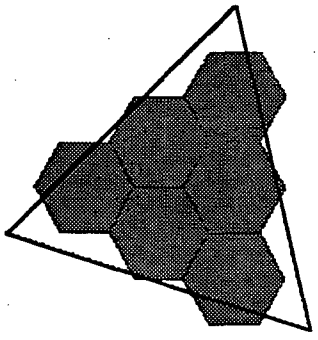

6(120-48)

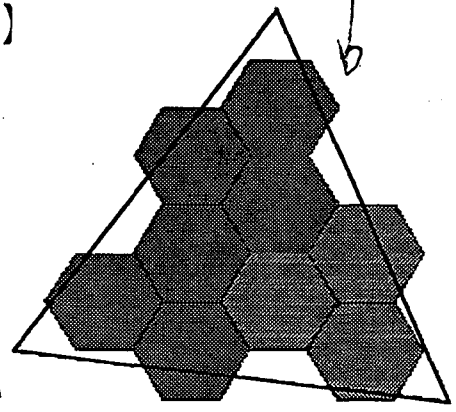

9(180-72)

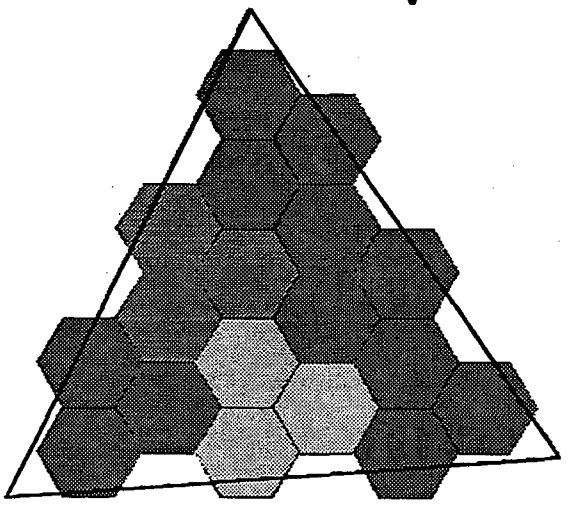

18(360-144)

# MARS-36

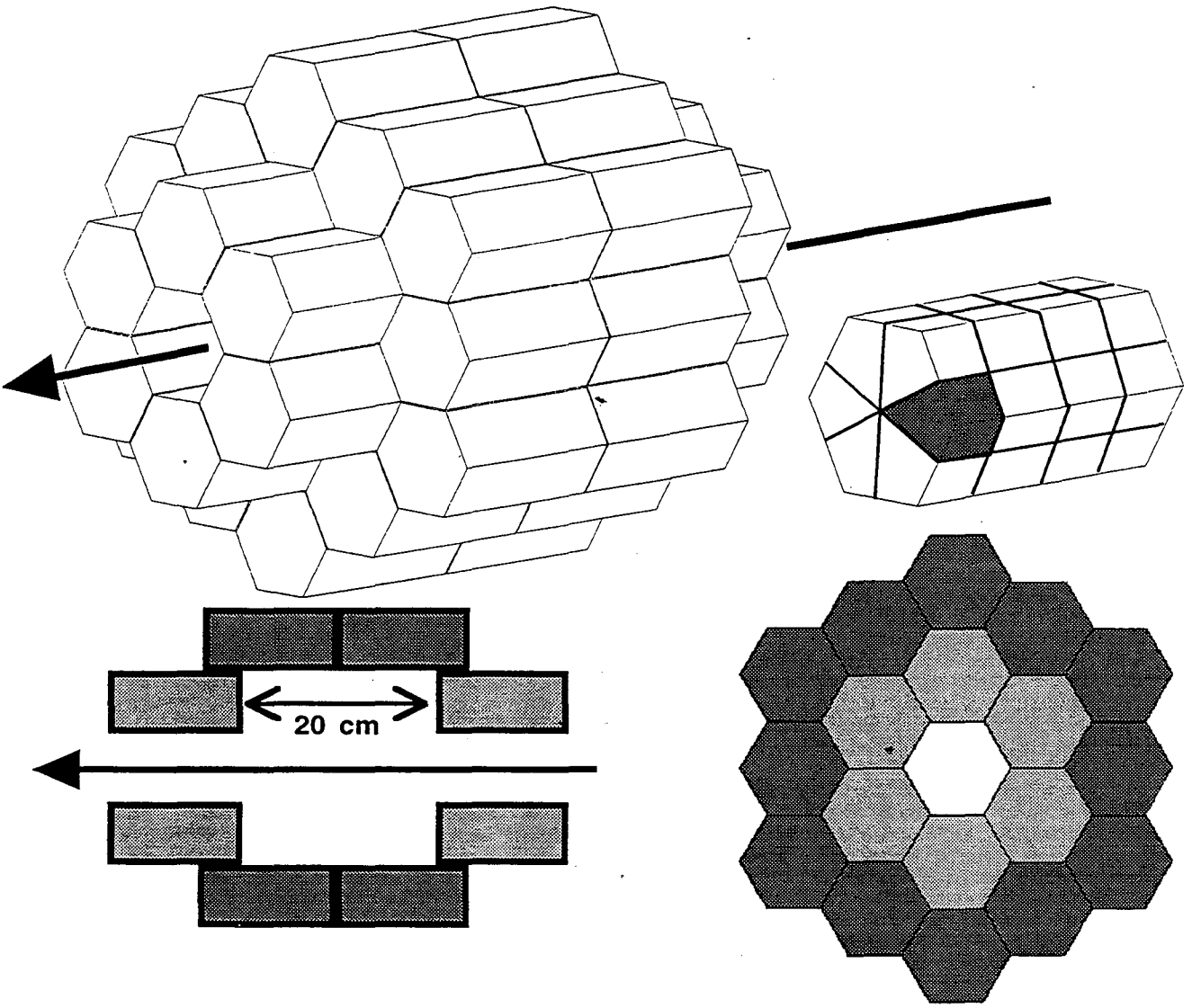


$R_i \sim$ 8-12 cm

$\Omega$ = 87.4 %

$\varepsilon$ = 29.5 %

PT= 45.8 %

$\Delta E$= 4.84(5.17)keV

$E_\gamma$=1.33 MeV $M_\gamma$=1 v/c=3%

Summing all detectors

4.84 using first hit
5.17 using max energy

L=12 cm

D=7 cm d=3.5 cm

3.1 kg ---> 2.5 kg 82% useful Ge mass

24 segments

# MARS-36
## Performance as a function of theta

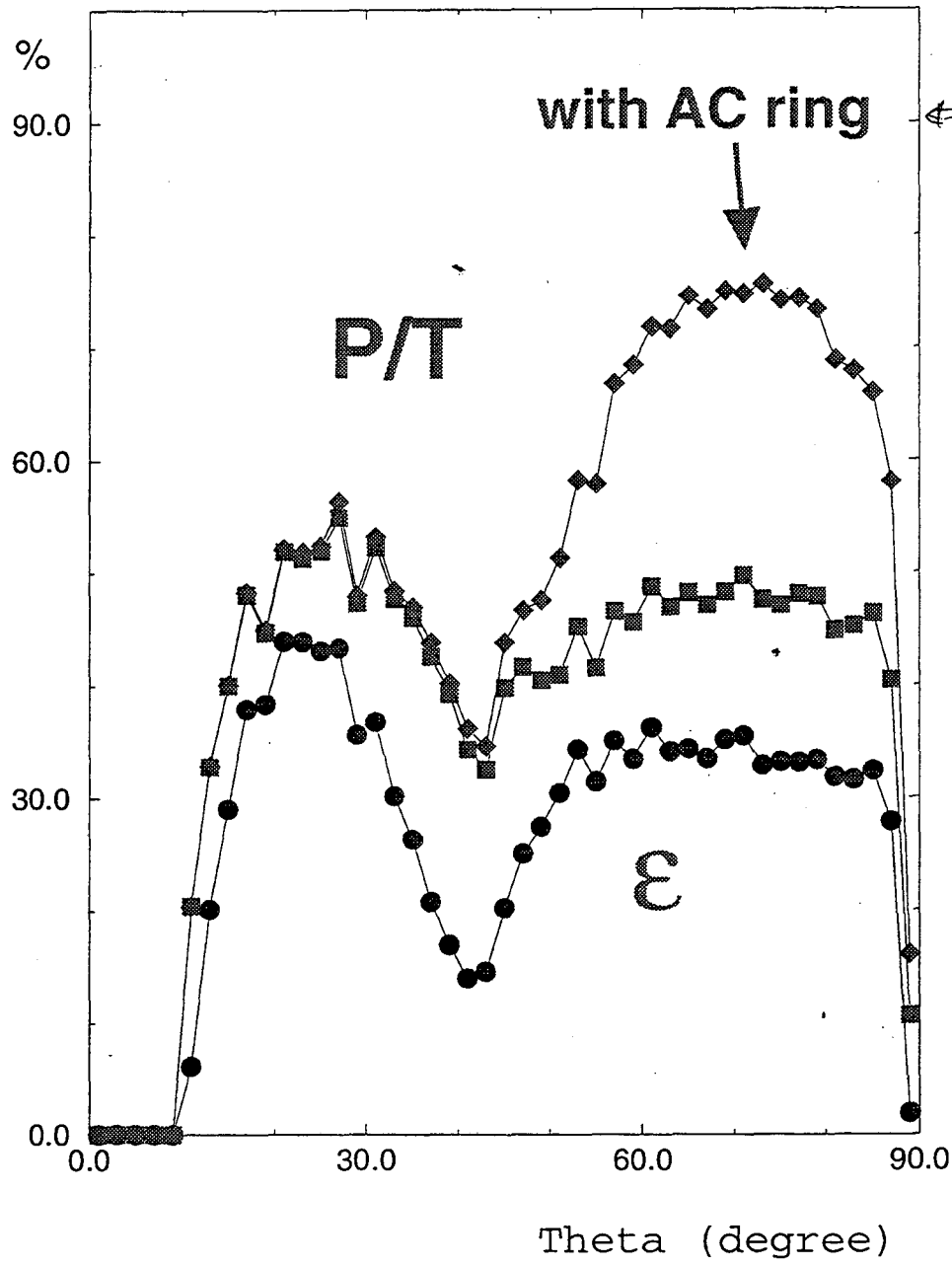


← 1 ring of 18 + 18 BGO detectors around the 12 + 12 central detectors

# MARS-54

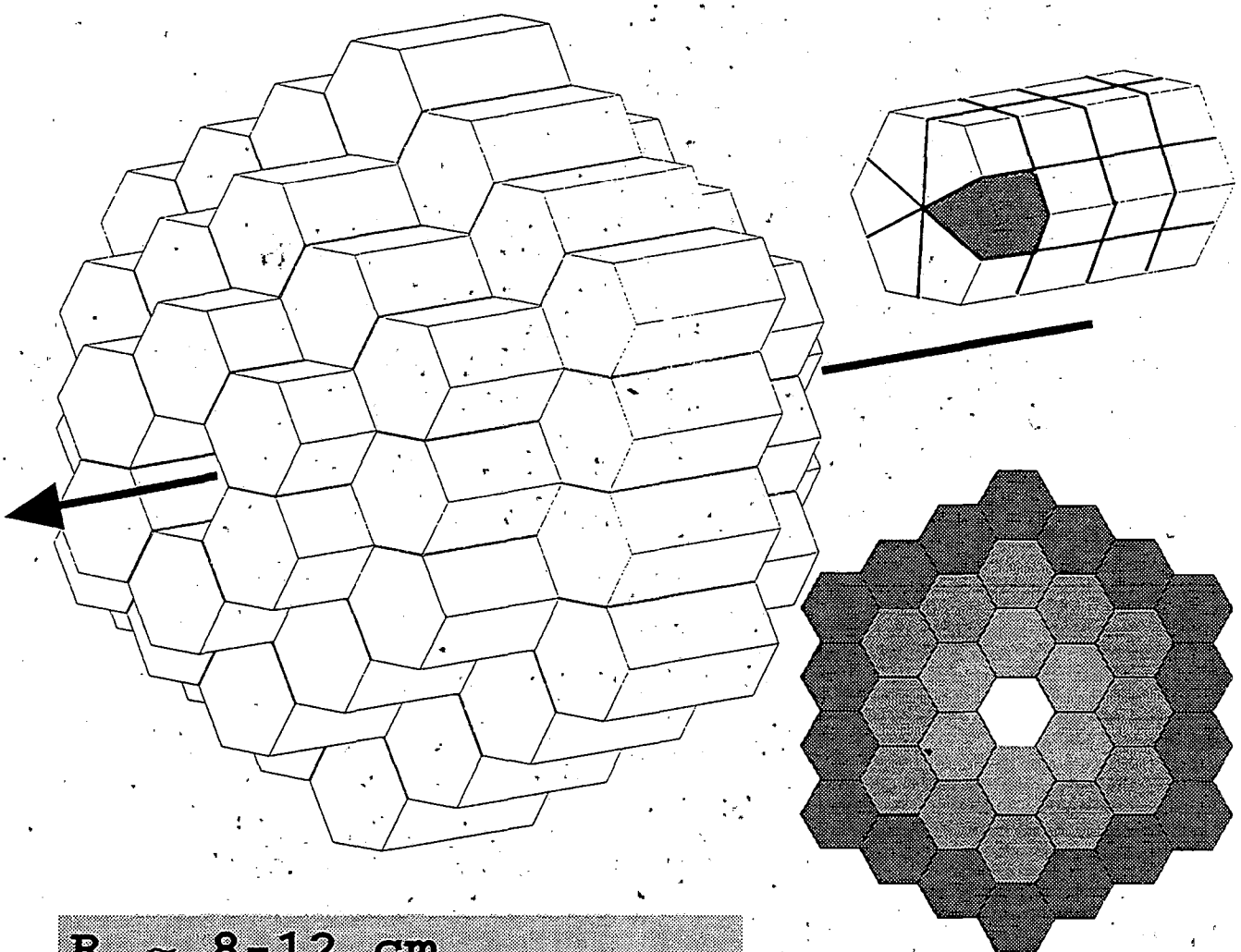

$R_i \sim 8\text{-}12$ cm

$\Omega = 92.9$ %

$\varepsilon = 36.3$ %

PT= 49.8 %

$\Delta E = 4.19(4.41)$keV

$E_\gamma$=1.33 MeV $M_\gamma$=1 v/c=3%

Summing all detectors

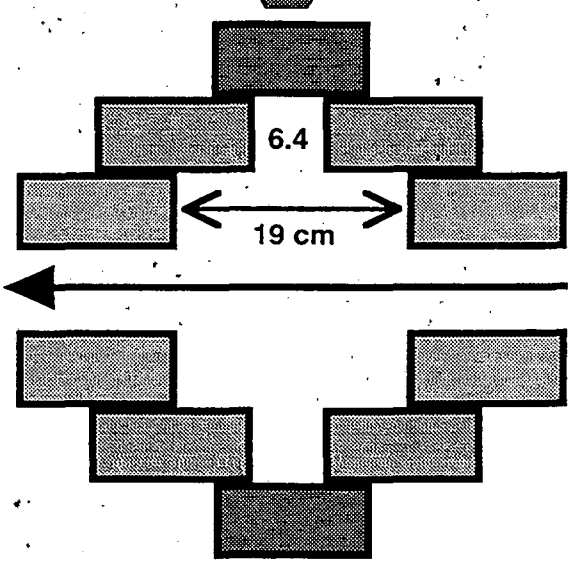

# MARS-54

## Performance as a function of theta

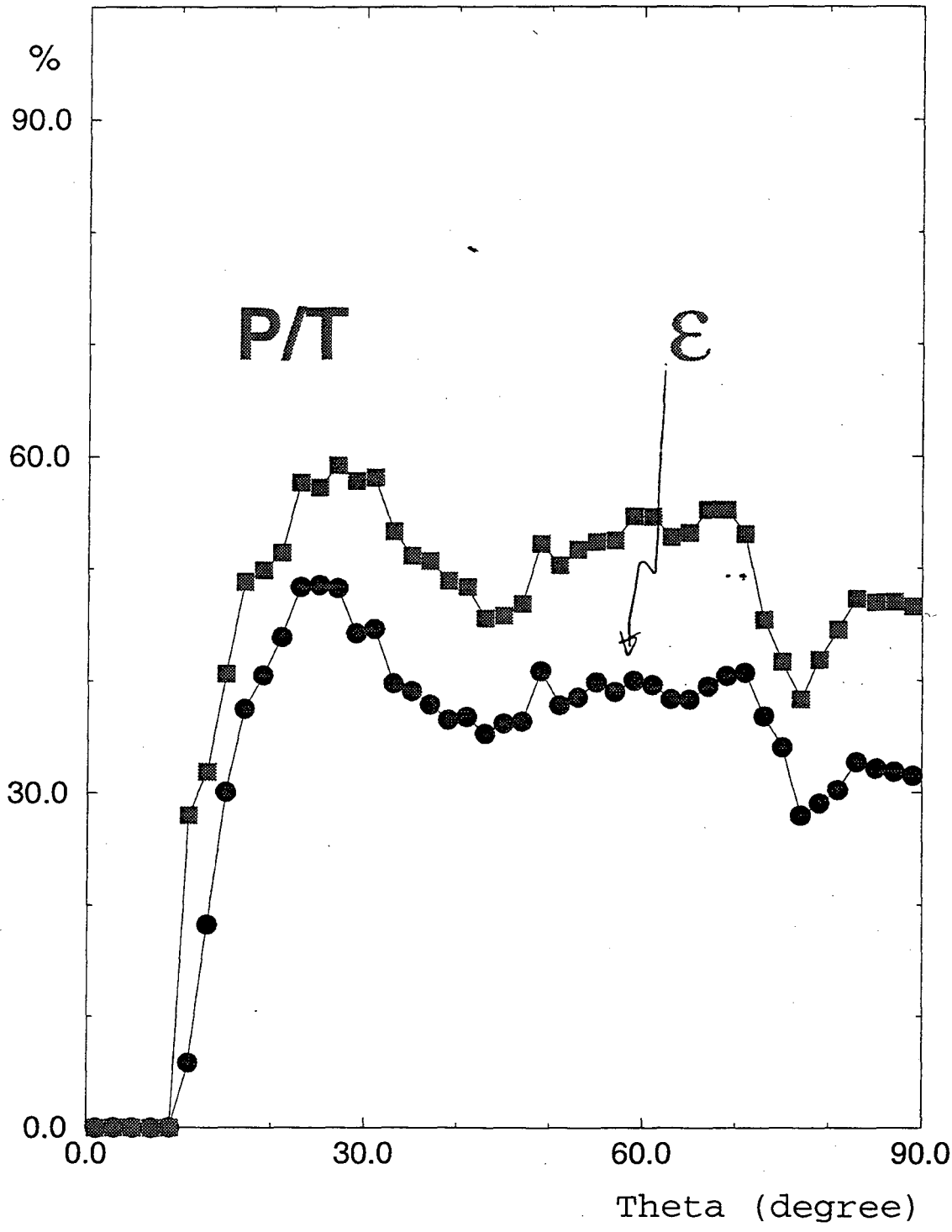

# MARS-36 world map

25 γ's shot into the array $E_\gamma = 1.333$ MeV
17 γ's detected
13 γ's fully absorbed (a particularly good event) 52%

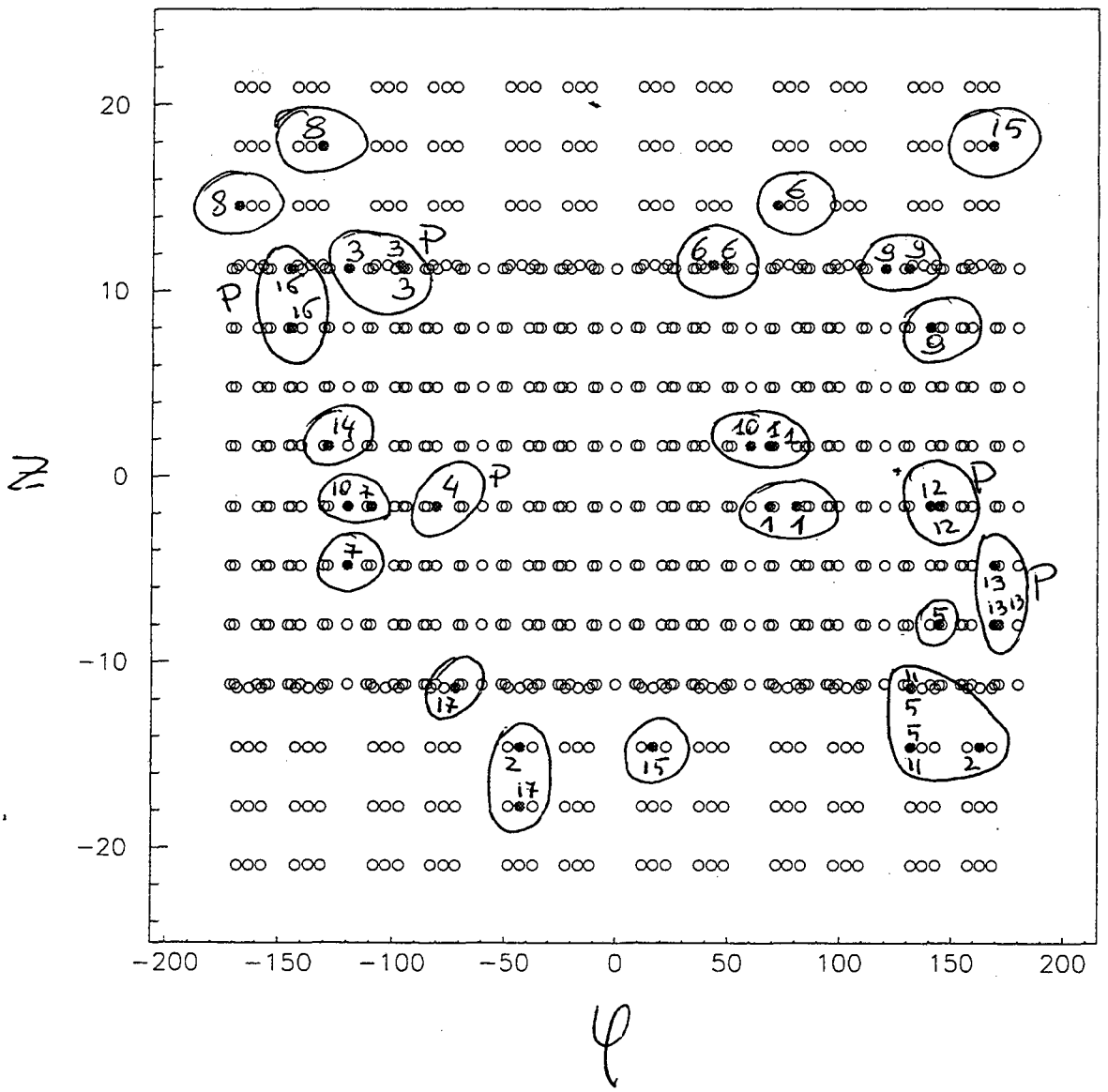


Clusterisation algorithm optimized for max efficiency
22 clusters found
(5 in peak) $\Longrightarrow \begin{cases} \varepsilon_{PH} = 20\% \\ P/T = 23\% \end{cases}$

# Response for High Gamma Ray Multiplicity

**Obtained with a clusterization algorithm optimized, for each fold, to produce "best" value for Efficiency and P/T**

| Conf. | 110 | | 36 | | 54 | |
|---|---|---|---|---|---|---|
| Mult. full | ε 27.5 | P/T 45.1 | ε 28.5 | P/T 45.8 | ε 36.3 | P/T 49.8 |
| 1 | 16.2 | 18.9 | 19.3 | 22.8 | 22.0 | 21.7 |
| 10 | 13.5 | 17.0 | 15.6 | 20.2 | 18.6 | 19.8 |
| 25 | 10.0 | 14.5 | 10.9 | 16.6 | 13.9 | 16.9 |

**Results are clearly insufficient mostly because of <u>long range scattering</u>.**

# Tracking needed

# Addback Effects with EB Clusters

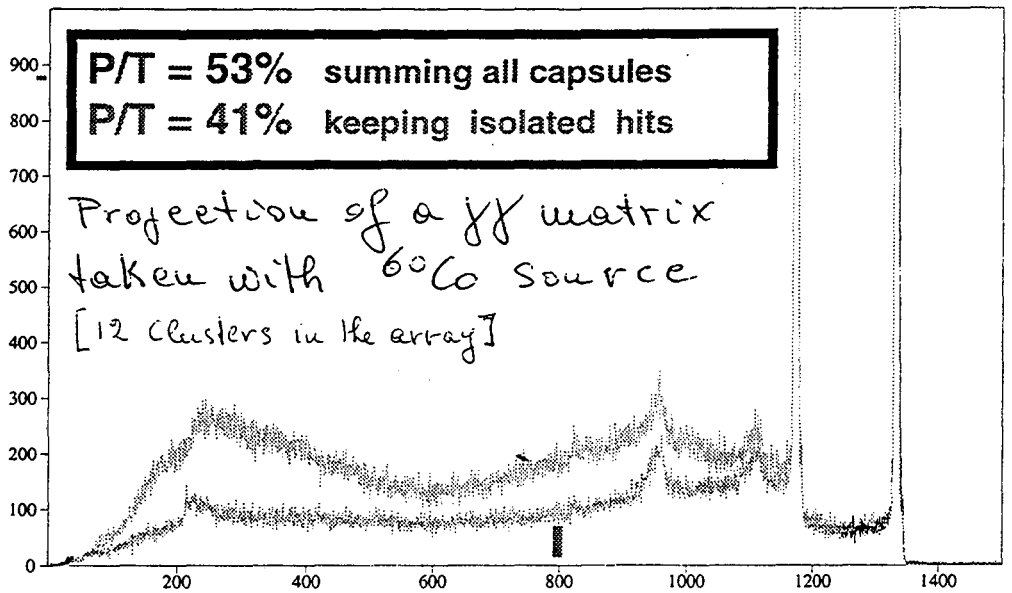


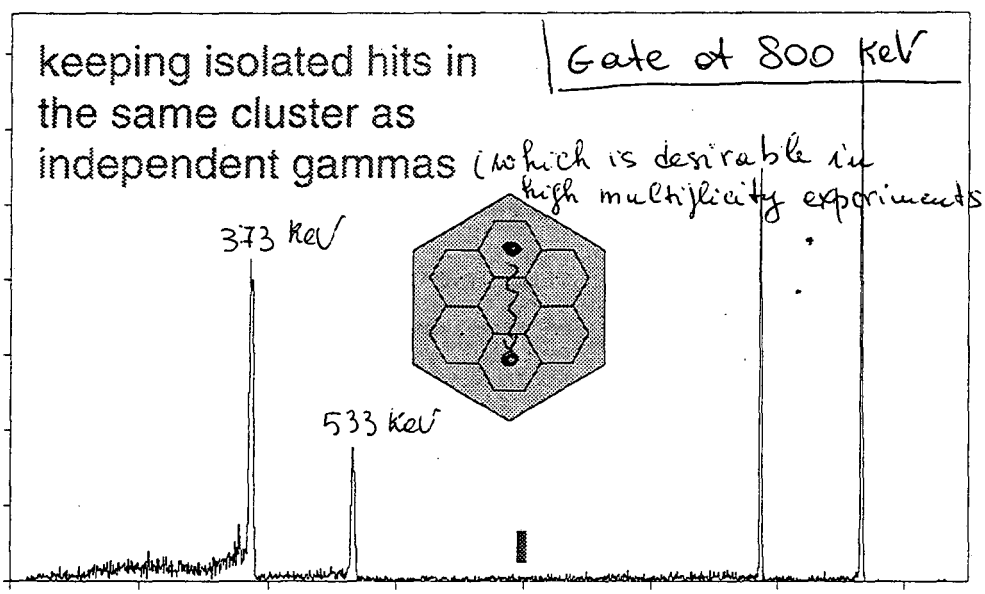


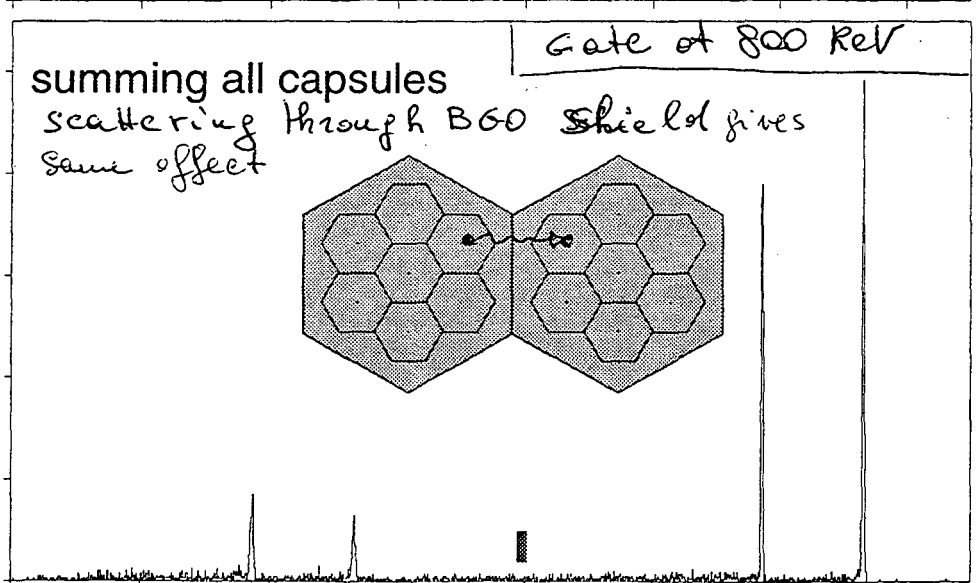


Same effect found also with Clovers and Tapered

# Hyperdeformation from $^{60}$Co source!?

## (summing all capsules in the Cluster)

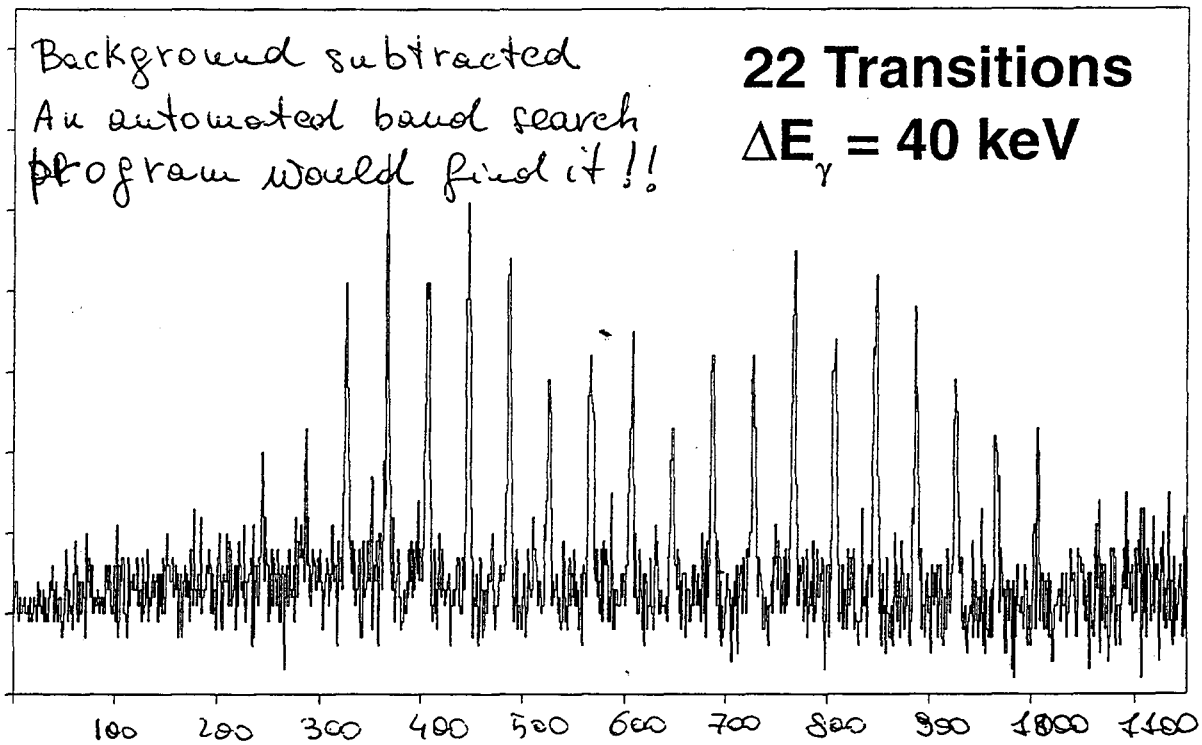


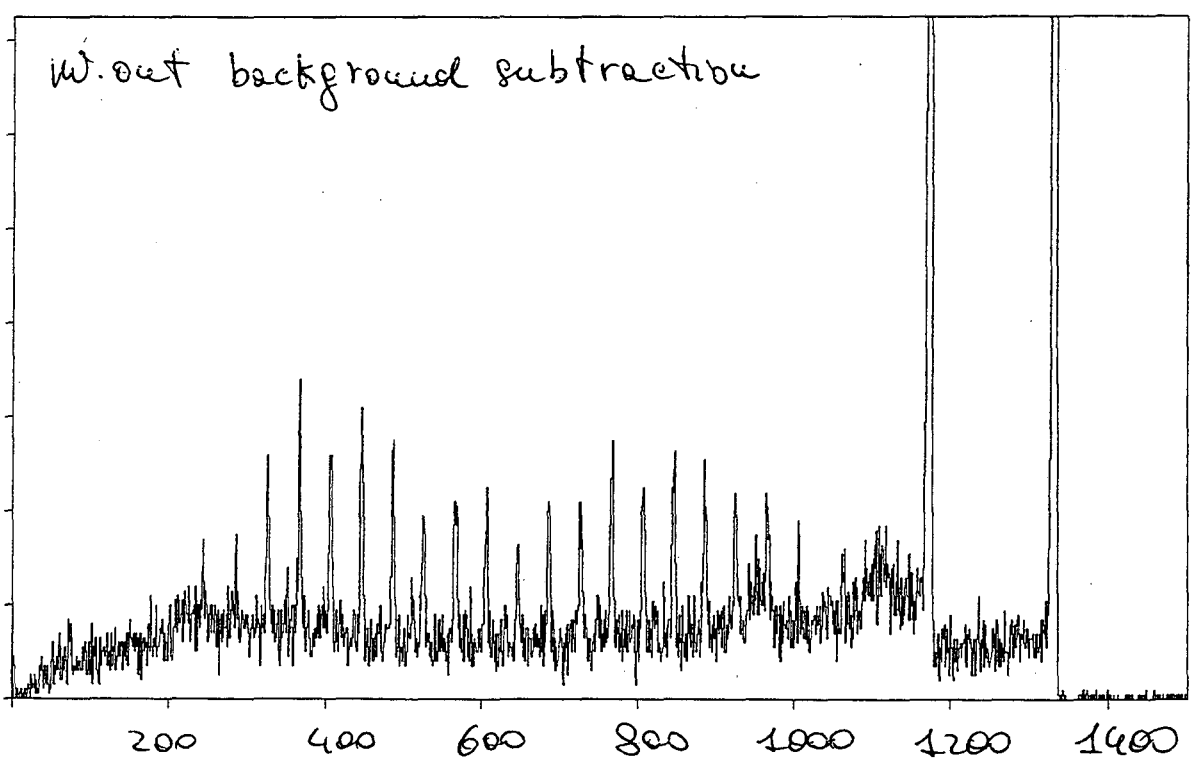

Thorsten Kröll

# Electric potential inside a closed-end coaxial germanium detector

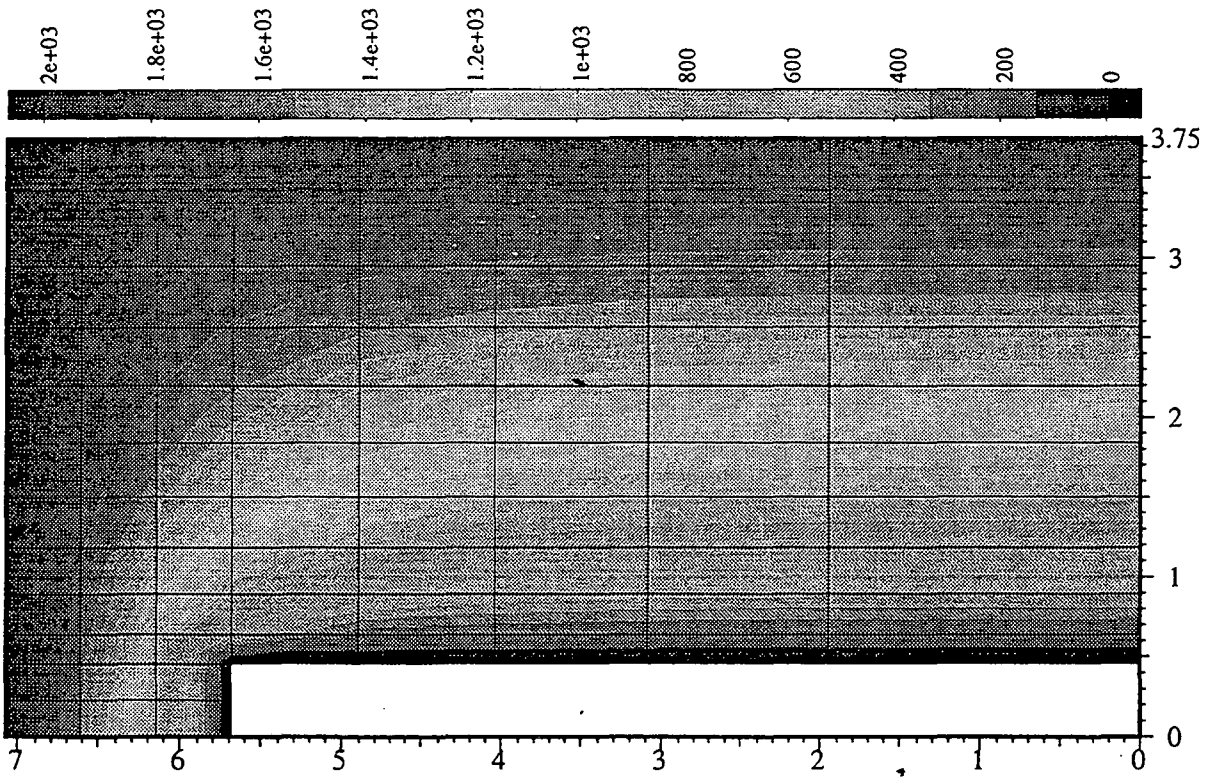


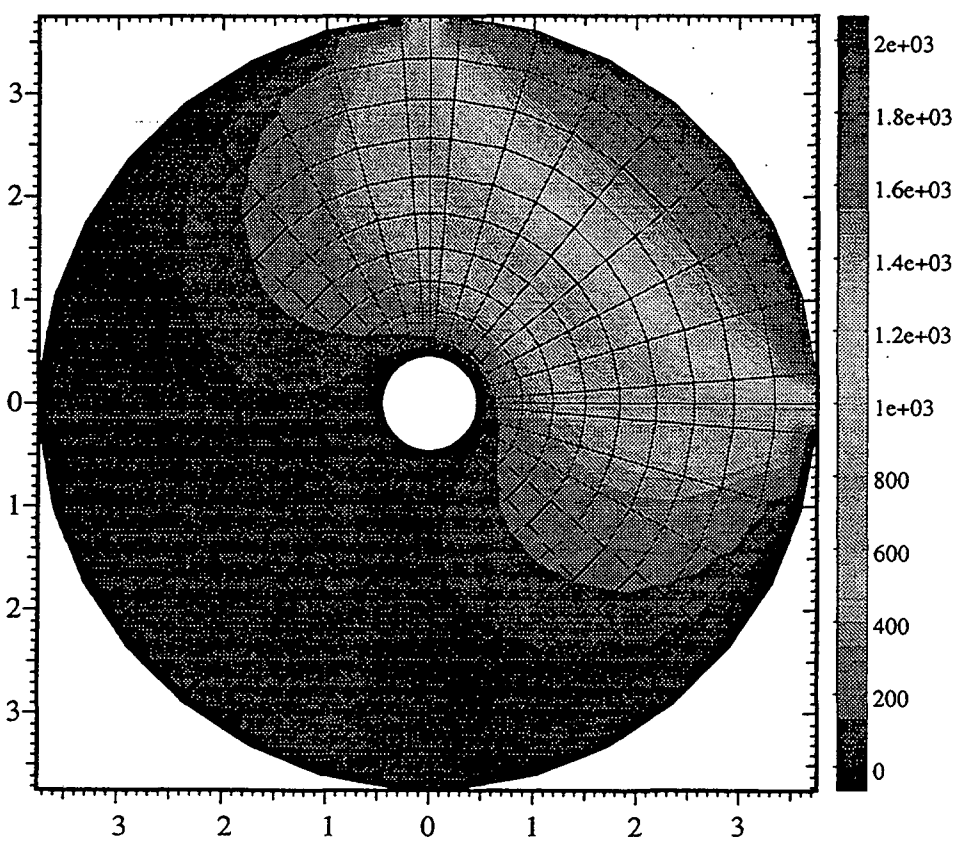


Weighting Field

induced current

# Pulse Shapes from a multiple interaction event

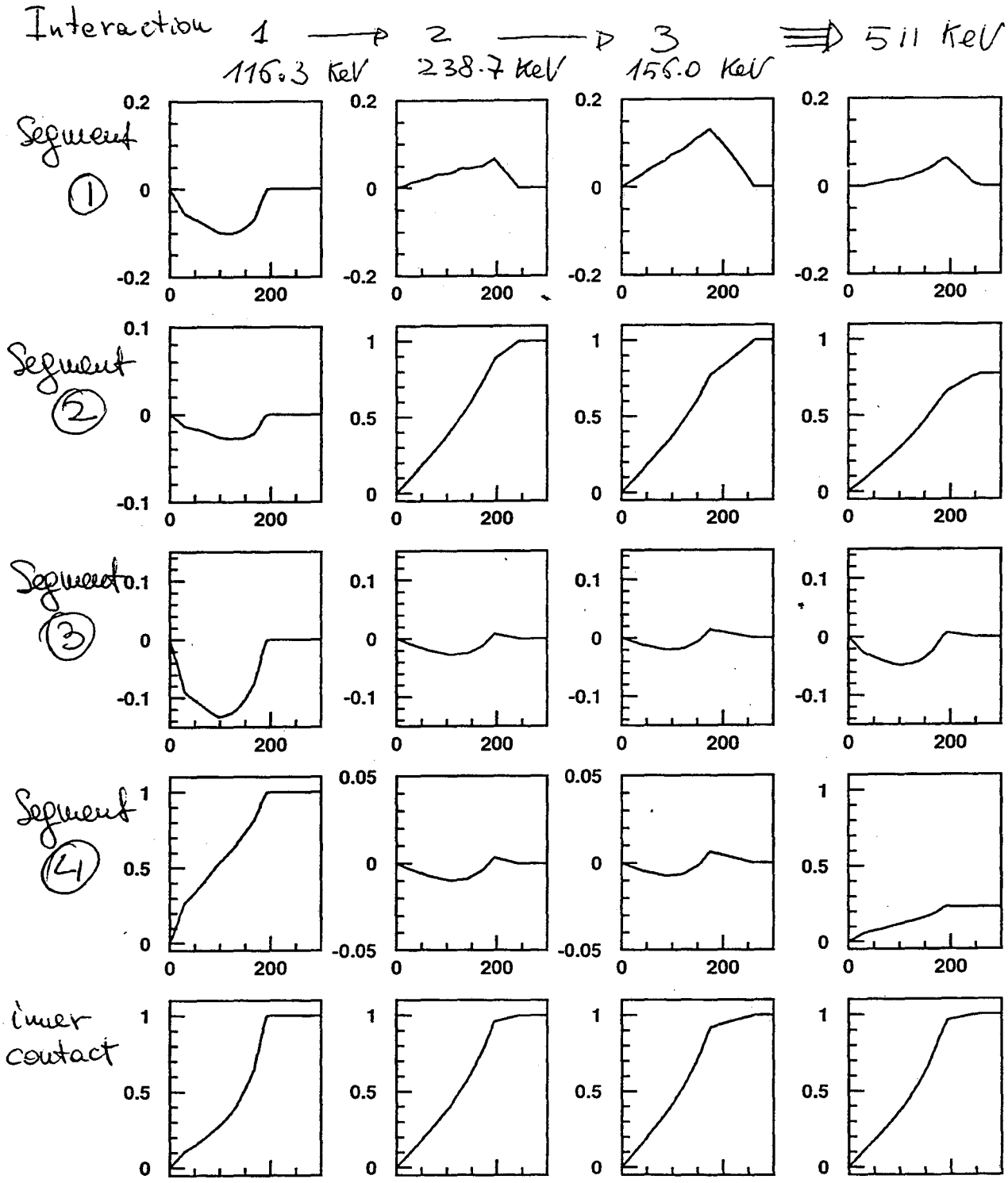


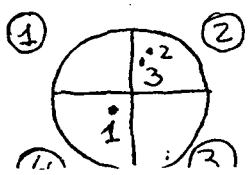


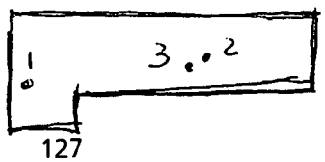

# Tracking with ANN

1) Artificial Neural Network (perceptron) trained to give the first point of interaction. Detector is not segmented and only a limited information from the pulse shape is us

Results for Radius r

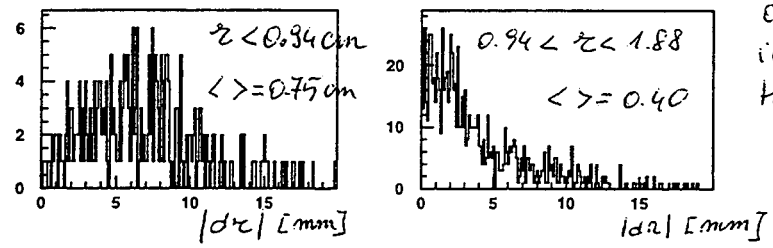


Global average deviation 0.41 cm

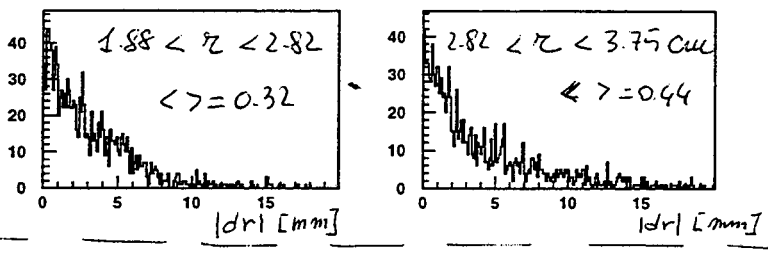


Results for Depth z

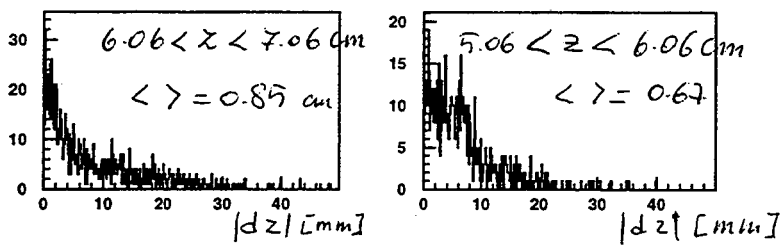


Global average deviation 0.9 cm

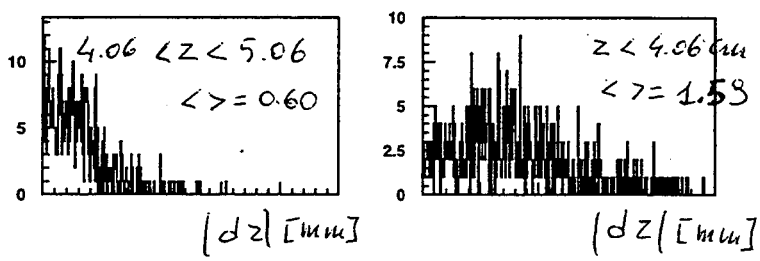


← Bad performance in the coax. part

2) Two dimensional (r and z) tracking by ANN

ANN (result)

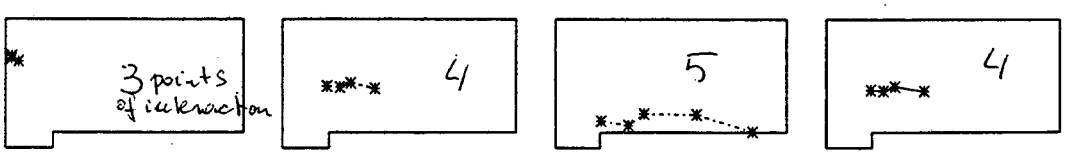


GEANT (input)

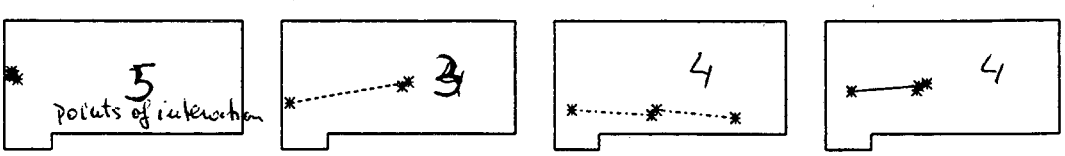

M. Bellato

# Inverse Fourier Transform

## Frequency cuts at 100, 40, 25, 10 MHz

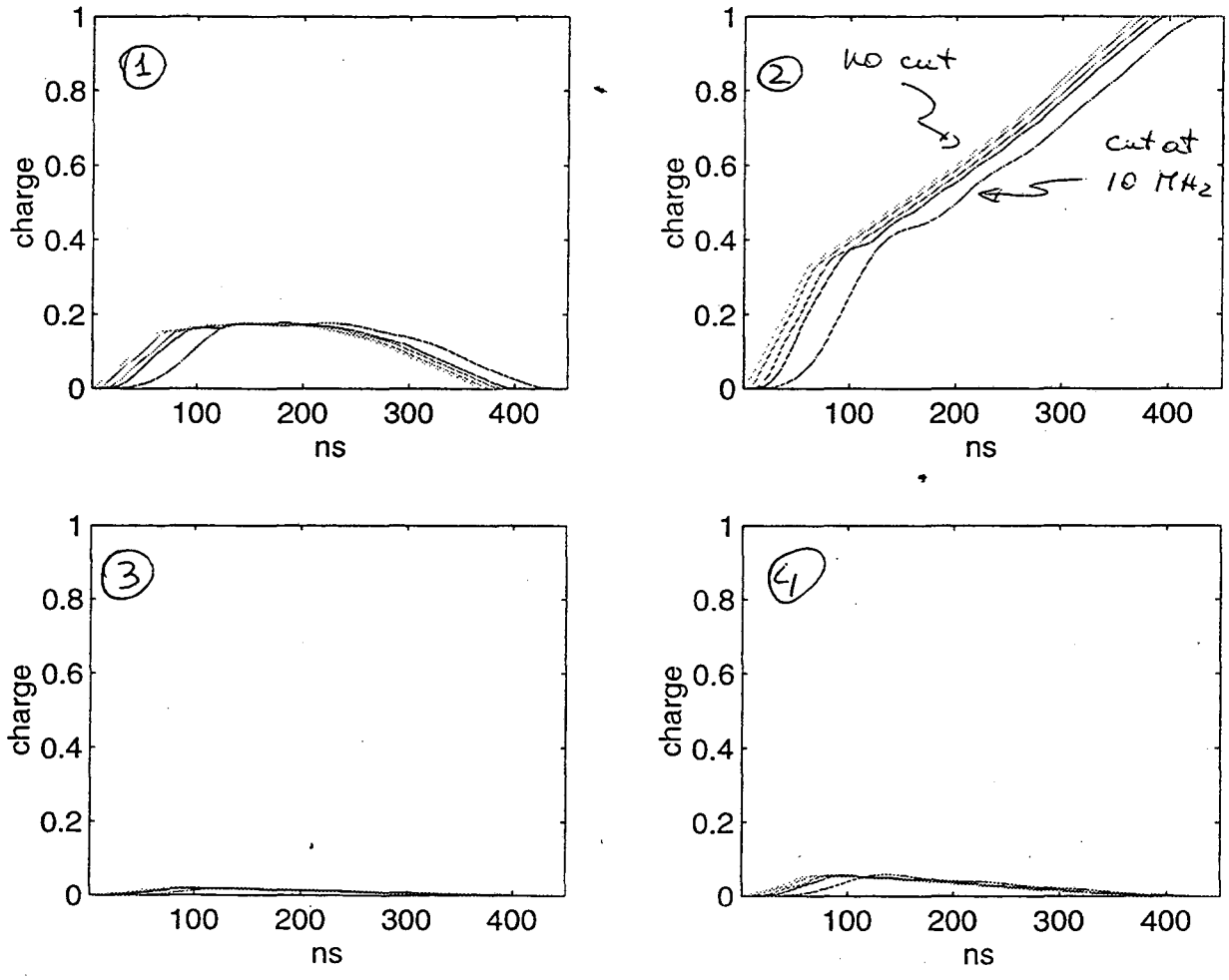


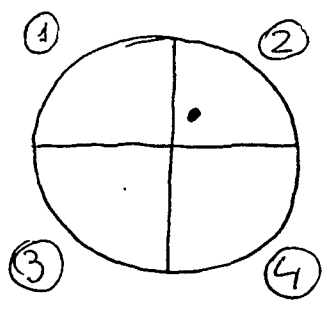


r = 1 cm
φ = 63°
coax region

# Two Interactions with equal energy

$r_1 = 1.5$ cm $\quad$ $r_2 = 2.17$ cm

$\varphi_1 = 53^0$ $\quad$ $\varphi_2 = 61^0$

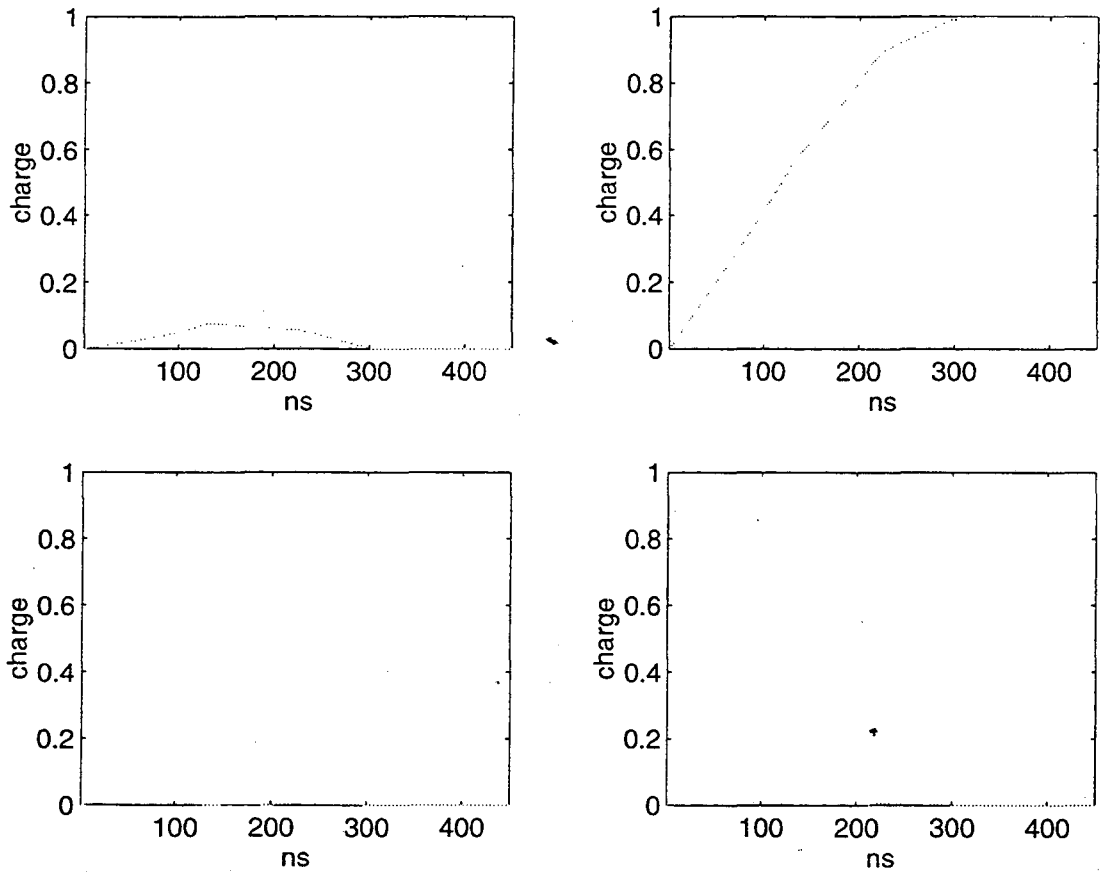


Deconvolution of signals into a base of calculated shapes

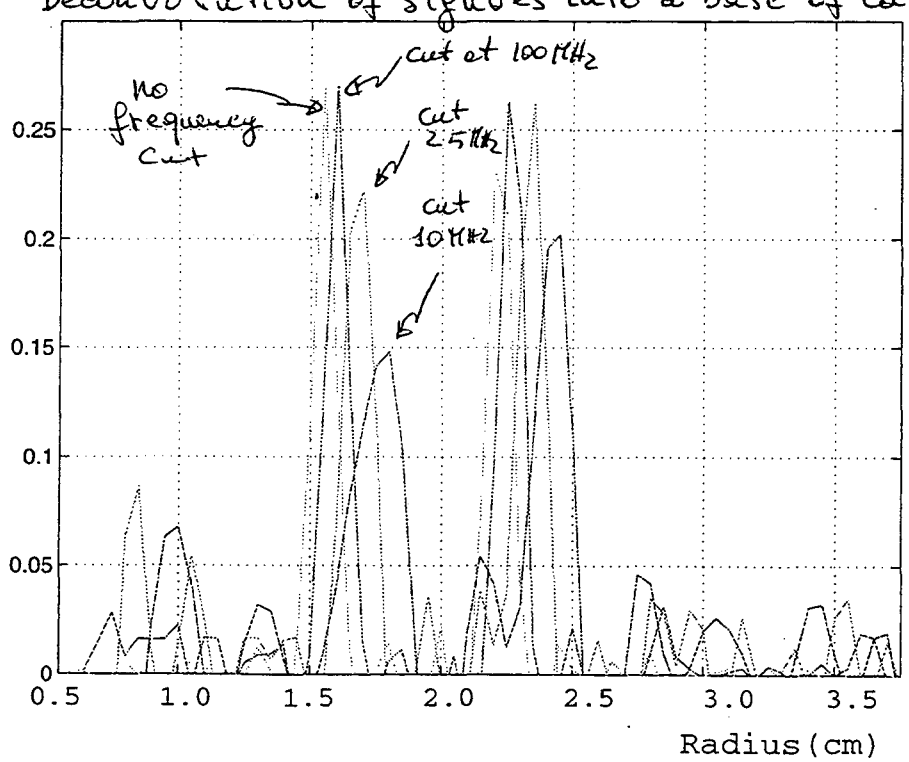


"Area" of compone
gives energy
partition

Main Component
give radial posit

G. Ripamonti

# Low Cost High Resolution Digital Pulse Processor

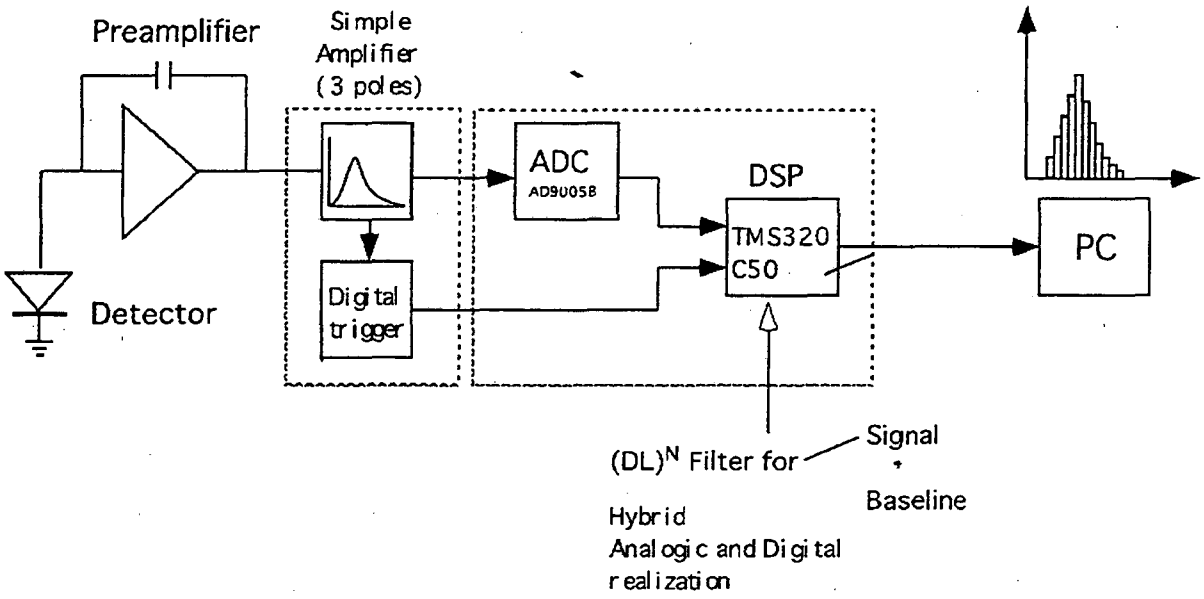


**For Pulse Shape a high sampling frequency FADC (10 bits, 100 Ms/s) is being considered**

# The Prototype Ge Detector

Efficiency > 75%

Closed end geometry

24 segments (6 in $\varphi$)x(4 in depth)

25 cold FET's for optimum energy resolution

Separate vacuum chamber for FET's

Fast, low power, small size, preamplifier

Mechanically compatible with GASP Ge's

Order placed to Eurisys

Delivery before summer

# Future perspectives

- Geant simulations
  - Other geometries and packing schemes
  - Tracking
- Tests of prototype detector
- Experimental study of pulse shapes
- Prototypes of electronics
- Data Acquisition System
- Write a proposal in 1998-1999
- Funding? ask for in 1999
- If project will be funded, construction could begin in year 2000 or 2001.
- Major man power problems to solve.

S.Frauendorf

Rotation beyond the standard scenario.

# Rotation beyond the standard scenario

standard: near axial
reflection symmetric
rotation about principal axis
well deformed
monopole pairing between like particles

shape

## GRETA'S Shopping list

- octupole deformations → low def
  → super def

  E1 in the signal
  Banana mode

- orientation degree of freedom
  loss of K quantum number

  cross talk between high K bands X

- triaxiality, moderate spin

  chiral rotations
  chiral vibrations X

- triaxiality, very high spin
  What can we see of the Jacobi instability?

- deliniate the regions of magnetic rotation N, Z, $E^*$
- transition suprafluid to normal X
- rotation of unpaired nuclei X
- pn - pairing X
- isospin symmetry and rotation X
- detailed spectroscopy of super def. (relative mergies and spins)

# Reorientation of the Spin

- erosion of K quantum number
- dynamics of the orientation degree of freedom

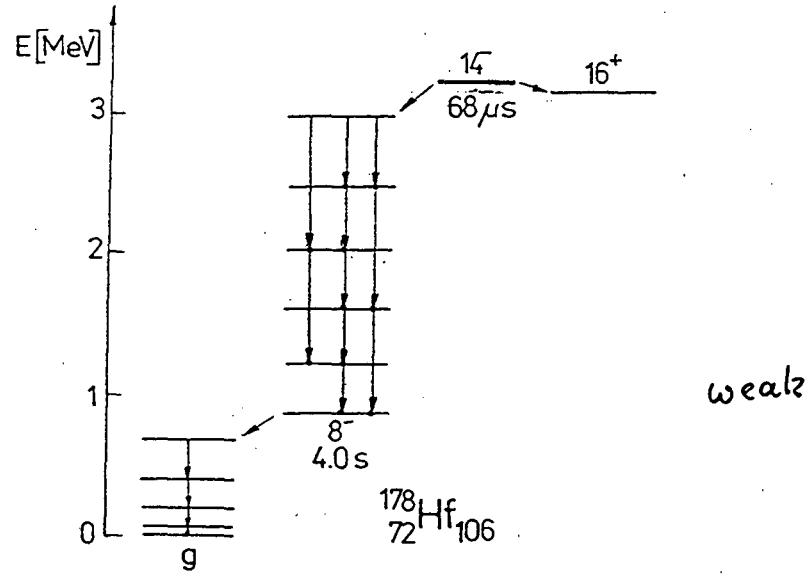


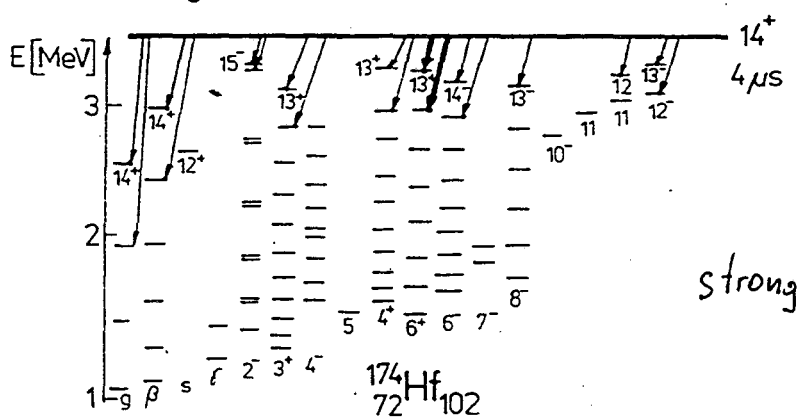


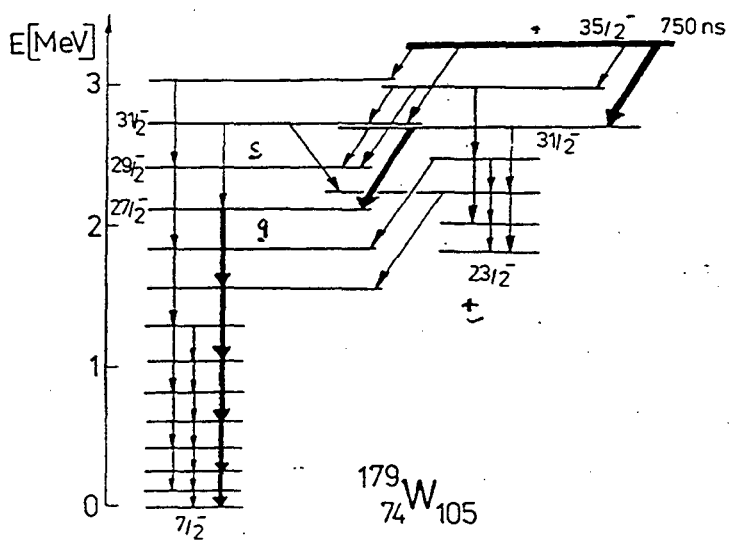


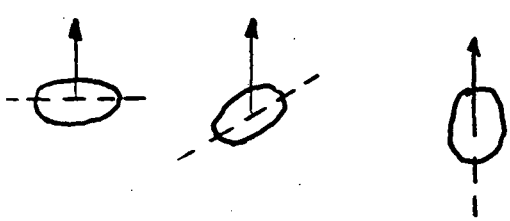

$^{178}_{74}W_{104}$

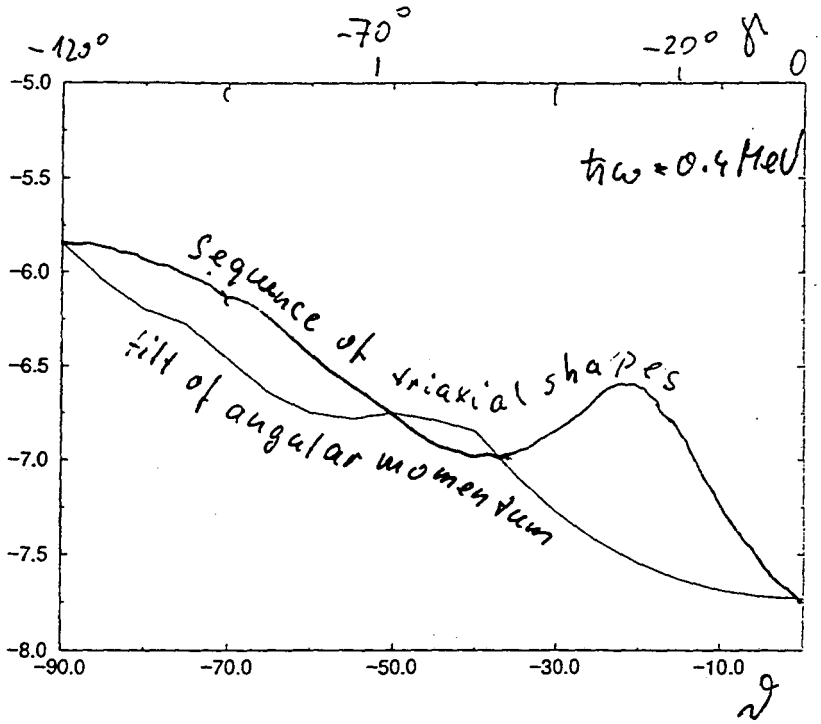


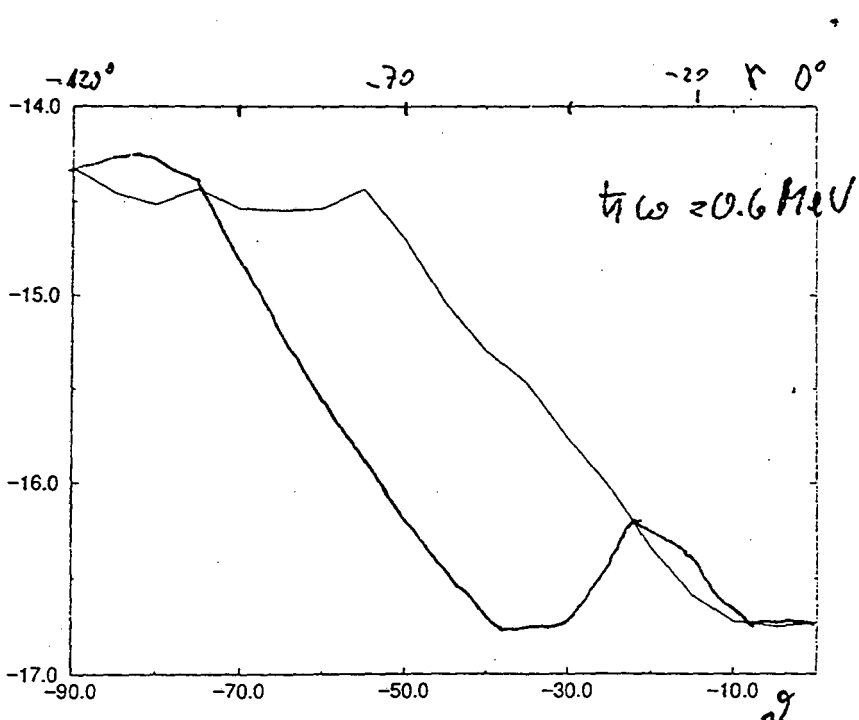


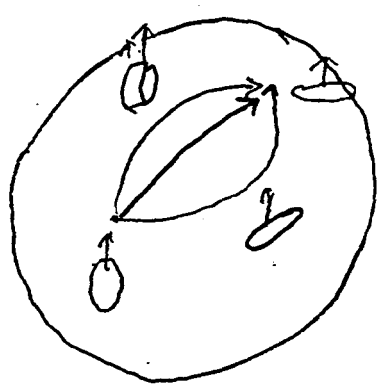

which is the dynamics?

$^{178}$W N=104 prots + neuts: $\pi$= 1 $\alpha$=0 I=30

step=0.5000 min = 5.193

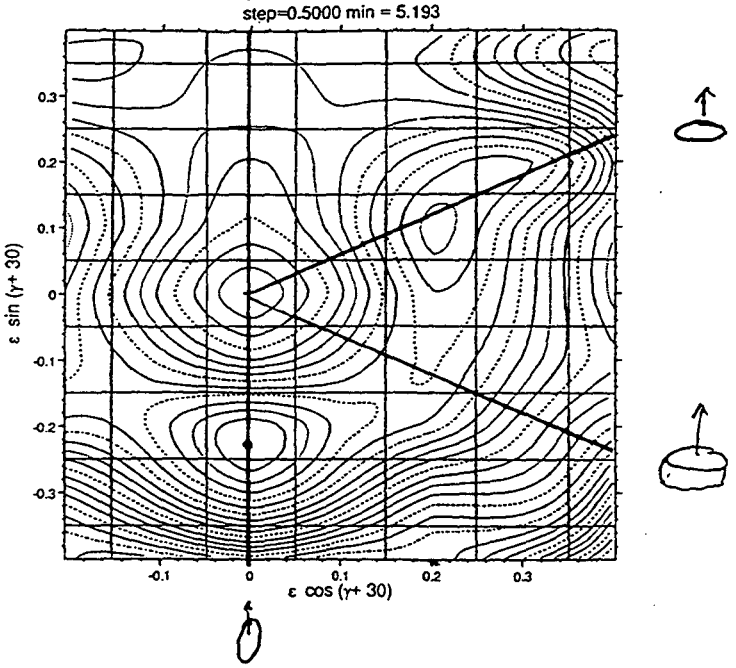


$^{178}$W N=104 prots + neuts: $\pi$= 1 $\alpha$=0 I=40

step=0.5000 min = 9.862

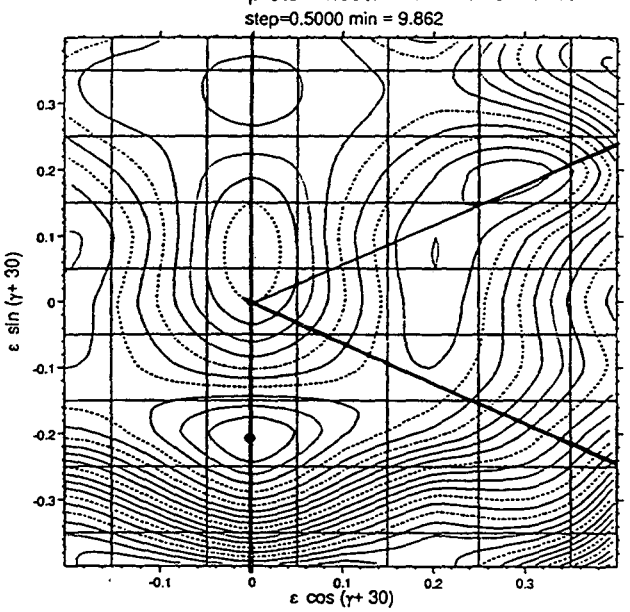


$^{178}$W N=104 prots + neuts: $\pi$= 1 $\alpha$=0 I=50

step=0.5000 min = 15.332

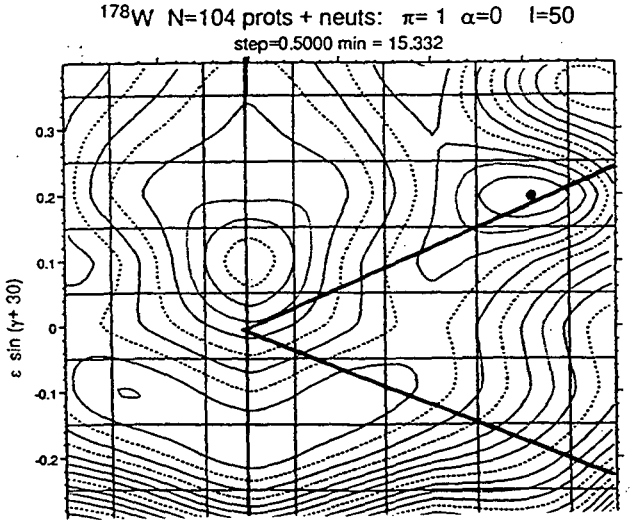

# • Chiral rotation and vibration of triaxial nuclei

- new example of chirality
- particle physics
  chemistry

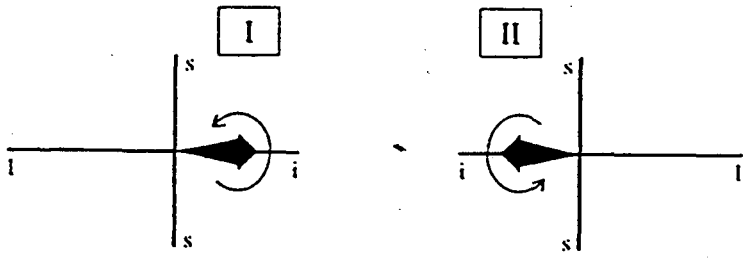


achiral

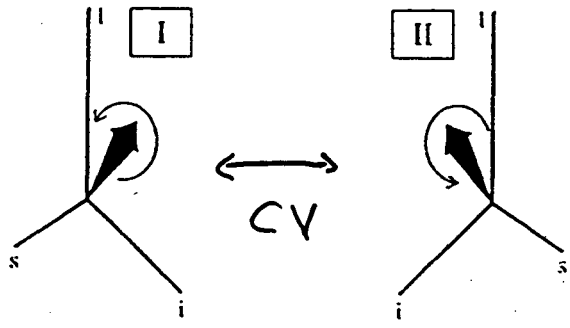


chiral

right - handed

CR

left - handed

CR

experimental signature

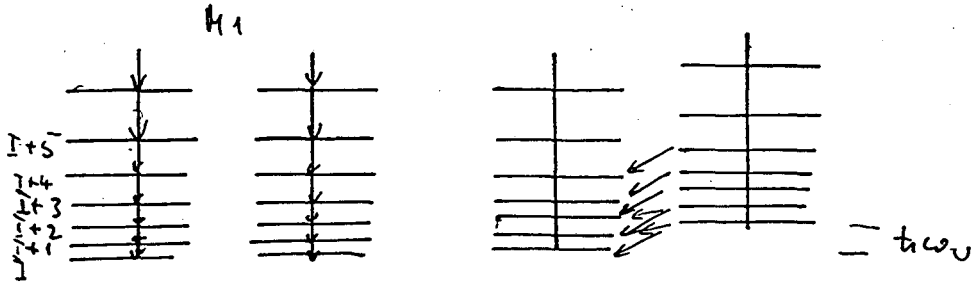


same parity

Chiral rotation

strong chiral symmetry

Chiral vibration

weak chiral symmetry

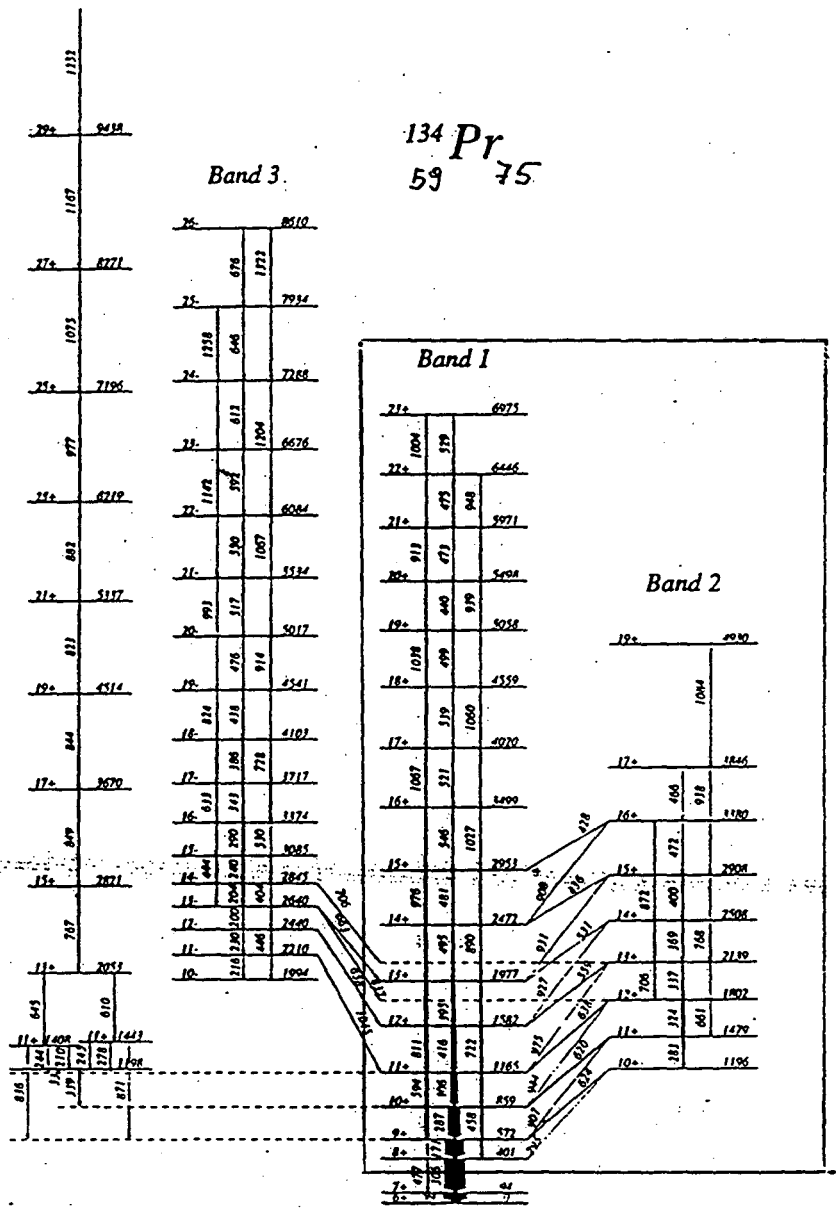


C.M. Petrache et al.
Nucl. Phys. A597 (1996) 106

GASP

$^{134}_{59}Pr_{75}$ $\hbar\omega = 0.35$ MeV

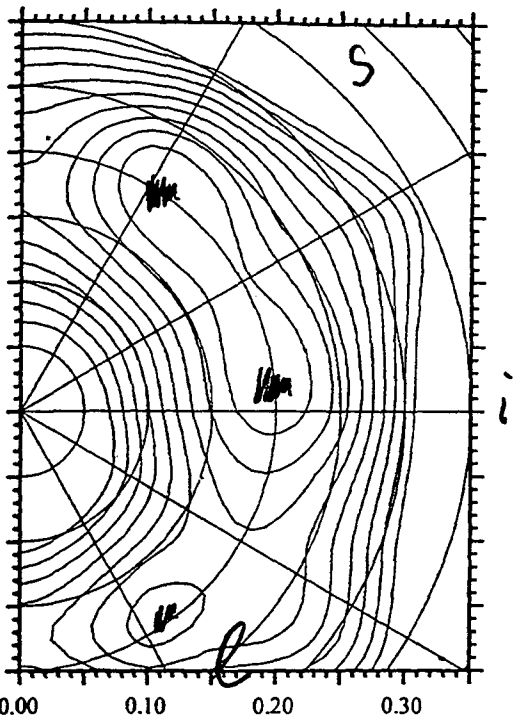


step = 0.2 MeV

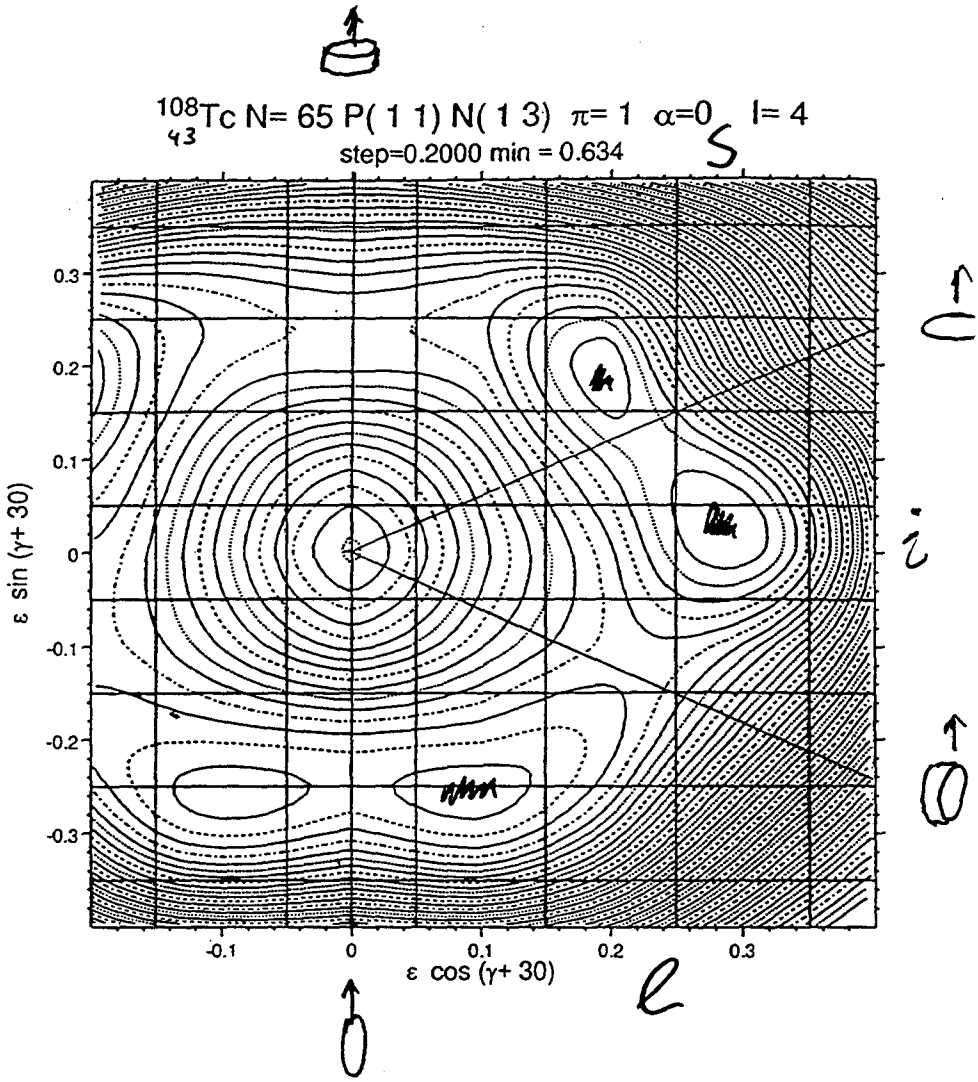


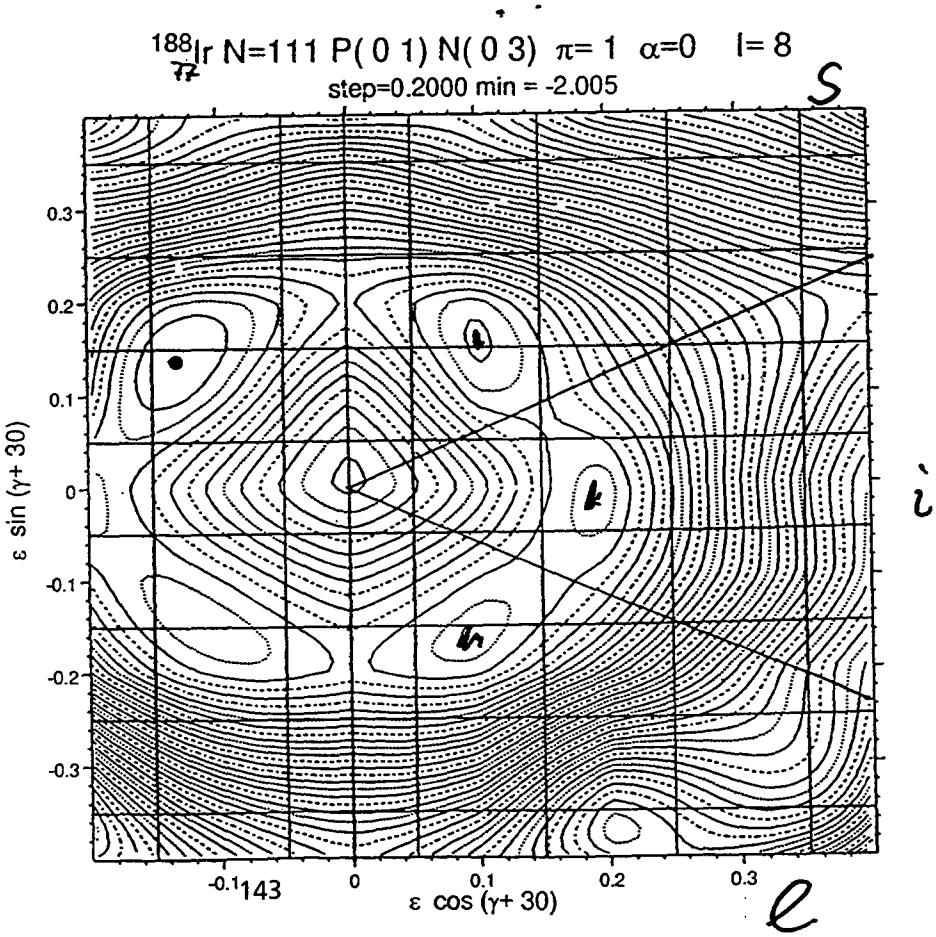


chirality:

- moderate I
- odd odd best
- not very long

Regions of Triaxiality / Chirality

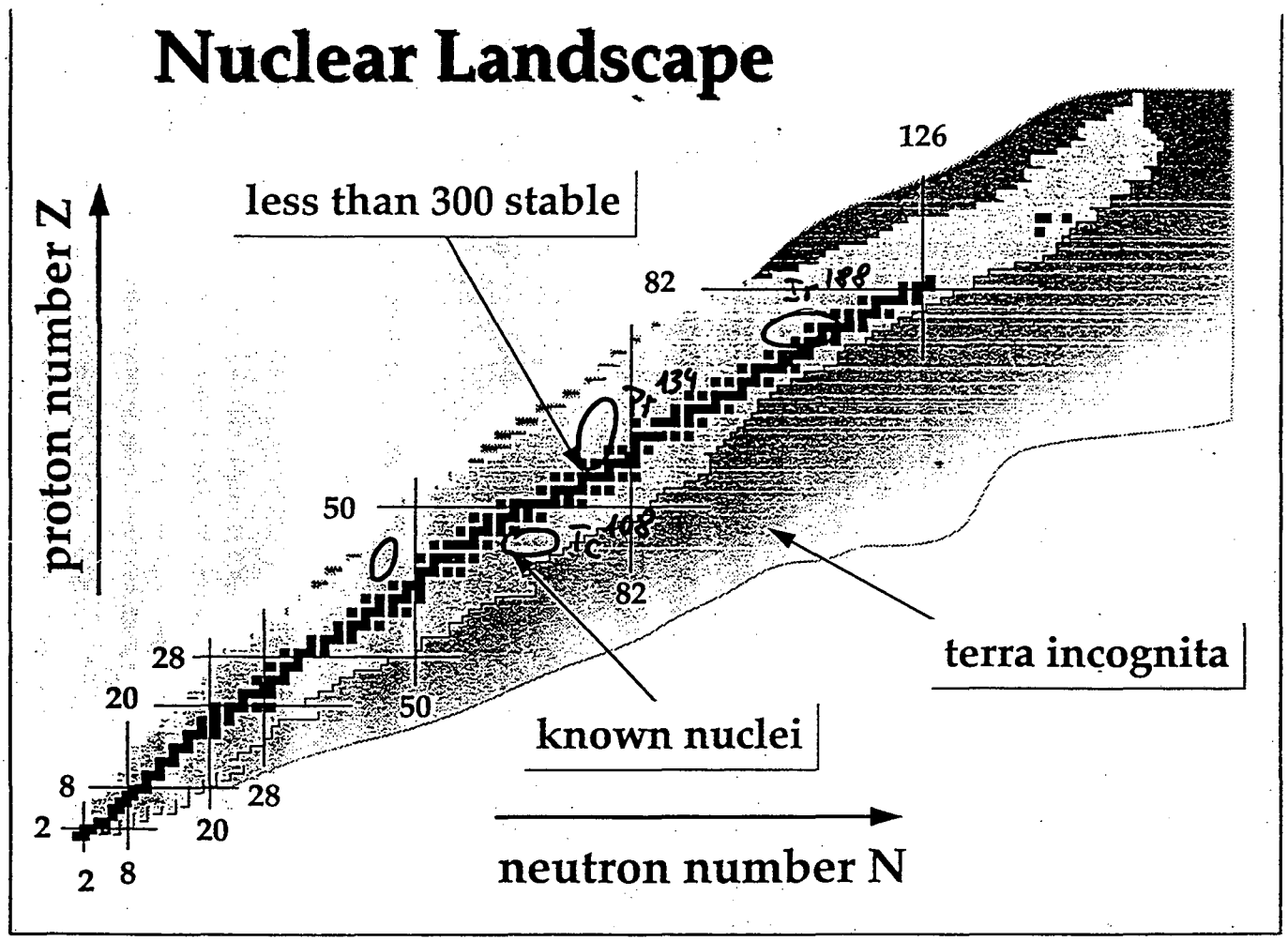

# Transition suprafluid normal

nucleus is a small system $\leftrightarrow$ small superconductors

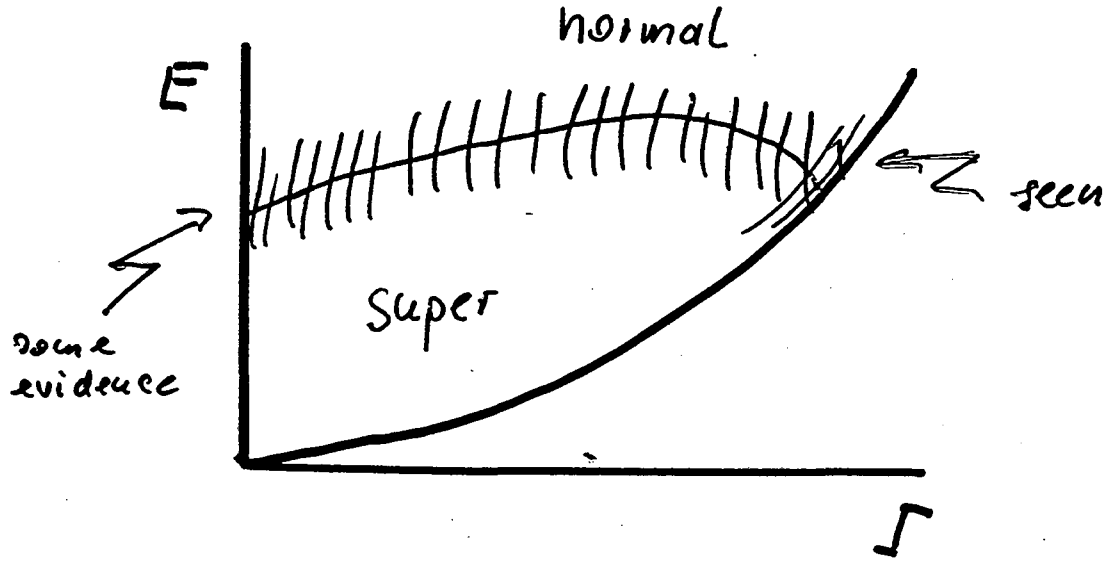


reasonable definition: HFB $\Delta \to 0$ "quenching of static pairing"

Signal: quenching of alignments and band crossings AB, ...
+ ??

- high spin, near yrast
  neutron blocking, protons?

- moderate spin, discrete excited bands
  do the crossings appear at $\hbar\omega_c$? ($\hbar\omega \sim 0.2 - 0.3$ MeV)

- low spin, high E
  level densities $S = \ln(\rho) = S(E)$ "equation of state"
  $J^{(2)}$ from $\gamma$-$\gamma$ correlations

What remains of phasetransition?

heat capacity

High K bands in $^{178,179}$W

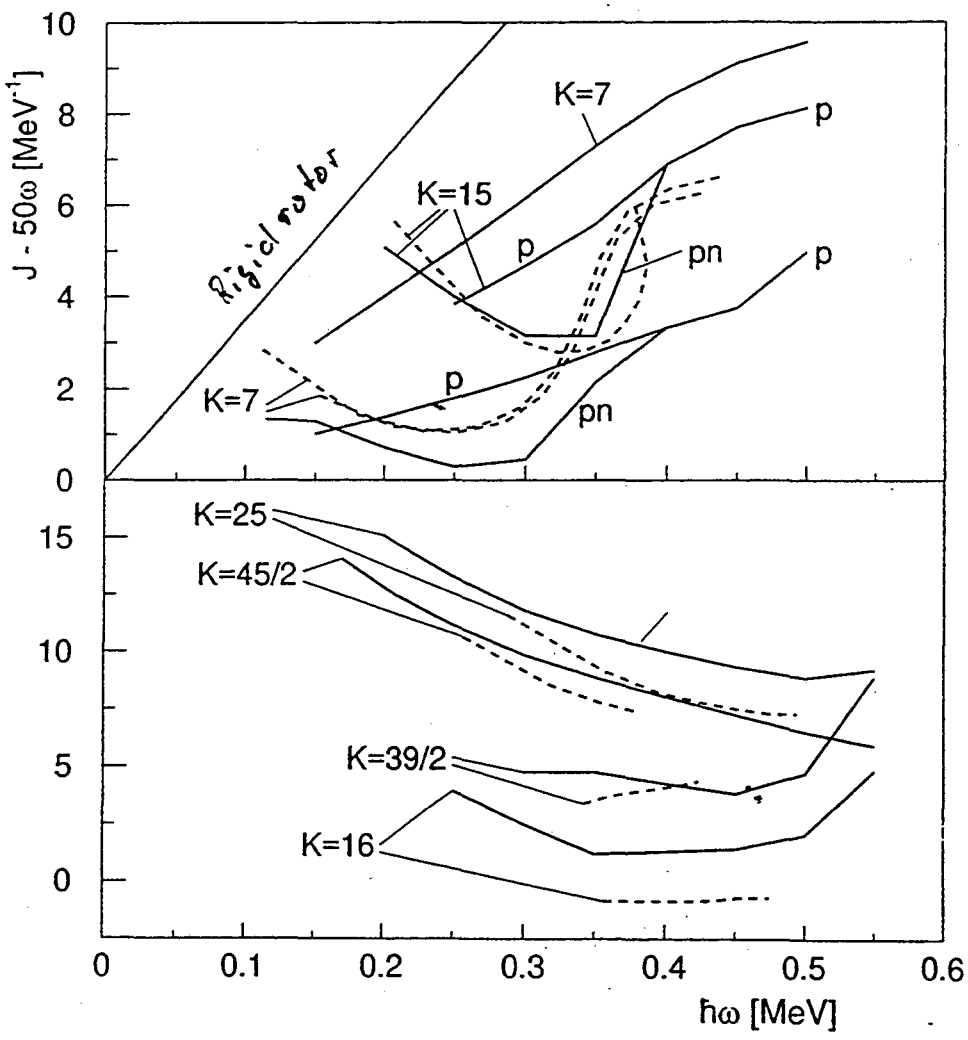


J. Sheikh et al.

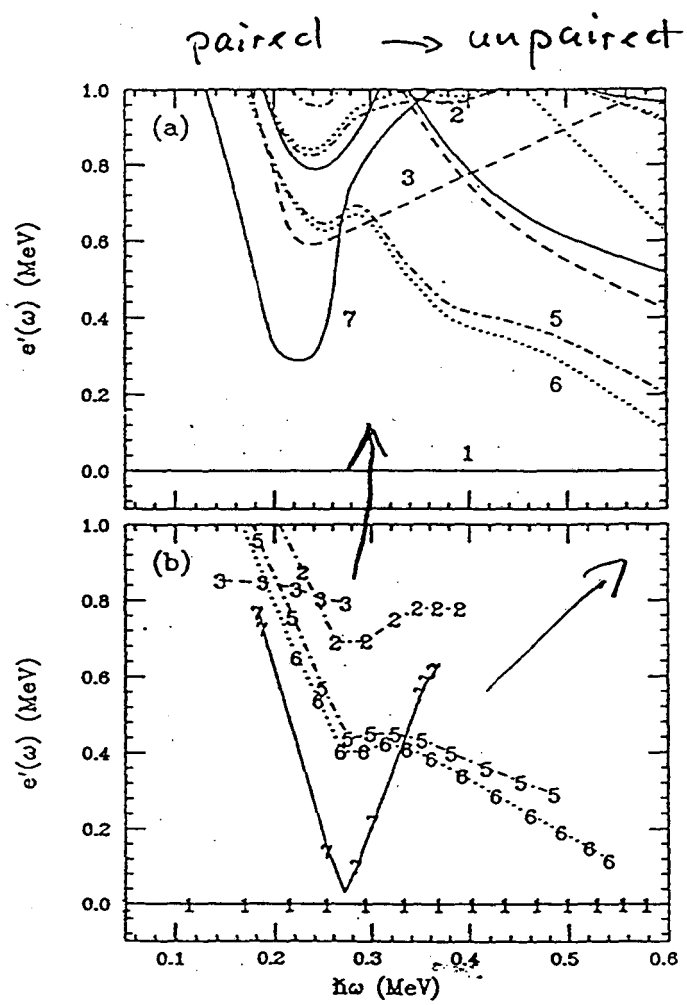


FIG. 3. Band structure of $^{166}$Yb. (a) Calculation with decreasing $\Delta$. (b) Experimental results [12]. The line conventions are the same as in Fig. 2.

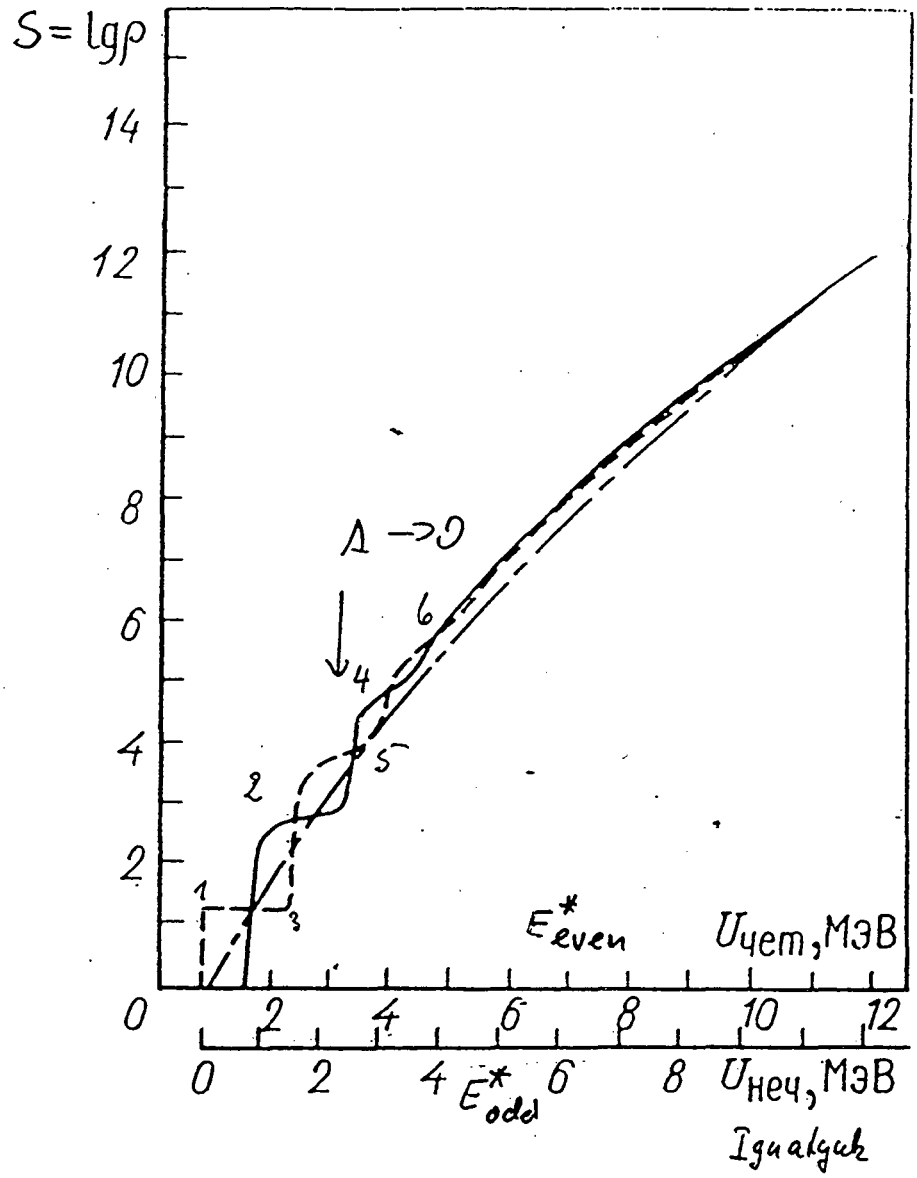
S = lgρ
14
12
10
8
6
4
2
0
Δ → 0
1
2
3
4
5
6
$E^*_{even}$
$U_{чет}$, МэВ
0 2 4 6 8 10 12
0 2 4 6 8
$E^*_{odd}$
$U_{неч}$, МэВ
Igualgak

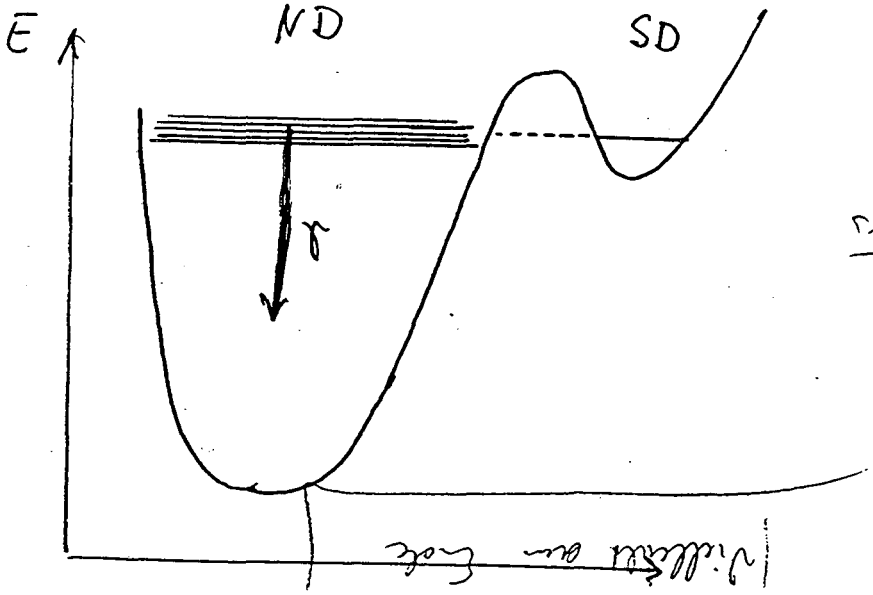
E
ND
SD
γ

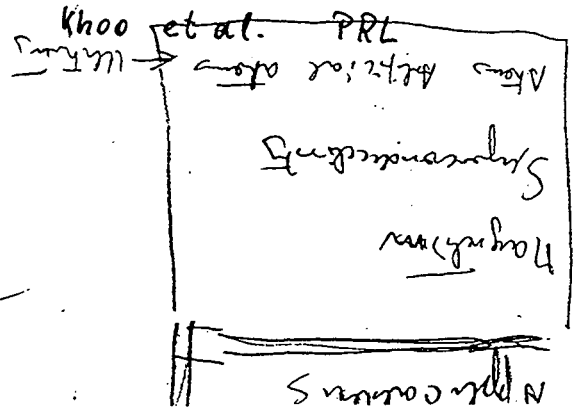
Khoo et al. PRL

# Rotation in the normal state

- not rigid (mesoscopic point of view)
  nature of the currents → finite size (magnetism of clusters and dofs)
  → spin orbit

- Cranked Shell model analysis (microscopic point of view)

  - Is the rotating local potential really sufficient? $h' = t + V(\text{def}) - \vec{\omega}\vec{J}$

  - Do mean field models as Skyrme HF, Relativistic HF describe the deviations?

  - New kind of correlations (no hidden by strong monopole pairing)
    Soft pairmodes with $J > 0$

  - relevance for super deformation

High K bands in $^{178}$Hf (16), $^{178}$W (22, 25), $^{179}$W (45/2)

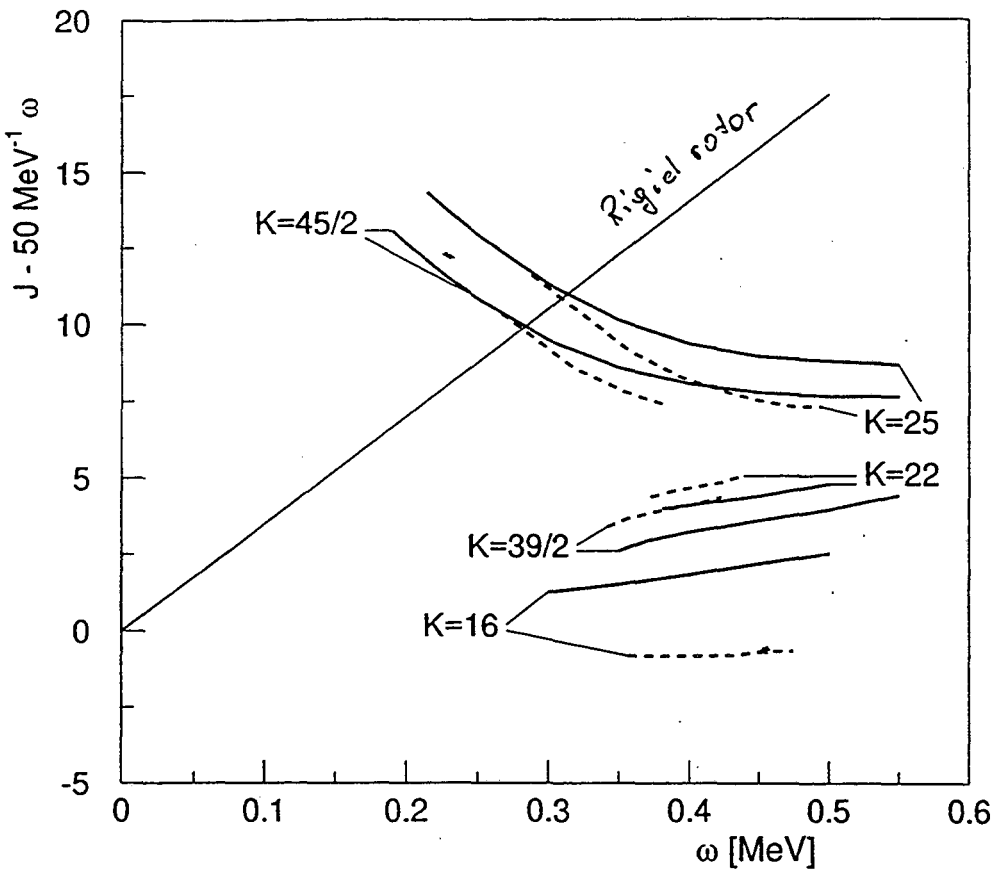


--- experiment

—— TAC calculation, no pairing

J. Sheikh et al.

Moments of inertia extracted from
Yrast levels (last 10 levels)

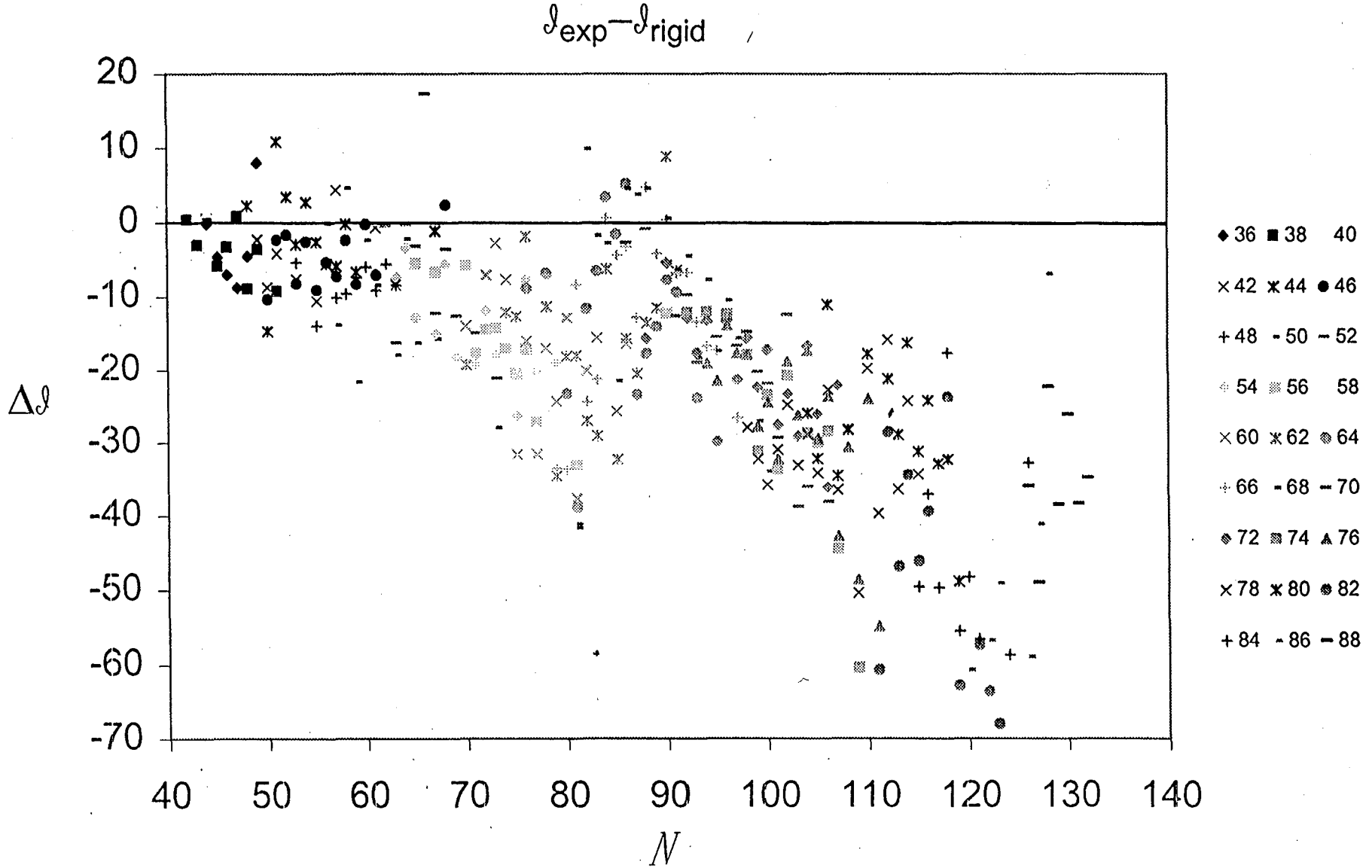


F. Chu et al.

$\Theta_{SH} \sim \Delta\mathcal{J}$

$\left.\frac{\Theta_{SH}}{E_{SH}}\right|_{N=126}$ : $\eta_\beta \sim 5$ 2 for $\Delta$ 13 for $\cap$

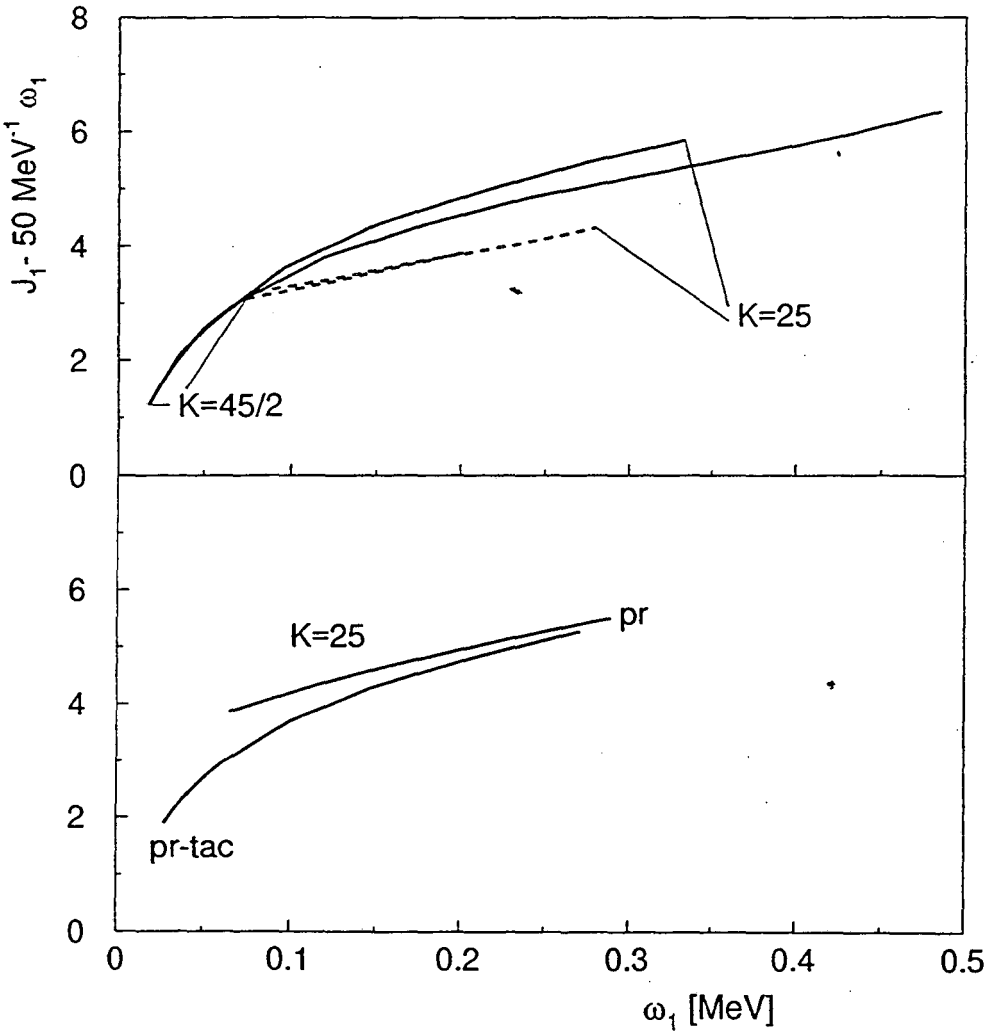
8
6
4
2
0
6
4
2
0
$J_1$- 50 MeV$^{-1}$ $\omega_1$
K=25
K=45/2
K=25
pr
pr-tac
0
0.1
0.2
0.3
0.4
0.5
$\omega_1$ [MeV]

# pn- pairing and rotation for $N \approx Z$

- rotational bands contain information (pp, nn!)

- turnover from $T=0$ pairing to
  $T=1$ pairing around $A \approx 60$ (low spin)

HFB mean field
Shell model
Algebraic model

- delayed backbend in $N \approx Z$
  seen in $^{72}_{36}Kr_{37}$ (Gasp)

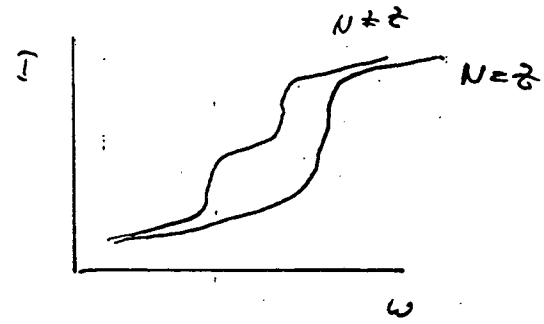


$T=1$ effect (Shell model)
physics ?

- How does pairfield develop if $N \to Z$ ? $\Delta_{nn}, \Delta_{pp} \to$ ?
  $A > 60$ $T=1$ regime (low spin)

- Spontaneous breaking of isospin symmetry
  pn pairing – a symmetry effect

- CSM at $N = Z$

- $J > 0$ pair correlations important at high spin

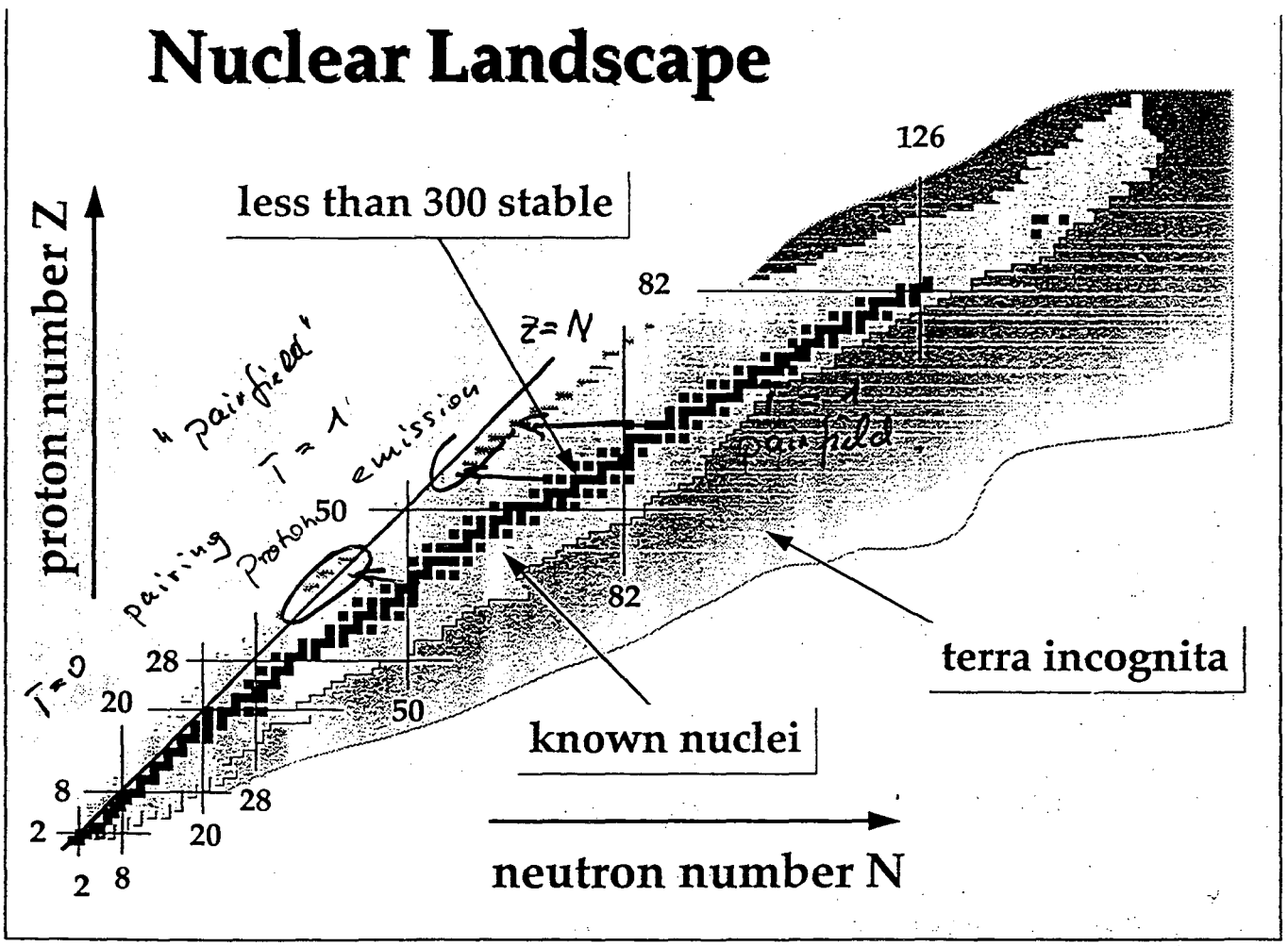
Nuclear Landscape
less than 300 stable
proton number Z
neutron number N
known nuclei
terra incognita
126
82
50
28
20
8
2
Z = N
T = 0
T = 1
pairing
Proton emission
pairfield
pairfield

# nucleonic Cooper pairs

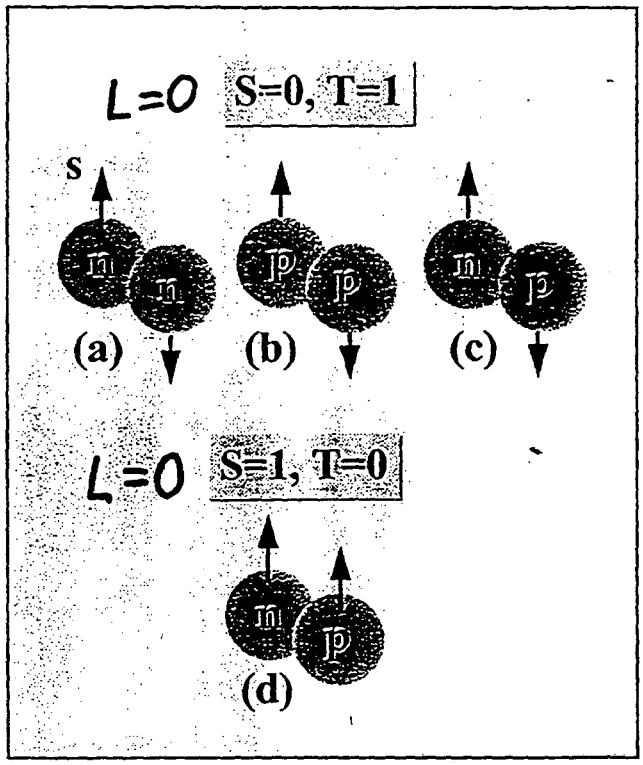


light nuclei

ls - coupling

no dineutron

T=0 more attractive

deuteron

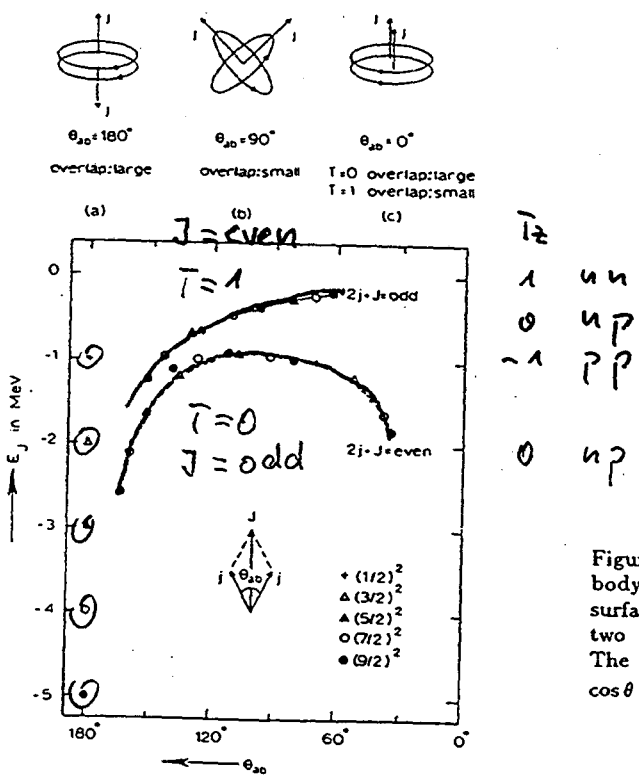


| $T_z$ | |
|---|---|
| 1 | nn |
| 0 | np |
| -1 | pp |
| 0 | np |

heavy nuclei

jj - coupling

T=1 more attractive

Figure 1: Diagonal two body matrix elements of the surface $\delta$ - interaction for two nucleons in a $j$ shell. The angle is defined as $\cos\theta = \frac{J(J+1)}{2j(j+1)} - 1$. Taken from ref. [2].

[ ψ(1) ψ(2) ]

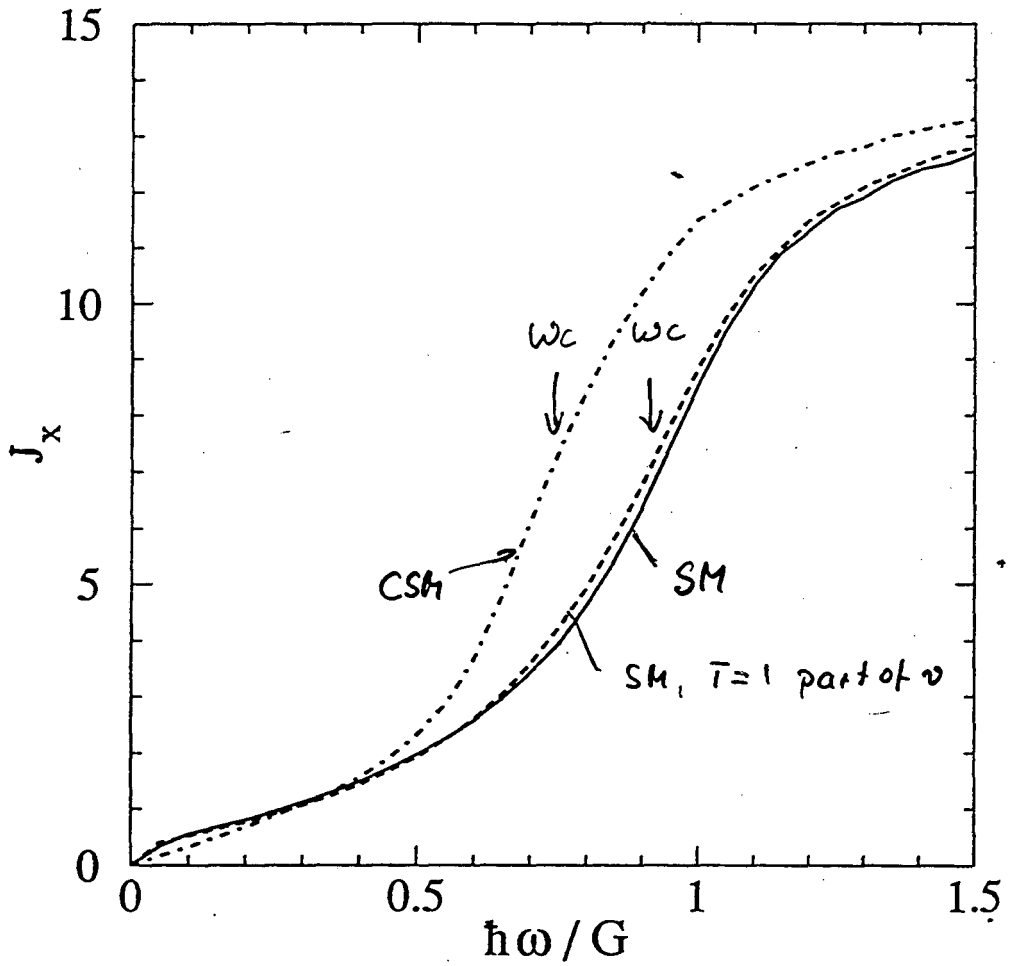


$N = Z = 0$ $T=0$ yrast

$[0]_{T=0} \rightarrow [ab\,1\,B]_0$ double alignment

Shift of $\omega_c$ : "dynamical pairing" $T=1$ pn pairing

experimental evidence for delayed backbend for $N \rightarrow Z$

# Spontanous breaking of isospin symmetry

$\lambda_\tau = 0$ :

$\Delta_{T=1,T_z}$ is a vector in isospace

all its orientations are equivalent intrinsic solutions

$$\Delta_{J,M,T=1,T_z=\pm1} = \mp\Delta_{J,M,T=1}\sin\theta\exp\mp i\phi/\sqrt{2}$$
$$\Delta_{J,M,T=1,T_z=0} = \Delta_{J,M,T=1}\cos\theta \qquad (7)$$

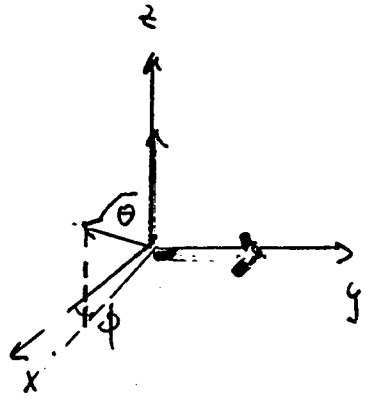


$\Delta_{nn} = \Delta_{pp} = 0 \quad \Delta_{np} \neq 0$

$\Delta_{nn} = \Delta_{pp}, \quad \Delta_{np} = 0$

- The relative strengthes of $\Delta_{nn}, \Delta_{np}, \Delta_{pp}$ are not well defined!
- $\lambda_\tau \neq 0 \qquad \Delta_{10} = 0$

<u>Restoration of isospin symmetry</u> $\longrightarrow$ reappearance of pn correlation

- $T=0$ states : $\quad |\tau=0\rangle = \frac{1}{\sqrt{4\pi}}\int d\phi \sin\theta d\theta \quad |\theta,\phi\rangle$

Equal amount of pp, nn, np correlation energy

- $\tau = \tau_2 \neq 0$ states: vibrations around y axis

pn correlation energy

= gs corr. energy of vibration

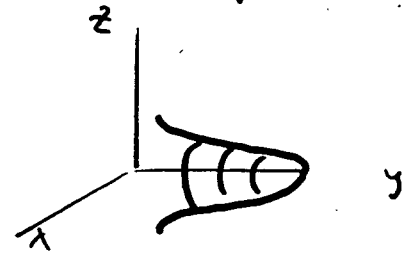


$E_{corr} \to 0$ with $|\tau_2|$

# Rotating Quasiparticles at $N = Z$ (CSM)

$T = 1$ regime

$\Delta_{nn} = \Delta_{pp} = \Delta$ only $\quad \Delta_{np}$ by symmetry

number parity known $\quad \alpha^+_{1n} \cdots \alpha^+_{\nu n} |0\rangle \quad \begin{matrix}\text{odd}\\ \text{even}\end{matrix}\ \nu \longleftrightarrow \begin{matrix}\text{odd}\\ \text{even}\end{matrix}\ N$

<u>$N = Z = A/2$ odd odd</u>

$T = 0$ states $\quad$ standard CSM + "isosignature" selection

$T = 1$ states $\quad$ isobar analogue of $T_z = 1 \quad N = A/2 + 1 \quad Z = A/2 - 1$
even-even

lowered by $2\Delta$ $\quad$ (pn by symmetry)

pushed up by $1/\Theta_T \quad \Theta_T = d\langle T_z\rangle / d\omega_T$

"isorotational energy"

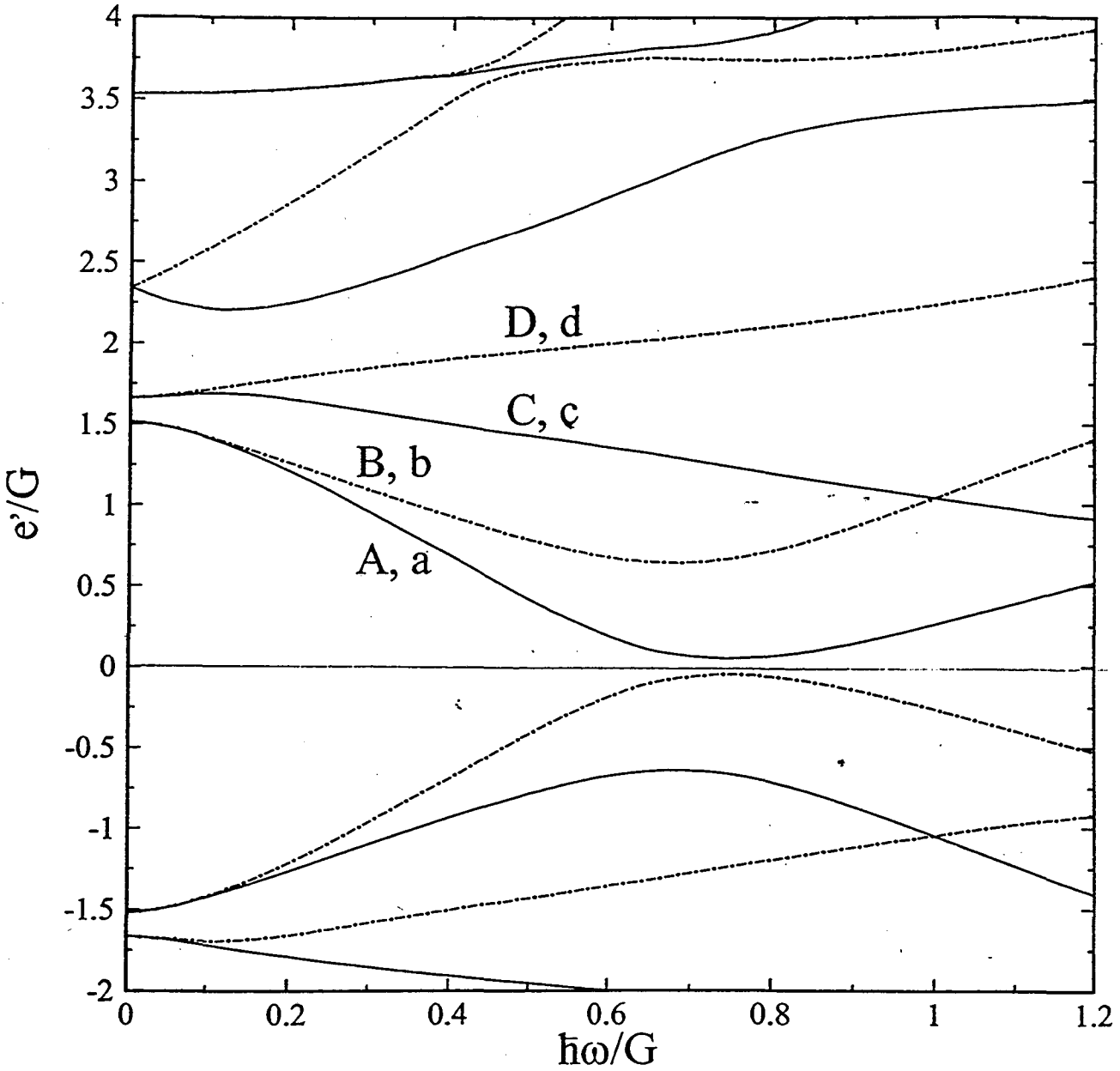


Quasiparticles in $f_{7/2}$ shell

$\langle \hat{N} \rangle = \langle \hat{Z} \rangle = 4$

$\Delta_{nn} = \Delta_{pp} \approx$ HFB value at $\omega = 0$

$\Gamma(\omega = 0)$ included

$f_{7/2}$ shell $\quad H = V_{def} + G\delta(\vec{r}_1 - \vec{r}_2) - \omega j_x$

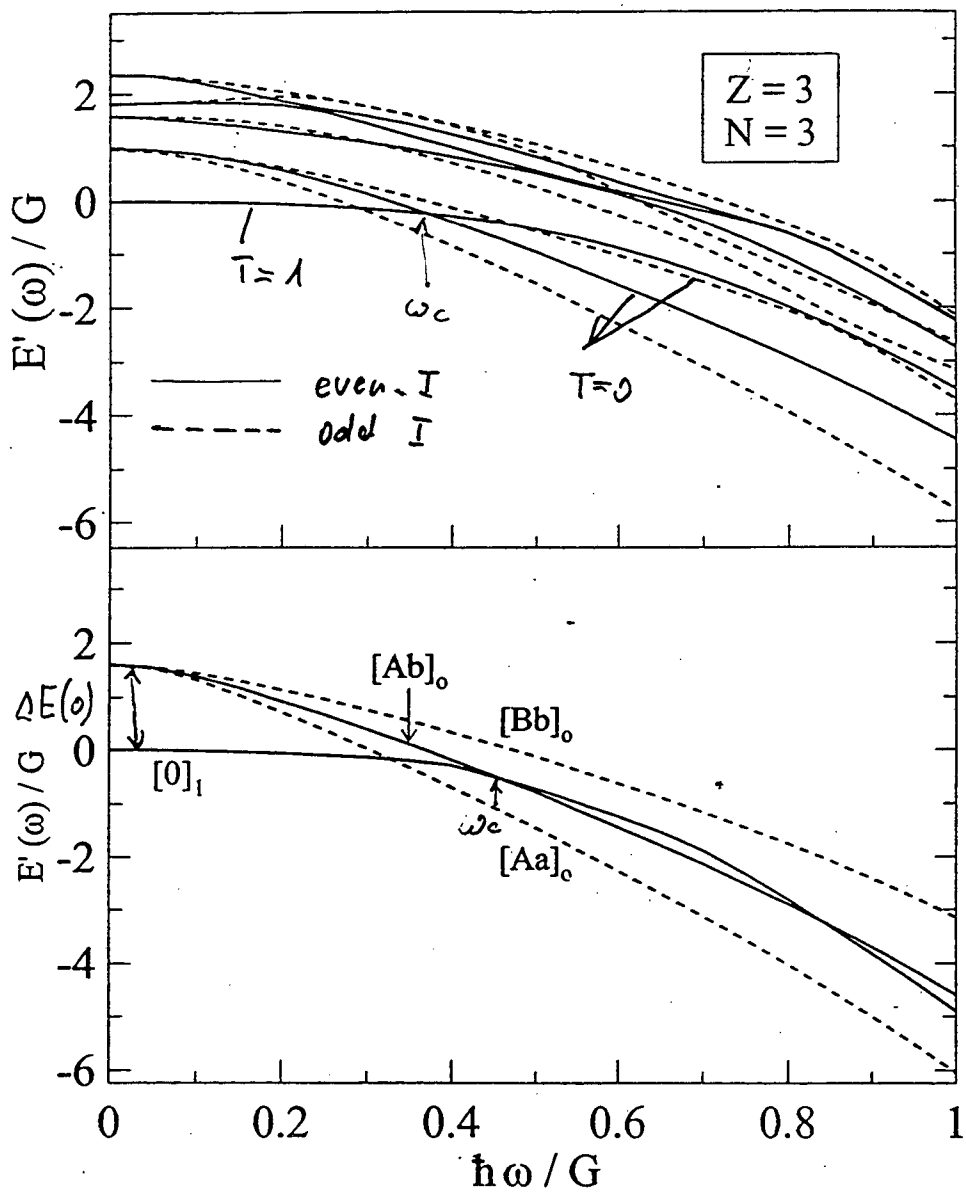


$\omega_c|_{SM} \lesssim \omega_c|_{CSM}$ $\qquad$ T=0 pn pairing (in [Ab])

$\Delta E(0)|_{SM} < \Delta E(0)|_{CSM}$ $\qquad$ T=1 dynamical p. (?)

$[Ab]_0$ correct $\frac{1}{\sqrt{2}}([Ab] + [aB])$ $\quad e^{i\pi \hat{T}_y}|\phi_+\rangle = |\phi\rangle$

not allowed $\frac{1}{\sqrt{2}}([Ab] - [aB])$ $\quad e^{i\pi \hat{T}_y}|\phi_-\rangle = -|\phi\rangle$

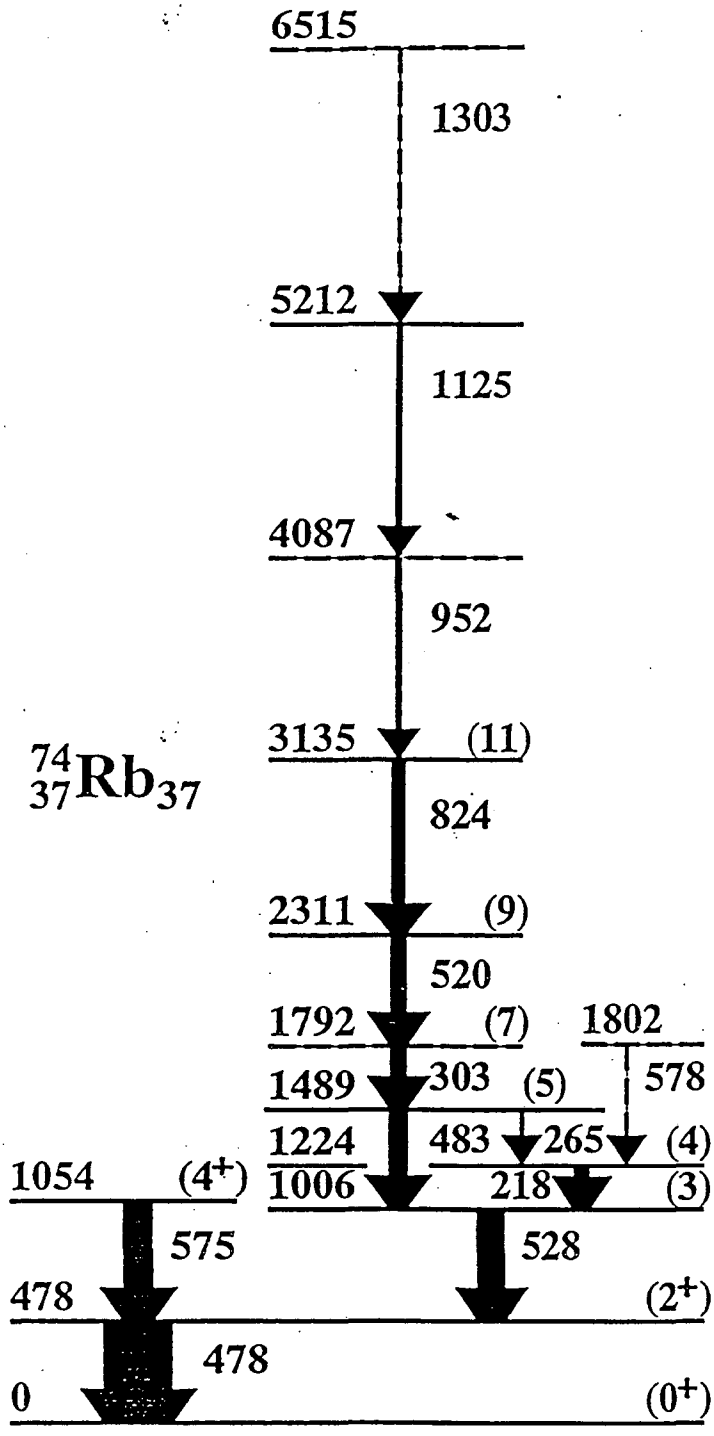


D. Rudolph et al.
PRL 76 (96) 376

## Model system : $f_{7/2}$ shell

Exact solutions (SM) for

$$H' = h' - g\delta(\hat{r}_1 - \hat{r}_2) \tag{1}$$

where,

$$h' = -4\kappa\sqrt{\frac{4\pi}{5}}Y_{20} - \omega J_x \tag{2}$$

<u>The HFB equations</u>

$$\sum_k (h_{jk}u_{ik} + \Delta_{jk}v_{ik}) = \tilde{\epsilon}_i u_{ij}$$
$$\sum_k (-\Delta^*_{jk}u_{ik} - h^*_{jk}v_{ik}) = \tilde{\epsilon}_i v_{ij} \tag{3}$$

where

$$h_{ij} = (h'_{ij} + \Gamma_{ij})\delta_{\tau_i\tau_j} - (\lambda + \lambda_\tau \tau_i)\delta_{ij} \tag{4}$$
$$\Gamma_{ij} = \sum_{kl} < ik|v_a|jl > \rho_{lk} \tag{5}$$
$$\Delta_{ij} = \frac{1}{2}\sum_{kl} < ij|v_a|kl > t_{kl} \tag{6}$$

isospin label $\tau = 1, -1$

mass constraint $< A >$ $\lambda = (\lambda_n + \lambda_p)/2$

# Spontaneous vs. external symmetry breaking

External breaking of isospin symmetry by Coulomb field

Standart estimate: Admixture of isovector monopole mode ($T=1$)
$\hbar\omega \sim 20$ MeV
impurity $\lesssim 1\%$ $\quad N = Z < 50$

New: Admixture of $T=2$ isorotational level
$E = \frac{T(T+1)}{2\vartheta} \sim 3$ MeV $\quad \frac{1}{\vartheta} \sim 1$ MeV ($Rb^{74}$)

causes anisotropy of pair field

- <u>Tests of isospin purity</u> $I(\omega)$ for $T_z = \pm 1/2$ (mirror nuclei)
$T_z = 0, 1^+ (-1)$

| | $E_\gamma$ | $\mathcal{J}$ | $E_\gamma$ | $\mathcal{J}$ |
|---|---|---|---|---|
| $2 \to 0$ | 0.478 MeV | 6.3 MeV$^{-1}$ | 0.456 MeV | 6.6 MeV$^{-1}$ |
| $4 \to 2$ | 0.575 MeV | 9.5 MeV$^{-1}$ | 0.558 MeV | 9.9 MeV$^{-1}$ |
| | $^{74}Rb$ $T=1$ $T_z=0$ | | $^{74}Kr$ $T=T_z=1$ | |

Rich field for study

W.Satula

The mean field: can it still surprise ?

# THE MEAN-FIELD:

## can it still surprise?
(or do we really understand
self-consistent mean-fields?)

W. SATUŁA
(with Jacek Dobaczewski &
Witek Nazarewicz)

- The 'logic':

Example of pairing filter:

$\frac{1}{4}(-1)^N$

| | | | |
|---|---|---|---|
| 1 | -3 | 3 | -1 |

Z ↑ N →

$$\propto B(Z,N-2) - 3B(Z,N-1) + 3B(Z,N) - 3B(Z,N+1)$$

$$\Rightarrow \Delta_\nu$$

- This filter measures neutron pairing. In other words, it is supposed to remove all other effects, in particular those associated with mean-field.

- We all are probably aware that the above is not fully true, that pairing although weak as compared to HF mean-field (it constitutes few percent of nuclear mass) is not a perturbative correction. But ...

WHO CARES ...

CALCULATIONS:

- HF - Skyrme model with
  SLy4
  SIII
  (SkM*) forces

- F, ..., Ni ($Z = 9, \ldots, 28$)
  nuclei with $N-Z = -2, \ldots, 6$
  ($N-Z = 0, 1$ with SkM*)

- BASIS (relatively small, but we are interested in relative masses)
  : 11 H.O. Shells in $^{40}Ca$ :
  (spherical)

- two versions of calculations:
  - full model
  - including only time-even (T.E.) components of Skyrme force

- WEAK POINT :

  - it is difficult to find an "absolute" minimum particularly in soft, transitional nuclei

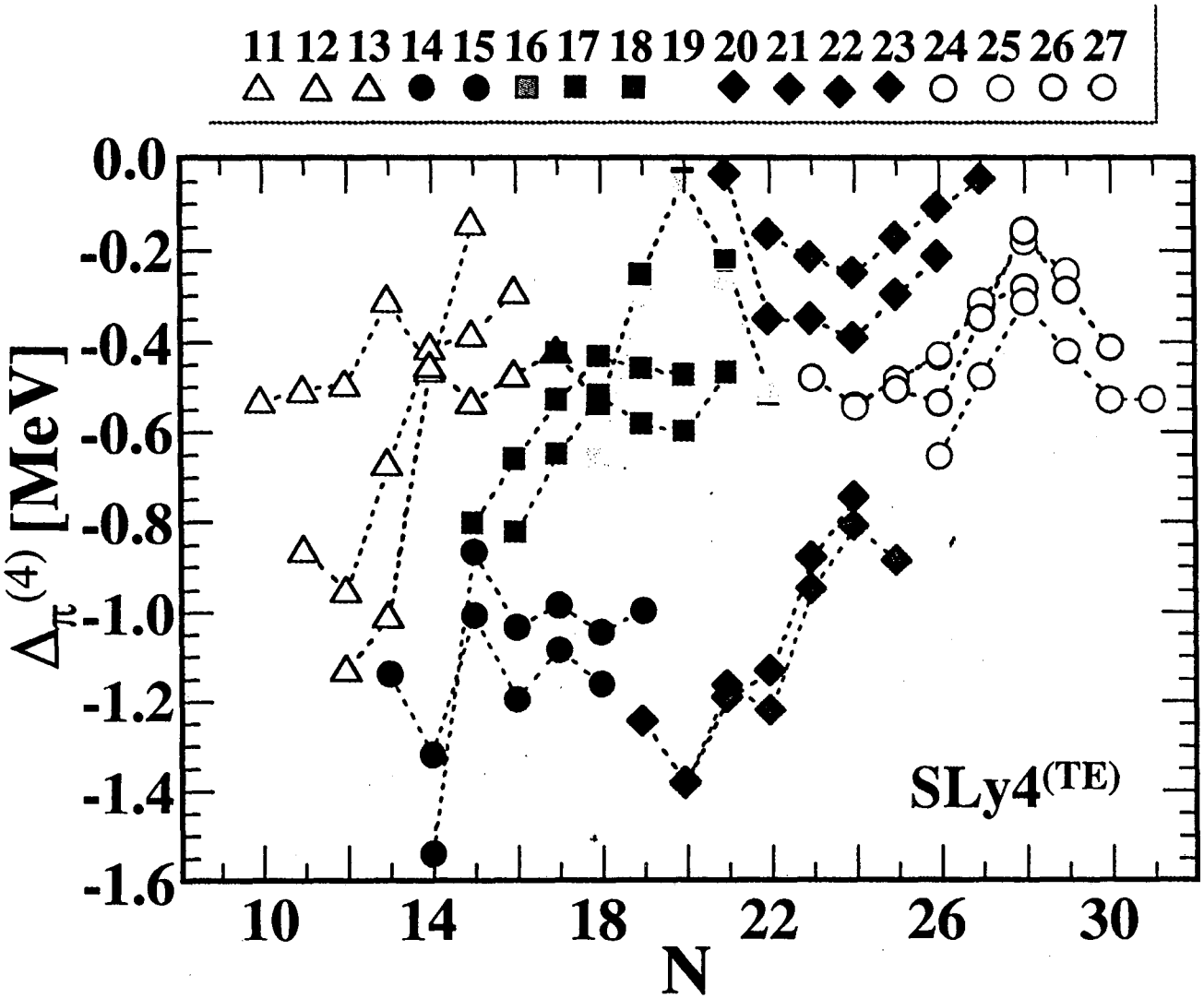
11 12 13 14 15 16 17 18 19 20 21 22 23 24 25 26 27
0.0
-0.2
-0.4
-0.6
-0.8
-1.0
-1.2
-1.4
-1.6
$\Delta_\pi^{(4)}$ [MeV]
10
14
18
22
26
30
N
SLy4(TE)

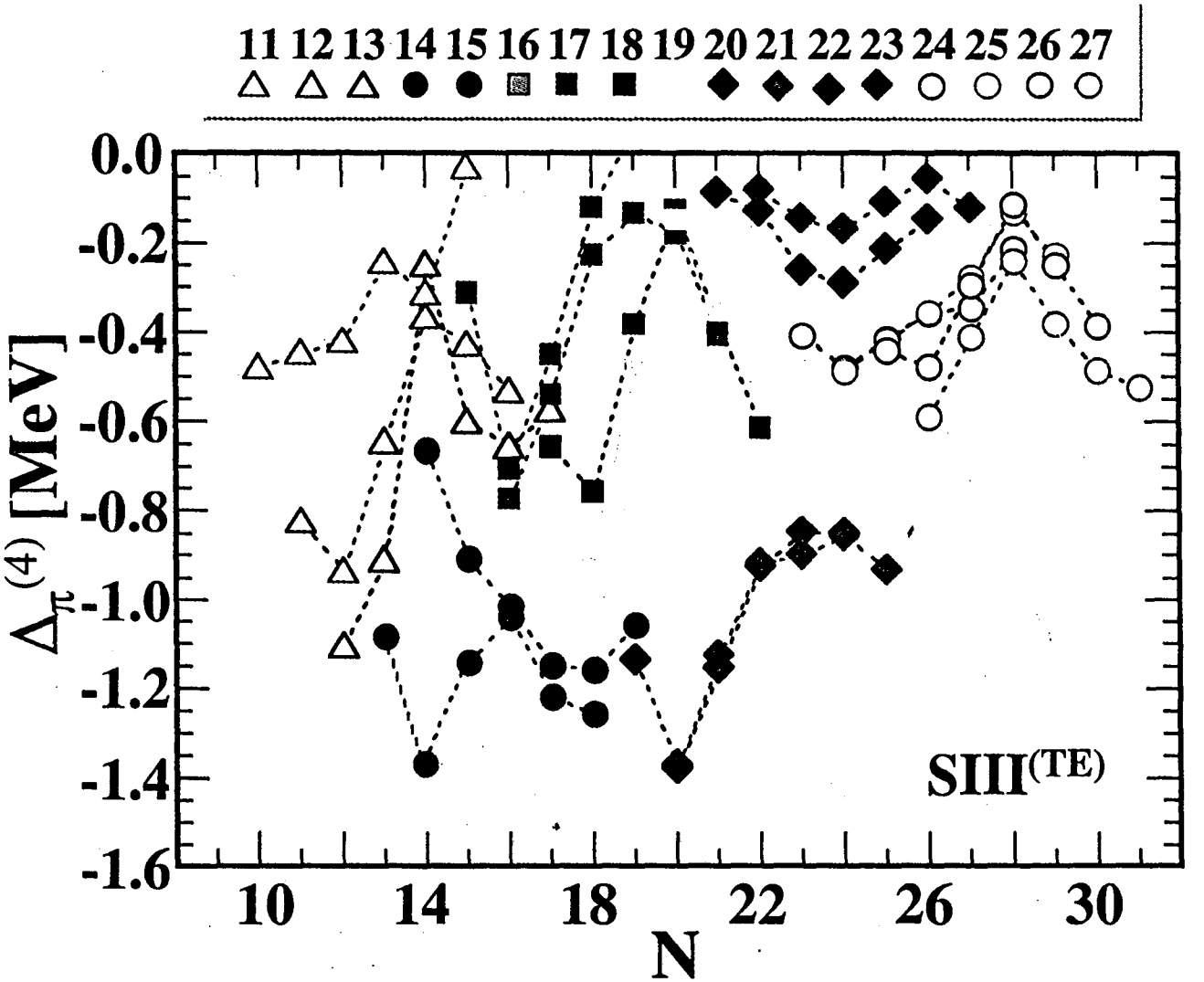
11 12 13 14 15 16 17 18 19 20 21 22 23 24 25 26 27
0.0
-0.2
-0.4
-0.6
-0.8
-1.0
-1.2
-1.4
-1.6
$\Delta_\pi^{(4)}$ [MeV]
10
14
18
22
26
30
N
SIII(TE)

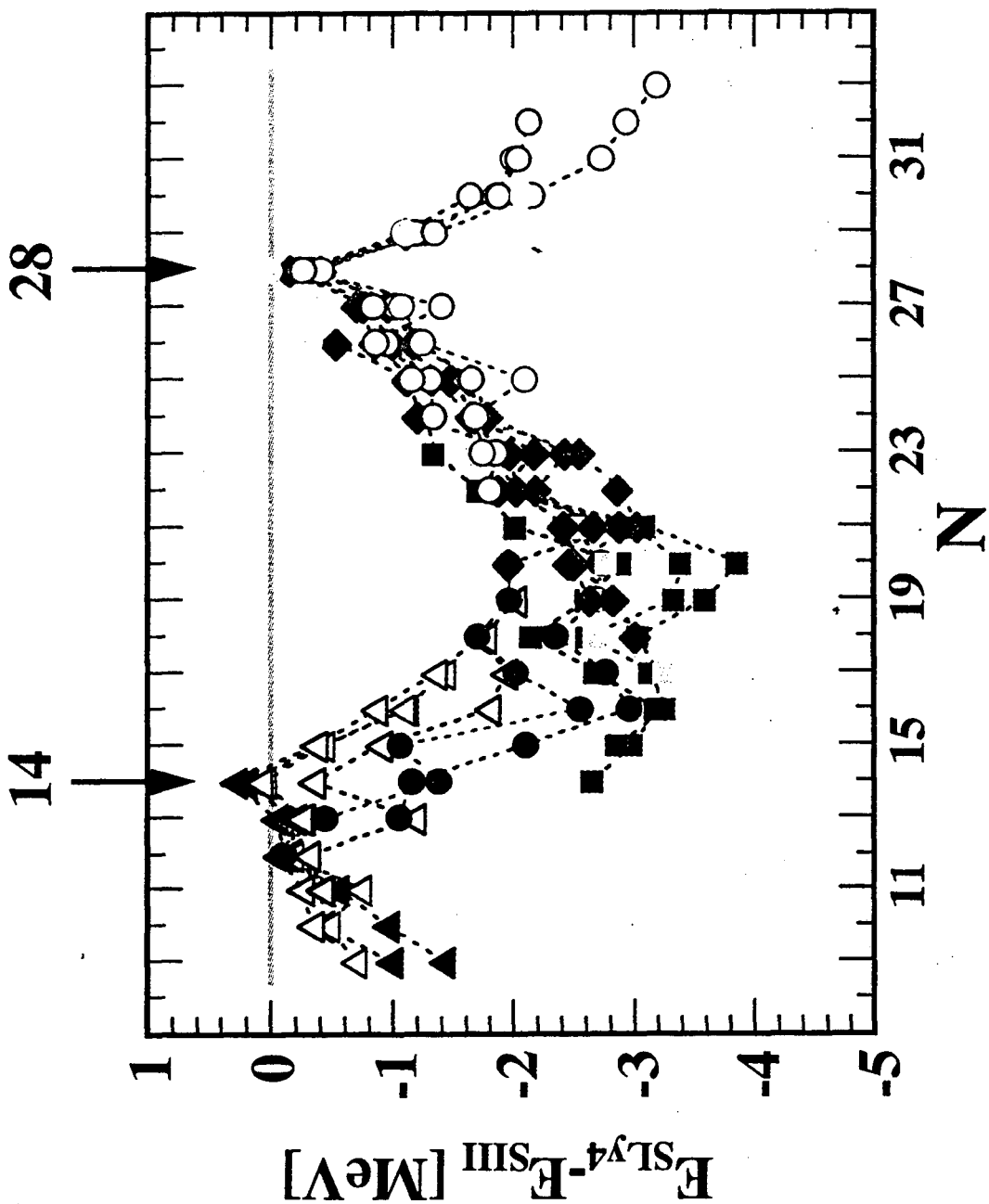
14
28
1
0
-1
-2
-3
-4
-5
11
15
19
23
27
31
N
$E_{SLy4}$-$E_{SIII}$ [MeV]

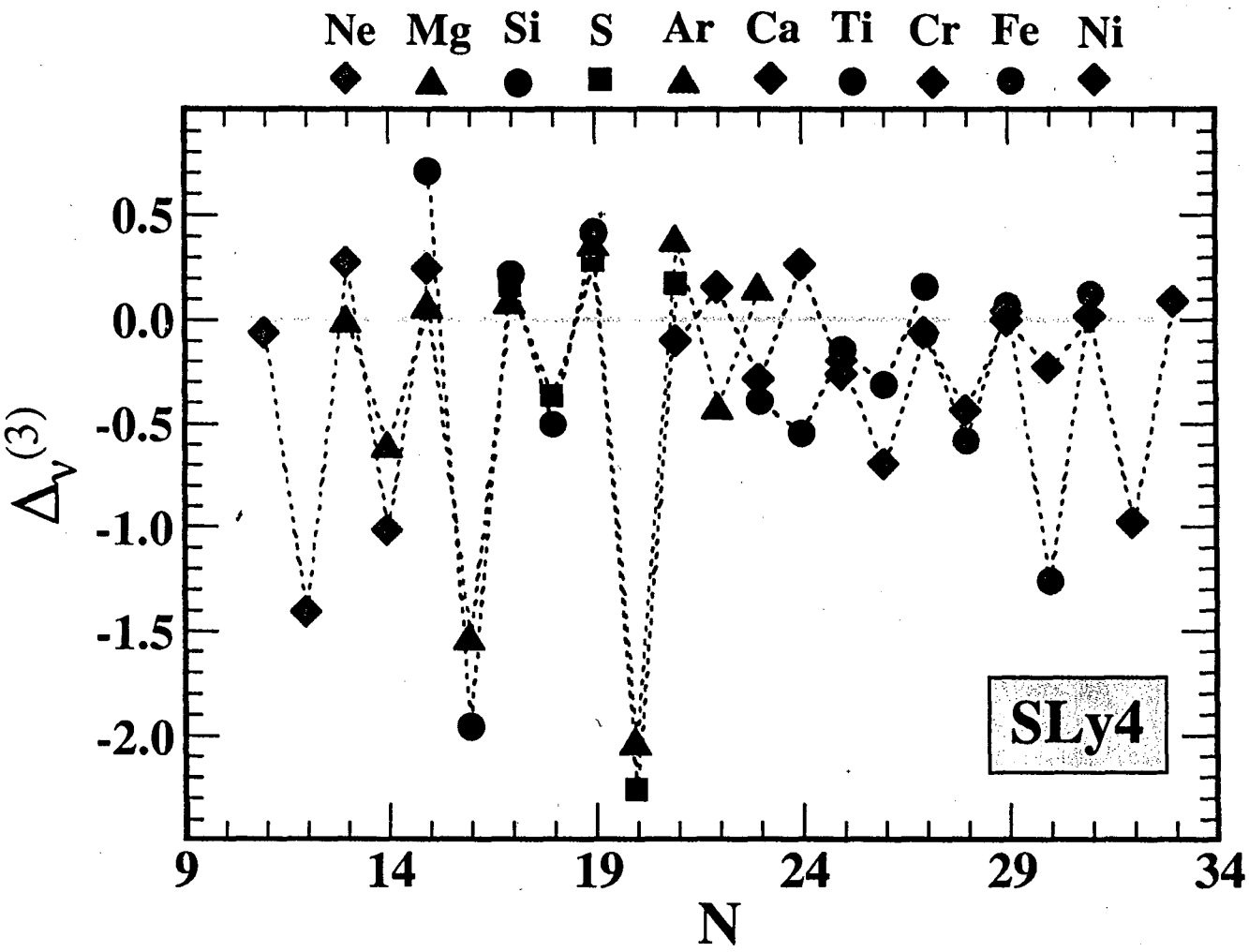
Ne
Mg
Si
S
Ar
Ca
Ti
Cr
Fe
Ni
0.5
0.0
-0.5
-1.0
-1.5
-2.0
$\Delta_\nu^{(3)}$
9
14
19
24
29
34
N
SLy4

Are there any systematic effects (fields) which, on the level of HF approximation, can lead to odd-even mass staggering?

- the answer is:
  'in principle yes -
  - these are time-odd fields:'

Two-body spin-spin interaction:

$$V_{\vec{s}\cdot\vec{s}} = \frac{1}{4} g\, \vec{s}\cdot\vec{s}^{+}$$

$$(T V_{\vec{s}\vec{s}} T^{+} = V_{\vec{s}\cdot\vec{s}})$$

$\longrightarrow$ mean-field counterpart:

$$\frac{1}{4} g \left( \langle \vec{s} \rangle \cdot \vec{s}^{+} + \langle \vec{s}^{+} \rangle \vec{s} \right)$$

$$= \frac{1}{2} g \langle \vec{s} \rangle \vec{s}$$

number (must be adjusted self-consistently)

time-odd!

- "One-dimensional 'topology'" of HF solutions:

$$\frac{1}{4}(-)^N \left\{ B(Z,N-2) - 3B(Z,N-1) + 3B(Z,N) - B(Z,N+1) \right\}$$

$$\equiv \frac{1}{4}(-)^N \left\{ [B(Z,N-2) - 2B(Z,N-1) + B(Z,N)] - [B(Z,N-1) - 2B(Z,N) + B(Z,N+1)] \right\}$$

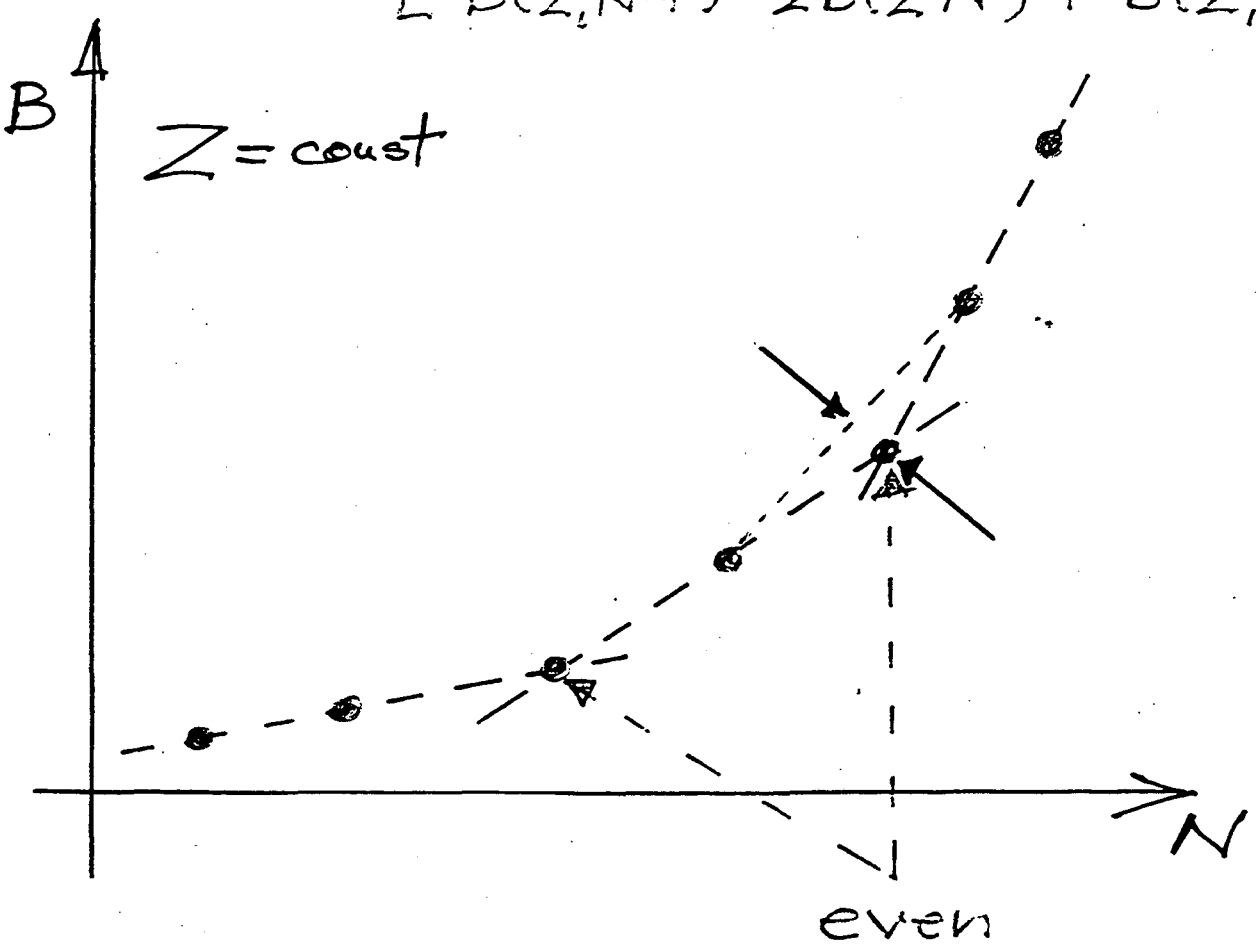

- MINIMAL MICROSCOPIC SCENARIO
  - EFFECTIVE M.F. MODEL

| | even-N | odd-N |
|---|---|---|
| N+1 | $2\varepsilon_1+\varepsilon_2$ | $2\varepsilon_1$ |
| N | $2\varepsilon_1$ | $\varepsilon_1$ |
| N-1 | $\varepsilon_1$ | 0 |
| | 'Local core' | 'Local core' |

$$\Rightarrow \Delta_\nu^{(3)} = \frac{1}{2}(-)^N \left\{ B(N-1) - 2B(N) + B(N+1) \right\}$$

$$= \begin{cases} \frac{1}{2}(\varepsilon_2-\varepsilon_1)\left[\ \ \right] + \Delta_\nu \left[\ \ \right] & \text{even-N} \\ 0 \qquad \left[\ \ \right] + \Delta_\nu \left[\ \ \right] & \text{odd-N} \end{cases}$$

$$\Rightarrow \Delta_\nu^{(4)} = \frac{1}{4}(\varepsilon_2-\varepsilon_1)\left[\ \ \right] + \Delta_\nu \left[\ \ \right]$$

- MACROSCOPIC SCENARIO:

$$\Delta_\nu^{(3)} = \Delta_\nu - \underbrace{\alpha_s}_{\text{symmetry energy}}(-)^N$$

$$\Delta_\nu^{(4)} = \Delta_\nu$$

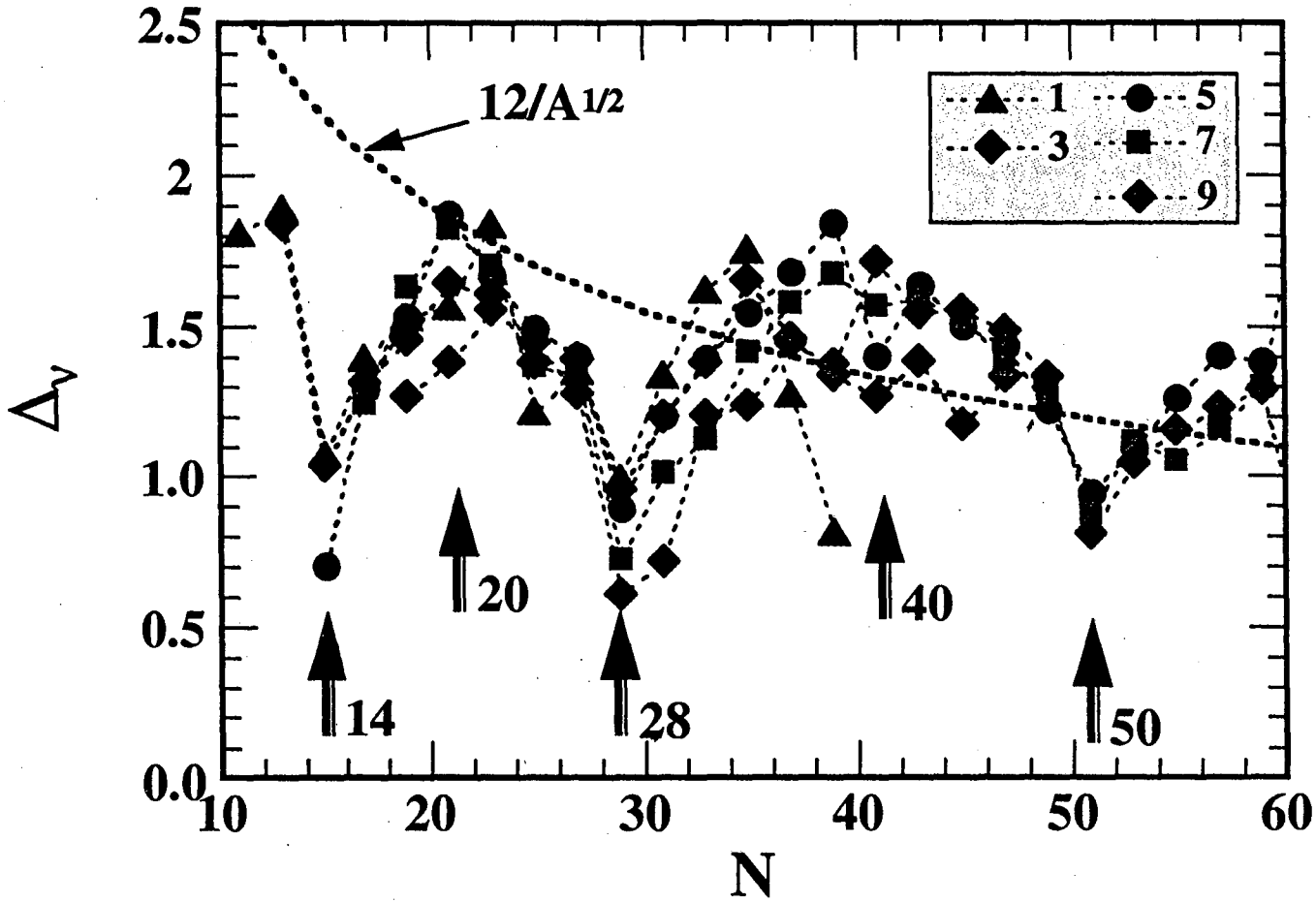
2.5
2
1.5
1.0
0.5
0.0
10
20
30
40
50
60
N
$\Delta_V$
$12/A^{1/2}$
1
5
3
7
9
14
20
28
40
50

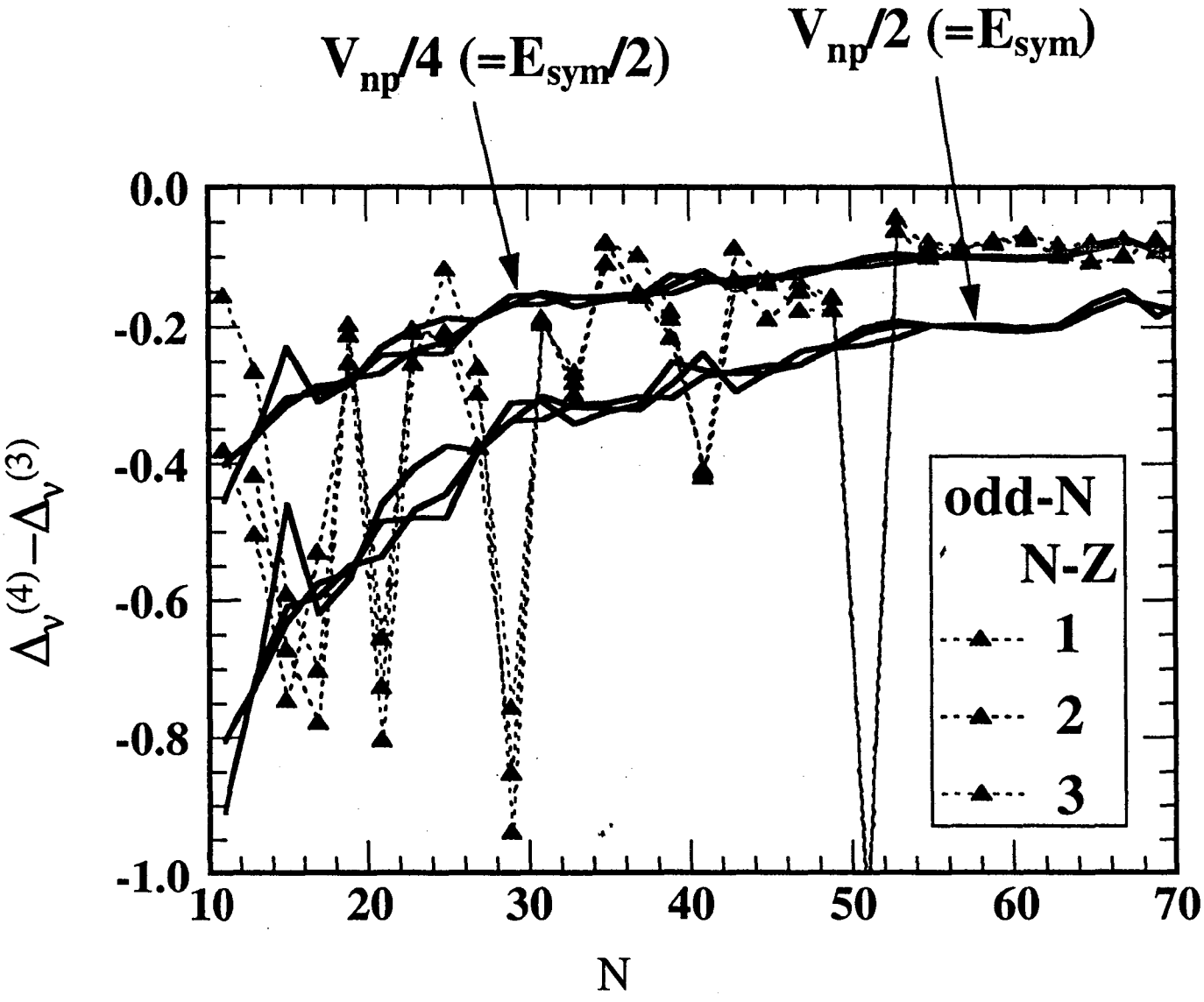
$V_{np}/4$ (=$E_{sym}/2$)
$V_{np}/2$ (=$E_{sym}$)
0.0
-0.2
-0.4
-0.6
-0.8
-1.0
10
20
30
40
50
60
70
N
$\Delta_\nu^{(4)} - \Delta_\nu^{(3)}$
odd-N
N-Z
1
2
3

M.Riley

# Reaching for the sky with GRETA: how high in spin can nuclei go and what do they do up there ?

# REACHING FOR THE SKY WITH GRETA: HOW HIGH IN SPIN CAN NUCLEI GO AND WHAT DO THEY DO UP THERE?

MARK A. RILEY
FLORIDA STATE UNIVERSITY

Physica Scripta, Vol. 10A, 13–20, 1974

# Some Current Themes in Nuclear Research

A. Bohr

The Niels Bohr Institute, University of Copenhagen, Denmark

B. R. Mottelson

Nordita, Copenhagen, Denmark

*Received July 3, 1974*

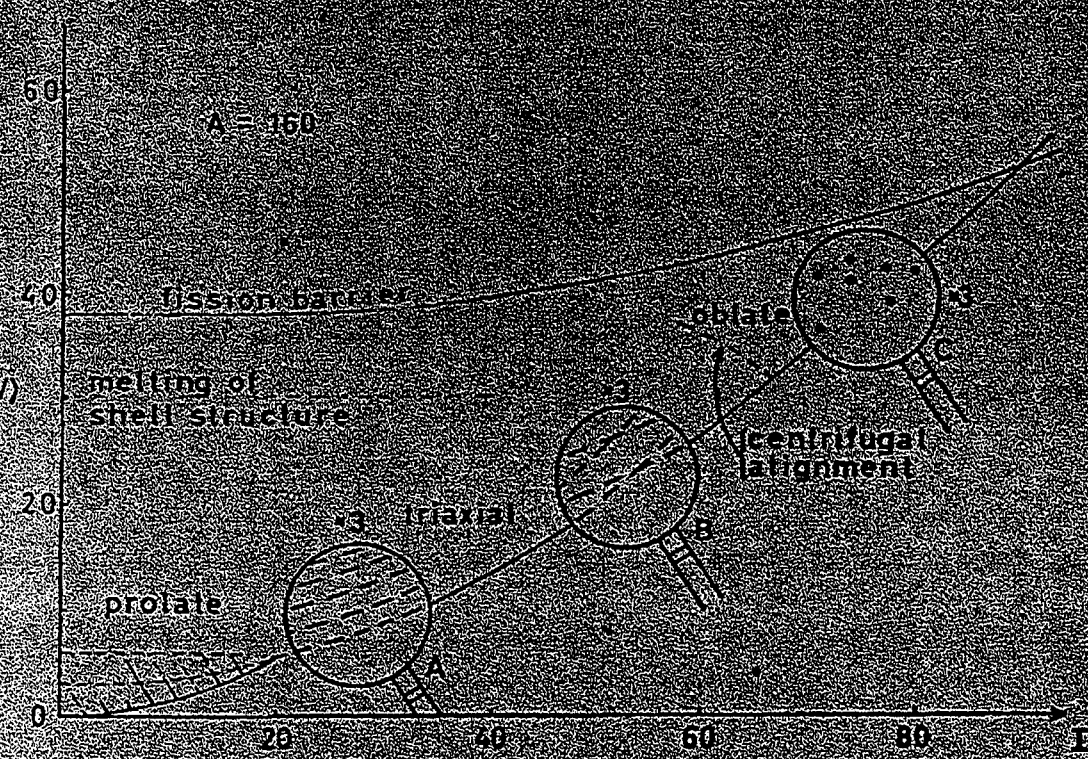


*Fig. 11.* Nuclear phases a a function of angular momentum and excitation energy (schematic).

The picture sketched in Fig. 11 is admittedly highly conjectural; however, with the ingenious experimental approaches that are being developed, we may look forward with excitement to the detailed spectroscopic studies that will illuminate the behavior of the spinning quantized nucleus.



Riley 09 25GM

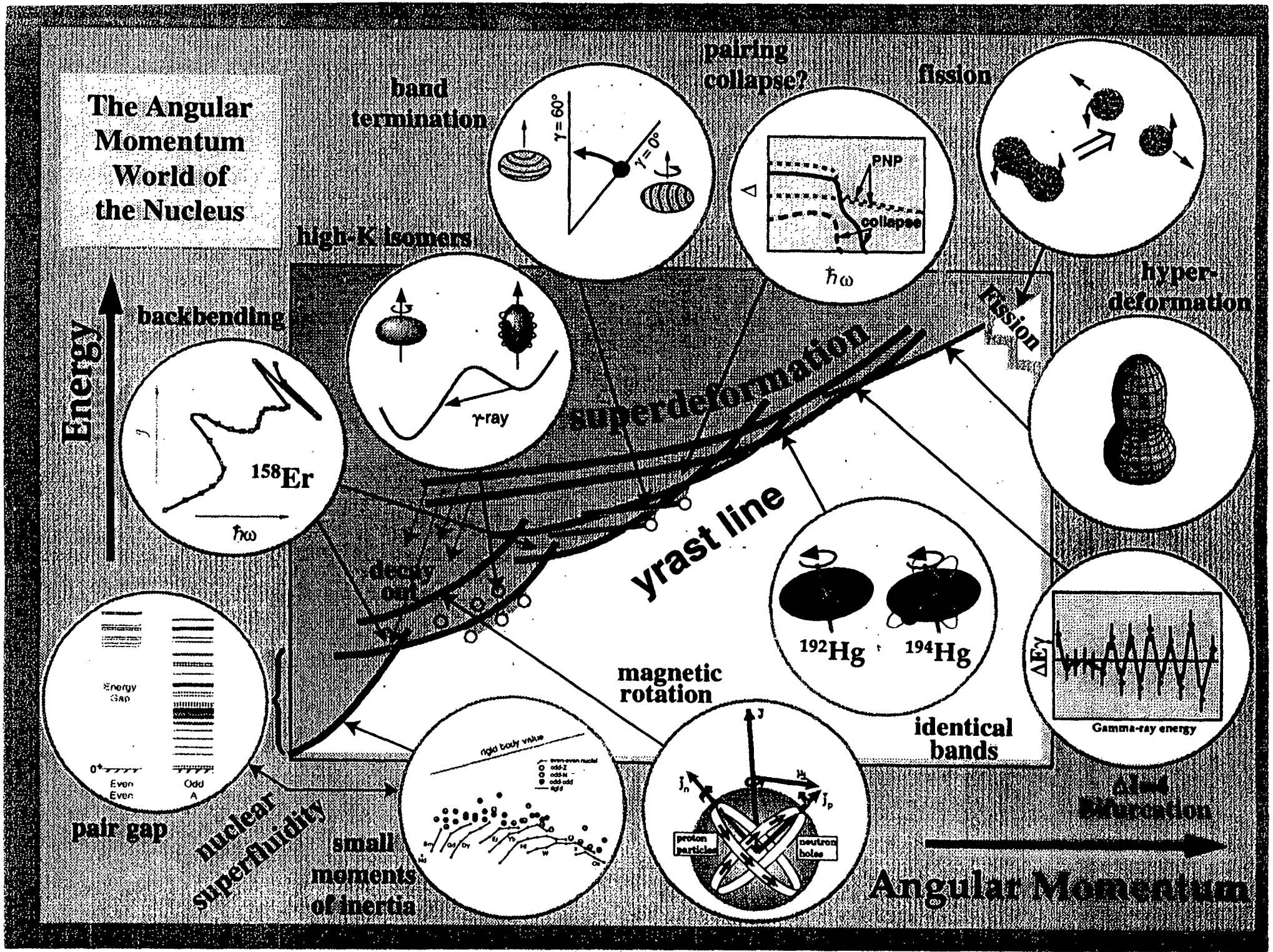
The Angular Momentum World of the Nucleus
band termination
pairing collapse?
fission
high-K isomers
backbending
Energy
superdeformation
Fission
hyper-deformation
yrast line
decay out
magnetic rotation
identical bands
pair gap
nuclear superfluidity
small moments of inertia
Angular Momentum
γ=60°
γ=0°
PNP
collapse
ħω
γ-ray
158Er
192Hg
194Hg
Energy Gap
Even Even
Odd A
rigid body value
proton particles
neutron holes
Gamma-ray energy

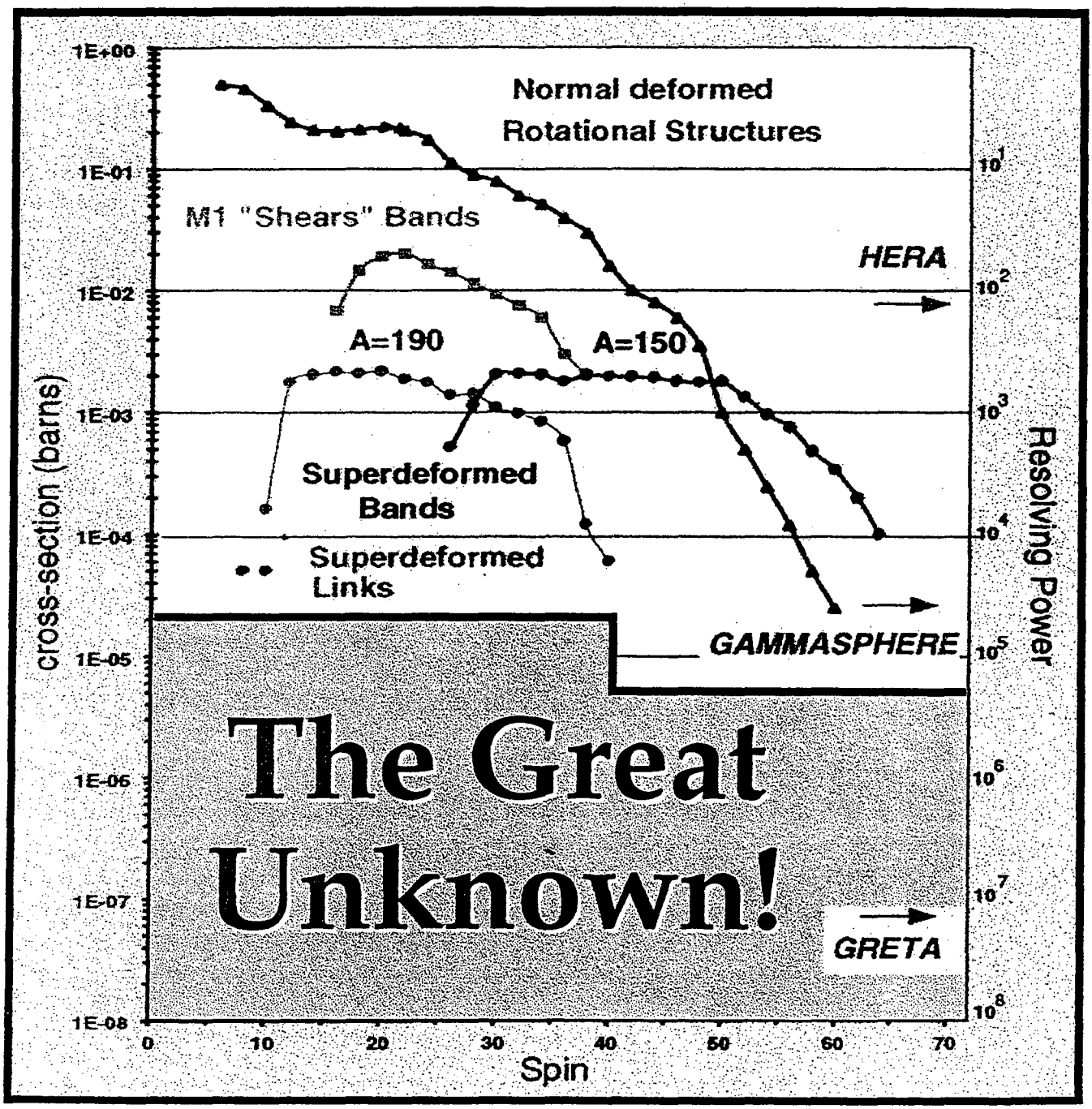
Normal deformed
Rotational Structures
M1 "Shears" Bands
HERA
A=190
A=150
Superdeformed
Bands
Superdeformed
Links
GAMMASPHERE
GRETA
The Great
Unknown!
cross-section (barns)
Resolving Power
Spin
1E+00
1E-01
1E-02
1E-03
1E-04
1E-05
1E-06
1E-07
1E-08
0
10
20
30
40
50
60
70

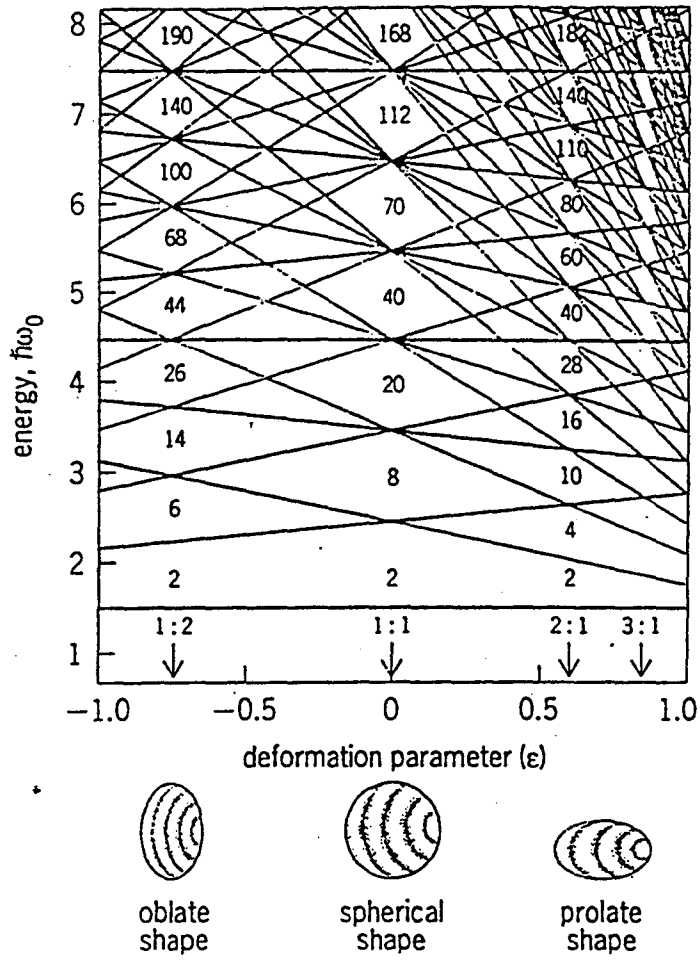


SD has been good to us!

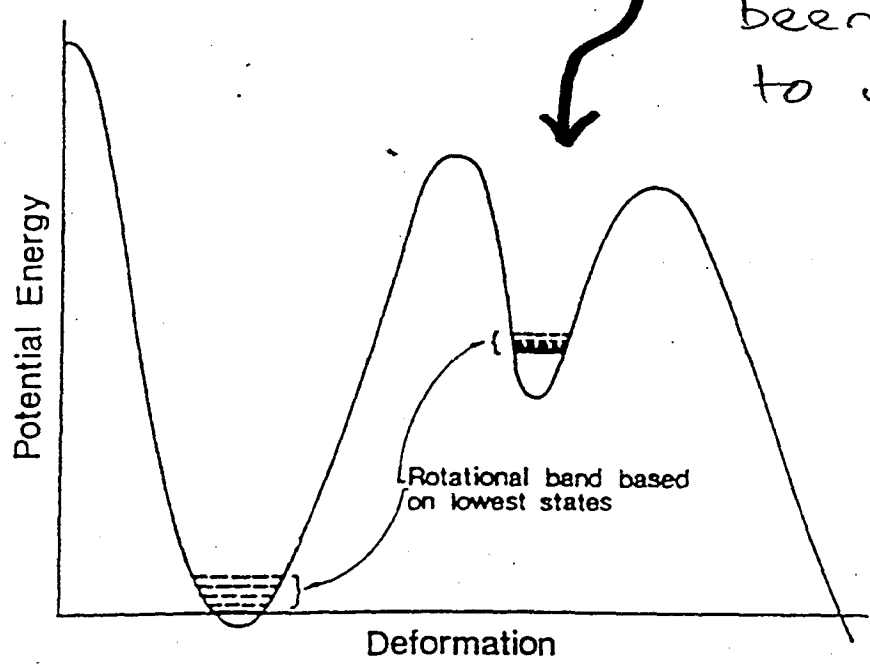

# $^{152}$Dy : A "Doubly Magic SD Nucleus."

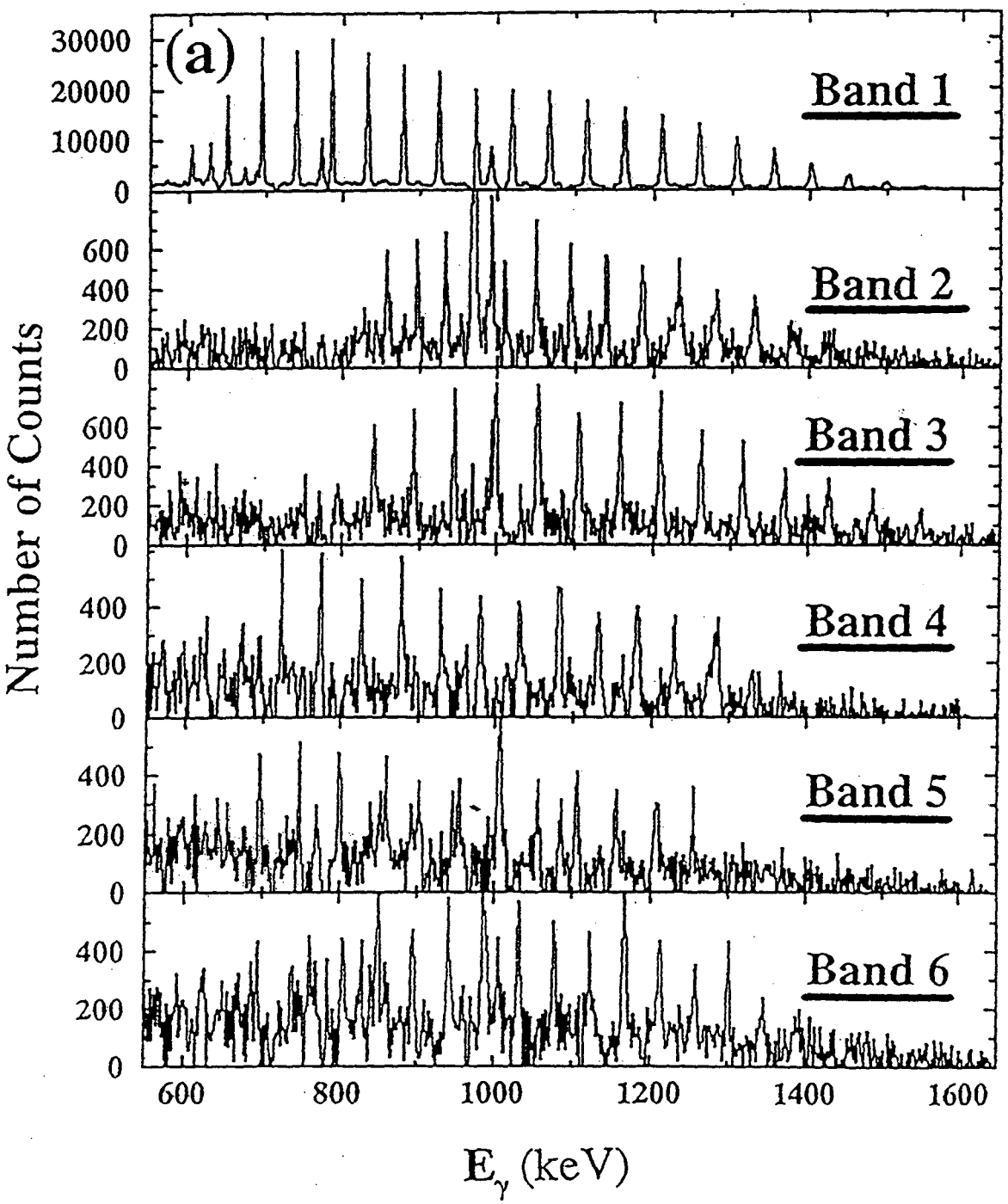


EUROGAM - LIVERPOOL GROUP

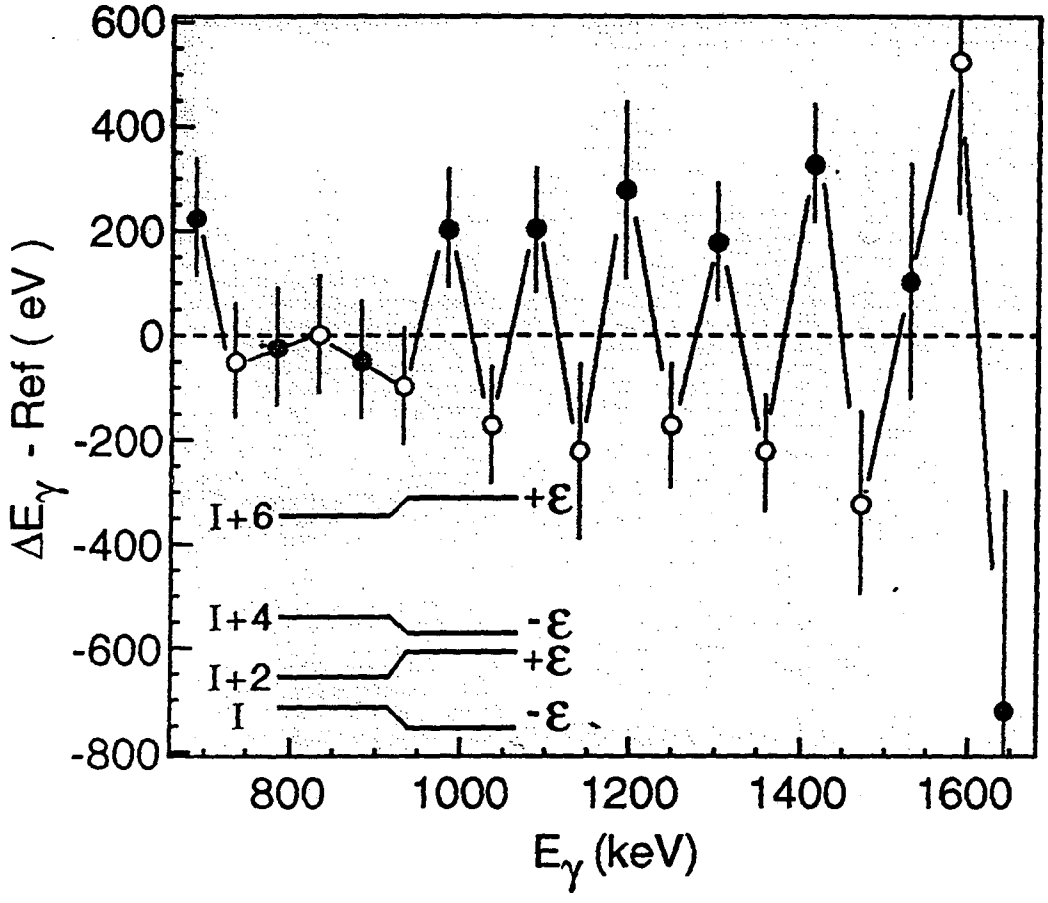


$E_\gamma$ shifts of 1 in ~ 6000 ▽ ○

$E_x$ " " 1 in ~ $10^{-6}$ ▽ ○

Ben: "a revelation"



Riley 02 19KF

"DISCOVERY HIGHLIGHTS OF THE LAST 5 YEARS"

PHYSICS TODAY DEC 91

# A LESSON IN HUMILITY

Daniel Kleppner

If you should suddenly feel the need for a lesson in humility, try forecasting the future of physics. I acquired this little bit of wisdom rather painfully a few years ago when fate tossed me onto the Brinkman committee—one of those panels that is assembled in the US roughly once a decade to survey physics. To prepare for the task, I looked into the previous survey to see how well it had done in my pet field of atomic physics. The performance was unimpressive. Apparently nobody noticed that the laser was about to revolutionize atomic physics and propel optics into the mainstream of physical science. Single-particle traps, clusters, high-resolution scattering and lots of other advances were also missed. My gorge rising against the clods who did my field such an injustice, I looked up the list of members of the atomic physics panel. Smack in the middle was my own name.

When you get down to it, about the only thing scientists can forecast with much accuracy is an eclipse. Understanding this, veteran science forecasters invariably qualify their discussions with some cautionary statement to the effect that because the most exciting discoveries are unpredictable, their predictions cannot begin to do justice to the glorious potential of their particular fields. Such a disclaimer allows one to exaggerate while appearing to display a becoming humility. Nevertheless, scientific discoveries generally do exceed expectations. By way of evidence for this, note that although it is hardly more than five years since the last physics survey—the Brinkman report—there is already an impressive list of advances that we either underestimated or simply failed to foresee. One can view this as evidence that physicists are shortsighted or that nature is inexhaustible. Naturally I vote for the latter. To support my point, here is a list of some things that we missed.

*High-T$_c$ superconductivity.* The discovery of high-temperature superconductivity by two scientists with an apparently eccentric interest in a totally unfashionable material—the copper oxides—is already a legend. It confirms the great tradition of individual scientists' pursuing their own goals in their own way and demonstrates that miracles in science really occur now and then. It also demonstrates that apparently simple systems can be subtle and complex, for five years and 18 000 papers later, the basic physics of high-temperature superconductivity remains an enigma and the early visions of levitated trains and superconducting power lines remain unfulfilled. Nevertheless, recognition of the two-dimensional nature of the underlying superconducting structure has led to an understanding of thin film behavior, and this has opened the way to practical thin film devices. Achieving the large currents needed for more general applications requires overcoming the limitations of the underlying two-dimensional superconducting structure. One hopes for the best.

*Supernova 1987A.* Since supernovae light up in the Milky Way approximately once every 300 years, the occurrence in 1987 can be described as astounding but not miraculous. However, the detection of 15 of the roughly $10^{57}$ neutrinos that were ejected as the star's core collapsed, traveled for 170 000 years and arrived within a few seconds of one another approaches a miracle—a windfall from the search for proton decay in Japan and the US. The agreement between the neutrino signals and the theory for the supernova's explosive collapse is a triumph of neutrino physics. The supernova now glows with light powered from the radioactive decay of cobalt-57, though in its few short years its luminosity has dropped dramatically. Here again the measurements are in extraordinary agreement with the theoretical scenario, and this story is heading straight for the textbooks.

*Atom cooling and atom optics.* It is hardly news that light can push around atoms, but nobody seemed to recognize that the interplay of optical fields with the internal dynamics of an atom would make it possible to cool atoms to temperatures of a few microkelvin, suspend them in space, toss them around like tennis balls or let them collide in a new world of ultraslow motion. A fountain of such cold atoms has already produced a resonance signal 50 times sharper than that in the best atomic clock. Out of this line of research has grown the discipline of atom optics, loosely centered around the interaction of atomic waves with mechanical structures, optical fields or both. Mirrors made of light have reflected beams of atoms, and a new art of interferometry has been created based on coherent beams of atoms.

*Buckyballs.* The Brinkman report paid suitable homage to clusters—those small chunks of matter, somewhere between individual atoms and solid structures, that can be generated in supersonic beams—but the anomalous peak in the carbon spectrum at mass 60 had yet to be discovered. Observation of $C_{60}$ and identification of its soccer ball structure—the "buckyball"—led to a rumble of excitement, and when it was discovered that the material could be made in bulk, that in fact it has been around since time immemorial as a major component of soot, the rumble turned into a roar. Chemistry has a new building block, and the excitement is reminiscent of the excitement that followed the discovery of high-temperature superconductivity. $C_{60}$ is only one member of a novel class of molecules called the fullerenes. The

**Daniel Kleppner** is the Lester Wolfe Professor of Physics and associate director of the Research Laboratory of Electronics at MIT.



© 1991 American Institute of Physics

opportunities for chemistry and materials science created by the discovery of this new state of carbon are, for now, beyond comprehension.

*Complexity, chaos and nonlinear dynamics.* Given that physicists generally esteem simplicity, it is remarkable that the study of complexity has moved to center stage, but such are the ironies of nature. Complexity encompasses everything from the growth of crystals to the dynamics of neural systems. Its central theme—the elaboration of forms from the repetition of simple operations—is being recognized as a fundamental organizing principle of nature. Several commentators have used this column to spread the good tidings of complexity (Leo P. Kadanoff in March 1991, Philip W. Anderson in July, and I in August). But the term was not even mentioned in the last physics survey. Nonlinear dynamics has also moved to center stage. Its origins go back to Henri Poincaré's work at the turn of the century; the origins of chaos likewise go back for several decades. Only in the past few years, however, have nonlinear dynamics and chaos theory entered the mainstream of physics. The last physics survey hardly noticed that classical mechanics was on the threshold of a renaissance.

*Superdeformed nuclei.* Although their existence was anticipated by theory, until they were discovered experimentally it did not seem likely that nuclei really could be stable in sausage-like geometries while spinning so fast that they are on the verge of flying apart. However, when calcium-48 and palladium-108 ions collide they can fuse to form a dysprosium nucleus that boils off a few neutrons and settles down into such a state of $^{152}$Dy. The ratio of major to minor axes is approximately 2:1, and the angular momentum is extraordinary—approximately $60\hbar$. The $^{152}$Dy methodically emits a series of gamma rays, producing a spectrum so regular that it is almost picket fence. When the angular momentum is about $26\hbar$, the $^{152}$Dy suddenly flips its shape and behaves like a conventional nucleus. Similar behavior has now been discovered in many other nuclei, so the phenomenon is by no means isolated. On the contrary, superdeformed nuclei are now recognized as a new state of nuclei, an unexpected happy event in the nuclear family.

*Large-scale structure of the universe.* The uniformity of the early universe has been one of the more comforting thoughts of modern cosmology. Measurements by the Cosmic Background Explorer, for instance, gave spectacular confirmation of the blackbody spectrum and isotropy of the cosmic microwave radiation. Aside from a small correction due to local motion, the radiation was uniform across the sky to better than 1 part in $10^4$. In view of this uniformity, the recent discovery of large-scale structures of the universe—voids in the distribution of galaxies, sheets of galaxies and large, foam-like structures—was totally unexpected. Possibly the structures bear the signature of dark matter, or possibly the present scenario for the evolution of fluctuations in the early stages of the universe is completely wrong. In any case, our view of the universe has altered in the last few years.

*Mesoscopic physics.* A new world of physics has been discovered in mesoscopic systems, structures that are large on the atomic scale but so small on the laboratory scale that quantum effects are important. When the distance needed for an electron to exchange energy becomes large compared with the size of the system, electron transport turns into a coherent process, and the transmission coefficient that determines the conductance is determined by a sum of Feynman paths over all the random paths through the system. In this regime, any change in phase leads to a macroscopic change in conductance. If some parameter such as the magnetic field is changed, the conductance—no matter what its size—fluctuates by a universal value, $-e^2/h$. Such universal conductance fluctuations can generate $1/f$ electronic noise due to the migration of one atom. In the mesoscopic world, the charge of a single electron can alter the potential of an electrode enough to cause macroscopic changes in behavior. Out of this simple idea have already emerged a single-electron "transistor" and other single-electron devices.

This account hardly exhausts the list of surprises from physics in the last five years, but it should at least suggest Nature's abundance. The lesson is that scientific discoveries invariably exceed the power of our imaginations. Learning this over and over again should school us in humility, though it is more likely to leave us feeling exhilarated than humble. In either case, the lesson can help us to keep up our spirits in these times of deferred hopes and faltering institutions.

• • •

*I thank my numerous colleagues who helped me to prepare this column by sharing their wisdom and their excitement over these advances and discoveries.* ■

BEN: "One of the gems of the subject"
Spt c

## THEORETICAL ATTEMPTS TO EXPLAIN IDENTICAL BANDS

- Weak Coupling and Rotational Alignment
- Strong Coupling Limit
- Particle Rotor Model
- Decoupled Pseudo-Spin
- Interacting Boson-Fermion Model
- Deformed Shell Model
- Cranked Hartree-Fock
- Cranked Relativistic Mean Field
- Mean Field Configuration Mixing
- Fermion Dynamical Symmetry Model
- Pseudo-SU(3)
- Supersymmetric Models

## NO SATISFACTORY ANSWER YET!

- It seems some very subtle cancellations are taking place or more interestingly that these degeracies are the result of some underlying symmetry not yet recognized!

HEROIC

BEN: ⇒ pseudo-spin alignment?
Sp 93

NON-HEROIC
- pairing - def. cancella
- out of numerical cancellations a heroi

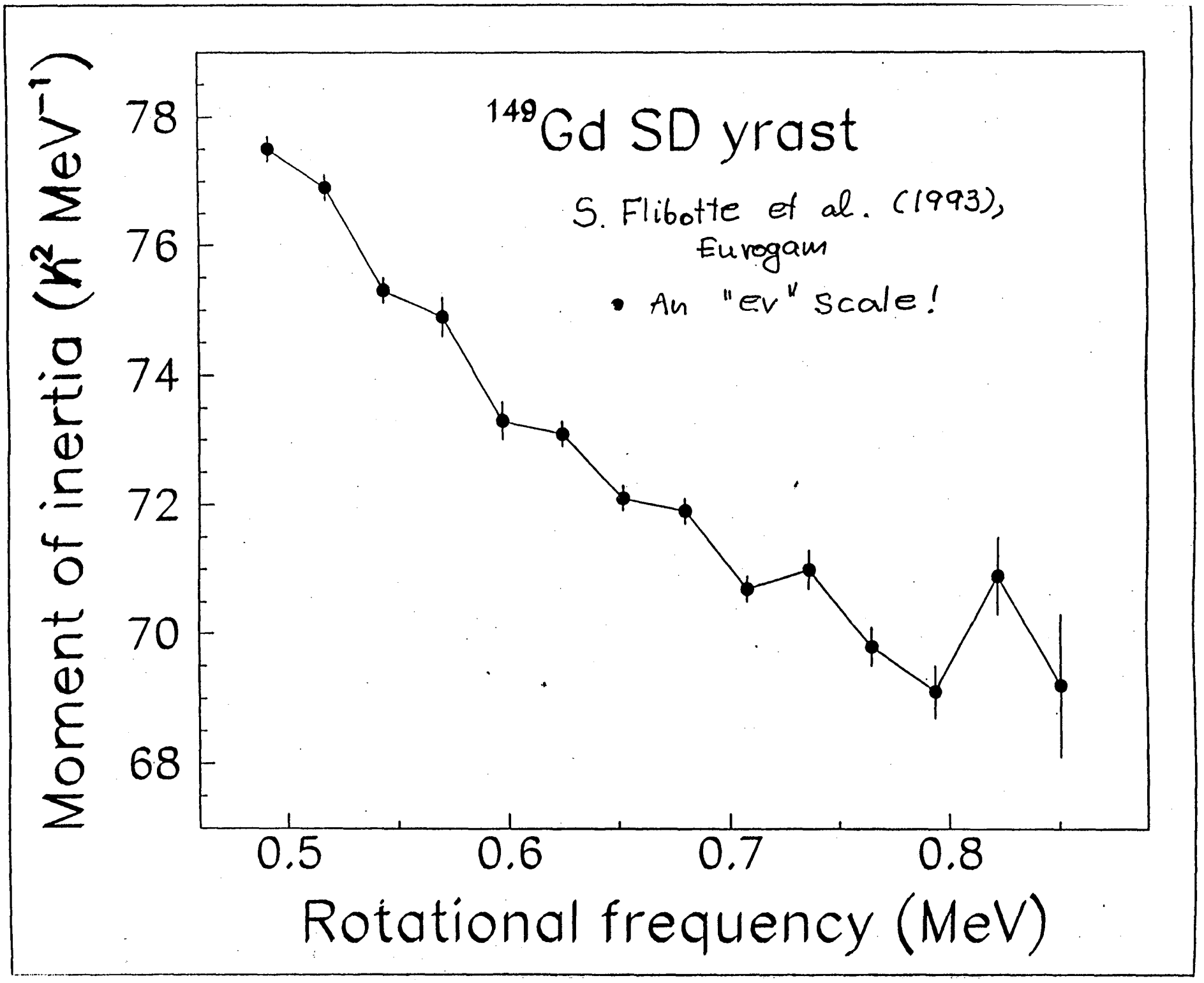
$^{149}$Gd SD yrast
S. Flibotte et al. (1993), Eurogam
• An "ev" scale!
Moment of inertia ($\hbar^2$ MeV$^{-1}$)
78
76
74
72
70
68
0.5
0.6
0.7
0.8
Rotational frequency (MeV)

Haslip et al (97)

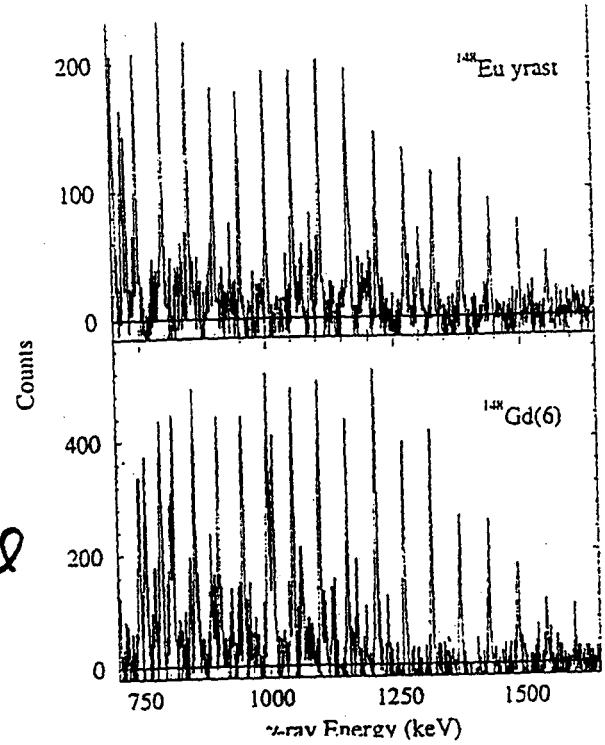


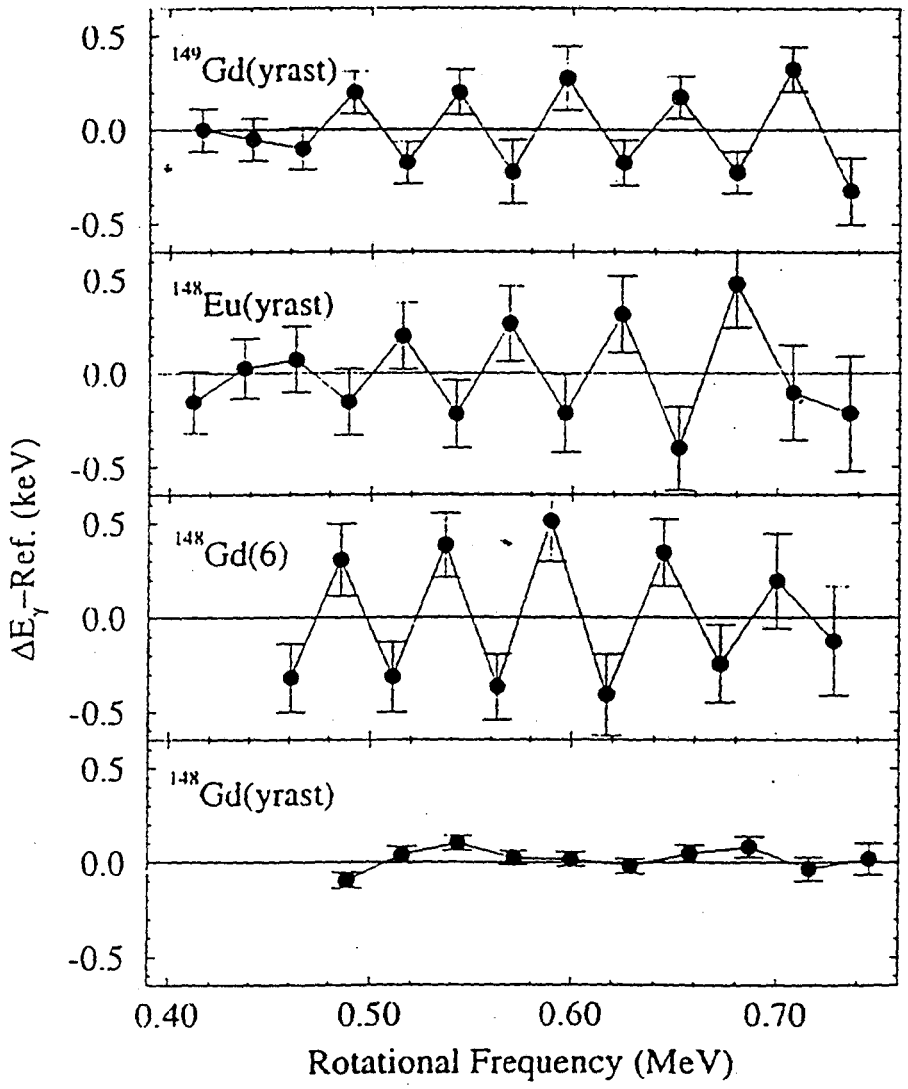


Reference: one thing the other bands are useful for!

FIG. 3. Staggering plots for the SD bands $^{149}$Gd(yrast), $^{148}$Eu(yrast), $^{148}$Gd(6), and $^{148}$Gd(yrast). For $^{149}$Gd(yrast), only the data in the same frequency range as the other bands

# Δ =4 Bi urcation in den ic l Superdeformed Bands

ΔI=4 bifurcation, in which alternate levels in a super-deformed band are perturbed by one part in a million, in opposite directions.

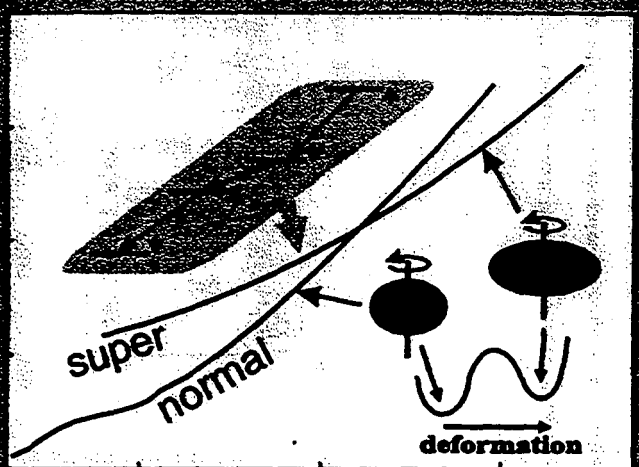


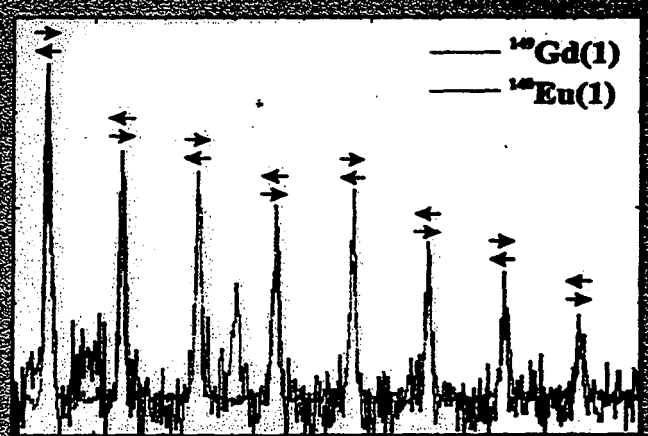


The transitions in these neighboring nuclei are nearly identical, but the direction of the tiny shift is reversed.

When the small shifts in three bands are plotted as a function of spin, they show a remarkable correlation which is not fully understood at this time.

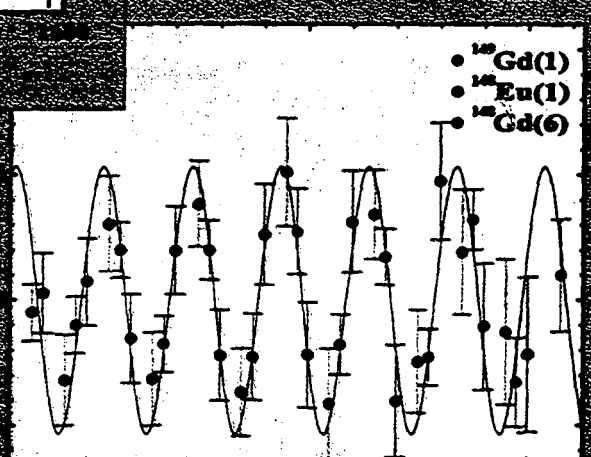

SD DECAY

NOLAN, BECK & FOSSAN ANNU. REV. NUCL. PART. SCI 1994, 45:561



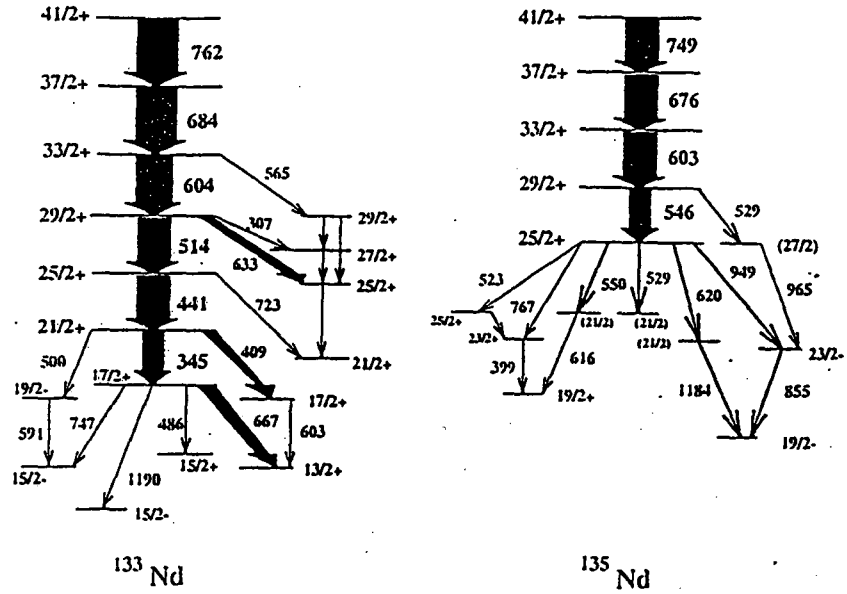


*Figure 21* The linking transitions found between super- and normal-deformed states in (*a*) $^{133}$Nd (data from GASP) and (*b*) $^{135}$Nd (data from GAMMASPHERE).

BAZZACCO et al PRC 49 (94) R2281

DELAPLANQUE et al PRC 52 (95) R2302

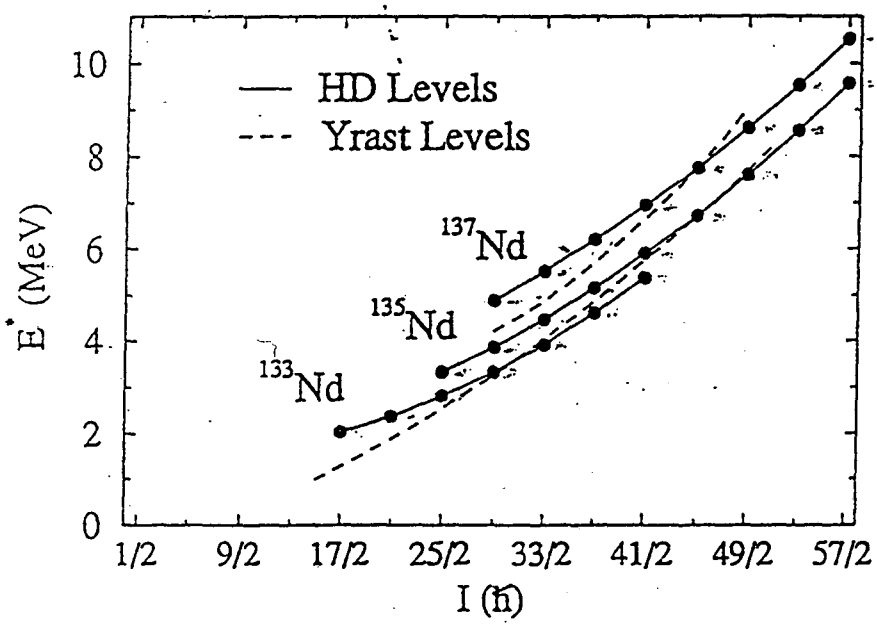

# Decay Out of the High-Spin Superdeformed Minimum

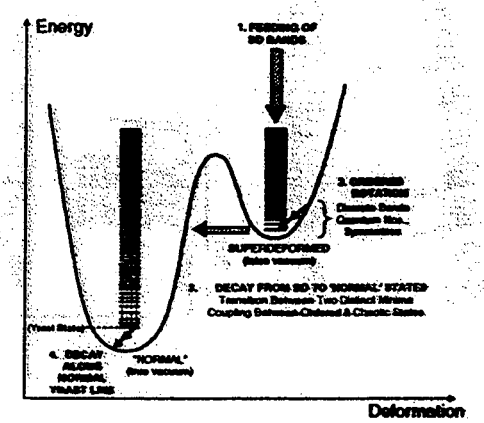


Nuclei can have an excited minimum (or false vacuum) in the potential energy at large deformation. Superdeformed (SD) states in the minima decay by tunneling through a barrier, aprocess possible only in very small objects governed by quantum mechanics.

Khoo et al. PRL 76, 1583(96)

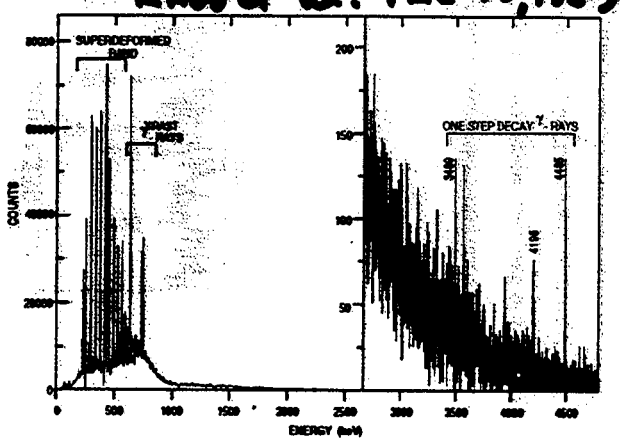


Spectrum (above) showing the weak direct one-step discrete high energy (3.4-4.5 MeV) decays linking the superdeformed and normal deformed minima.

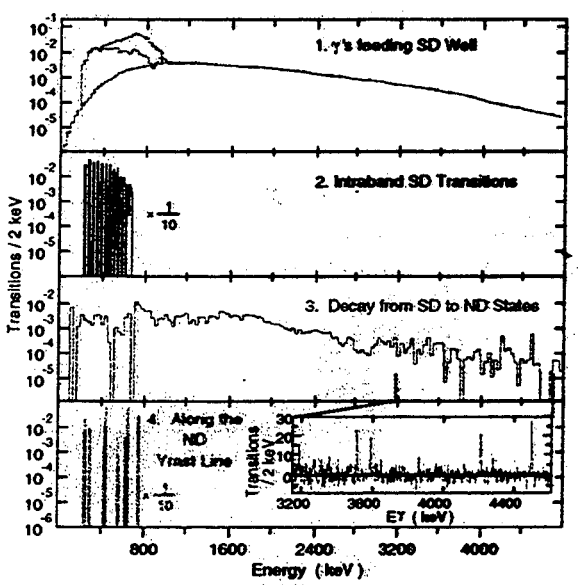


The spectra emitted in the feeding and decay of a superdeformed band show a unique double cycle of chaos-to-order transition.

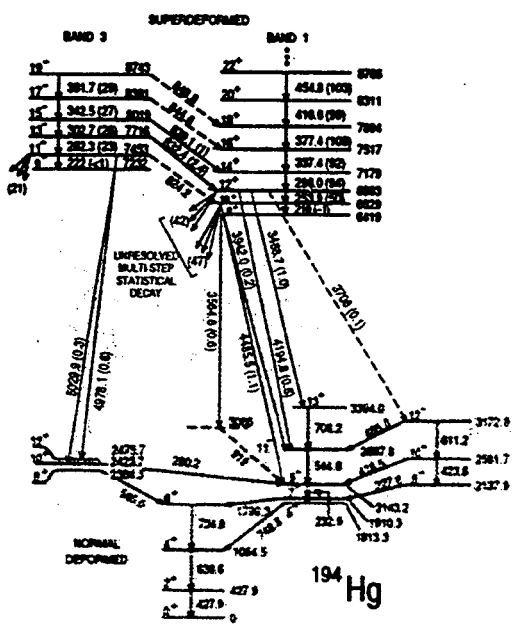


This observation unambiguously defined the excitation energies, spins and probable parities of bands in the A=190 region for the first time.

Tentatively scheduled for 1 April 1998, Physical Review C, Volume 57, Number 4

---

Shell effects in superdeformed minima

P.-H. Heenen, J. Dobaczewski, W. Nazarewicz, P. Bonche, and T. L. Khoo

Recent and planned experiments aiming at the observation of the direct links between superdeformed and normal-deformed structures in the $A$$\sim$190 mass region may offer a unique information on the absolute nuclear binding energy in the 2:1 minima, and hence on the magnitude of shell effects in the superdeformed well. In the present paper, the self-consistent mean-field theory with density-dependent pairing interaction is used to explain at the same time the two-particle separation energies in the first and second wells, and the excitation energies of superdeformed states in the $A$$\sim$190 and $A$$\sim$240 mass regions.

© 1998 The American Physical Society.

---

# Single-Step Linking Transition from Superdeformed to Spherical States in $^{143}$Eu

A. Ataç[1], A. Axelsson[1], I. Bearden[2], M. Bergström[2], B. Herskind[2], J. Nyberg[3], M. Palacz[4,5], J. Persson[1], M. Piiparinen[6], C. Fahlander[3], G. Hagemann[2], S. Leoni[2], M. Lipoglavšek[1,7], P. Nolan[8], E. Paul[8], N. Redon[9], L. Roos[1], G. Sletten[2], K. Tuček[3]

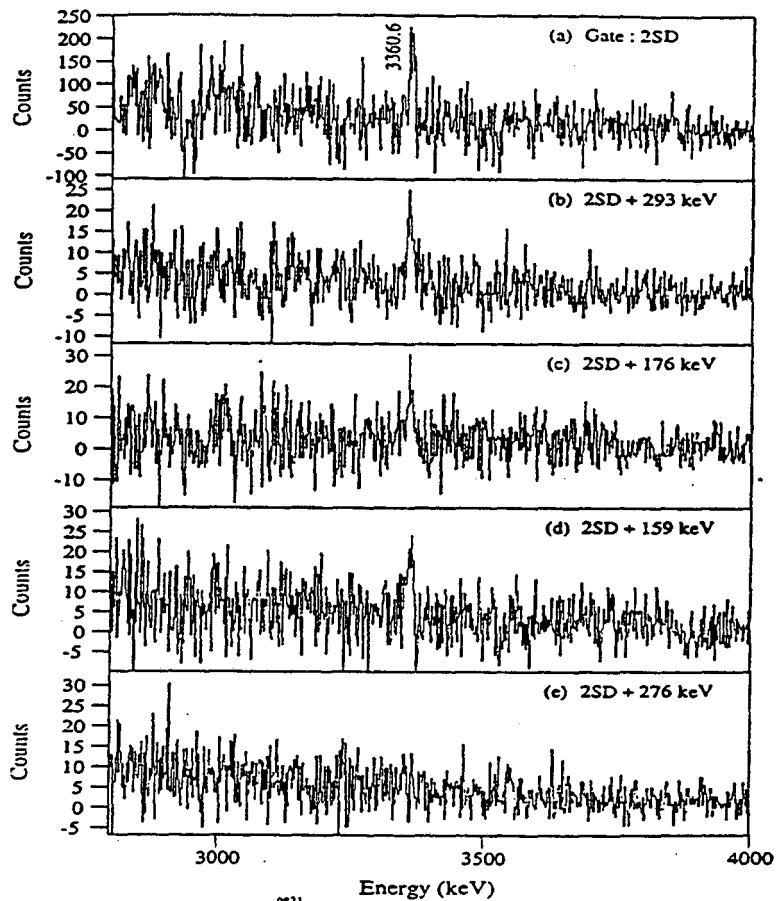


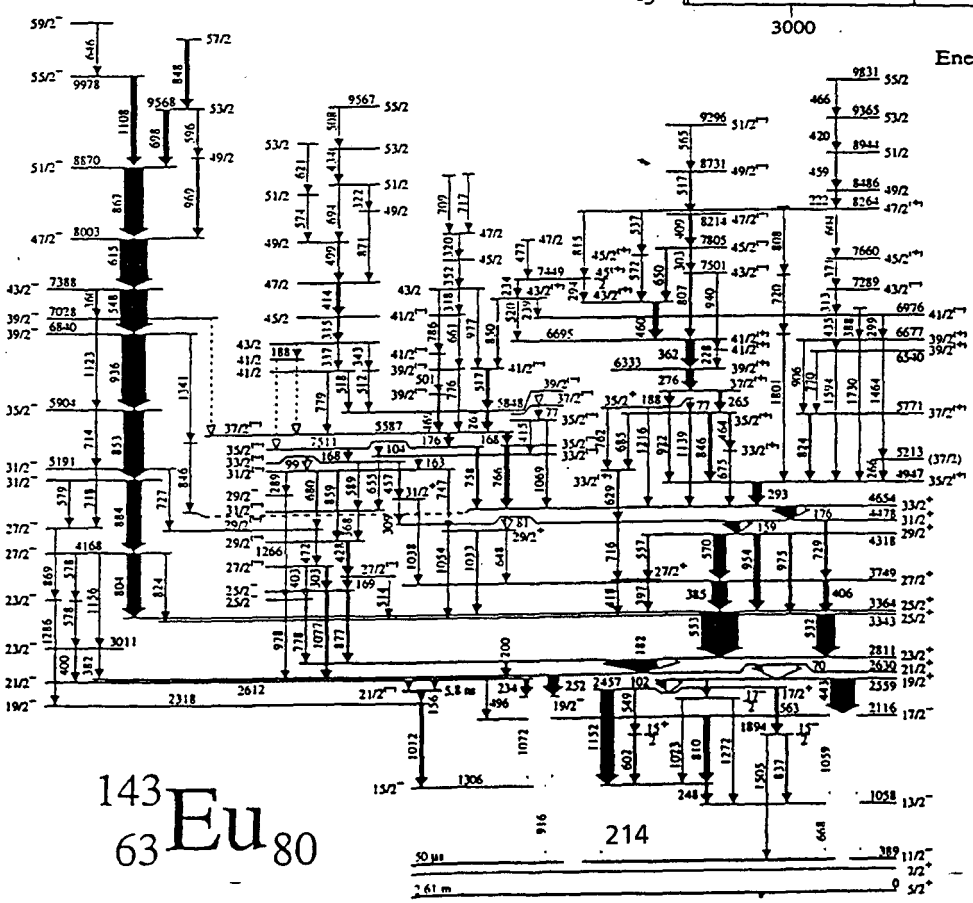

# 194Hg and 192Hg (band−1)

(one/two step decay−out line search)

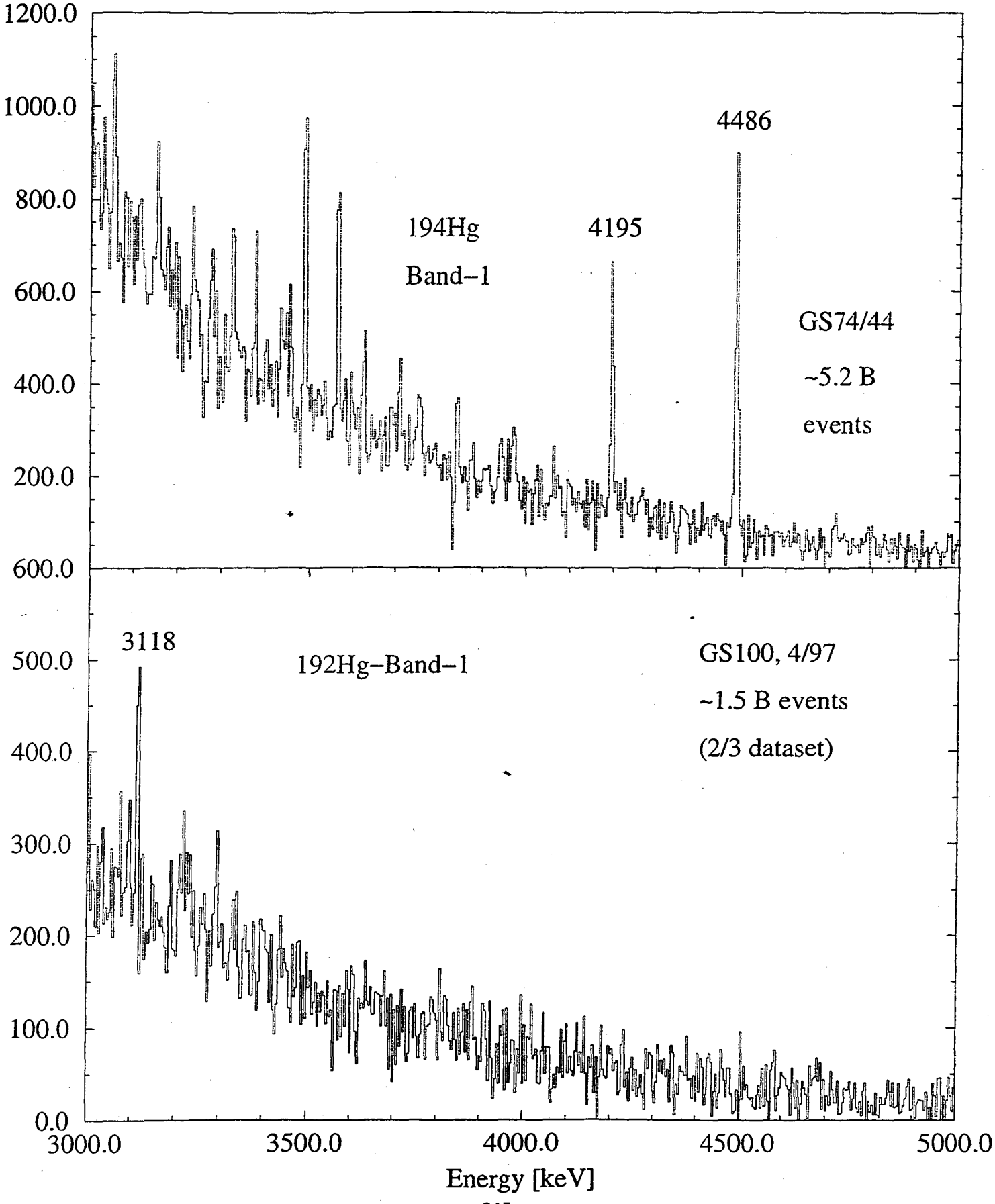

# What about other regions?

60

80

130 ($^{132}$Ce etc)

140 - 150

190 ($^{192}$Hg etc)

In order to say we understand the 2nd minimum we need to the fundamental properties $E_x$, $I^\pi$ etc of the bands

WE NEED GRETA!

# Superdeformed Bands in the A~80 region

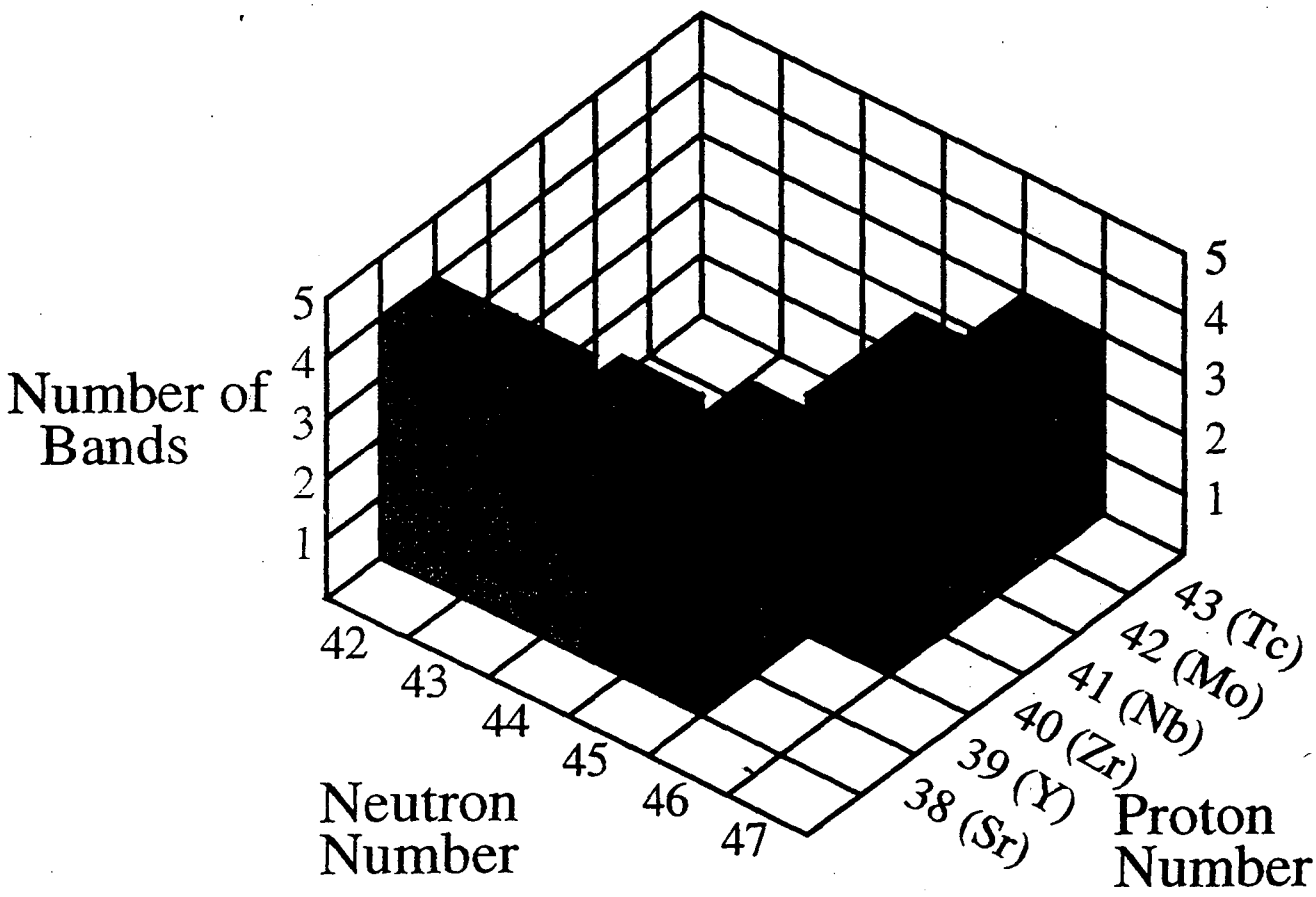

# Superdeformation

## *The Regions of Superdeformation*

Superdeformed bands have been observed throughout the nuclear chart. The moments of inertia, after scaling to $A^{5/3}$, are all similar due to the fact that the shape (deformation) of a SD band is largely independent of the mass. The shell gaps, which define the SD shape, depend on the underlying symmetry of the nucleus, and occur at near-integer axis ratios.

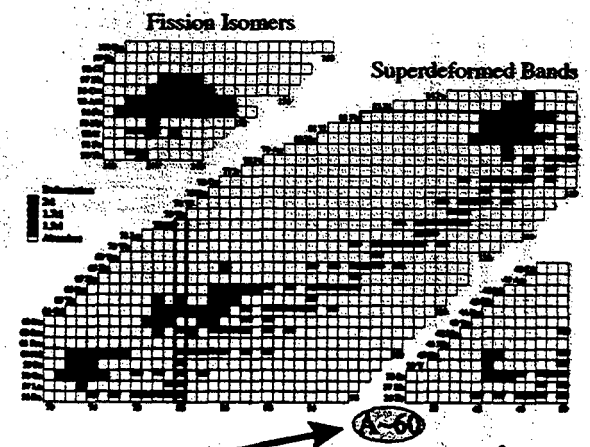


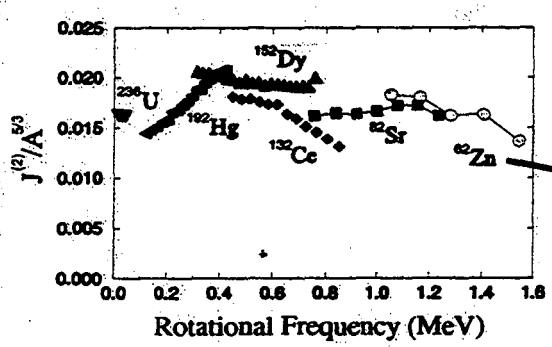


Swensson et al PRL 79 (97)

Recent observation, with Gammasphere, of a new region of superdeformation (N~Z~30) opens up many exciting opportunities, including the possibility to study the most collective states known with a "Shell" model description.

## *Precise Measurement of Superdeformed Band Properties*

RDM is used to determine the lifetimes of SD states at low spins.

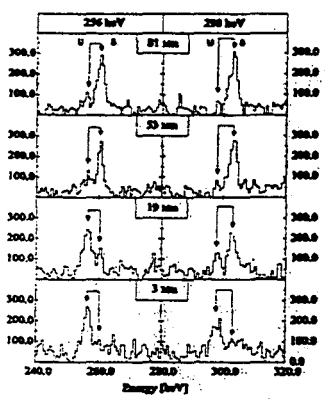

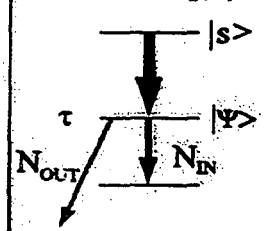


SD bands decay due to a mixing with states in first minimum. To know the extent of this mixing, precise lifetimes (decay probabilities) are required. Such expts. have been carried out with Gammasphere.

WHAT CAN WE LEARN FROM THE LIFETIMES ?

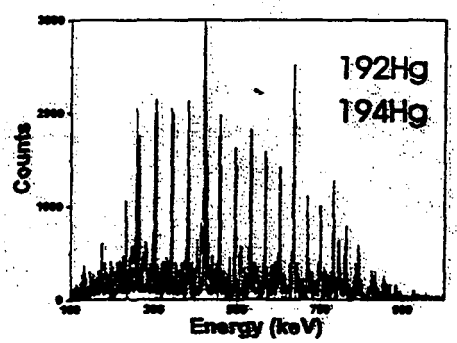


DSAM is used to determine the lifetimes (quadrupole moment, deformation) of nuclear "high-spin" states.

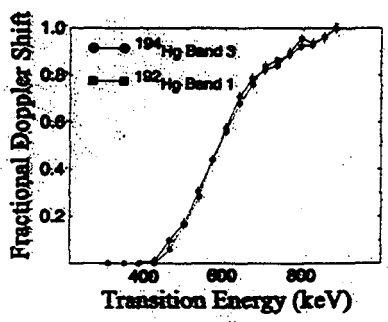


Gammasphere data has shown that SD bands in $^{192}$Hg and $^{194}$Hg not only have the same transition energies (they are "identical bands")(middle figure), but also the same lifetimes, and hence the same deformation. Other precision measurements have been made in A=80, 130, 150 regions.

I. Ragnarsson

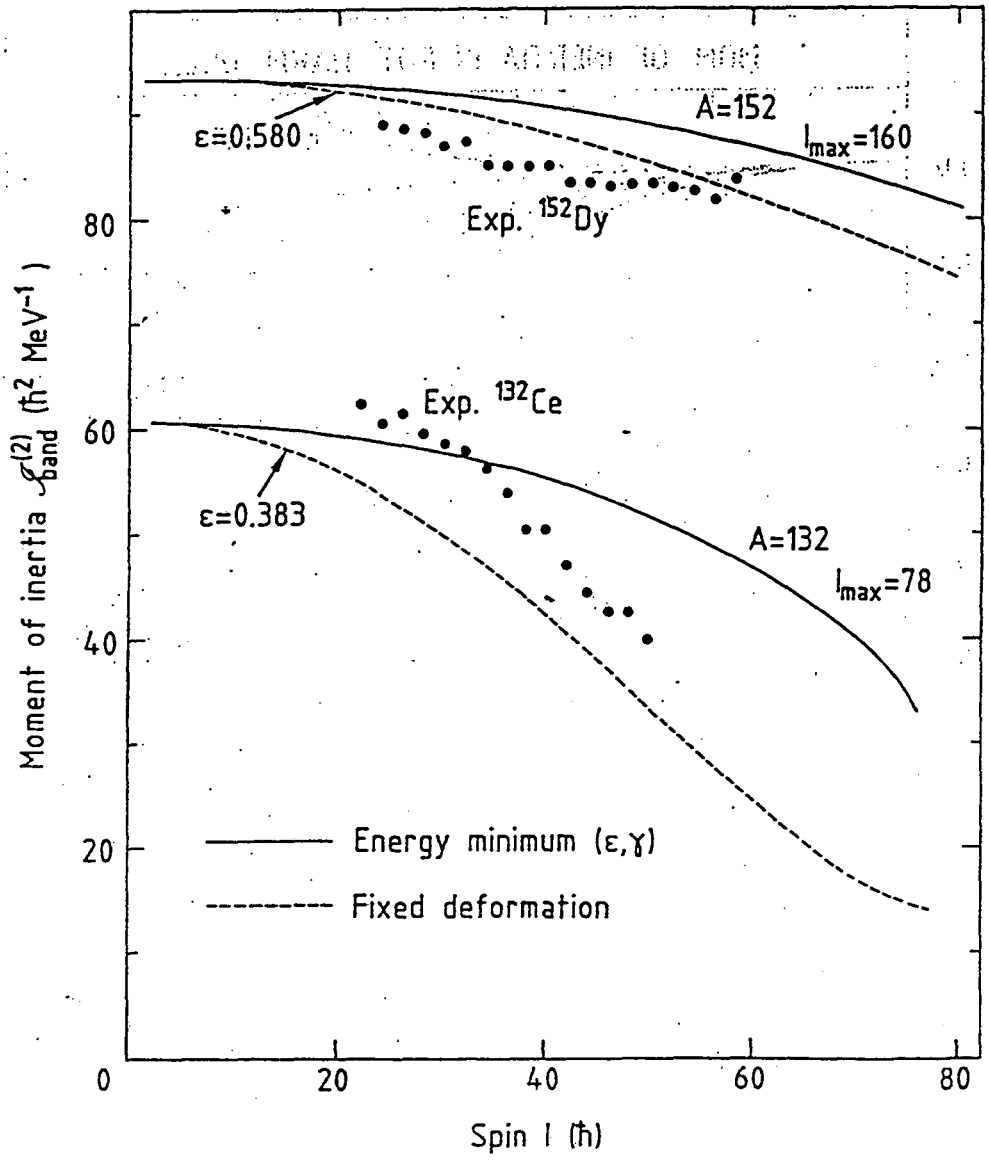


- Figure 3 -

# Light Nuclei (A=20-50)

- Lund group (and others) have been telling us about the wild things that light nuclei can do.
- Beautiful opportunity to test and compare models
  eg. Shell Model ⟷ Mean Field
- But $E_\gamma$'s very high > few MeV
  ⇒ Need high efficiency array
  ⇒ NEED GRETA!

# Quantum Chaos in Nuclei

Garrett 97

Nuclear level repulsion,

Order vs Chaos

Conserved quantum #'s

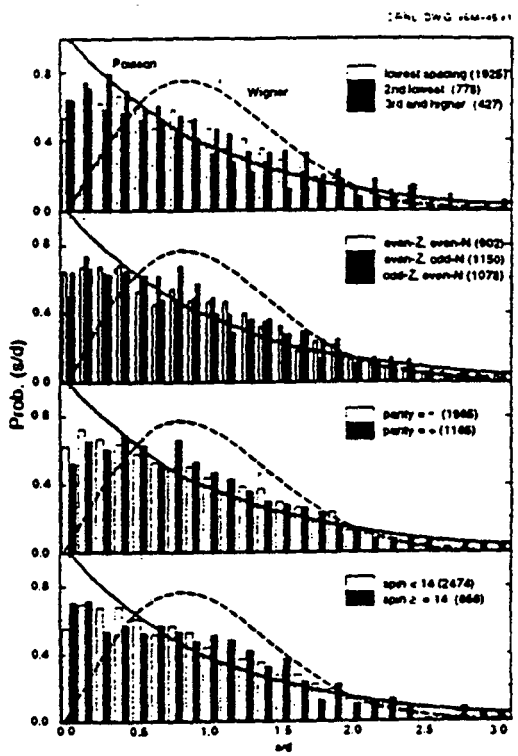


**Figure 1** Level-spacing distributions as a function of excitation energy, nuclear-type, parity, and angular momentum.

Åberg – "ERGODIC" bands
Spectacular new phenomenon!

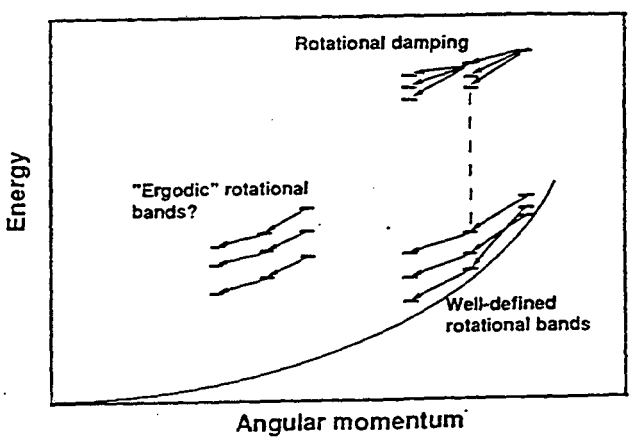


- Well-defined rotational bands:
  -regular states
  -regular decay
- Rotational damping:
  -chaotic states
  -chaotic decay
- "Ergodic" rotational bands:
  -chaotic states
  -regular decay

NORMAL DEF.
WHAT WE CAN DO
WITH ALL THE
BANDS?

$^{163}$Er

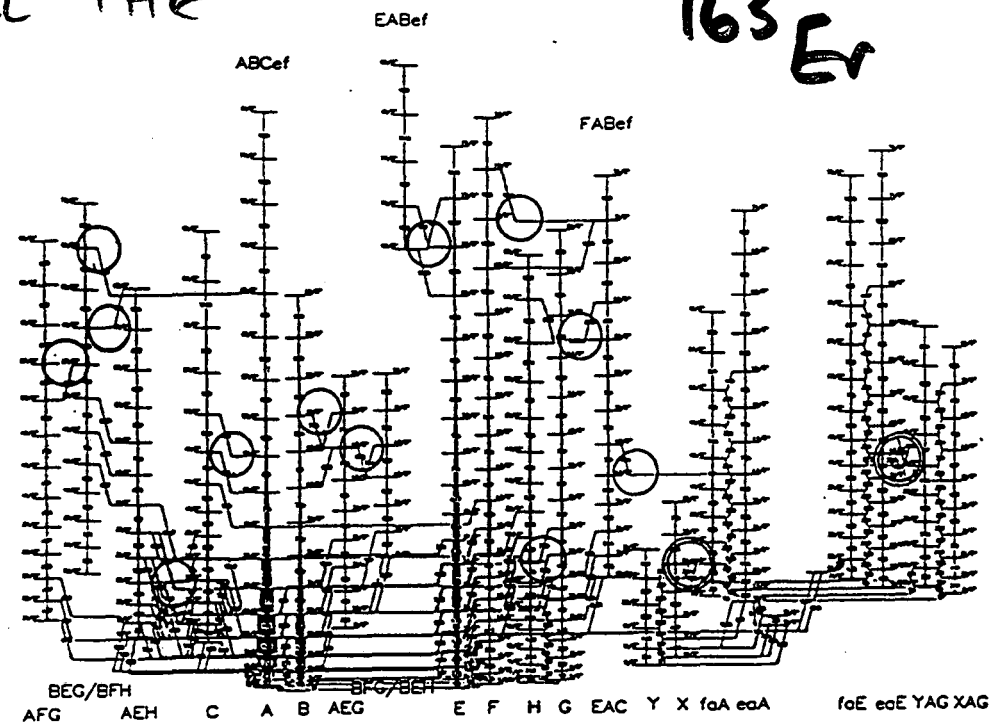


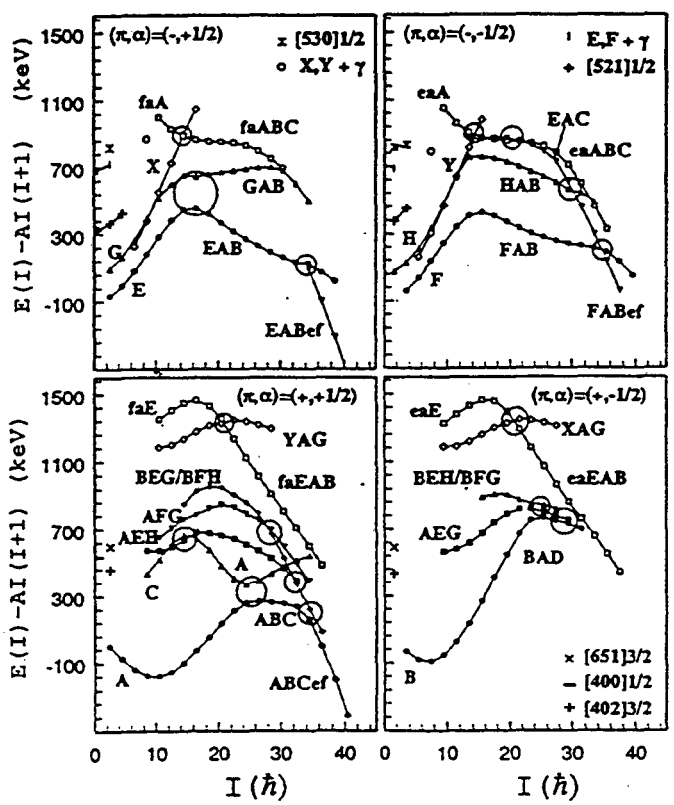


Hagemann et al. 97.

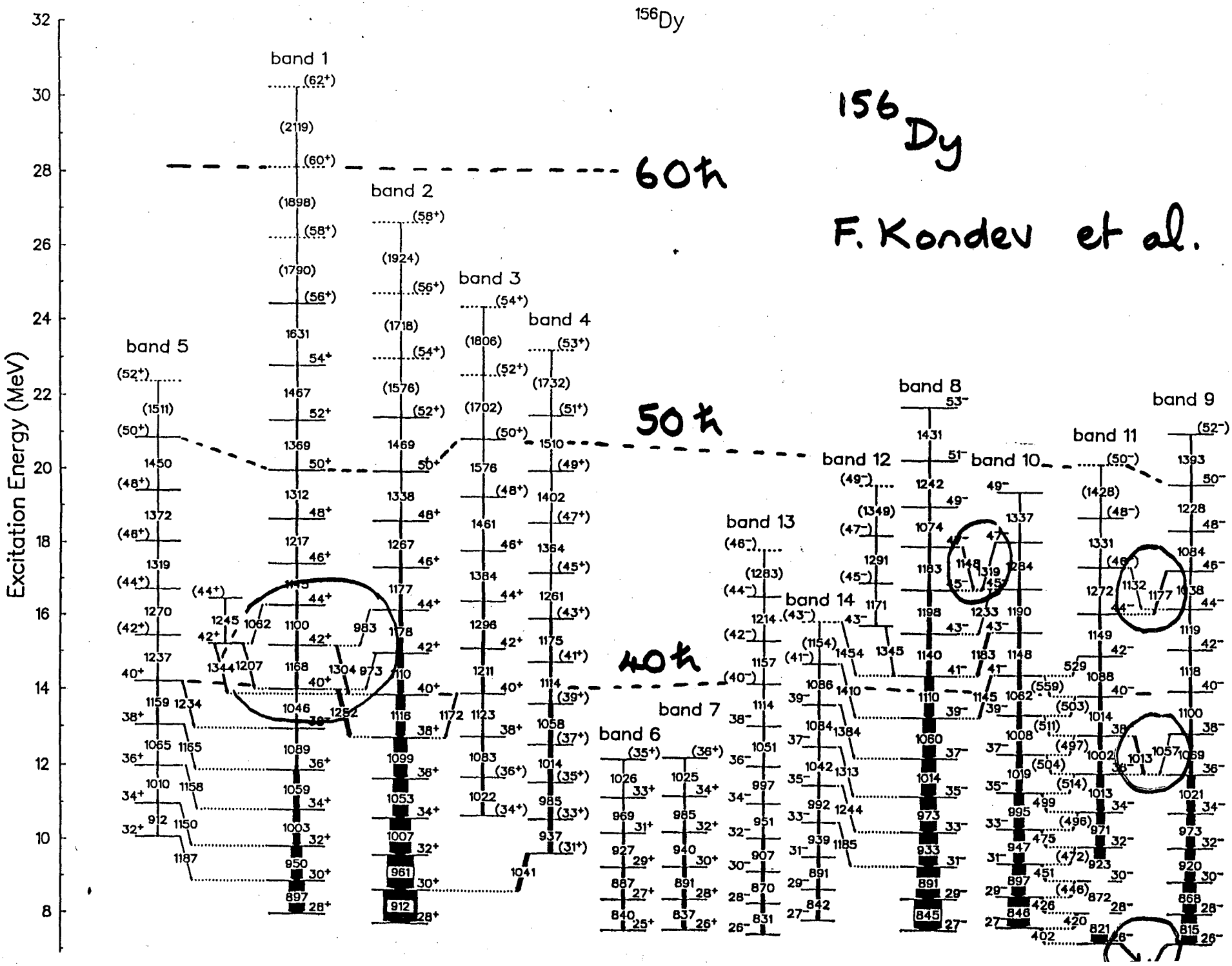
156Dy
156 Dy
F. Kondev et al.
60ħ
50ħ
40ħ
Excitation Energy (MeV)
band 1
band 2
band 3
band 4
band 5
band 6
band 7
band 8
band 9
band 10
band 11
band 12
band 13
band 14

increase with spin?

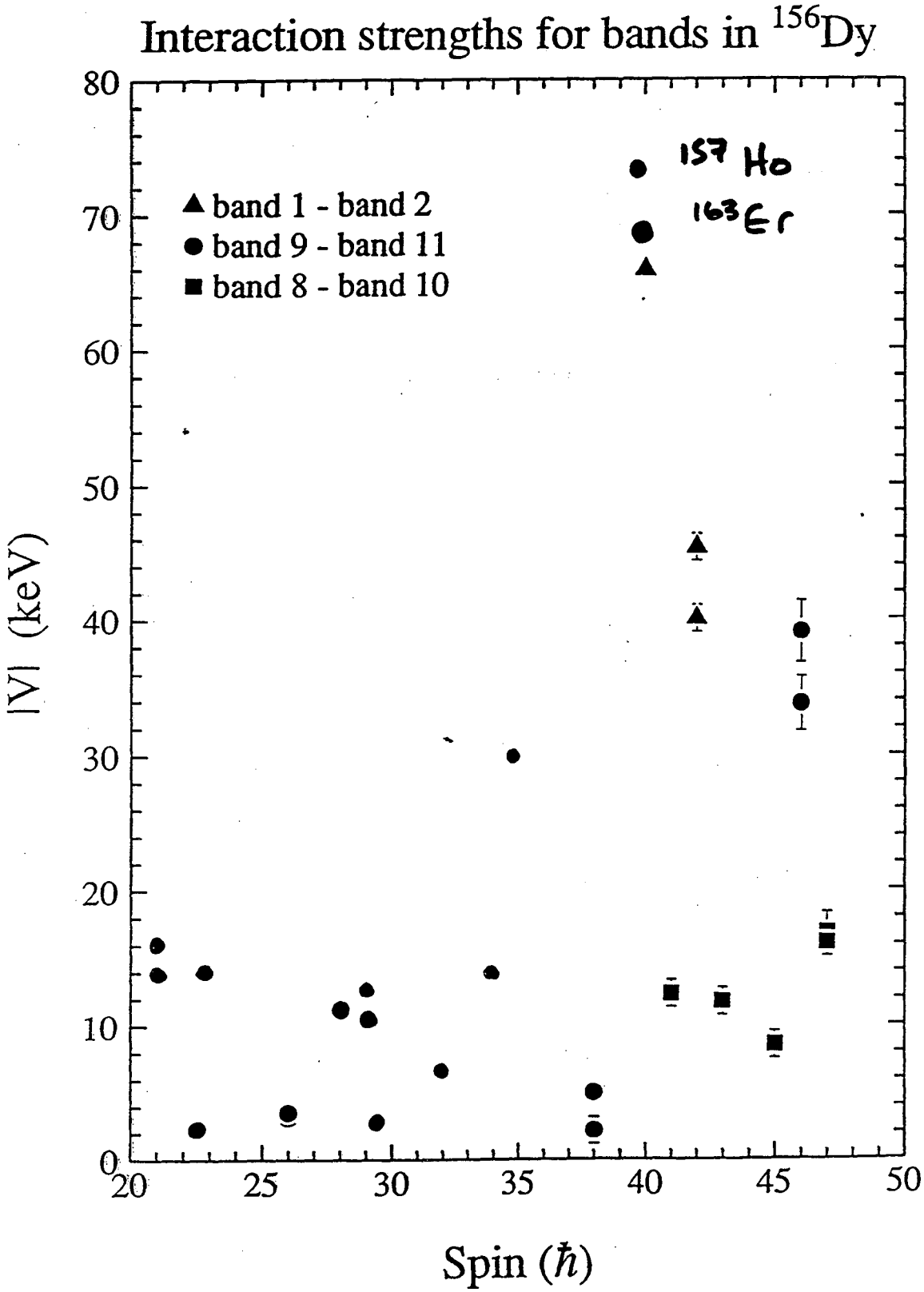

# OW HIGH IN SPIN CAN NUCLEI GO?

fundamental question

limits now 60ħ ND $^{156}$Dy
~65ħ SD $^{149}$Gd
~70ħ

how high above yrast do discrete bands go?
how fast do they melt into chaos?

where does all the intensity go?

$I_{input}$ ~70-80ħ but $I_{discrete}$ ~30-40ħ

need GRETA to unravel the continuum.
(BENT)

how close to the Edge are we?

nice A~190 SD indicator –
but is this it?
what about other regions?

need GRETA to pull the weak signal of survival out of the sea of fission

our "funding fathers" has spent a lot of time studying this question

∴ it must be interesting!

need GRETA to answer it.

# Magnetic Rotation a
# "Shears Mechanis

Equally spaced gamma-ray transitions, normally imply collective rotational motion due to a non-spherical nuclear shape. However for a band in $^{199}$Pb (amongst others) collective rotation is not the answer. The nuclear shape is near-spherical and a new mechanism has been proposed to generate angular momentum, the so-called "Shears Mechanism".

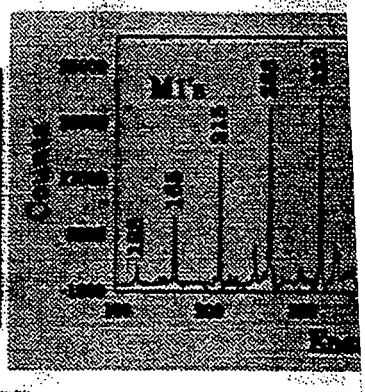


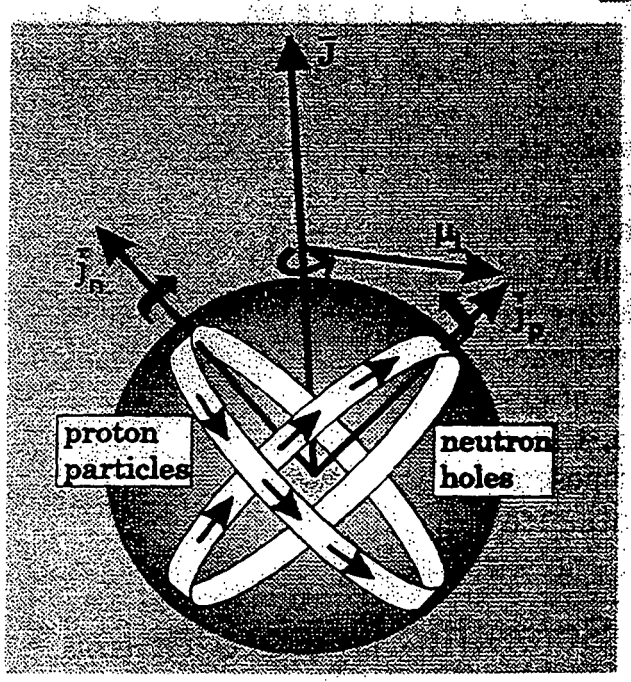


It has been suggested that
new type of rotation wher
broken by the anisotropic
currents. A few valence pr
couple to form two "long"
$j_n$ (blades of the shears) wh
the total spin J. Increasing s
the angle between $j_p$ and $j_n$.
which rotates around the to
characteristic M1 radiation.
become known as magnetic

The strength of the M1 transition is proportional to the size of the perpendicular component of the magnetic moment $\mu_\perp$. Confirmation of the "Shears Mechanism" came with the observation in a GAMMASPHERE experiment that the strength of the Magnetic Dipole Transition rates *DECREASE* with increasing rotational speed.

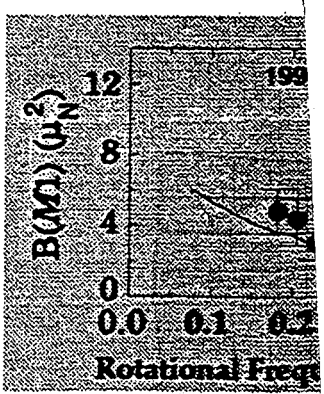

# HOW HIGH IN SPIN CAN NUCLEI GO?

- fundamental question
- limits now 60ħ ND $^{156}$Dy
  ~65ħ SD $^{149}$Gd
  ~70ħ
- how high above yrast do discrete bands go? how fast do they melt into chaos?
- where does all the intensity go?

  $I_{input}$ ~70-80ħ but $I_{discrete}$ ~30-40ħ

  need GRETA to unravel the continuum. (BENT)
- how close to the Edge are we?

  nice A~190 SD indicator –
  but is this it?
  what about other regions?

  need GRETA to pull the weak signal of survival out of the sea of fission
- our "funding fathers" has spent a lot of time studying this question

  ∴ it must be interesting!

  need GRETA to answer it.

# Magnetic Rotation and the "Shears Mechanism"

Equally spaced gamma-ray transitions, normally imply collective rotational motion due to a non-spherical nuclear shape. However for a band in $^{199}$Pb (amongst others) collective rotation is not the answer. The nuclear shape is near-spherical and a new mechanism has been proposed to generate angular momentum, the so-called "Shears Mechanism".

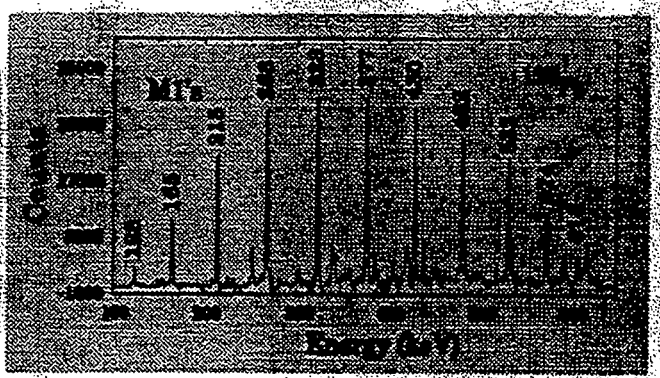


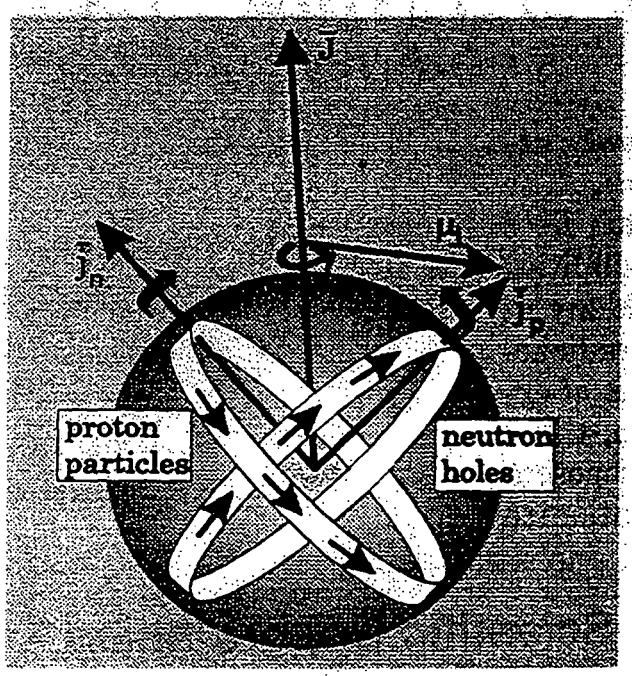


It has been suggested that these bands arise due to a new type of rotation where rotational symmetry is broken by the anisotropic arrangement of nucleonic currents. A few valence proton and neutron holes couple to form two "long" angular momenta, $j_p$ and $j_n$ (blades of the shears) which in turn couple to give the total spin J. Increasing spin is generated by closing the angle between $j_p$ and $j_n$. A magnetic moment arises which rotates around the total spin giving the characteristic M1 radiation. This phenomenon has become known as magnetic rotation.

The strength of the M1 transition is proportional to the size of the perpendicular component of the magnetic moment $\mu_\perp$. Confirmation of the "Shears Mechanism" came with the observation in a GAMMASPHERE experiment that the strength of the Magnetic Dipole Transition rates *DECREASE* with increasing rotational speed.

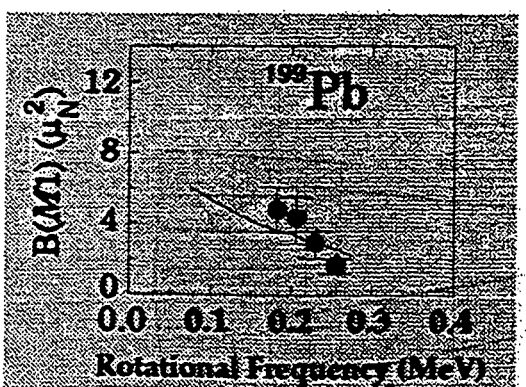

WHERE DOES ALL THE INTENSITY GO?

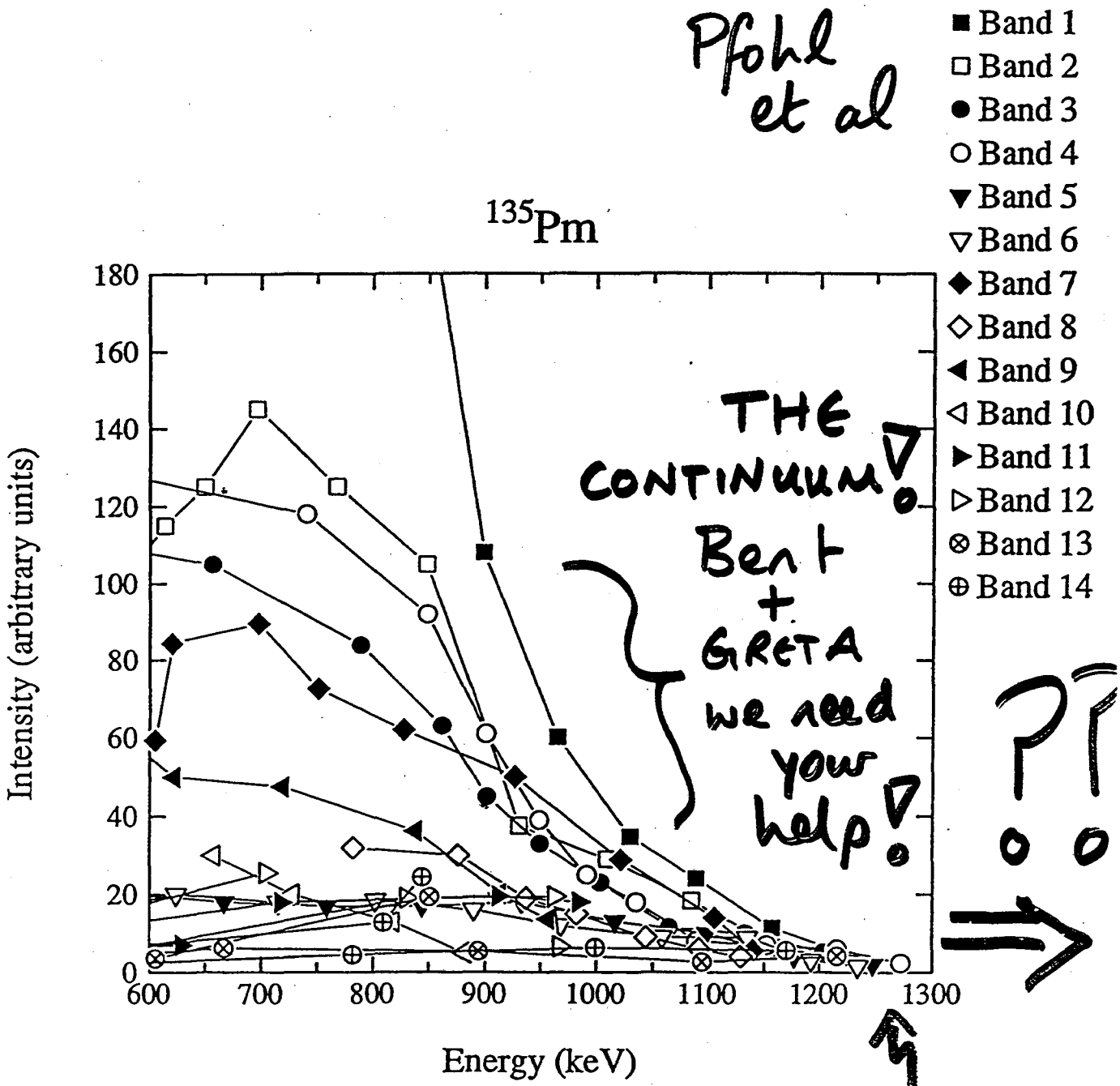


$L_{input} \sim 75k$

35k



ntensity.cmd

# Limits of Angular Momenta

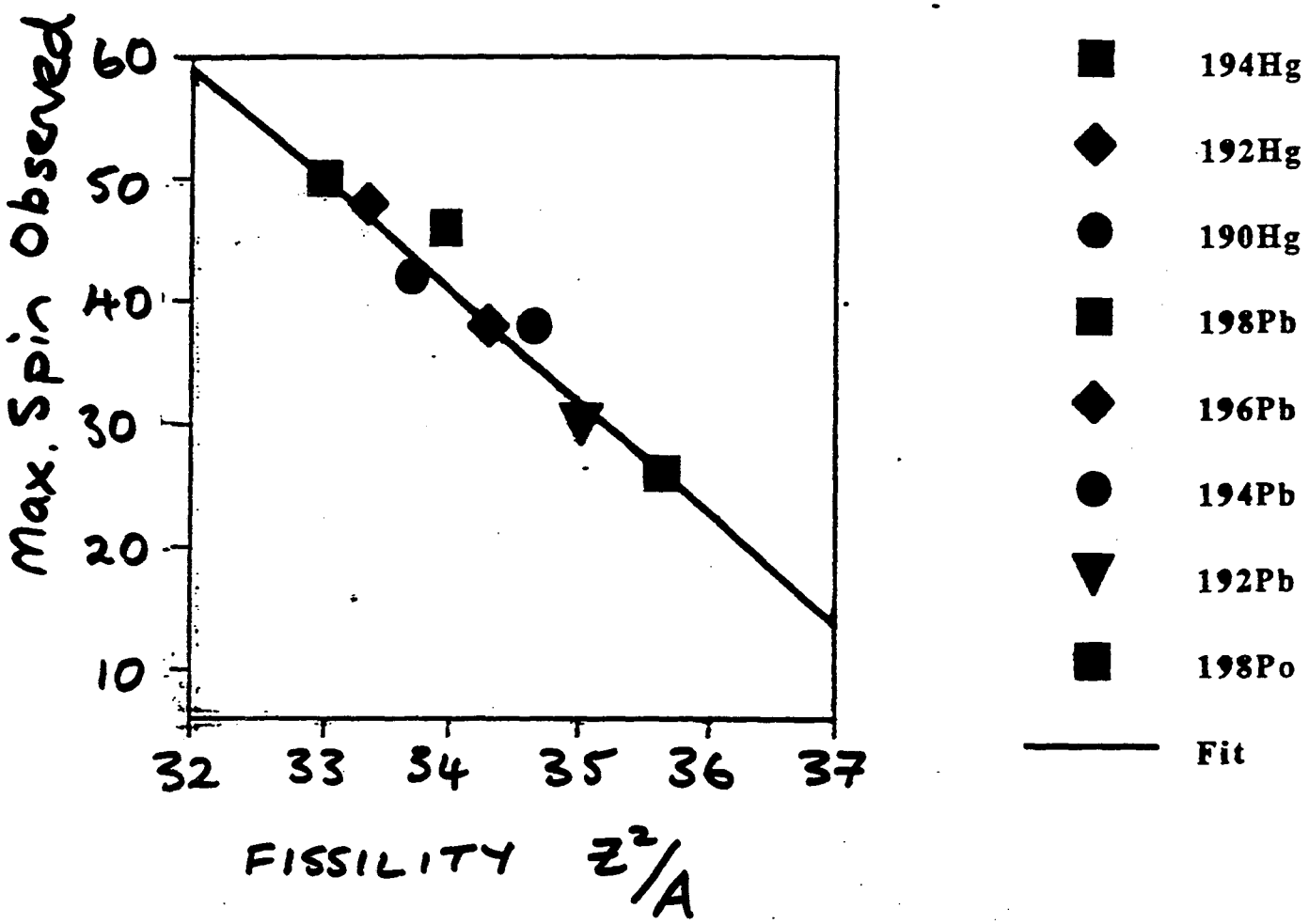


Ciżewski et al.

PHYSICAL REVIEW C VOLUME 29, NUMBER 3 MARCH 1984

## Rapid Communications

# Angular-momentum-dependent fission barriers in the rare-earth region

F. Plasil, T. C. Awes, B. Cheynis,* D. Drain,* R. L. Ferguson,
F. E. Obenshain, A. J. Sierk,† S. G. Steadman,‡ and G. R. Young
*Oak Ridge National Laboratory, Oak Ridge, Tennessee 37831*
(Received 7 November 1983)

Fission and evaporation residue excitation functions of $^{153}$Tb and $^{181}$Re compound systems are investigated in the context of angular-momentum-dependent fission barrier calculations in which effects of the finite range of the nuclear force and of the diffuseness of the nuclear surface are included. Carbon- and neon-induced reactions are studied in both the $^{153}$Tb and $^{181}$Re cases. Reasonable agreement is found between experimental and calculated excitation functions without adjustments of the theoretical fission barriers.

PHYSICAL REVIEW C VOLUME 28, NUMBER 5 NOVEMBER 1983

# Fission of polonium, osmium, and erbium composite systems

J. van der Plicht,* H. C. Britt, M. M. Fowler, Z. Fraenkel,† A. Gavron, and J. B. Wilhelmy
*Los Alamos National Laboratory, Los Alamos, New Mexico 87545*

F. Plasil, T. C. Awes, and G. R. Young
*Oak Ridge National Laboratory, Oak Ridge, Tennessee 37830*
(Received 5 July 1983)

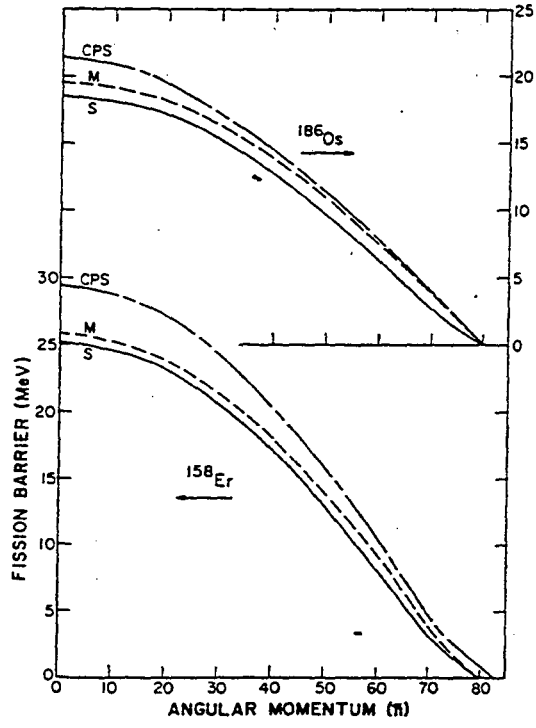


FIG. 14. Calculated fission barriers as a function of angular momentum from Sierk (S) (Ref. 12), Mustafa *et al.* (M) (Ref. 21), and Cohen, Plasil, and Swiatecki (CPS) (Ref. 11).

# THEME FOR THE FUTURE

"Study of Nuclei at Extremes"

HYPERDEFORMATION

Deformation

Spin

HYPER-DEFORMATION

HD

Dudek, Werner, Riedinger Phys. Lett. B211, 2 (1

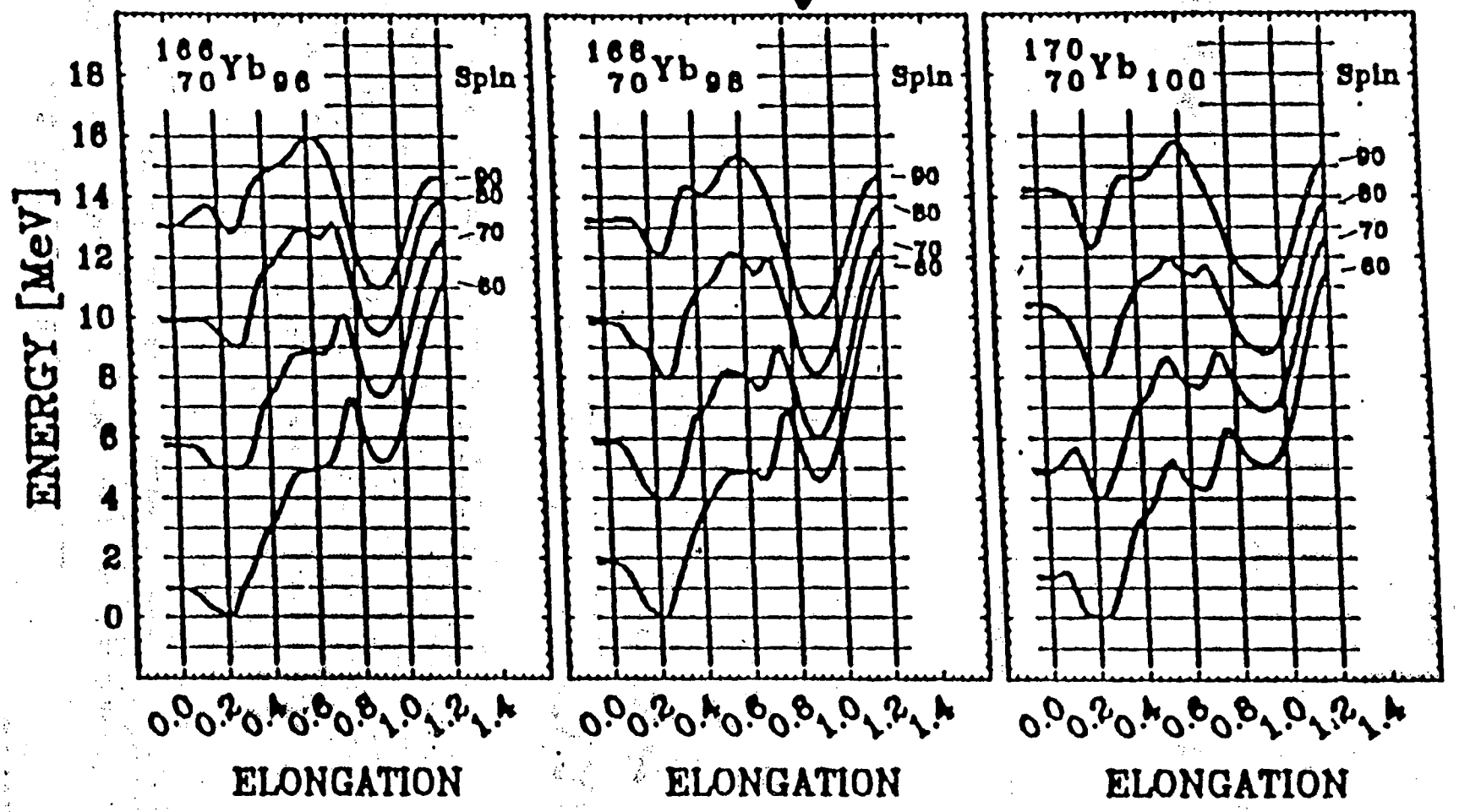

# Search for hyperdeformation in $^{168}$Yb

J. N. Wilson,[1] S. J. Asztalos,[2] R. A. Austin,[1] B. Busse,[2] R. M. Clark,[2] M. A. Deleplanque,[2] R. M. Diamond,[2] P. Fallon,[2] S. Flibotte,[1] G. Gervais,[1] D. S. Haslip,[1] I. Y. Lee,[2] R. Kruecken,[2] A. O. Macchiavelli,[2] R. W. MacLeod,[2] J. M. Nieminen,[1] G. J. Schmid,[2] F. S. Stephens,[2] O. Stezowski,[3] C. E. Svensson,[1] K. Vetter,[2] and J. C. Waddington[1]
[1]*Department of Physics and Astronomy, McMaster University, Hamilton, Ontario, Canada L8S 4M1*
[2]*1 Cyclotron Road, Lawrence Berkeley Laboratory, Berkeley, California*
[3]*Institut de Recherche Subatomique, Strasbourg Cedex 2, France*
(Received 5 May 1997)

The nucleus $^{168}$Yb, and its near neighbors, have been studied at the very highest angular momenta using the full Gammasphere array. The experiment was performed in order to search for evidence for the existence of hyperdeformed states, which have predicted nuclear axis ratios of ~3:1. After exhaustive searching for both discrete and continuum $\gamma$ rays associated with a hyperdeformed shape, using a wide variety of different analysis techniques, no evidence for the existence of hyperdeformation has been found. This search of unprecedented sensitivity has been carried out with the full Gammasphere, and was performed on arguably the best candidate nucleus. A maximum achievable observational limit of ~0.02% of the $^{168}$Yb channel has been calculated for this particular experiment, using Monte Carlo simulations of the response of Gammasphere. [S0556-2813(97)02410-2]

$^{48}$Ca + $^{124}$Sn @ 215 MeV
$\ell_{max}$ ~ 87ħ

56

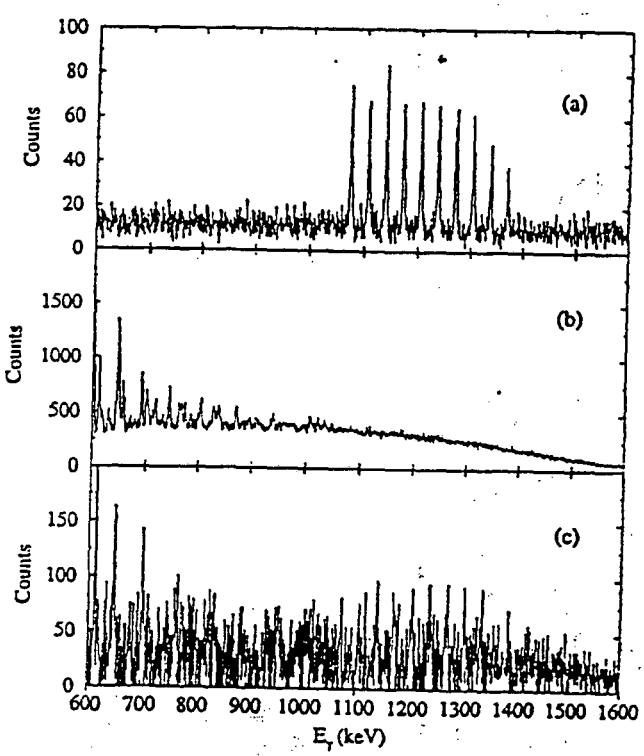


FIG. 4. (a) Triply gated spectrum created from the sum of 10 gates on 70 000 events of simulated hyperdeformed data, where the simulated band had ten transitions and the gates were 1 FWHM wide. (b) Triply gated spectrum created from exactly the same sum of ten gates applied to the real data containing 500 million events in the full database. (c) The sum of the spectra (a) and (b), after a suitable high-statistics background spectrum has been subtracted. The peaks in the simulated band are not particularly prominent in this spectrum, which corresponds to a band of 0.014% intensity. The limit of sensitivity for one data point is calculated from spectra such as (a) and (b).

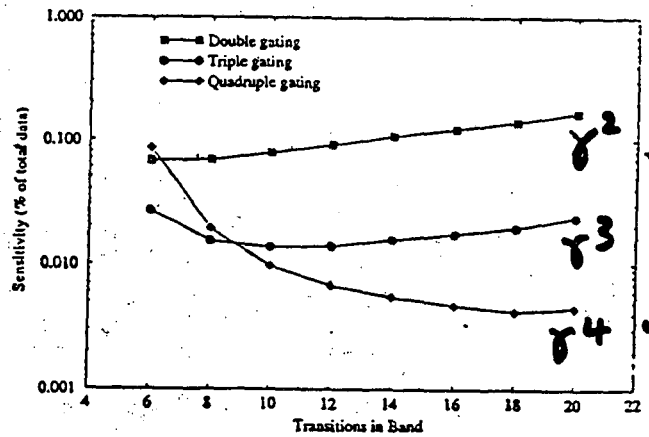


FIG. 5. Plot of the limit of sensitivity of the full Gammasphere for this particular reaction, given the assumptions of the Monte Carlo simulation. This limit will vary from experiment to experiment due to changes in the amount of data collected, and the strength of continuum background, but the major factor in affecting the limit is the total photopeak efficiency for Gammasphere (taken here as 10.0% in the range of the simulated band). Note that the limit of sensitivity for the $^{168}$Yb channel is ~5 times higher than these values, as this comprises only 20% of the data set.

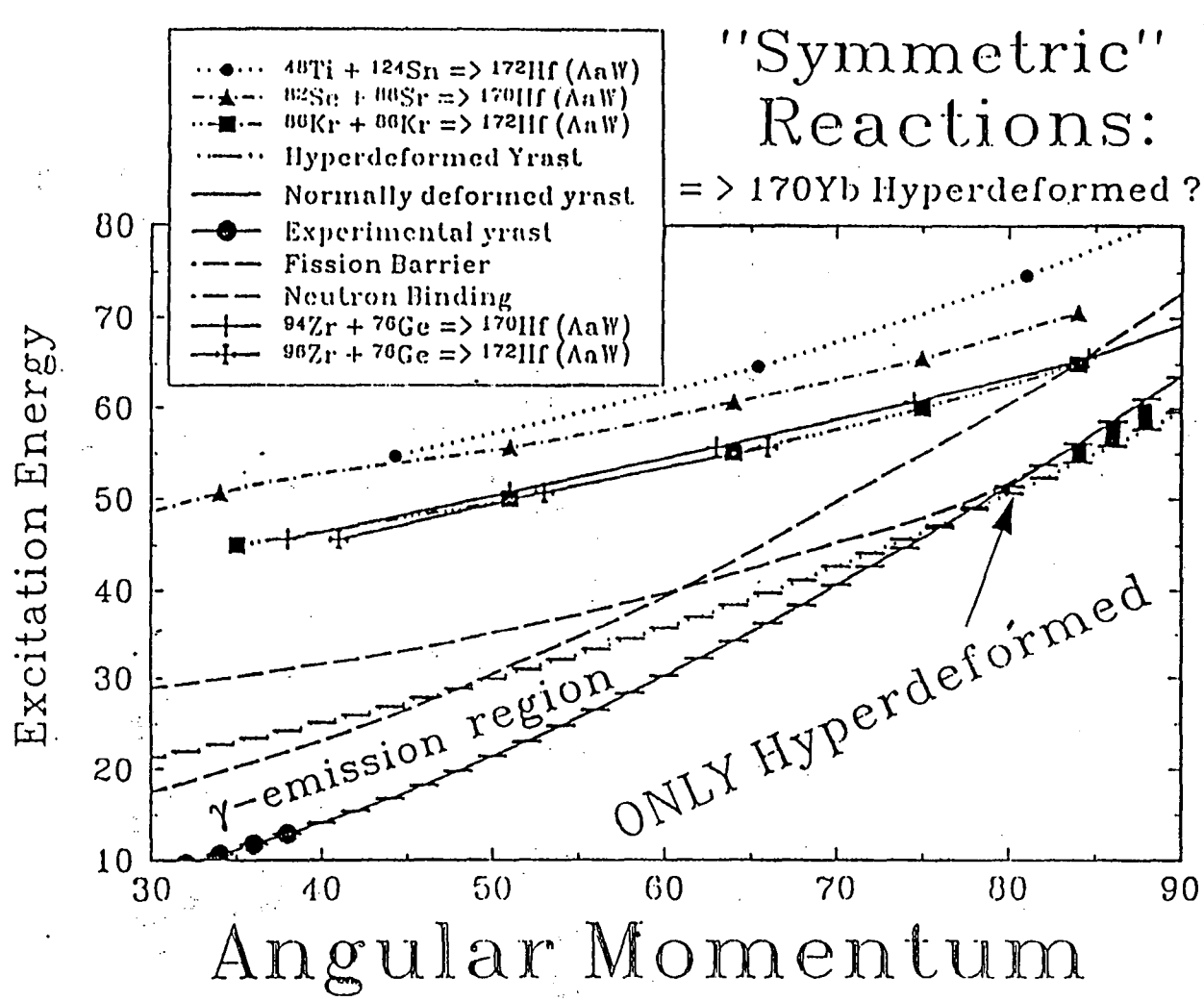


Fig. 1. Schematic energy diagram illustrating the population of hyperdeformed states in $^{168}$Yb. The $L_{max}$ of possible reactions are shown with filled circles, triangles, boxes, and crosses, as calculated by the new fusion model of Aa. Winther [3].

Don't forget
HD
predicted in
other regions too!

# "FISSION FOR HYPERDEF"

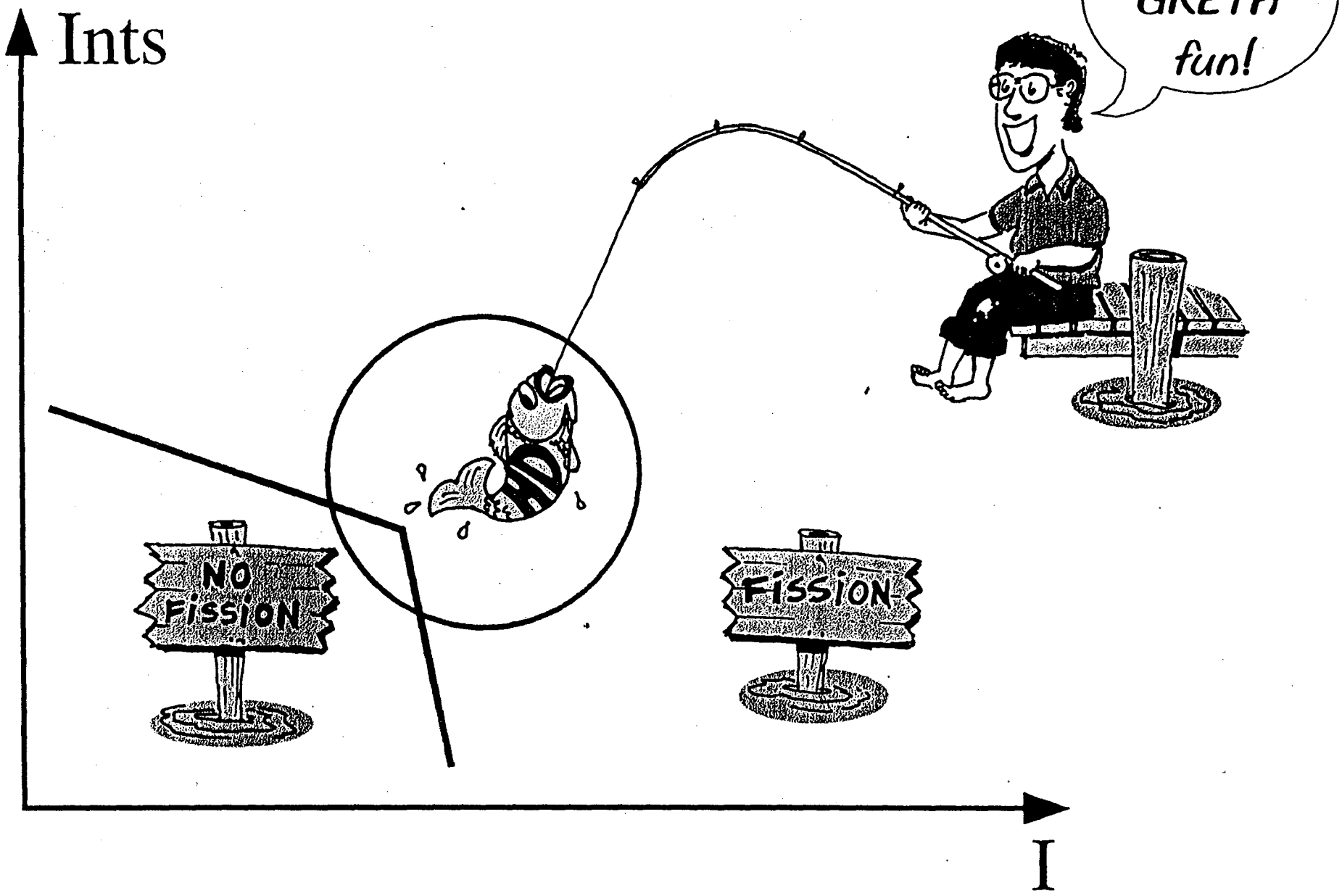

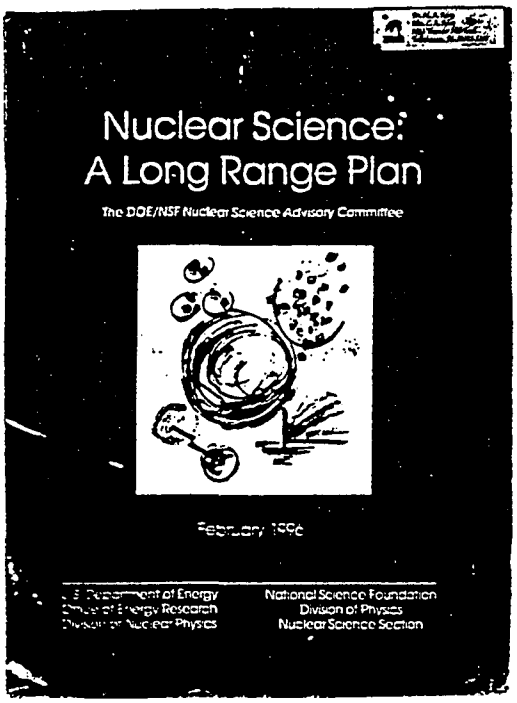


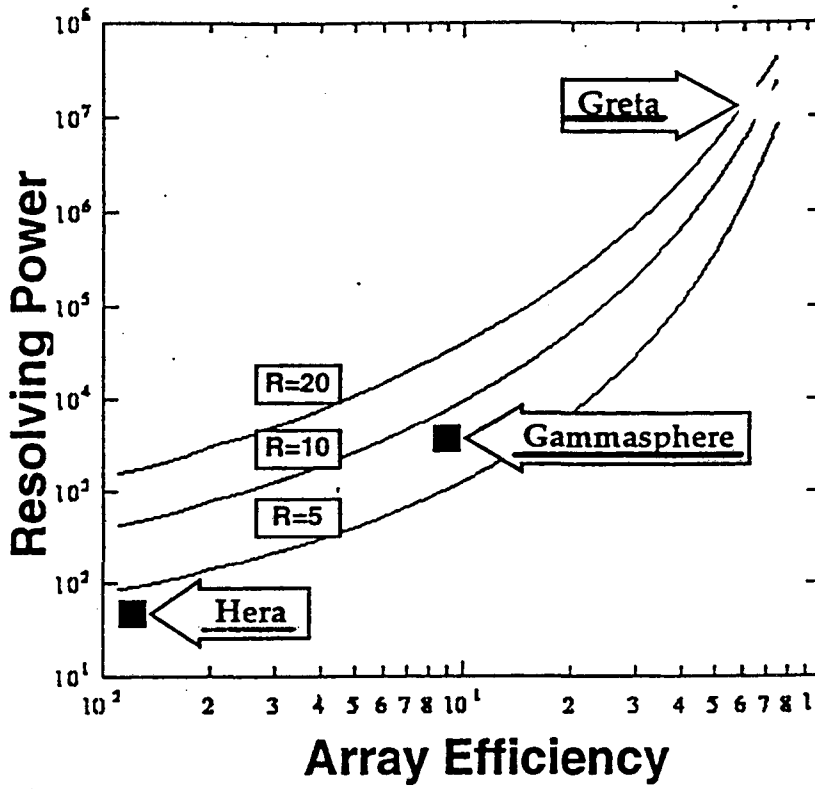


Experimental progress arises from newly developed instrumentation and capabilities. The most important future directions for this field should capitalize on new physics possibilities made possible by technical advances. Many of these arise from the opportunities with radioactive beams and will exploit the capabilities of existing and planned facilities. In addition, there are powerful new gamma-ray detectors proposed, such as GRETA, that promise to revolutionize many areas.

## Scientific Opportunities with an Advanced ISOL Facility

***GRETA***

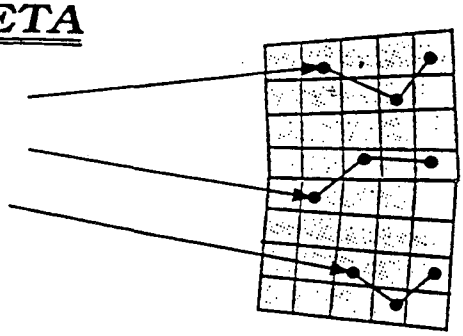

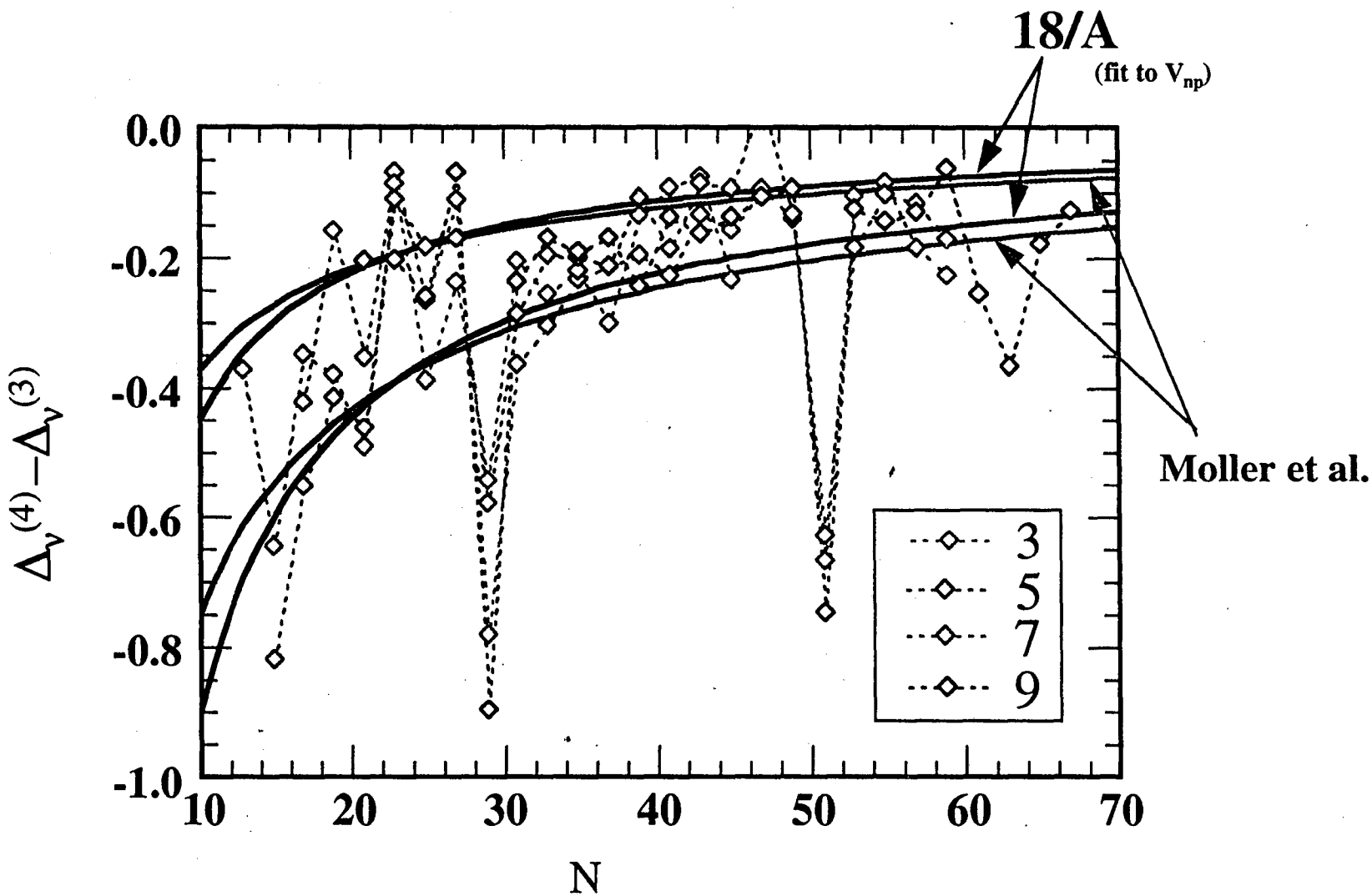
18/A
(fit to $V_{np}$)
Moller et al.
0.0
-0.2
-0.4
-0.6
-0.8
-1.0
10
20
30
40
50
60
70
N
$\Delta_v^{(4)} - \Delta_v^{(3)}$
3
5
7
9

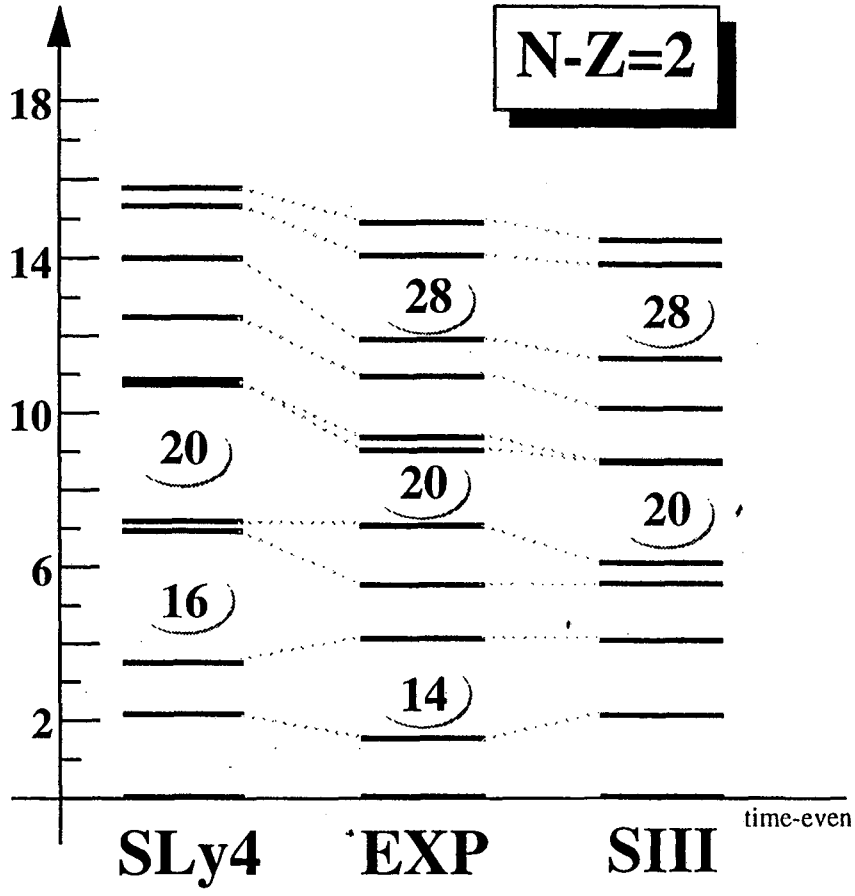


W. Satula
1-24-98

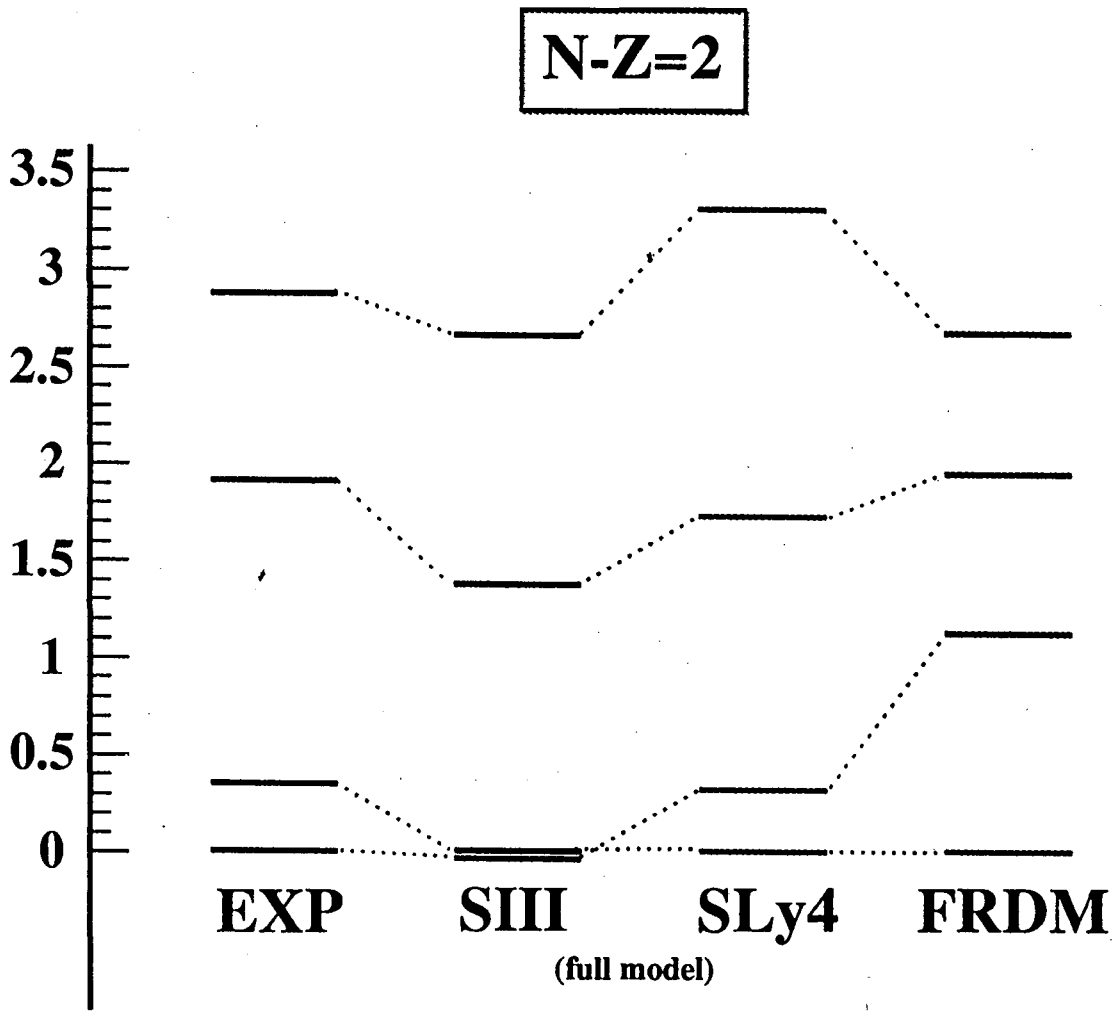
N-Z=2
3.5
3
2.5
2
1.5
1
0.5
0
EXP
SIII
SLy4
FRDM
(full model)

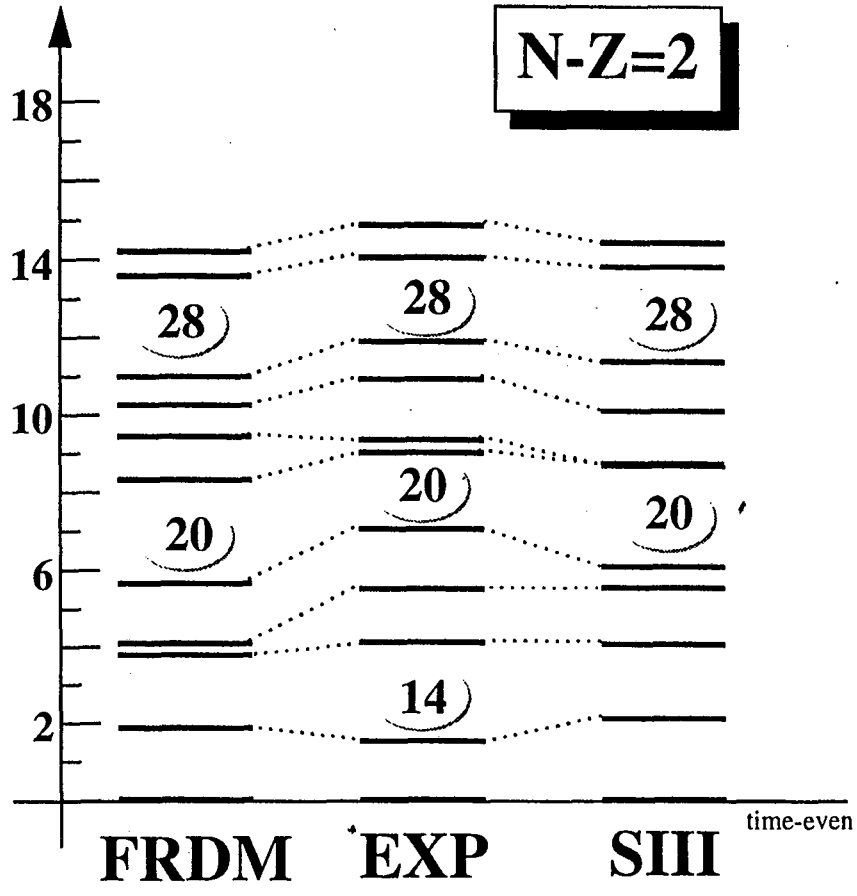


W. Satula
1-28-98

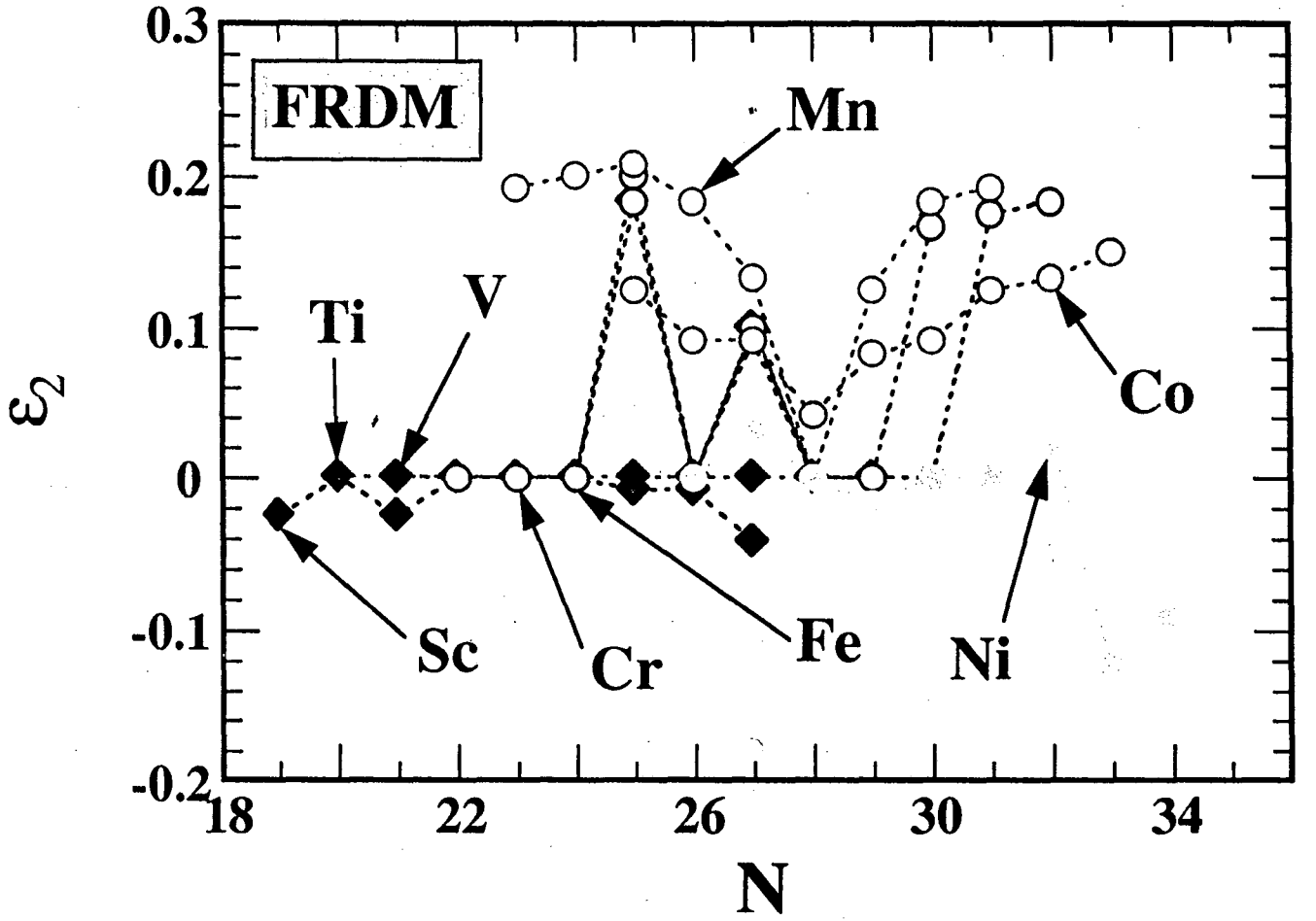


W. Satula
1-30-98

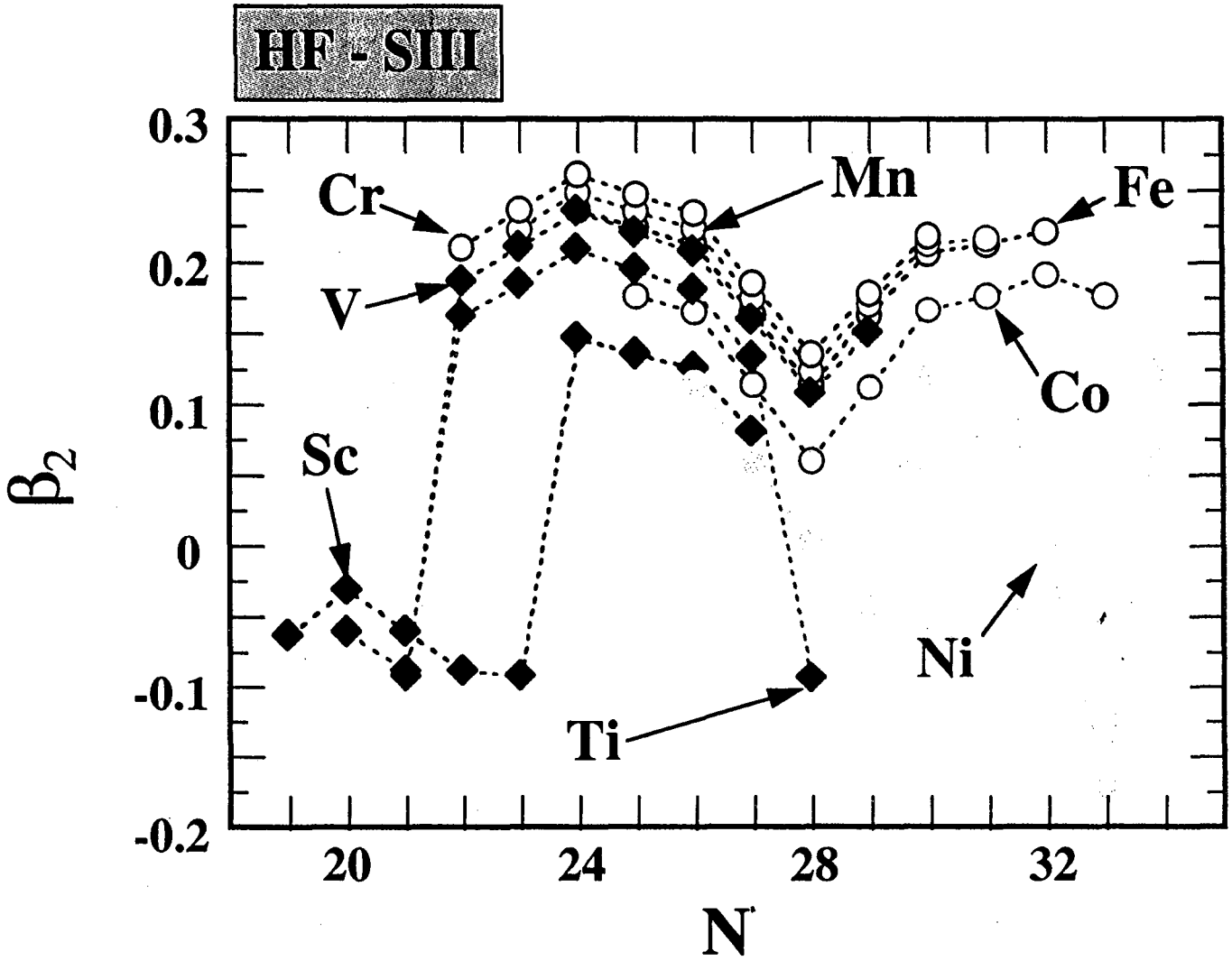
HF - SIII
0.3
0.2
0.1
0
-0.1
-0.2
$\beta_2$
20
24
28
32
N
Cr
Mn
Fe
V
Co
Sc
Ni
Ti

'PLANAR TOPOLOGY' OF THE HF SOLUTIONS:

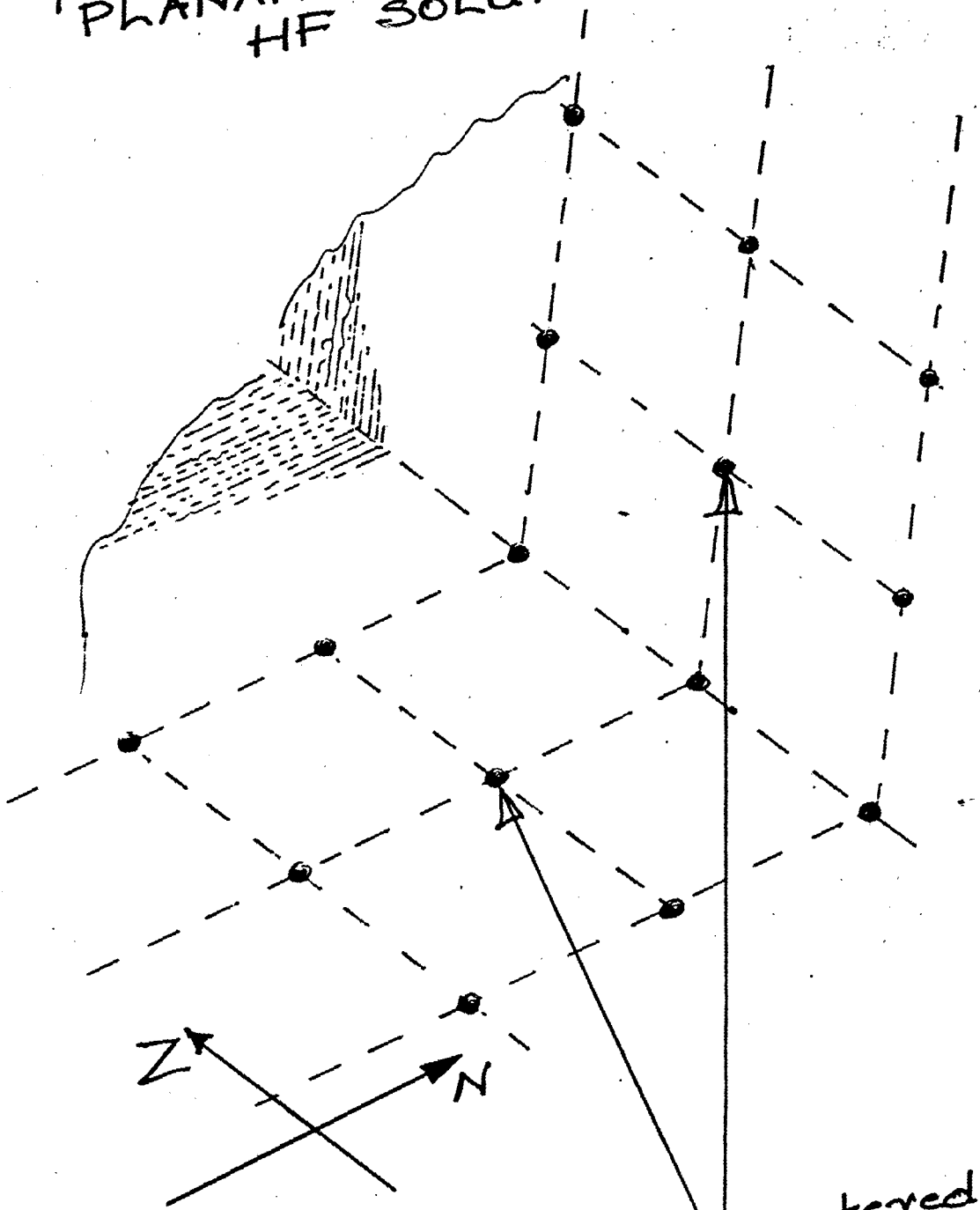


centered around odd-odd nuclei:

$$\alpha N + \beta Z + \gamma N \cdot Z + \delta |N-Z| + \text{const} \; (+ \chi Z^2)$$

↳ weak. Coulomb

- FILTERS:
  (probing 'planar topology')

(i) $\frac{1}{4}(-)^{A}$

| | | |
|---|---|---|
| 1 | −2 | 1 |
| −2 | 4 | −2 |
| 1 | −2 | 1 |

$\sim \delta_{np}$

(probes np interaction in odd-odd nucleus)

(ii) $\frac{1}{2}$

| | | |
|---|---|---|
| | −1 | |
| 1 | 0 | 1 |
| | −1 | |

$\sim \Delta^{(3)}_{\pi} - \Delta^{(3)}_{\nu}$

(probes Coulomb but only if N & Z are of the same parity)

(iii) $\frac{1}{4}$

| | | |
|---|---|---|
| 1 | | −1 |
| | | |
| −1 | | 1 |

$\sim V_{pn}$

probe symmetry energy in N:Z (directio

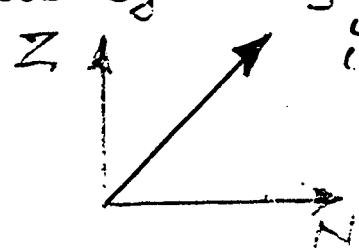

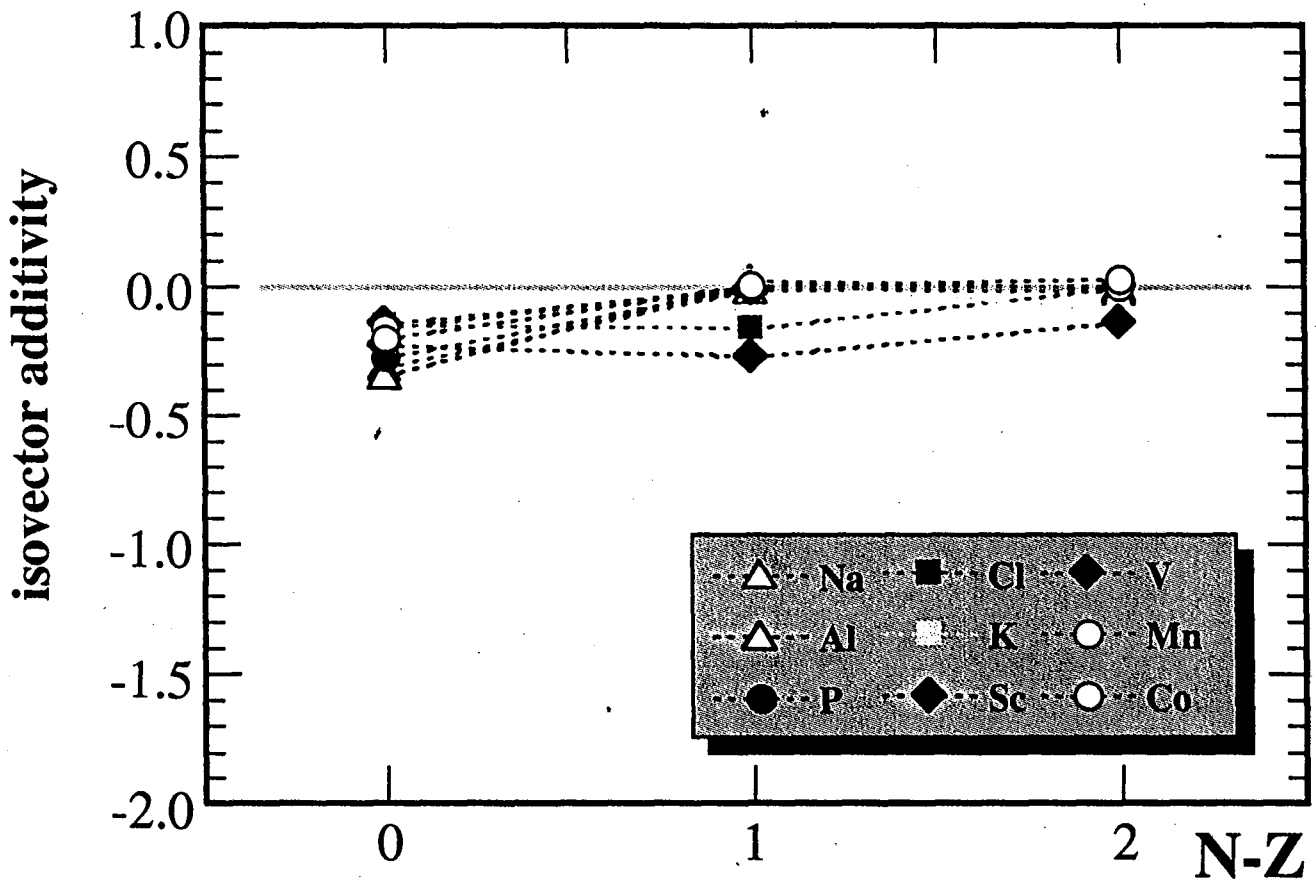
isovector additivity
1.0
0.5
0.0
-0.5
-1.0
-1.5
-2.0
0
1
2
N-Z
Na
Cl
V
Al
K
Mn
P
Sc
Co

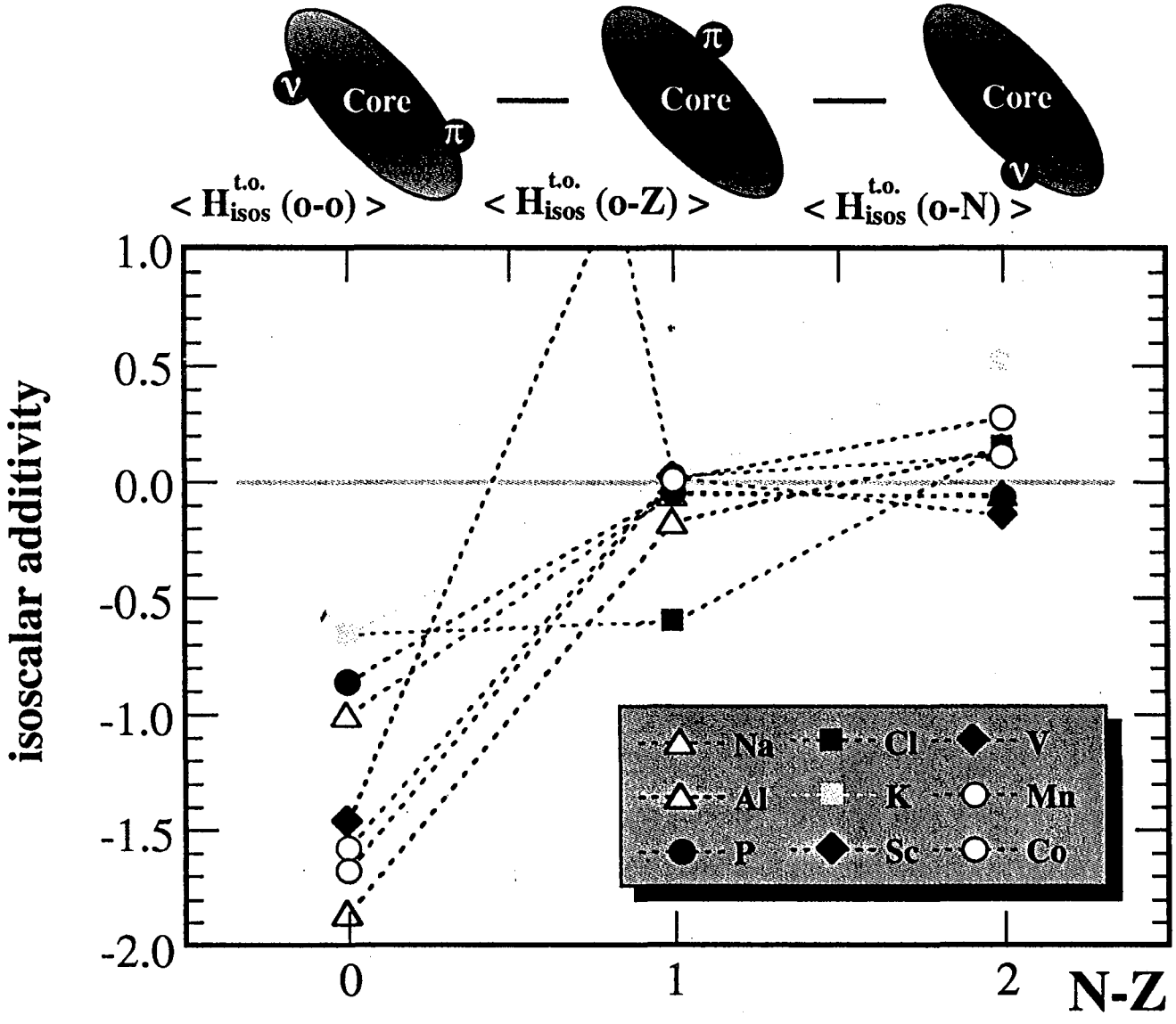
Core
ν
π
Core
π
Core
ν
< H^t.o._isos (o-o) >
< H^t.o._isos (o-Z) >
< H^t.o._isos (o-N) >
isoscalar additivity
1.0
0.5
0.0
-0.5
-1.0
-1.5
-2.0
0
1
2
N-Z
Na
Cl
V
Al
K
Mn
P
Sc
Co

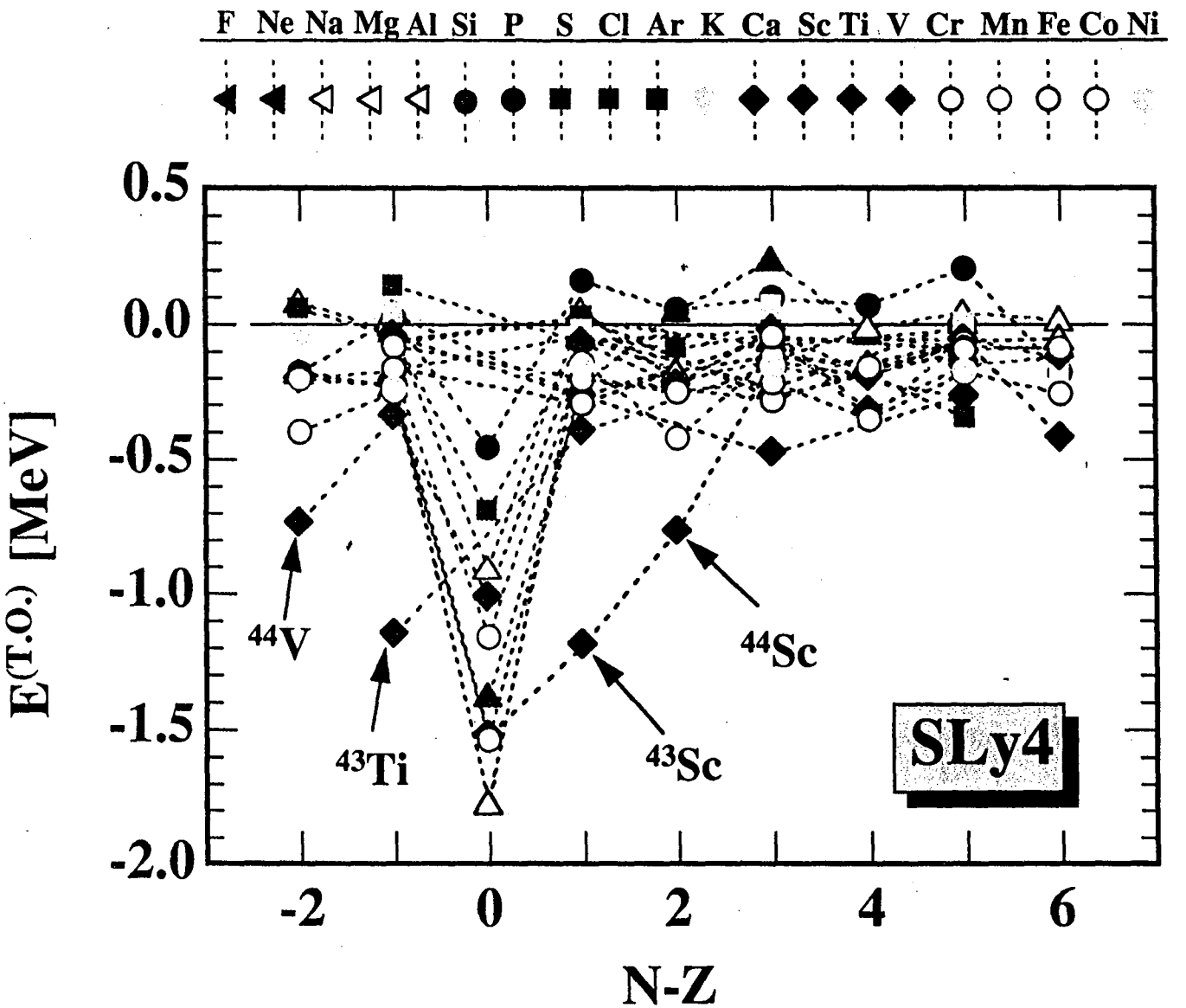
F Ne Na Mg Al Si P S Cl Ar K Ca Sc Ti V Cr Mn Fe Co Ni
0.5
0.0
-0.5
-1.0
-1.5
-2.0
E(T.O.) [MeV]
-2
0
2
4
6
N-Z
44V
43Ti
43Sc
44Sc
SLy4

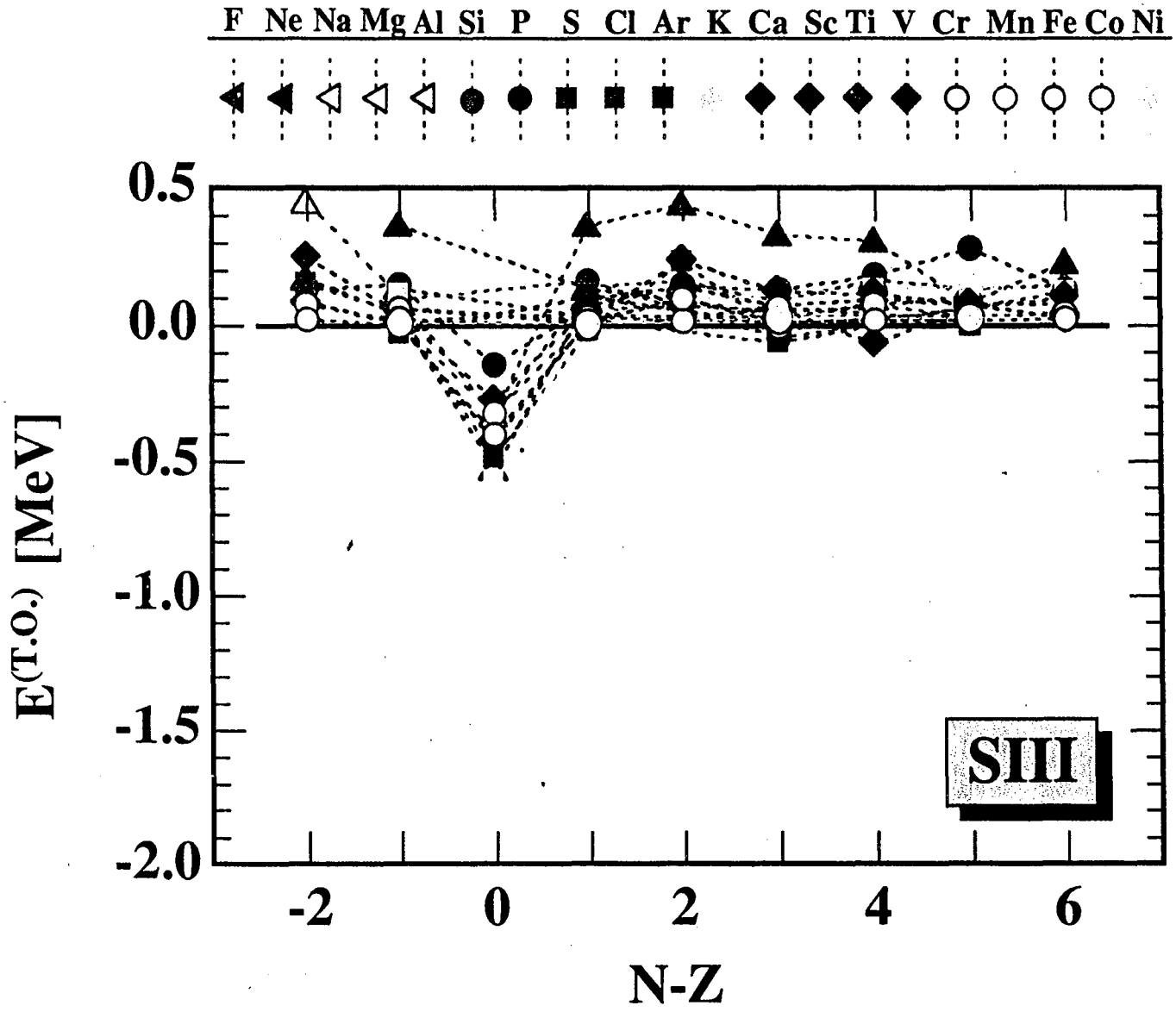
F Ne Na Mg Al Si P S Cl Ar K Ca Sc Ti V Cr Mn Fe Co Ni
0.5
0.0
-0.5
-1.0
-1.5
-2.0
E(T.O.) [MeV]
-2
0
2
4
6
N-Z
SIII

# SIII - time-even

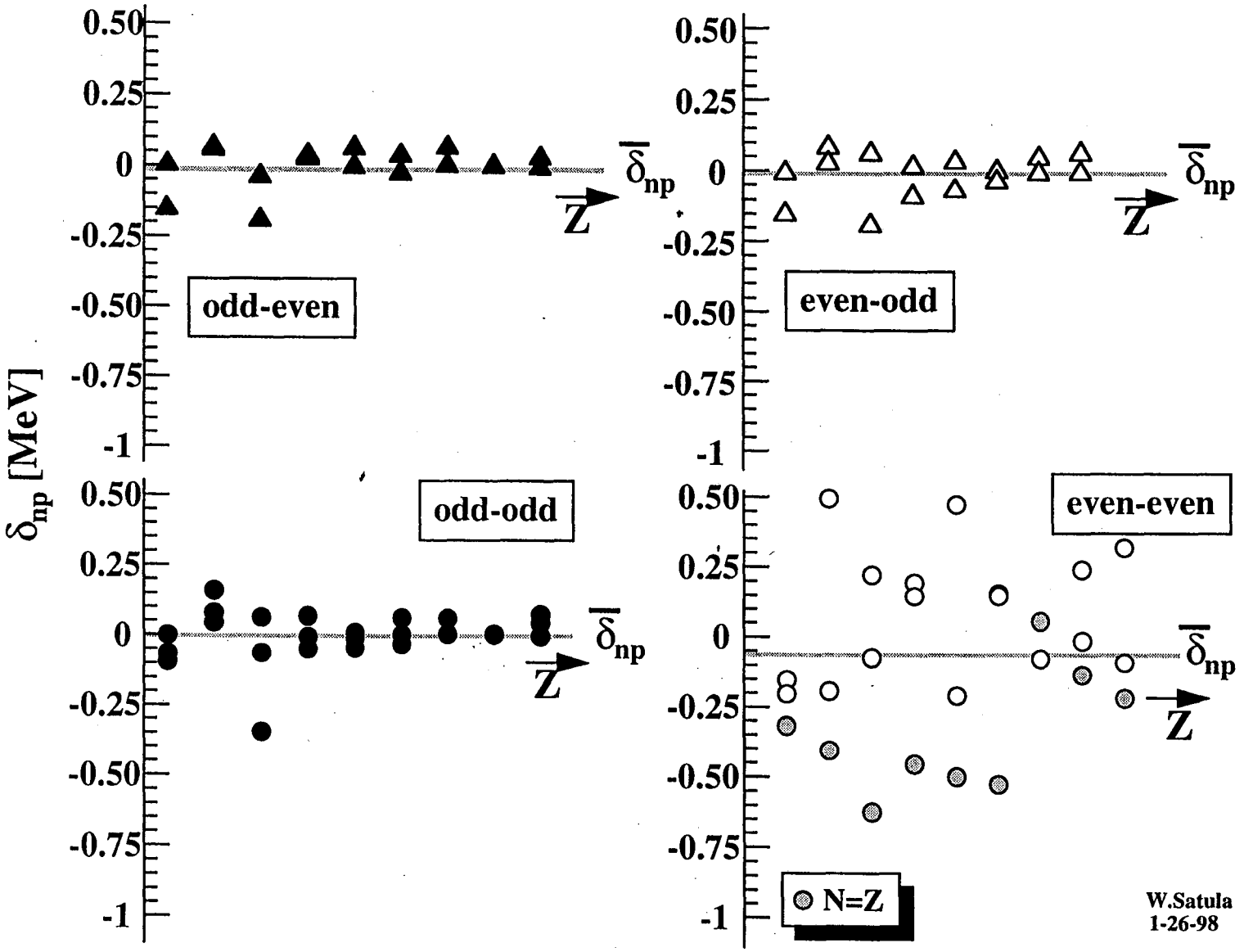

# SIII

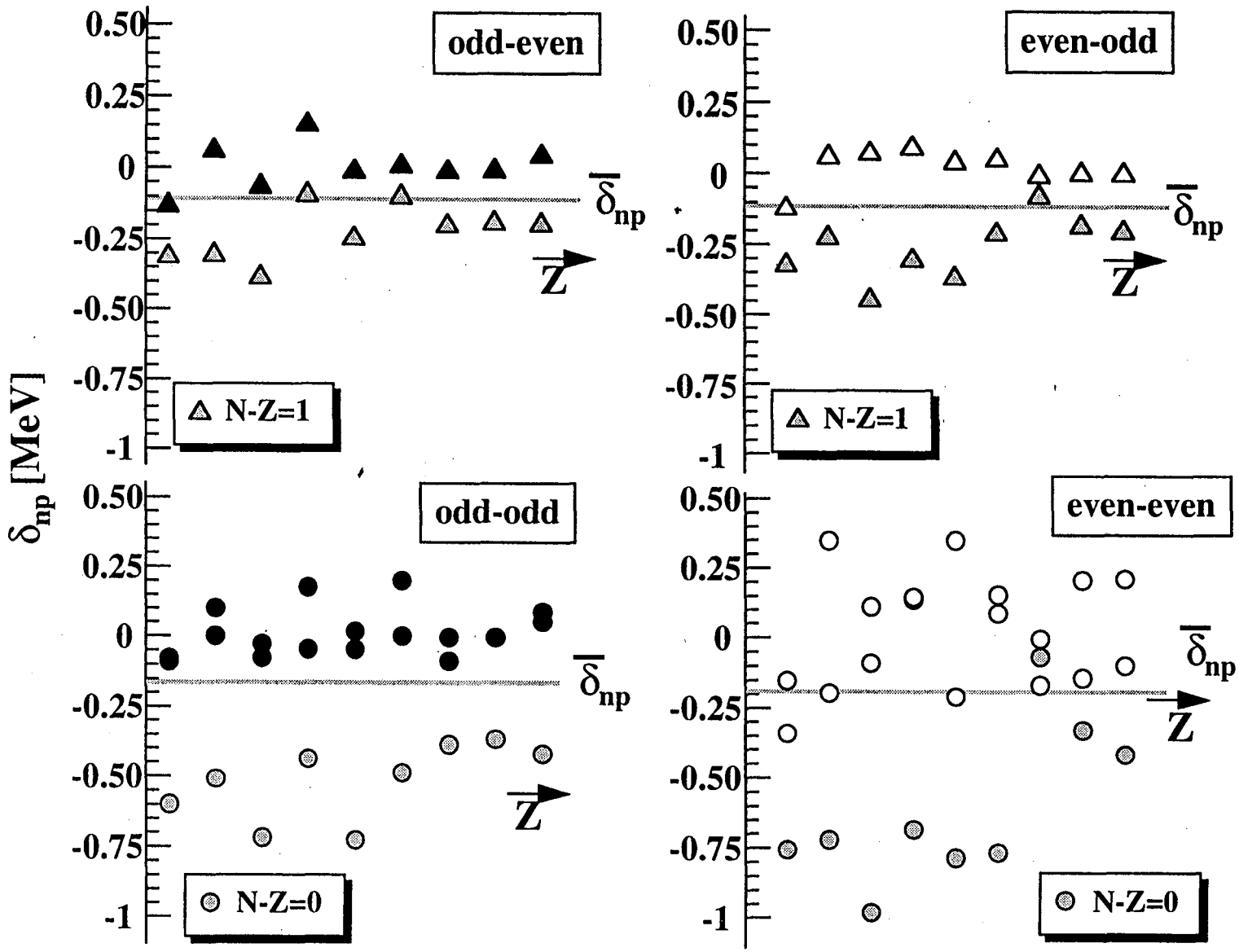


W.Satula
1-27-98

ON THE TIME-ODD FIELDS:

- Skyrme energy densities (t.e.)

$$\mathcal{H}_t^{odd}(\vec{r}) \simeq C_t^{\vec{s}}(\rho)\, \vec{s}_t^{\,2}(\vec{r}) + C_t^{\Delta\vec{s}}\, s_t \cdot \Delta\vec{s}_t$$

dominant

$$+ \ldots$$

where
$\vec{s}_t(\vec{r})$ is a local spin density
and $t = 0\,(1)$ denotes isospin

| | $C_t^{\vec{s}}(\rho=0)$ [MeV fm$^5$] | $C_t^{\vec{s}}(\rho=\rho_{NM})$ [MeV fm$^5$] | $C_t^{\Delta\vec{s}}$ [MeV fm$^5$] |
|---|---|---|---|
| SkM* | | | |
| t=0 | 271.1 | 31.7 | 17.1 |
| t=1 | 330.6 | 91.2 | 17.1 |
| SIII: t=0 | 14.1 | 56.4 | 17.0 |
| t=1 | 141.1 | 98.8 | 17.0 |
| SLy4: | | | |
| t=0 | −207.8 | 153.4 | 47.1 |
| t=1 | 311.1 | 99.6 | 14.3 |

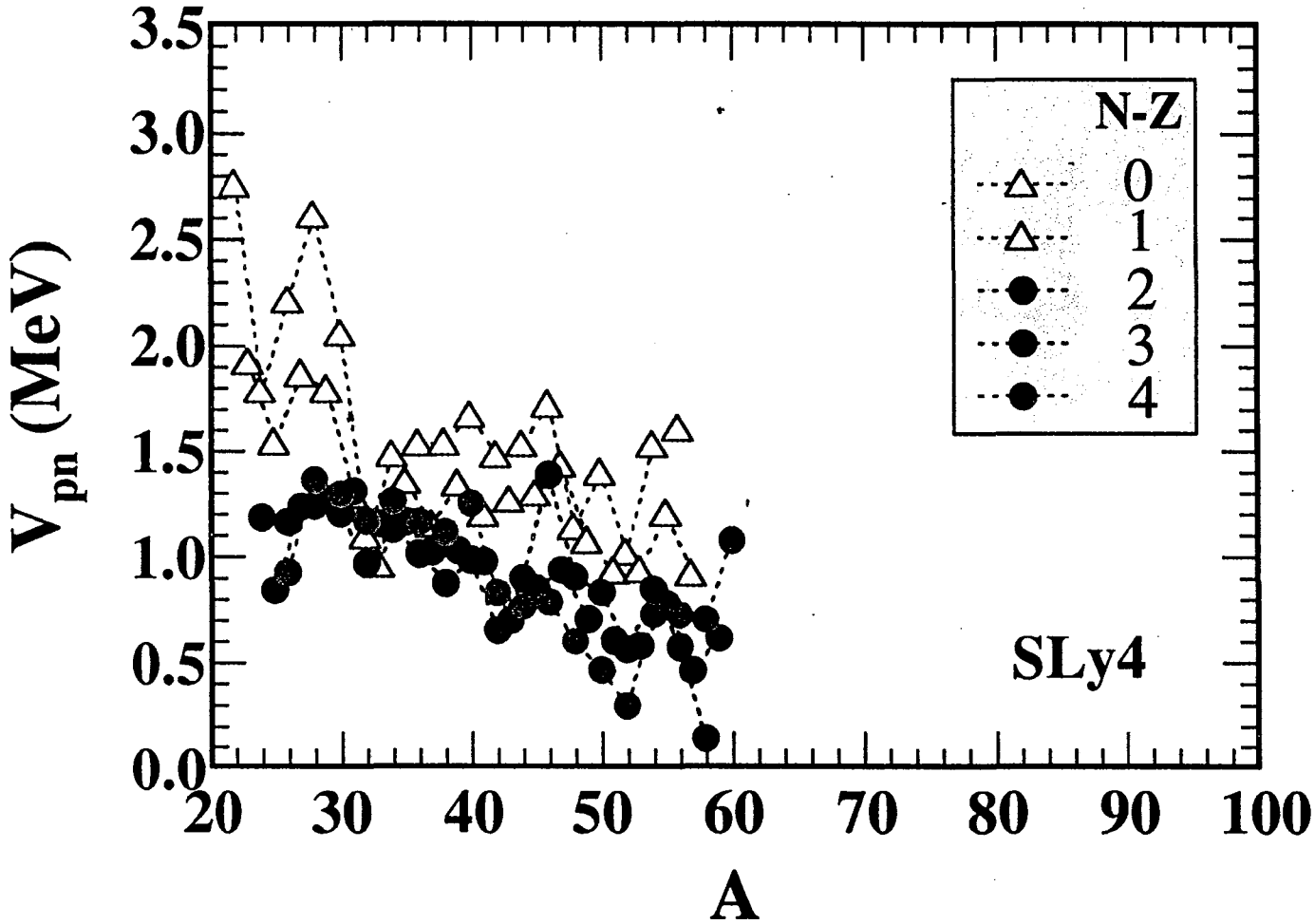
3.5
3.0
2.5
2.0
1.5
1.0
0.5
0.0
20
30
40
50
60
70
80
90
100
A
$V_{pn}$ (MeV)
N-Z
0
1
2
3
4
SLy4

C.Baktash

Nuclear structure near the N=Z line.

# Nuclear Structure Near the N=Z Line

*Cyrus Baktash*

ORNL, Munich, McMaster, Washington U., UTK, JIHIR, LBNL, Koln, Madrid

# *OUTLINE OF PHYSICS TOPICS*

$^{56}$Ni and its neighbors: The Bridge

» Spherical, deformed, & superdeformed states

» Effective interactions

» Proton emission from the 2$^{nd}$ well

» March toward $^{32}$S

Astrophysics (rp-process)

T=0 pairing

N=Z nuclei (rapid structural changes, superallowed β decay)

$^{100}$Sn region

Proton radioactivity and spectroscopy beyond the drip line (recoil-decay tagging)

Summary: The need for more powerful gamma-detectors

# *MOTIVATION*

$^{56}$Ni is the only doubly-magic nucleus above $^{40}$Ca that may be studied with stable beams and significant cross section.

$^{56}$Ni and its neighbors provide important input for the *large-scale shell model calculations*

- The predicted *deformed* multi particle-hole states (with respect to N,Z=28) provide a unique set of data to test, compare, and relate the predictions of widely different theoretical approaches; namely, large-scale shell model, mean field, and cluster model calculations.

Nuclei along the N=Z line near and beyond $^{56}$Ni may provide insight into the question of *neutron-proton pairing*.

## $^{36}Ar + ^{28}Si$ at 136 MeV

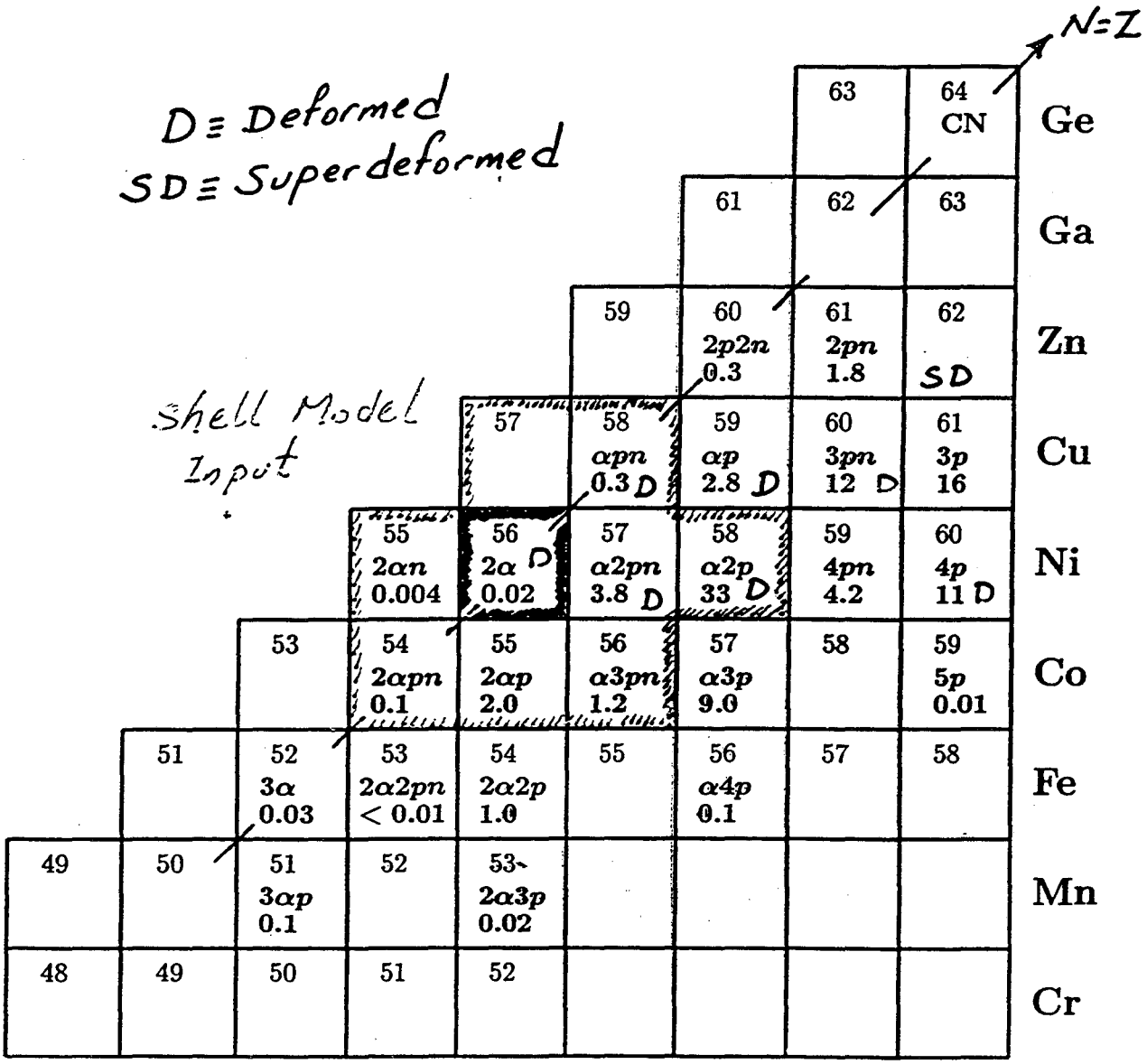


Figure 3: Experimental relative cross-sections [%] of the reaction $^{36}Ar + ^{28}Si$ at 136 MeV beam energy deduced from the thin target GAMMASPHERE experiment. The total cross section amounts to $\sigma_{tot} \approx 1000$ mb and the uncertainties reach from 5 % (strong channels) to 20 % (weak channels). The proposed reaction $^{24}Mg + ^{40}Ca$ leads to the same compound nucleus $^{64}Ge$.

- The A=55 Mirror Nuclei: The heaviest mirror pair yet studied

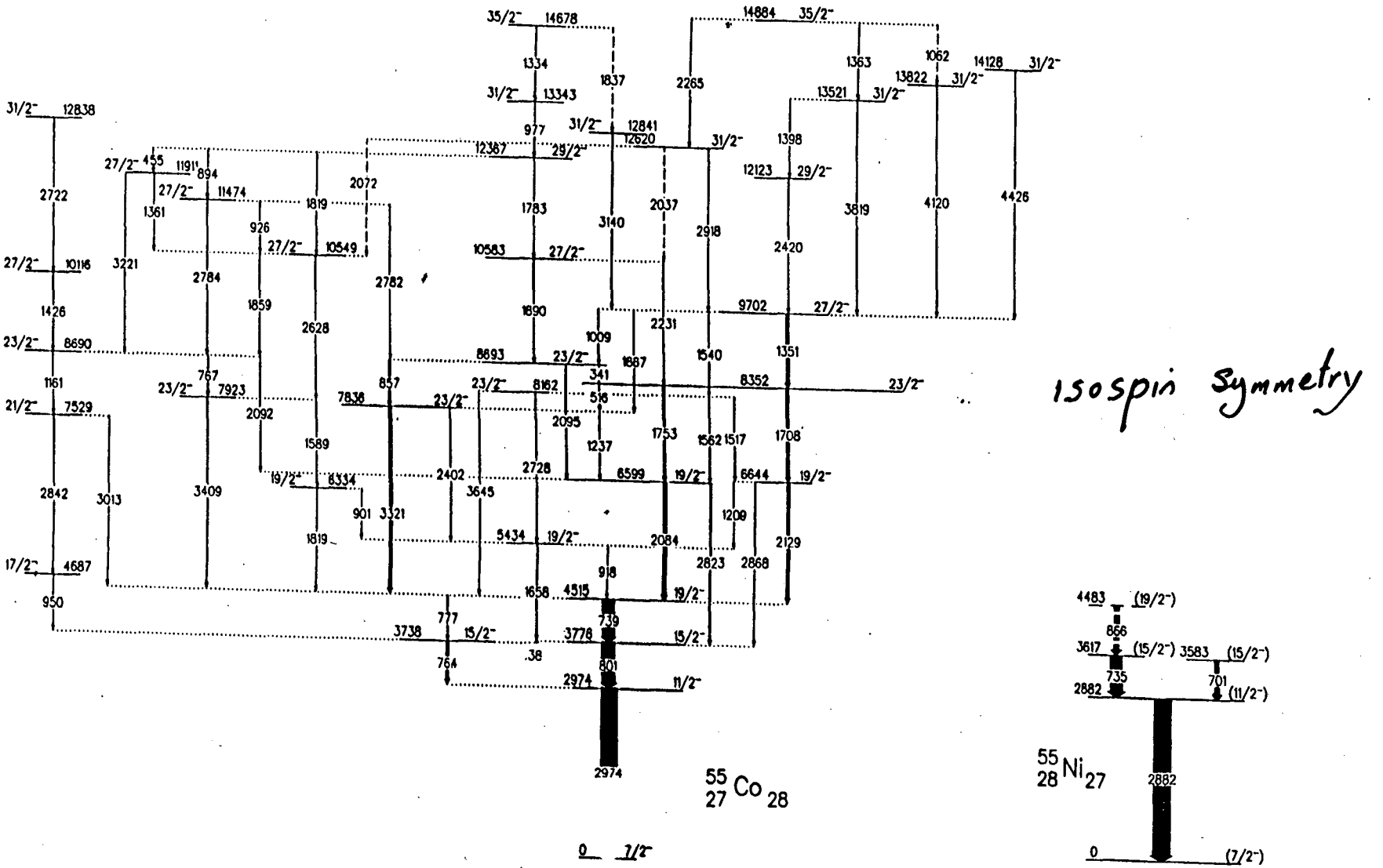

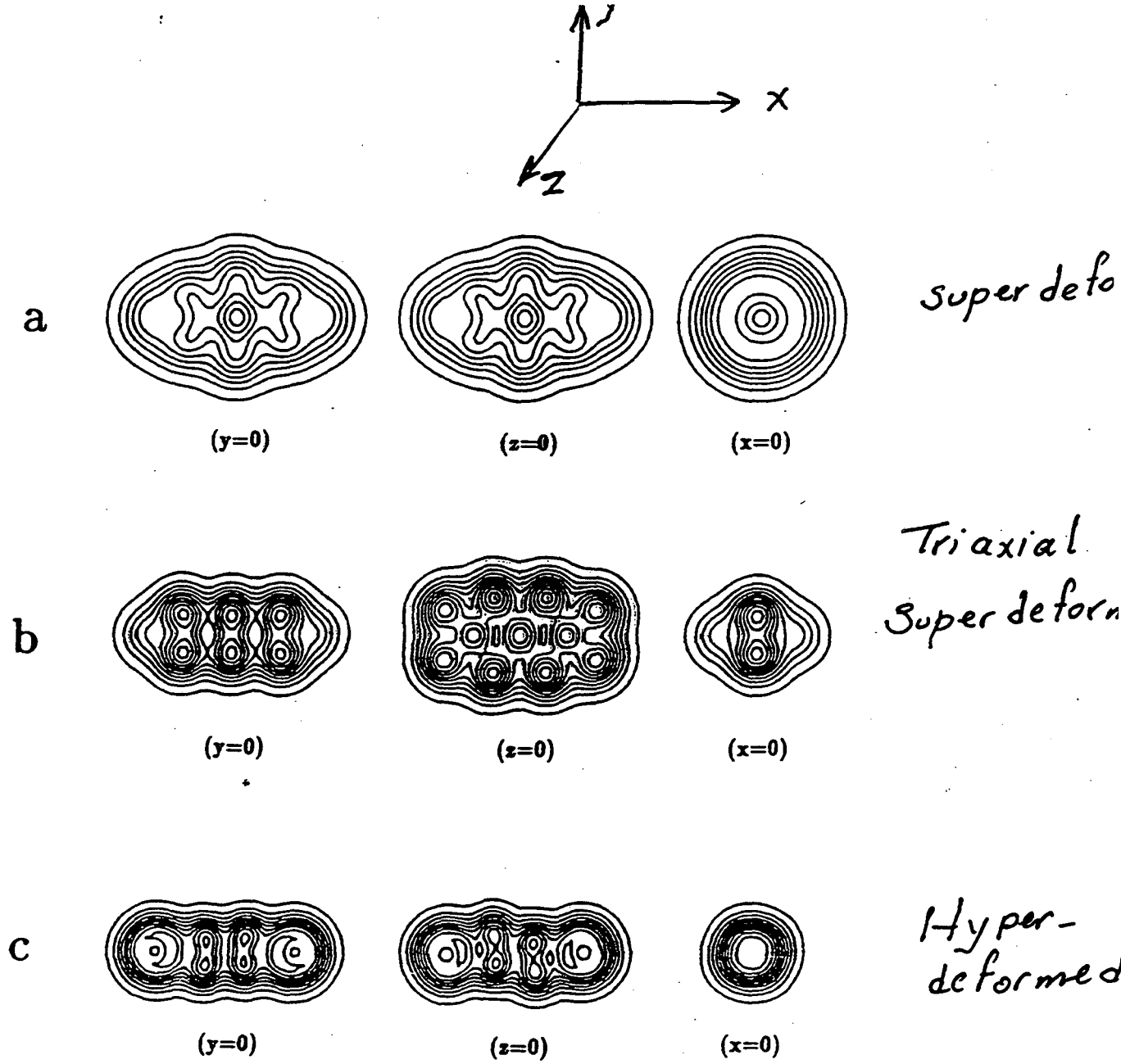


**FIG. 1. Density profile contours for (a) 2:1, (b) triaxial, and (c) 3:1 alpha-cluster configurations in $^{56}$Ni, from the Bloch-Brink alpha-cluster model calculations.**

Rudolph et al.

$\pi g_{9/2} \otimes \nu g_{9/2}$

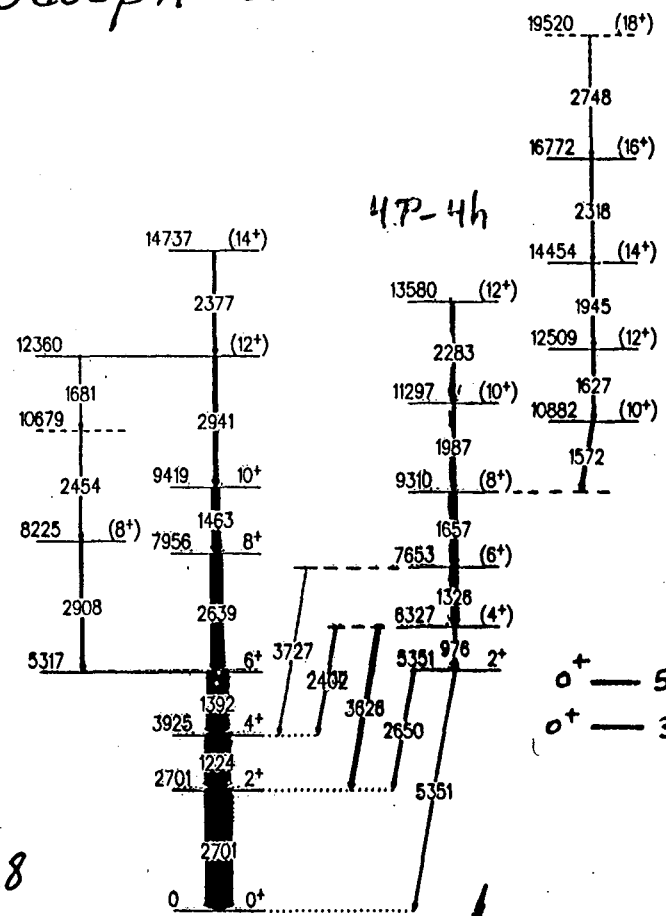


$^{56}_{28}Ni_{28}$

$0^+$ — 5003 (P,t)

$0^+$ — 3956 ($^3$He,n)

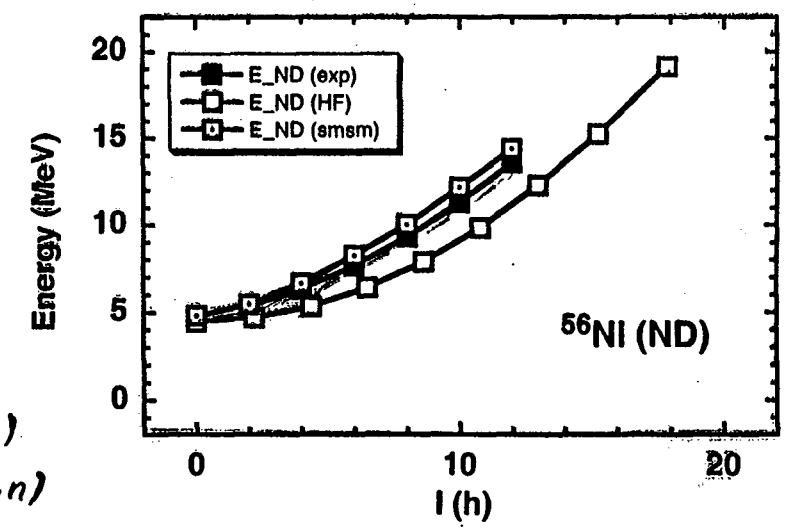


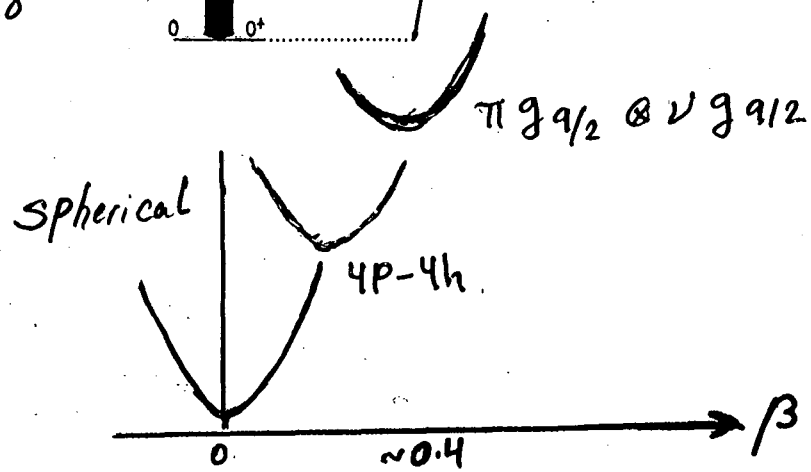

paul et. al.

Positive Parity Band in (N=Z+1) Nucleus $^{79}Y$ $\left\{ \begin{array}{l} J^{(1)} = J^{(2)} \\ \text{Rigid Rotor} \end{array} \right.$

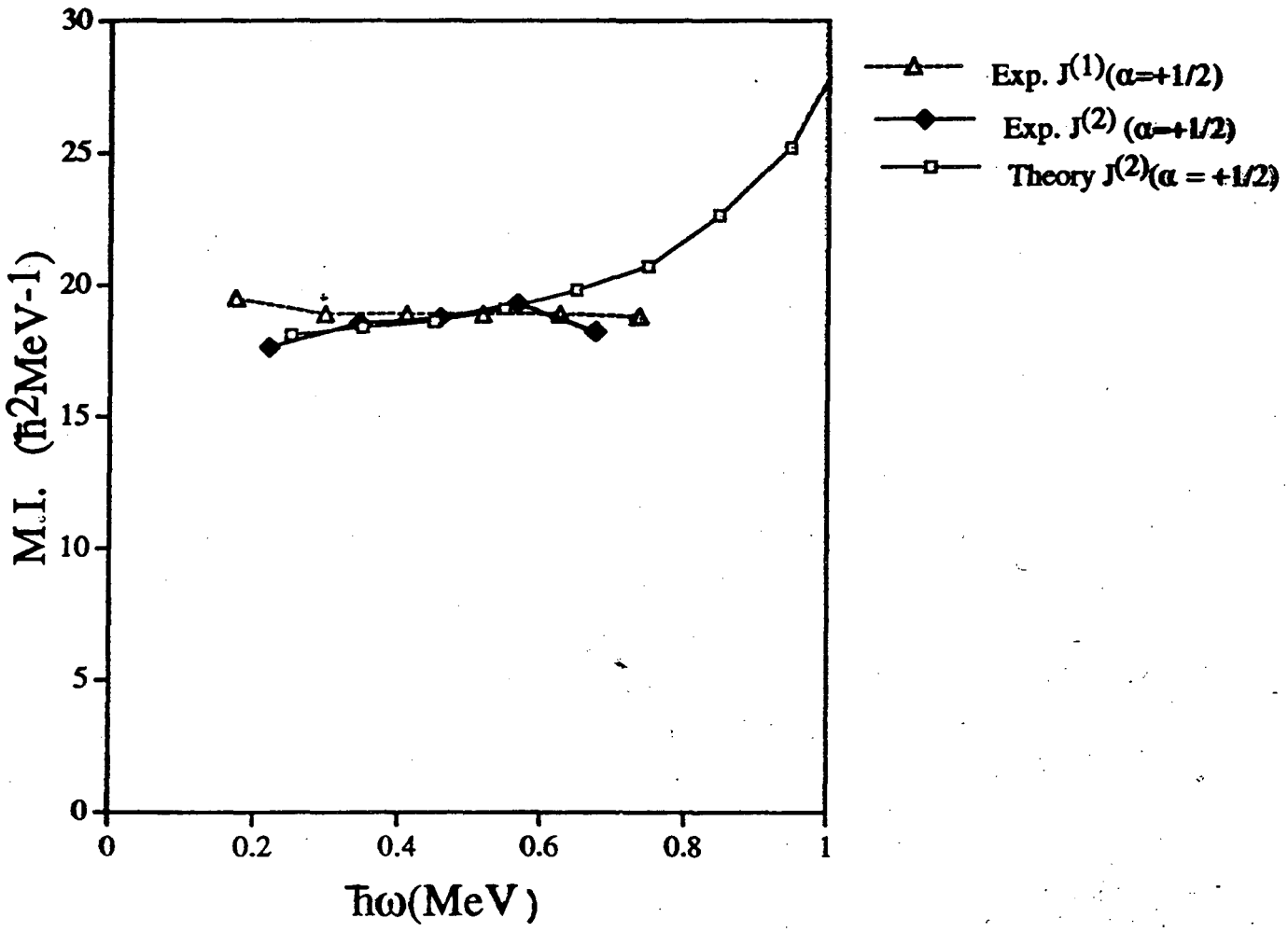

# Onset of $T$=0 Pairing and Deformations in High Spin States of the $N$=$Z$ Nucleus $^{48}$Cr

J. Terasaki, R. Wyss
The Royal Institute of Technology, Institute of Physics Frescati
Frescativägen 24, S-104 05 Stockholm, Sweden

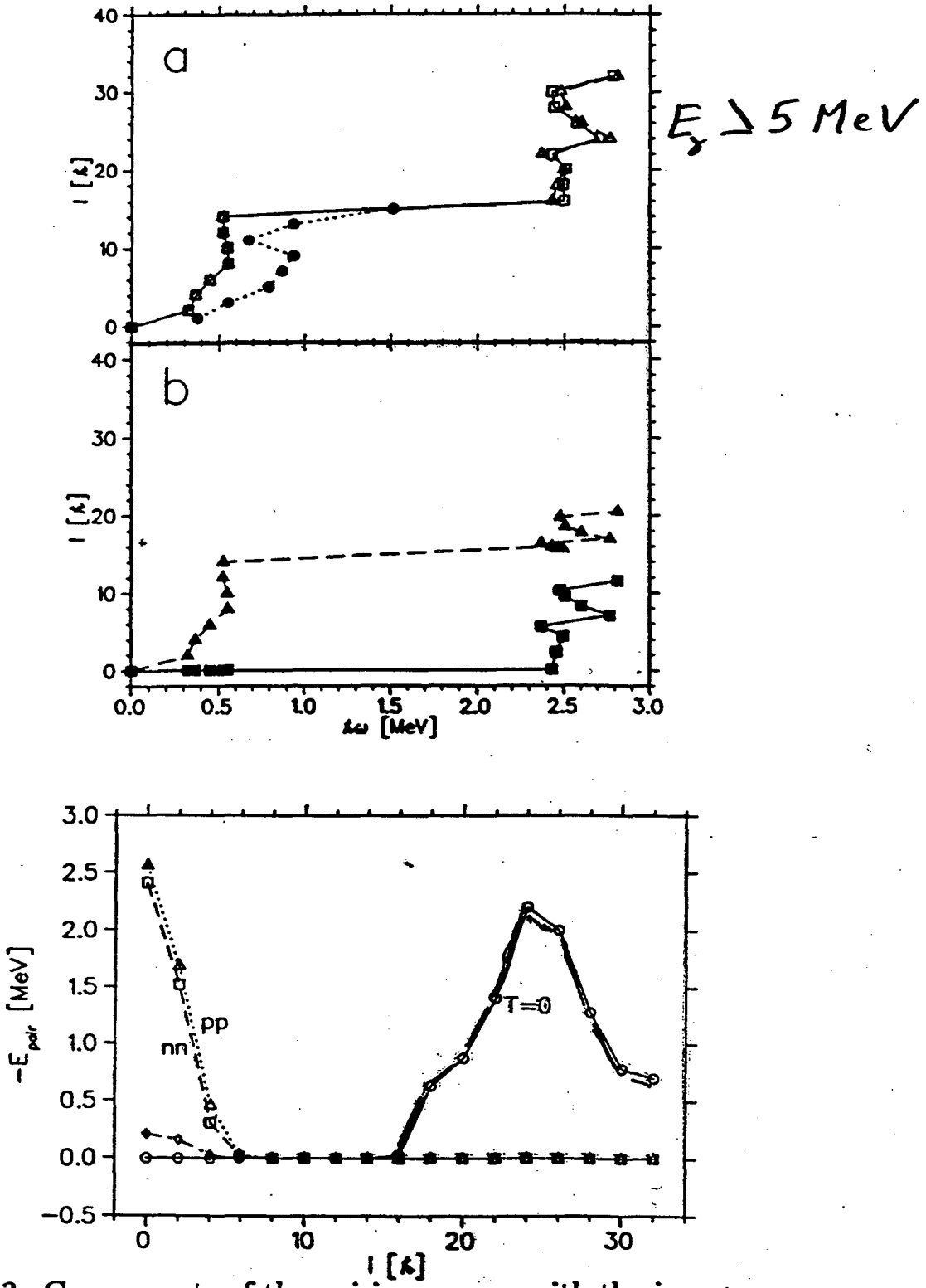


FIG. 3. Components of the pairing energy with the inverted sign. The diamonds are the $T = 1, T_z = 0$ (np) component.

Proton spectrum in coincidence with 830 keV gate in deformed band.

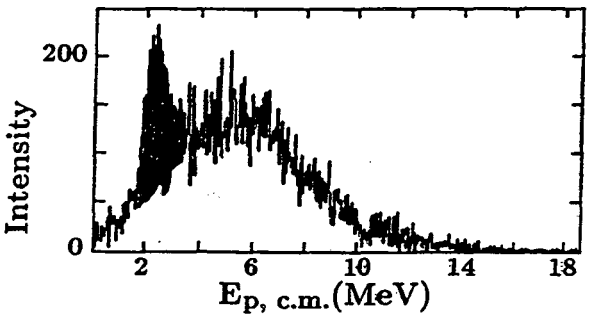


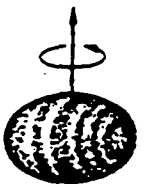

Deformed Band

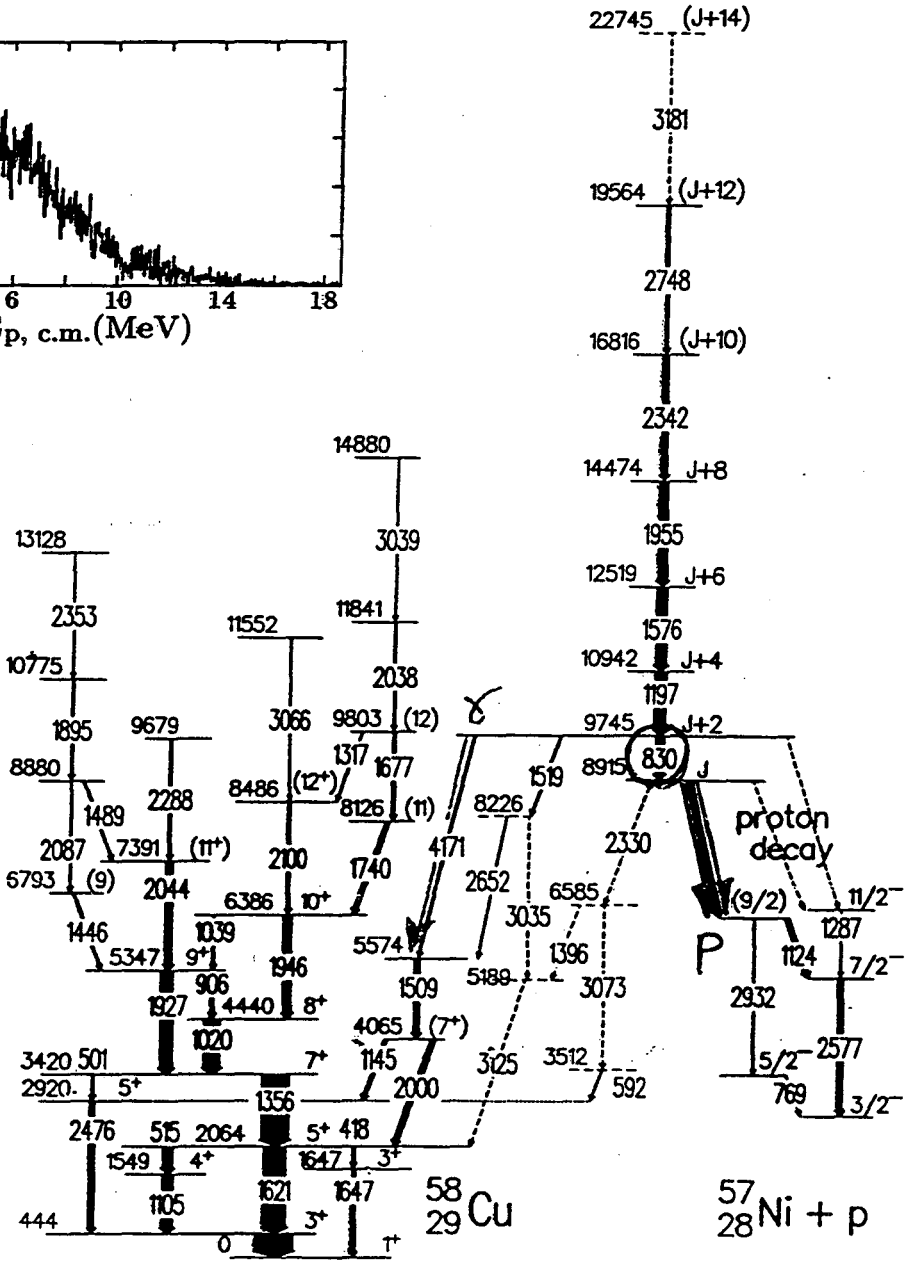


Rudolph et al.

Rudolph et al.

SD Band in $^{58}Cu$

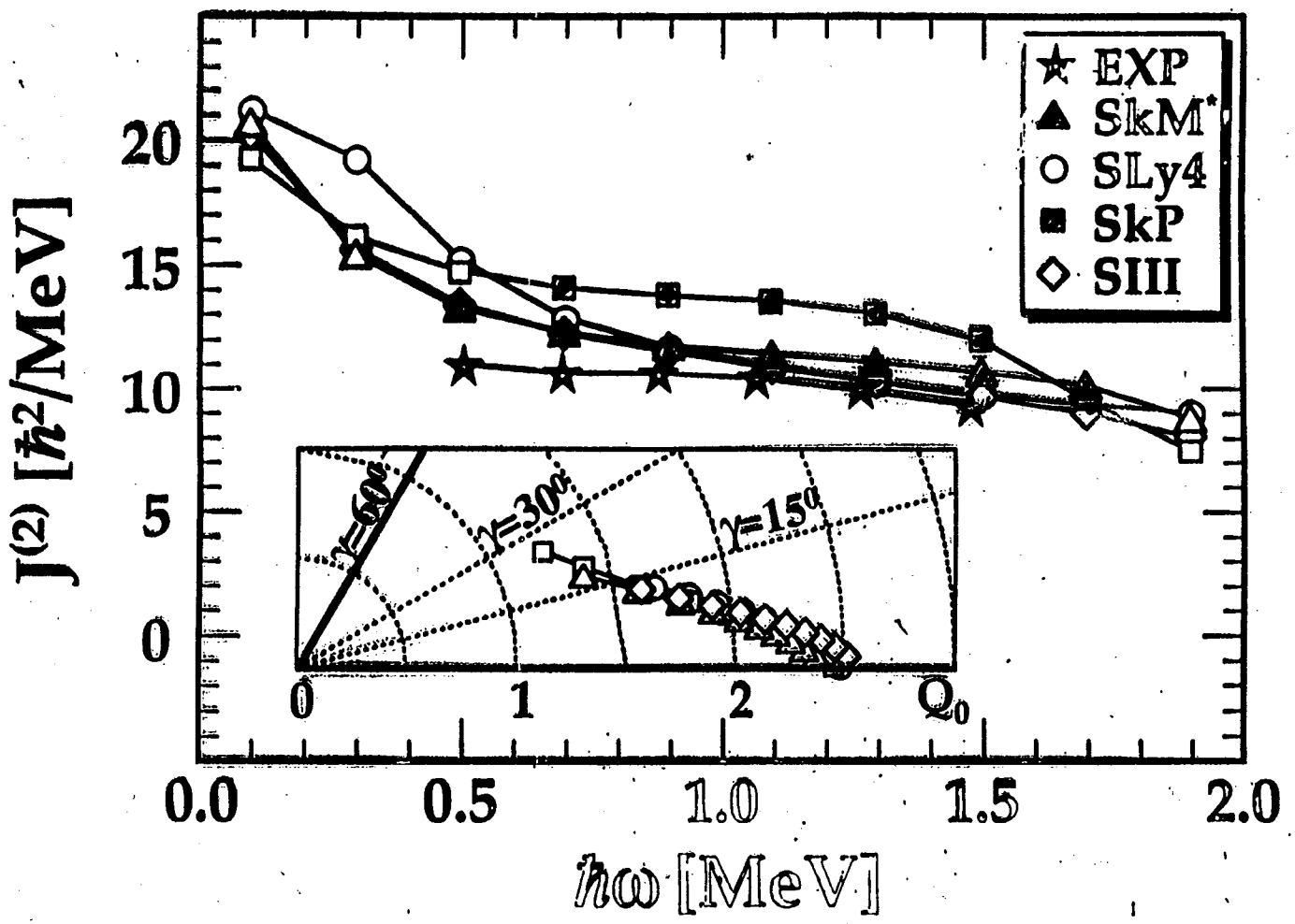

Dobaczewski
Satula
Zazarewicz

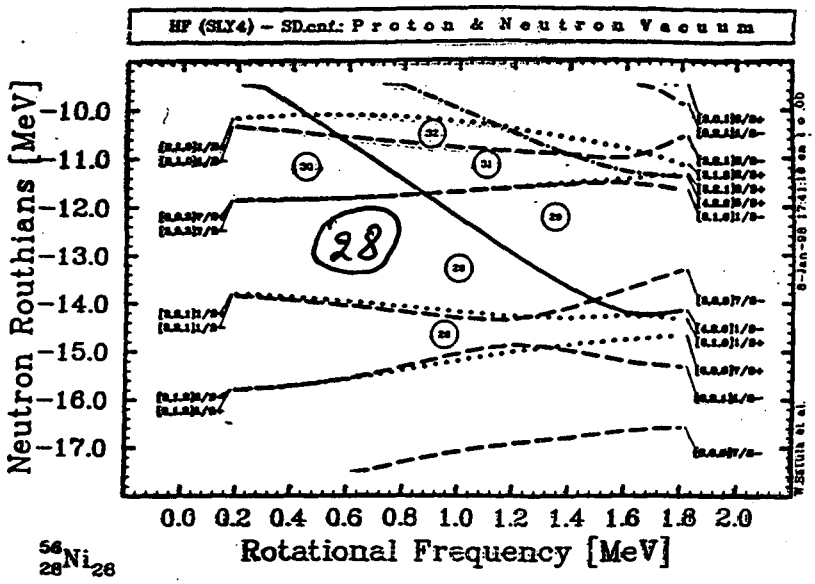


$^{56}_{28}Ni$

SM in
$f_{7/2}, f_{5/2}, g_{9/2}$
space

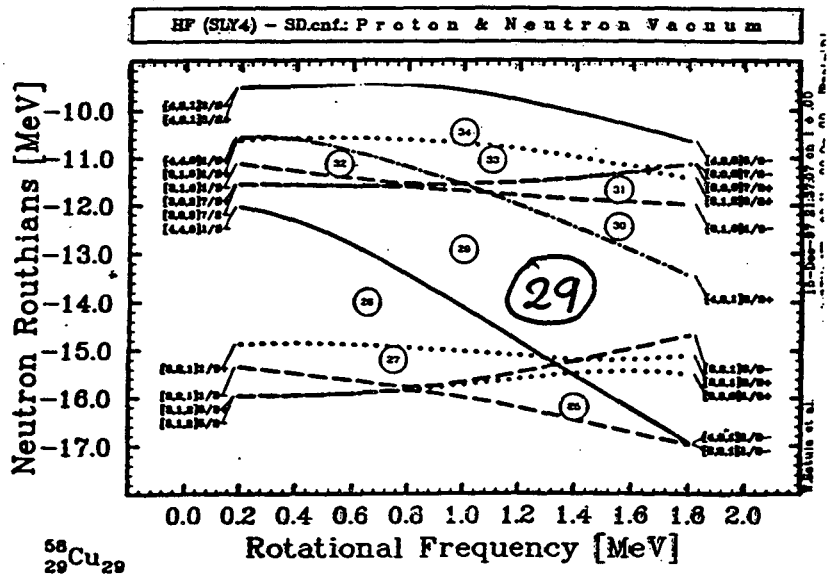


$^{58}_{29}Cu$

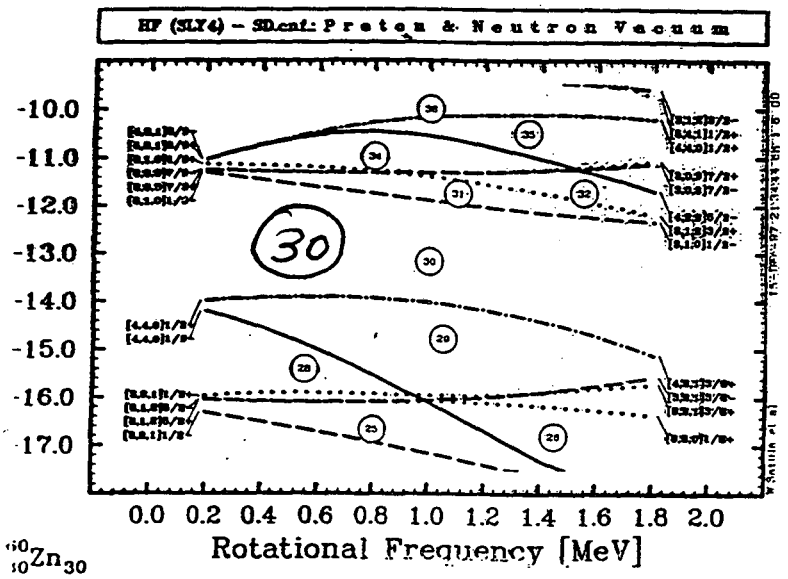


$^{60}_{30}Zn$

SD Gaps

# Superdeformed Nuc ear Rotors...

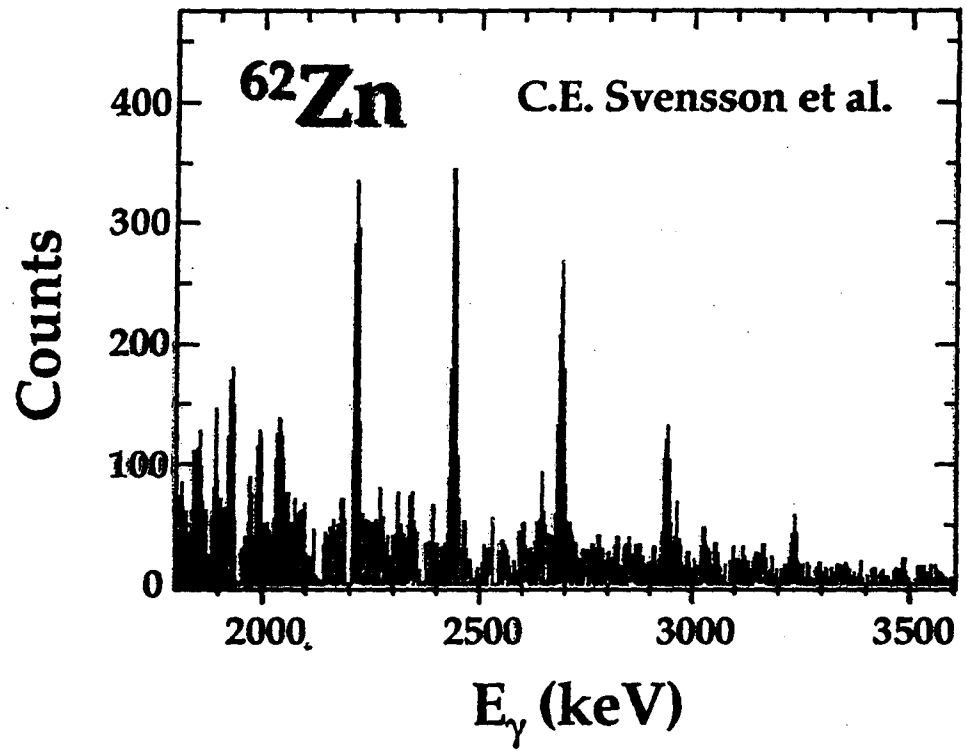

γ sphere

μ ball

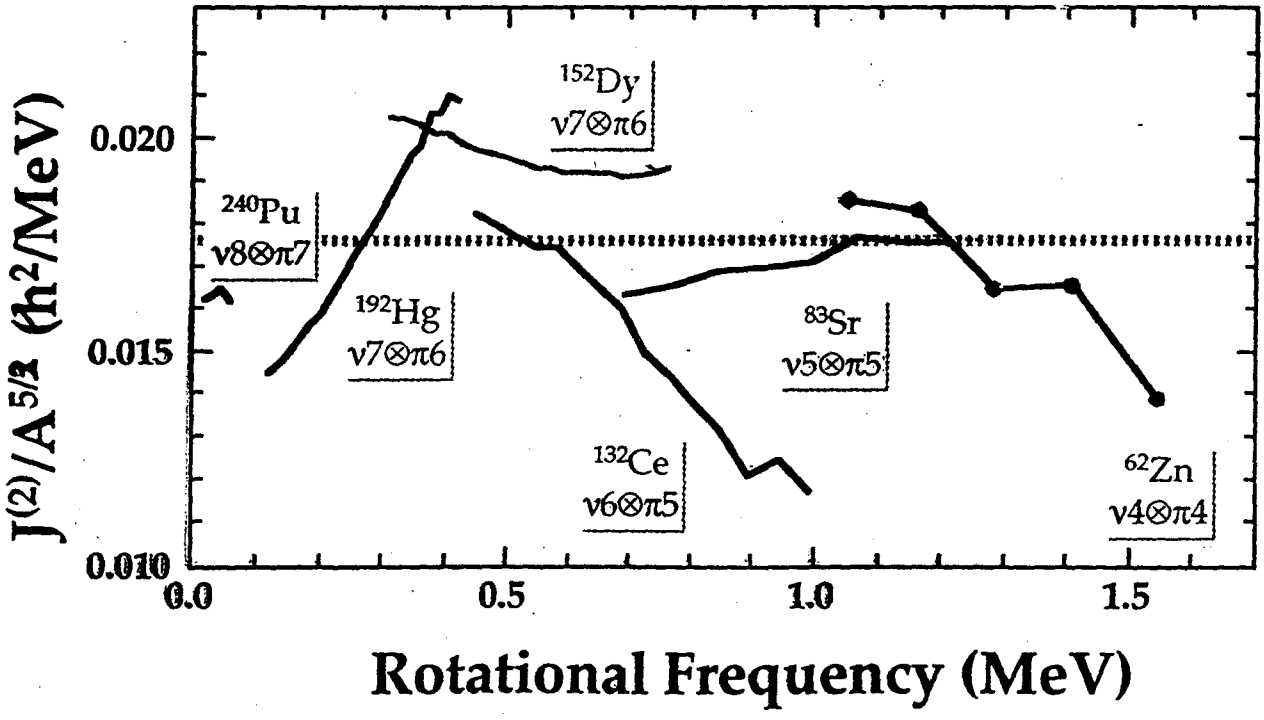

Dobaczewski

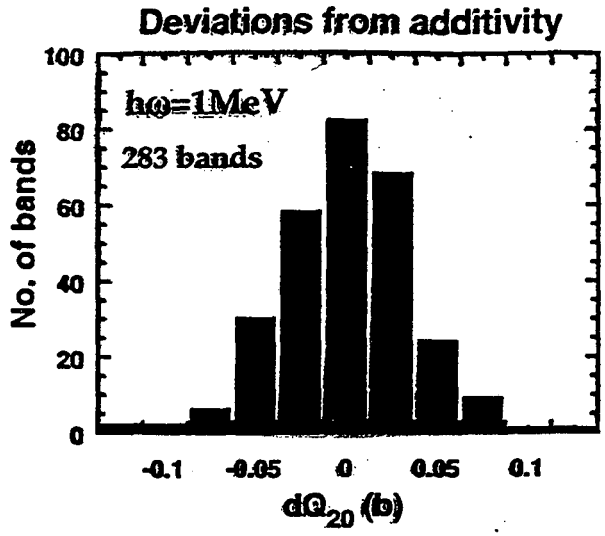


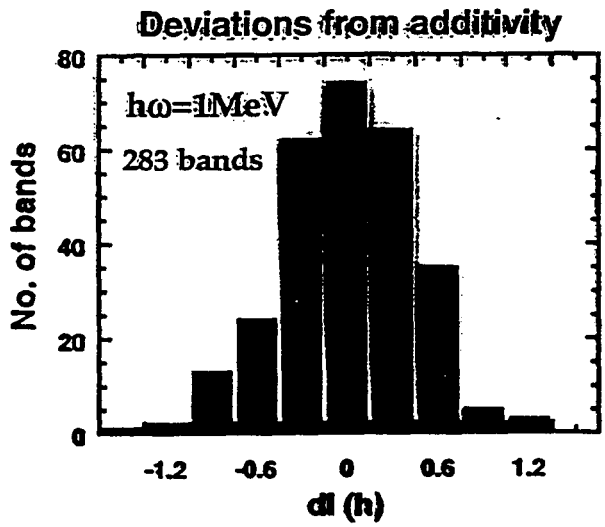


59Cu vs 58Cu

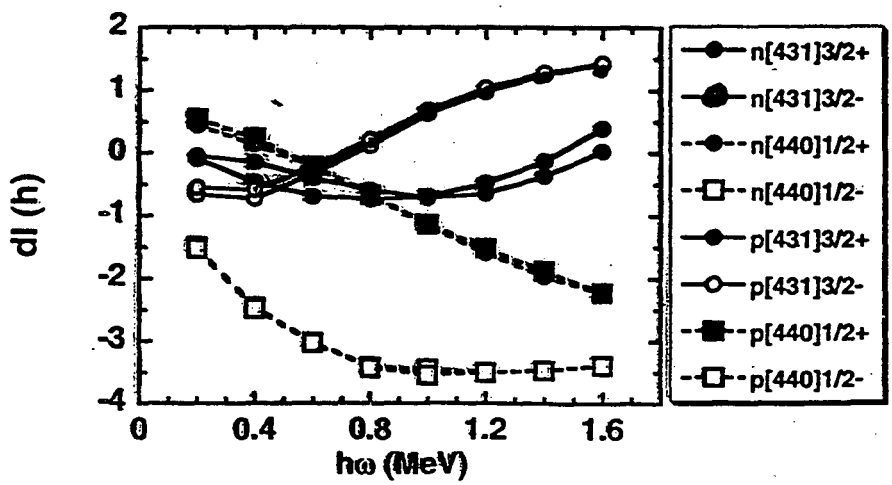

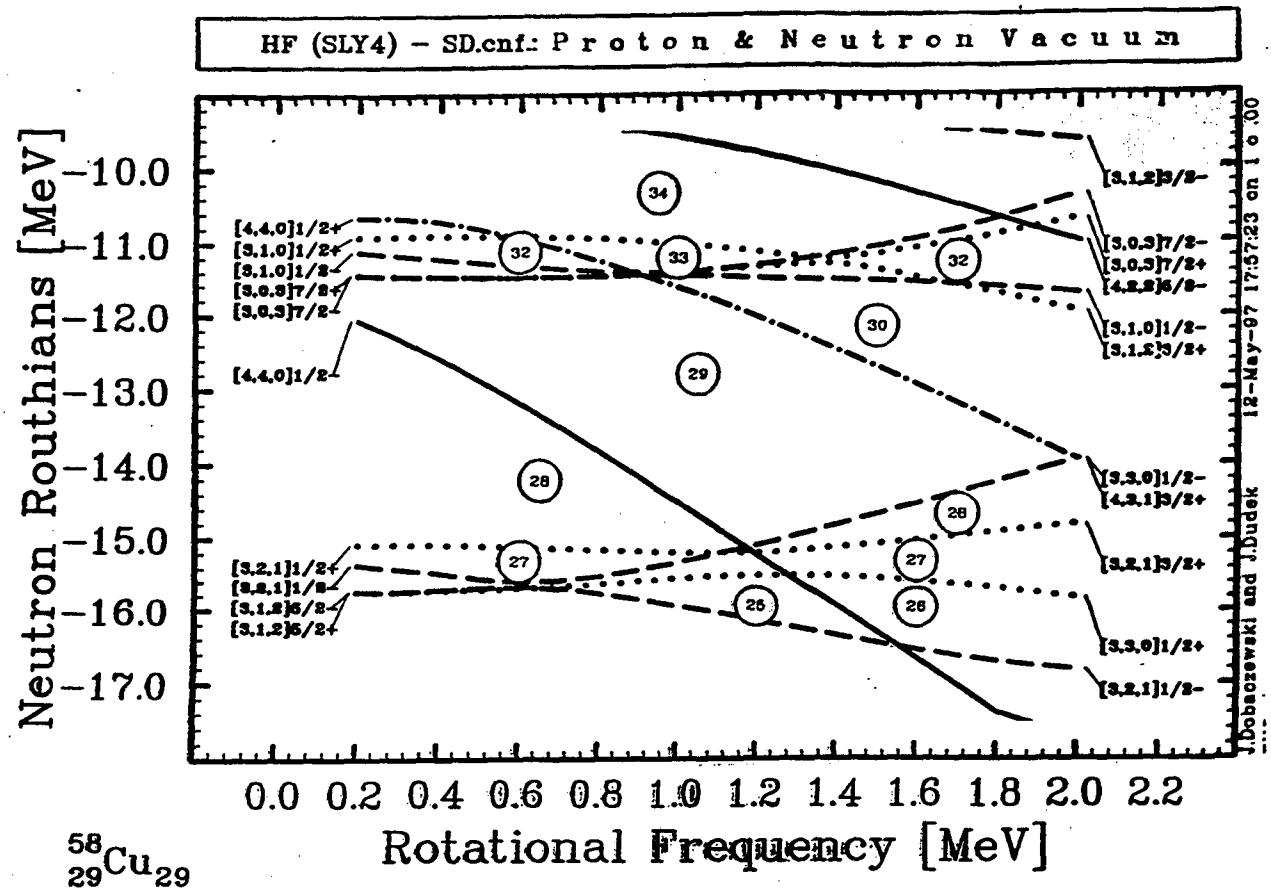
HF (SLY4) – SD.cnf.: Proton & Neutron Vacuum
Neutron Routhians [MeV]
Rotational Frequency [MeV]
$^{58}_{29}Cu_{29}$
[4,4,0]1/2+
[3,1,0]1/2+
[3,1,0]1/2-
[3,0,3]7/2+
[3,0,3]7/2-
[4,4,0]1/2-
[3,2,1]1/2+
[3,2,1]1/2-
[3,1,2]5/2-
[3,1,2]5/2+
[3,1,2]3/2-
[3,0,3]7/2-
[3,0,3]7/2+
[4,2,2]5/2-
[3,1,0]1/2-
[3,1,2]3/2+
[3,3,0]1/2-
[4,3,1]3/2+
[3,2,1]3/2+
[3,3,0]1/2+
[3,2,1]1/2-
J.Dobaczewski and J.Dudek
12-May-97 17:57:23 on 1 o .00

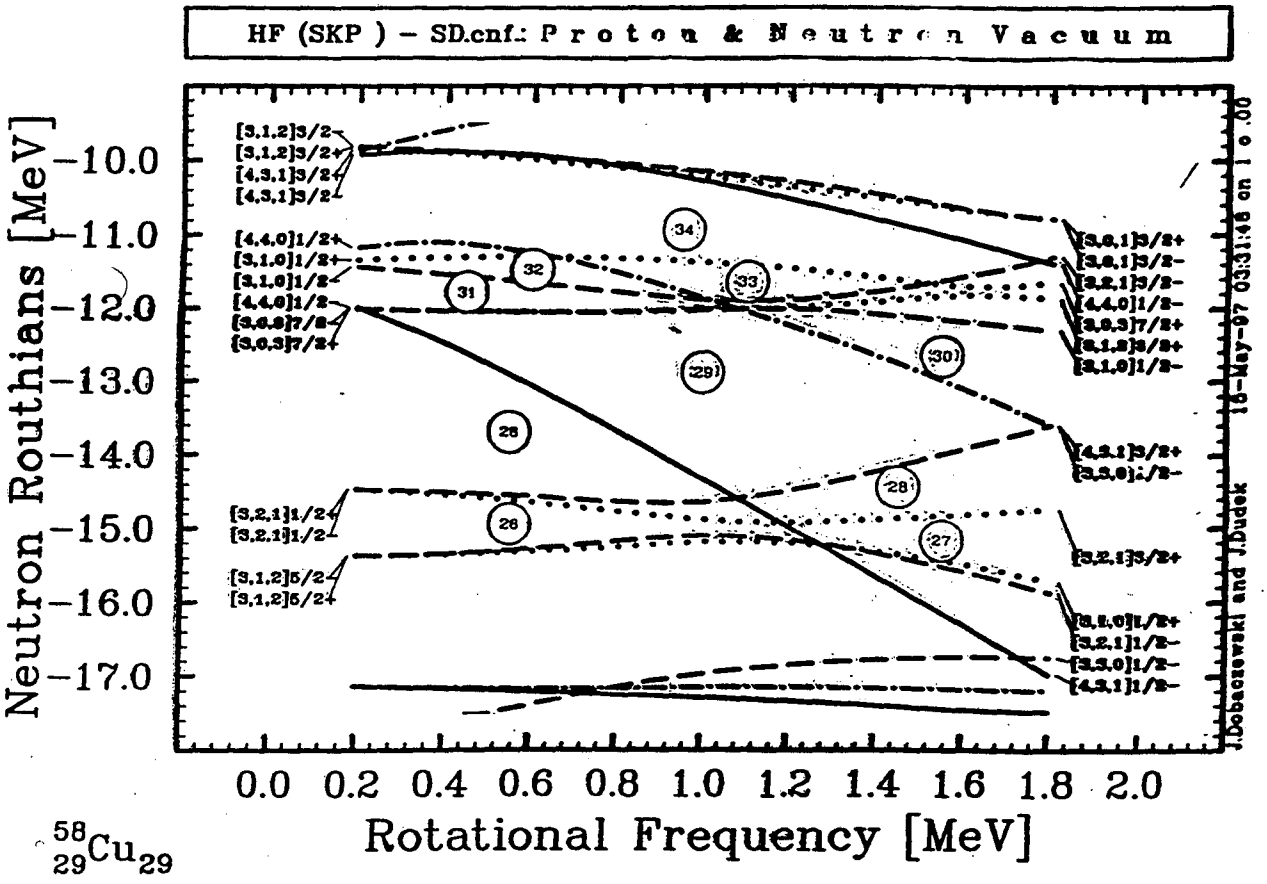
HF (SKP ) – SD.cnf.: Proton & Neutron Vacuum
Neutron Routhians [MeV]
Rotational Frequency [MeV]
$^{58}_{29}Cu_{29}$
[3,1,2]3/2-
[3,1,2]3/2+
[4,3,1]3/2+
[4,3,1]3/2-
[4,4,0]1/2+
[3,1,0]1/2+
[3,1,0]1/2-
[4,4,0]1/2-
[3,0,3]7/2-
[3,0,3]7/2+
[3,2,1]1/2+
[3,2,1]1/2-
[3,1,2]5/2-
[3,1,2]5/2+
[3,0,1]3/2+
[3,0,1]3/2-
[3,2,1]3/2-
[4,4,0]1/2-
[3,0,3]7/2+
[3,1,2]3/2+
[3,1,0]1/2-
[4,3,1]3/2+
[3,3,0]1/2-
[3,2,1]3/2+
[3,1,0]1/2+
[3,2,1]1/2-
[3,3,0]1/2-
[4,3,1]1/2-
J.Dobaczewski and J.Dudek
16-May-97 03:31:46 on 1 o .00

# Prompt Proton Decay
## of a
# Well-Deformed Band in $^{58}$Cu

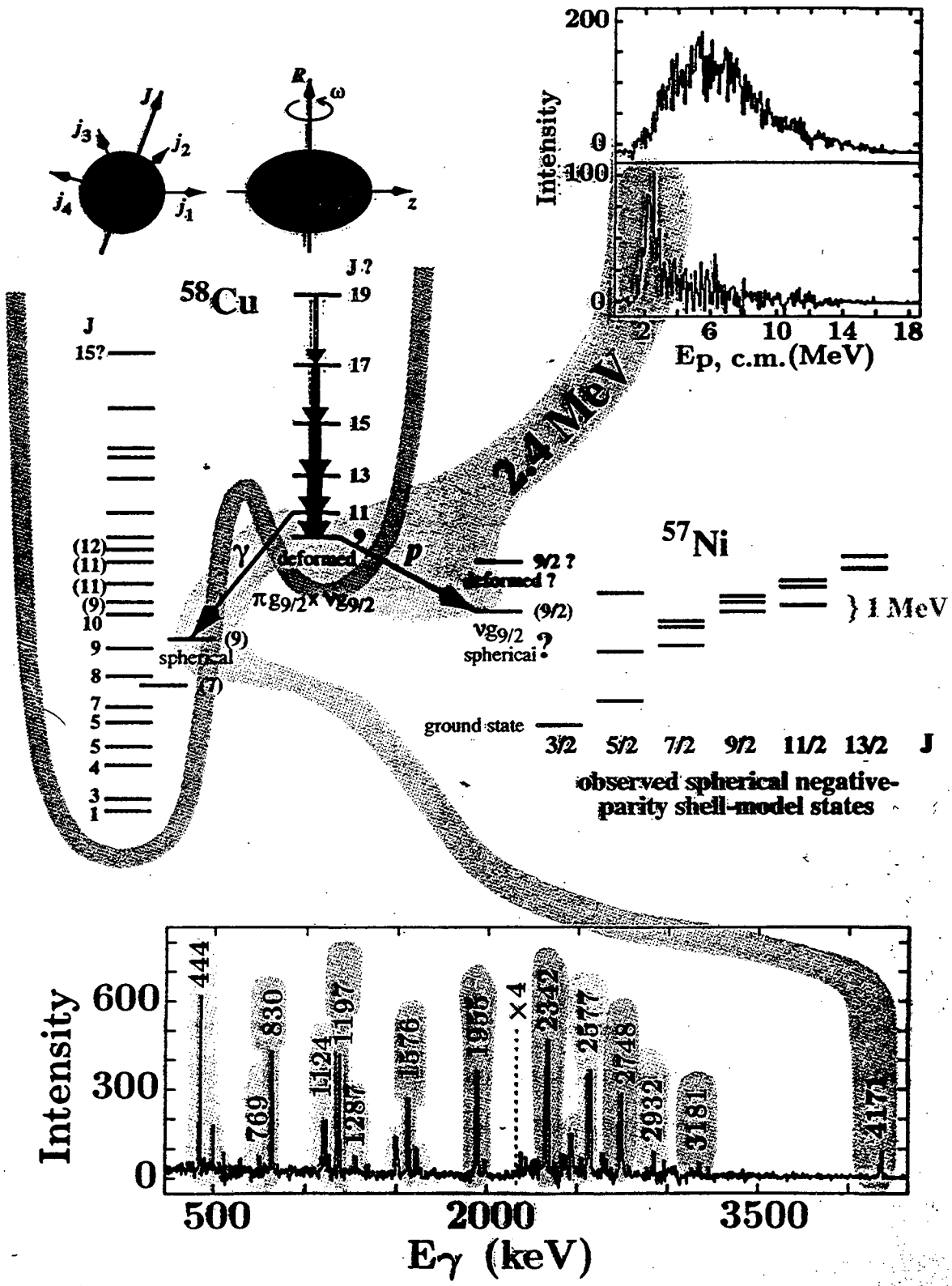

# Proton Radioactivity

First observation of p-radioactivity from the decay of the spin-gap isomer in $^{53}$Co. It has remained the only known p-emitter below Z=50 (Cerny et al., 1970).

near p-drip line

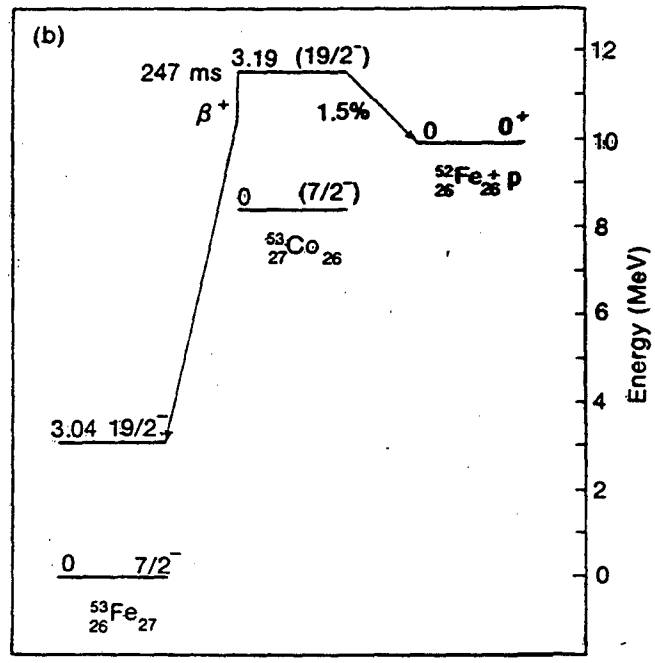


Aberg et al.

Comparison of the experimental and theoretical spectroscopic factors for the p-emitters in the Z=53-83 region (Aberg et al.). Except for the weakly deformed $^{109}$I and $^{113}$Cs, they are all believed to be spherical nuclei.

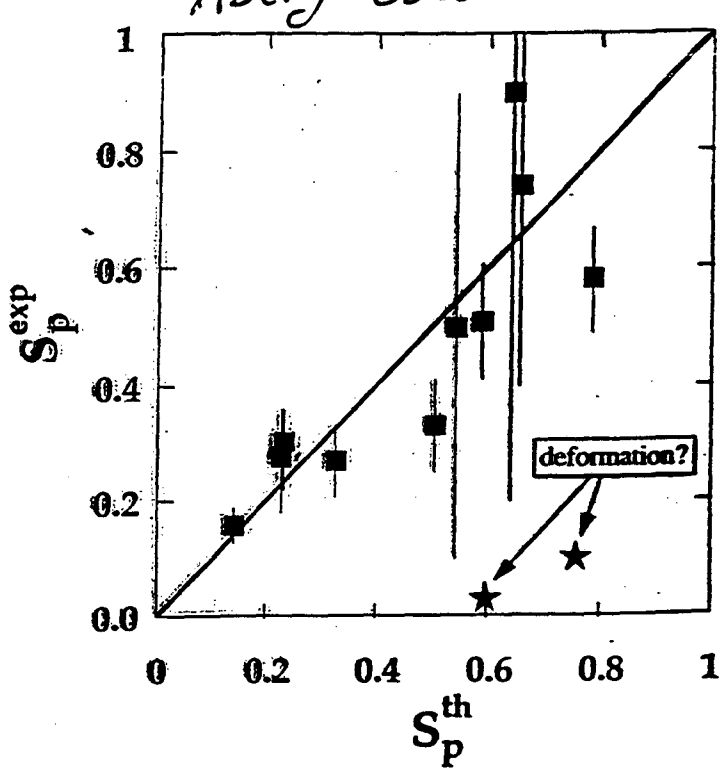


beyond p-drip line

RDT : band structure

# Excited States in $^{176,178}$Hg and Shape Coexistence in Very Neutron-Deficient Hg Isotopes

M. P. Carpenter,[1] R. V. F. Janssens,[1] H. Amro,[1,2] D. J. Blumenthal,[1] L. T. Brown,[1,3] D. Seweryniak,[1] P. J. Woods,[4] D. Ackermann,[1] I. Ahmad,[1] C. Davids,[1] S. M. Fischer,[1] G. Hackman,[1] J. H. Hamilton,[3] T. L. Khoo,[1] T. Lauritsen,[1] C. J. Lister,[1] D. Nisius,[1] A. V. Ramayya,[3] W. Reviol,[5] J. Schwartz,[1,6] J. Simpson,[7] and J. Wauters[5]

$\epsilon_\gamma \simeq 1\%$

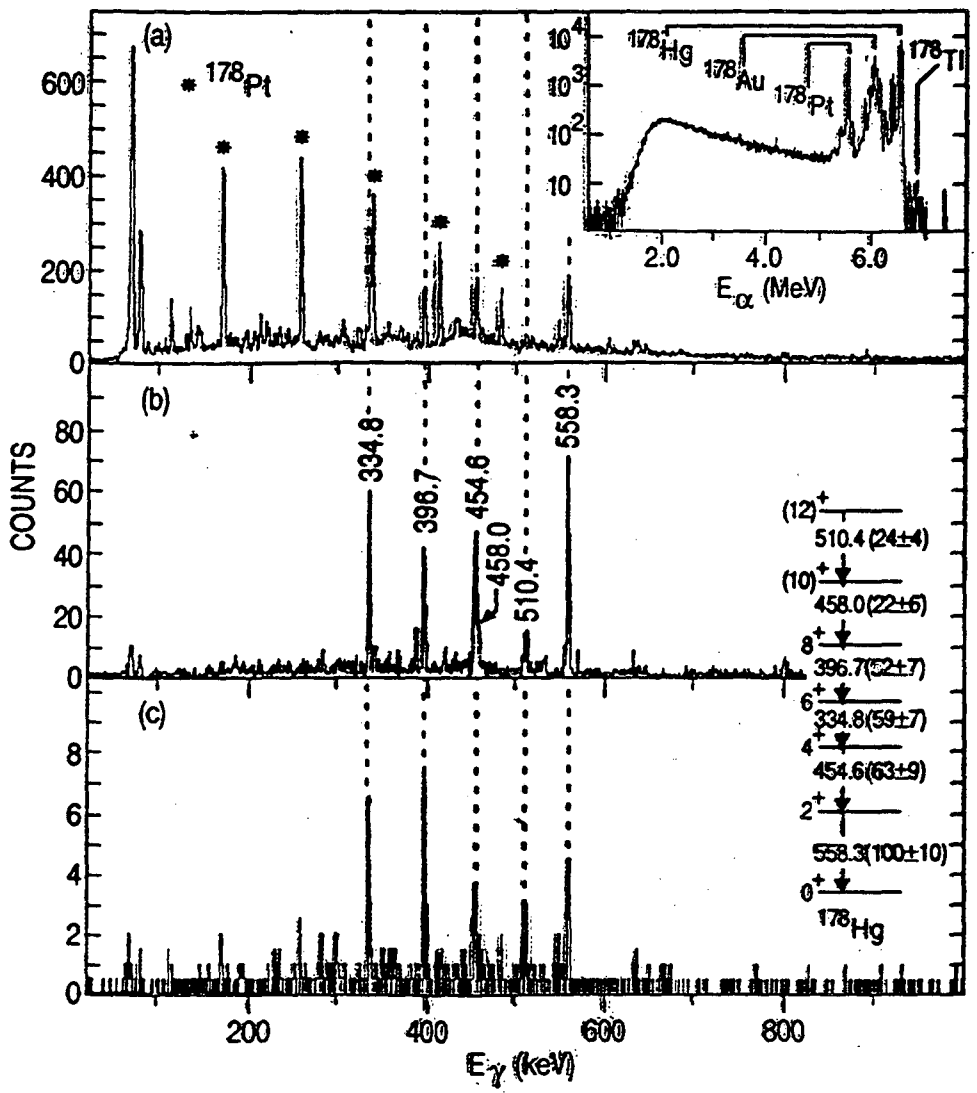


FIG. 1. Sample spectra relevant for the $^{178}$Hg data: (a) projection of all $\gamma$ rays in coincidence with mass $A = 178$; (b) $\gamma$ rays correlated with the $^{178}$Hg $\alpha$ decay (the charged-particle spectrum is shown in the top inset); (c) sum of coincidence spectra gated on the transitions assigned to the $^{178}$Hg level scheme given in the second inset. The measured total intensities are given in parenthesis next to the transition energies in the level scheme. See text for a detailed discussion.

# Proton emission from deformed nuclei

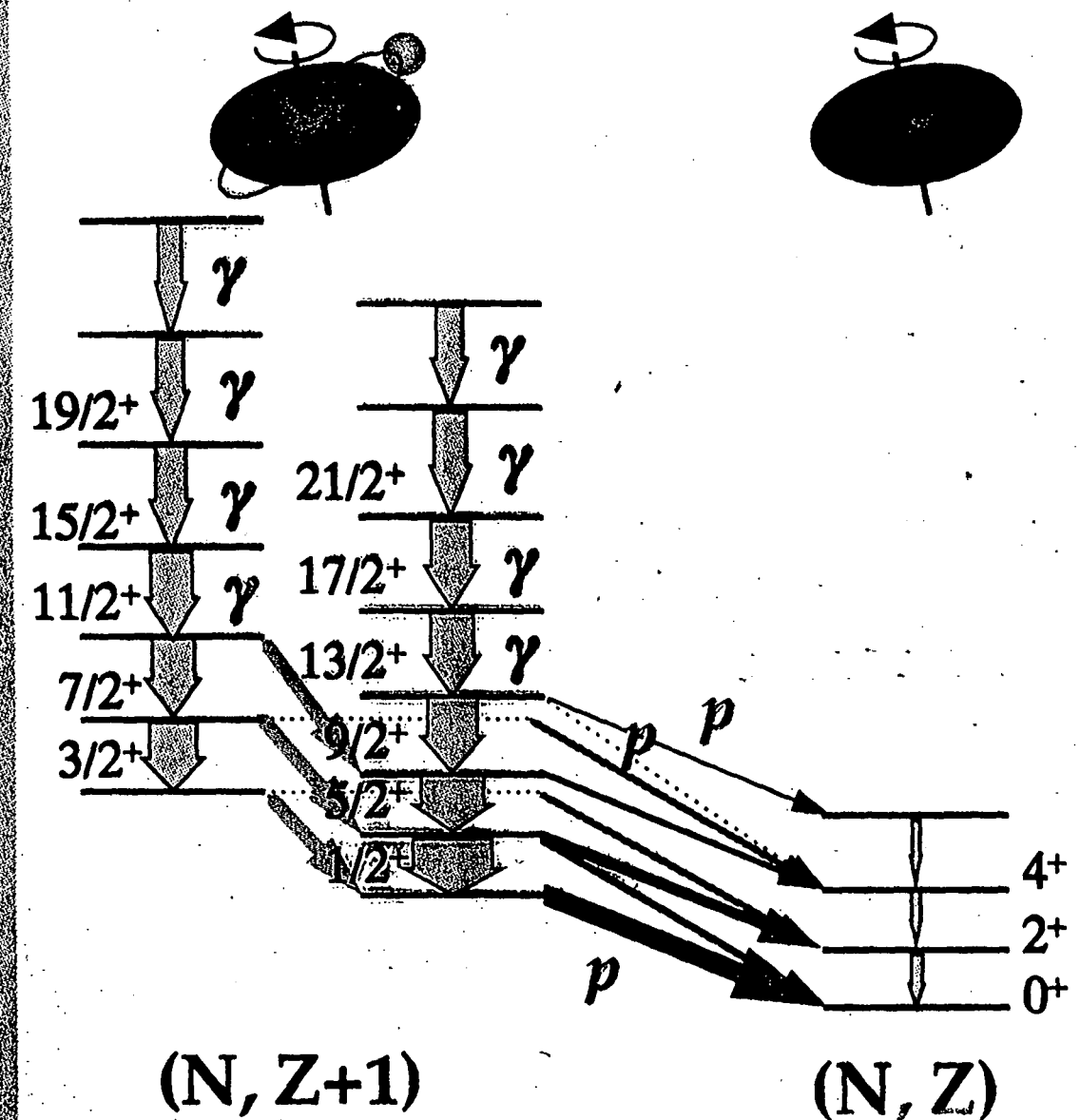


- Competition between gammas and protons (very narrow energy window!)
- Strong dependence of proton width on:
  - ☆ deformation
  - ☆ angular momentom
  - ☆ residual interaction
- Angular momentum dependent coupling between bound states and narrow resonances
- Very clean three-dimensional tunelling through the deformed barrier
- Non-standard approach to Nilsson orbitals!

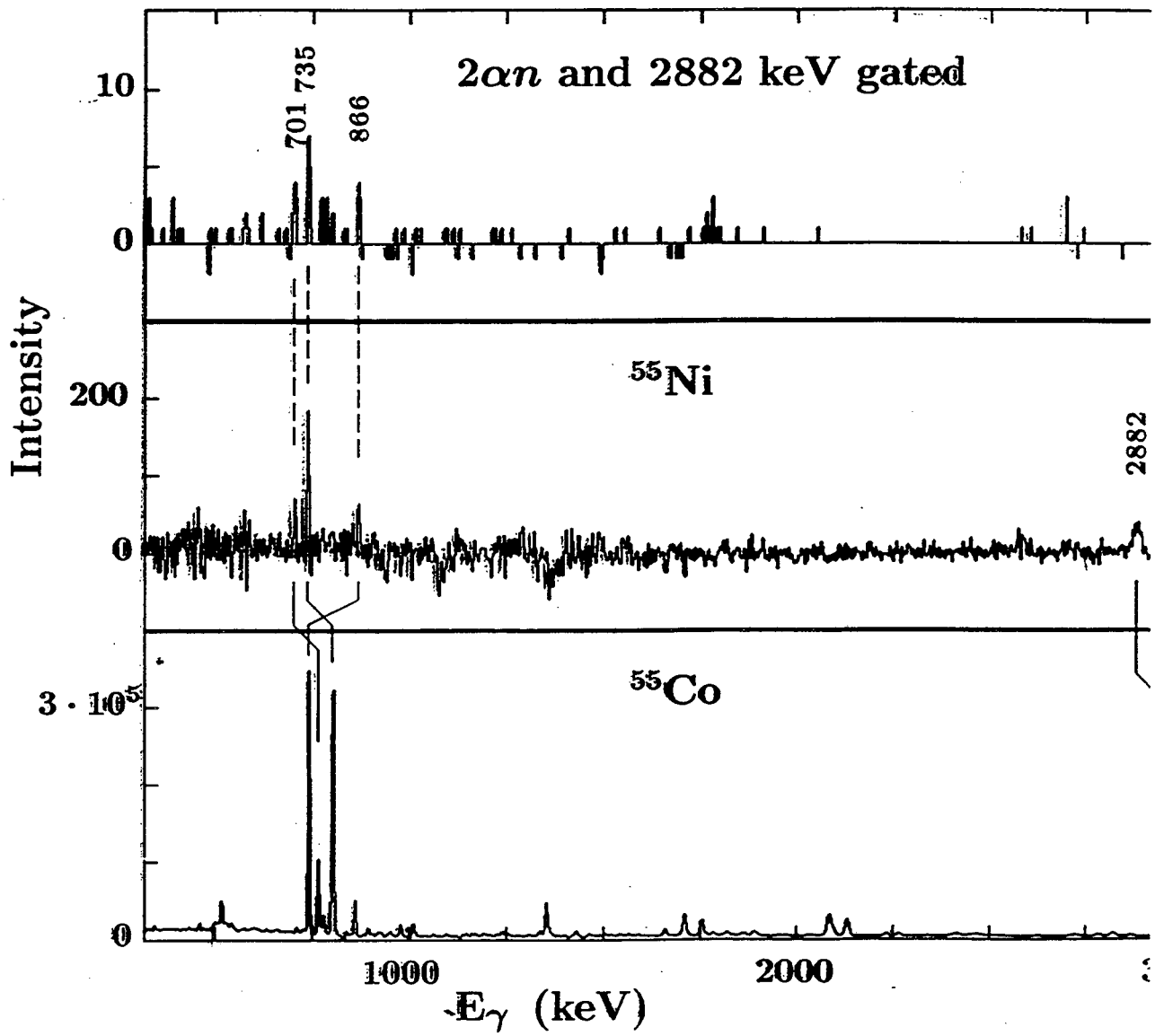


$^{55}Ni$ $\begin{cases} \sigma \simeq 40\,\mu b \\ GS\ (^{57}Ge) \end{cases}$

$^{57}Cu$ : few $\mu b$

Beyond GS

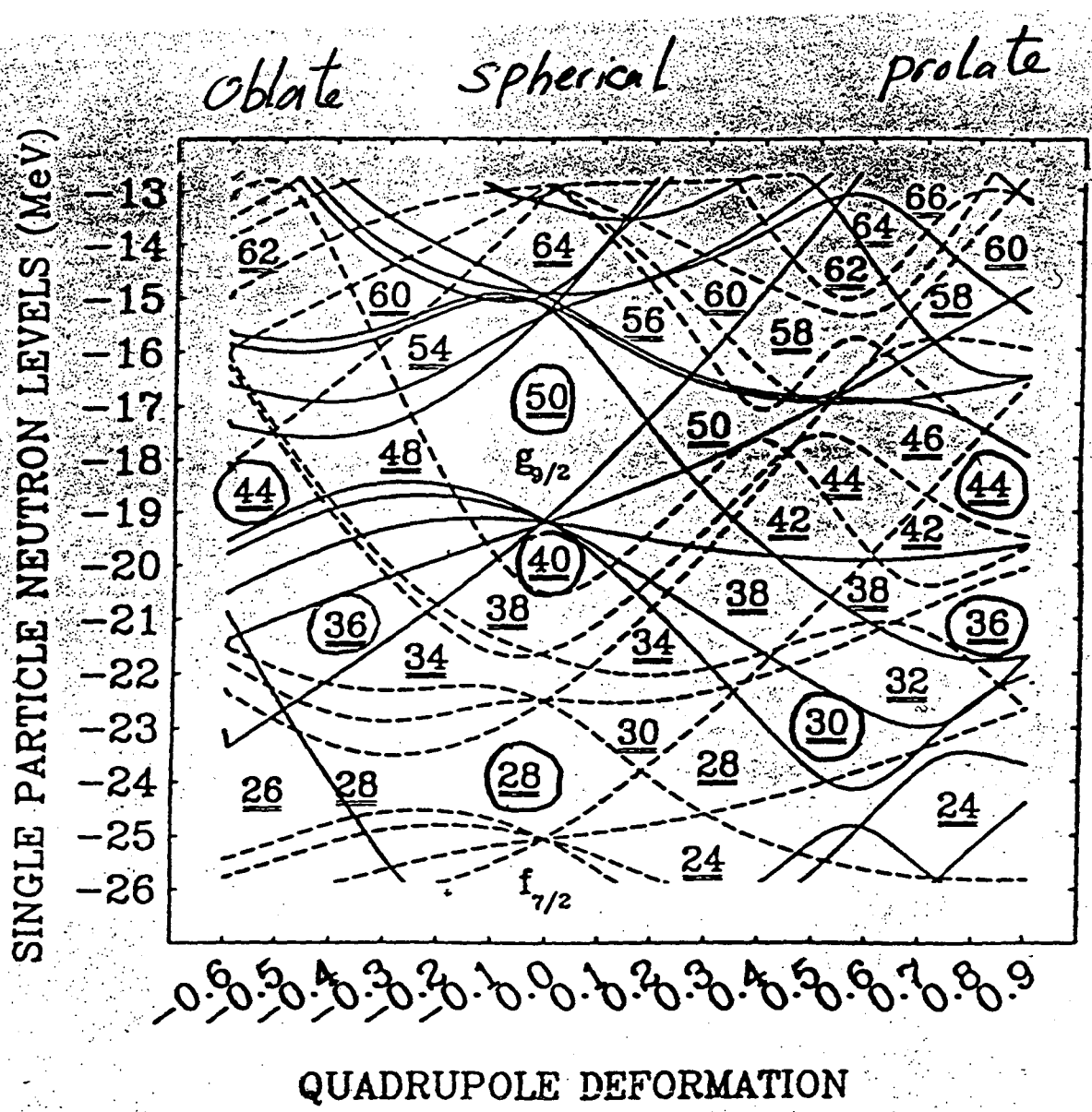


- The proton- & neutron shell gaps occur *simultaneously* in N=Z nuclei and give rise to a variety of distinct shapes and structures.

- These structures change rapidly with N, Z, and I.

- These changes provide a strong challenge to microscopic models.

Gelletly et al

Vampir : prolate g.s.
excited oblate

Nazarewicz : γ-soft
3 minima @ $\epsilon = \begin{cases} -0.08 \\ -0.27 \\ +0.30 \end{cases}$

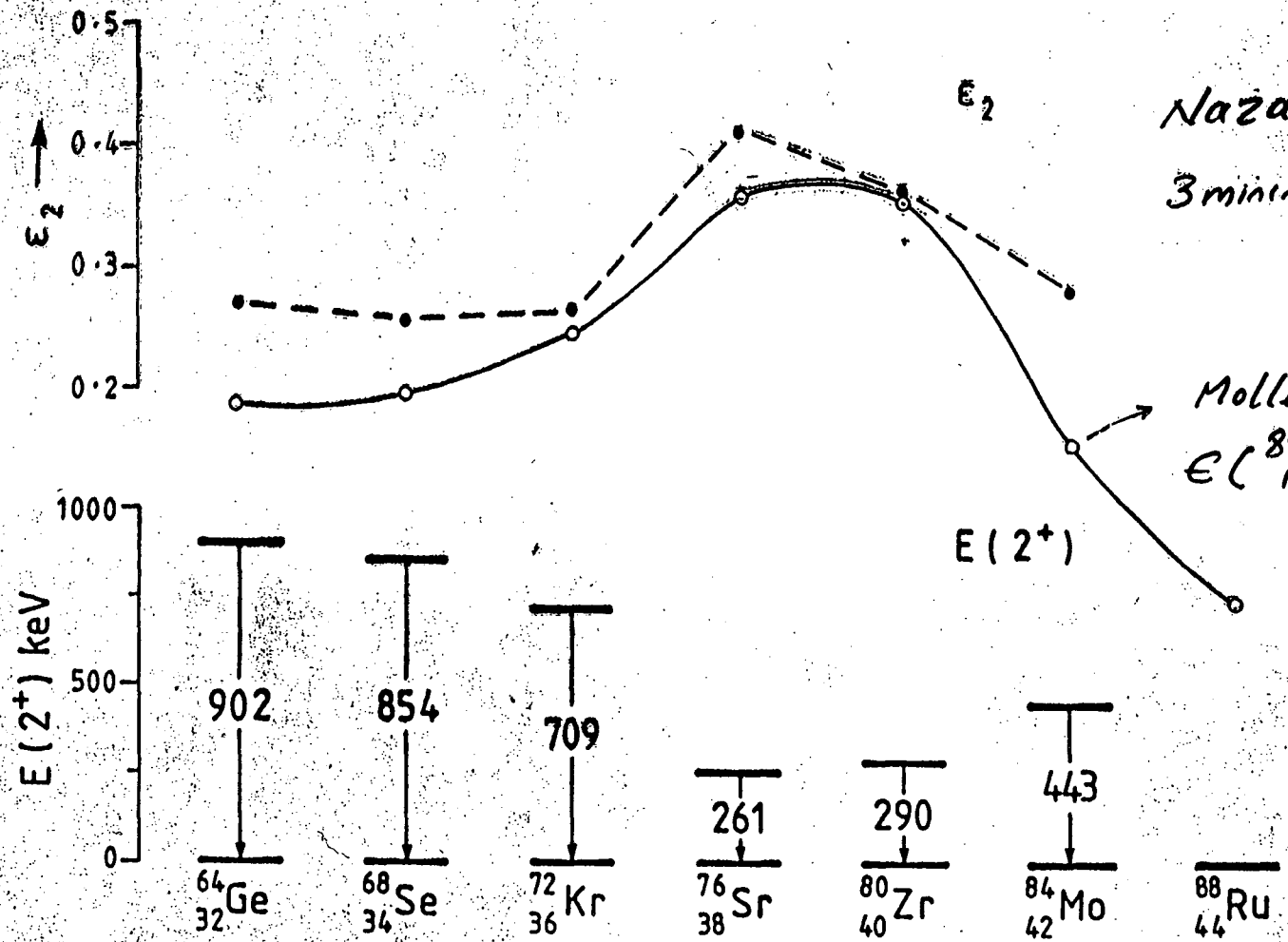


Moller & Nix
$\epsilon(^{84}Mo) = -0.18$

Triaxial

prolate – oblate
shape co-existence

very large
prolate

?

?

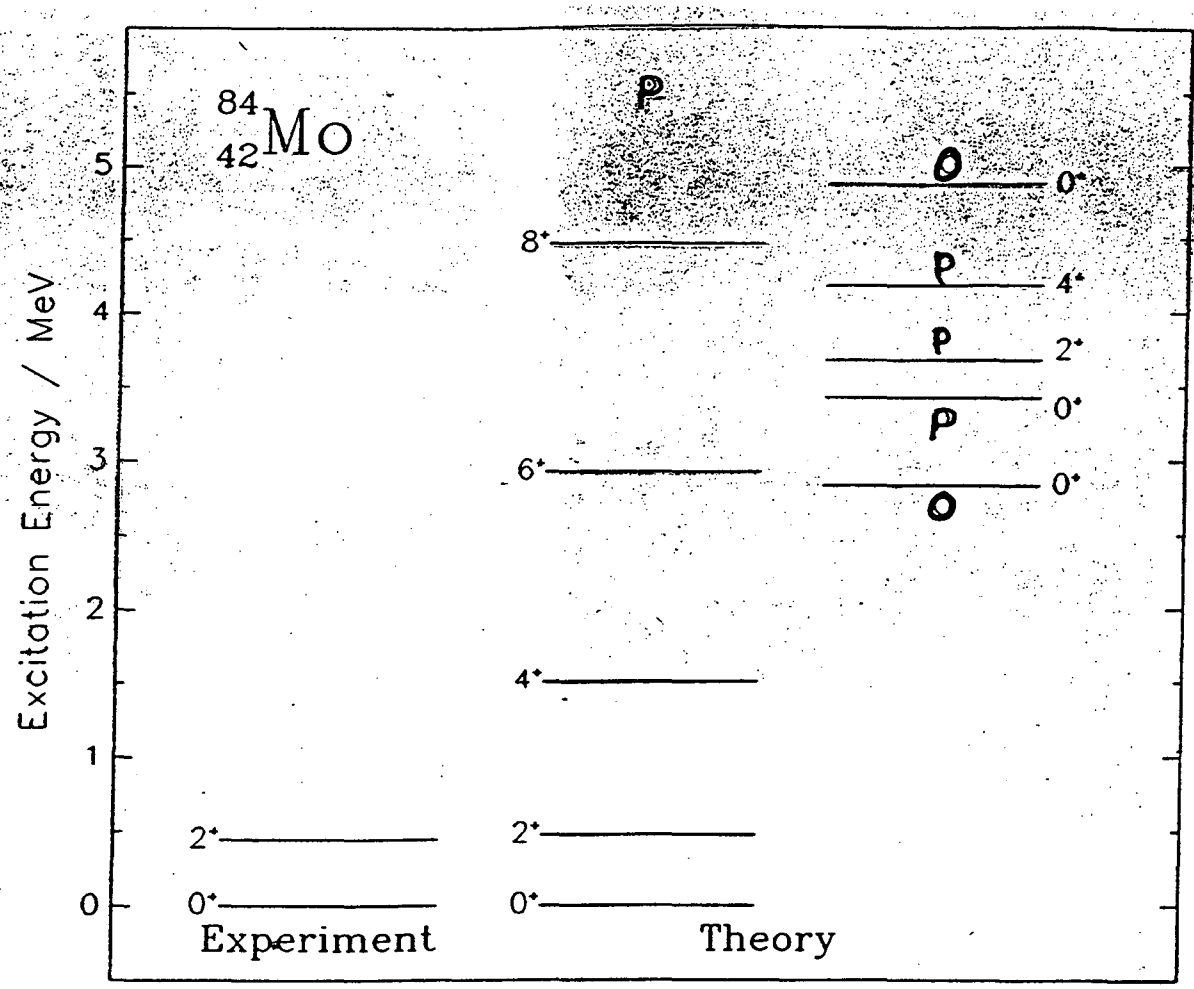
$^{84}_{42}$Mo
Excitation Energy / MeV
0
1
2
3
4
5
2+
0+
Experiment
8+
6+
4+
2+
0+
Theory
P
O
0+
P
4+
P
2+
P
0+
O
0+

VAMPIR

Gelletly et al

Heavier N=Z ; σ ≈ 10 μb ⇒ Requires High Selecti

- Mass separator

* Z - selector

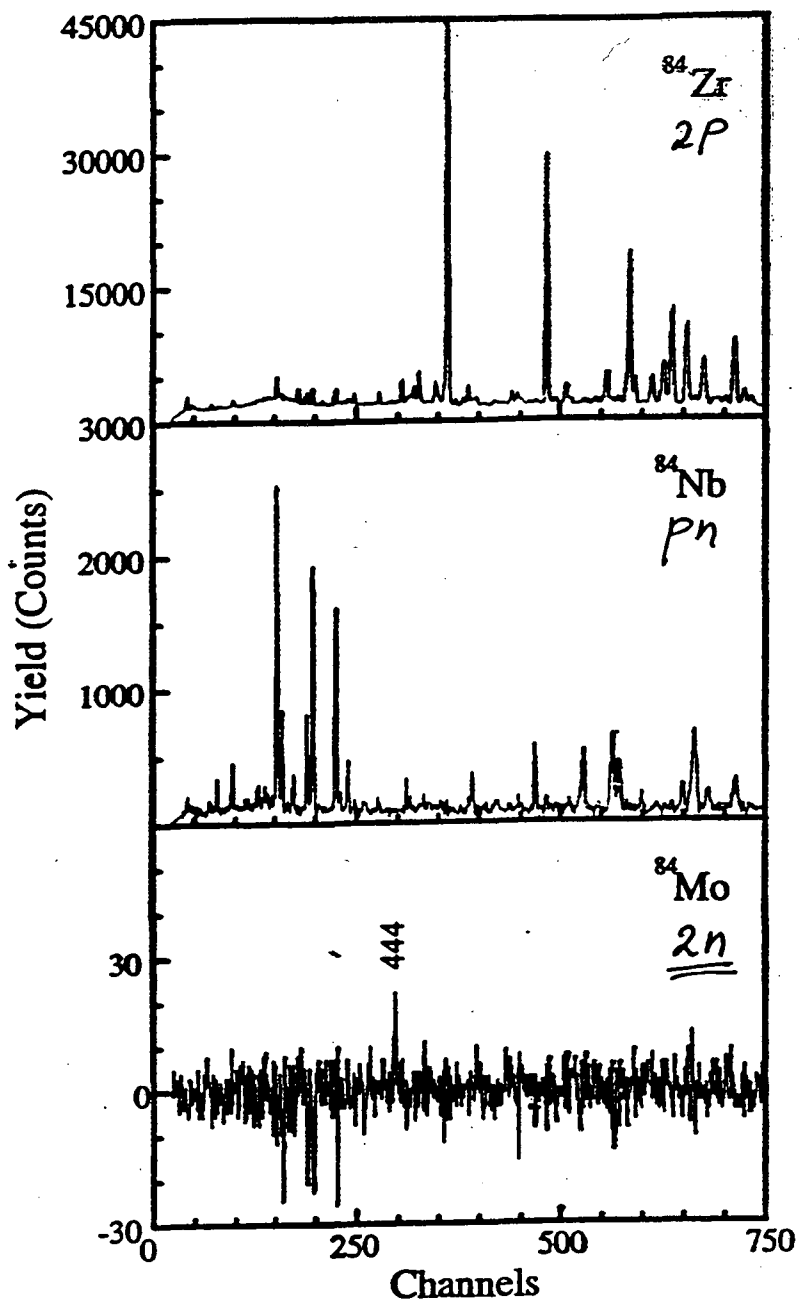


Recall that GS + γ Ball was not good enough

- Remains to be seen if addition of n-detector would help.

# Proton Drip Line Nuclei

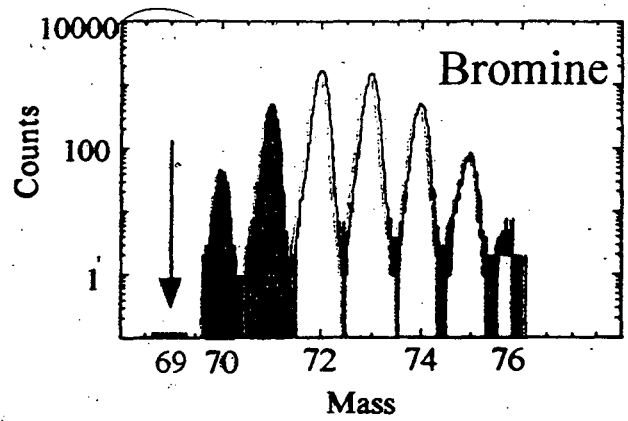


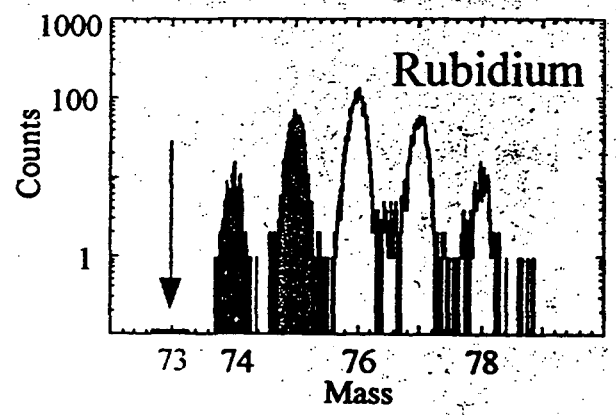


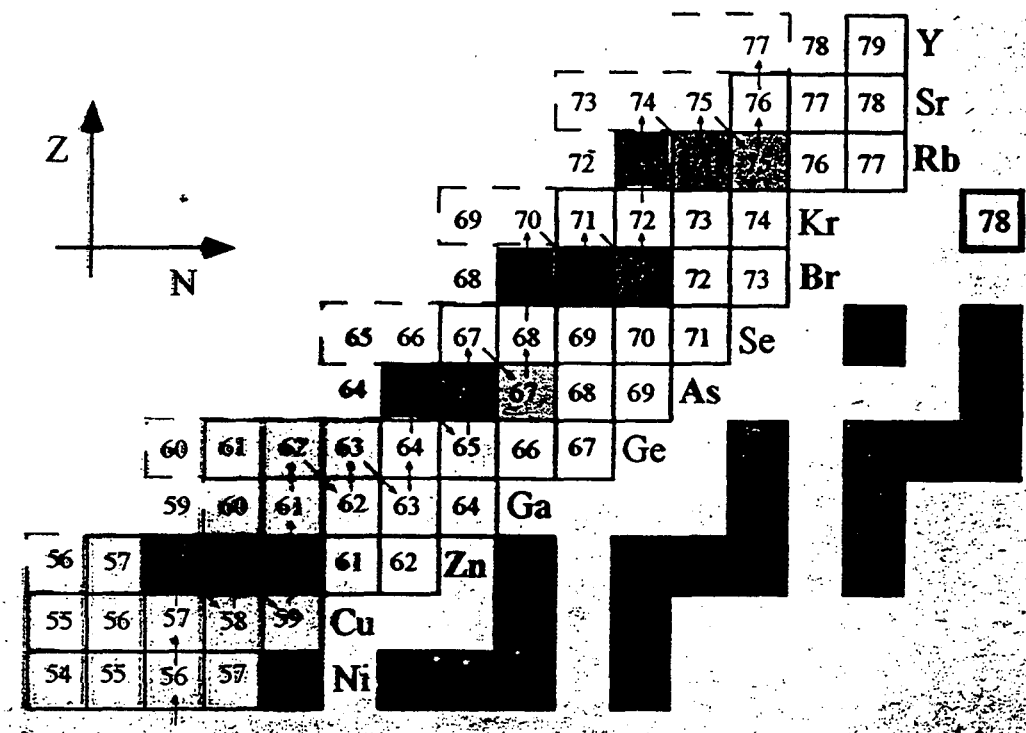


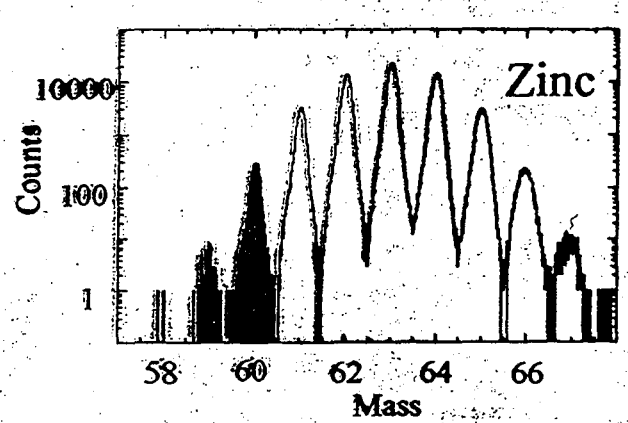


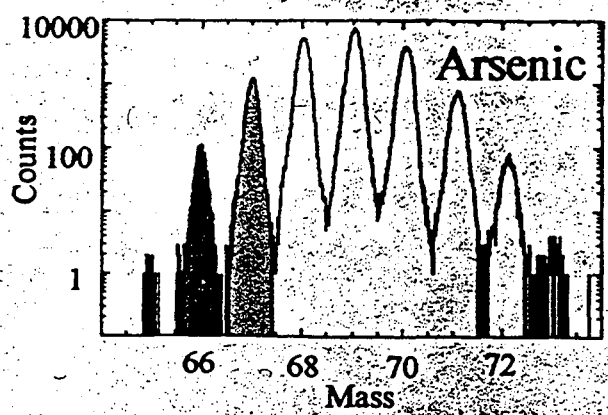

# Single Particle Levels

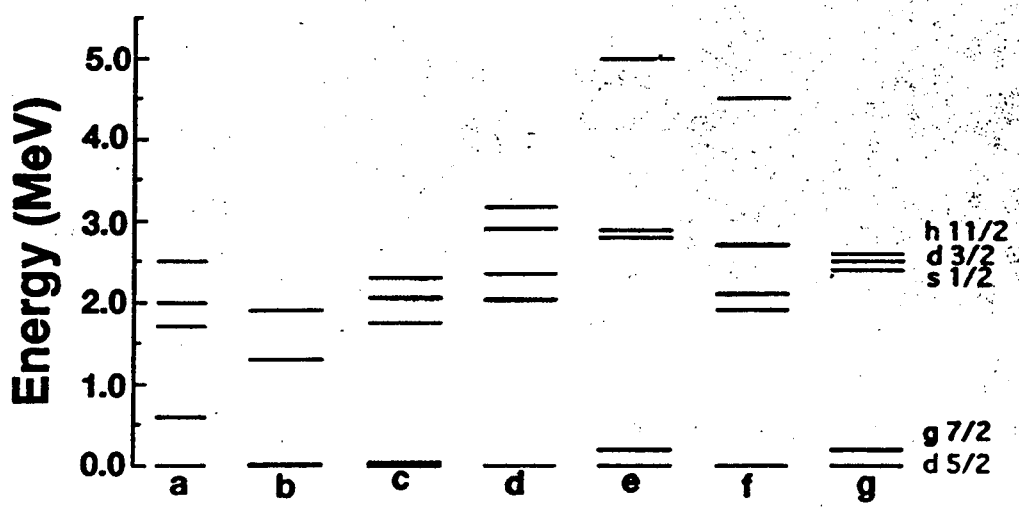


a) Ogawa et al.
b) Skouras & Manakos
c) Brown & Rykaczewski
d) Kamerdhziev et al.
e) Schubart et al.
f) Dobaczewski & Nazararewicz
g) Grawe et al.

## $^{64}$Ga + $^{40}$Ca @ 235 MeV

**ν SPE**
**πν TBME**
**ππ TBME**

| | | | | | | |
|---|---|---|---|---|---|---|
| | | | | Sb | | |
| Sn | | | ● | 10 | | |
| In | | | | 161 | 207 | 2 |
| Cd | | | 71 | 235 | 5255 | 508 |
| Ag | | | 1658 | 409 | 3008 | 2673 |
| Pd | | 54 | 824 | 3949 | 13 | 497 |
| Rh | | 141 | | 315 | | |
| Ru | 1 | 5 | | 1 | | |
| | 46 | 48 | 50 | | 52 | |

# SUMMARY

* Discussed the outlines of many fascinating physics topics that need to be explored in proton-rich (N~Z) nuclei.

» Some may be addressed with:

GRETA & stable beams (+ Aux. detecto

» Some require:

GS & Radioactive Beams

» Best Results for:

GRETA + Radioactive Beams

I.Ahmad

Structure and stability of the heaviest elements.

# Structure and Stabilities of the Heaviest Elements

I. Ahmad

February 4, 1998

# Outline

I. There is a need to improve the calculation of the stability of the Superheavy Elements

II. For better calculations, more experimental data are needed, in particular the single-particle level energies and deformation parameters.

III. GRETA will have the sensitivity for such measurements up to $Z = 108$.

# Recent Calculations

Strutinsky Method:

Nilsson et al., Nucl. Phys. A115, 545 (1968)
Moller and Nix, J. Phys. G20, 1681 (1994)
Smolanczuk et al., Phys. Rev. C52, 1871 (1995)
Chasman and Ahmad, Phys. Lett. B392, 255 (1997)

Other Methods:

Cwiok et al., Nucl. Phys. A611, 211 (1996)
Rutz et al., Phys. Rev. C56, 238 (1997)
Myers and Swiatecki, Nucl. Phys. A601, 141 (1996)

Rutz et al., Phys. Rev. C56, 238 (1997)

"Doubly magic spherical nuclei are searched in the region Z=110-140 and N=134-298. They are found at (Z=114, N=184), (Z=120, N=172) , or at (Z=126, N=184), depending on parametrization"

Structure of Actinide Nuclei

$Z = 90 - 100$ (Th - Fm)

$N = 132 - 157$

well Studied

Superheavy Elements

$Z \sim 114$

$N \sim 184$

Trans-Superheavy Elements

$Z \sim 126$

$N \sim 184$

Rev. Mod. Phys. 49, 833 (1977)

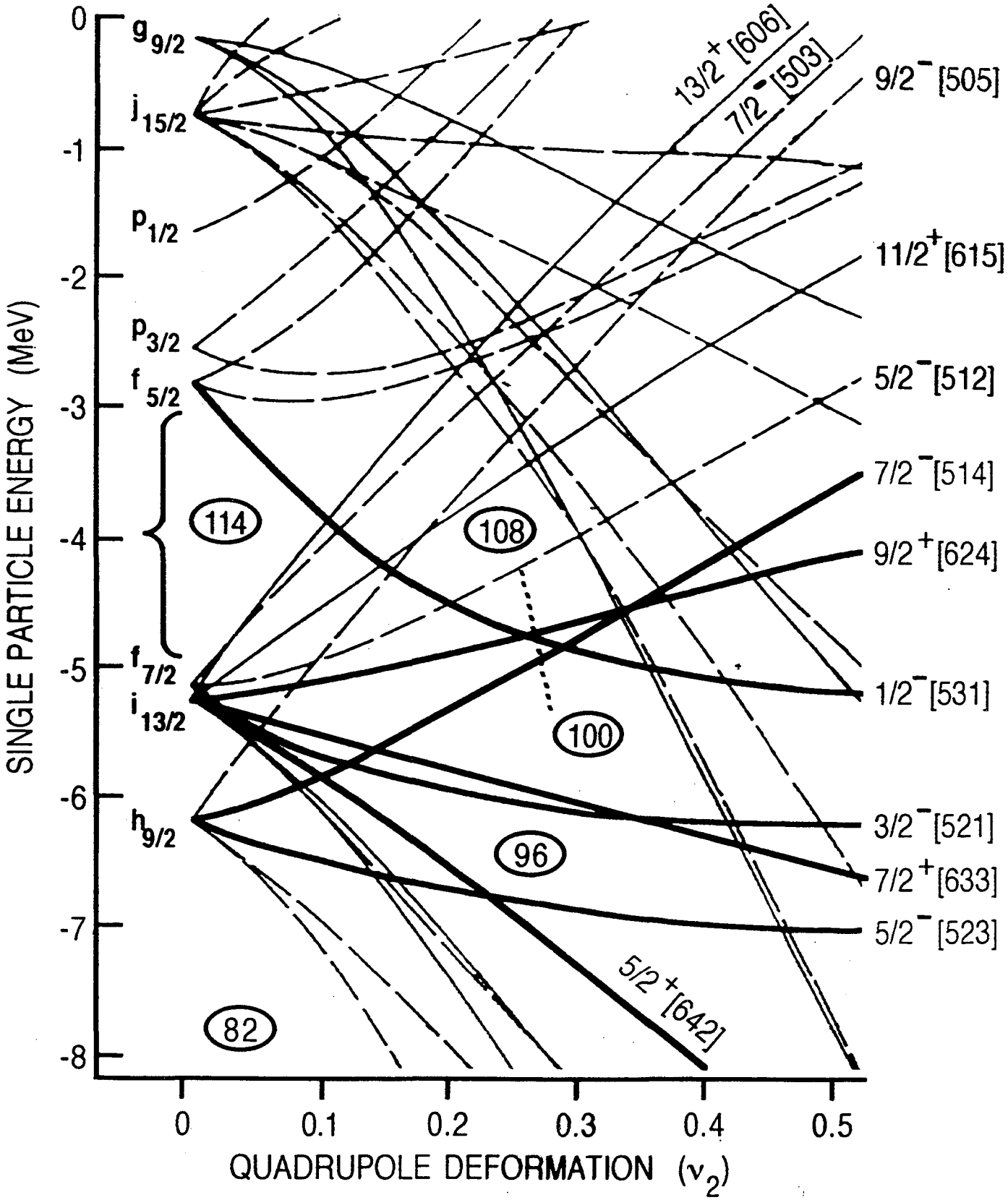

Rev. Mod. Phys. 49, 833 (1977)

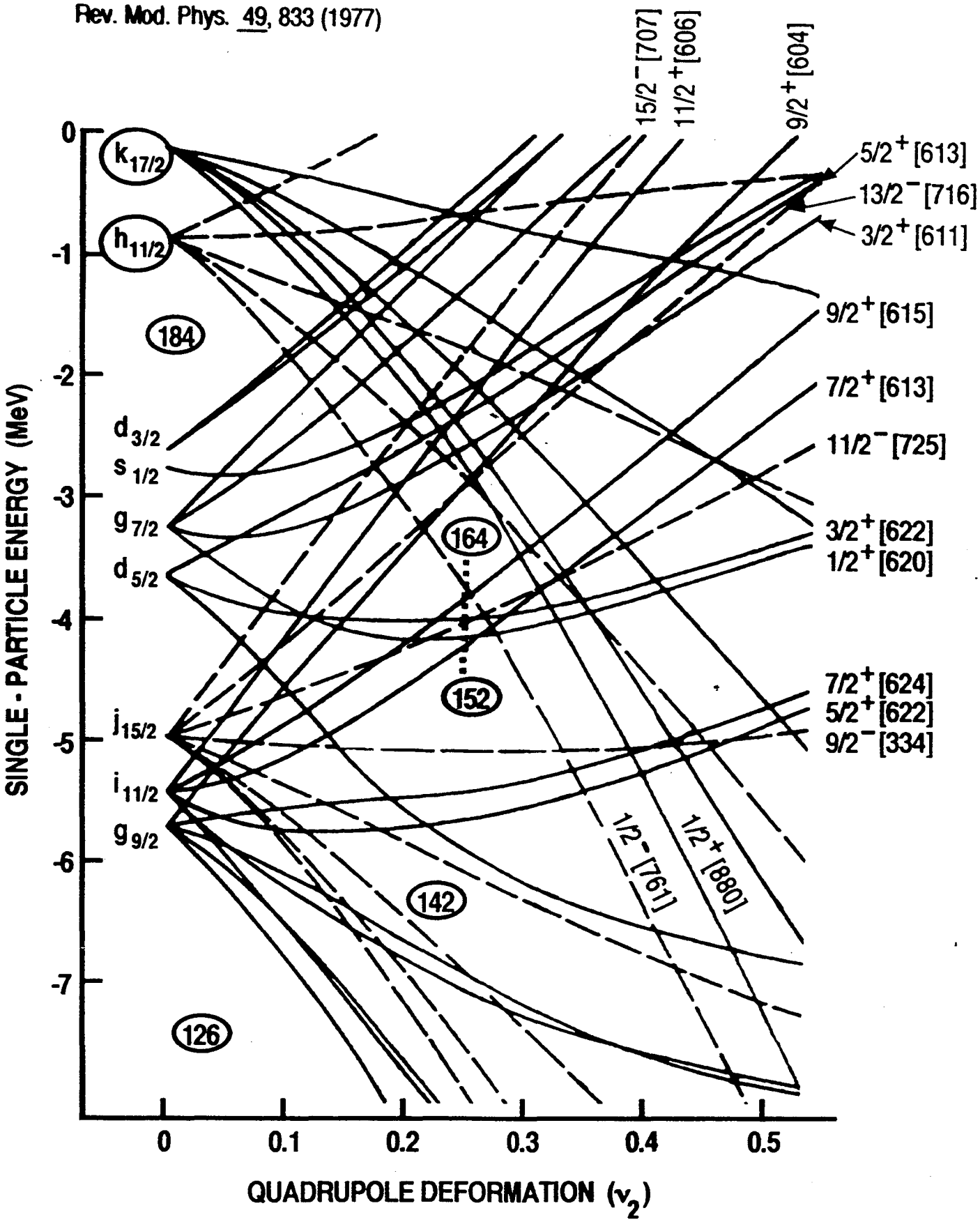

Rev. Mod. Phys. 49, 833 (1977)

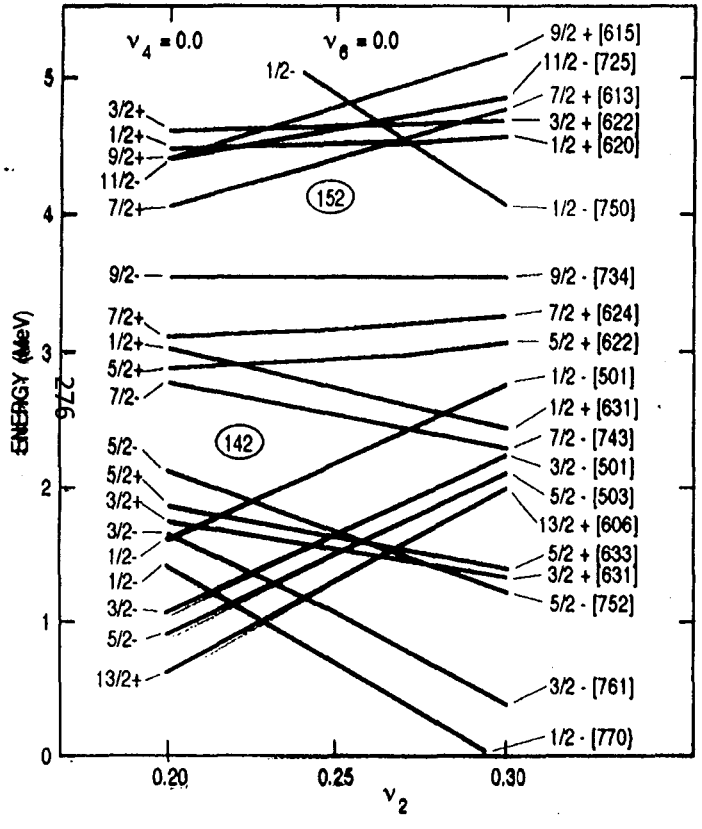


Rev. Mod. Phys. 49, 833 (1977)

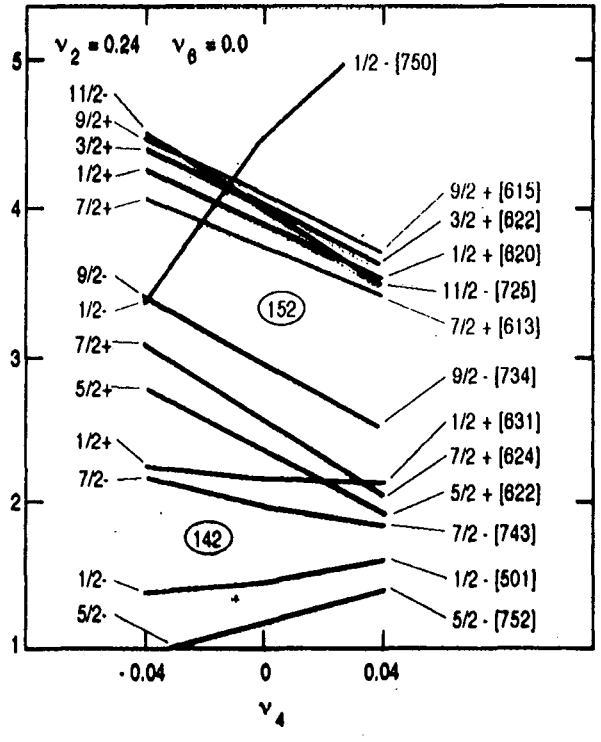


Rev. Mod. Phys. 49, 833 (1977)

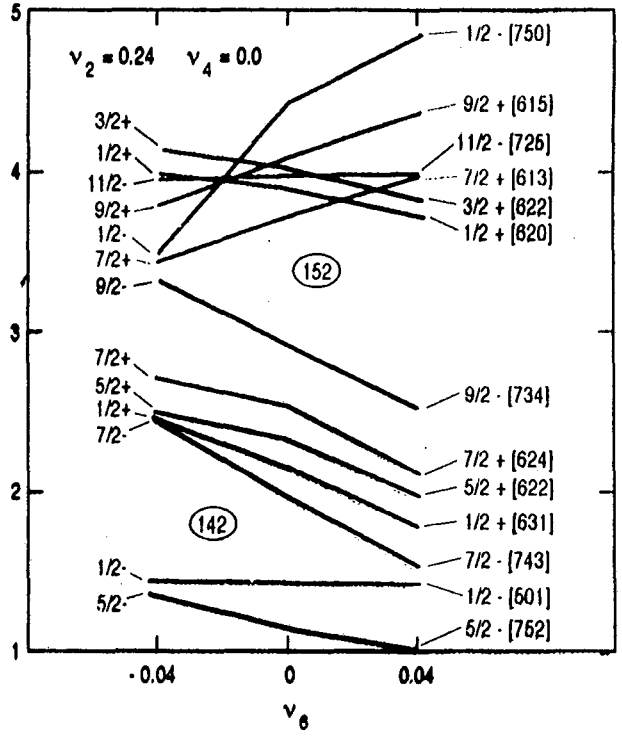

ANL-P-21,975

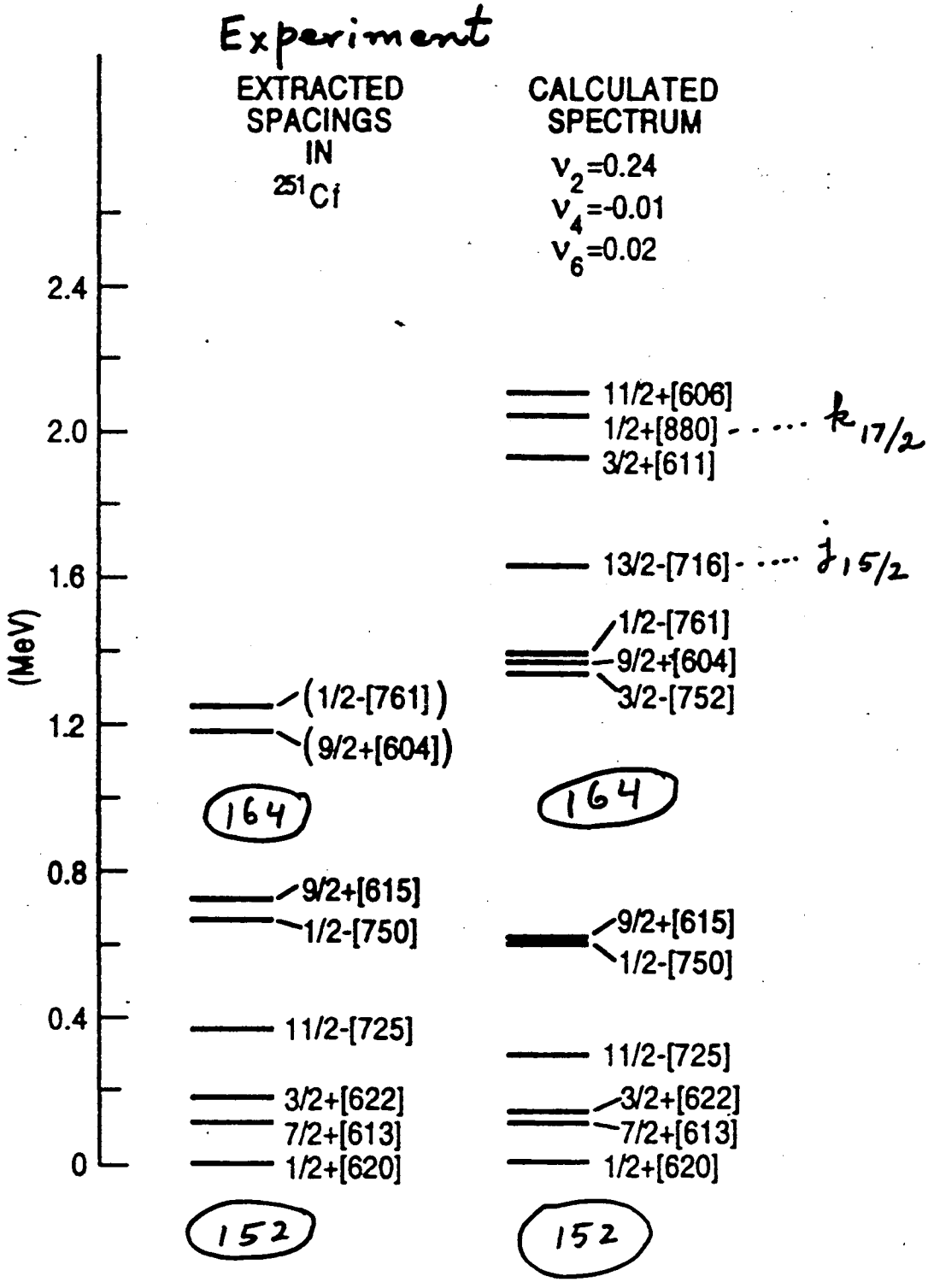
Experiment
EXTRACTED SPACINGS IN $^{251}$Cf
CALCULATED SPECTRUM
$\nu_2$=0.24
$\nu_4$=-0.01
$\nu_6$=0.02
(MeV)
2.4
2.0
1.6
1.2
0.8
0.4
0
11/2+[606]
1/2+[880]
3/2+[611]
k 17/2
13/2-[716]
j 15/2
1/2-[761]
9/2+[604]
3/2-[752]
(1/2-[761])
(9/2+[604])
164
164
9/2+[615]
1/2-[750]
9/2+[615]
1/2-[750]
11/2-[725]
11/2-[725]
3/2+[622]
7/2+[613]
1/2+[620]
3/2+[622]
7/2+[613]
1/2+[620]
152
152

Chasman & Ahmad, PL B392, 255 (1997)

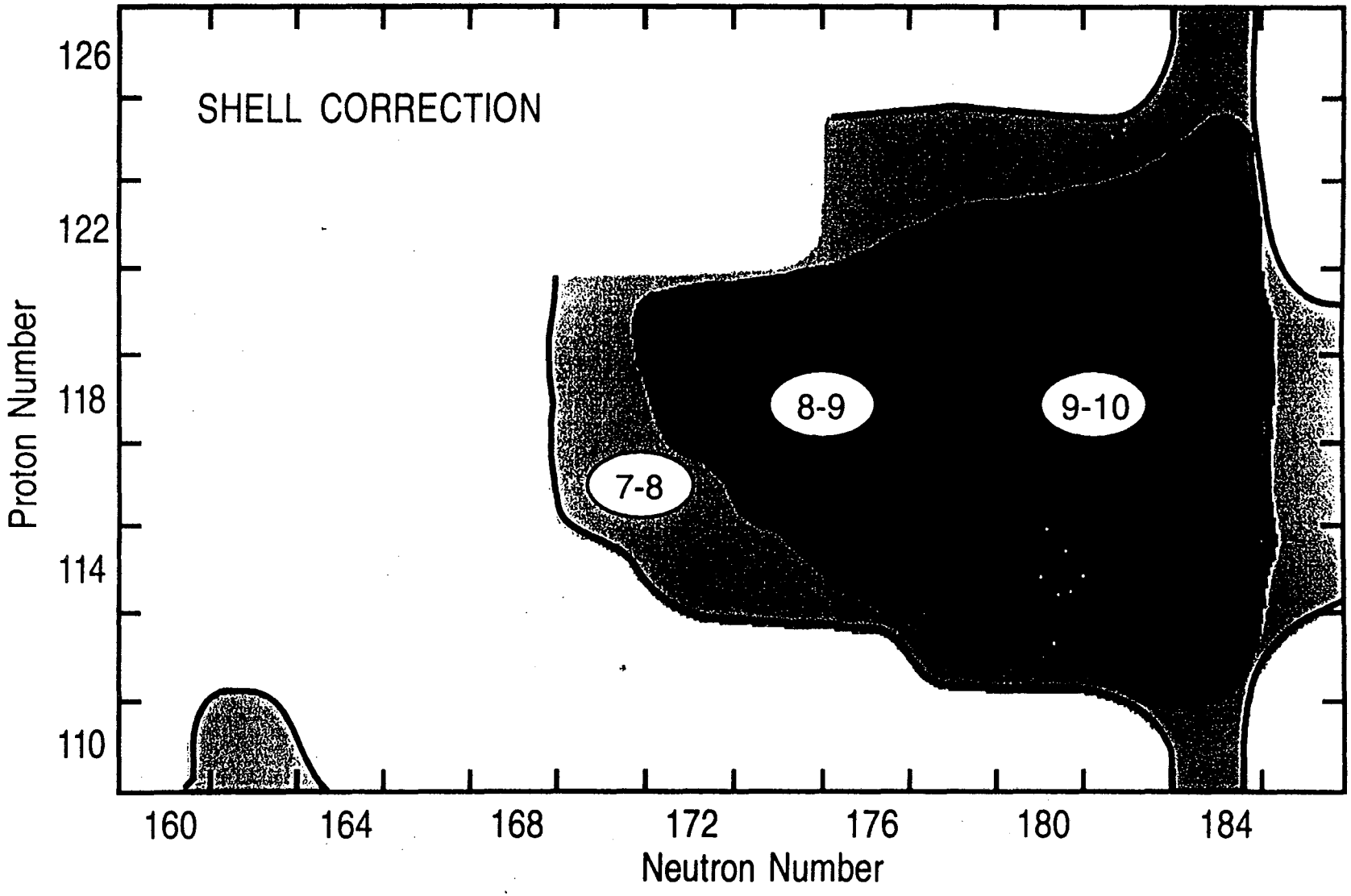

# ALPHA DECAY HALF-LIVES

Chasman & Ahmad, PL B392, 255 (1997)

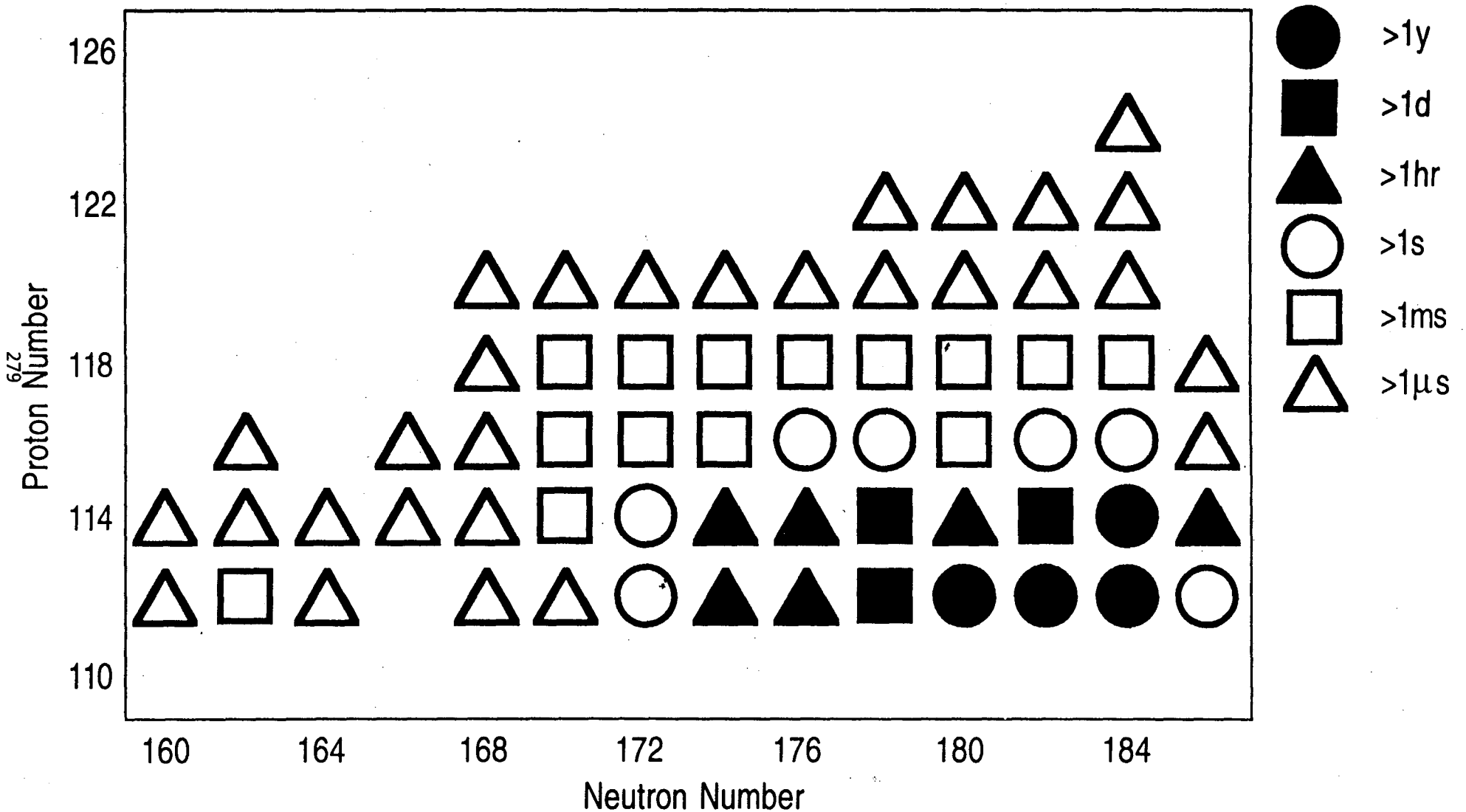

# Structure Studies of

# Z = 100 – 108

A. At the Target position

Beam current ~ 10 pnA

B. At the focal plane of

Recoil Mass Separator

like

SHIP

Favored α decay

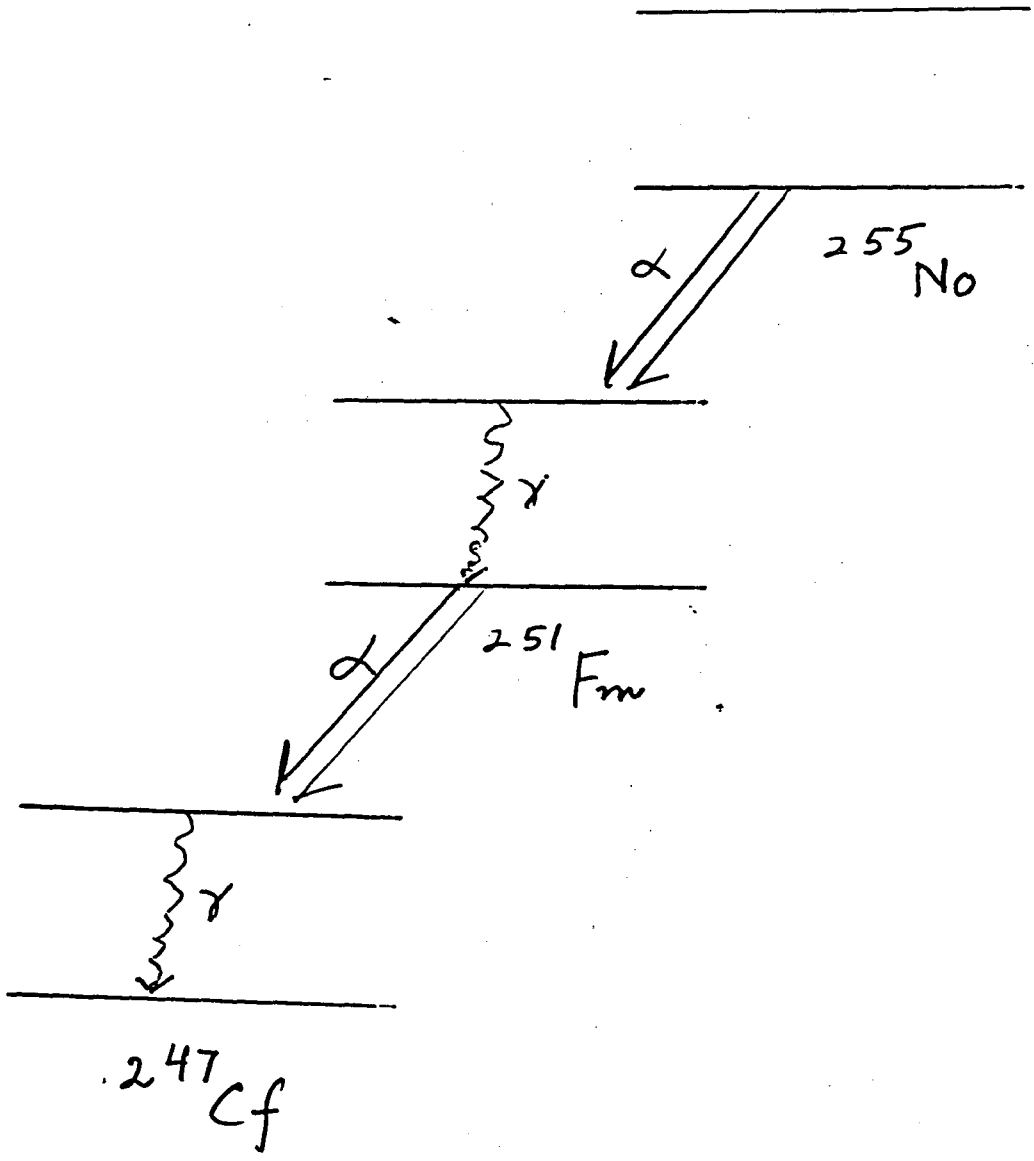

Assume 100 $\alpha$ decays in the focal plane

Favored $\alpha$ branch ~ 50%

Conversion coefficient ~ 2

$\alpha$ detection efficiency ~ 80%

$\gamma$ detection efficiency ~ 80%

Counts in the coincidence peak

~ 10

# Reaction Details
# Dubna and GSI

GSI Cold Fusion
Typical Run

Beam: 0.5 pμA
Target: 0.5 mg/cm²
Time: 5 days

Production 1 atom/pb

Z. Phys. A350, 277 (1995)

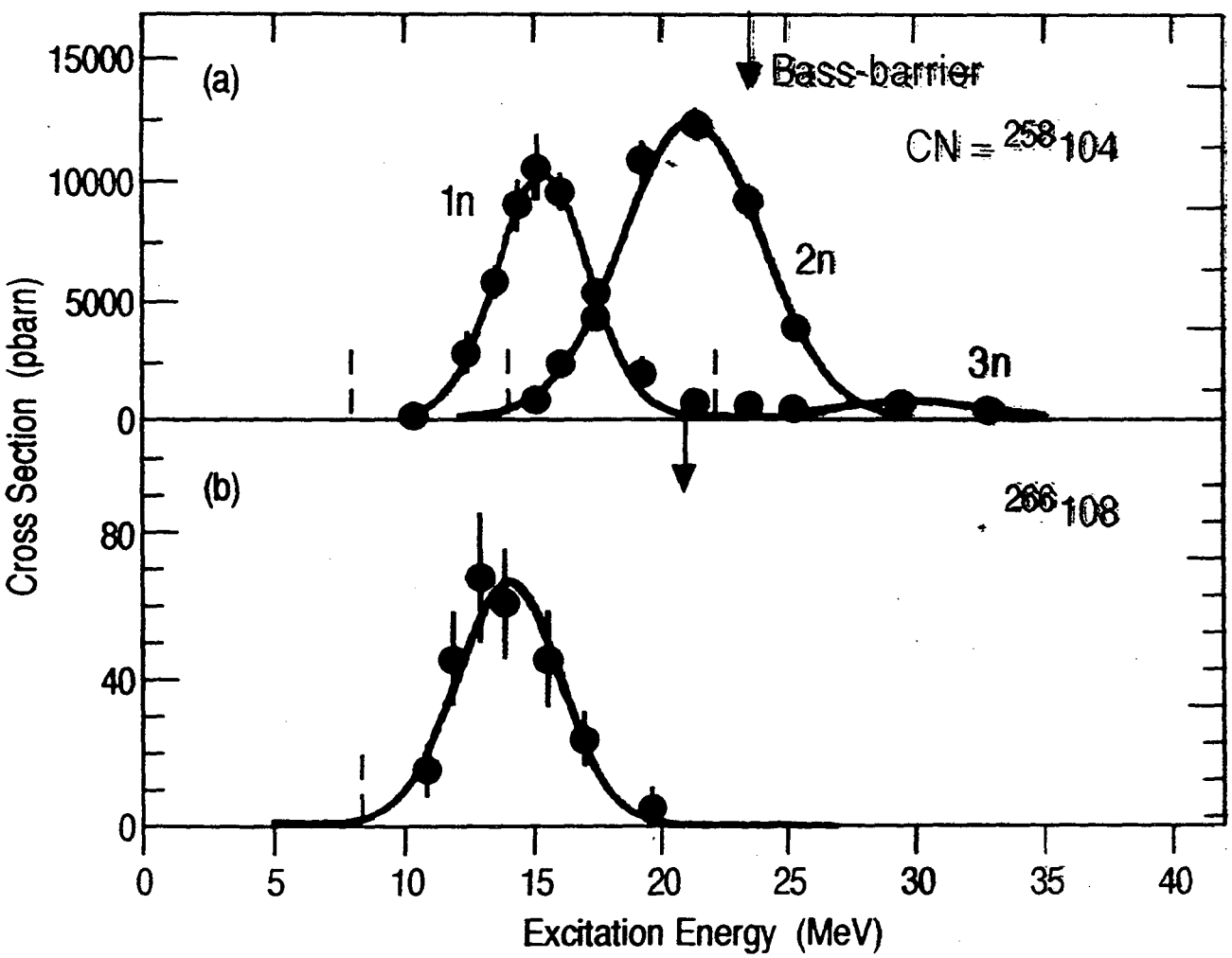

Z. Phys. A350, 277 (1995)

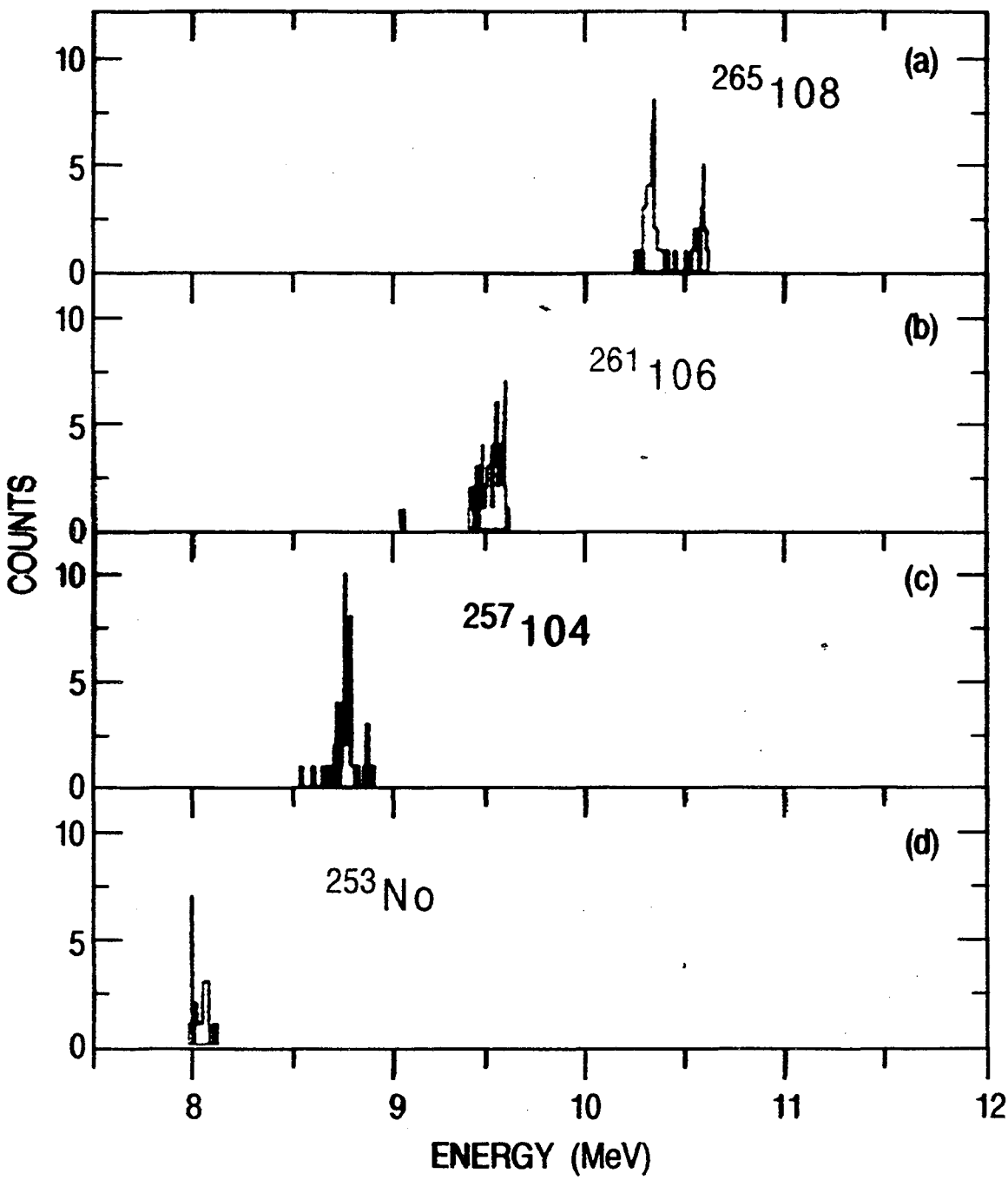

S. Hofmann (1997), Welch Foundation Lectures

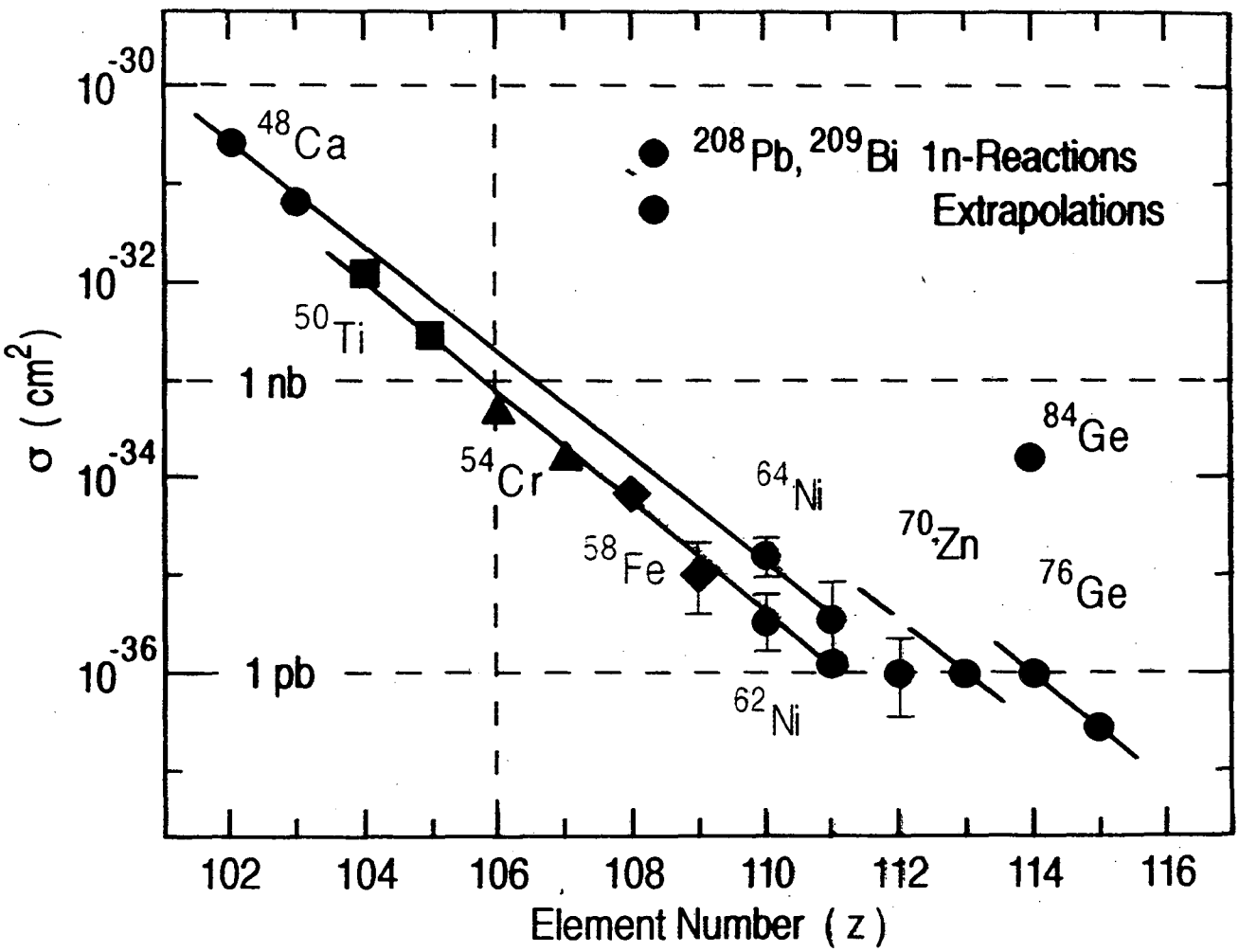

Vandenbosch & Huizenga, 1973, p.227

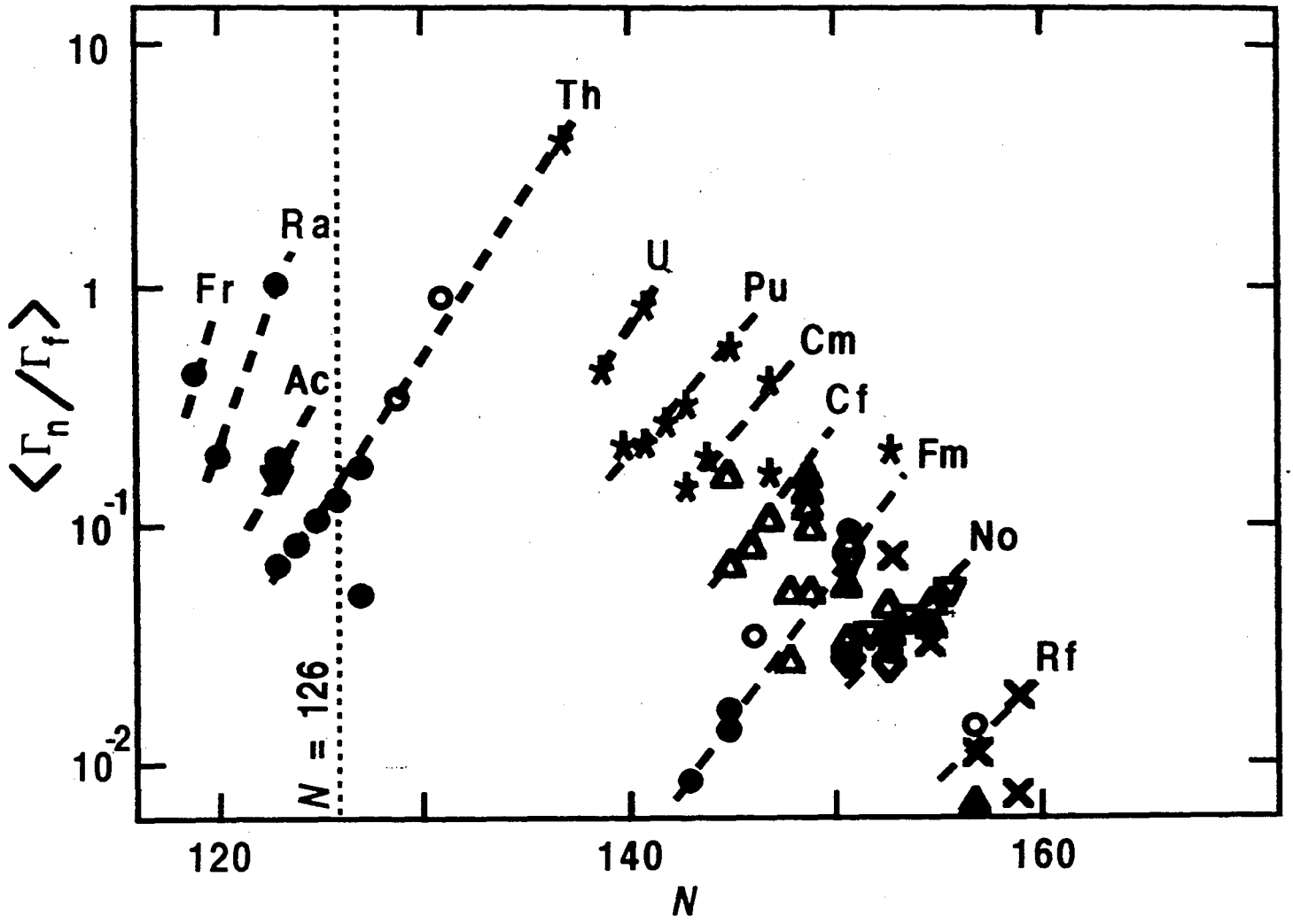

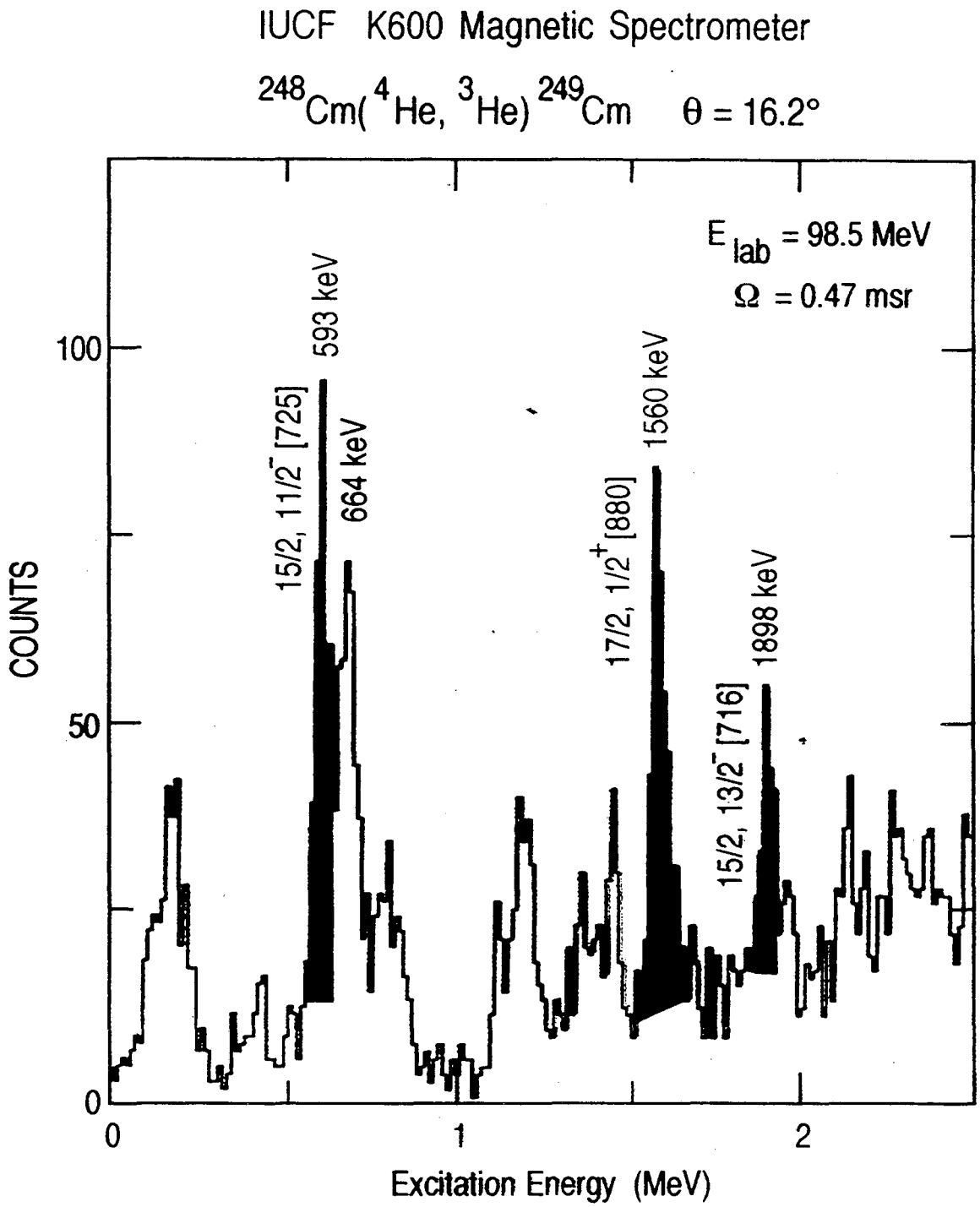
IUCF K600 Magnetic Spectrometer
248Cm(4He, 3He)249Cm θ = 16.2°
E lab = 98.5 MeV
Ω = 0.47 msr
593 keV
664 keV
15/2, 11/2− [725]
1560 keV
17/2, 1/2+ [880]
1898 keV
15/2, 13/2− [716]
COUNTS
100
50
0
0
1
2
Excitation Energy (MeV)

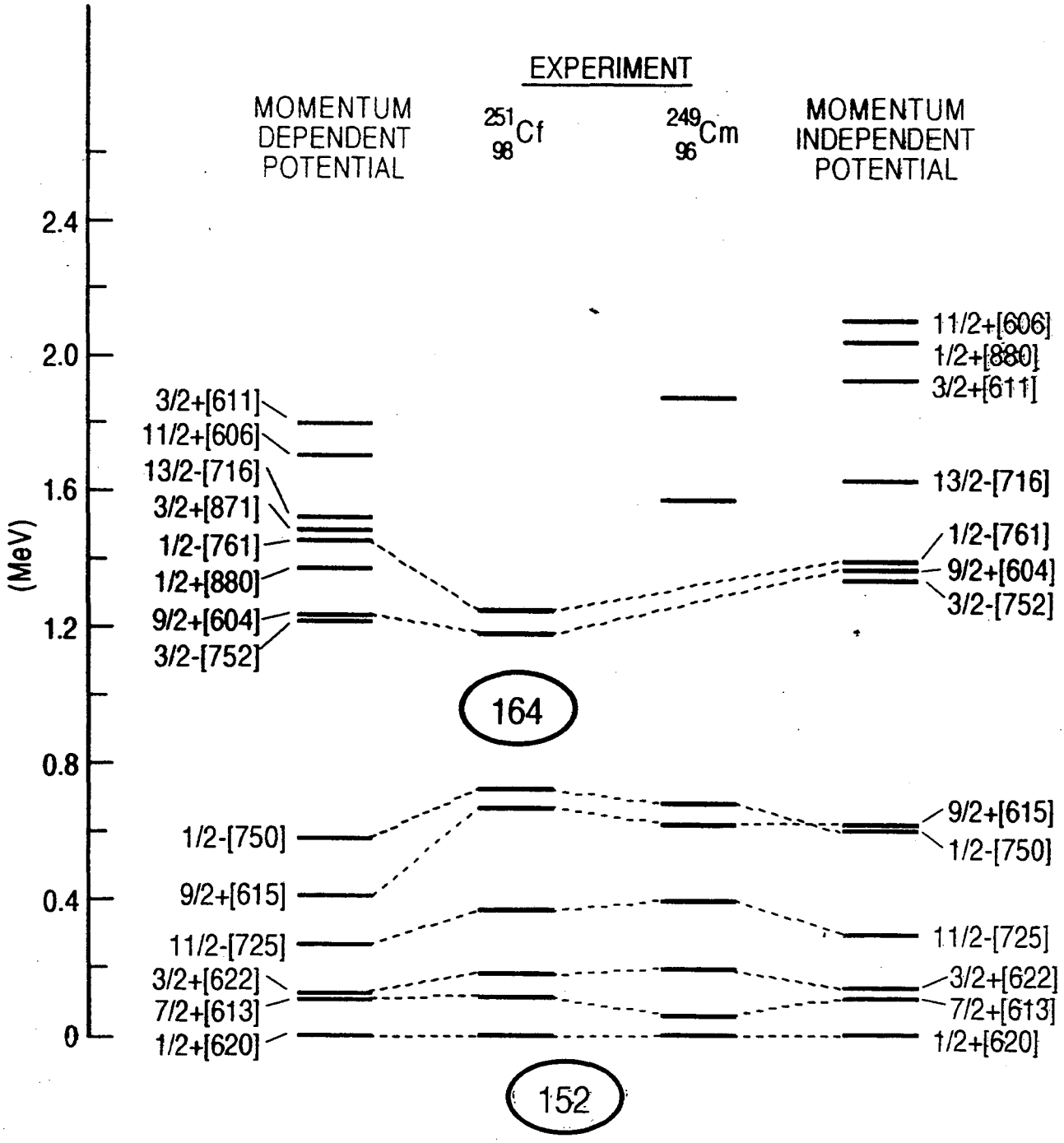
EXPERIMENT
MOMENTUM DEPENDENT POTENTIAL
251 98 Cf
249 96 Cm
MOMENTUM INDEPENDENT POTENTIAL
(MeV)
2.4
2.0
1.6
1.2
0.8
0.4
0
3/2+[611]
11/2+[606]
13/2-[716]
3/2+[871]
1/2-[761]
1/2+[880]
9/2+[604]
3/2-[752]
164
1/2-[750]
9/2+[615]
11/2-[725]
3/2+[622]
7/2+[613]
1/2+[620]
152
11/2+[606]
1/2+[880]
3/2+[611]
13/2-[716]
1/2-[761]
9/2+[604]
3/2-[752]
9/2+[615]
1/2-[750]
11/2-[725]
3/2+[622]
7/2+[613]
1/2+[620]

# $^{249}$Cm

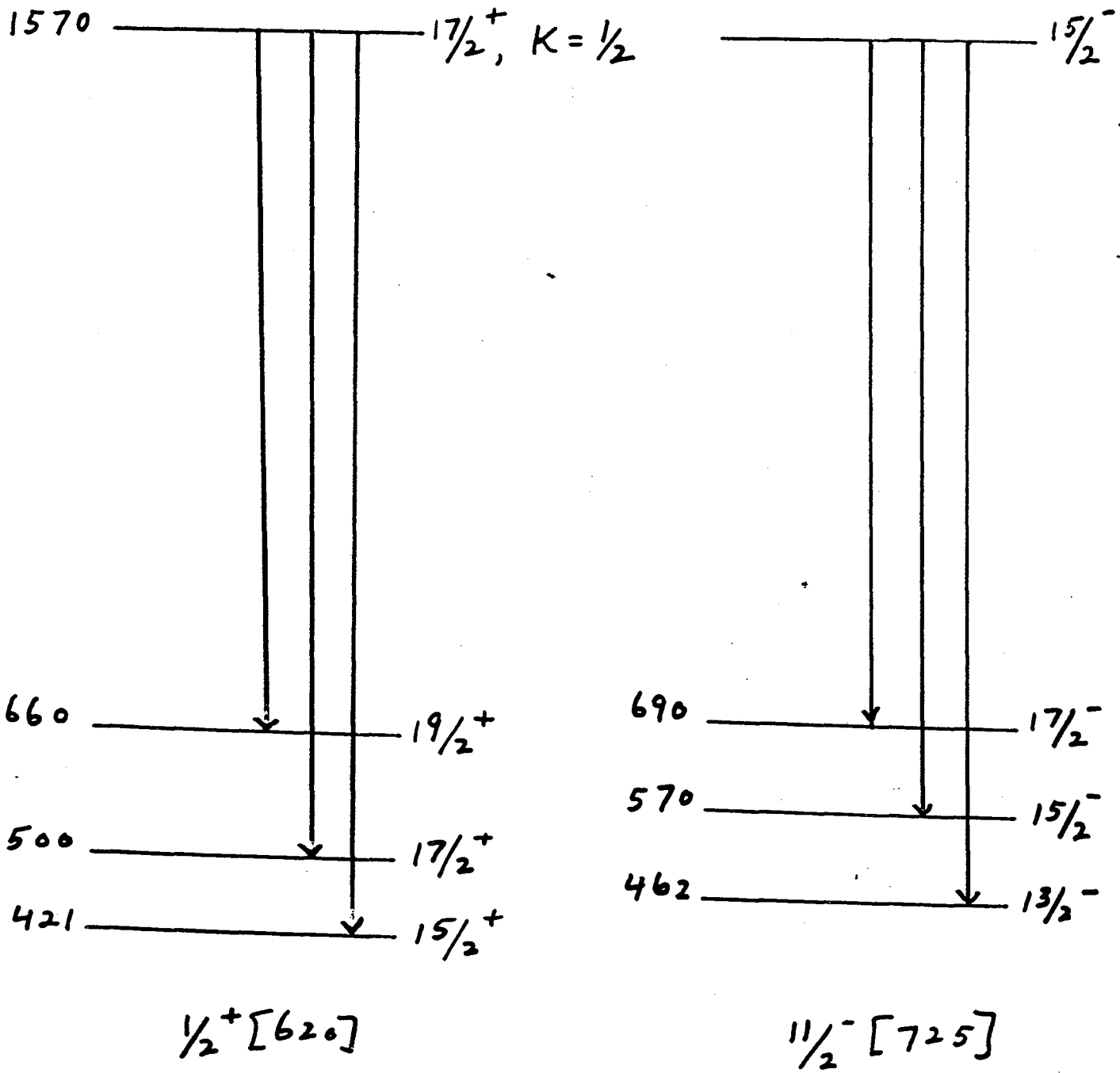


Chasman, Lanham, Lukbock, 1975

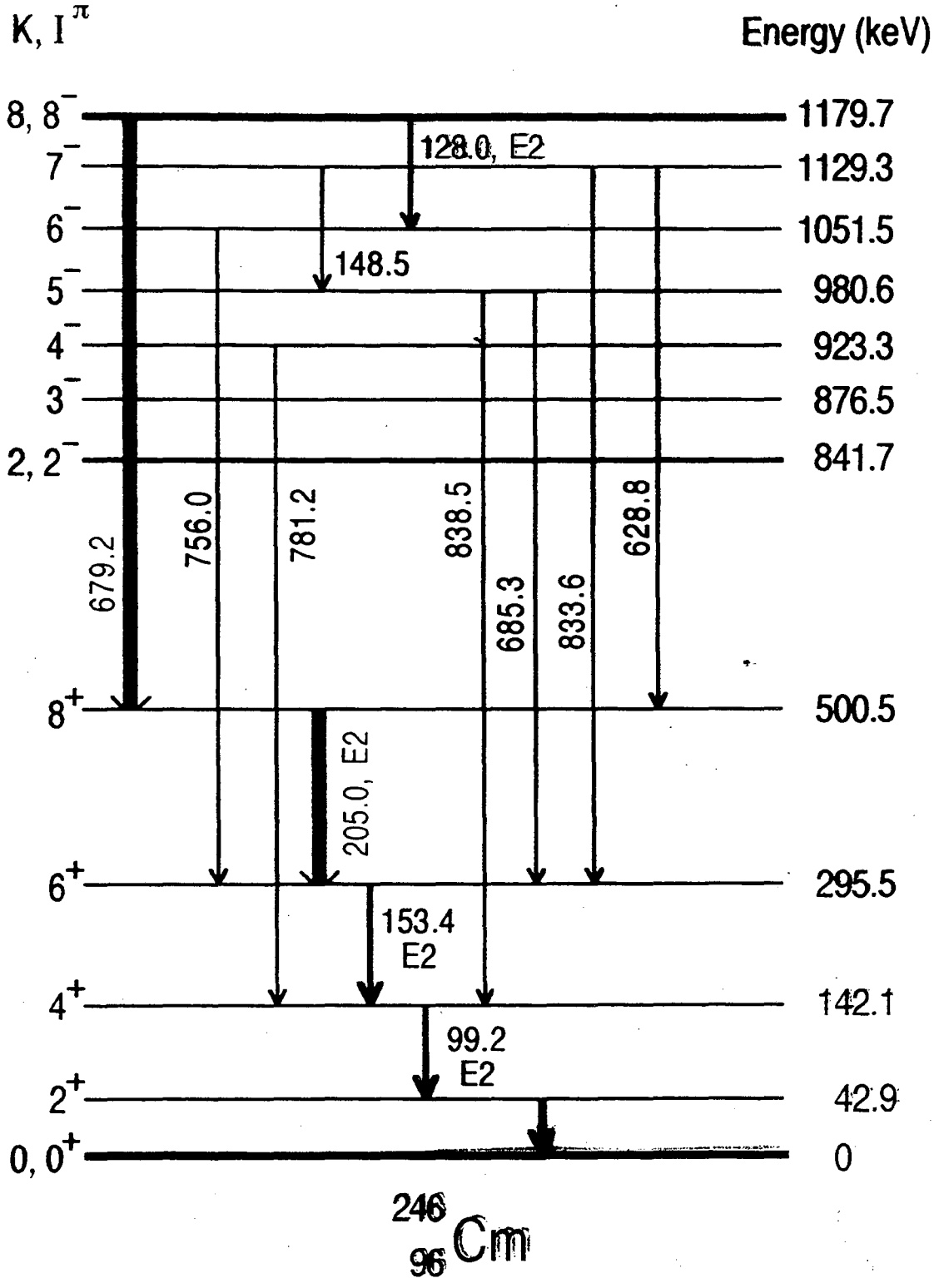
K, I^π
Energy (keV)
8, 8^−
7^−
6^−
5^−
4^−
3^−
2, 2^−
8^+
6^+
4^+
2^+
0, 0^+
1179.7
1129.3
1051.5
980.6
923.3
876.5
841.7
500.5
295.5
142.1
42.9
0
128.0, E2
148.5
679.2
756.0
781.2
838.5
685.3
833.6
628.8
205.0, E2
153.4
E2
99.2
E2
246
96
Cm

One rotational band

Large E1 rate

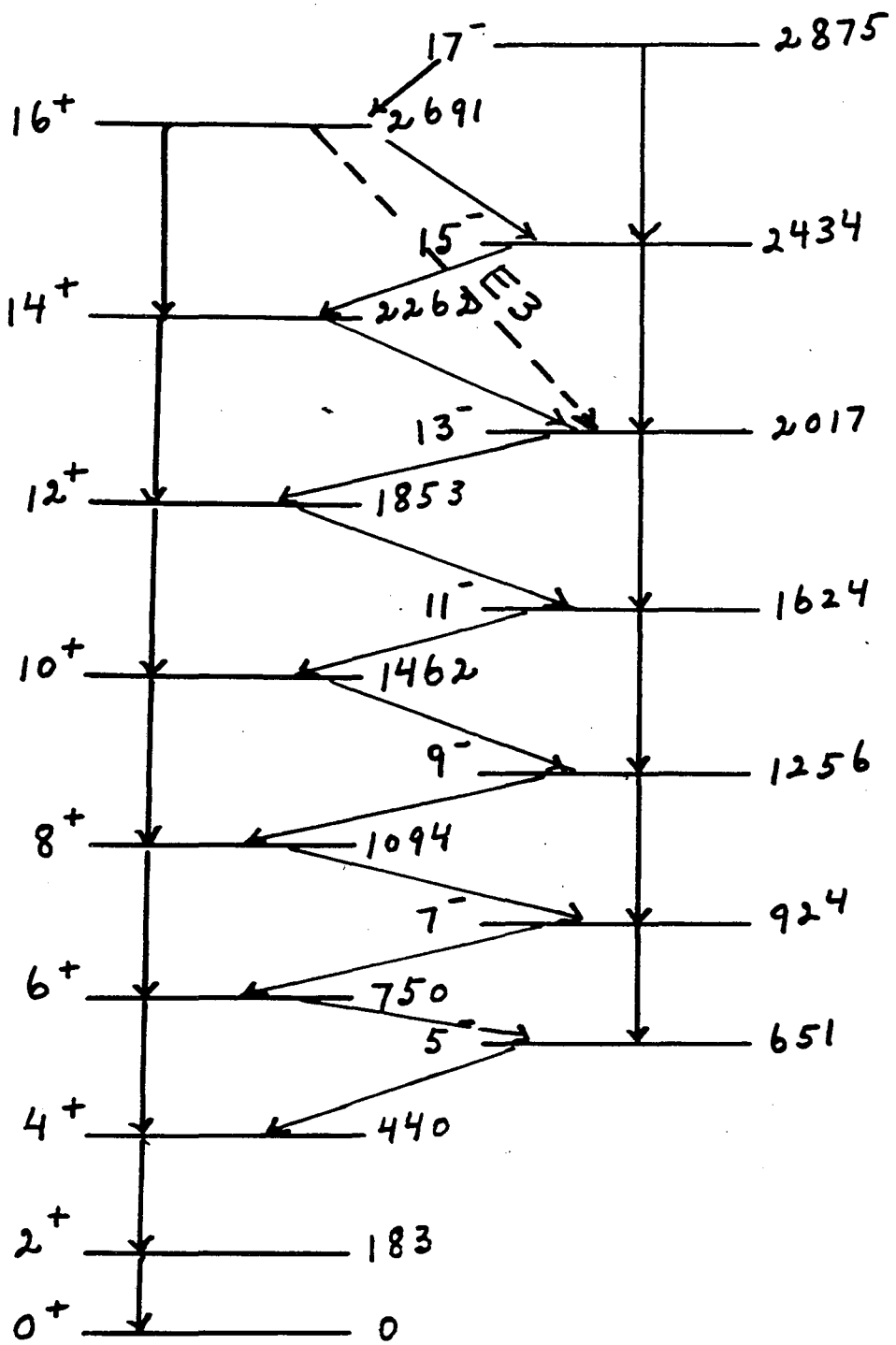


$^{222}_{90}Th$

? Schuler et al. Phys. Lett. 174B, 241 (1986)

# Summary

Using GRETA at the focal plane of a Recoil Mass Separator, we will be able to study single-particle states in nuclei up to $Z = 108$. These data will enable theorists to deduce the parameters of their models and thus will provide a more reliable prediction of the stability of Superheavy Elements.

B.Sherrill

Techniques for mapping halo wavefunctions.

# Nuclear wavefunction mapping with GRETA

## Determination of nuclear structure near the drip lines

- **Introduction**
  - Simple picture of nucleon knock-out
  - Importance of the breakup reaction mechanism
  - Examples
  - S800 Spectrograph
- **Measurements with γ-rays**
  - Determination of the reaction mechanism
  - Measurement of parentage to n+core states.
  - Examples
- **The need for GRETA**
  - Resolution: in heavier nuclei the g-cascades can be complicated
  - Efficiency: weak beams require near 100% efficiency

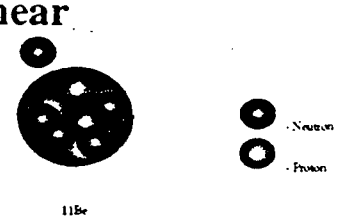

# Wavefunction Mapping in 1s Atomic Hydrogen

McCarthy and Weigold, Rep. Prog. Phys. 51 (1988) 299

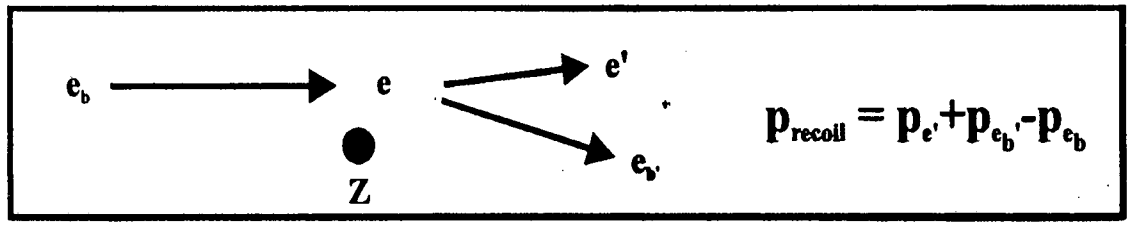


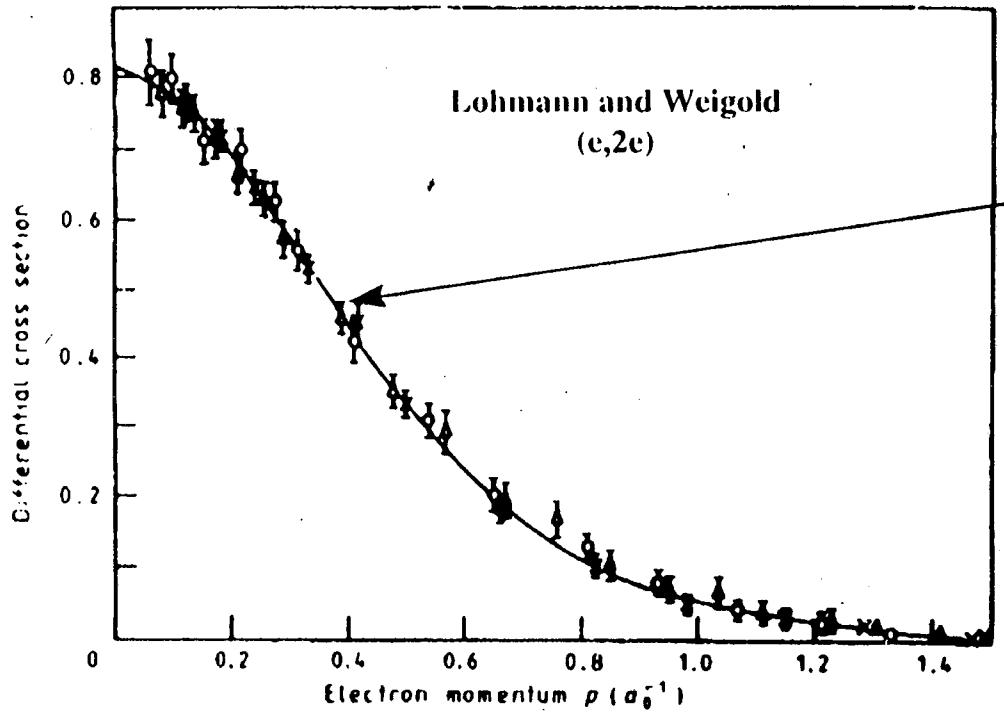


**1s hydrogen momentum wavefunction**

$$|\langle p|\Psi_0\rangle|^2 = \frac{8}{p^2(1+p^2)^4}$$

## Nuclear Physics:

**(e,ep)**
**(p,2p)**
**(p,p$\alpha$)**

# High-Momentum Protons in $^{208}$Pb

## (e,e'p)

**I. Bodeldijk et al. PRL 73 (94) 2684**

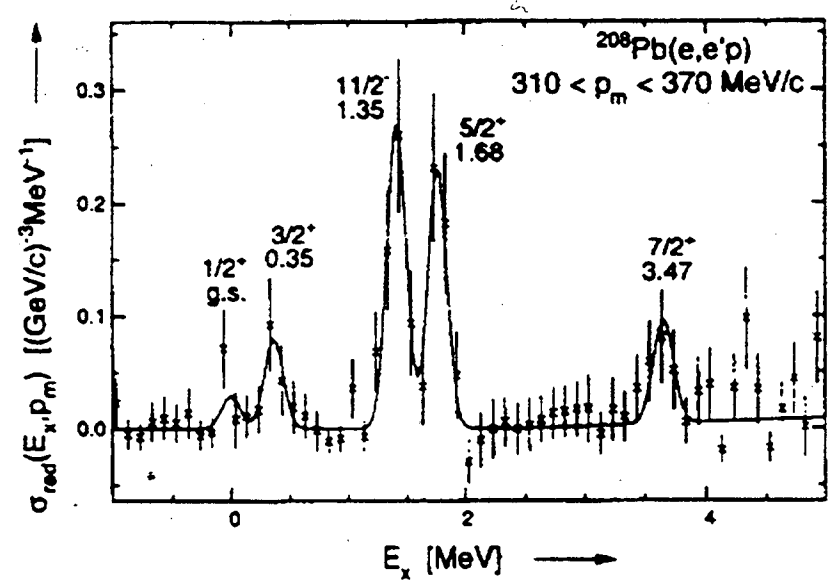


20[redacted]Tl States

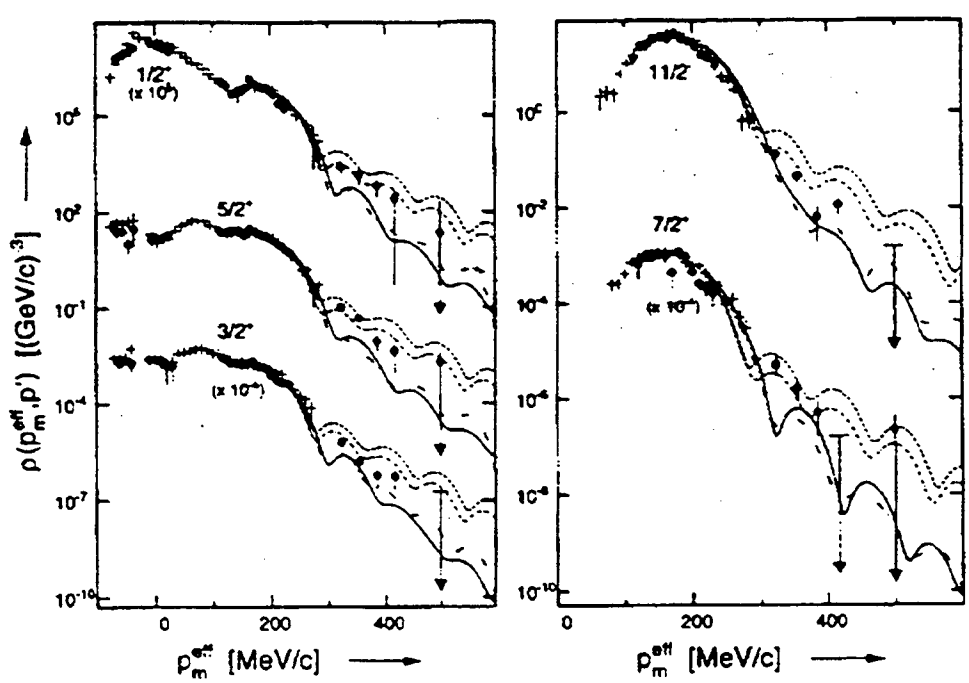


**There are higher momentum components than expected from nucleon mean-field models**

# Nucleons in the Nucleus

C.J.G. Onderwater et al., PRL 78 (97) 4839

**A long standing problem is that the probability of finding a nucleon is a given orbit is only 0.6.**

**Spectral functions for pair knockout in $^{16}O$**

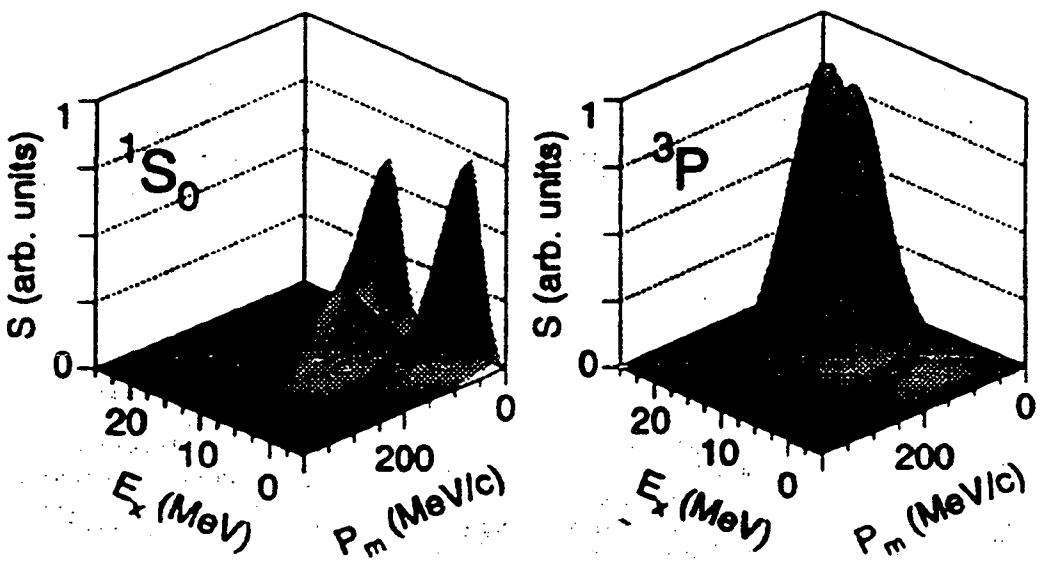


**Conclusion: Correlations are very important!**

# Parallel Momentum → Momentum wf

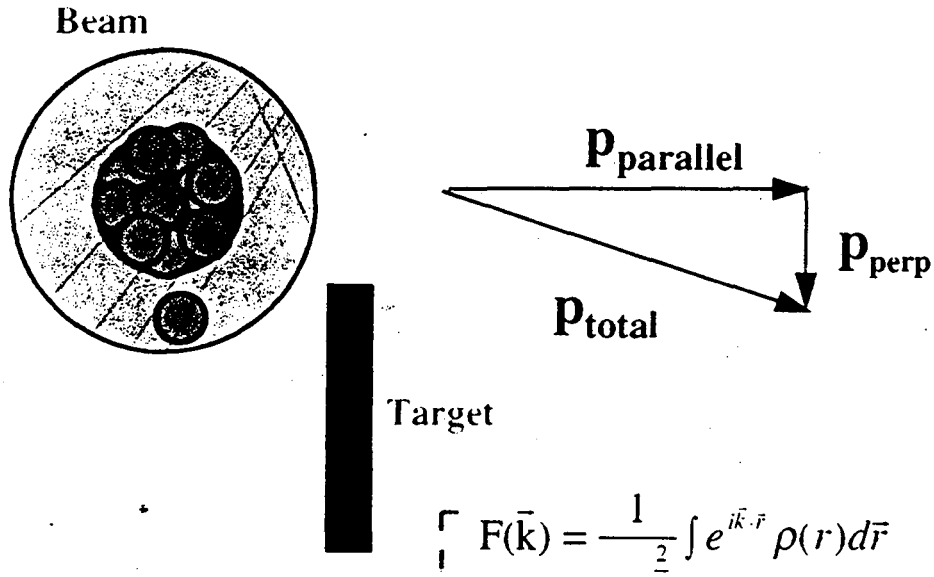


**Asymptotic 0s-wave:**

$$F(\vec{k}) = \frac{1}{2\pi^{\frac{2}{3}}} \int e^{i\vec{k}\cdot\vec{r}} \rho(r) d\vec{r}$$

$$p(r) = \frac{e^{-\rho r}}{r} \quad \text{"Yukawa"}$$

K. Riisager

$$|F(\vec{k})|^2 = \frac{h}{2\rho\pi^3} \frac{1}{(\frac{h^2}{\rho^2} + k^2)^2}$$

**General:**

$$F(\vec{k}) = \tilde{\Psi}(k) Y_{lm}(\theta, \varphi) \text{ where}$$

B.A. Brown
H. Esbensen

$$\tilde{\Psi}(k) = \sqrt{\frac{2}{\pi}} \frac{i^{-l}}{k} \int \Psi(r) j_l(kr) r^2 dr$$

**In both cases:**

$$P(k_p) = \frac{1}{2} \int |F(\vec{k})|^2 dk_r \qquad k^2 = k_p^2 + k_r^2$$

# Momentum and Spatial Wave functions for $^{11}$Be Halo and Core Neutrons

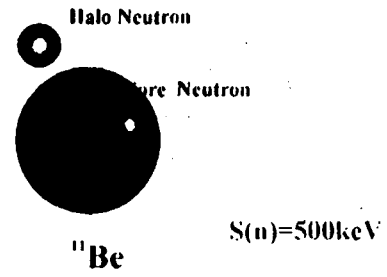


Data: J. Kelley et al., Phys. Rev. Lett. 74 (1995) 30.

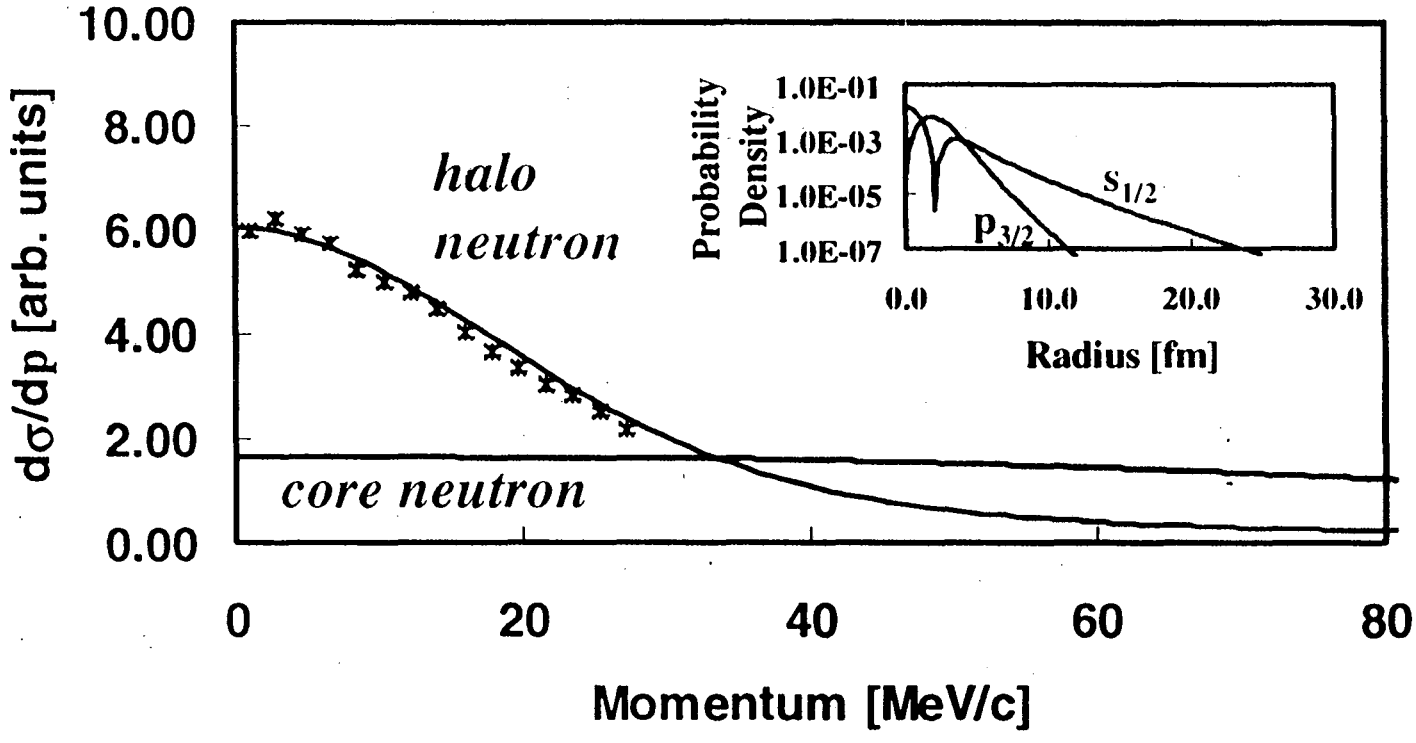

# Momentum Content of Single-Nucleon Halos

P.G. Hansen PRL 77 (1996) 1016
H. Esbensen PR C53 (1996) 2007
K.Henken, G. Bertsch, H. Esbensen PRC 54, 3043 (1996)

"...collisions with a nuclear target cannot explore all parts of the halo's spatial wave function with equal probability."

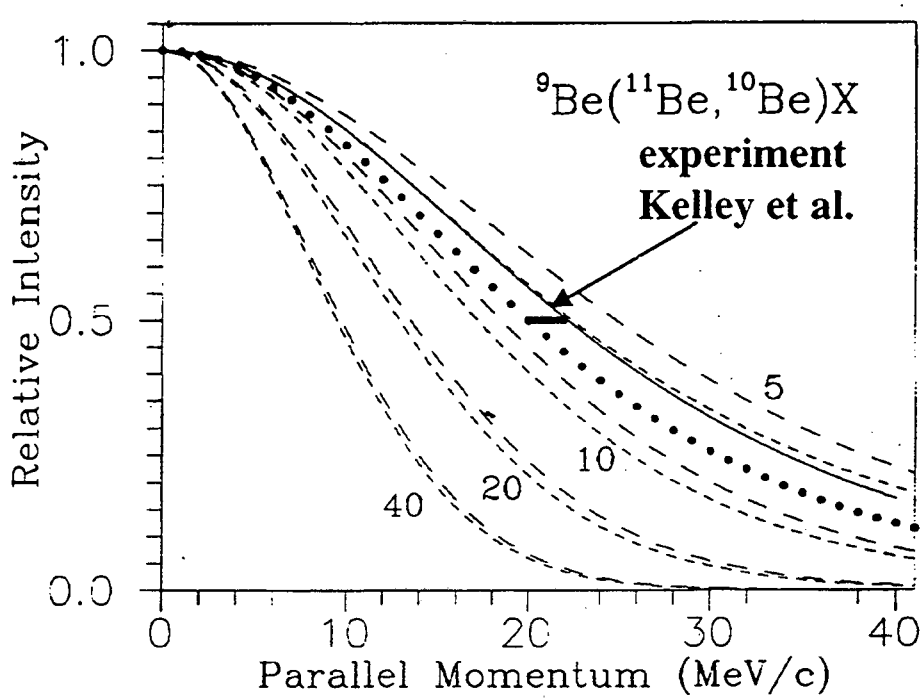


..... full differential cross section
----- contributions from different impact parameters
—— intrinsic wave-function

# Summary of the Nuclear Landscape

Doubly Magic Nuclei (proton and neutron number magic)

**Well known cases:**

$^{4}He$, $^{16}O$, $^{40,48}Ca$, $^{208}Pb$

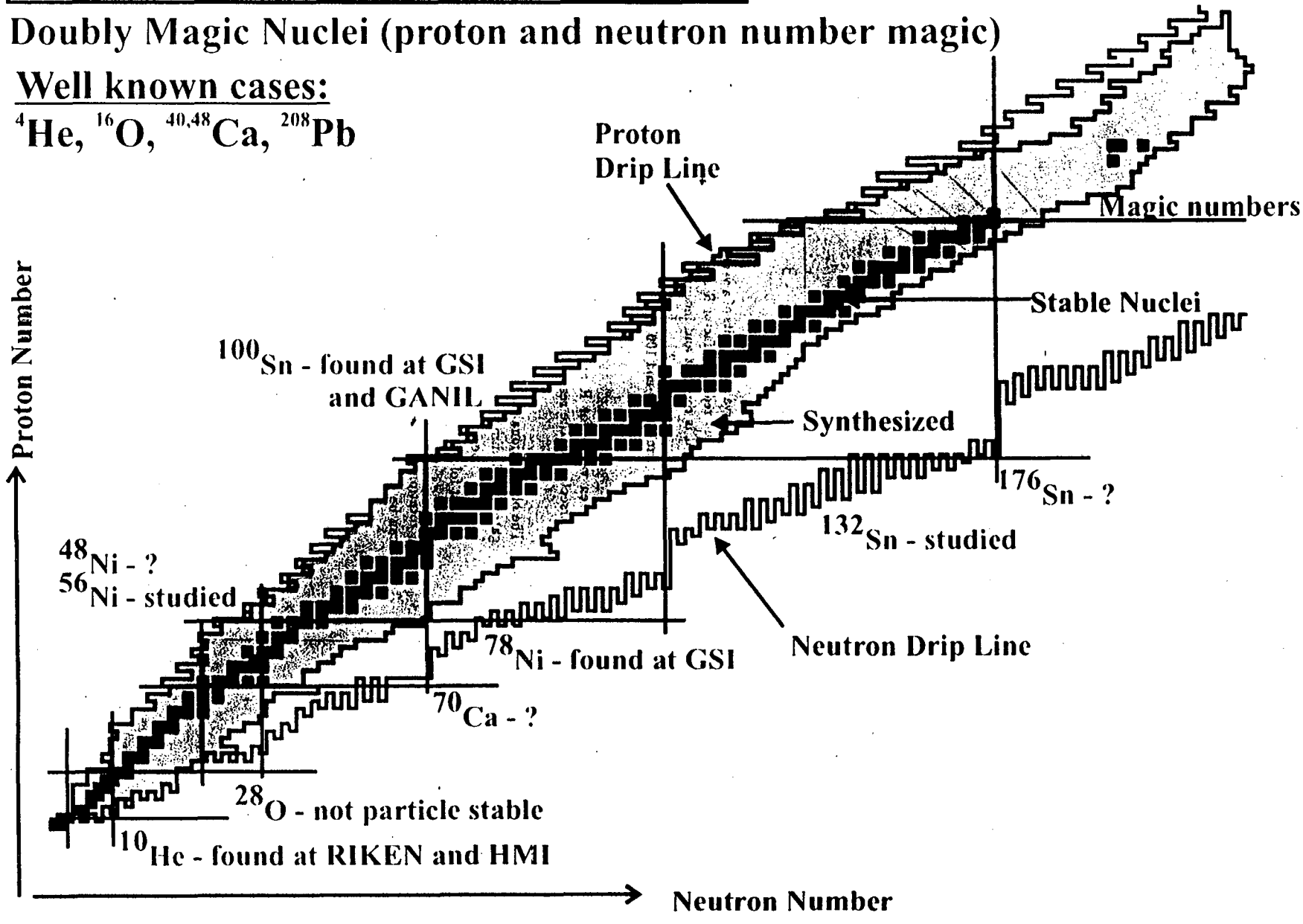

# The NSCL Coupled Cyclotron Proposal

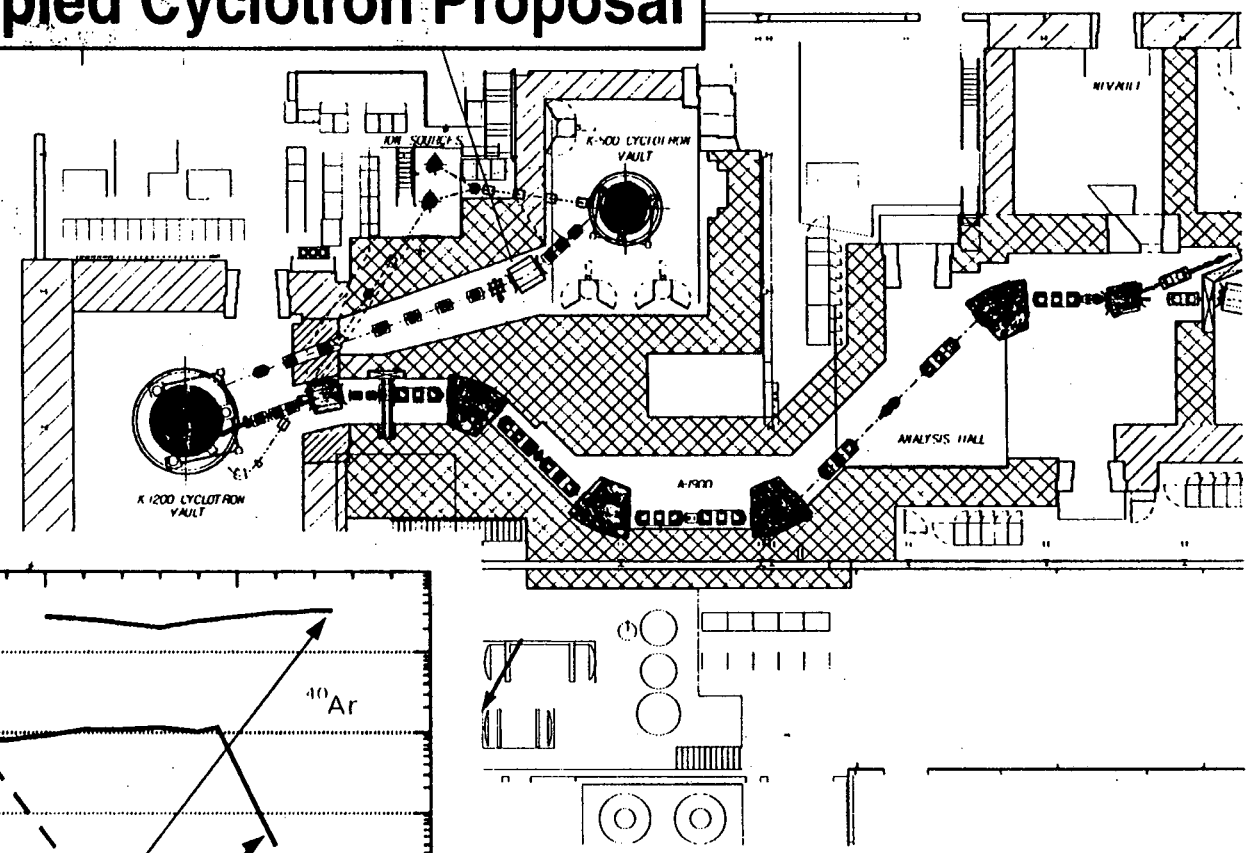


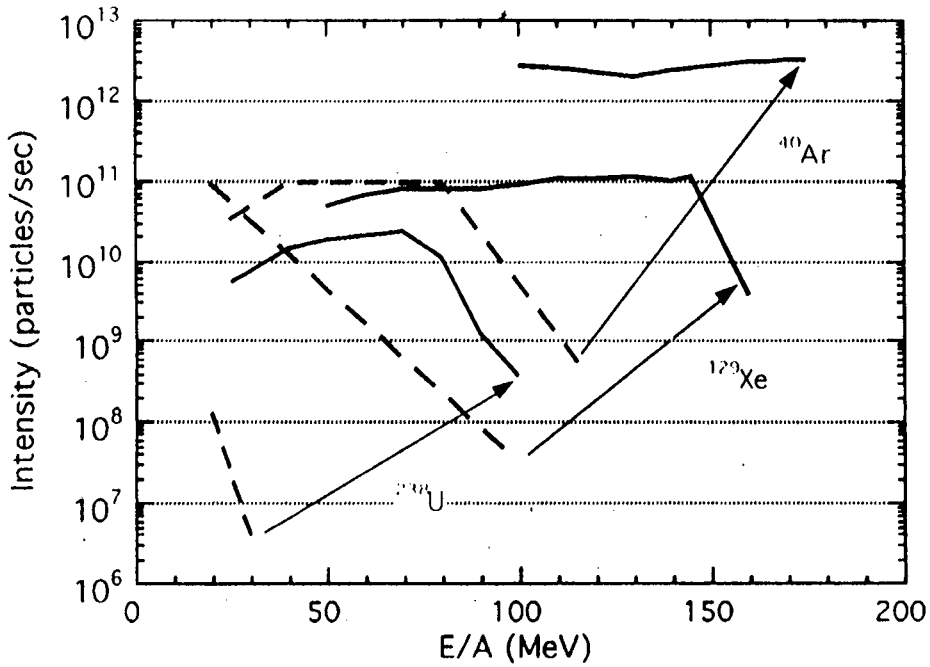


present

upgrade

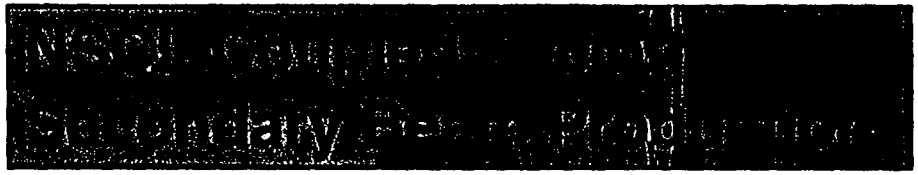

**Sample Beams** (Ions/s)

| Ion | K1200 | K500xK1200 |
|---|---|---|
| $^{11}Li$ | $2.5 \times 10^3$ | $4 \times 10^6$ |
| $^{19}Ne$ | $6 \times 10^7$ | $1 \times 10^{10}$ |
| $^{32}Mg$ | $1.2 \times 10^3$ | $3 \times 10^6$ |
| $^{56}Ni$ | $7 \times 10^4$ | $1 \times 10^8$ |
| $^{132}Sn$ | 2 | $4 \times 10^4$ |

Nuclei at or near the neutron drip line

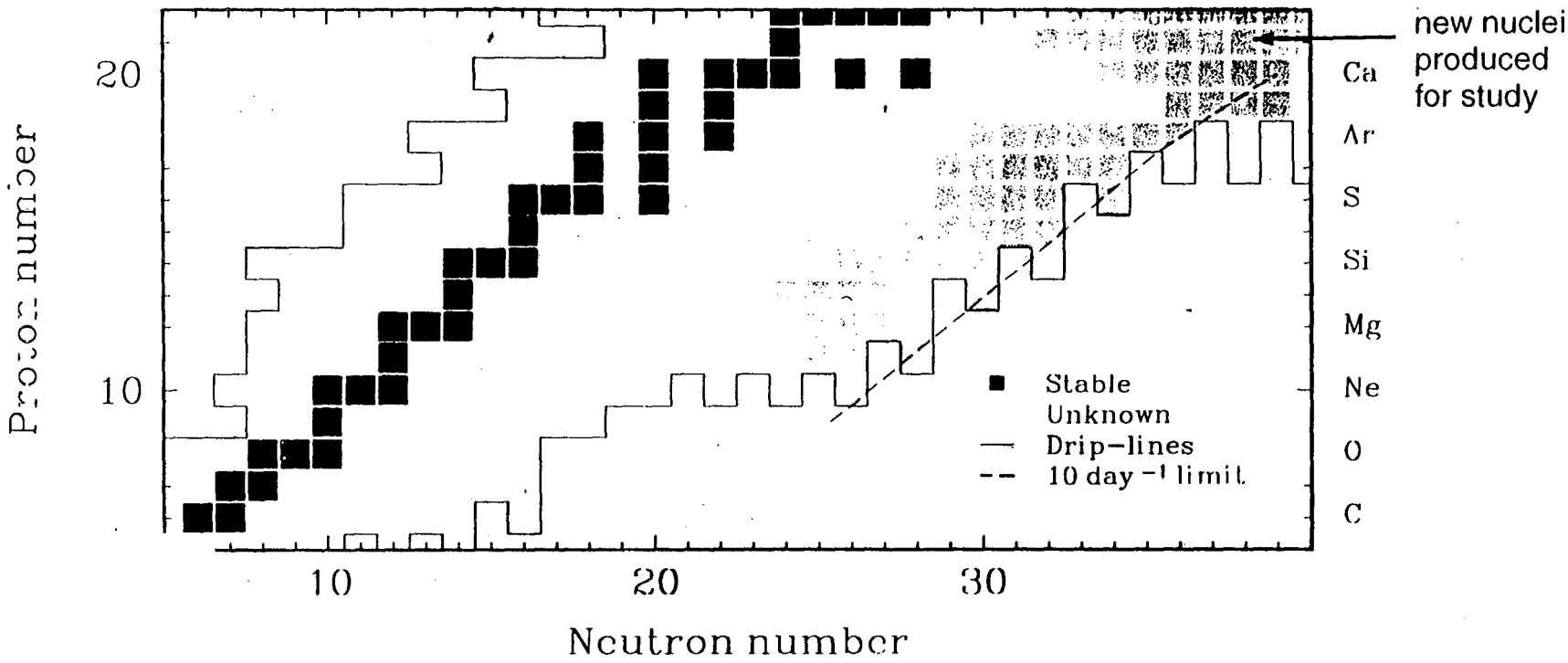

# Prospects for Searching for Halo Nuclei

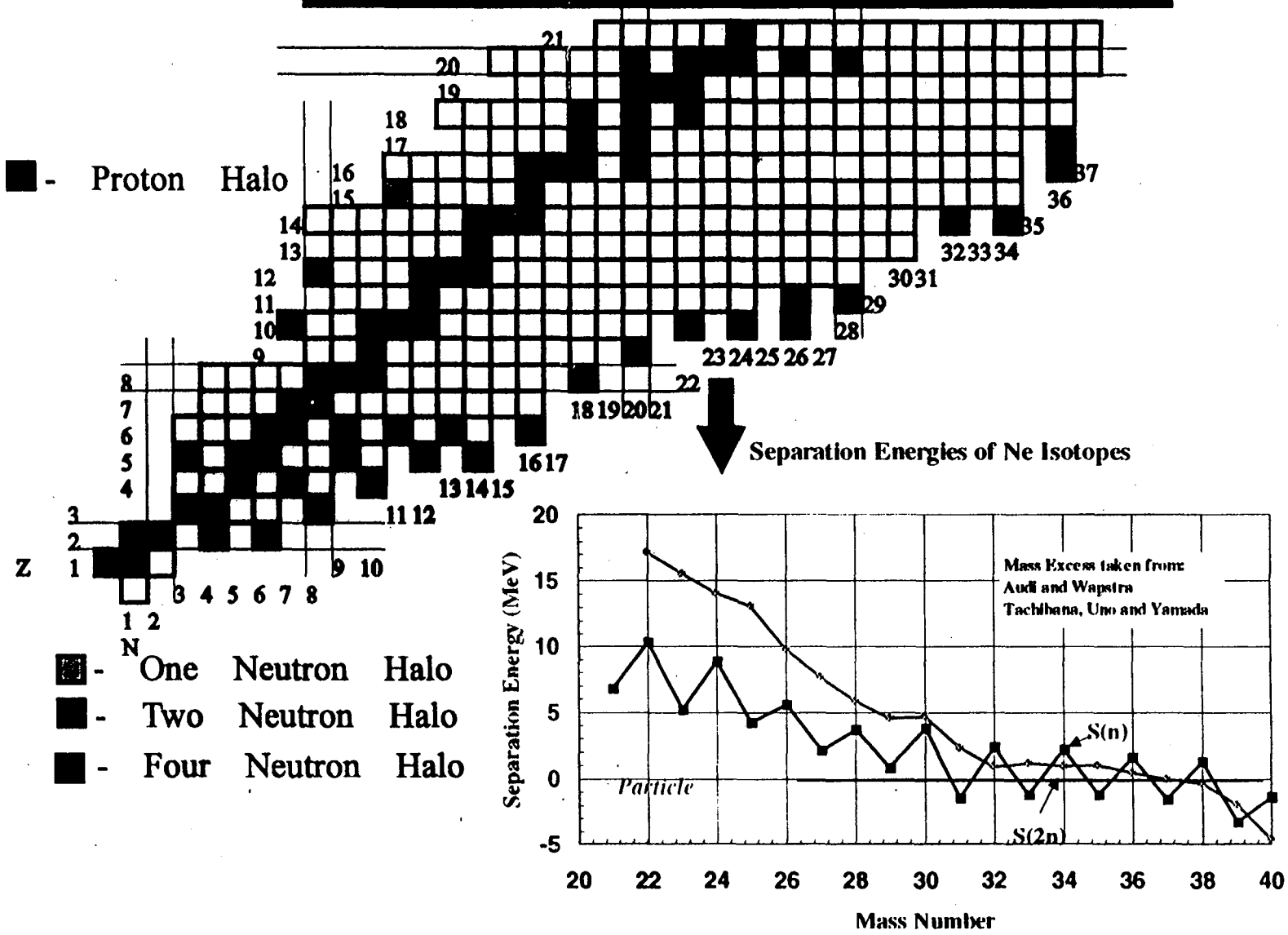

# Neutron Removal Mechanisms

## Diffractive dissociation:

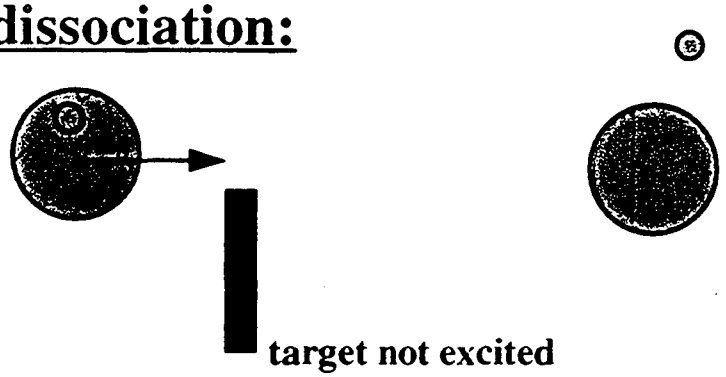


## Stripping:

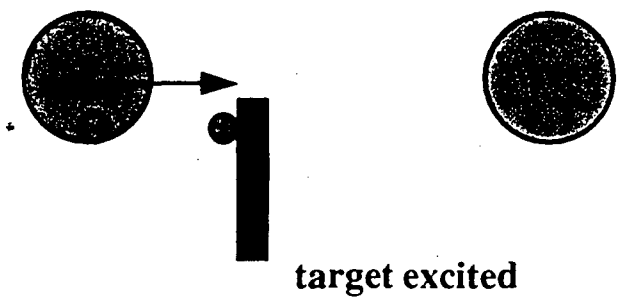


## Sequential:

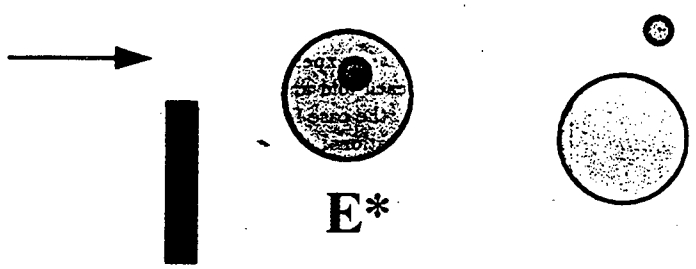


## Coulomb Excitation:

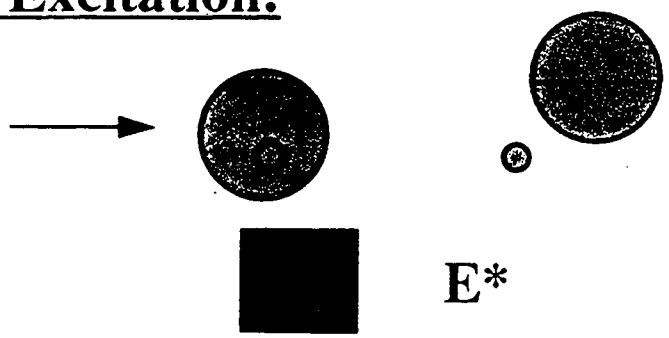

# Determination of all components of the valence wave function

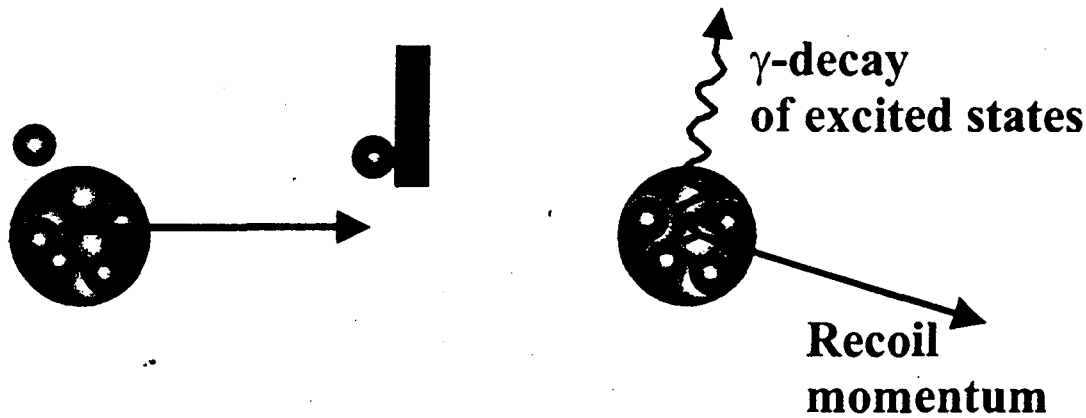


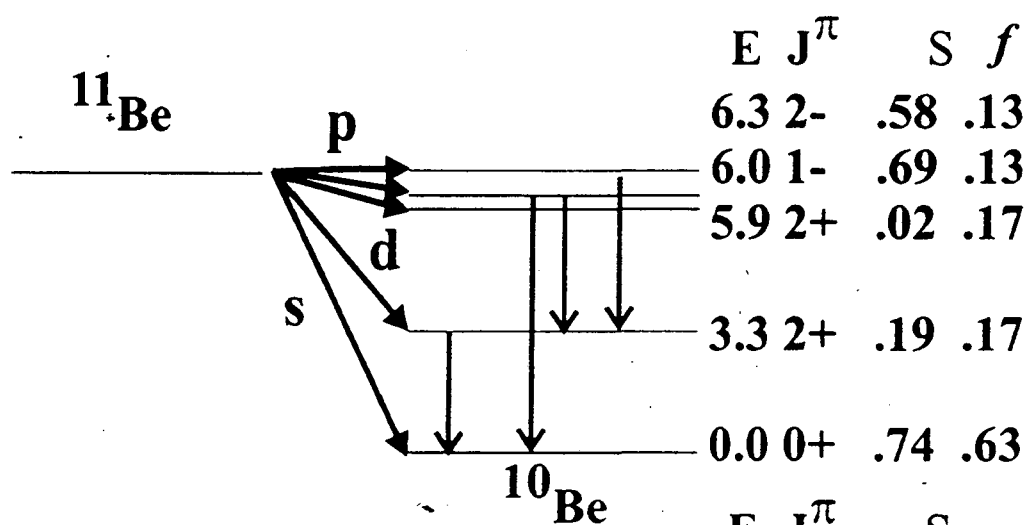


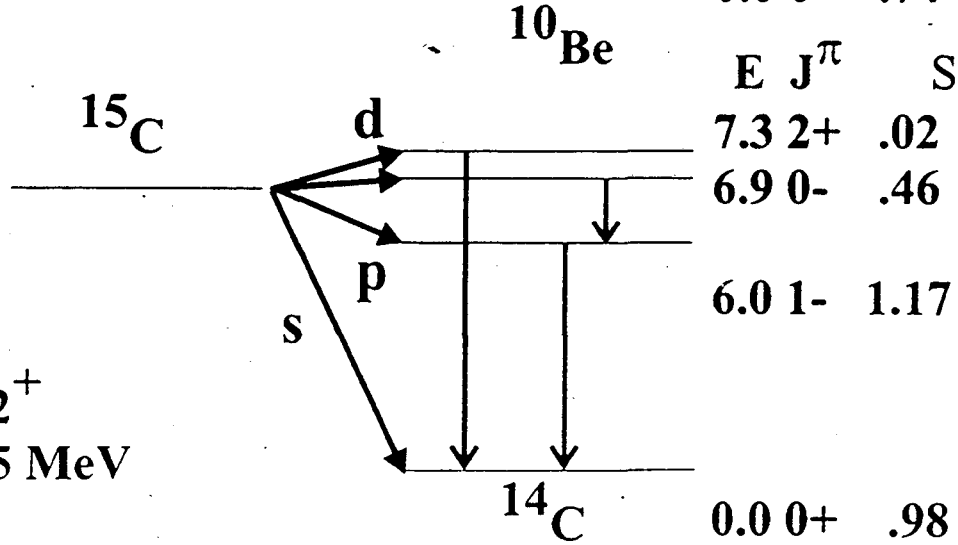


**Beams:**

$^{11}$Be $1/2^{+}$
S(n) = 0.5 MeV

$^{15}$C $1/2^{+}$
S(n) = 1.2 MeV

# Core Knock-out Contribution to the Recoil Momentum

H.Sagawa and
K. Yazaki
PL B244 (90) 149.

S, P, and D
contributions

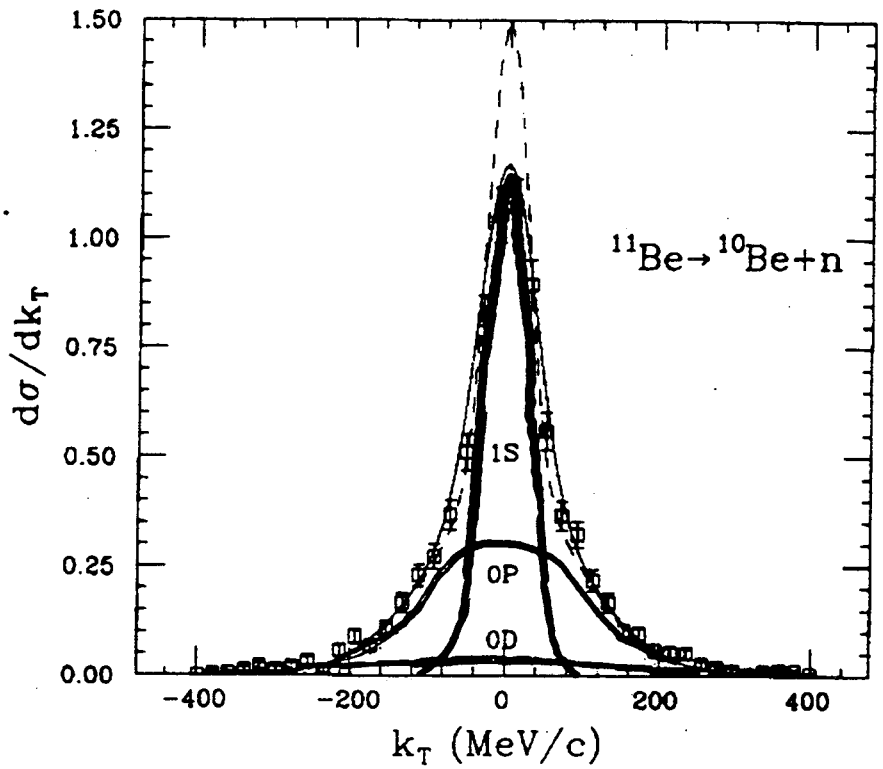


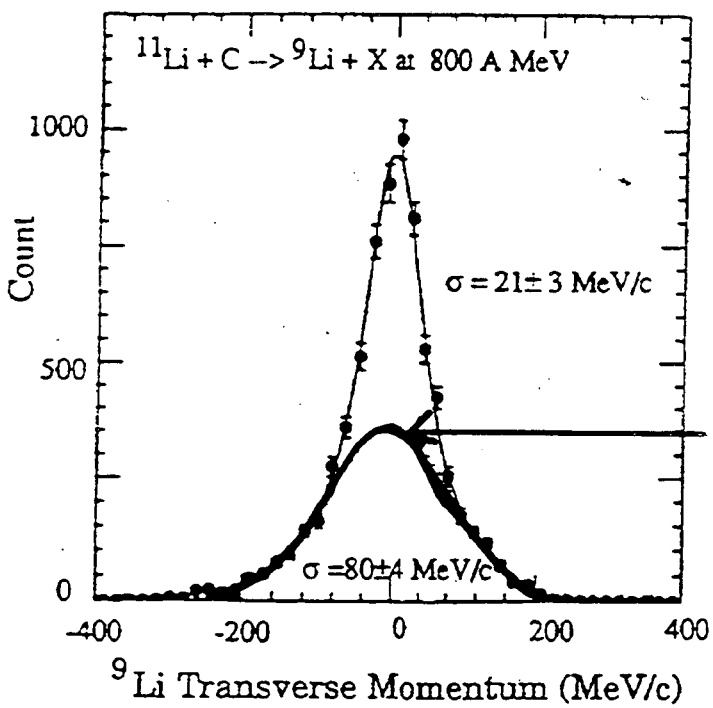


T. Kobayashi et al.
PRL 60 (88) 2599.

Core removal
contribution

# Position-sensitive NaI(Tl) photon detection array

- Array of 38 NaI(Tl) crystals (with two phototubes each) surrounding the target
- Measures energies and interaction points of photons up to 8 MeV
- Detectors from former PET machine (Washington University, St. Louis)

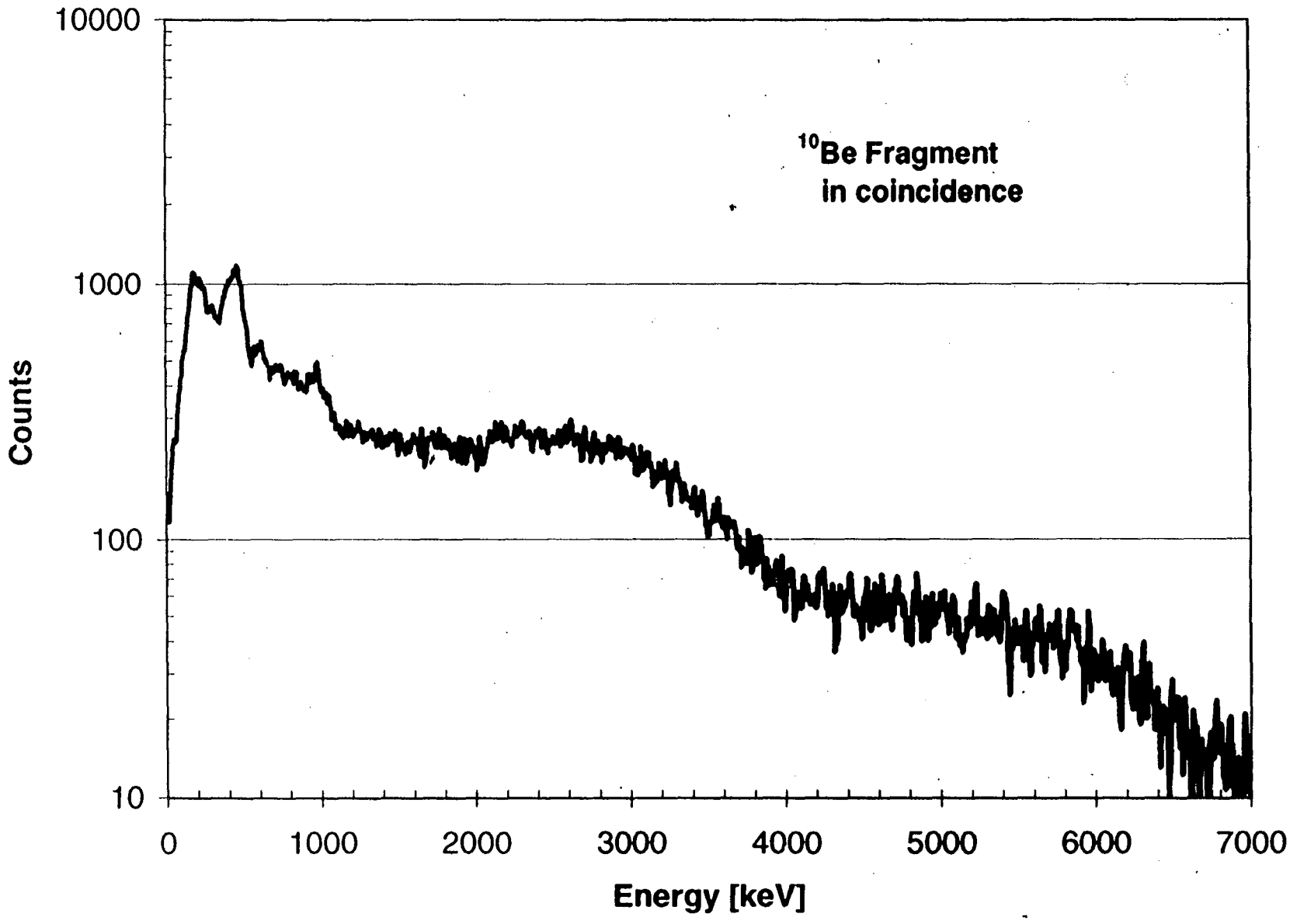
10000
1000
100
10
Counts
0
1000
2000
3000
4000
5000
6000
7000
Energy [keV]
$^{10}$Be Fragment
in coincidence

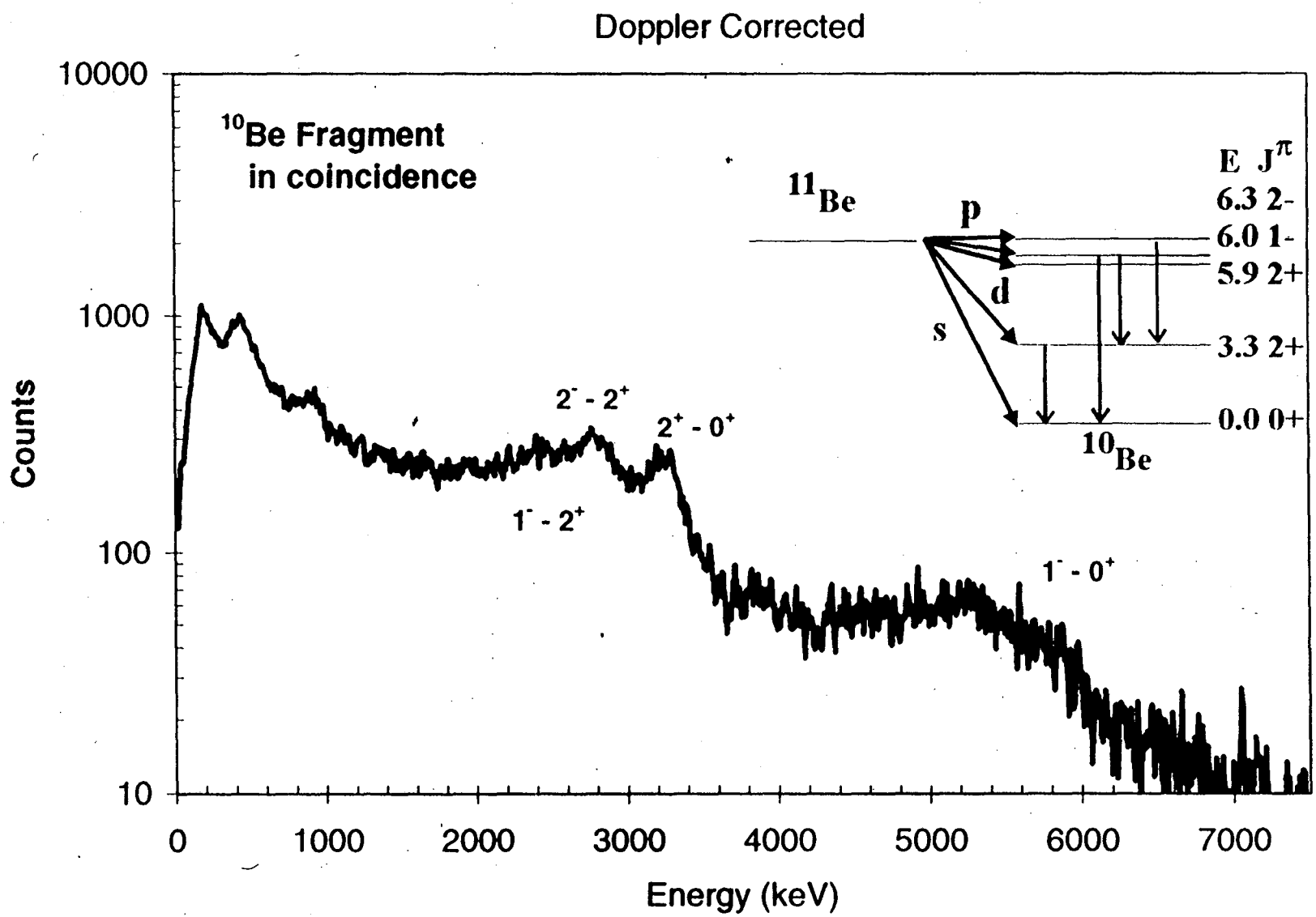
Doppler Corrected
10000
1000
100
10
Counts
0
1000
2000
3000
4000
5000
6000
7000
Energy (keV)
10Be Fragment
in coincidence
2- - 2+
2+ - 0+
1- - 2+
1- - 0+
11Be
p
d
s
E Jπ
6.3 2-
6.0 1-
5.9 2+
3.3 2+
0.0 0+
10Be

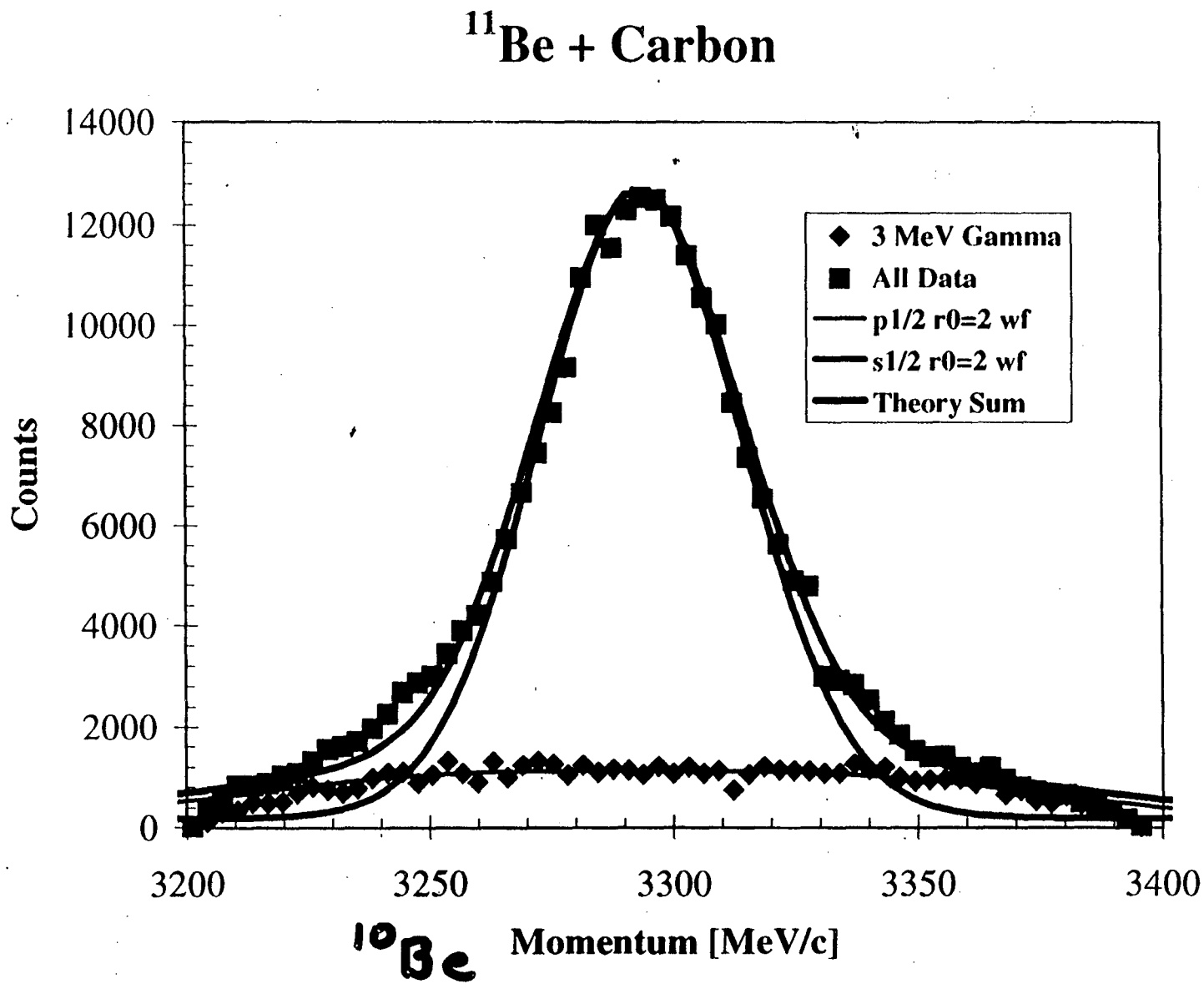
$^{11}$Be + Carbon
14000
12000
10000
8000
6000
4000
2000
0
Counts
3200
3250
3300
3350
3400
Momentum [MeV/c]
3 MeV Gamma
All Data
p1/2 r0=2 wf
s1/2 r0=2 wf
Theory Sum
$^{10}$Be

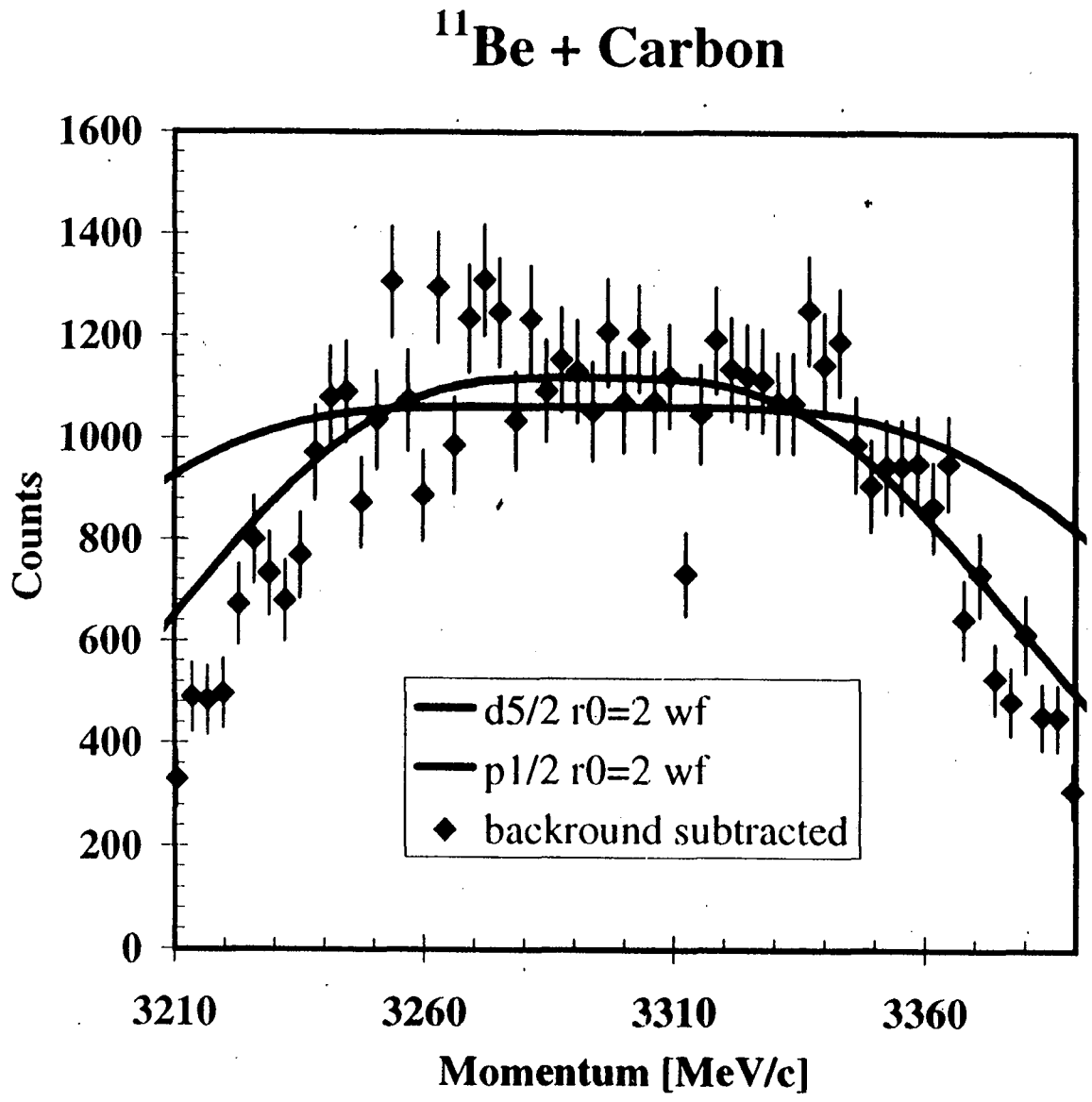
$^{11}$Be + Carbon
1600
1400
1200
1000
800
600
400
200
0
Counts
3210
3260
3310
3360
Momentum [MeV/c]
d5/2 r0=2 wf
p1/2 r0=2 wf
backround subtracted

# Ground State Structure of 17C

$^{17}C + ^{9}Be \rightarrow ^{16}C + X$

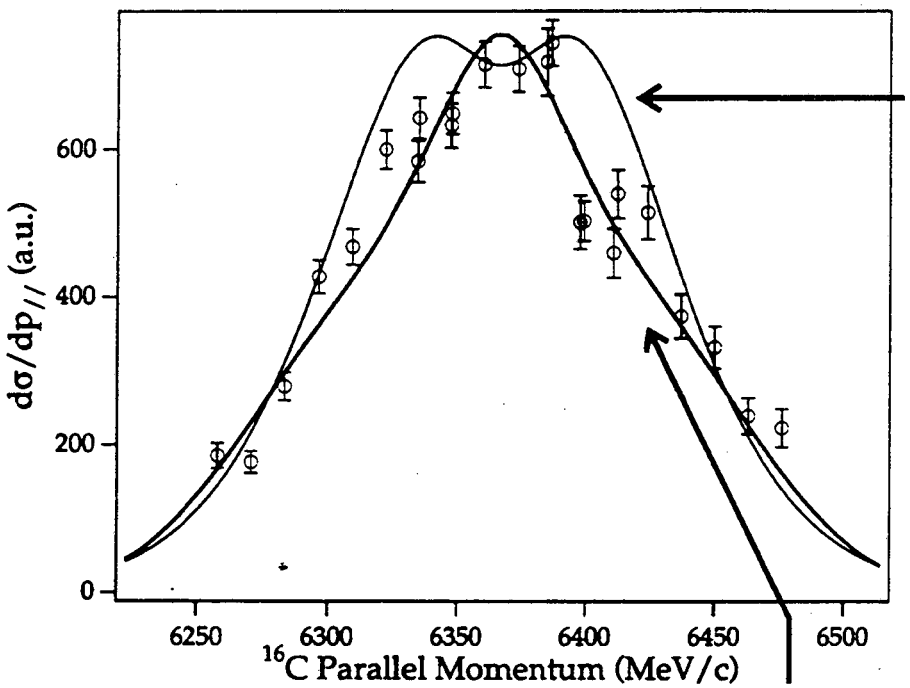


G. Hansen
l=2 wavefunction
with cutoff

$^{17}C$ $(3/2^+)$ with fractional parentage to $^{16}C$ $(2^+)$

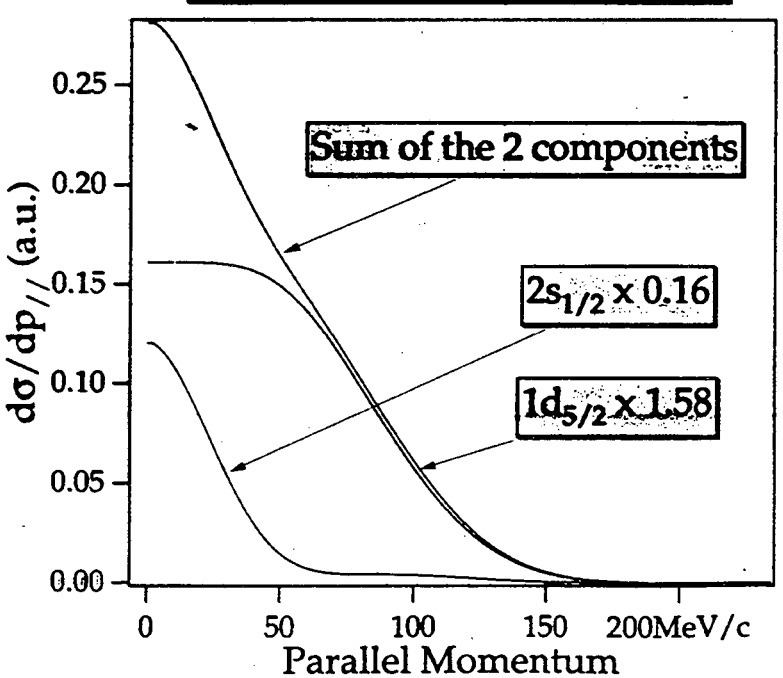


**D. Bazin,**
**B.A. Brown,**
**G. Hansen et al.**
Phy. Rev. C

# What is the limit of the technique?

Reminder: (p,d) studies will require 1000/s for a few day run.

(d,p) at lower energy require 10,000/s.

Advantages:

Large breakup cross sections - 300 mb
Thick targets (same Z same v) - 300 mg/cm2
100% efficiency for fragments (S800)

Event Rate:

Based on the numbers above the interaction probability is: 6%

For a beam intensity of 20/day we would have 1 event/day.

GRETA full energy efficiency of 43% for a 2.0 MeV gamma-ray

20 day experiment (?)

# Conclusions

- **We have a technique for the determination of valence wave functions**
  - Works well in light nuclei
  - Reaction mechanism effects are important
  - We have seen unusual parentage in $^{17}C$
  - Have measured $^{11}Be$, $^{14}B$, $^{15,17,19}C$, $^{26,27,28}P$
- **Need Measurements with γ-rays**
  - S800 available for momentum measurement
  - Measurement of parentage to n+core states.
  - Need high efficiency, doppler correction and good energy resolution
  - Need GRETA

M.Thoennessen
Giant resonances.

# High Resolution Studies of Giant Resonances?

- GDR Built on Excited States
- GDR and GQR Built on the Ground State
- GDR in Exotic Nuclei

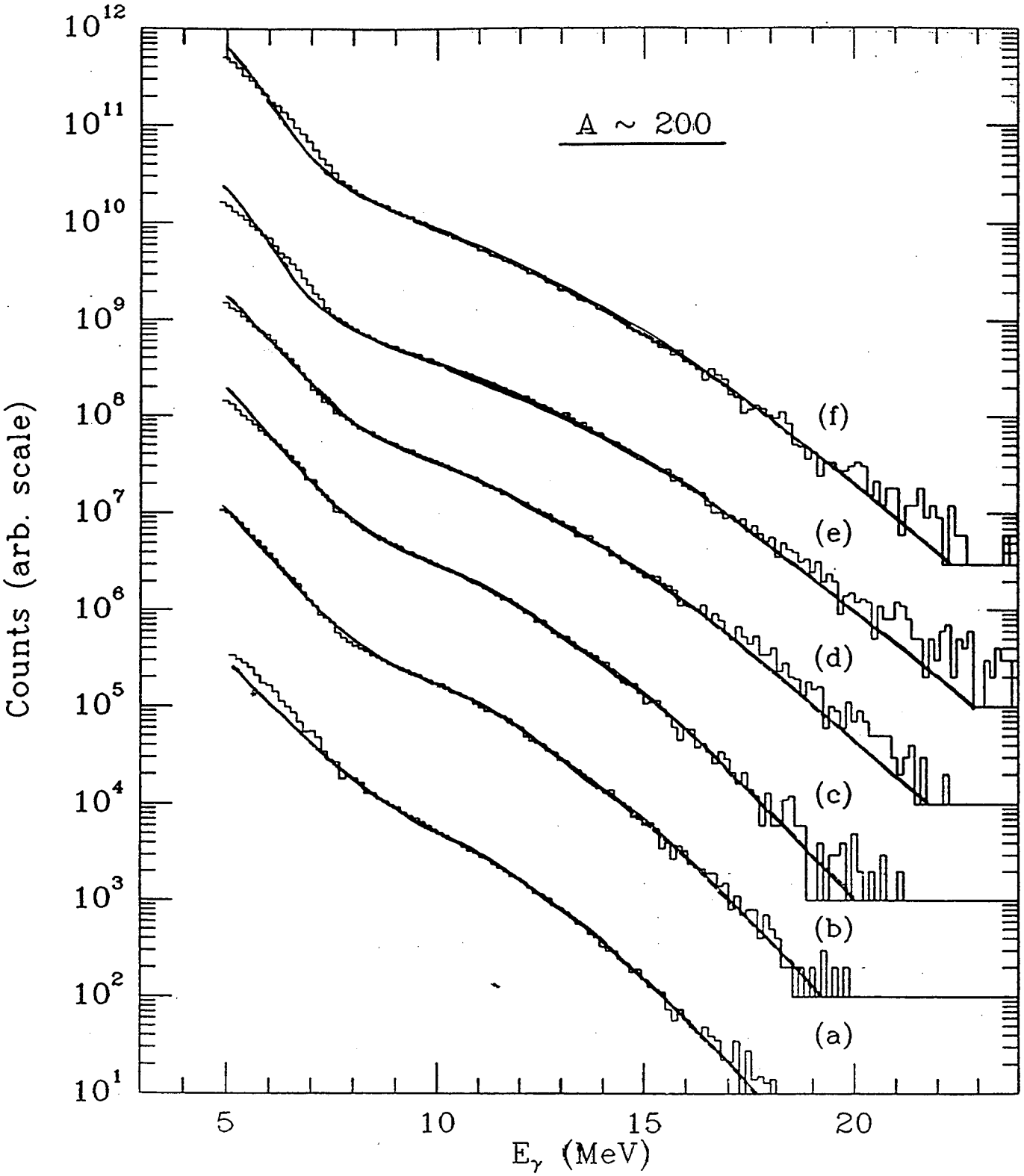


(a) $^{19}F + ^{181}Ta$ 93 MeV
(b) $^{16}O + ^{nat}W$ 100 MeV
(c) $^{19}F + ^{181}Ta$ 105 MeV
(d) $^{19}F + ^{181}Ta$ 126 MeV
(e) $^{16}O + ^{nat}W$ 140 MeV
(f) $^{19}F + ^{181}Ta$ 141 MeV

## PROBLEM:

— The $\gamma$-decay of the GDR originates from a wide range of excitation energies and angular momenta.

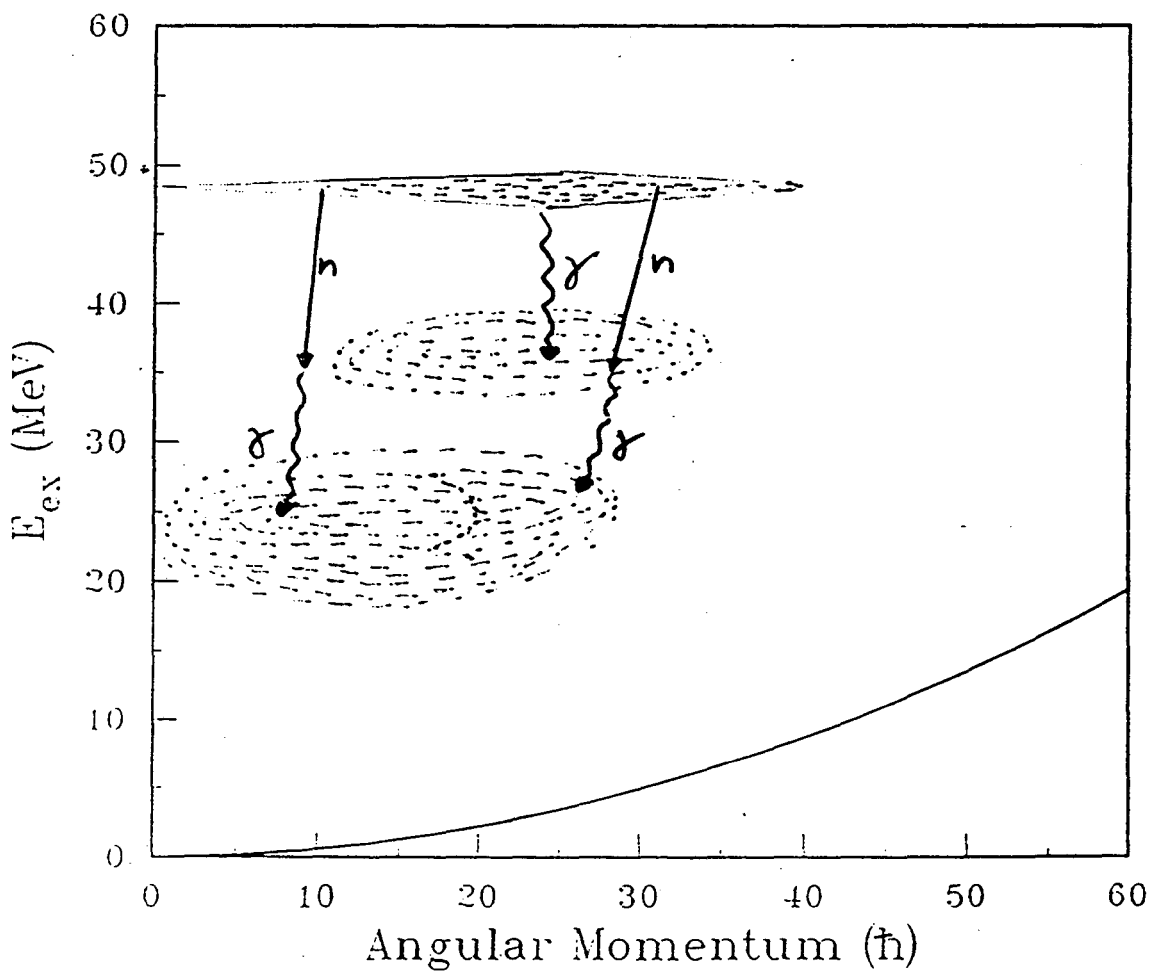

# Isolate Specific Channels

- Multiplicity Gates
  A. Bracco, Phys. Rev. Lett 74, 3748 (1995)
- Isomer Trigger
  J. P. S. van Schagen, Nucl. Phys. A581, 145 (1995)
- $\alpha$-Scattering
  E. Ramakrishnan, Phys. Rev. Lett. 76 2025 (1996)
- Discrete Transitions
  G. Viesti et al., Phys. Rev. C55, 1594 (1997)

High energy γ-spectra gated on normal and superdeformed transitions

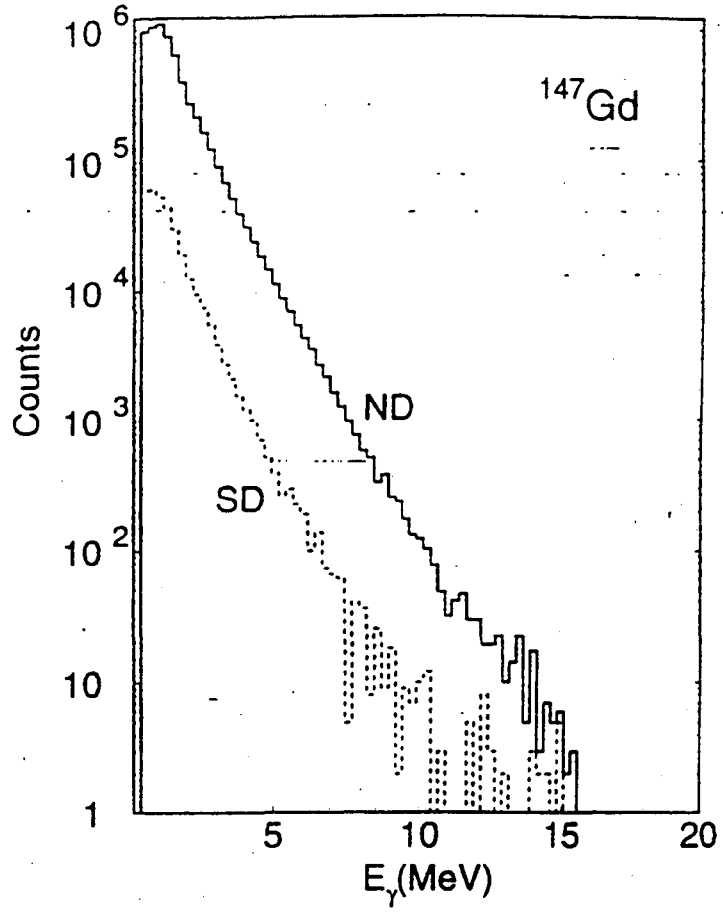


L. H. Zhu et al., Phys. Rev. C55, 1169 (1997)

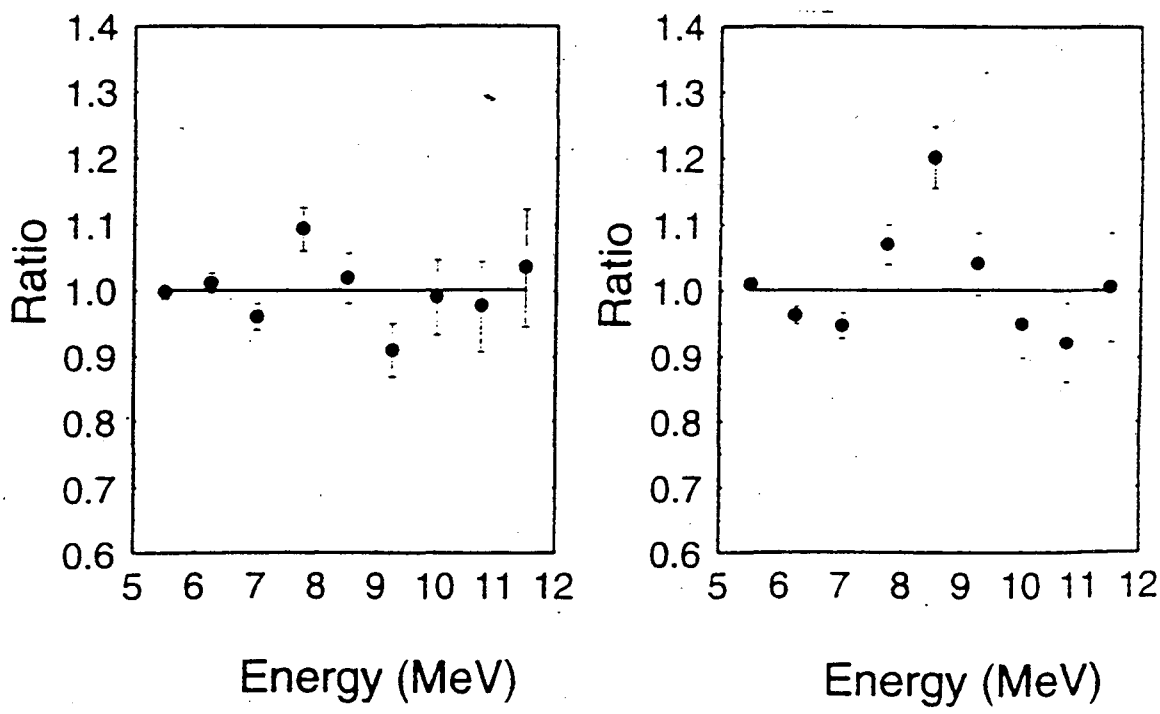


F. Camera et al., Act. Phys. Pol. B28, 207 (1997)

# High Resolution High Energy γ-Ray Detectors

- Large NaI: ~2%
- Ge+BaF2: 1.6%

  A. Krasznahorkay et al. NIM A316, 306 (1992)
- Ge+BGO: 0.7%

  F. Camera et al. NIM A351, 401 (1994)

# Detecting High Energy γ-Rays With HPGe Detectors

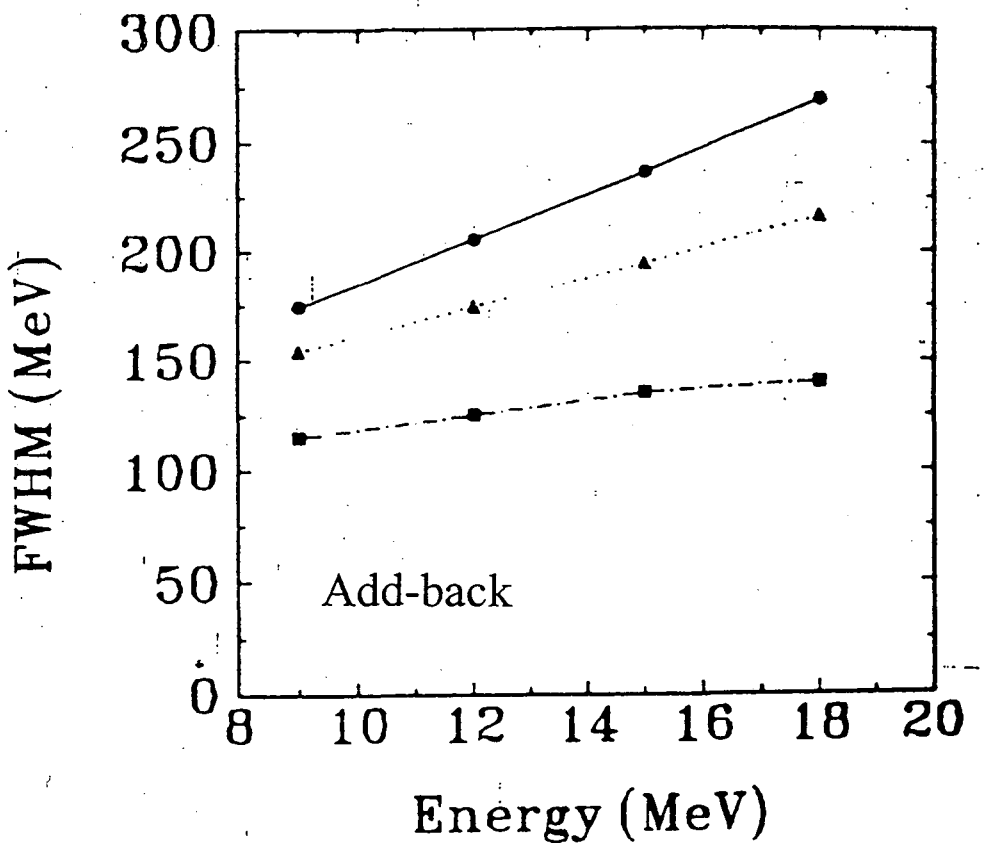


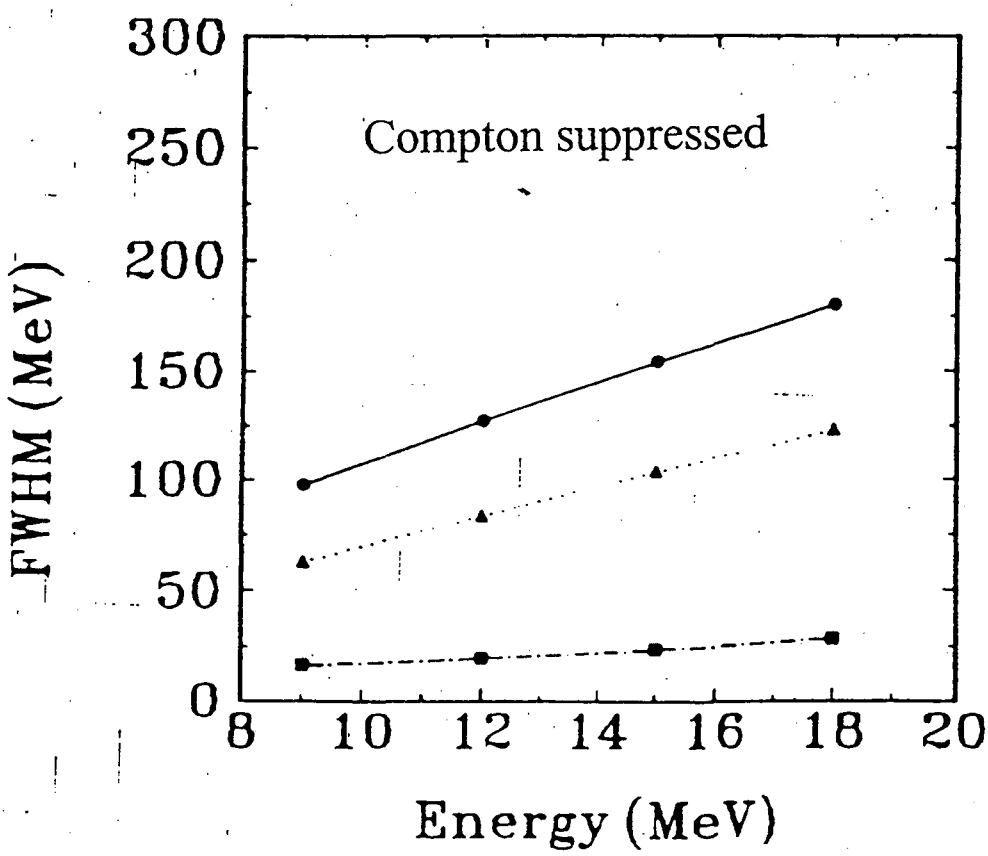


F. Camera et al., Act. Phys. Pol. B26, 479 (1995)

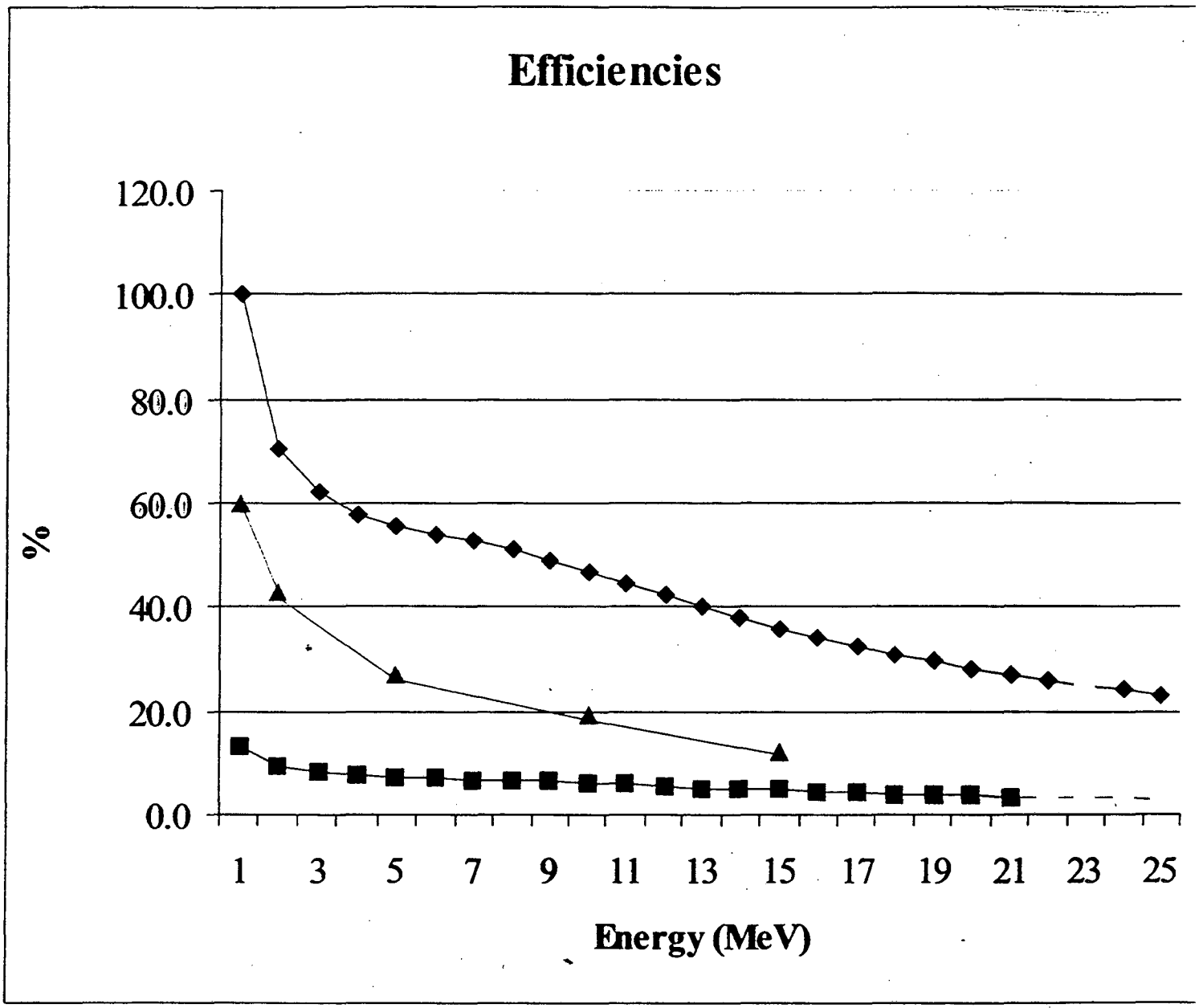


$BaF_2$ Intrinsic Efficiency

GRETA Shell

ORNL/MSU/TAMU $BaF_2$ Wall

# GRETA for the GDR built on Excited States

- Tagging of low energy transitions
- Simultaneous detection of high energy γ-rays
- Large detection efficiency

S. S. Dietrich and B. L. Berman, At. Data Nucl. Data Tables 38, 199 (1988)

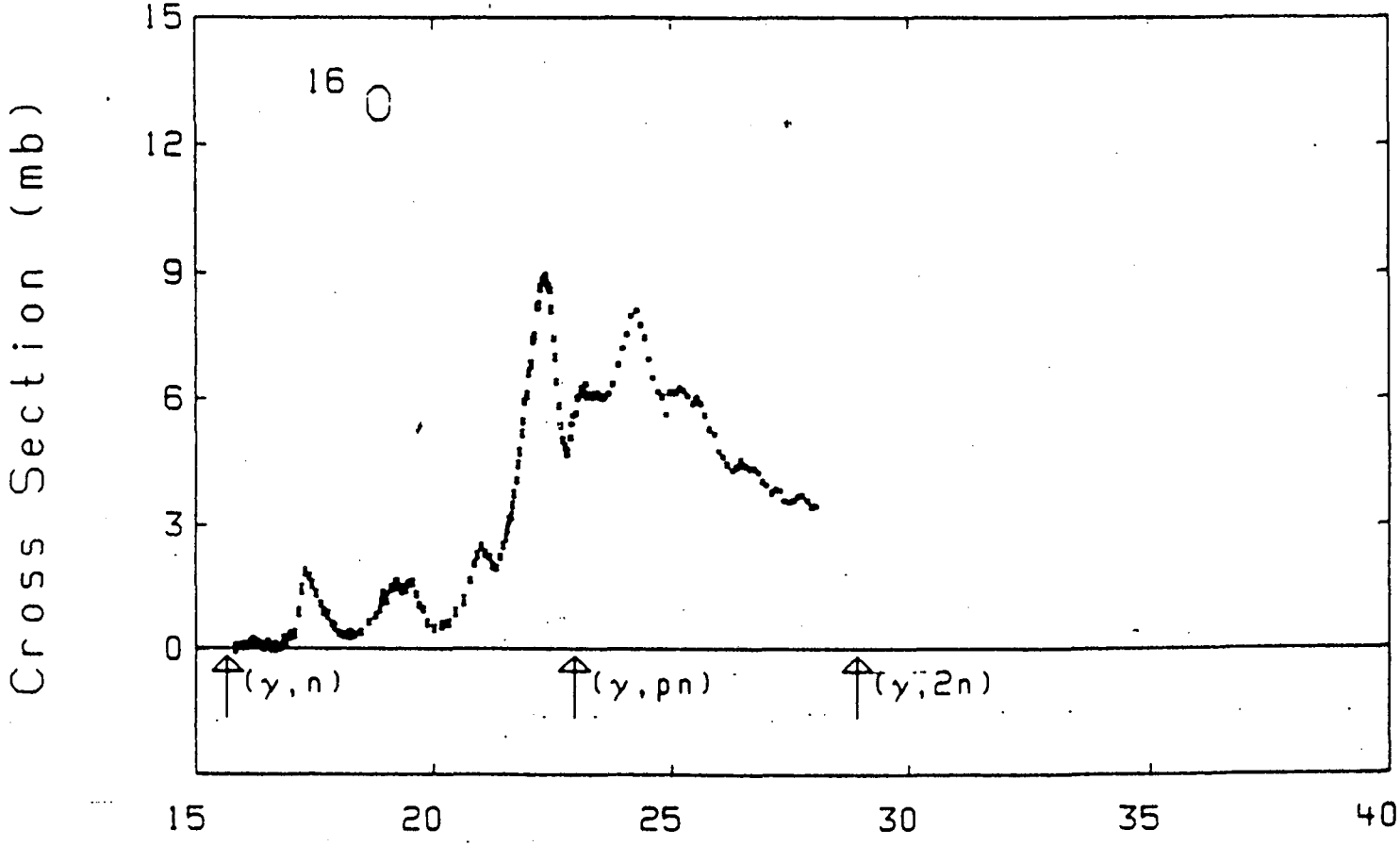


GDR in Stable Nuclei

# GDR is BROAD

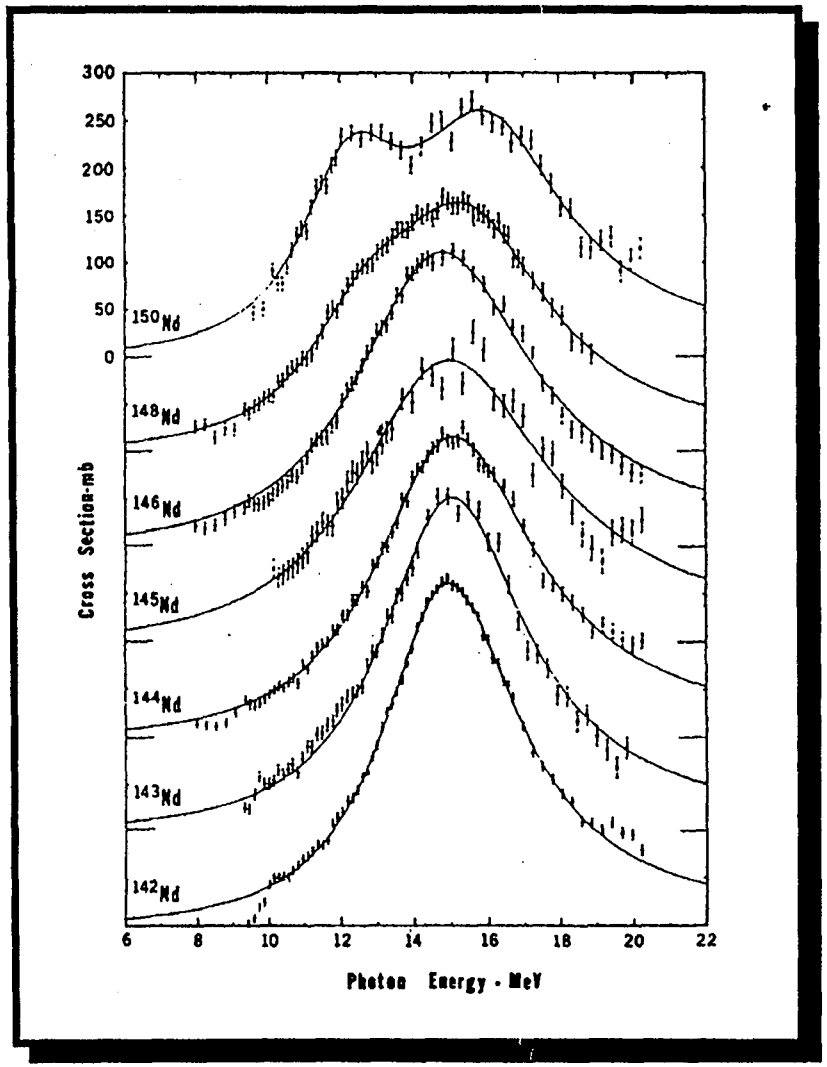


B. L. Berman and S. C. Fultz,
Rev. Mod. Phys. 47(1975)713

ORNL 22 MeV/nucleon

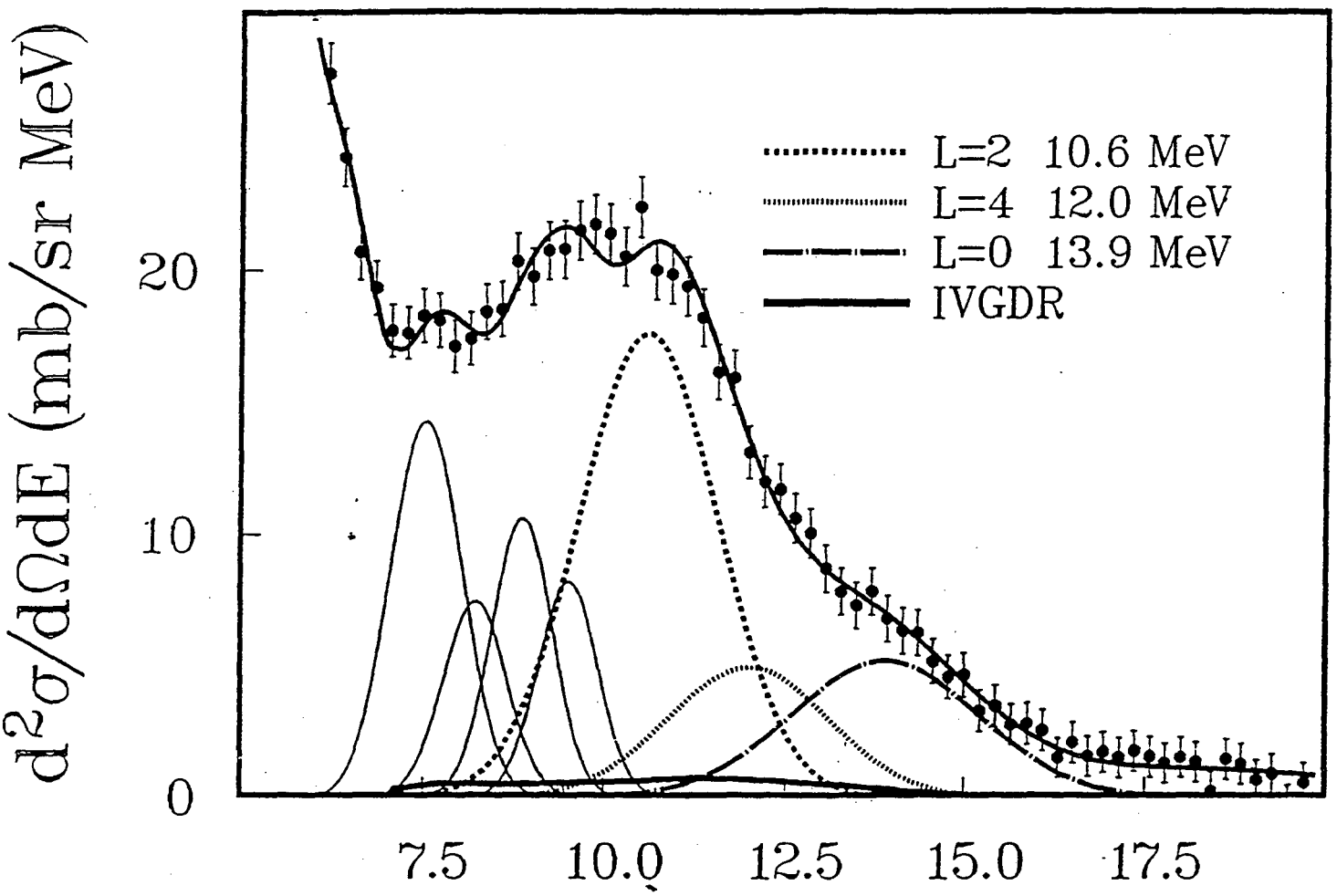


Singles: (Background subtracted)

J. R. Beene *et al.*, Phys. Rev. **C 39**, 1307 (1989).

# Multipole Selectivity of Giant Resonance Decay

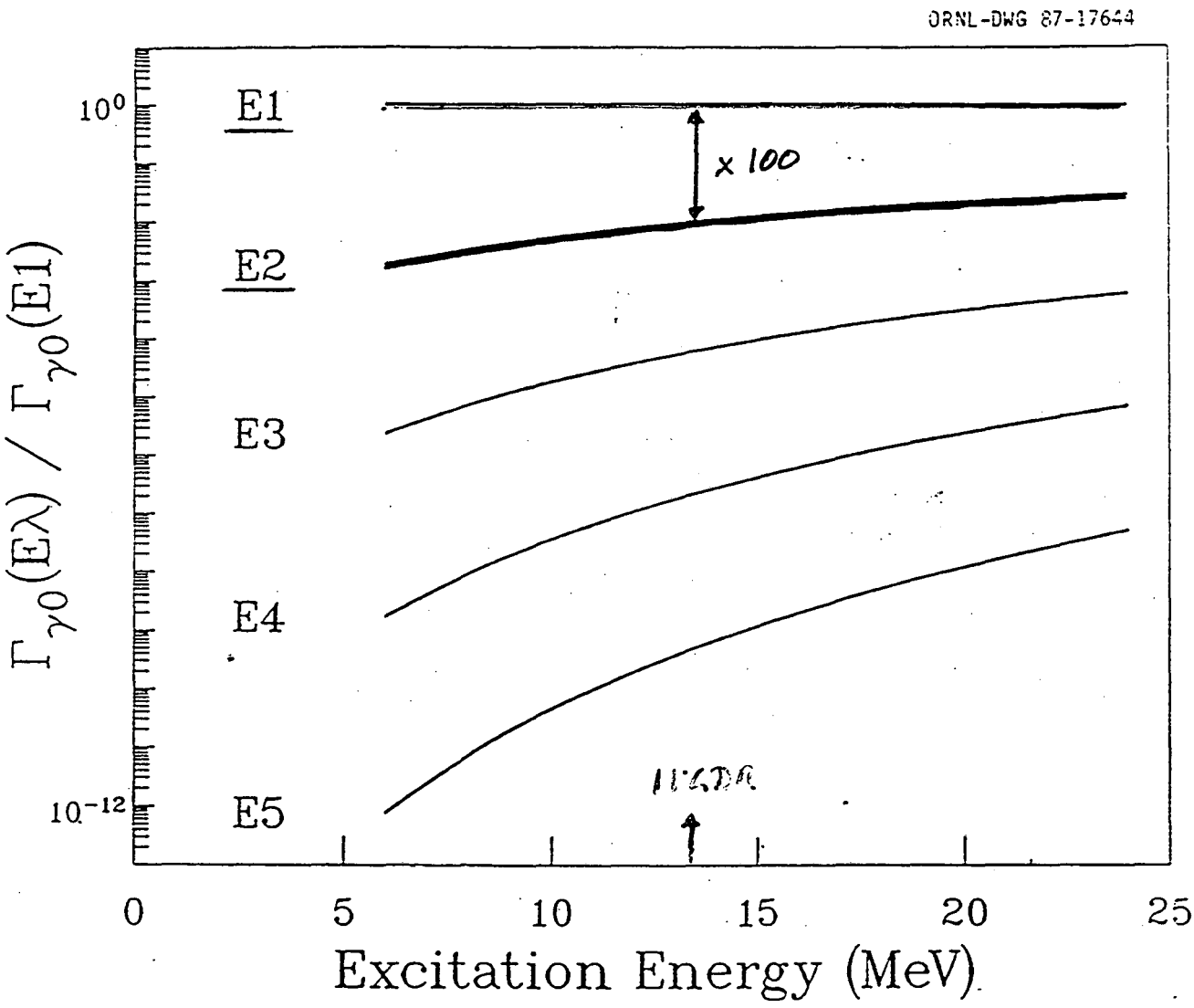

# Giant Dipole Resonance Decay

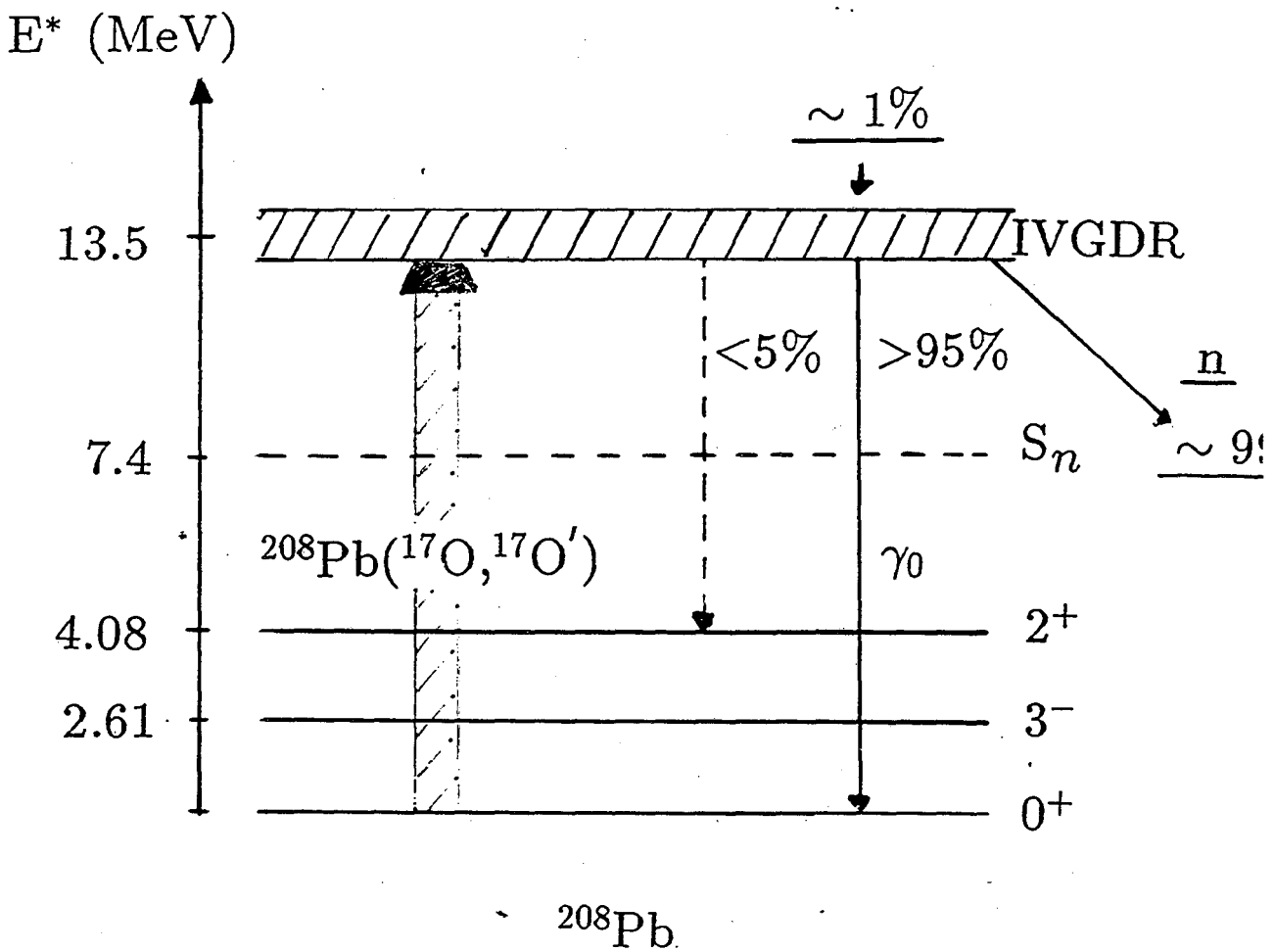

# Experimental Setup:

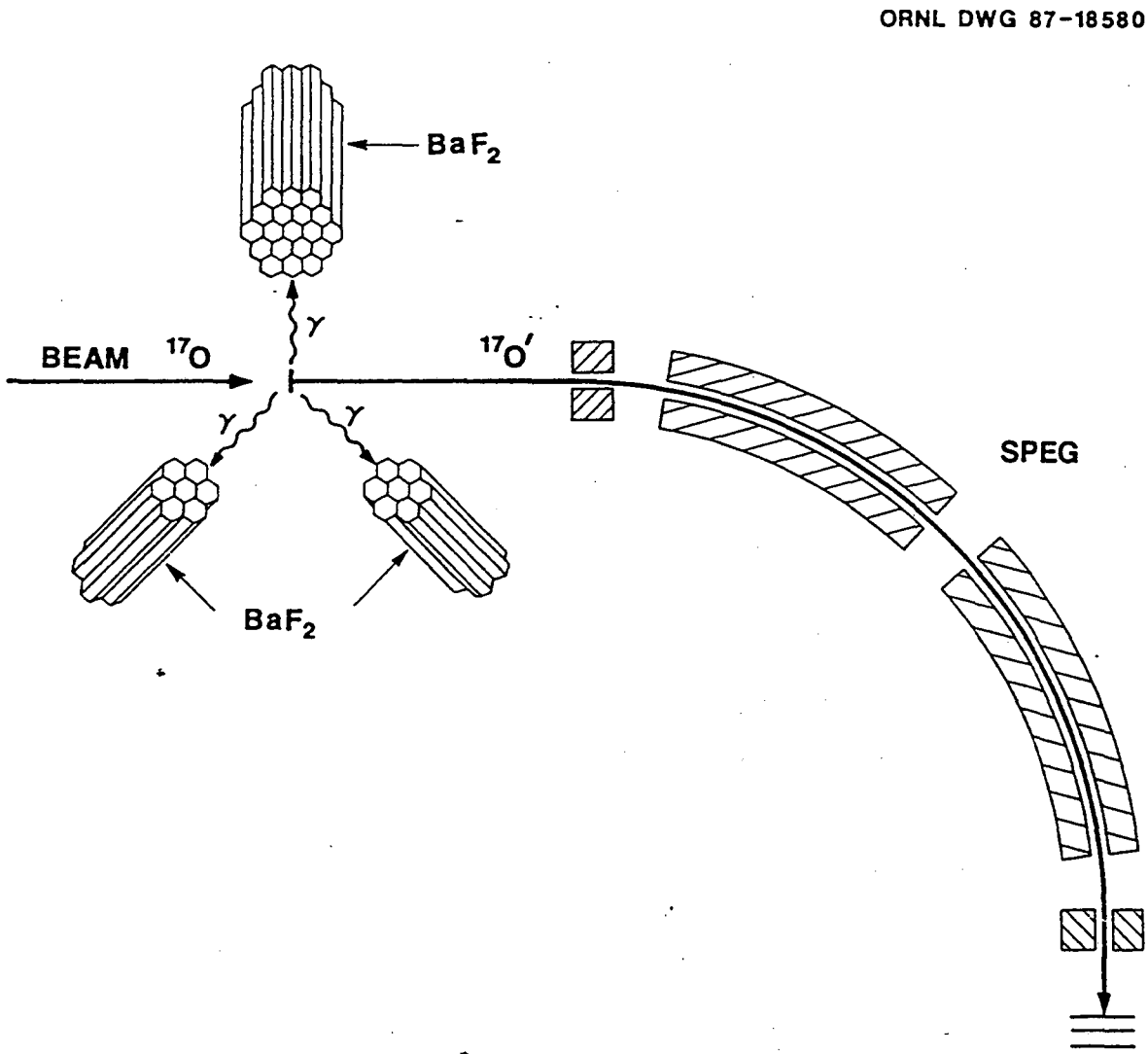


SPEG: Angular Range: 1.5° - 5.0°
Energy Resolution: 800 keV

$BaF_2$: 6 clusters of 7 detectors 8.7cm × 14cm
3 clusters of 19 detectors 5.7cm × 20cm

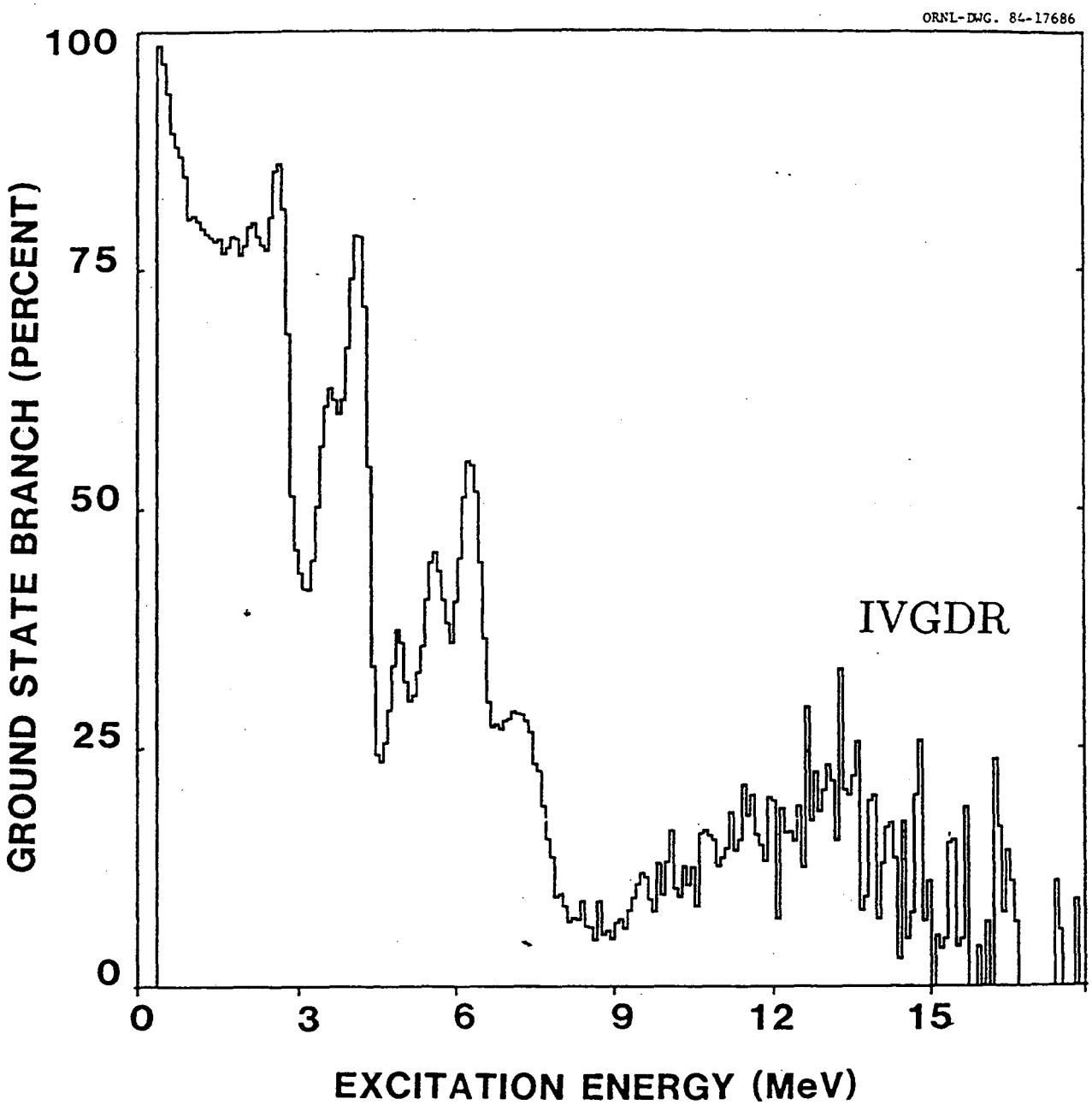
ORNL-DWG. 84-17686
100
75
50
25
0
GROUND STATE BRANCH (PERCENT)
IVGDR
0
3
6
9
12
15
EXCITATION ENERGY (MeV)

# Excitation of Giant Resonances:

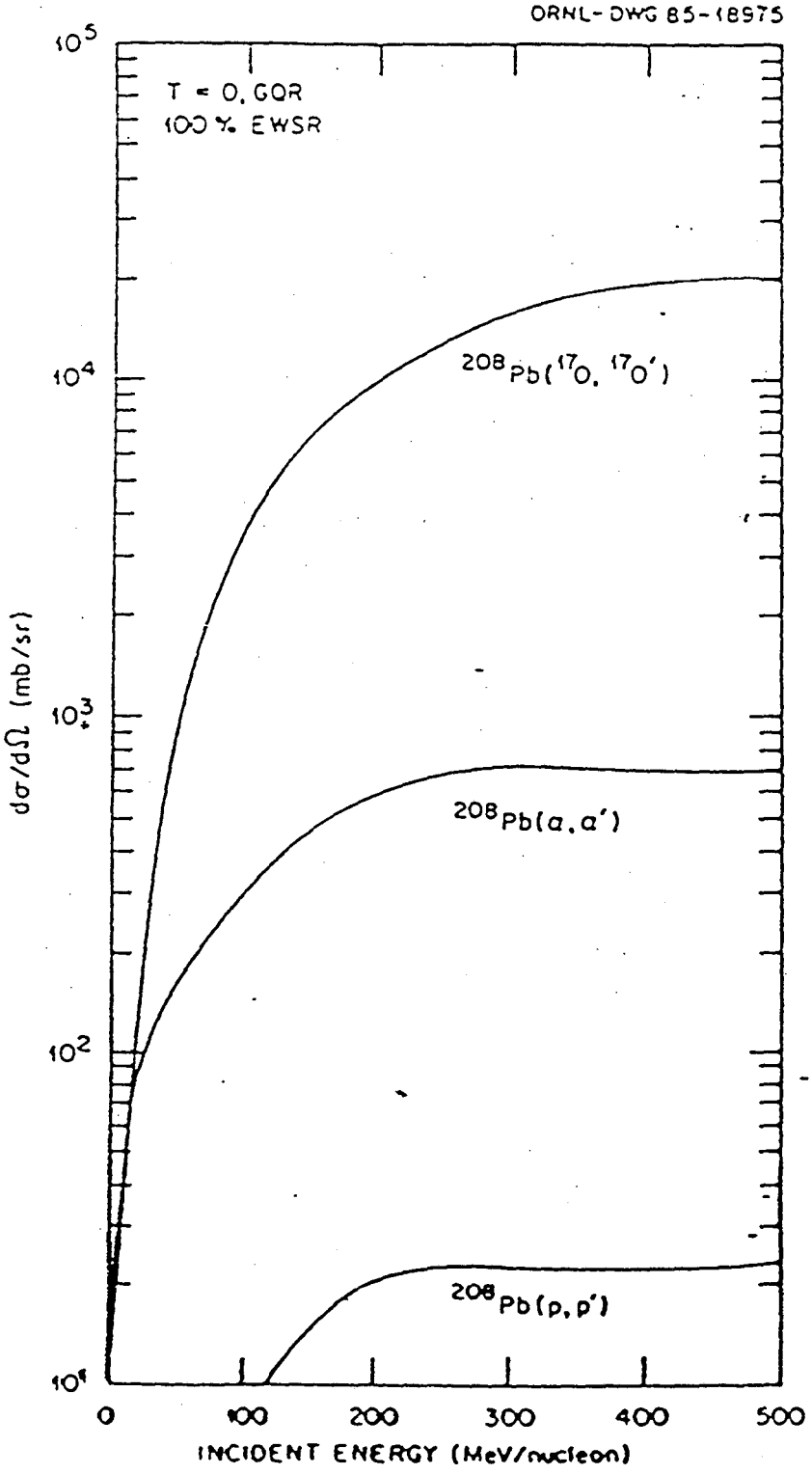


Large Cross Sections ==> – Heavy Ions
– High Beam Energies

# GRETA for GR's at/near the Ground State

- Isolate specific resonance by gating on no/low energy transition: (E1 ==> $\gamma_0$ , E2 ==> $\gamma_3$-)
- Simultaneous detection of low and high energy $\gamma$-rays ==> Large efficiency
- Coulomb Excitation ==> High Beam Energies (100-150 MeV/u)
- Coincidence with High Resolution Spectrometer

# Giant Resonances in Exotic Nuclei

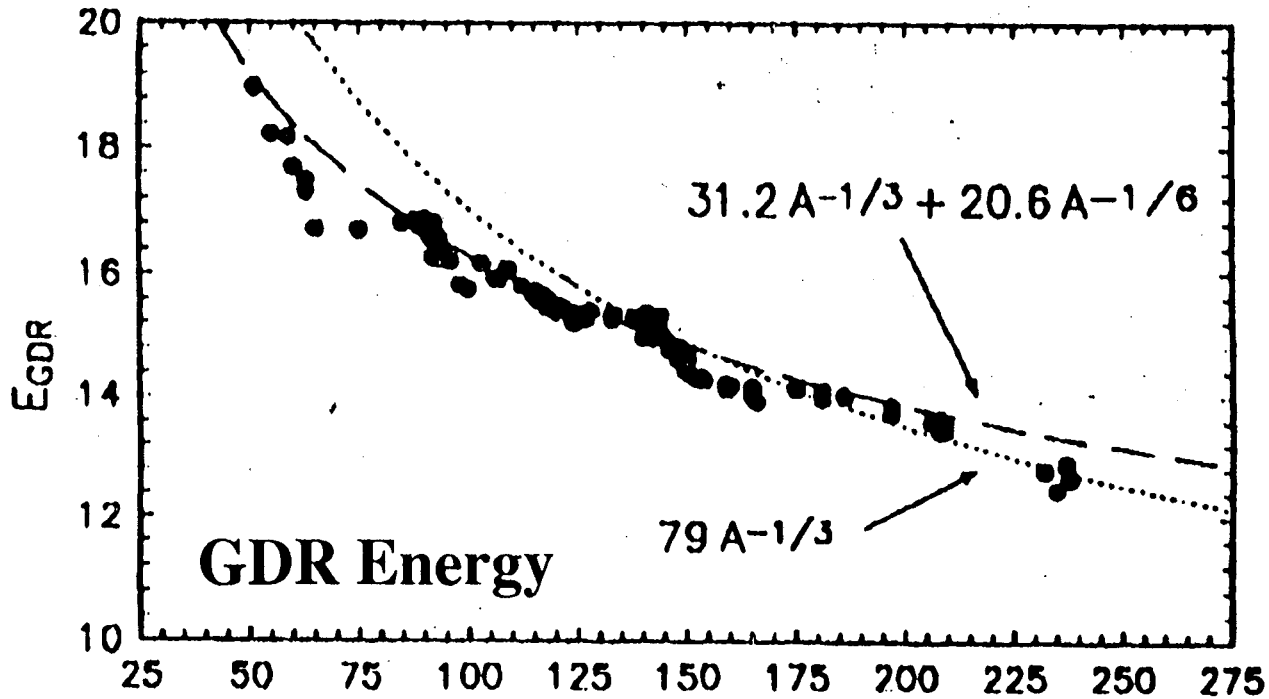


**A-dependence, but no Z and N dependence**

J. J. Gaardhøje, Ann. Rev. Nucl. Part. Sci., 42(1992)483

# $^{11}Li$ - E1 Strength Function

# $^{11}Li$ - Photo Absorption Cross Section

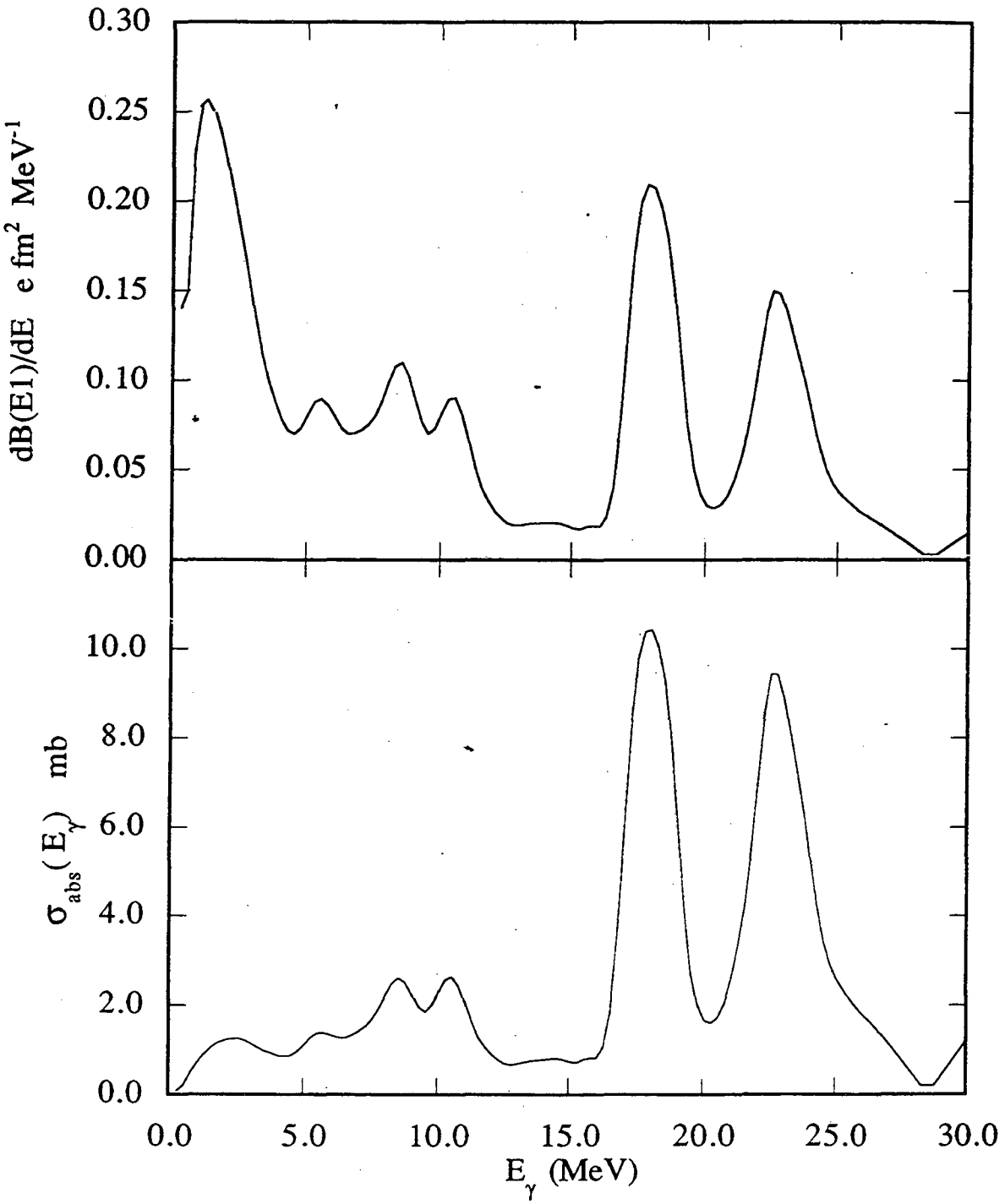

# *Projectile Excitations*

***Study of Deexcitation of Projectiles in Peripheral Heavy-Ion Collisions***

***Excitation via Virtual Photon Field***

***Decay Studied by Reconstructing the Decay Products***

***Two-Phonon Giant Dipole Resonance:***

***Measure Total Energy (LAND)***

***(Virtual Photon Absorption)***

***Measure the real γ-decay back to the ground state (TAPS)***

# Excitation of the GDR

## Target Excitation

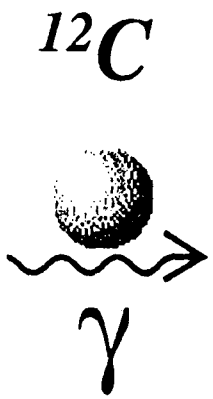


Absorption of **real** photons

## Projectile Excitation

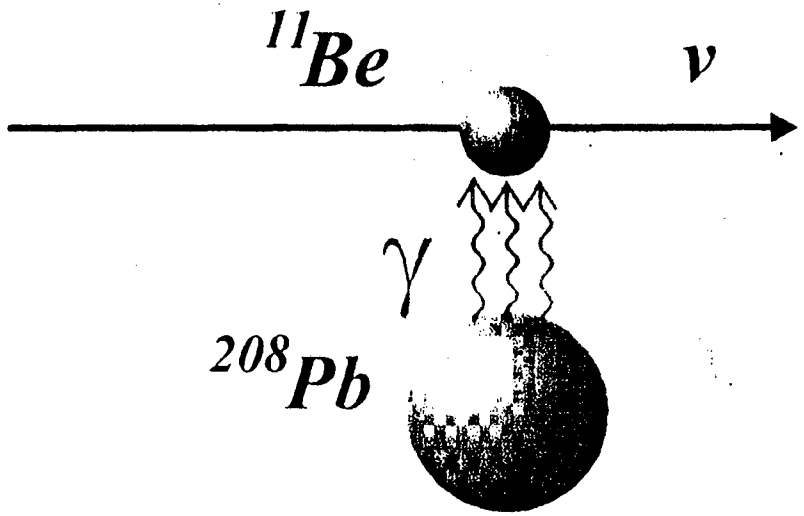


Coulomb excitation or absorption of **virtual** photons

# *Virtual Photon Scattering*

***Study of Exotic Nuclei: Projectiles!!***

***Low Intensities***

***Single Excitations of the GDR***

***Coulomb excitation***

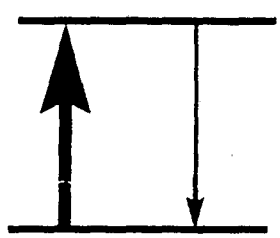

***$\gamma$ decay back to the ground-state***

→ ***S800***

***$BaF_2$ Array***

# *Prediction of the $^{208}Pb(^{11}Be,^{11}Be\gamma)$ Yield*

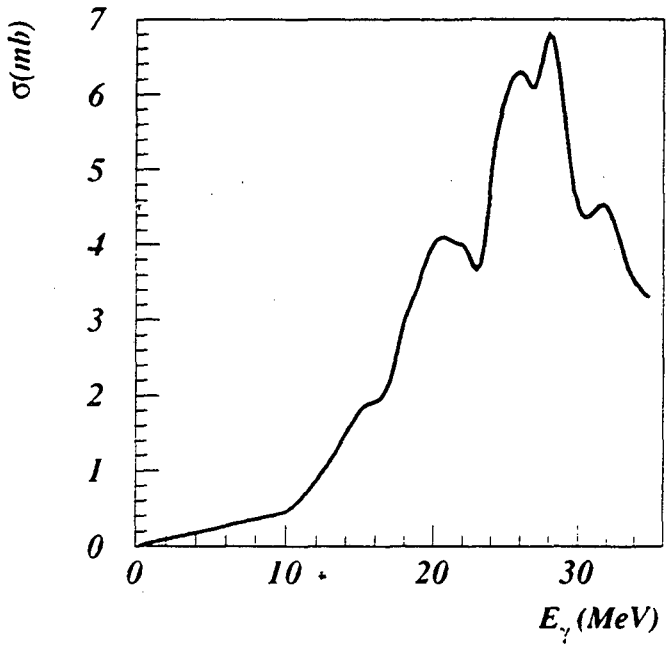


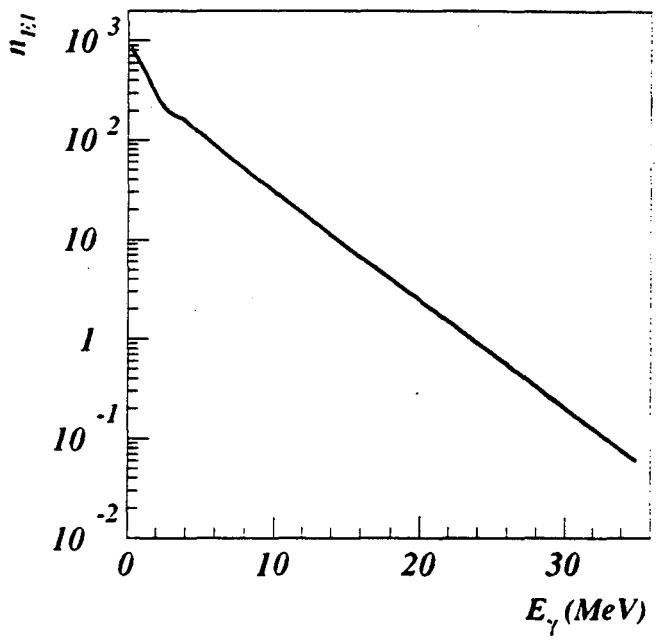


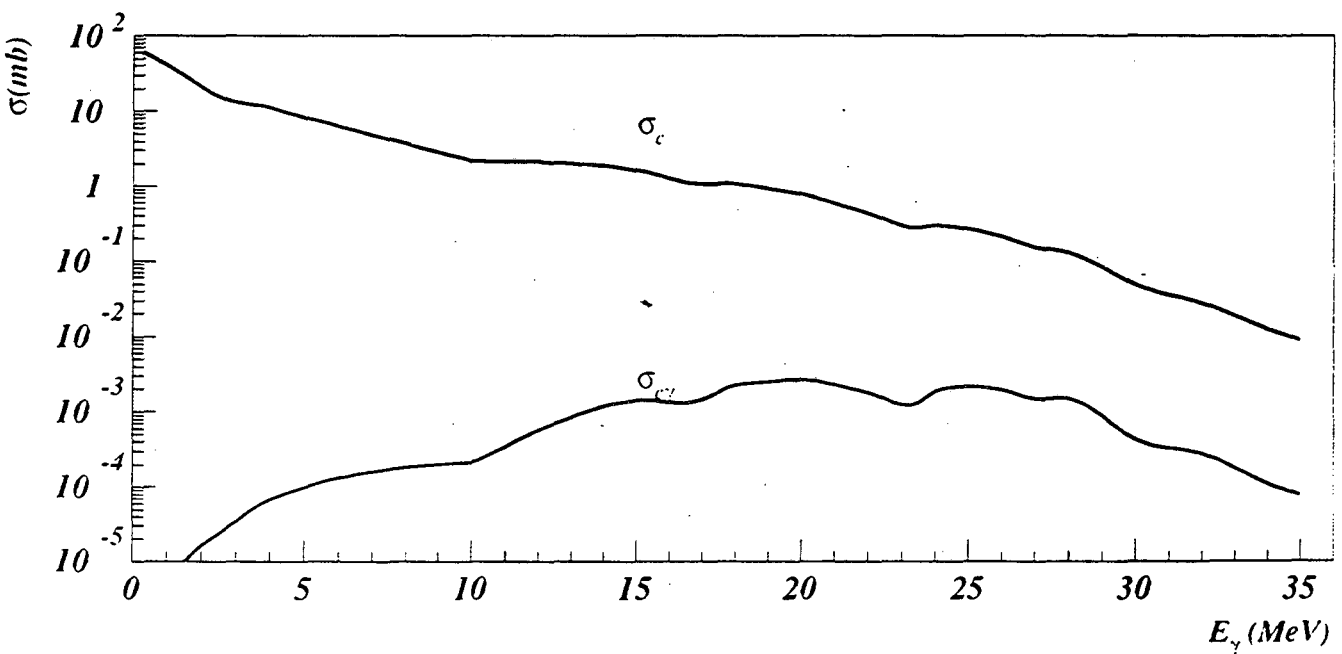

# *E1 - Inelastic Excitation of $^{11}Be$*

## *$10^6$ pps of 80 MeV/nucleon $^{11}Be$*
## *100 mg/cm$^2$ $^{208}Pb$*

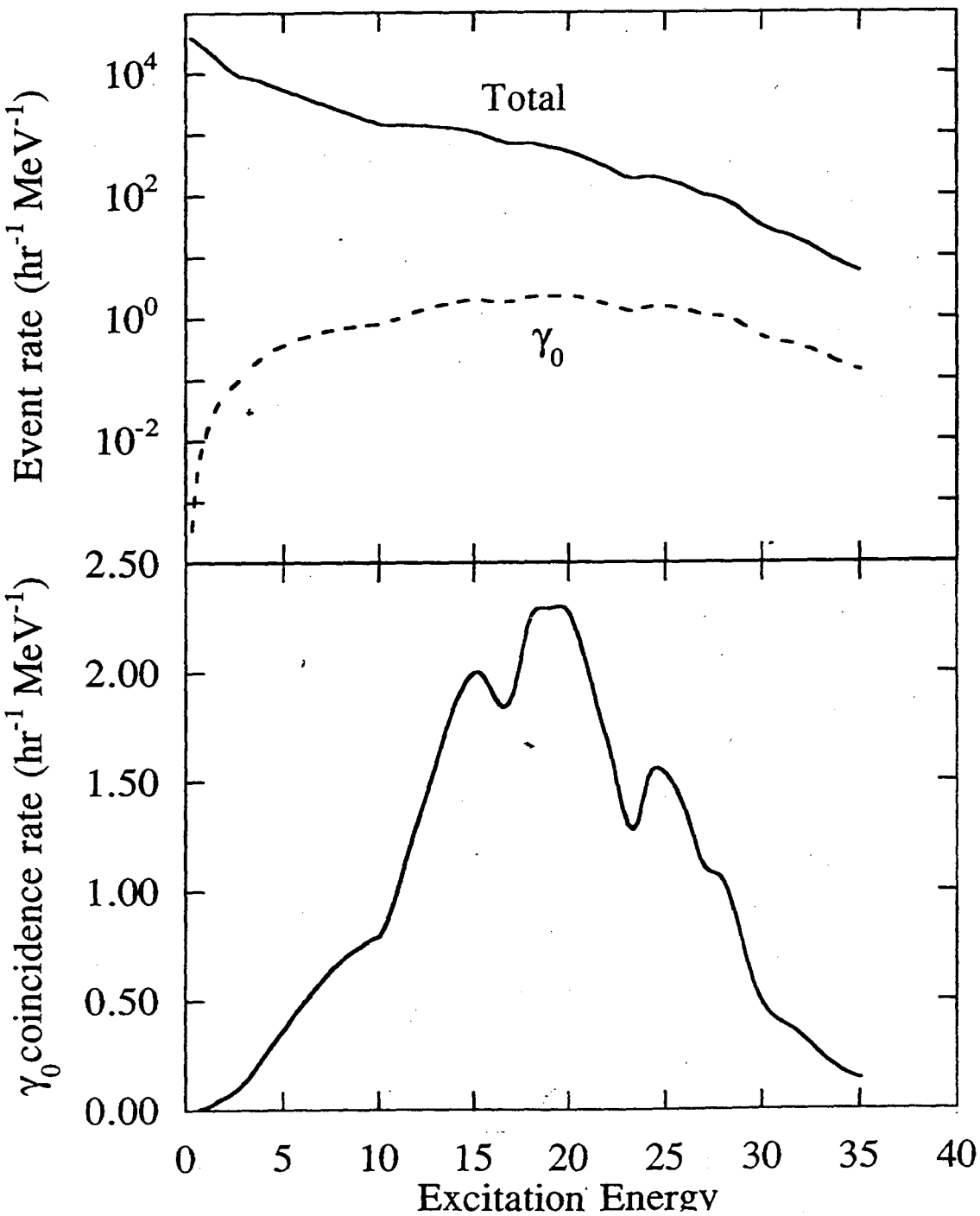

# $\gamma$-ray Angular Distribution

## 150 MeV/nucleon $^{11}Li$

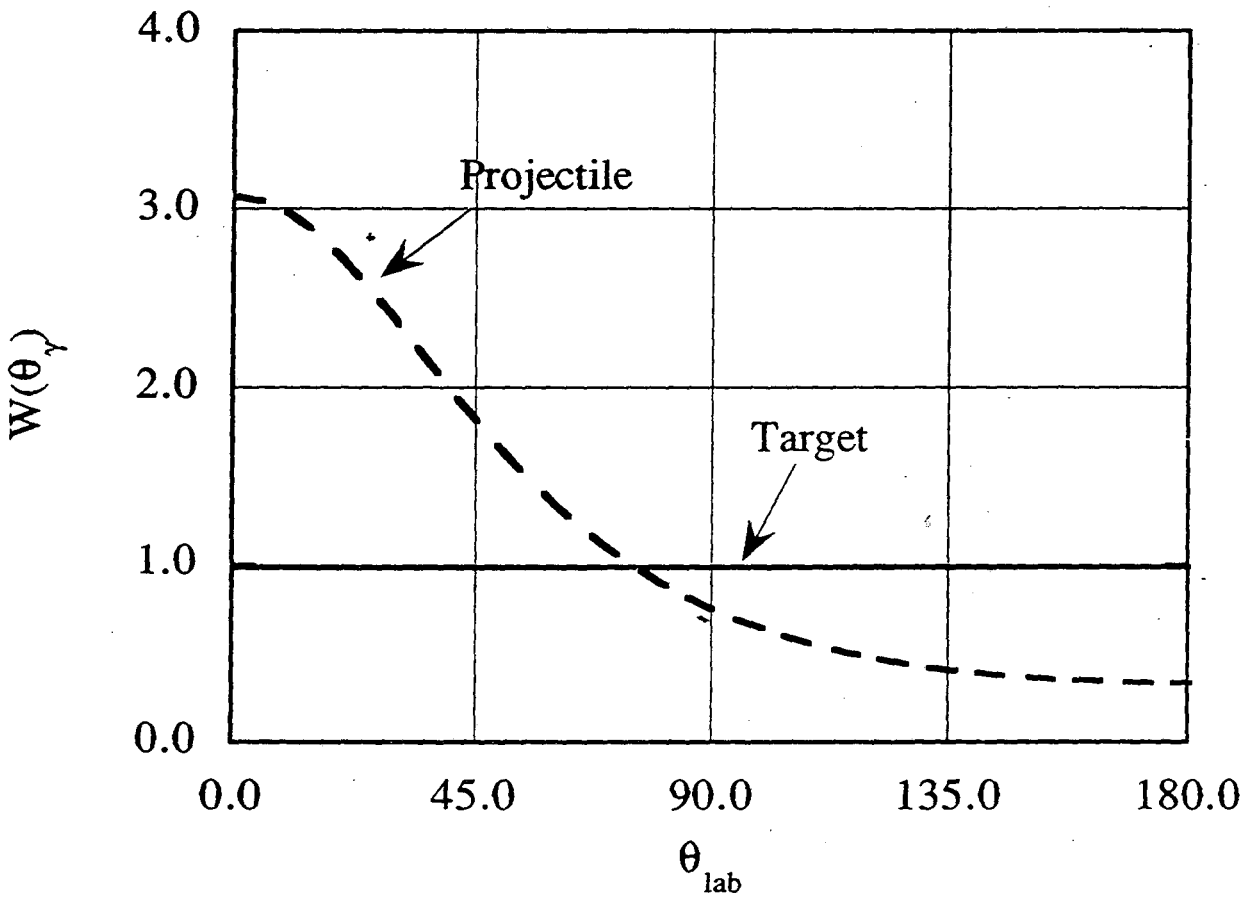

# Experimental Setup

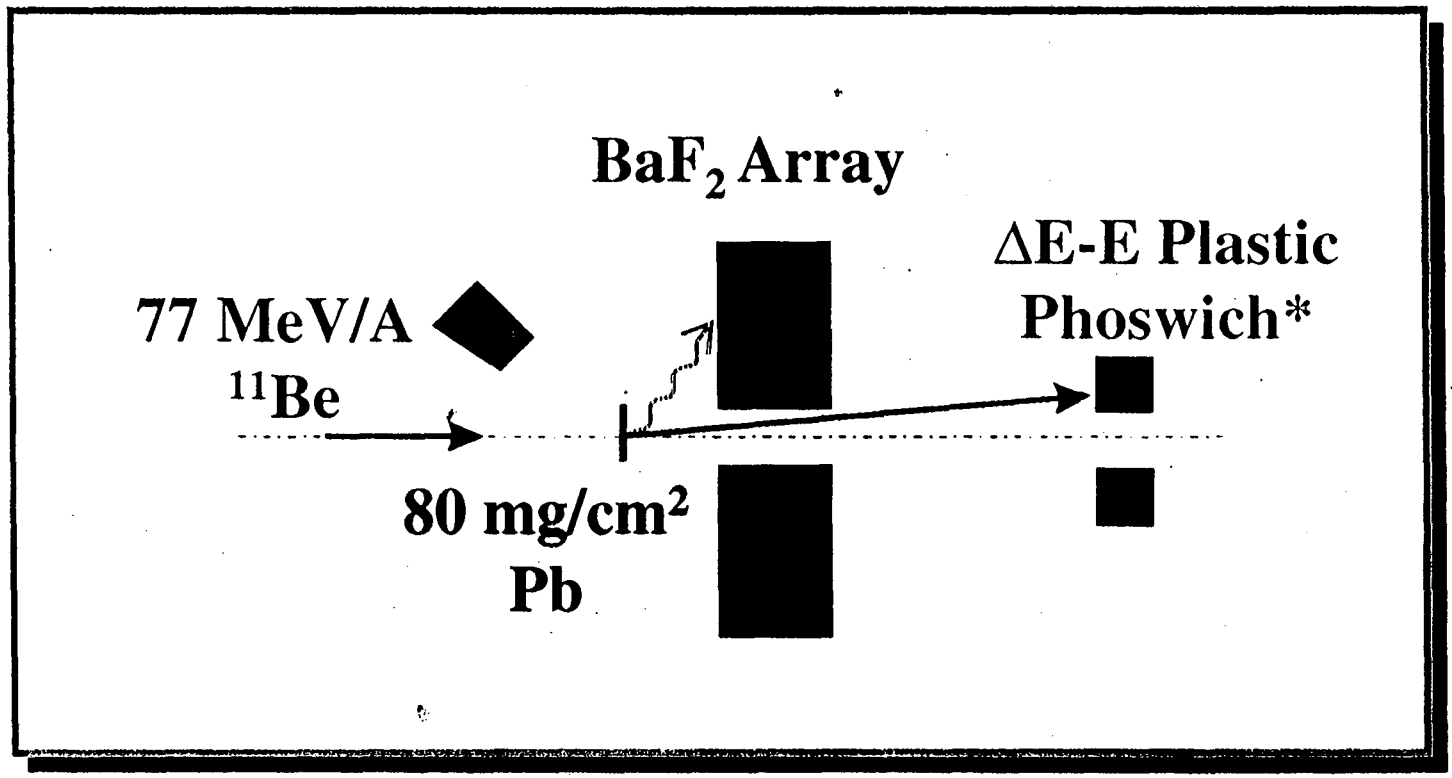


*G. Westfall, N. Stone

# $BaF_2$ Wall for $^{11}Be$ Excitation Experiment

**First use of ORNL-MSU-TAMU joint $BaF_2$ array**
**NSCL, May 1995**

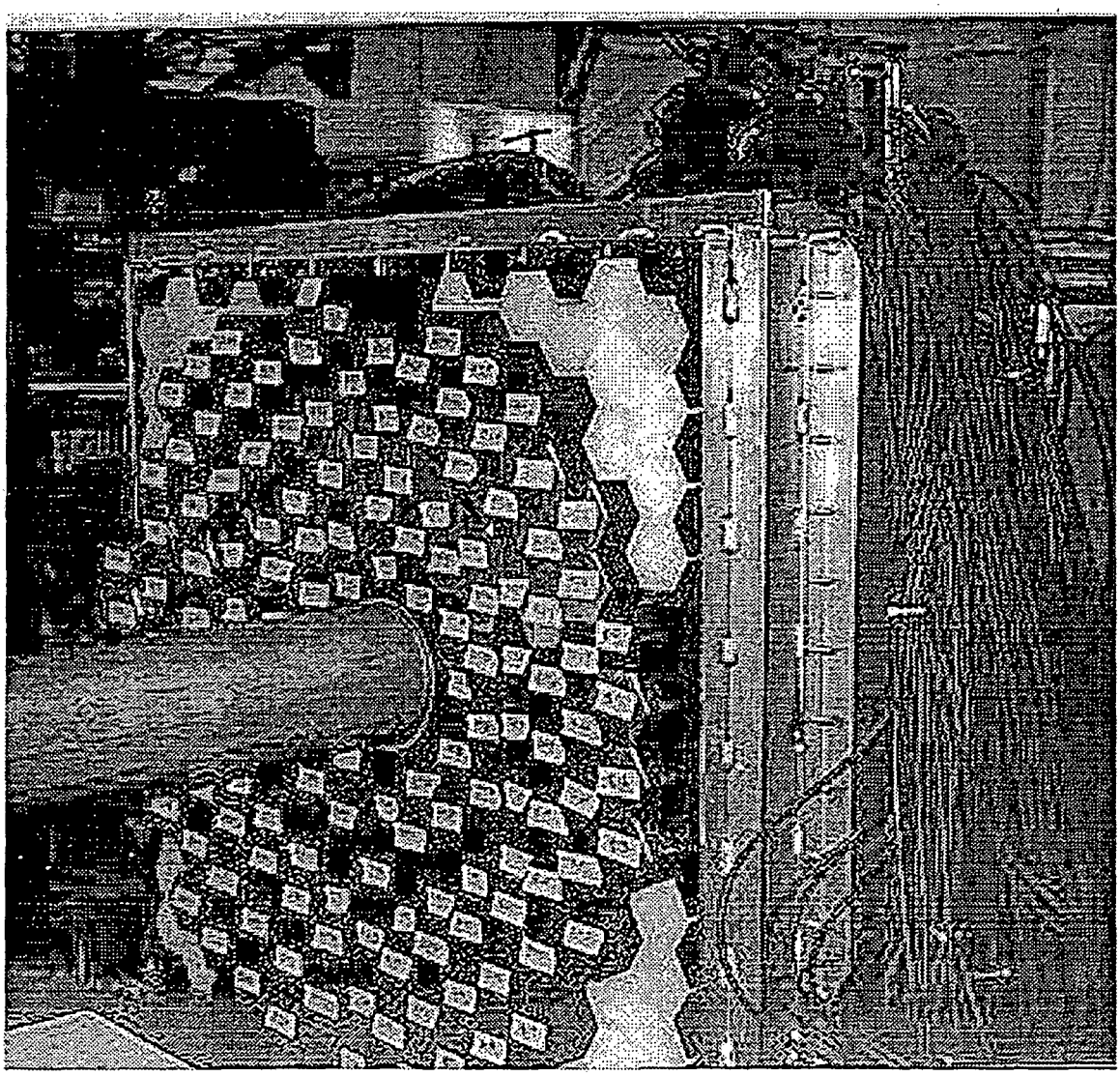

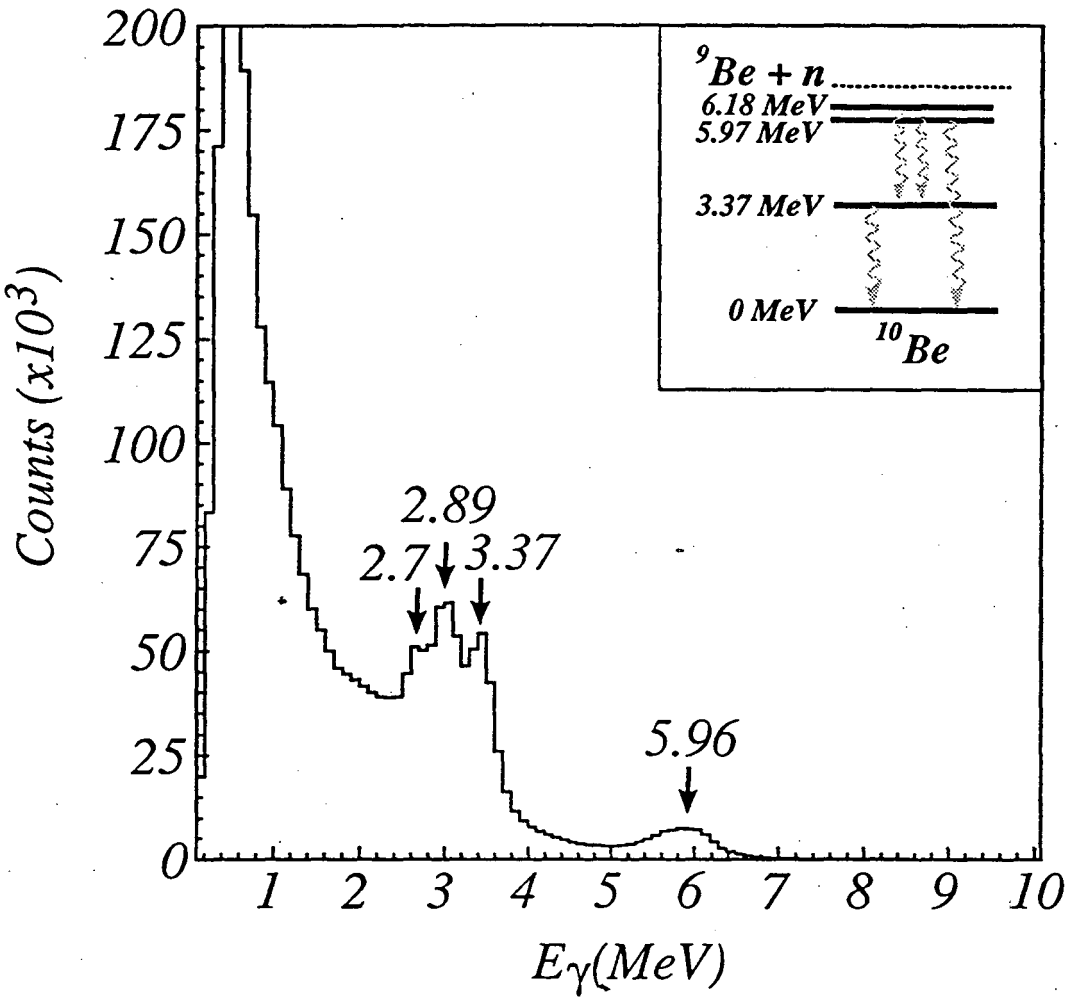
200
175
150
125
100
75
50
25
0
Counts (x10^3)
1
2
3
4
5
6
7
8
9
10
Eγ(MeV)
2.89
2.7
3.37
5.96
9Be + n
6.18 MeV
5.97 MeV
3.37 MeV
0 MeV
10Be

# GDR in $^{11}$Be

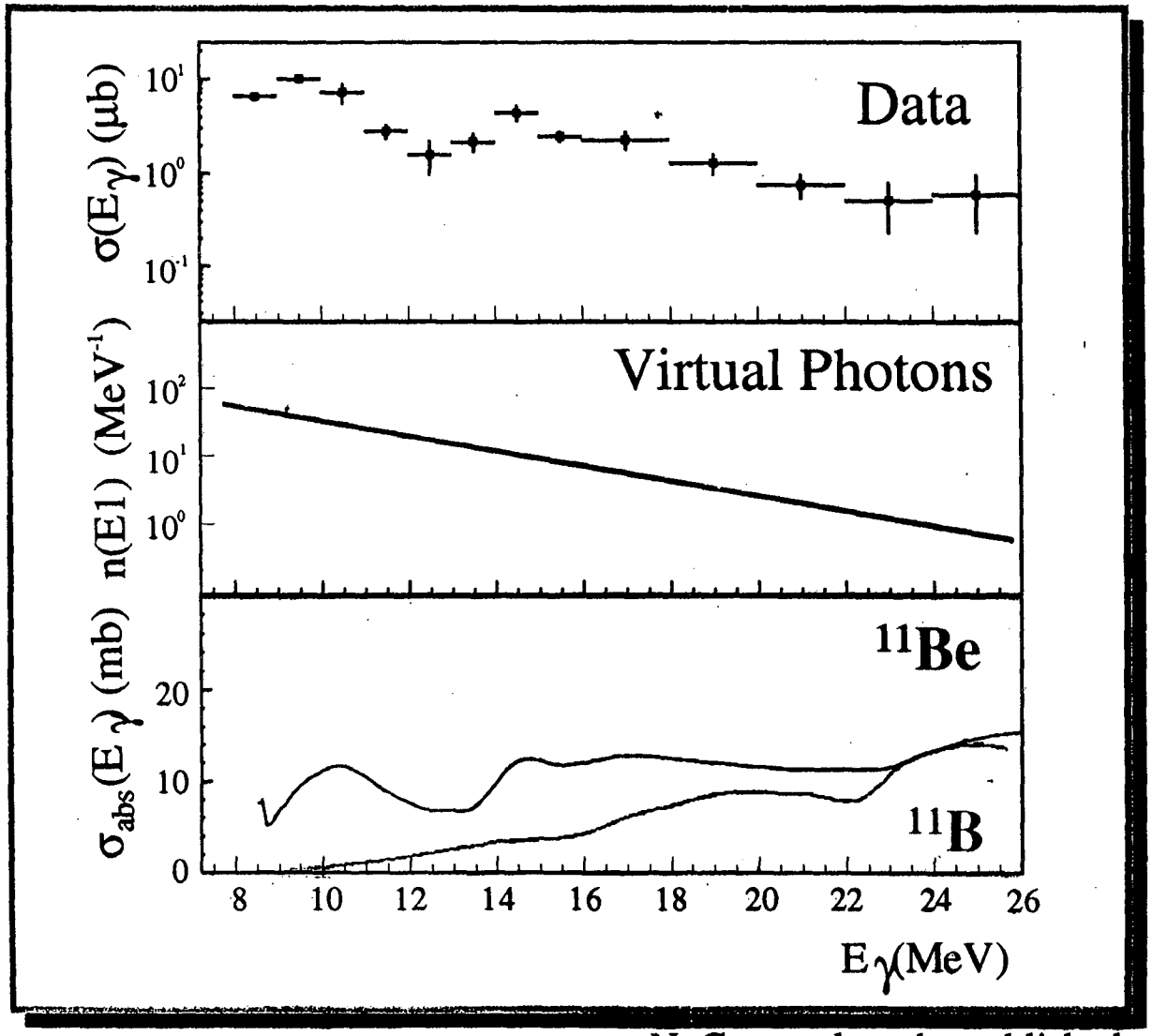


N. Gan et al., to be published

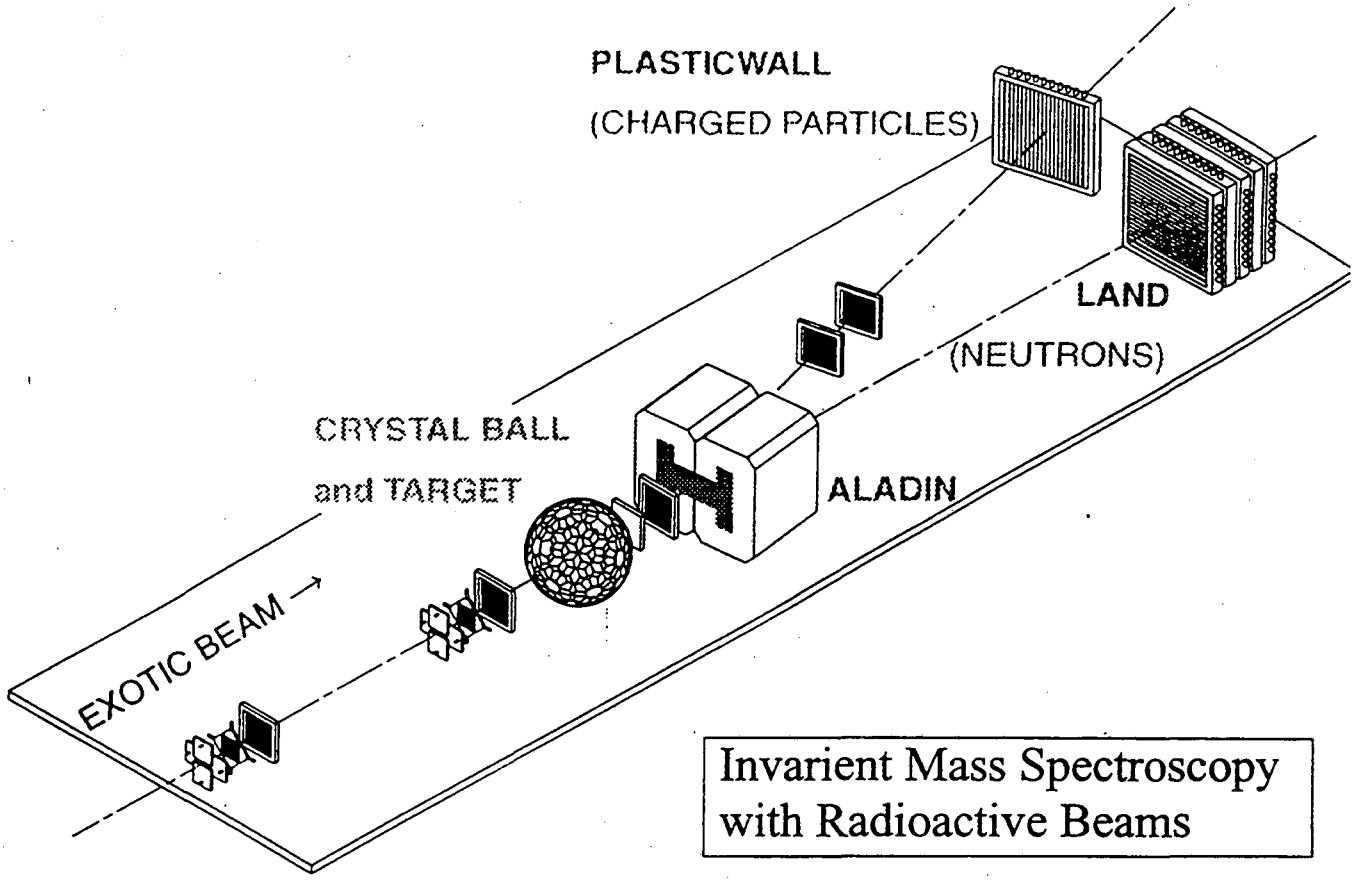


Invarient Mass Spectroscopy with Radioactive Beams

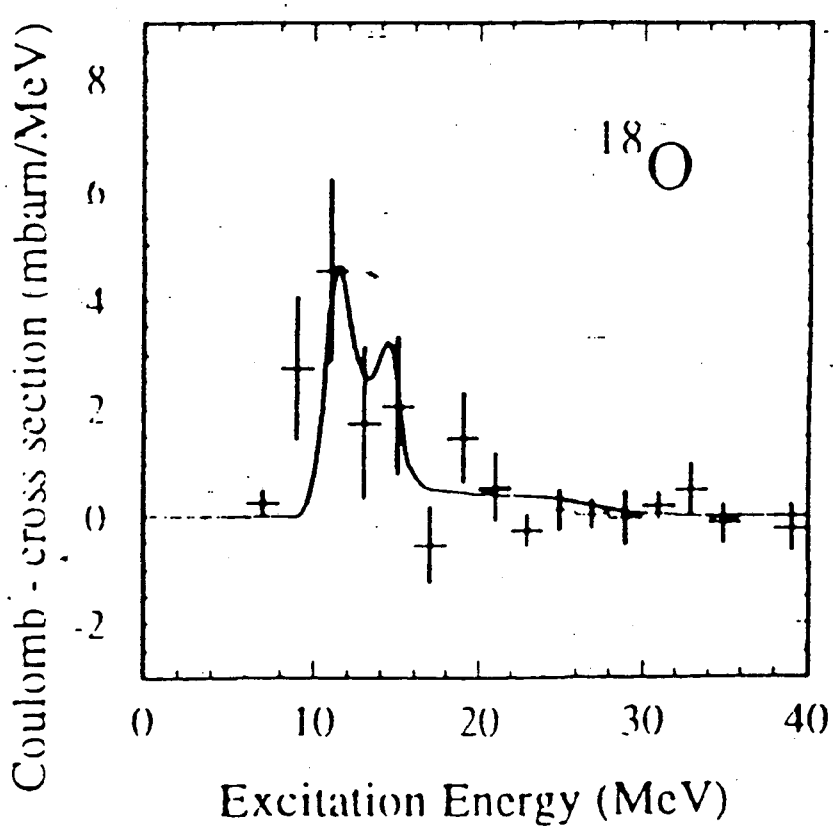


J. Cub et al., Act. Phys. Pol. B28, 367 (1997)

# Schematic Setup

$$^{11}Be + Target \Rightarrow {}^{9}Li + p + n + \gamma$$

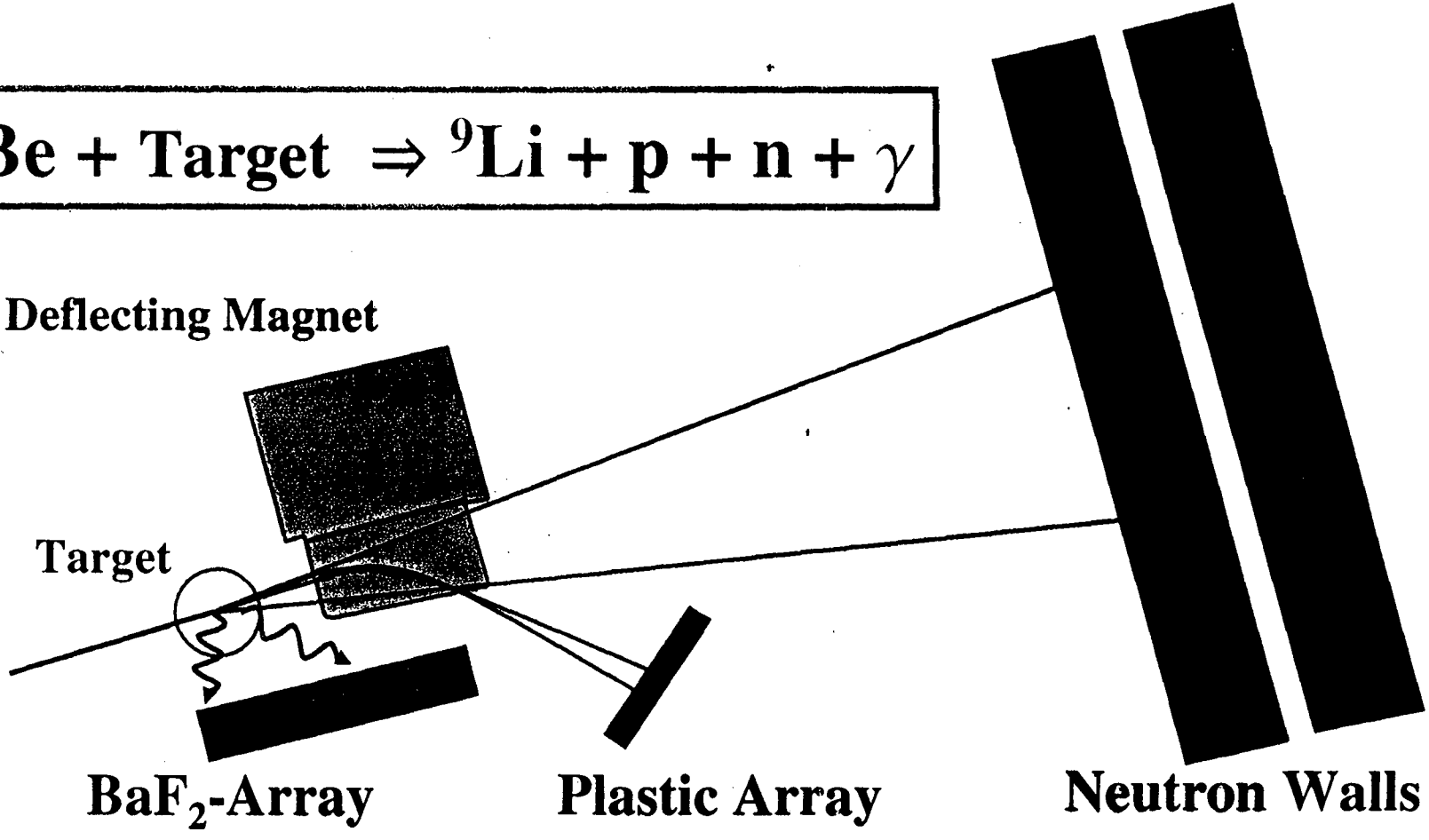

# Gamma Rays from $^{9}$Li

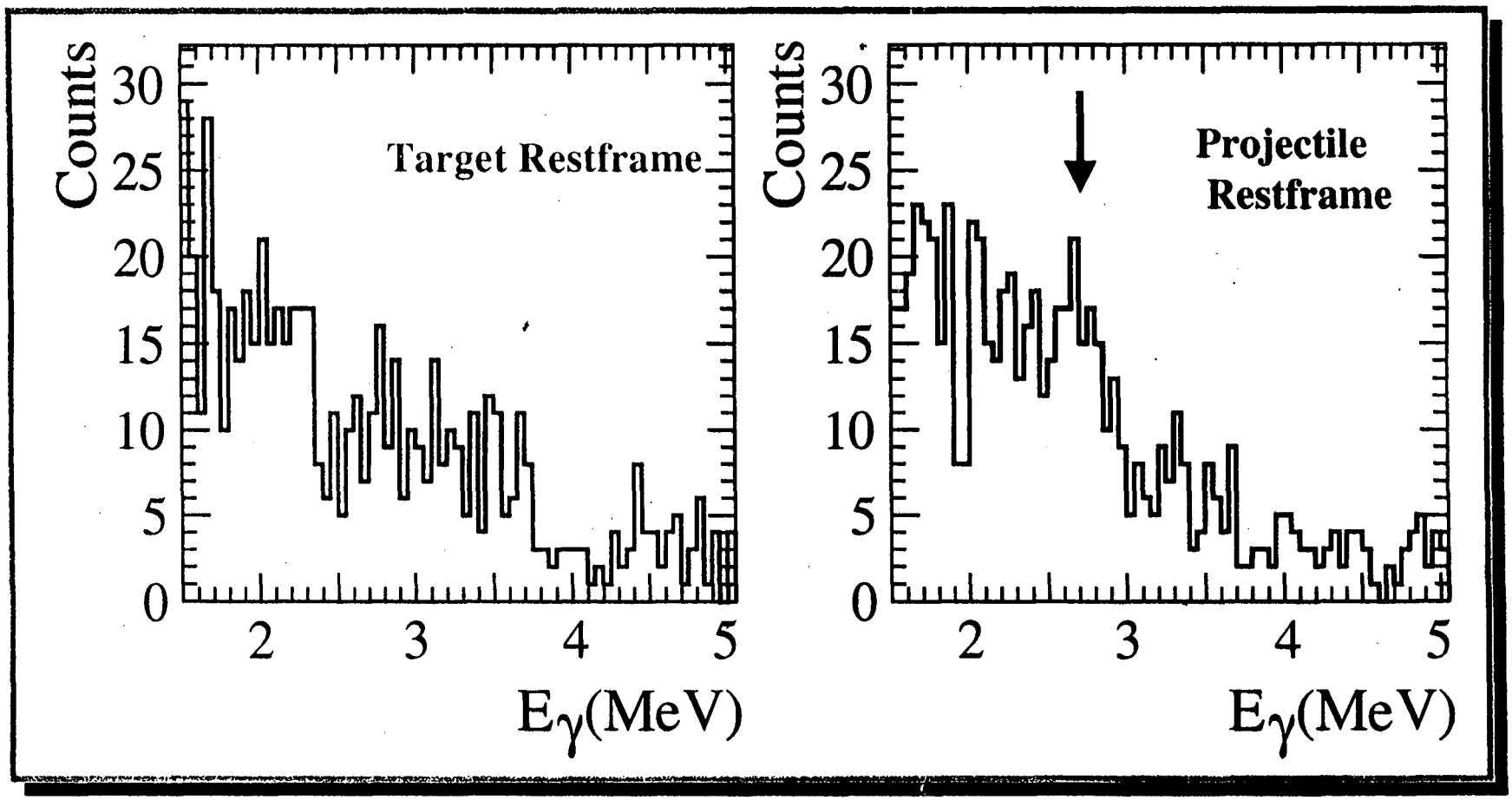

# Support for Low-lying *s*-wave in $^{10}$Li

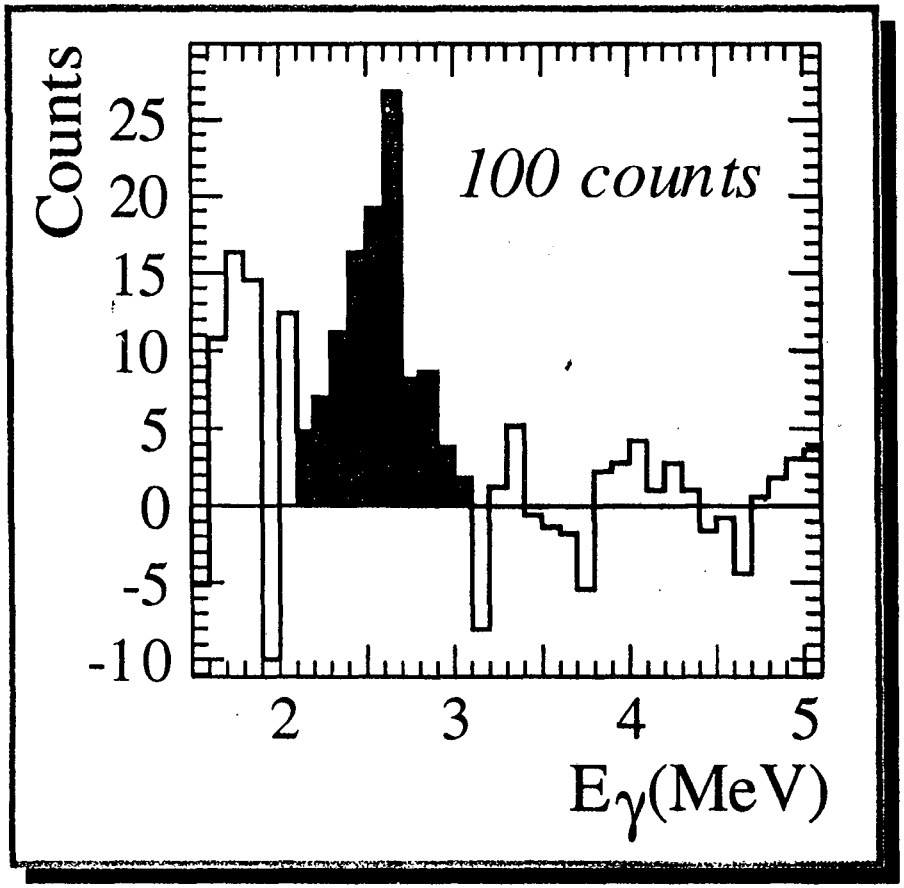


**From efficiency:**

**2.7 MeV state is populated only 5% of all decays.**

**⇒ Low lying s-wave strength must be the ground state of $^{10}$Li**

# GRETA for GDR of Exotic Nuclei

- Virtual Photon Scattering ==> Coincidence with Spectrometer
- Virtual Photon Absorption ==> Coincidence with Spectrometer and Neutron Wall
- Larger efficiency at forward angles
- Beam intensities of $10^6$-$10^7$/s

# Conclusions

- GDR Built on Excited States:
  - Tagging with low energy transitions
  - Stand-alone mode
- GDR and GQR Built on the Ground State:
  - Tagging to enhance specific resonances
  - Coincidence with spectrometer
- GDR in Exotic Nuclei:
  - Doppler correction
  - Coincidence with spectrometer/neutron wall

T.Glasmacher

The spectroscopy of neutron-rich nuclei with a gamma-ray tracking device.

# The spectroscopy of neutron-rich nuclei with a γ-ray tracking device

Thomas Glasmacher

*National Superconducting Cyclotron Laboratory and*
*Department of Physics and Astronomy at*
*Michigan State University, East Lansing, Michigan 48824*

February 6, 1998
Berkely, California

# Current status of the π(sd) shell

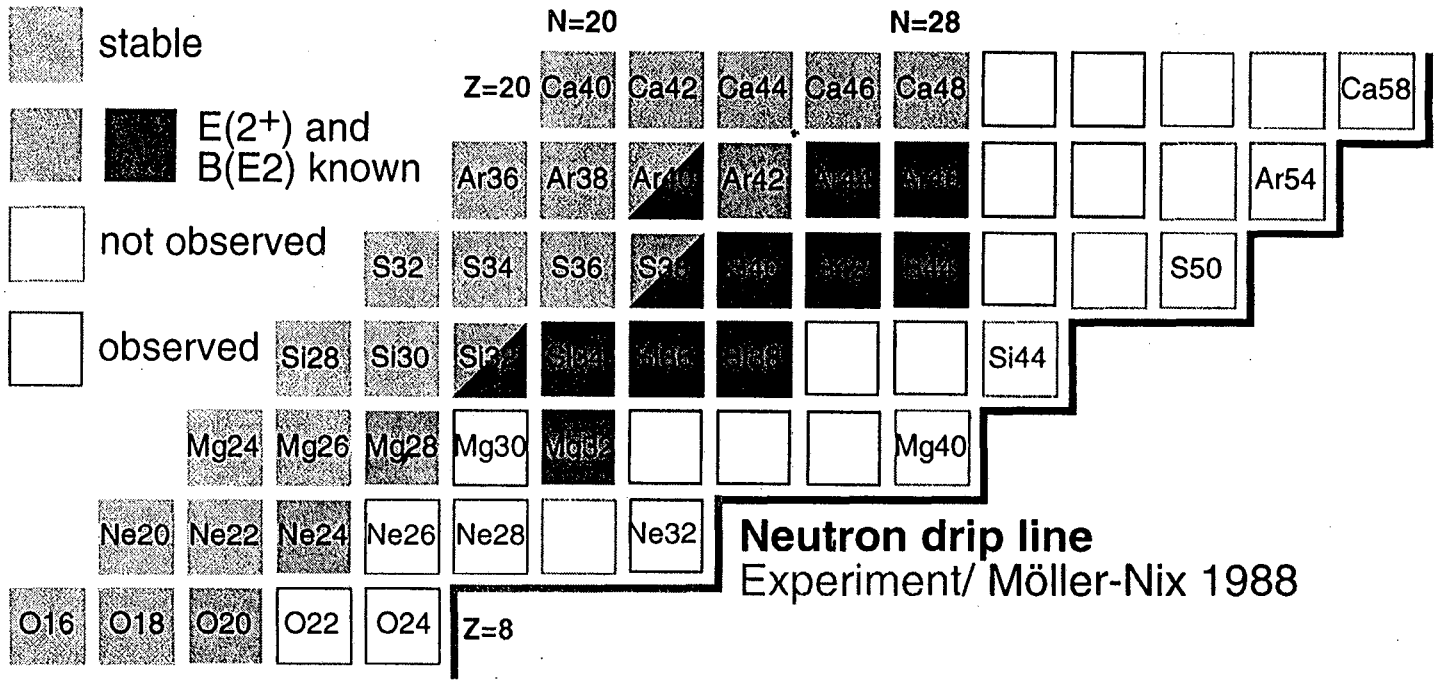


- T. Motobayashi *et al.*, Phys. Lett. **B 346** (1995) 9.
- H. Scheit *et al.* Phys. Rev. Lett. **77** (1996) 3967.
- T. Glasmacher *et al.* Phys. Lett. **B 395** (1997) 163.
- R. Ibbotson *et al.* Phys. Rev. Lett. (1998) in press

# Energy spectra in target and projectile frames for $^{40}S+^{197}Au$

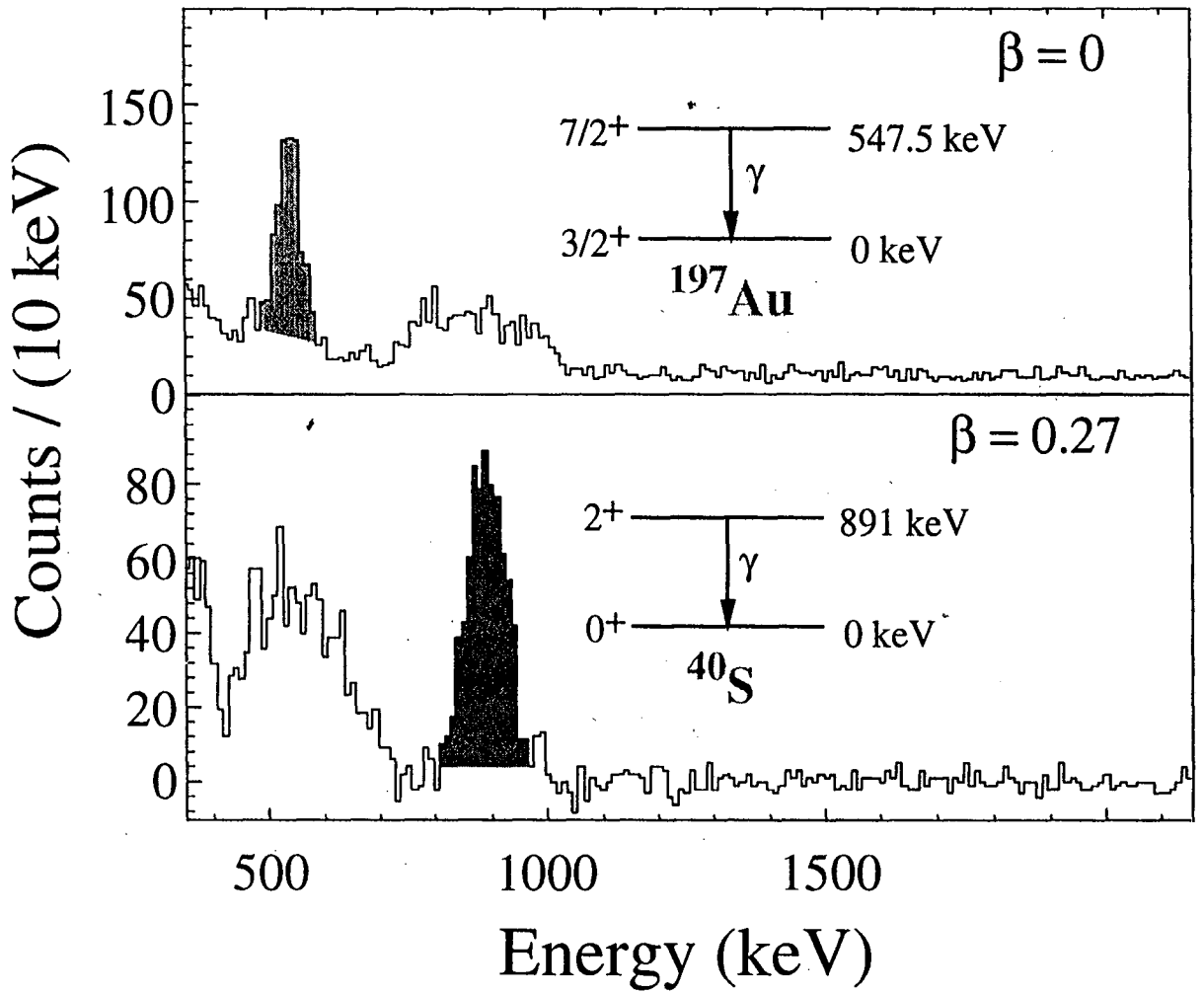

# Experimental signatures of *known* shell closure: the calcium isotopes (Z=20)

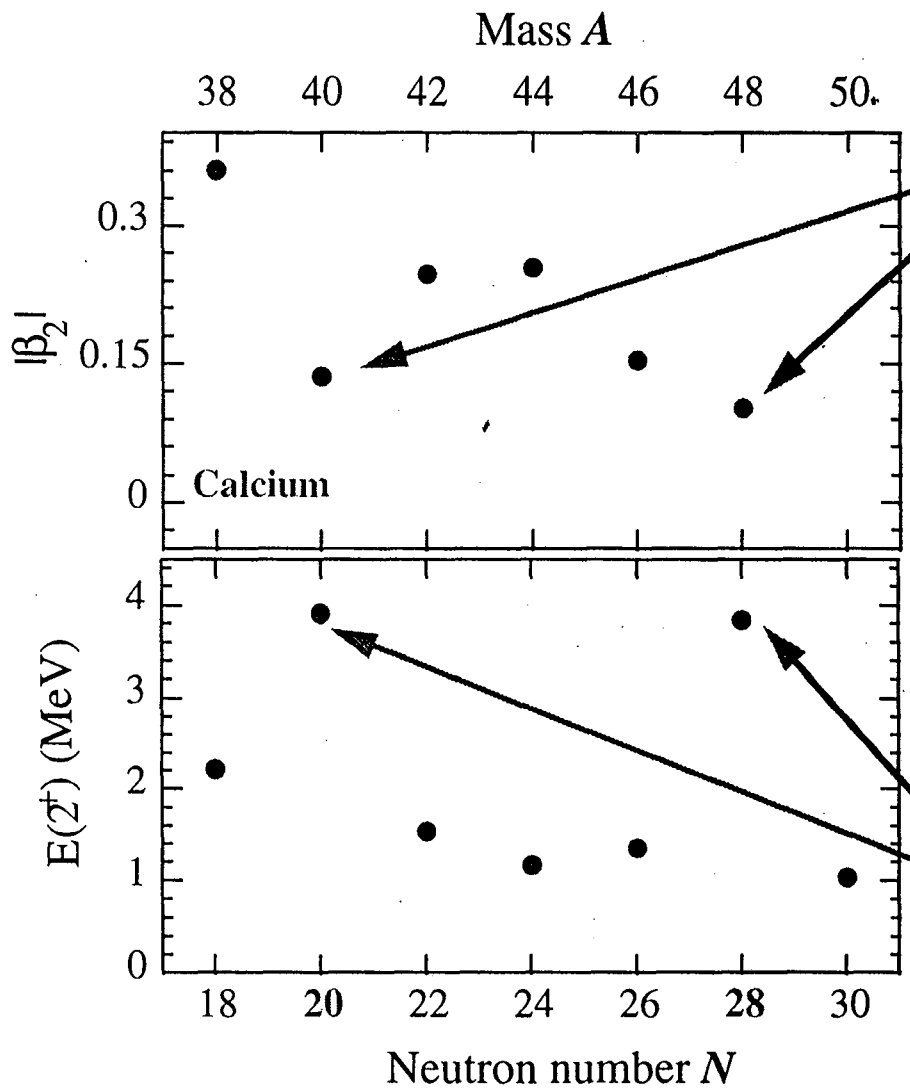


- small degree of collectivity $\beta_2$

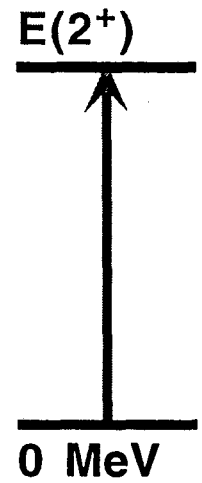


$\beta_2 \propto B(E2)^{1/2}$

$B(E2;0^+\rightarrow 2^+) = \langle \Psi_{2^+} \| E2 \| \Psi_{0^+} \rangle$

- high excitation energy $E(2^+)$

# Deformation parameters $\beta_2$ and excitation energies $E(2^+)$: $^{30}S - ^{44}S$

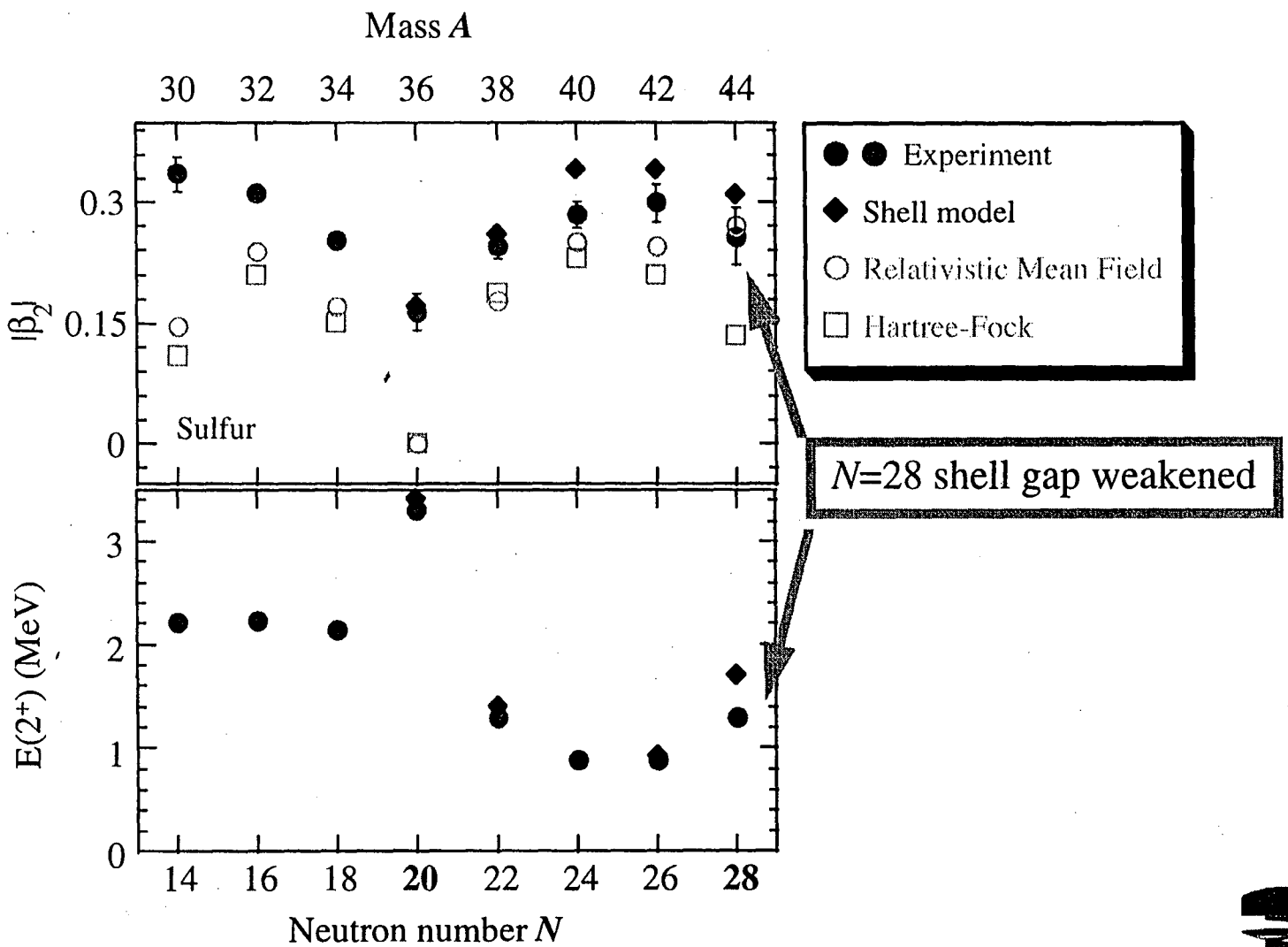

# Coulomb excitation - semiclassically

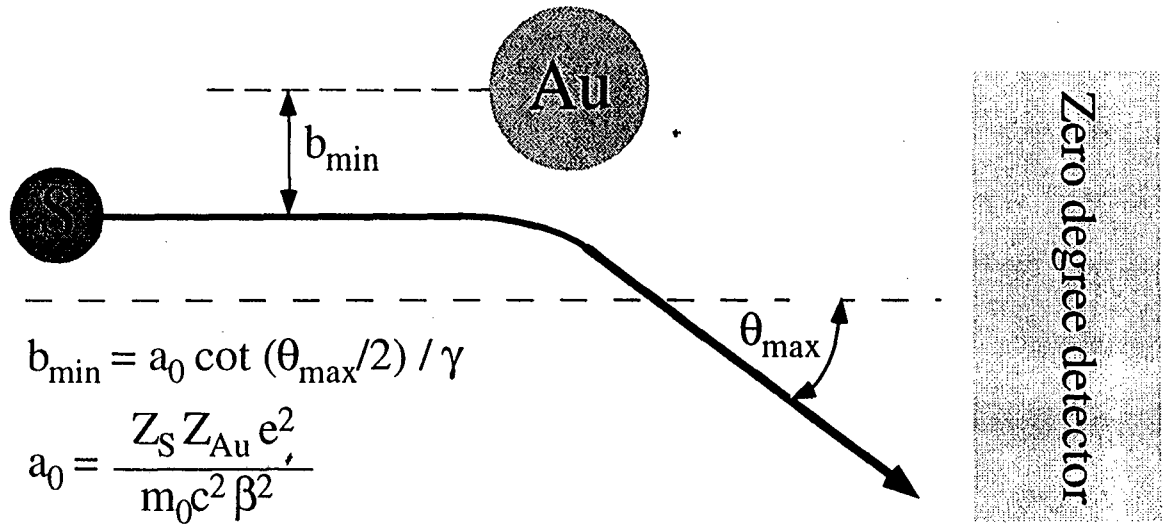


$$b_{min} = a_0 \cot(\theta_{max}/2) / \gamma$$

$$a_0 = \frac{Z_S Z_{Au} e^2}{m_0 c^2 \beta^2}$$

- $E_{beam} \approx 40$ MeV/nucl.
- $\beta \approx 0.3$, $g \approx 1.05$
- $b_{min} \approx 20$ fm
- "touching spheres" $1.2(A_S^{1/3}+A_{Au}^{1/3}) = 11$ fm


- K. Alder *et al.*, Rev. Mod. Phys. **28**, 432 (1956).
- A. Winther and K. Alder, Nucl. Phys. **A 319**, 518 (1979).
- C.A. Bertulani and G. Baur, Phys. Rep. **163**, 300 (1988).
- T. Glasmacher, Ann. Rev. Nucl. Part. Sci. (1998), in print.

# Intermediate energy Coulomb excitation to study structure of exotic nuclei

- Excite neutron-rich secondary beam particle in heavy target (e.g. gold) and detect de-excitation photon
- Measure the energy of first excited state $E(2^+)$ and extract $B(E2, g.s. \rightarrow 2^+)$ for exotic nuclei
- Method works at peak of exotic beam production cross-section for projectile fragmentation (50-100 MeV/nucl.)
- Schematic setup:

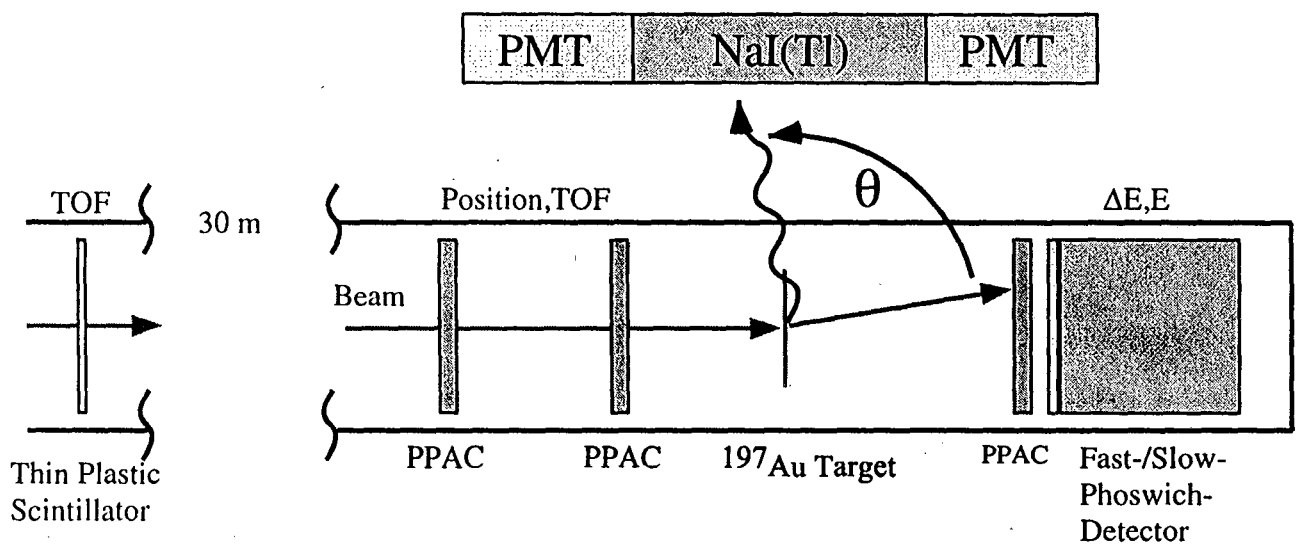

# The A1200 fragment separator at the NSCL at Michigan State University

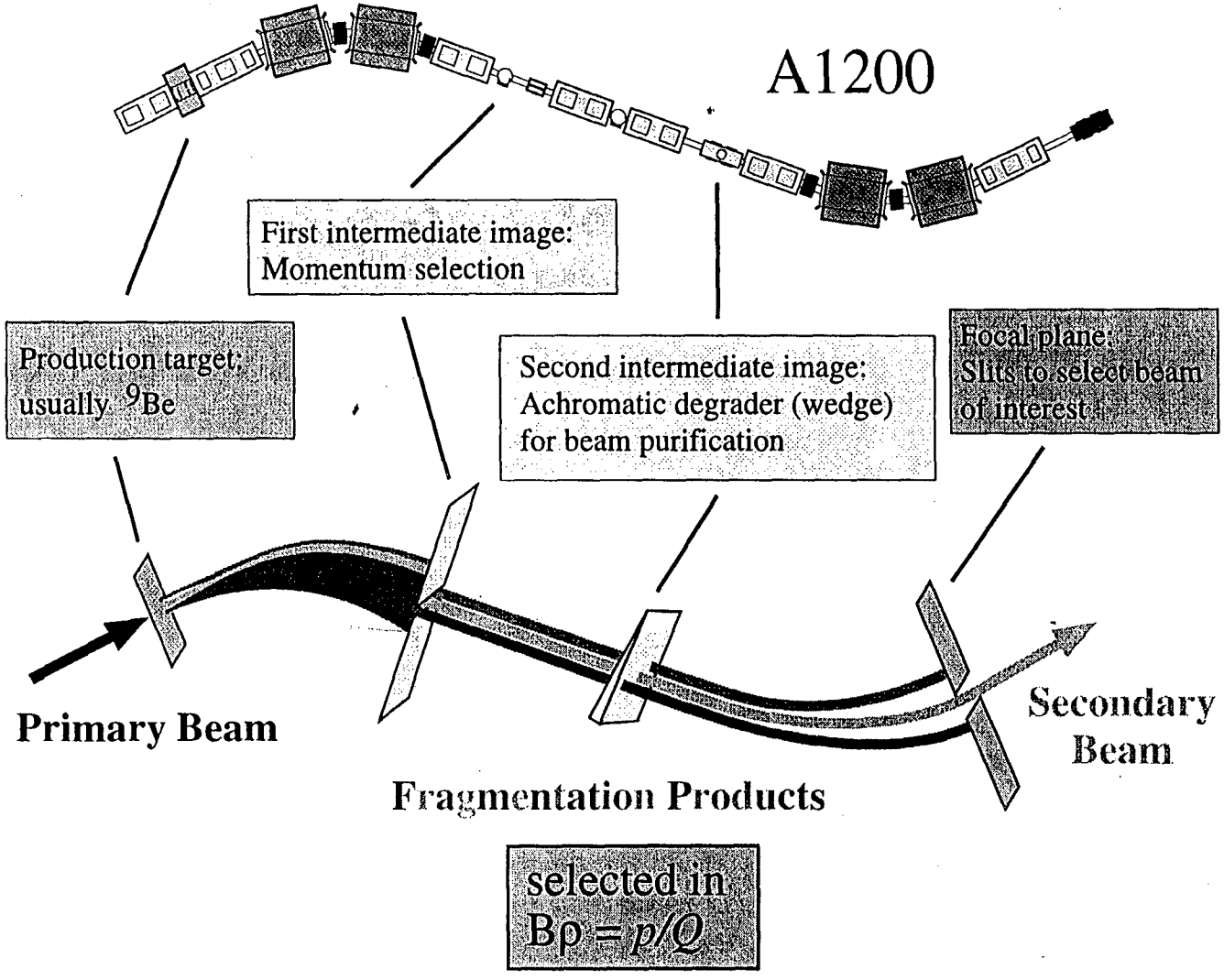

# Schematic view of the NaI(Tl) detector setup with shielding

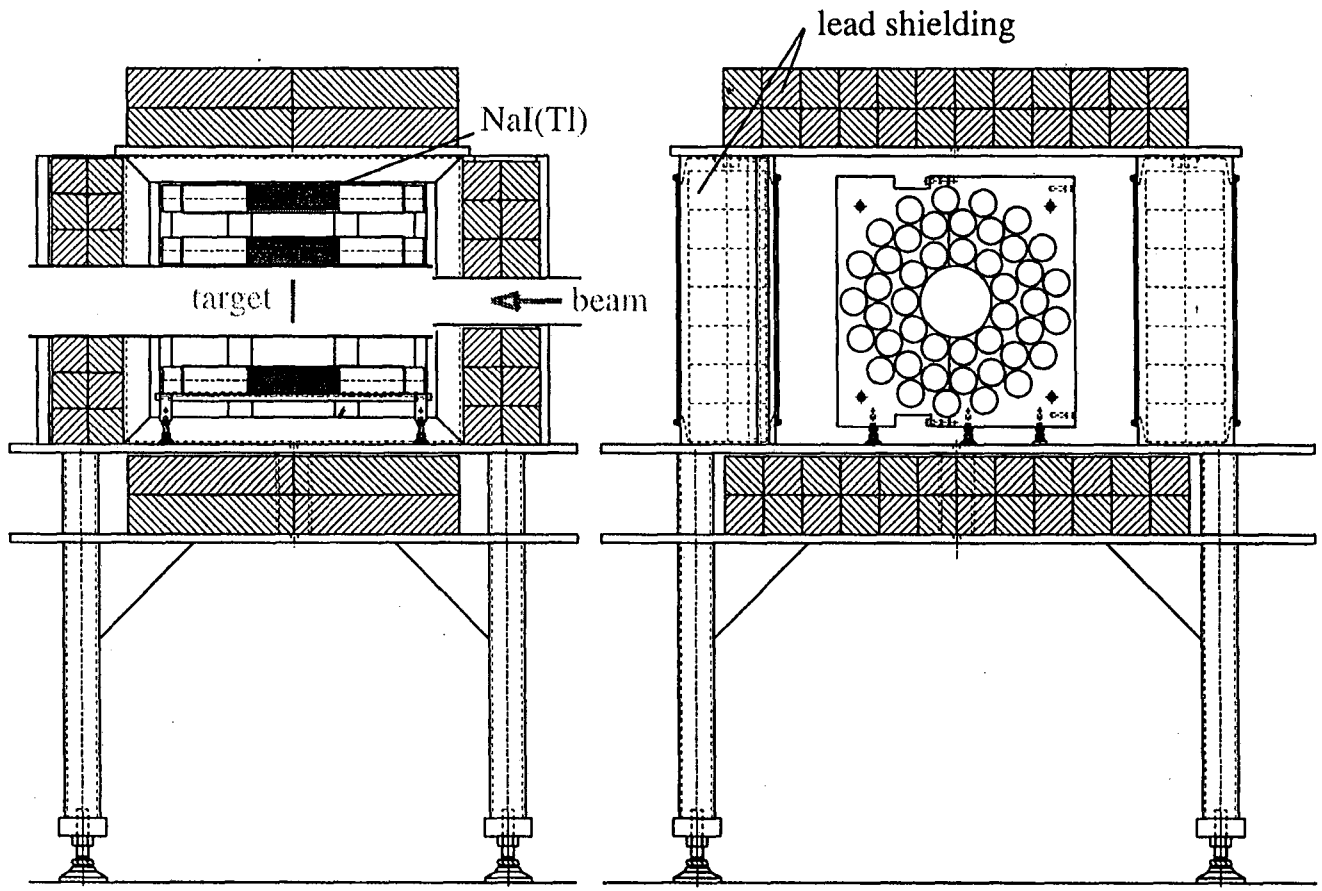

# Photon detection in reactions with intermediate-energy exotic beams

General properties of experiments with fast ($\beta \approx 0.3$-$0.5$) exotic beams:

- Low photon multiplicity
- Detect branching ratios of 10-100%
- Beam intensity not adjustable (maximum available)
- Beam energy constrained by production mechanism

Experimenter can choose:

- Target thickness
- Location of detector

**Optimize count rate versus energy resolution**

# Doppler shift at intermediate energies

$$E_\gamma = E_\gamma^{proj} \frac{\sqrt{1-\beta^2}}{1-\beta\cos\theta}$$

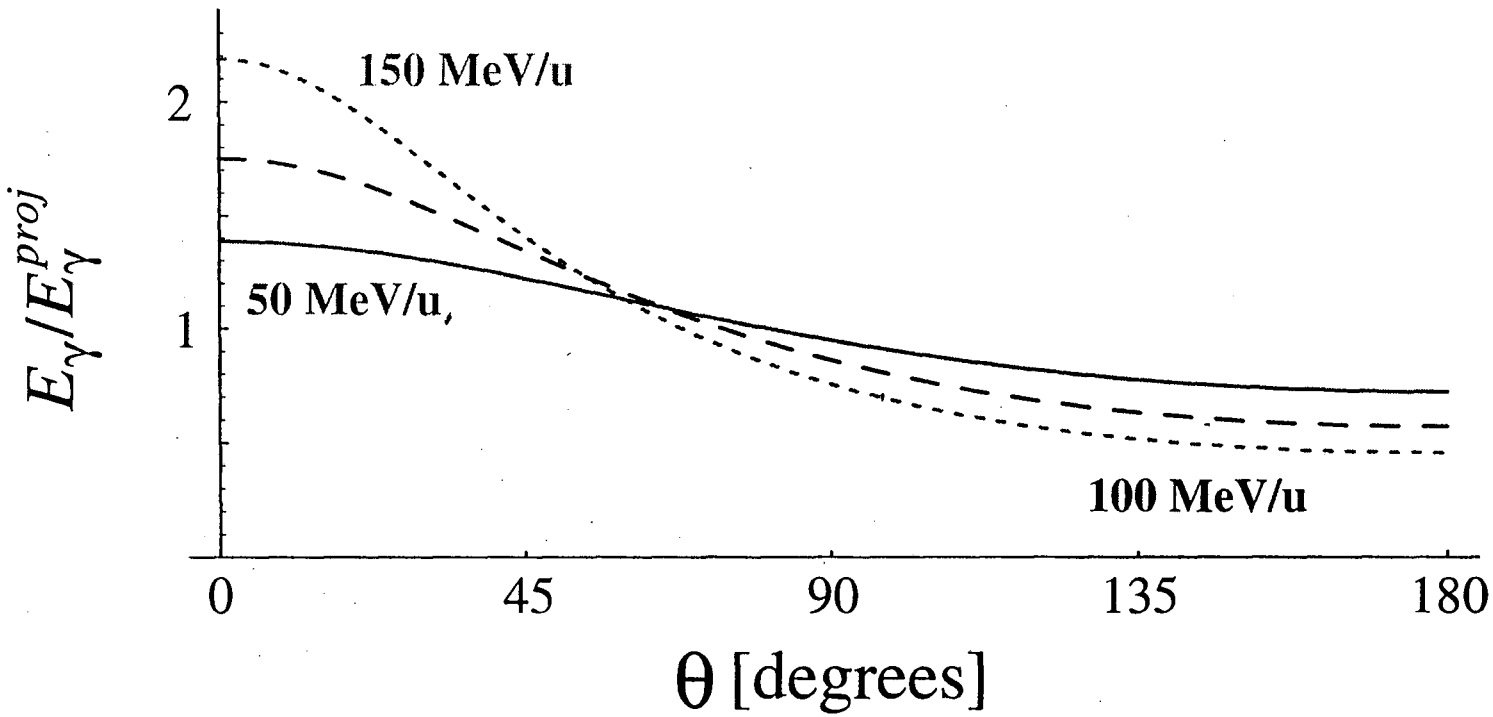


- Dynamic range of electronics needs to be 2.5 larger than highest expected γ-ray energy

# Contributions to final energy resolution

Four major contributions to final energy resolution of photon spectrum emitted from a fast ($\beta \approx 0.4$) source:

a) Intrinsic energy resolution of detector
→ detector material

b) Doppler broadening due to finite opening angle of detector
→ detector granularity and distance from target

c) Doppler broadening due to slowing down of projectile in target
→ target thickness (and element)

d) Doppler broadening due to angular spread of projectile caused by scattering in target
→ target thickness (and element)

# Doppler broadening due to finite opening angle of detector

$$E_\gamma = E_\gamma^{proj} \frac{\sqrt{1-\beta^2}}{1-\beta^* \cos\theta}$$

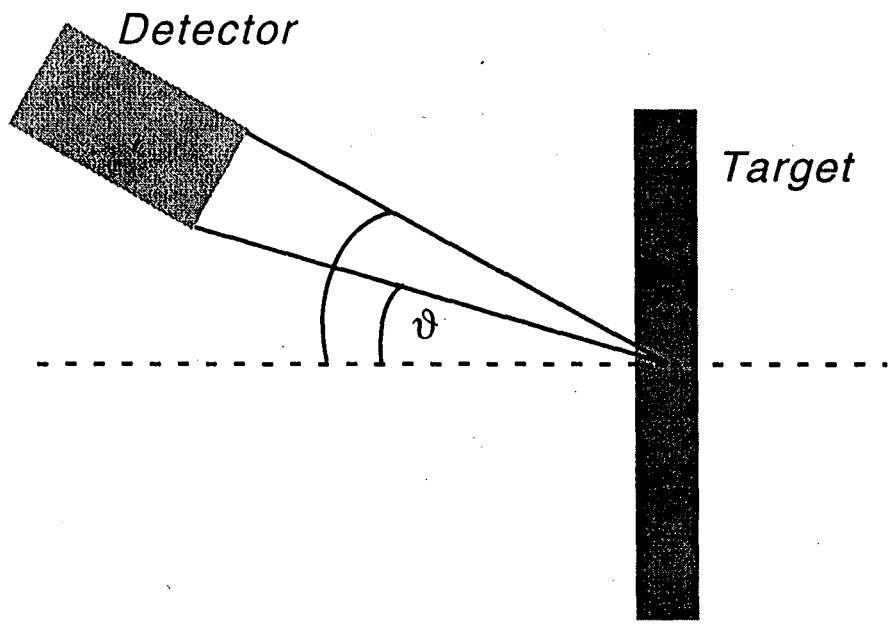

# Doppler broadening due to slowing down of projectile in target

$$E_\gamma = E_\gamma^{proj} \frac{\sqrt{1-\beta^2}}{1-\beta^* \cos\theta}$$

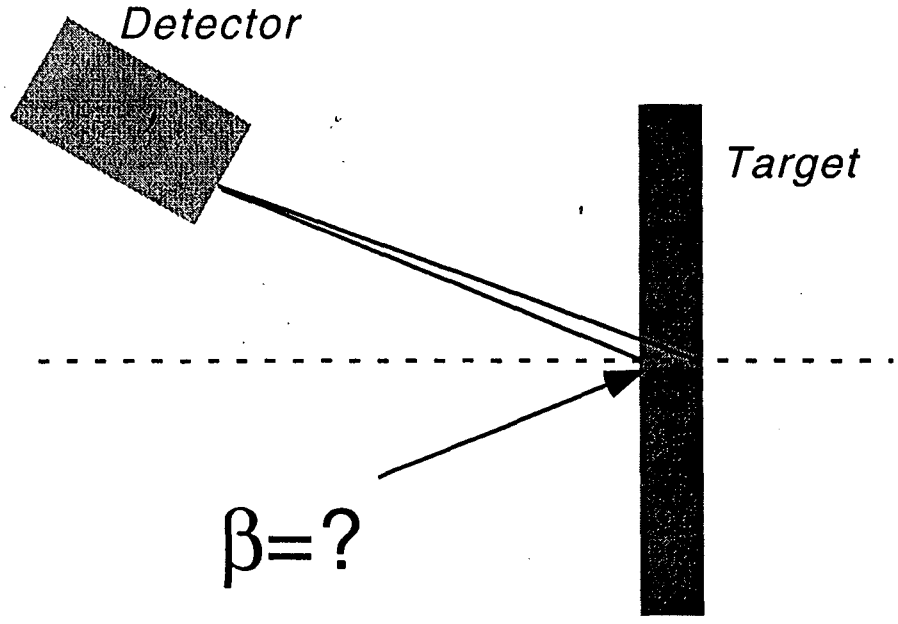

# Energy resolution considerations

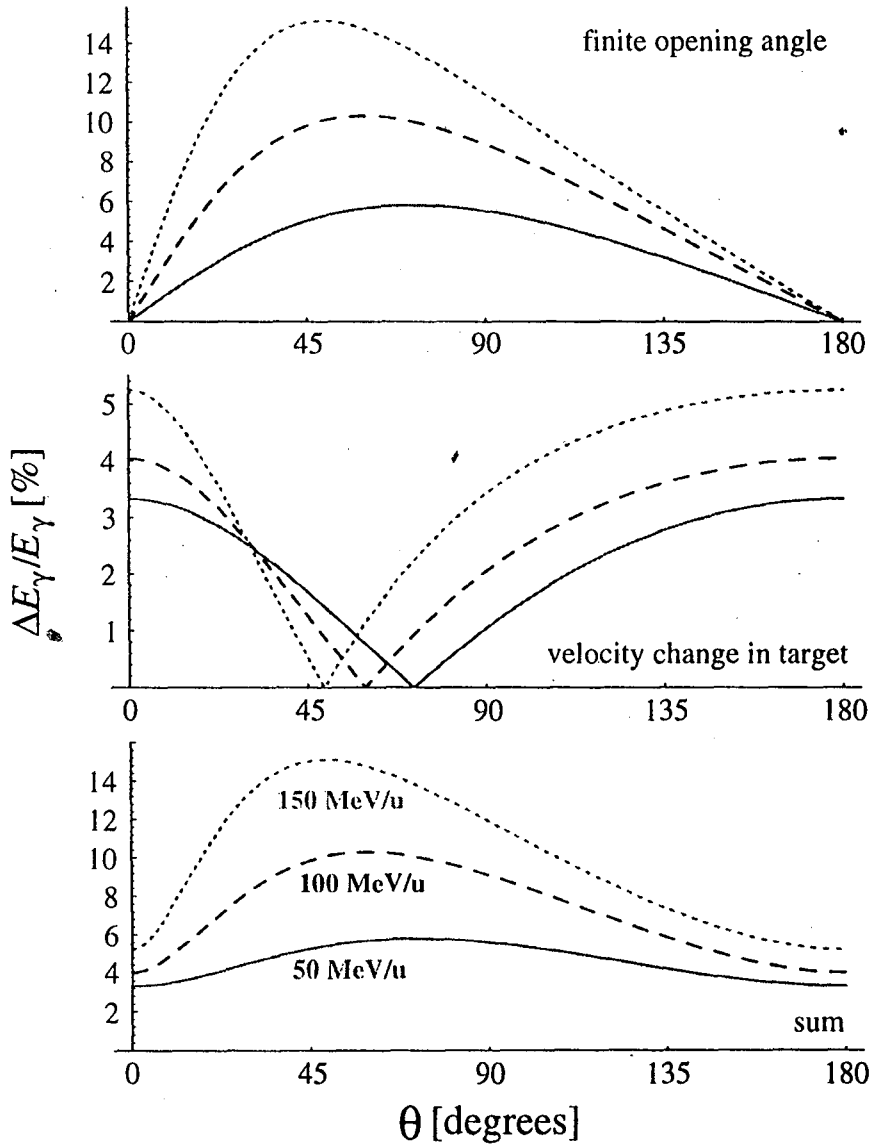


- Resolution in energy scales inversely with
  - uncertainty in scaterring angle $\Delta\theta$
  - uncertainty in beam velocity $\Delta\beta$
  - intrinsic detector resolution

- Uncertainty in position of first interaction point with respect to scattered beam will be primary constraint on final energy resolution

# Excitation cross sections versus beam energy for $2^+$, GDR, GQR

$^{40}S+^{197}Au$, $r_{min} = 16$ fm

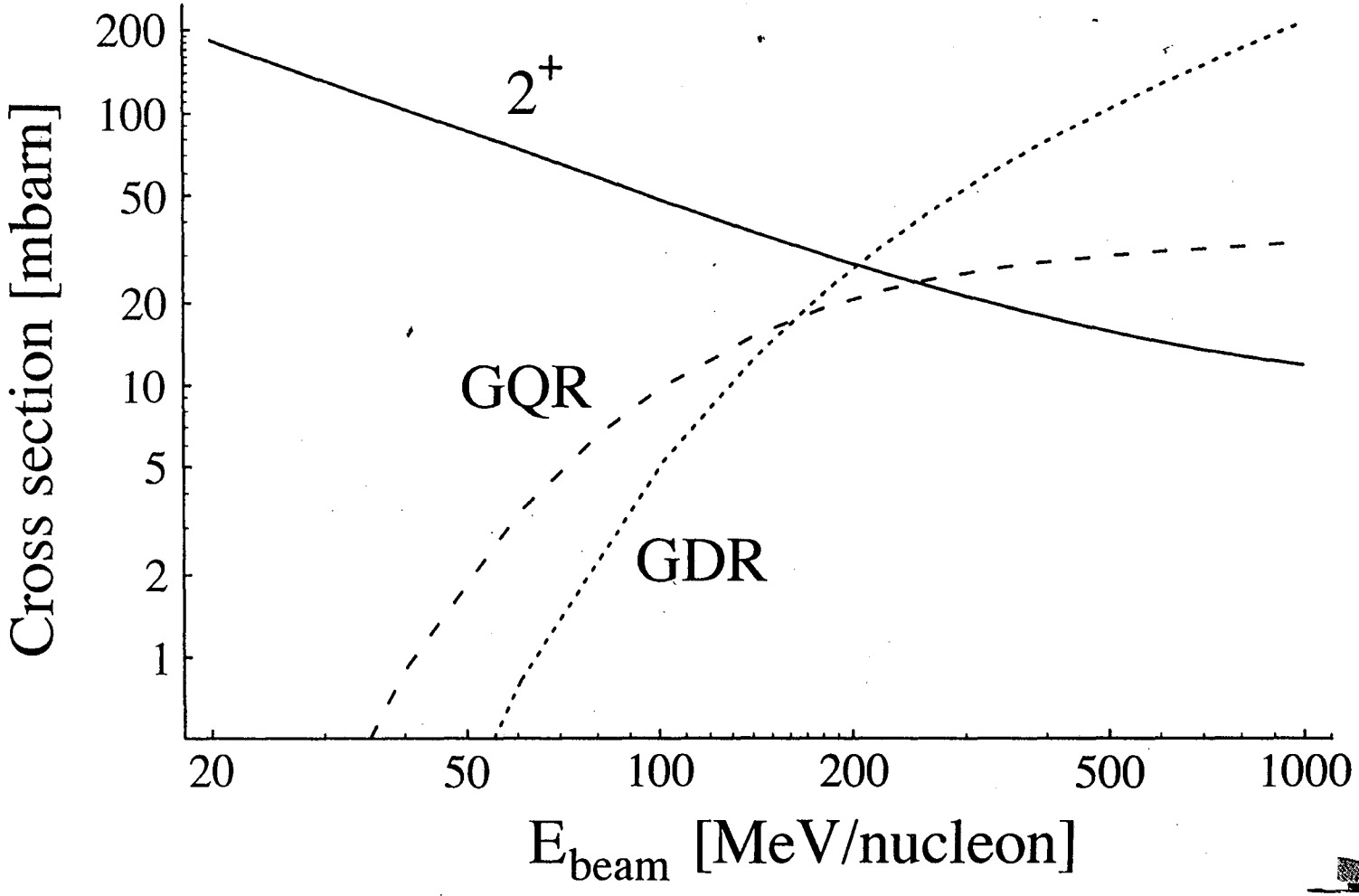

# Neutron-rich nuclei: slow and rapid neutron capture (*s*-process and *r*-process)

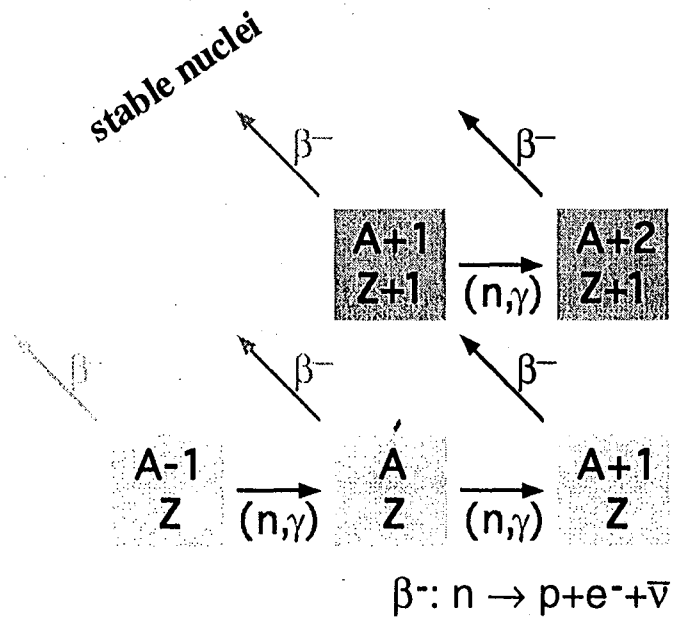


- Nuclear reaction network calculations
- assume (n,γ) ↔ (γ,n) equilibrium: $N_{r,prog}(Z)/T_{1/2}$ = const.
- shell closures act as bottle neck (low neutron separation energy and long half life)
- Nuclear physics input: masses, $T_{1/2}$, $P_n$

- slow neutron capture (*s*-process)
  - low neutron density ($n_n \approx 10^8$ cm$^{-3}$)
  - $\tau_\beta < \tau_{n,\gamma}$
- rapid neutron capture (*r*-process)
  - high neutron density ($n_n \approx 10^{20}$ cm$^{-3}$)
  - $\tau_\beta >> \tau_{n,\gamma}$
  - forms about half of the A≥70 galactic elements up to $^{209}$Bi
  - responsible for Th-U-Pu isotopes

# Energy resolution with fast beams for different target thicknesses

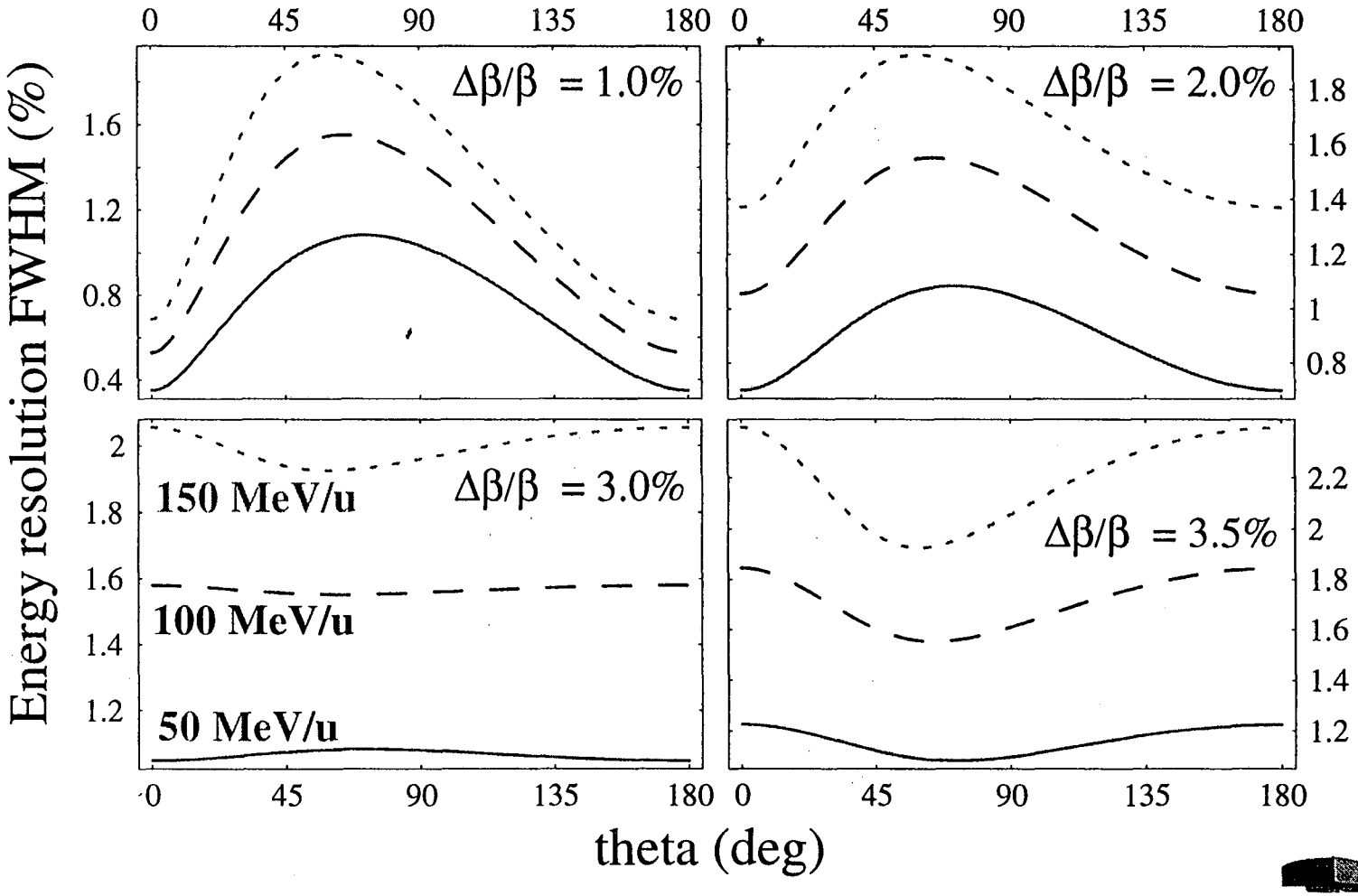

# Count rate estimate

## $^{40}S+^{197}Au$, $r_{min}$ = 16 fm

| E [MeV/u] | β | γ | d [mg/cm²] | σ [mbarn] | $N_{reaction}/N_{beam}$ | γ/(hr*beam part) |
|---|---|---|---|---|---|---|
| 50 | 0.315 | 1.05 | 80 | 90 | 0.0043 | 7.8 |
| 100 | 0.429 | 1.11 | 250 | 50 | 0.0075 | 13.5 |
| 150 | 0.508 | 1.16 | 500 | 32 | 0.0100 | 18.0 |

- Nreaction = Nbeam
- Need 100 counts in photopeak
- $\varepsilon_{photo} \approx 50\%$
- Can do intermediate-energy Coulex experiments with less than 1 particle/second and an energy resolution of 2%

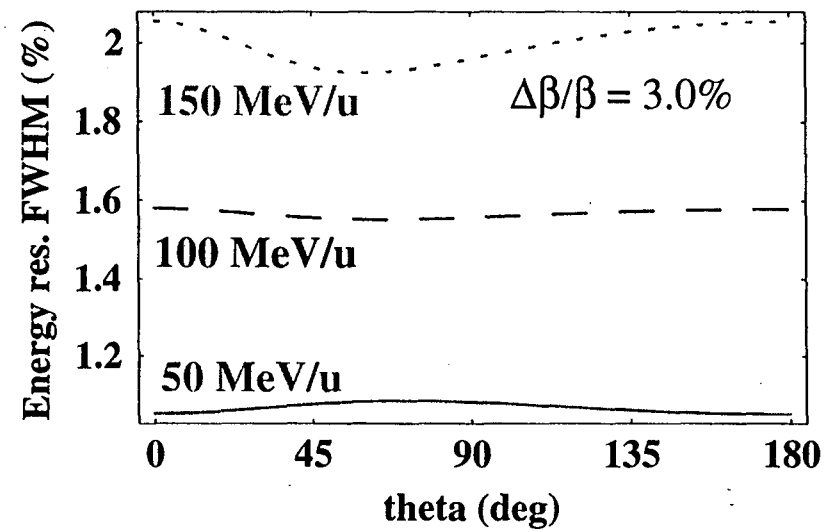

# Nuclei far from the valley of β-stability

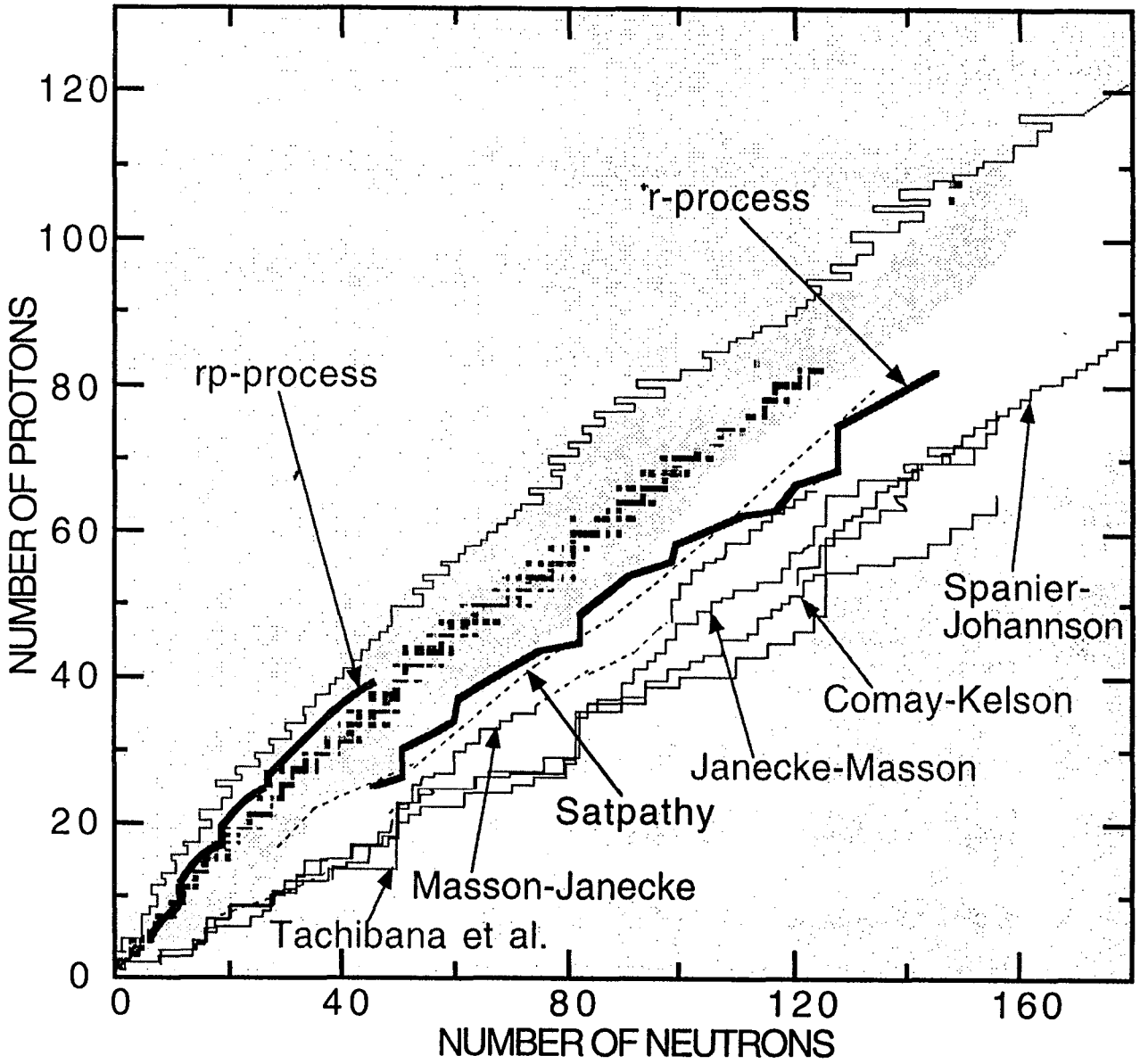

# Observed solar abundances and *r*-process network calculations

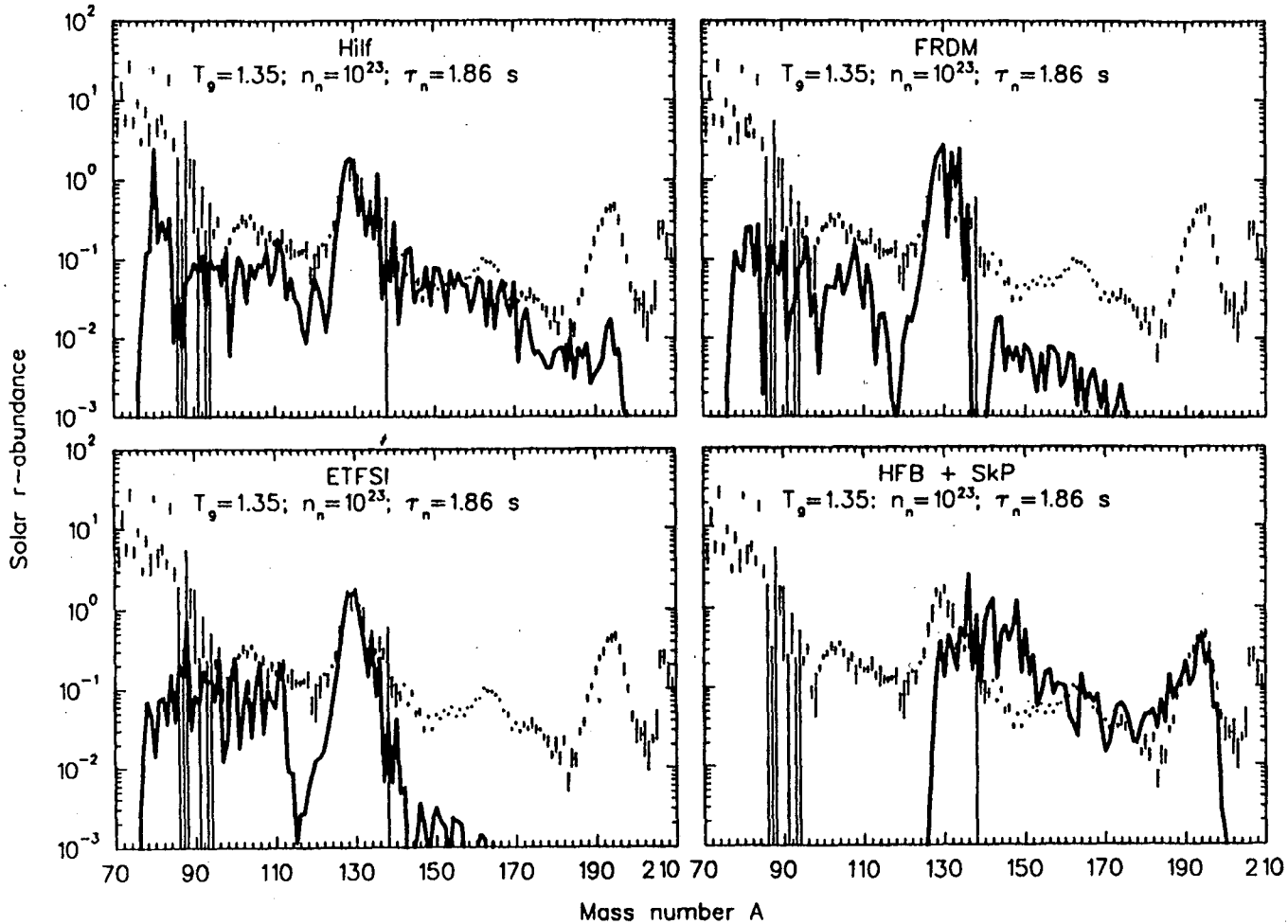


K.-L. Kratz, B. Pfeiffer, and F.-K. Thielemann, Nucl. Phys. A (1998), in print

# Width $\Gamma_\gamma$ of the 6.79 MeV $3/2^+$ state in $^{15}O$ and the $S_{1,14}$ factor in $^{14}N(p,\gamma)^{15}O$

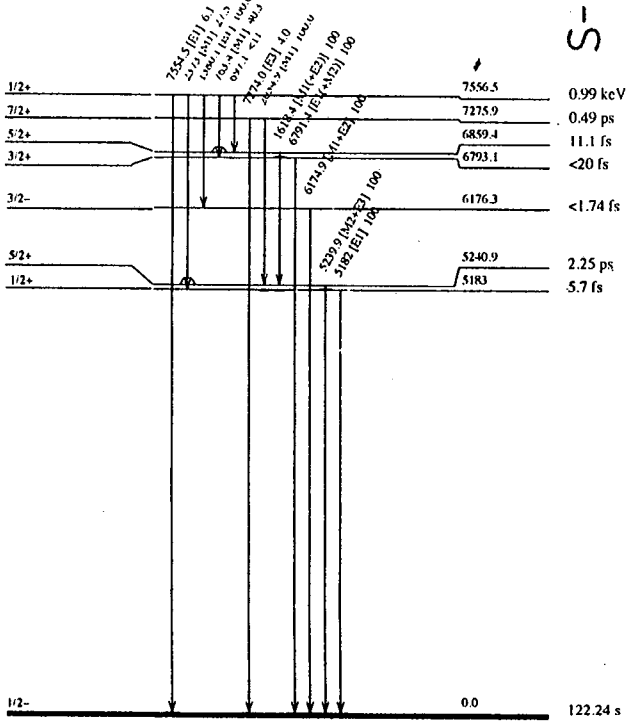


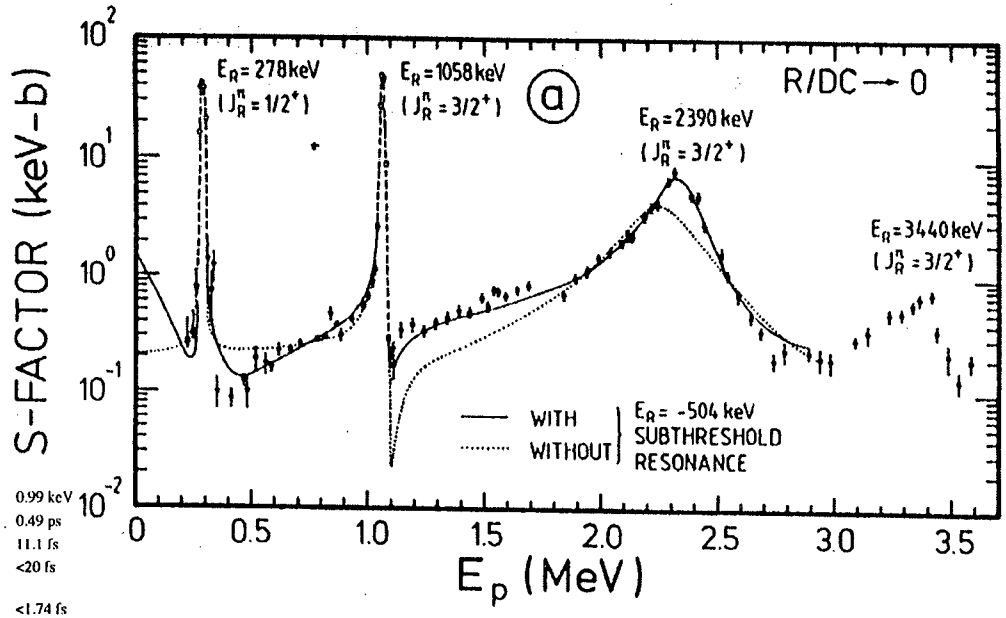


U. Schröder *et al.* NPA **467** (1987) 240

# Summary

- Physics topics:
  - Evolution of nuclear shells (rp-process path up to A≈130)
  - Determination of gamma width of individual states

- Technical points:
  - Position resolution of first interaction dominates energy resolution
  - dynamic range of electronics needs to be 2.5 larger than highest γ-ray energy
  - Forward cone or at least 12 degrees needs to be removable

D.Habs
Miniball physics.

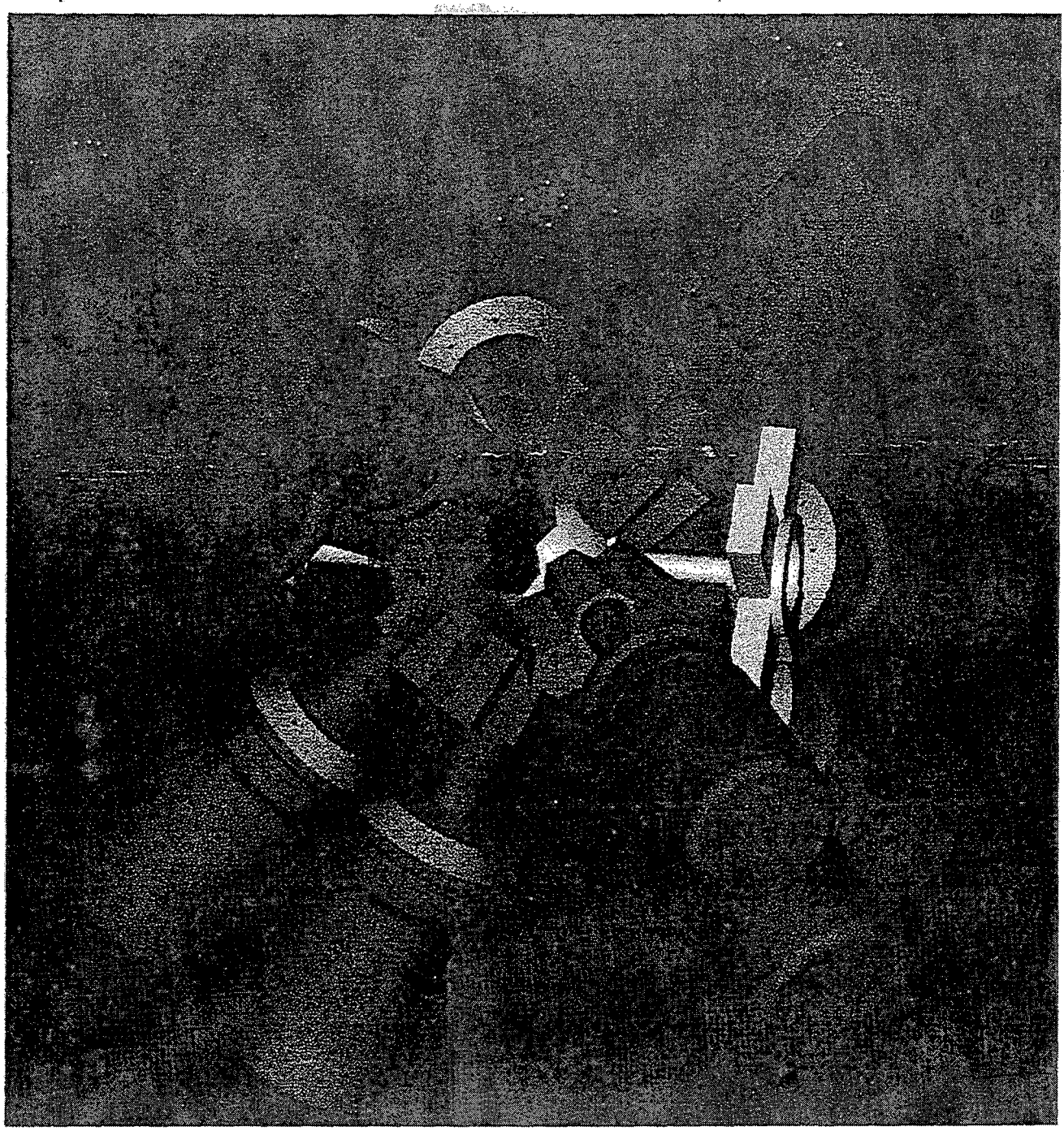

# γ- Efficiency of Miniball-detector

$^{24}Mg(p,n)\,^{24}Al \xrightarrow{\beta^+} {}^{24}Mg$

Photopeak efficiency
of central contact
+ segment efficiency

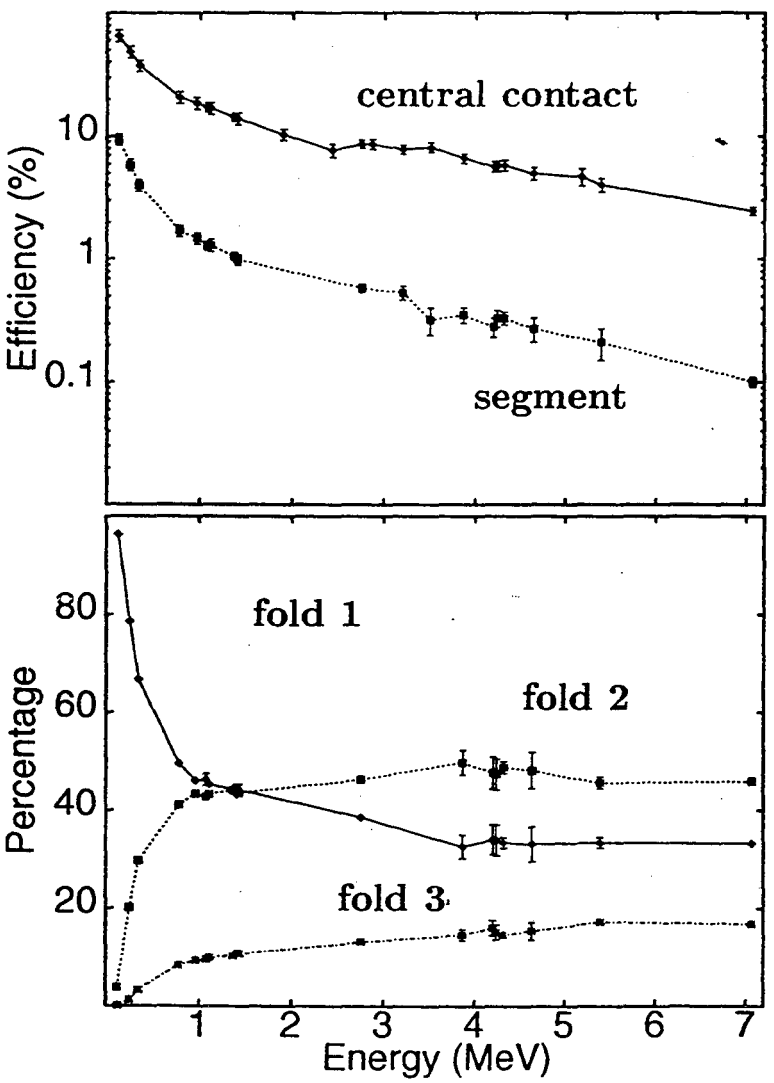


7.1 MeV

Central contact

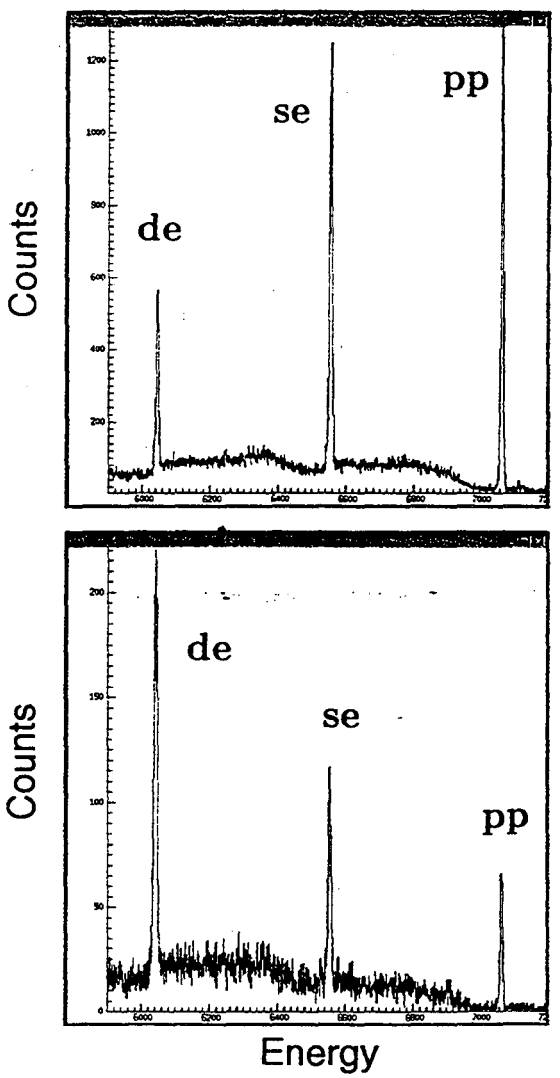


segment

# Radial position resolution from pulse shape

Collimated sources

Middle of segment

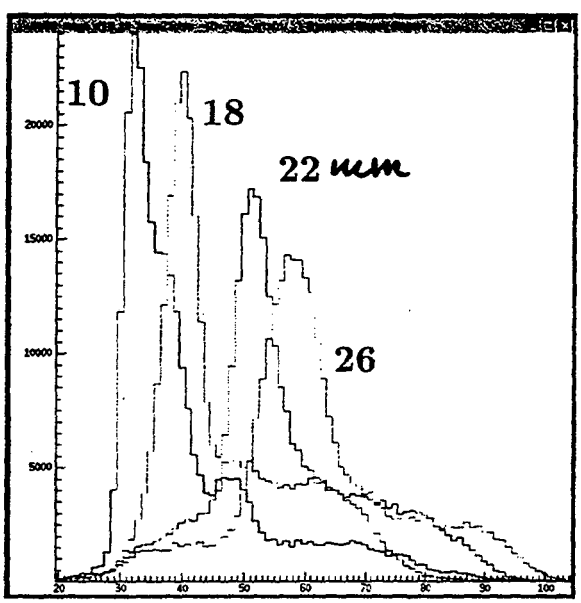


Boarderline between two segments

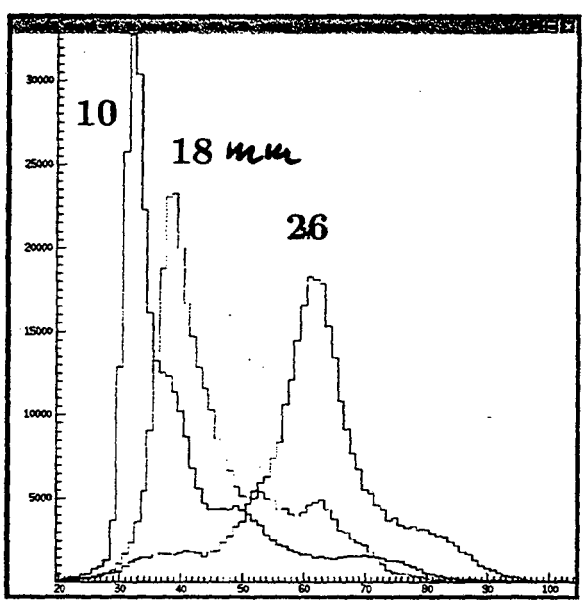


Time to Steepest Slope

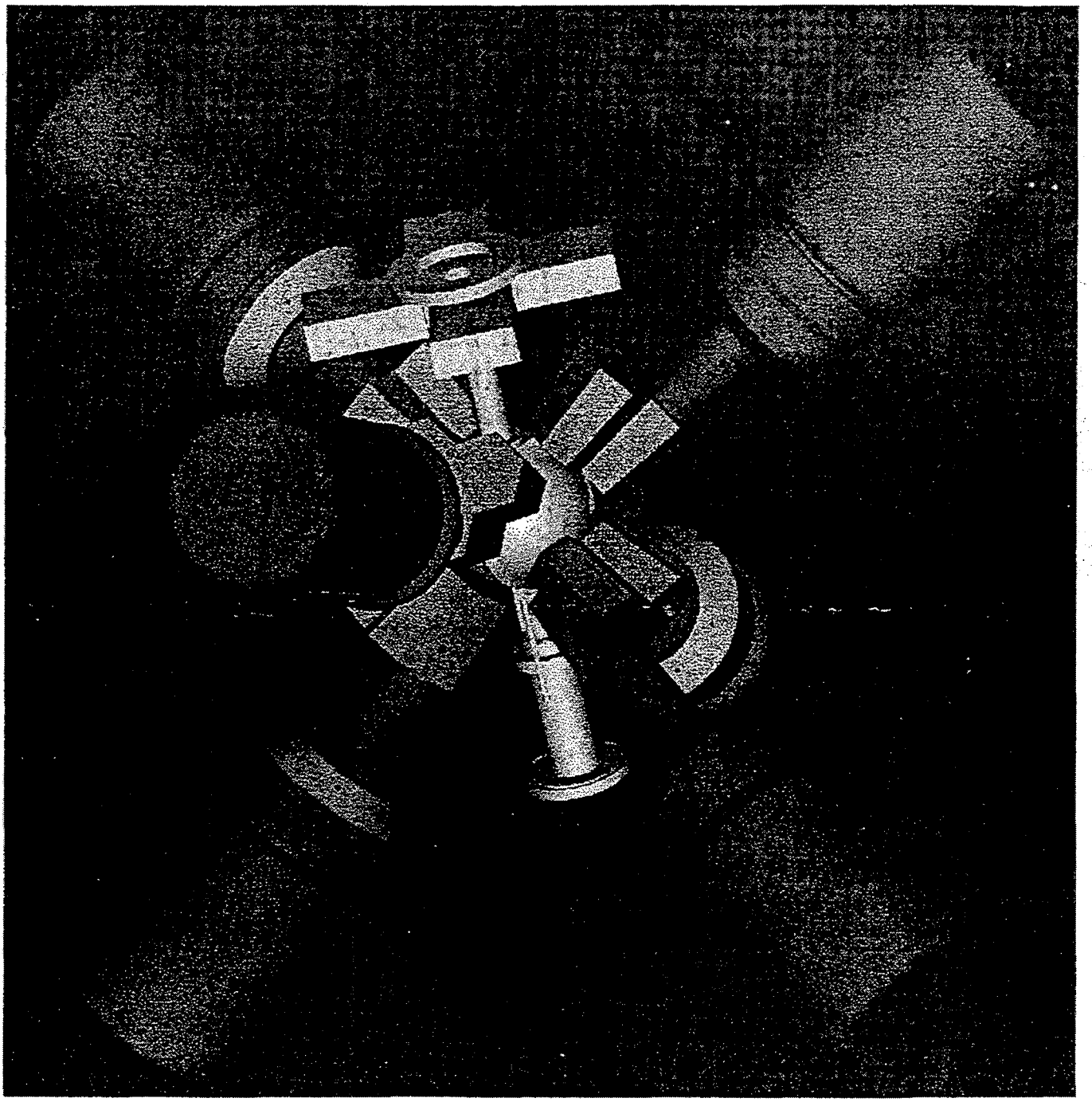

# MINIBALL Physics (I)

## Physics with radioactive beams

- Coulex and transfer with radioactive beams
  → REX-ISOLDE (Cern)
- Coulomb excitation of fission fragments (BE2)-value
  → PIAFE (Grenoble)
  → SFB (Munich)
- heavy ion fusion reactions with fission fragments
  (active Compton suppression shields)
  - High K-isomers ($A \approx 180$) z.B. $^{48}Ca(^{148}Ba, xn)$
  - second minimum in $^{208}Pb$ z.B. $^{82}Se(^{132}Sn, xn)$
- Relativistic Coulex with fast radioactive beams
  → FRS (GSI)
- Radiative p and α capture for radioactive beams
  → ARENAS$^3$ (Louvain-la-Neuve)

# Radioactive Beam EXperiment at ISOLDE

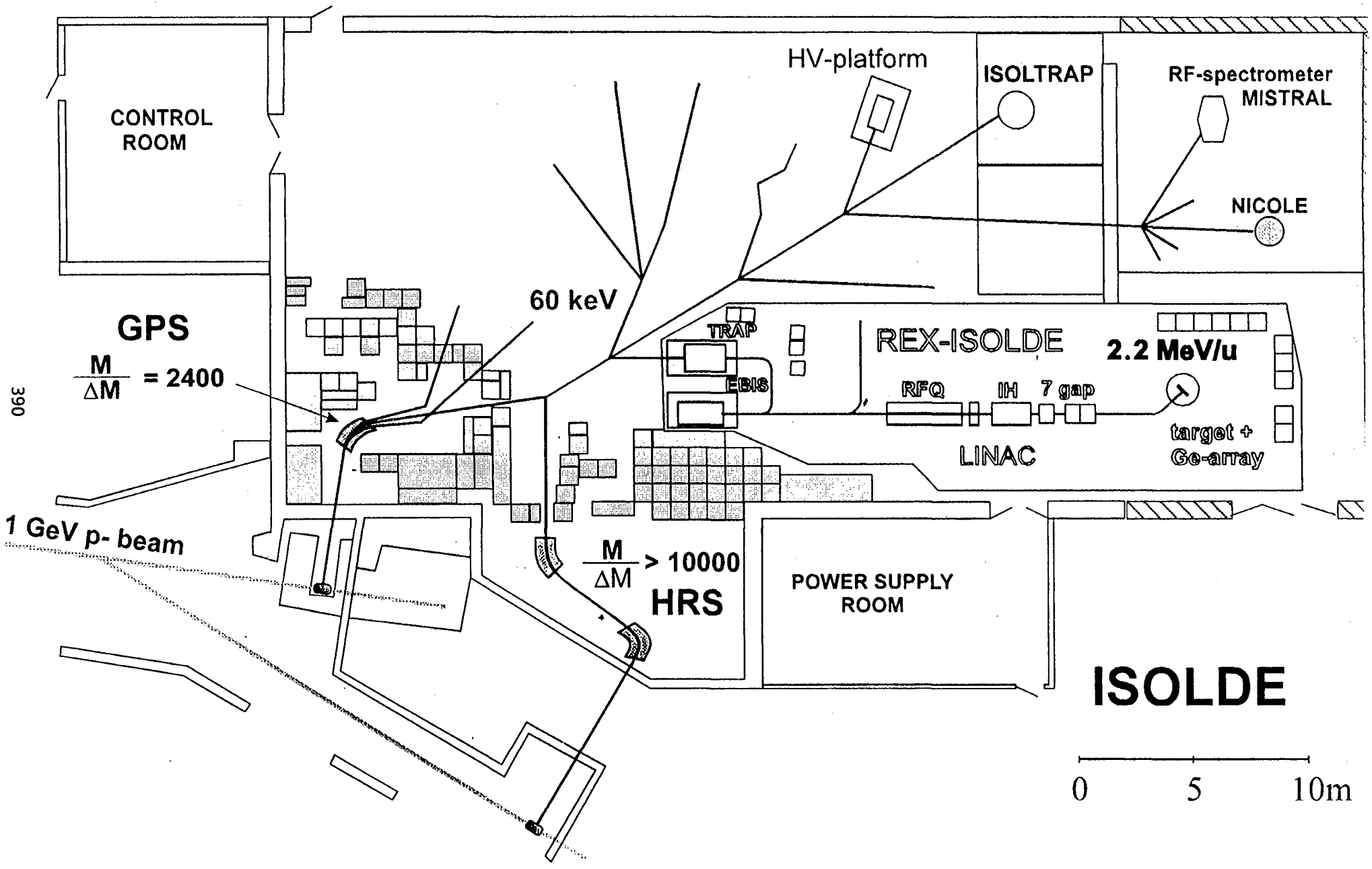

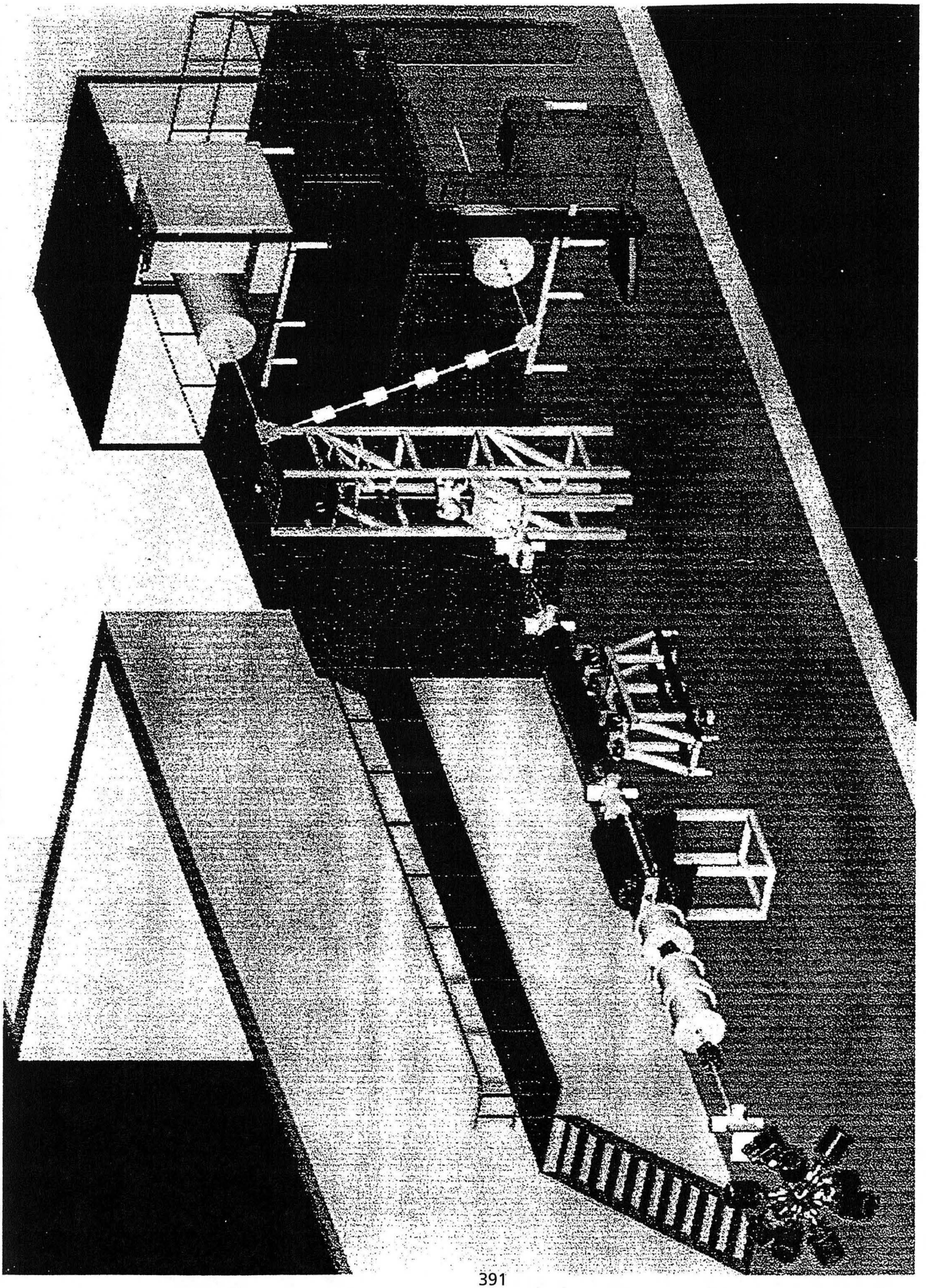

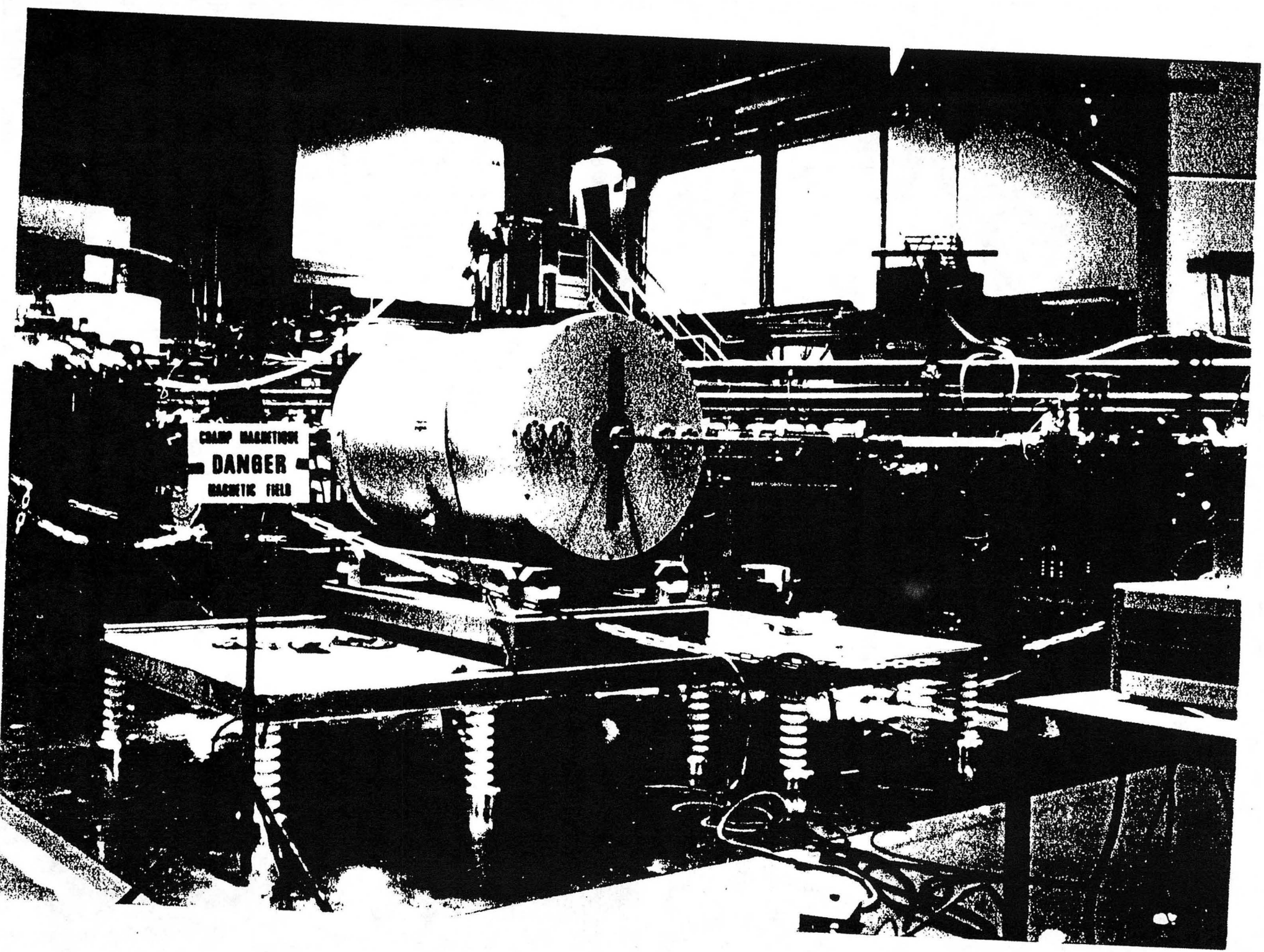
CHAMP MAGNETIQUE
DANGER
MAGNETIC FIELD

# CAPTURE AND LONGITUDINAL COOLING BY A BUFFERGAS

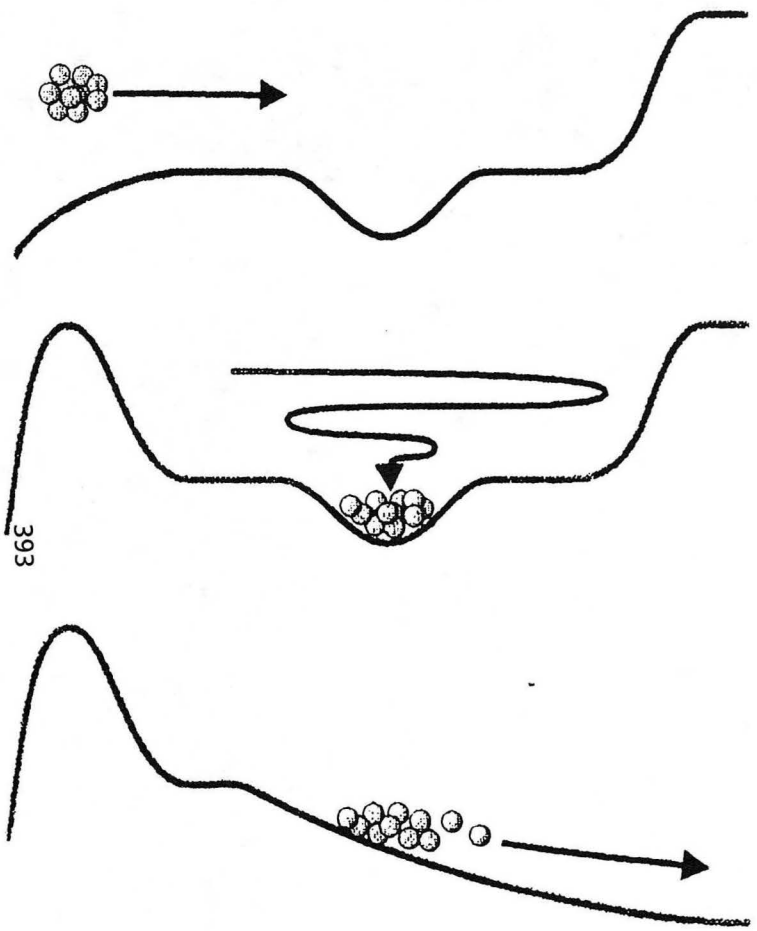

PULSED INJECTION

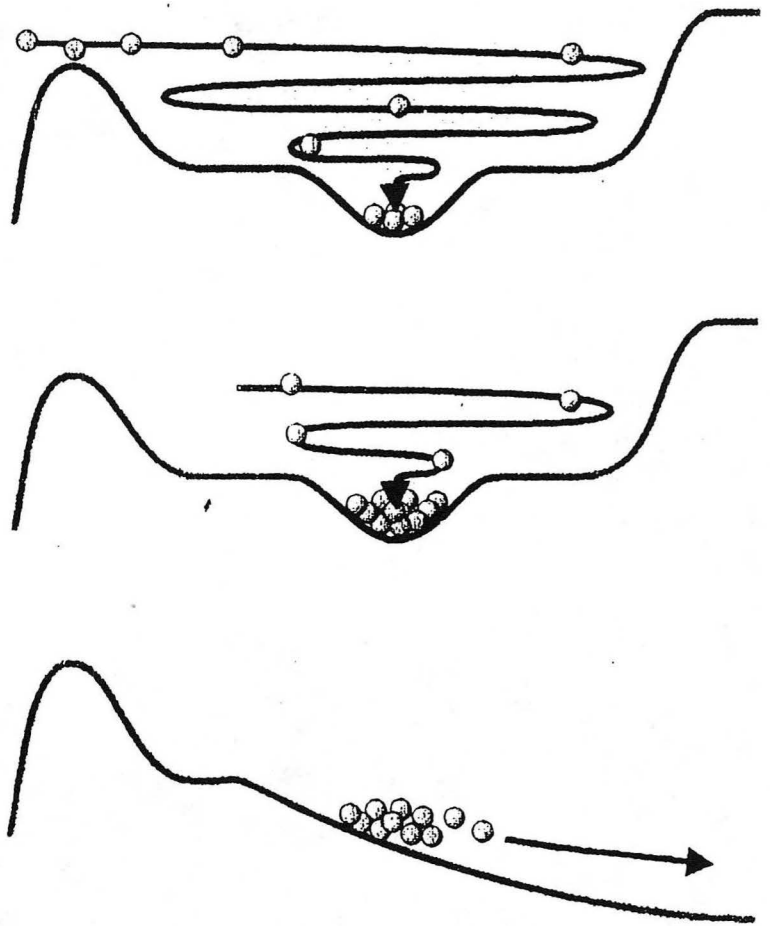

CONTINUOUS INJECTION

# Compact Disc (CD) — Coulex experiments REX — ISOLDE

Proposed detector specification

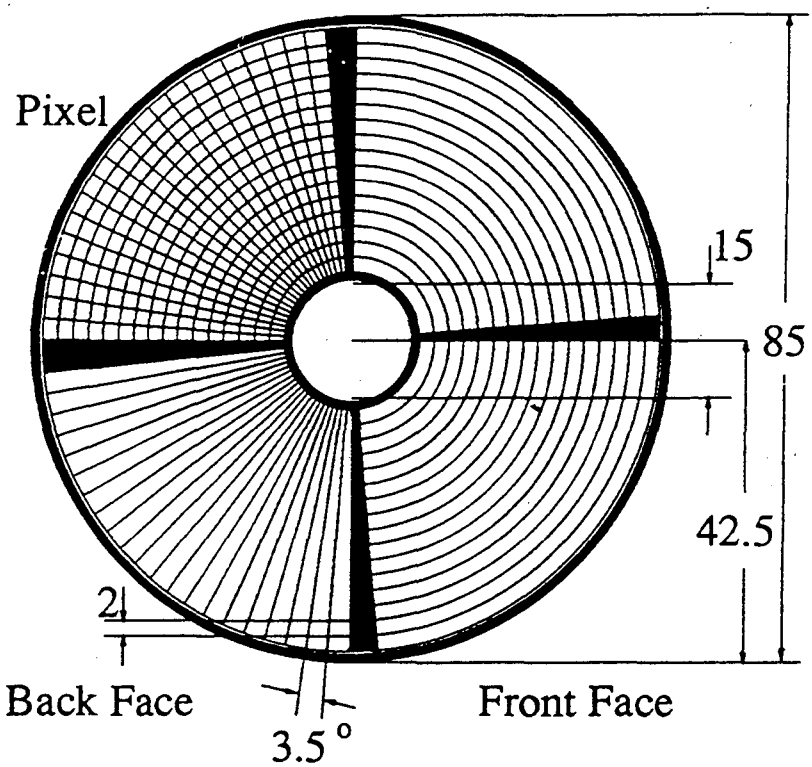


Double-sided silicon strip detector (DSSSD)

4 quadrants  Total Area 50cm$^2$ (~93% active)

16 annular p+ strips / quadrant @ 2mm pitch

24 sector n+ strips / quadrant @ 3.5° pitch

Total of 160 discrete detector elements

Wafer Thickness 60 - 1000 μ (transmission mounting)

Inter-strip distance 35 - 100 μ

Dead Layer ~ 0.3 - 0.8 μ

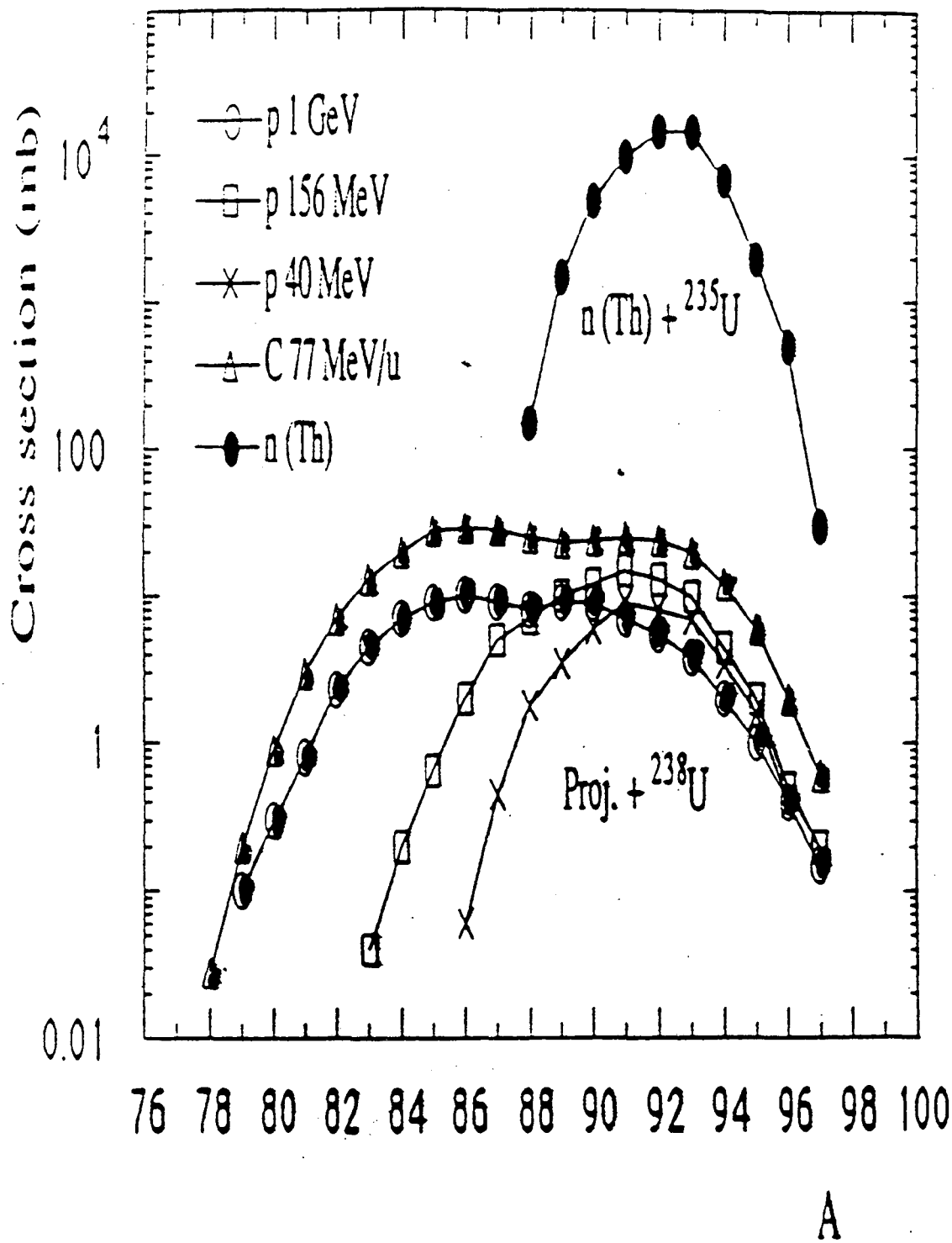
Cross section (mb)
$10^4$
100
1
0.01
p 1 GeV
p 156 MeV
p 40 MeV
C 77 MeV/u
n (Th)
n (Th) + $^{235}$U
Proj. + $^{238}$U
76 78 80 82 84 86 88 90 92 94 96 98 100
A

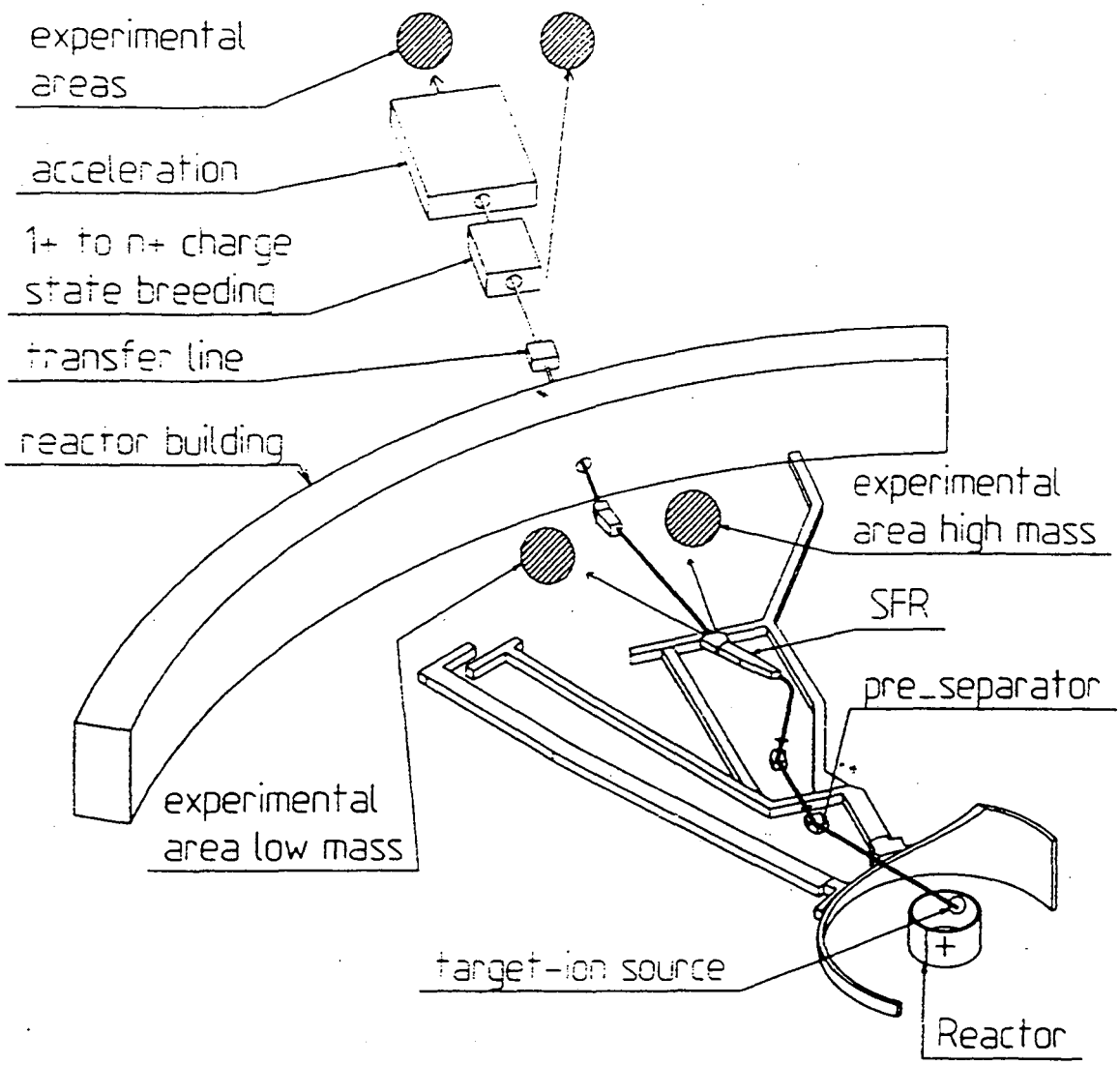


Overview of the PIAFE layout.

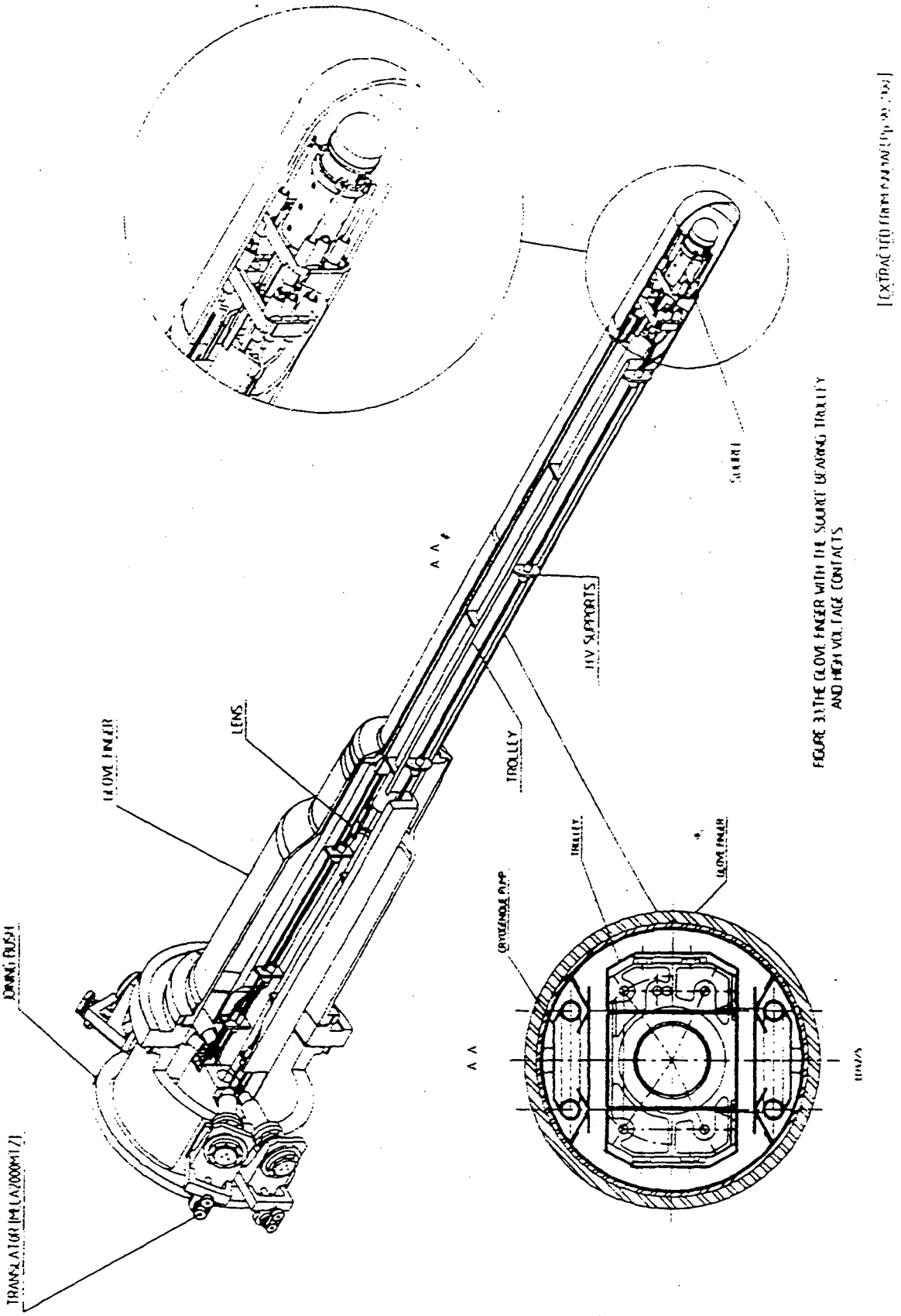


Figure 2: In-pile part of the PIAFE project.

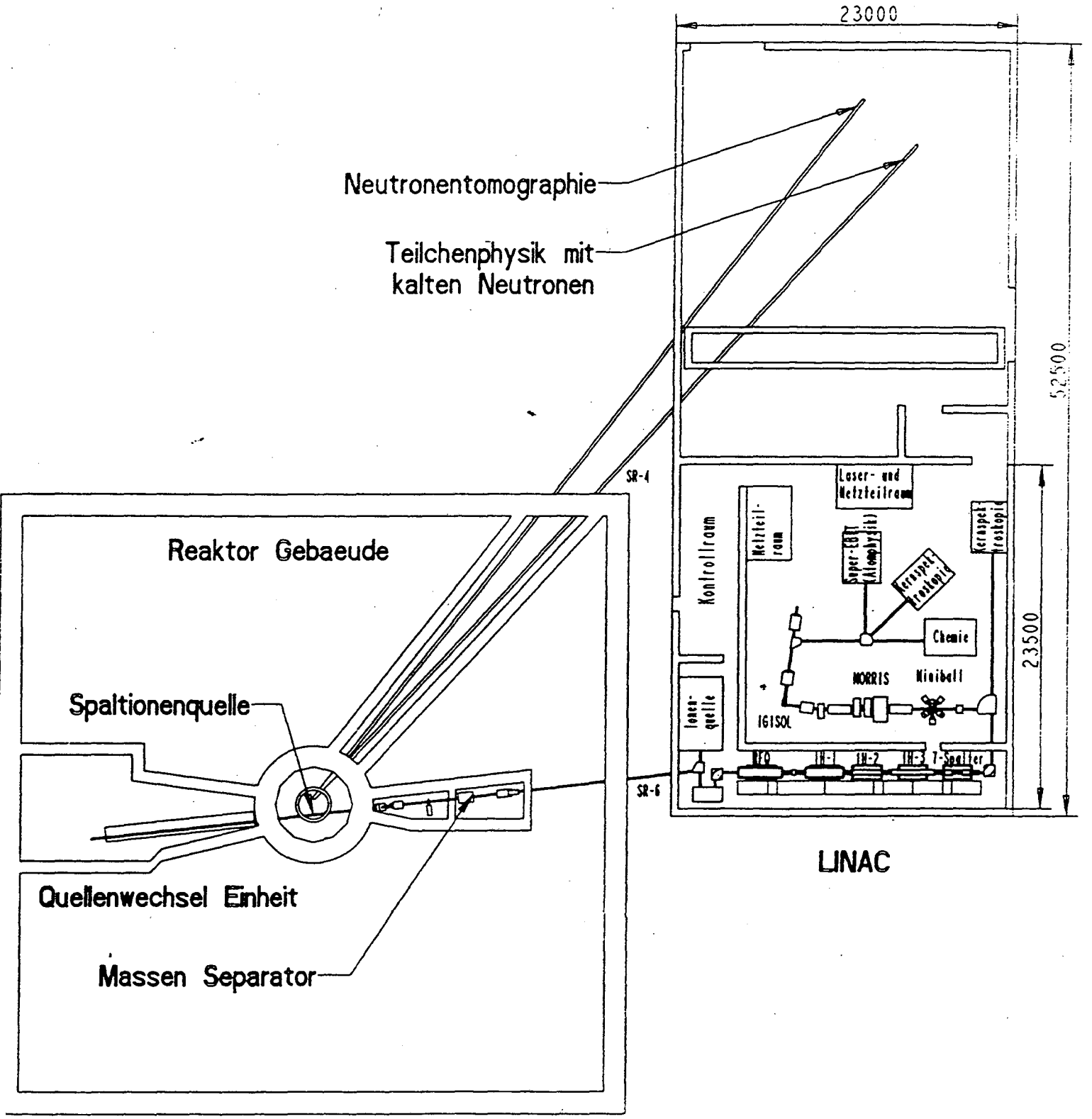
23000
Neutronentomographie
Teilchenphysik mit
kalten Neutronen
52500
SR-4
Laser- und
Netzteilraum
Kontrollraum
Netzteil-
raum
Super-EBIT
(Atomphysik)
Kerspektroskopie
Kerspektroskopie
Chemie
23500
MORRIS
Nineball
Ionen-
quelle
IGISOL
RFQ
IH-1
IH-2
IH-3
T-Spalter
SR-6
LINAC
Reaktor Gebaeude
Spaltionenquelle
Quellenwechsel Einheit
Massen Separator

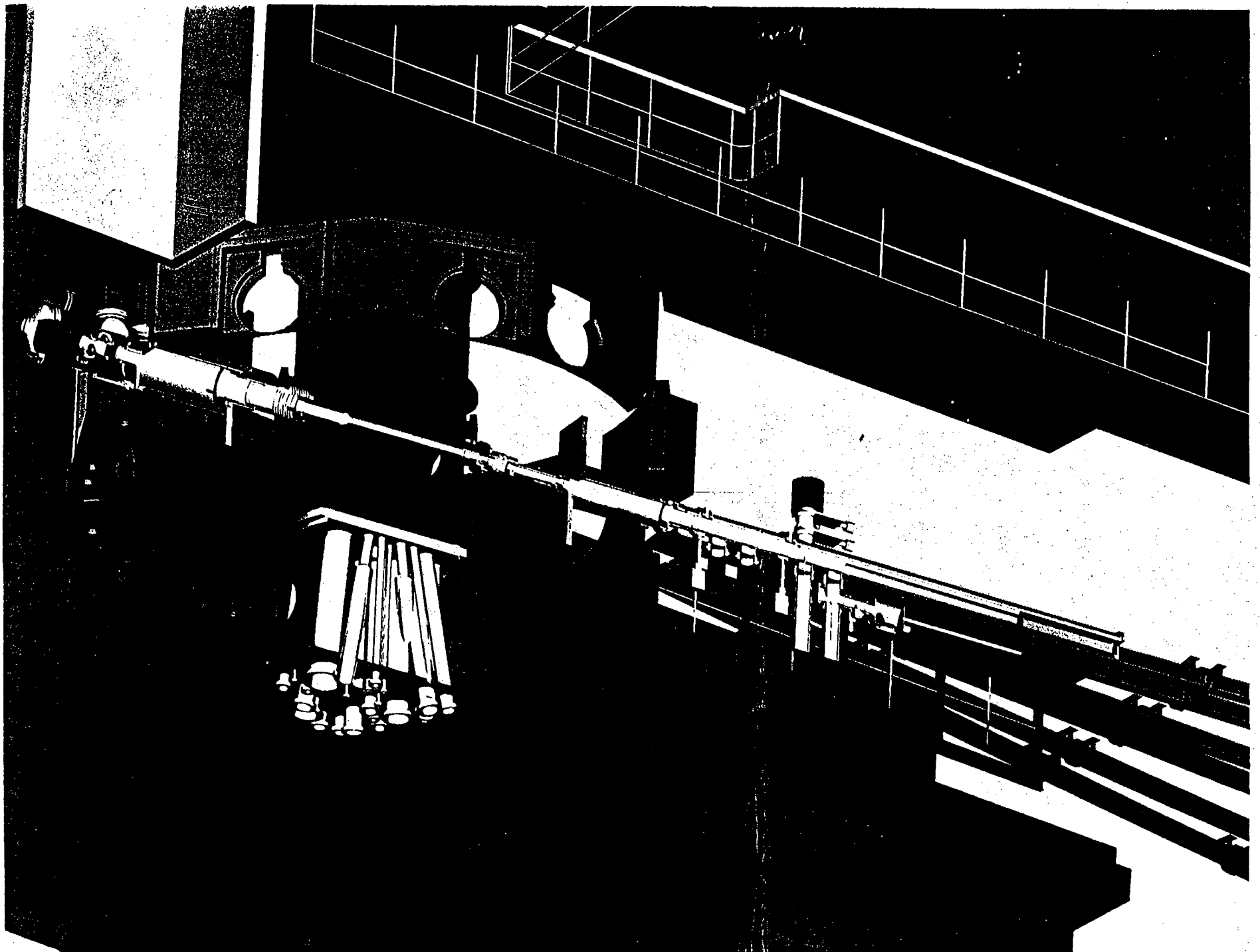

Yields of prominent isotopes at PIAFE compared to accelerator based RIB facilities. The primary beams are 10 $\mu$A of 1.15 GeV $^{12}$C for SPIRAL, 2.5 $\mu$A of 1 GeV protons (or 600 MeV protons for the SC respectively) for ISOLDE and 100 $\mu$A of protons for the ISL.

| Isotope | Prod. rate ($s^{-1}$) | Half-life (s) | Release (%) | Ioniz. (%) | PIAFE ($s^{-1}$) | SPIRAL ($s^{-1}$) | ISOLDE ($s^{-1}$) | ISL ($s^{-1}$) |
|---|---|---|---|---|---|---|---|---|
| $^{78}$Zn | $2.3 \cdot 10^{9}$ | 1.47 | 36 | 10 | $\mathbf{4 \cdot 10^{8}}$ | $2 \cdot 10^{6}$ | $1 \cdot 10^{6}$ SC | $6 \cdot 10^{6}$ |
| $^{82}$Ge | $1.2 \cdot 10^{11}$ | 4.6 | 48 | 10 | $\mathbf{6 \cdot 10^{9}}$ | | $2 \cdot 10^{5}$ SC | $1 \cdot 10^{8}$ |
| $^{91}$Kr | $3.3 \cdot 10^{12}$ | 8.6 | 89 | 15 | $\mathbf{4 \cdot 10^{11}}$ | $2 \cdot 10^{9}$ | $2 \cdot 10^{9}$ | $4 \cdot 10^{10}$ |
| $^{94}$Kr | $1.1 \cdot 10^{11}$ | 0.2 | 16 | 15 | $\mathbf{3 \cdot 10^{9}}$ | $3 \cdot 10^{7}$ | $4 \cdot 10^{6}$ | $6 \cdot 10^{9}$ |
| $^{97}$Rb | $3 \cdot 10^{10}$ | 0.17 | 10 | 80 | $\mathbf{2 \cdot 10^{9}}$ | $5 \cdot 10^{8}$ | $3 \cdot 10^{8}$ | $7 \cdot 10^{9}$ |
| $^{132}$Sn | $7 \cdot 10^{11}$ | 39.7 | 89 | 10 | $\mathbf{6 \cdot 10^{10}}$ | $6 \cdot 10^{6}$ | $8 \cdot 10^{7}$ SC | $1 \cdot 10^{10}$ |
| $^{142}$Xe | $5.2 \cdot 10^{11}$ | 1.24 | 7 | 25 | $\mathbf{1 \cdot 10^{10}}$ | $6 \cdot 10^{7}$ | $2 \cdot 10^{8}$ | $4 \cdot 10^{10}$ |
| $^{144}$Xe | $9.3 \cdot 10^{9}$ | 1.15 | 7 | 25 | $\mathbf{2 \cdot 10^{8}}$ | $1 \cdot 10^{6}$ | $5 \cdot 10^{6}$ | $2 \cdot 10^{10}$ |
| $^{144}$Cs | $4.3 \cdot 10^{11}$ | 1.0 | 47 | 80 | $\mathbf{2 \cdot 10^{11}}$ | $2 \cdot 10^{10}$ | $3 \cdot 10^{10}$ | $6 \cdot 10^{10}$ |

poor man's radioactive beam collider with radioactive targets

| | cumulative y. | target thickness | Detection limit (1 pnA ; 1 reaction/day) |
|---|---|---|---|
| 130 Sn | $3 \times 10^{11}/s$ | 1 $\mu g/cm^2$ | 320 nb |
| 134 Te | $2 \times 10^{12}/s$ | 135 $\mu g/cm^2$ | 3 nb |

# High-$K$ isomers

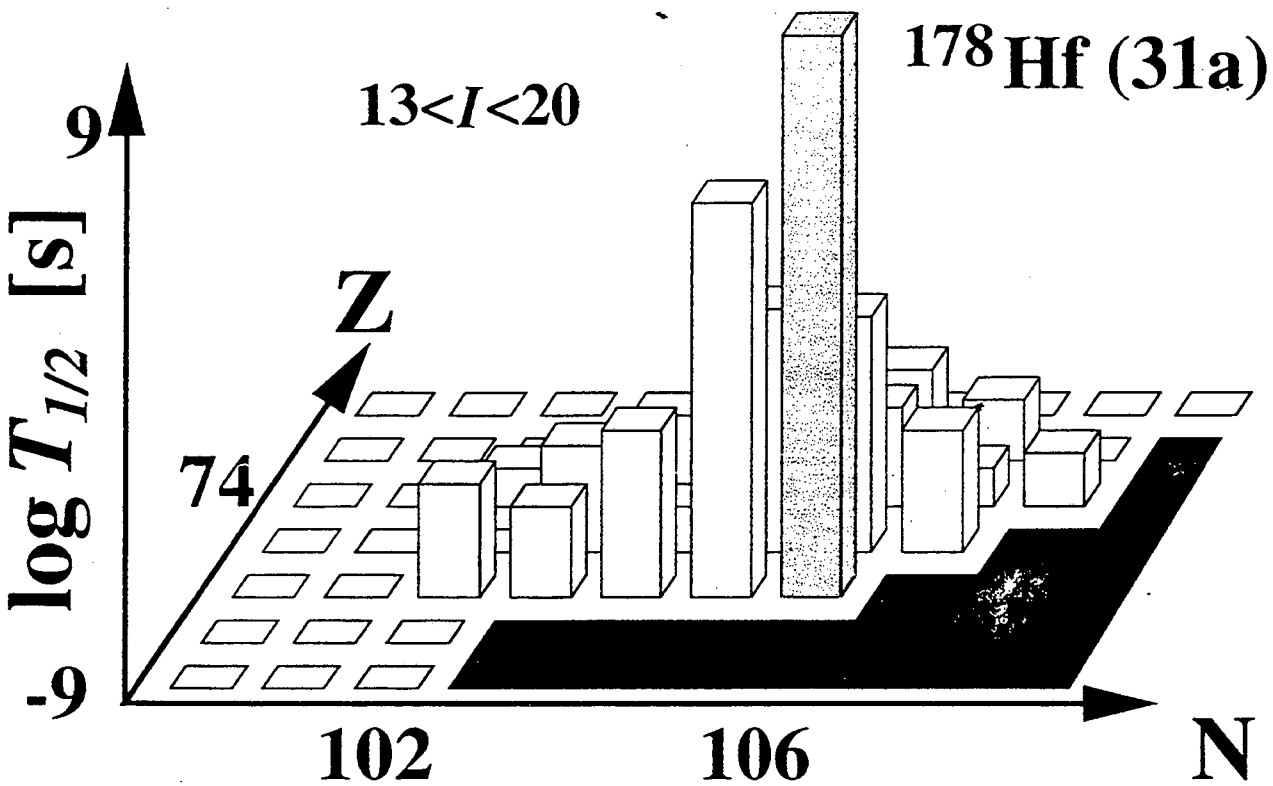

# Expected s.p. excitation scheme of $^{208}$Pb

**Low high-spin level density!**

**High-spin isomers?**

| $E_x$ (MeV) | $I$ | |
|---|---|---|
| ~25 | ~42 | 4p4h |
| ~19 | ~34 | 3p3h |
| ~13 | $26^+$ | 2p2h |
| 6.7 | $14^-$ | 1p1h |
| 0 | $0^+$ | |

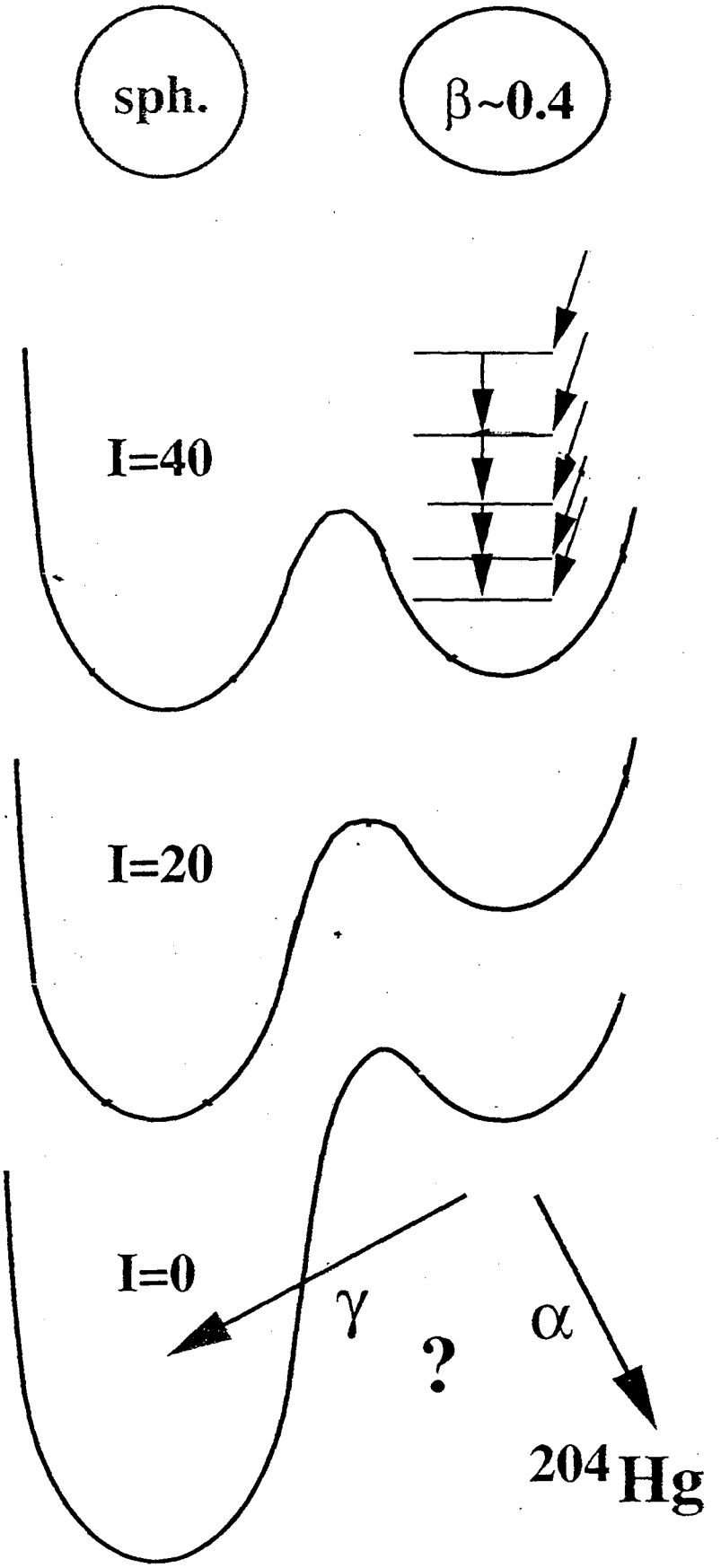

# MINIBALL Physics (II)

## Rare Decays

- γ-decay in the second minimum of fission isomers
  example (Heidelberg): $^{240m}Pu$ ; new e.g. $^{236m}U$
- γ-decay feeding isomers like the high-spin isomer in $^{178}Hf$
- complex decays of isomers
- double γ-decay.
- γ-decay of negative positronium

## Studies with low γ-ray multiplicities

- large nucleon-transfer in the actinide region
- Spectroscopy of very heavy elements
- γ-deexcitation following deep-inelastic reactions
- (γ,γ') studies
- β-delayed γ radiation far off stability e.g. $^{100}Sn$
  → SHIPTRAP
- isomeric γ-decay following fragment separation of close

D. Pansegrau (HD)

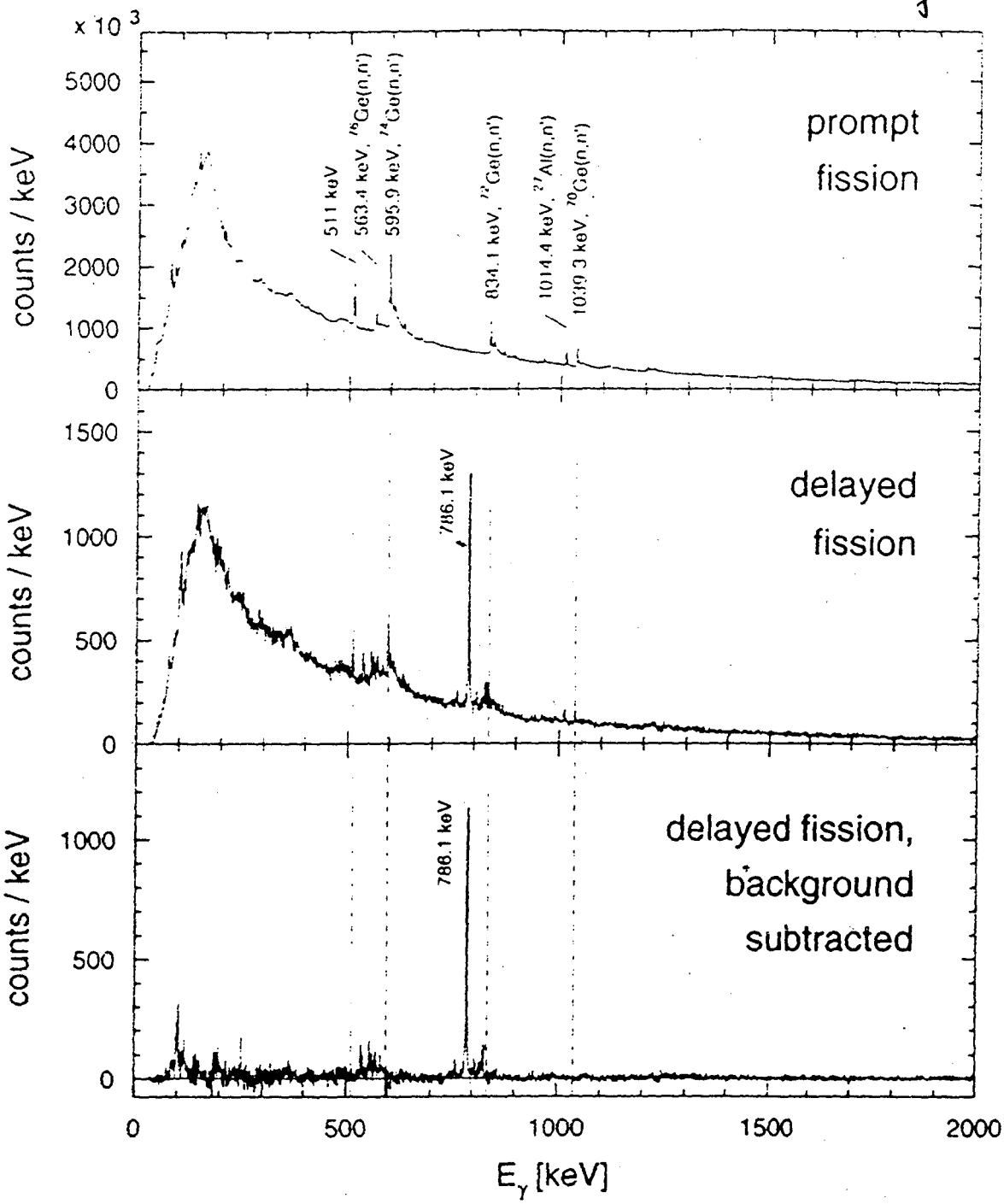


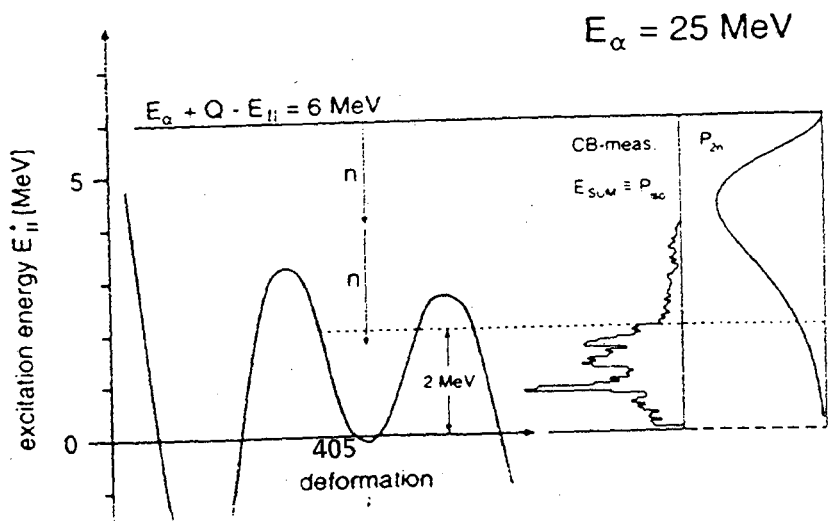

D. Pansegrau (HD)

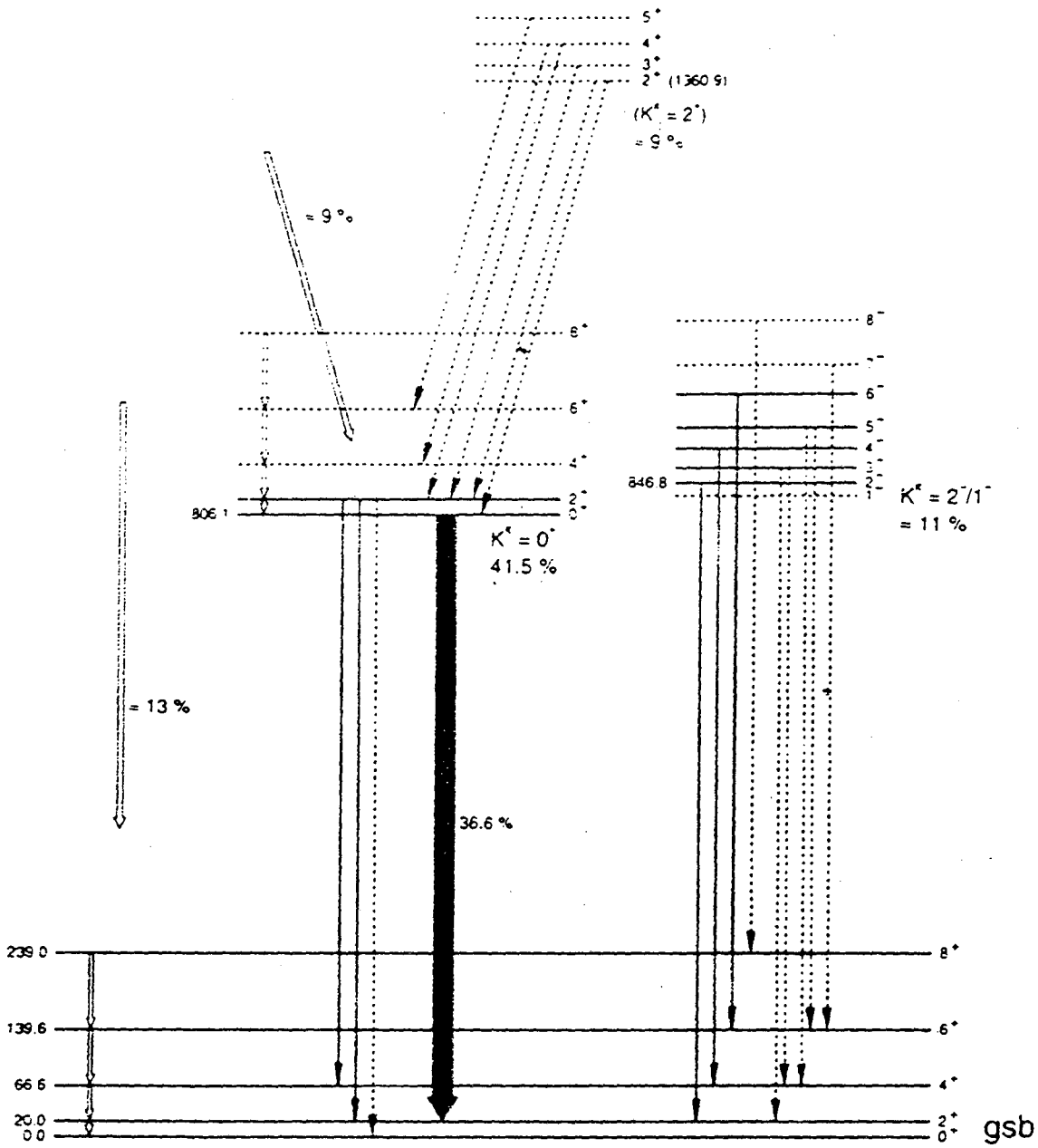


$^{240m}$Pu

# SHIPTRAP + MINIBALL

$\varepsilon = 50\%$

$\frac{\Delta A}{A} = 10^{-5}$

10-20 ms

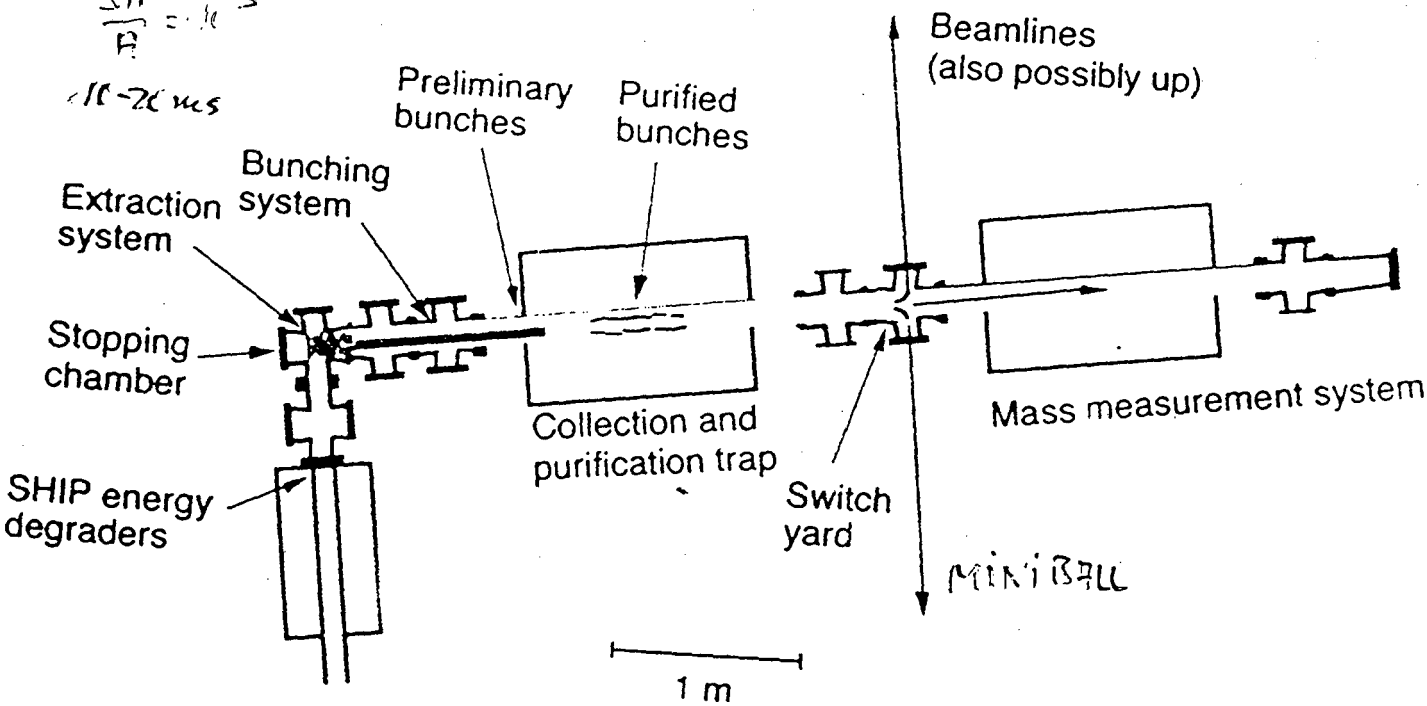


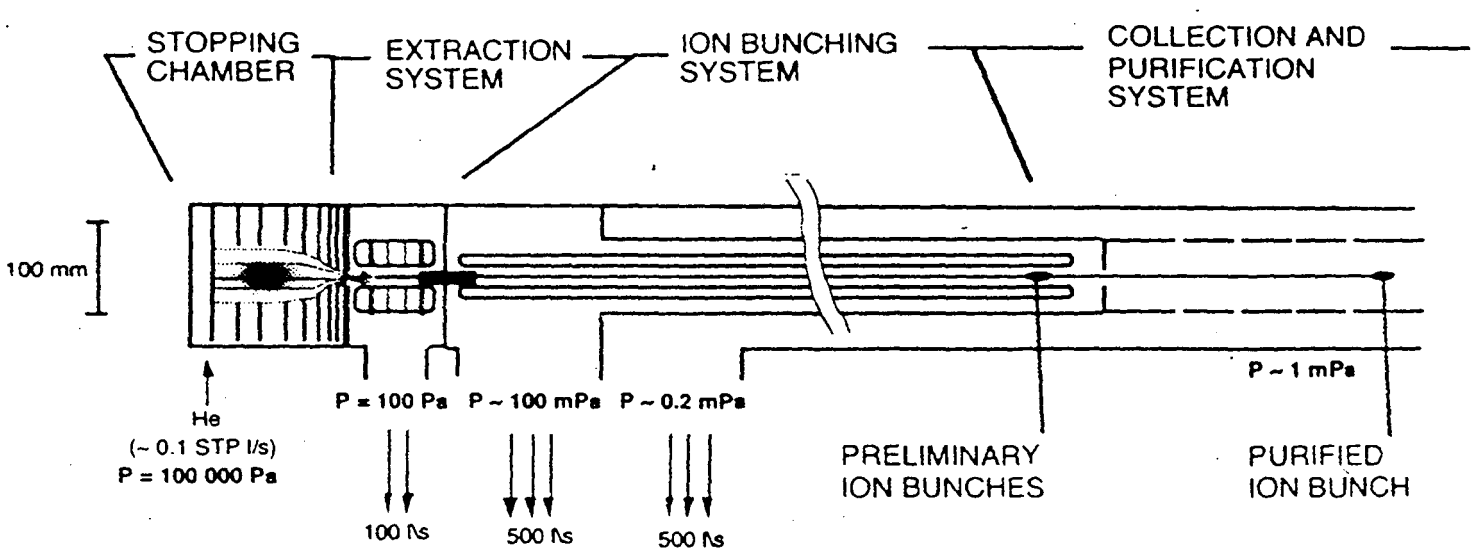

D.Cline

Spectroscopy of neutron-rich nuclei.

# NEUTRON-RICH NUCLEI

**D. Cline, M.W. Simon, C.Y. Wu**
Nuclear Structure Research Laboratory
University of Rochester

## Population of neutron-rich nuclei

- Quasi-elastic transfer reactions
- Strongly-damped reactions
- Fission fragmentation
- Nucleus fragmentation at high energy

## Technical innovation

- CHICO
- GRETA

## Quasi-elastic transfer reactions

## Fission fragmentation

## Conclusions

# CHICO

## Compact Heavy Ion Counter

M.W. Simon, R. Gray, D. Cline, C.Y. Wu, C. Long

Nuclear Structure Research Laboratory
University of Rochester

Funded by the National Science Foundation

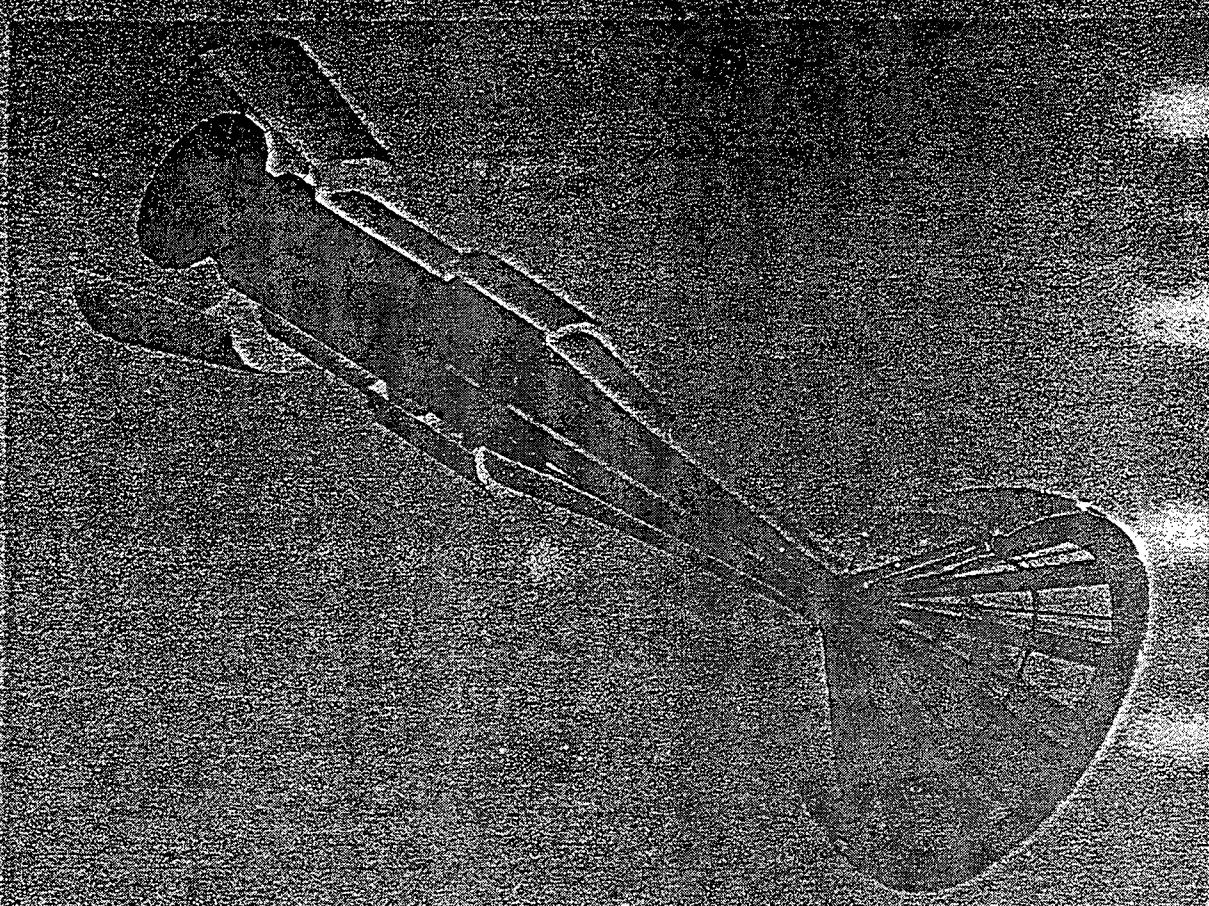

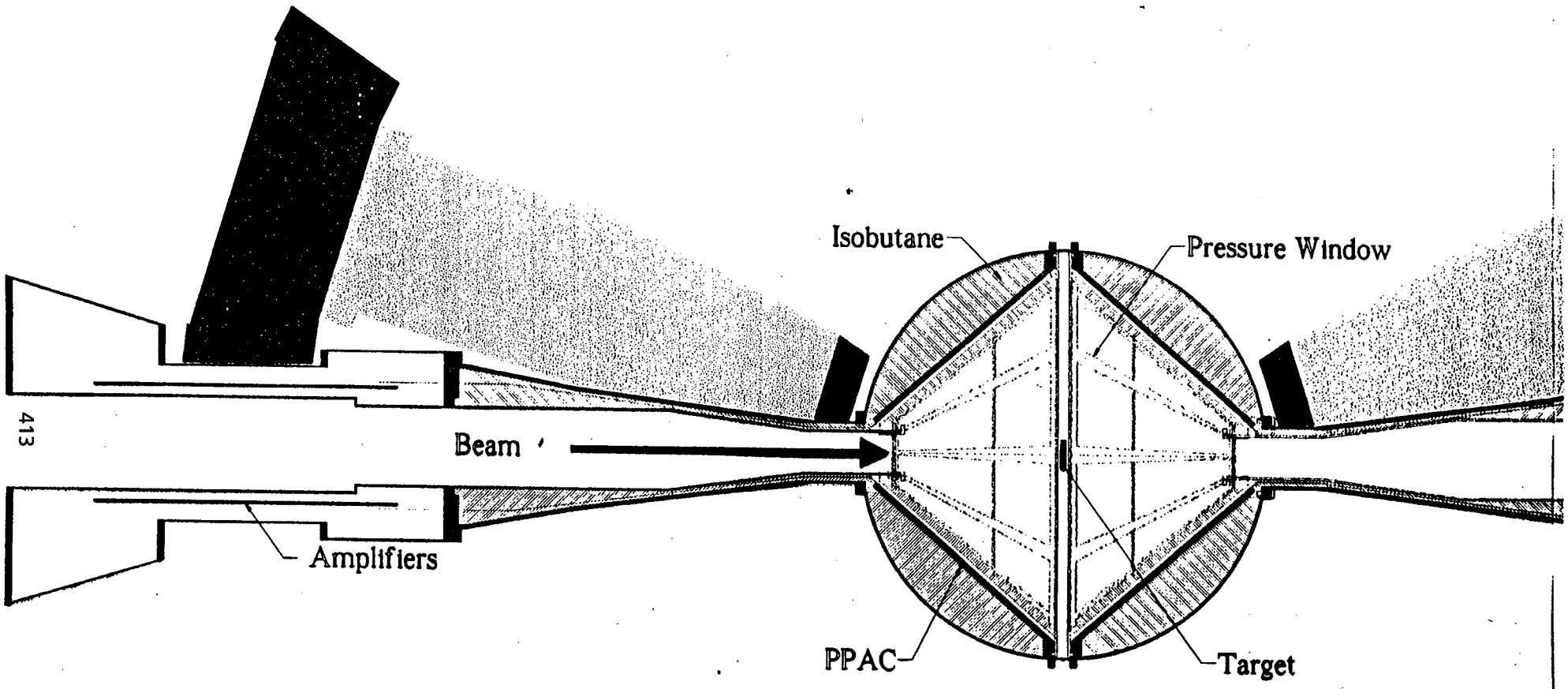
Isobutane
Pressure Window
Beam
Amplifiers
PPAC
Target

# CHICO AT GAMMASPHERE

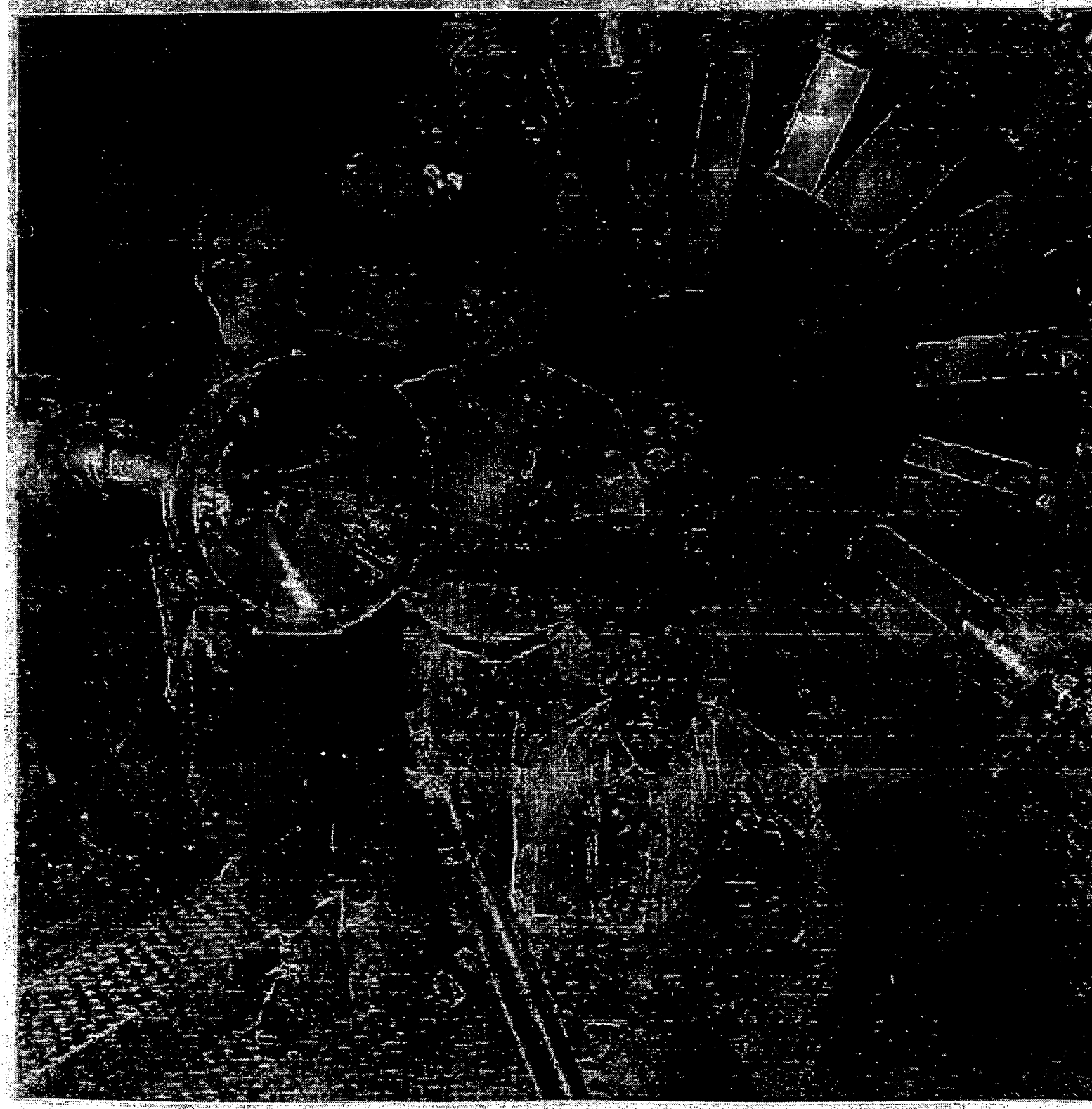

# SUMMARY

| | |
|---|---|
| **Geometry:** | Pentagonal symmetry of Gammasphere<br>Maximum flight path (13.5 cm)<br>Minimum mass to reduce photon scattering |
| **Solid angle:** | 8.5 sr (68% of $4\pi$) |
| **Angular range:** | $12^0 < \theta < 85^0$, $95^0 < \theta < 168^0$ |
| **Angular resolution:** | $\Delta\theta < 1^0$, $\Delta\phi = 9^0$ |
| **Time resolution:** | ~ 500 ps |
| **Binary reactions:** | |
| | Mass resolution $\Delta m/m = 5\%$<br>Q-value resolution = 19MeV |
| **Count rate:** | $>10^6$ /second |
| **Versatile:** | Coulomb excitation<br>Heavy-ion induced transfer reactions<br>Strongly-damped reactions<br>Fission products |

# Heavy-ion-gamma coincidence technique

## Advantages:

- Measure and select mass of reaction products
- Measure reaction Q value for binary collision
- Correct for Doppler shift
- Identify which recoiling nucleus emitted each gamma ray
- Clean $\gamma$-ray spectra
- Eliminates thick-target Doppler-broadened line-shape problems
- Measure p-$\gamma$ angular distributions
- Measure lifetimes directly
- Study prompt and isomeric transitions

## Disadvantage:

- Finite size of Ge detectors degrades $\gamma$-ray energy resolution for large recoil velocities.

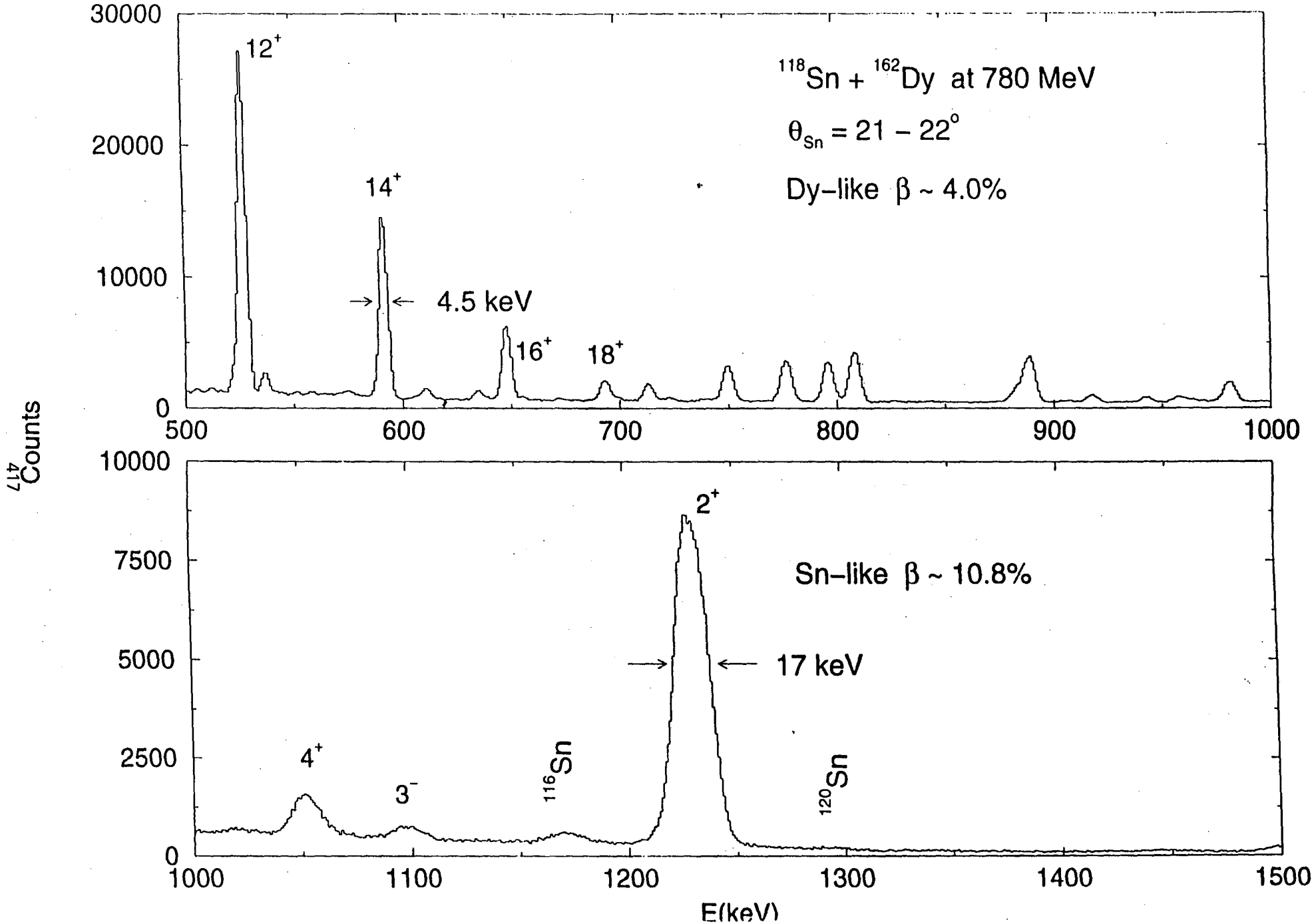
$^{118}$Sn + $^{162}$Dy at 780 MeV
$\theta_{Sn}$ = 21 – 22°
Dy–like β ~ 4.0%
12+
14+
4.5 keV
16+
18+
Sn–like β ~ 10.8%
2+
17 keV
4+
3−
$^{116}$Sn
$^{120}$Sn
Counts
E(keV)

# GRETA versus Gammasphere

## Doppler broadening:

| | |
|---|---|
| Gammasphere | $\Delta E_\gamma/E_\gamma \leq 1.4$ % FWHM |
| GRETA | $\Delta E_\gamma/E_\gamma = 0.2$ % FWHM |
| Improvement factor | ~ 7 |

## Peak/Compton ratio:

| | |
|---|---|
| Gammasphere | 2.1 |
| GRETA | ~9 |
| Improvement factor | ~ 4 |

## Peak efficiency:

| | |
|---|---|
| Gammasphere | 9.4% |
| GRETA | 51.% |
| Improvement factor | ~5.5 |

Use much higher fold
Excellent H and K resolution
Allow use of weak exotic beams
Improve true to random ratio

# Coulomb excitation sensitivity

**Minimum excitation probability, $\Delta P$, detected in Rochester group Coulomb excitation measurements**

| | $\Delta P$ |
|---|---|
| 1975 | $\sim 5\ 10^{-3}$ |
| 1985 | $\sim 5\ 10^{-4}$ |
| 1990 | $\sim 4\ 10^{-5}$ |
| GASP | $< 10^{-5}$ |
| Gammasphere | $\sim 5\ 10^{-7}$ |
| GRETA | $\sim 10^{-9}$ |

# HEAVY-ION REACTIONS AT BARRIER

## Quasielastic transfer reactions:

- Reaction mechanism simple direct transfer
- One-nucleon transfer sensitive probe of single-particle structure
- Two-nucleon transfer sensitive probe of pairing correlations.
- Interplay of shell and collective degrees of freedom.

## Damped reactions:

- Populate a wide range of nuclei near valley of stability
- Approximately binary-reaction kinematics

## Technique: CHICO + Gammasphere

Approximate binary-reaction kinematics:

- Masses
- Q-value
- Impact parameter

P-γ-γ:

- Identify both binary products
- Clean γ-ray spectra
- Identify γ-ray emitting nucleus
- H and K

# Production and spectroscopy of the neutron-rich nucleus $^{166}$Dy

**C.Y. Wu, M.W. Simon, D. Cline, G.A. Davis, A.O. Macchiavelli, K. Vetter**
(Physical Review, Submitted 1998)

$^{118}$Sn($^{162}$Dy,$^{164}$Dy)$^{116}$Sn and $^{118}$Sn($^{164}$Dy,$^{166}$Dy)$^{116}$Sn reactions at 4.81 MeV/nucleon.

## Reaction $Q_{gg}$ values and excitation probabilities

| Projectile | | Reaction product $^{160}$Dy | $^{162}$Dy | $^{164}$Dy | $^{166}$Dy |
|---|---|---|---|---|---|
| $^{162}$Dy | $Q_{gg}$ (MeV) | +0.5 | 0.0 | -2.3 | |
| | P = | (0.0065) | (1.000) | (0.0019) | |
| $^{164}$Dy | $Q_{gg}$ (MeV) | | +1.7 | 0.0 | -3.5 |
| | P = | | (0.011) | (1.000) | (0.0027) |

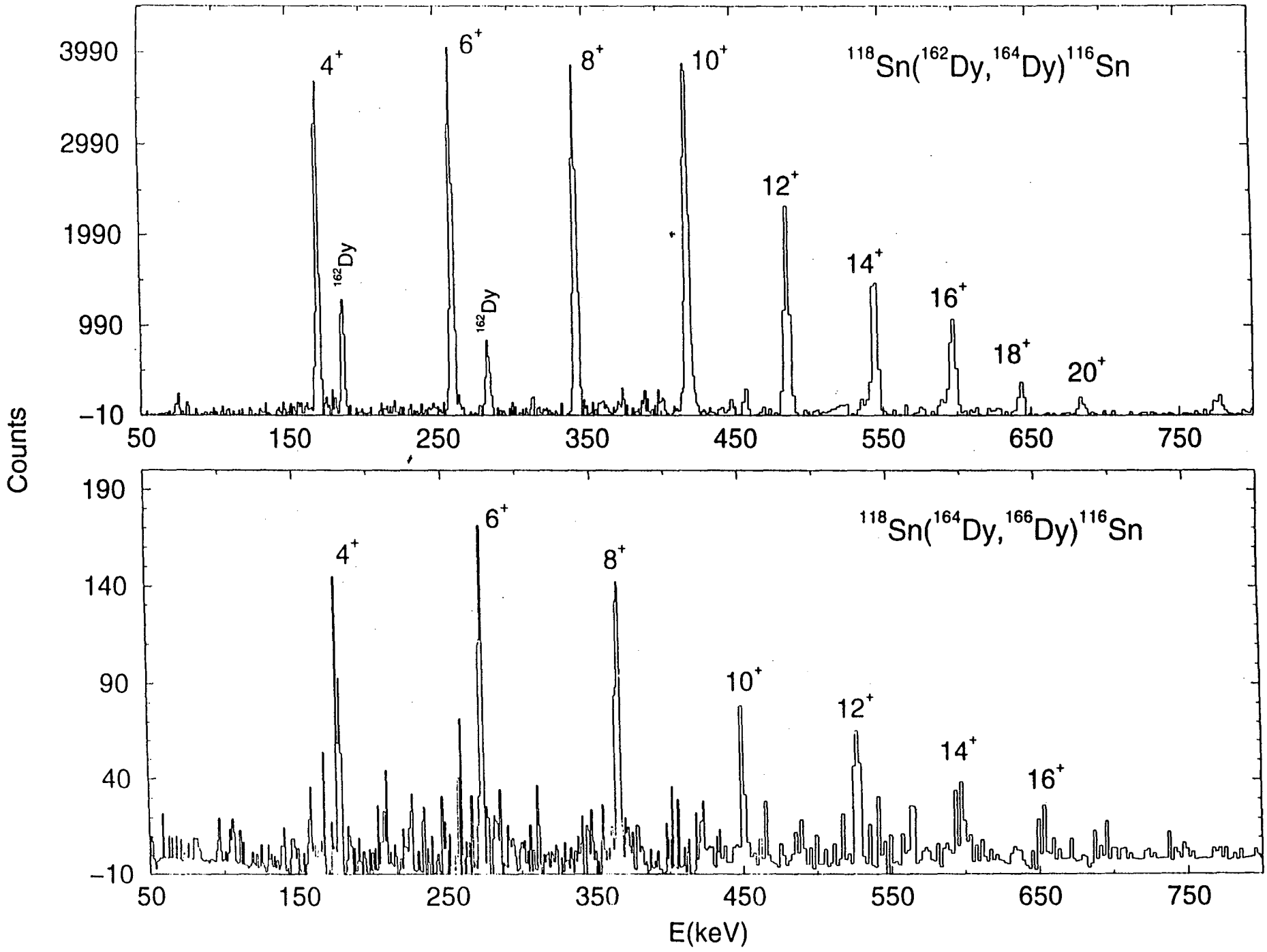
$^{118}$Sn($^{162}$Dy,$^{164}$Dy)$^{116}$Sn
4+
6+
8+
10+
12+
14+
16+
18+
20+
162Dy
162Dy
3990
2990
1990
990
−10
$^{118}$Sn($^{164}$Dy,$^{166}$Dy)$^{116}$Sn
4+
6+
8+
10+
12+
14+
16+
190
140
90
40
−10
50
150
250
350
450
550
650
750
Counts
E(keV)

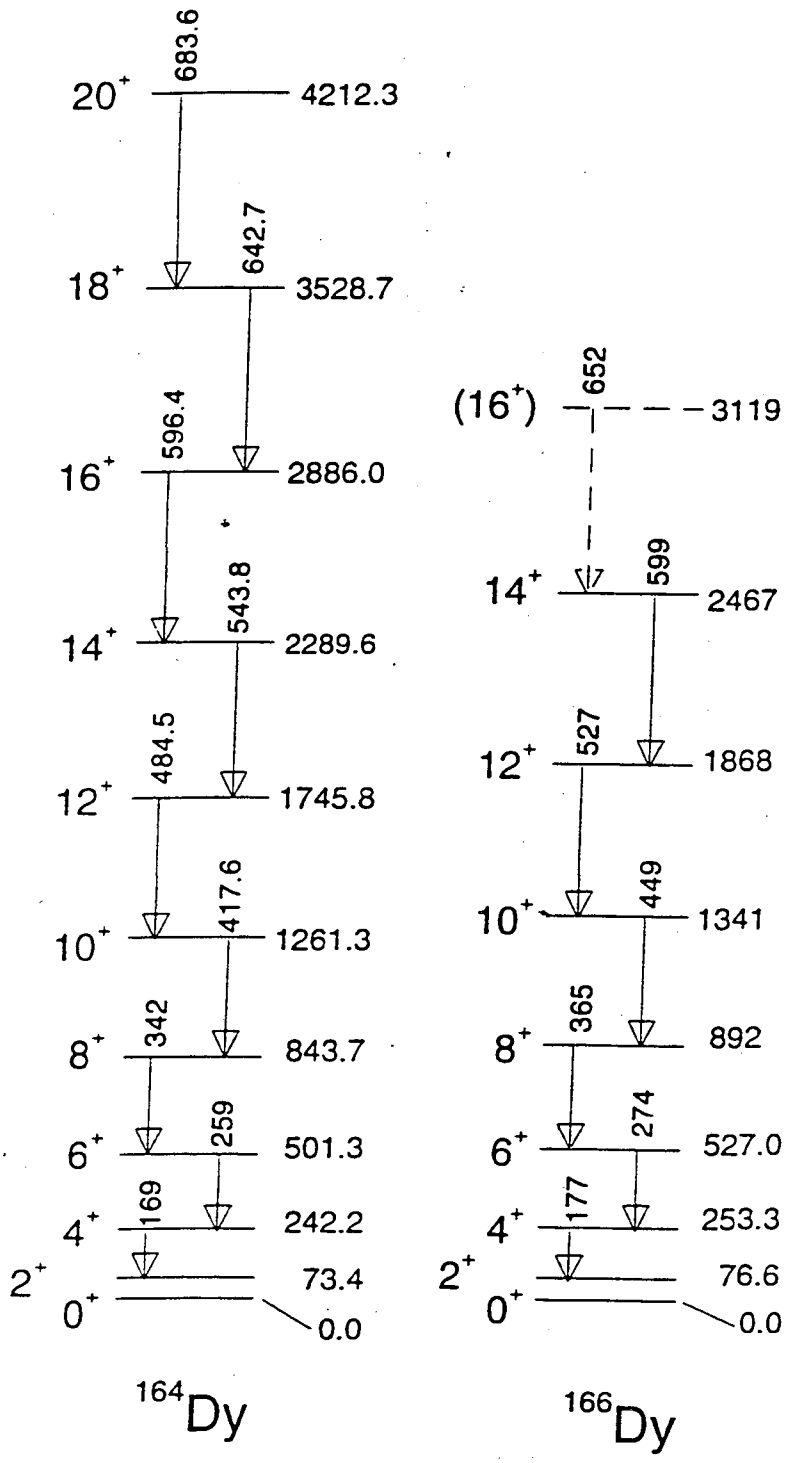
683.6
20+
4212.3
642.7
18+
3528.7
596.4
16+
2886.0
543.8
14+
2289.6
484.5
12+
1745.8
417.6
10+
1261.3
342
8+
843.7
259
6+
501.3
169
4+
242.2
2+
73.4
0+
0.0
164Dy
652
(16+)
3119
599
14+
2467
527
12+
1868
449
10+
1341
365
8+
892
274
6+
527.0
177
4+
253.3
2+
76.6
0+
0.0
166Dy

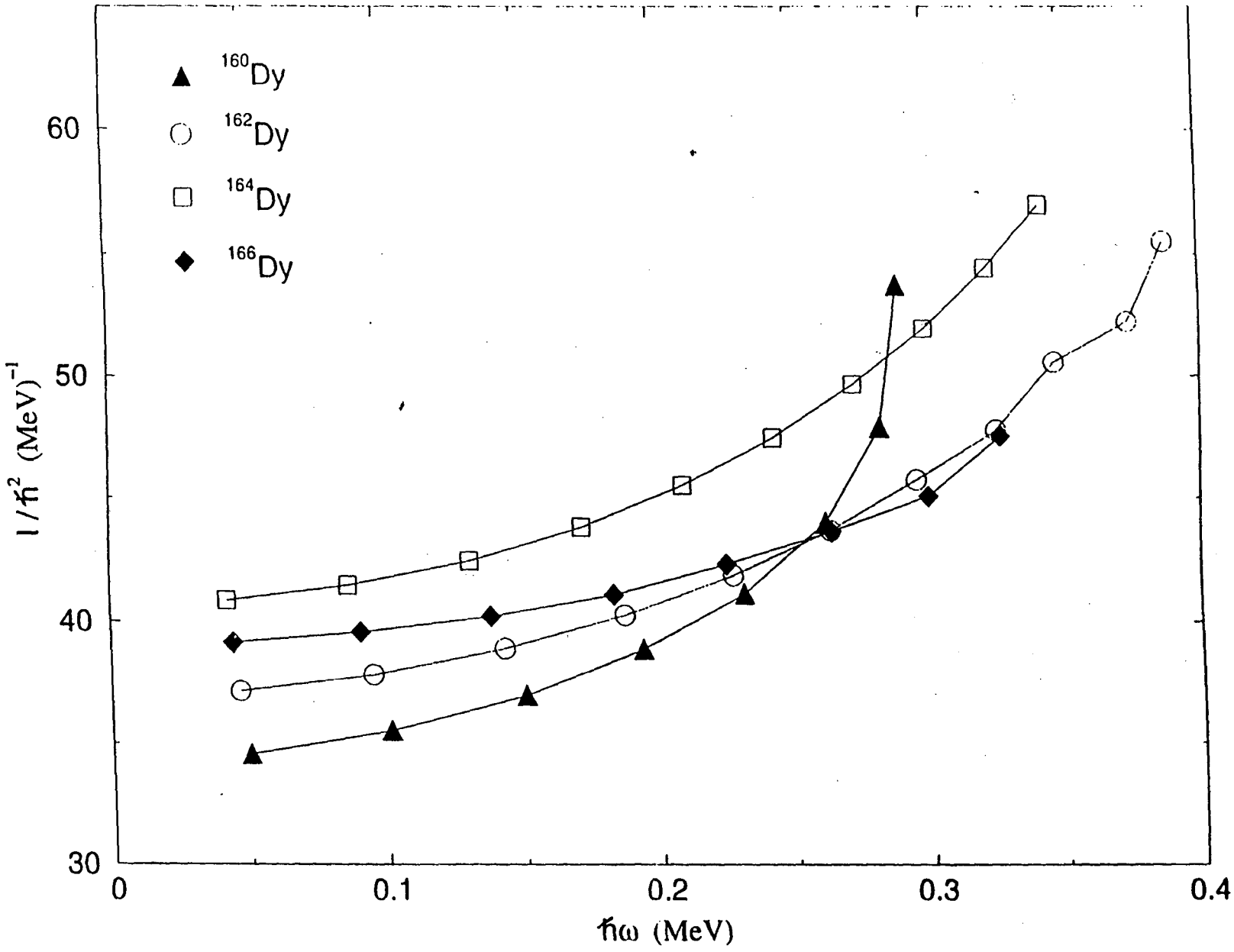
160Dy
162Dy
164Dy
166Dy
60
50
40
30
0
0.1
0.2
0.3
0.4
I / ħ² (MeV)⁻¹
ħω (MeV)

# HEAVY-ION REACTIONS AT THE BARRIER

## SUMMARY

1: Both quasi-elastic transfer and strongly-damped reactions can be used to populate neutron rich nuclei with comparable cross sections.

2: GRETA will allow study of heavy neutron-rich nuclei with 6 neutrons more than the heaviest stable isotope.

3: Quasi-elastic transfer has several advantages over strongly-damped reactions for spectroscopic studies:

- The reaction is more selective and gives cleaner $\gamma$-ray spectra.
- The simple direct reaction mechanism can be used to selectively map single-particle, pairing, and possible cluster modes.

4: H-K resolution sufficient to select temperature and spin distribution of directly-populated states.

5: Neutron halo of weakly-bound neutrons in neutron-rich nuclei provide excellent opportunity for studying neutron pairing via sub-Coulomb transfer reactions. Possible Josephson-type behavior in sub-Coulomb transfer reactions.

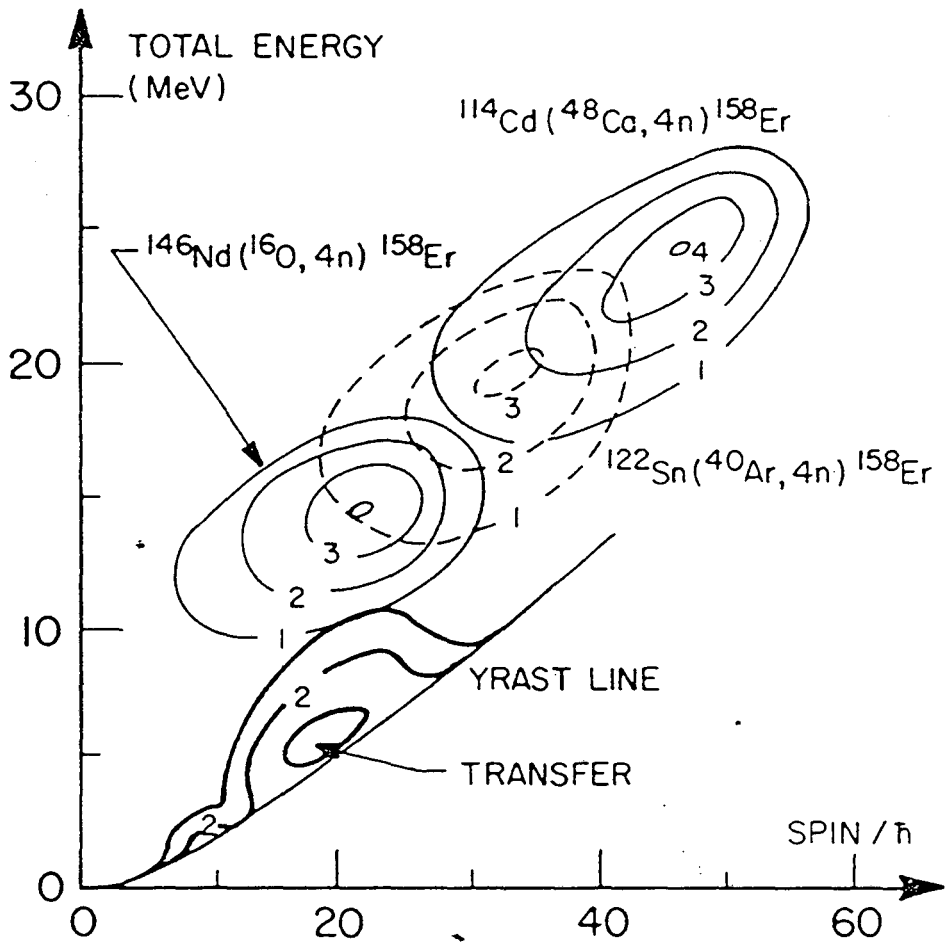


Fig.3-18. Population regions for fusion reactions and heavy-ion induced one-nucleon transfer reacti
leading to rare-earth final nuclei.

# FISSION FRAGMENTATION

Spectroscopic information from SF

● Stable Isotopes

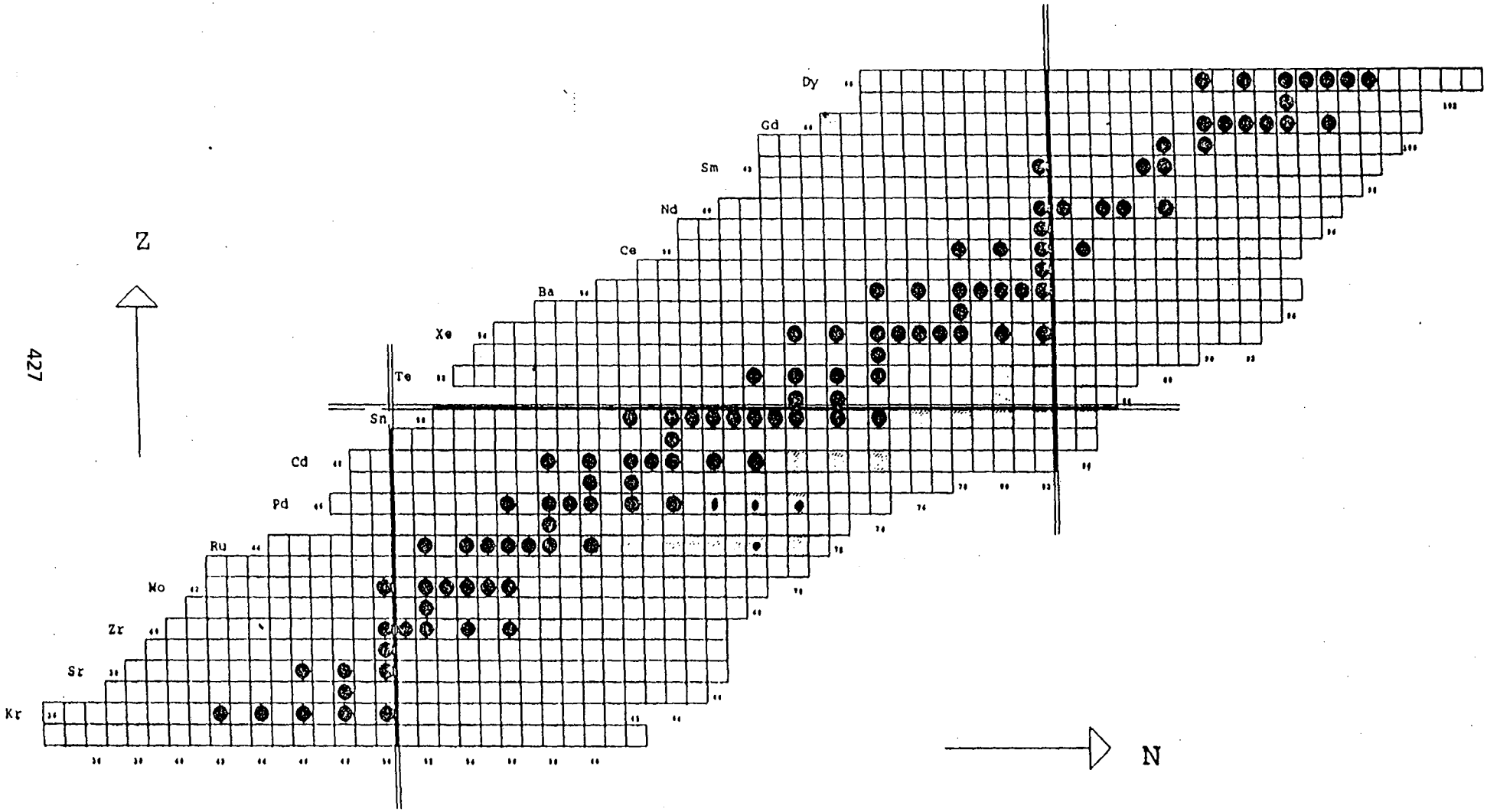

# Spectroscopy of Neutron Rich Nuclei with Fragment Detector (CHICO) and Gammasphere

*University of Rochester*
*Nuclear Structure Research Laboratory**
M. Simon, D. Cline, R. W. Gray, C. Y. Wu

*Lawrence Livermore National Laboratory*
M. A. Stoyer

*Lawrence Berkeley National Laboratory*
S. Asztalos, K. Gregorich, J. Gilat, I. Y. Lee, A. Macchiavelli, R. W. Macleod, K. Vetter

*Purdue University*
*Dept. of Chemistry and Physics*
C. T. Zhang, P. Bhattacharyya

* Supported by the NSF

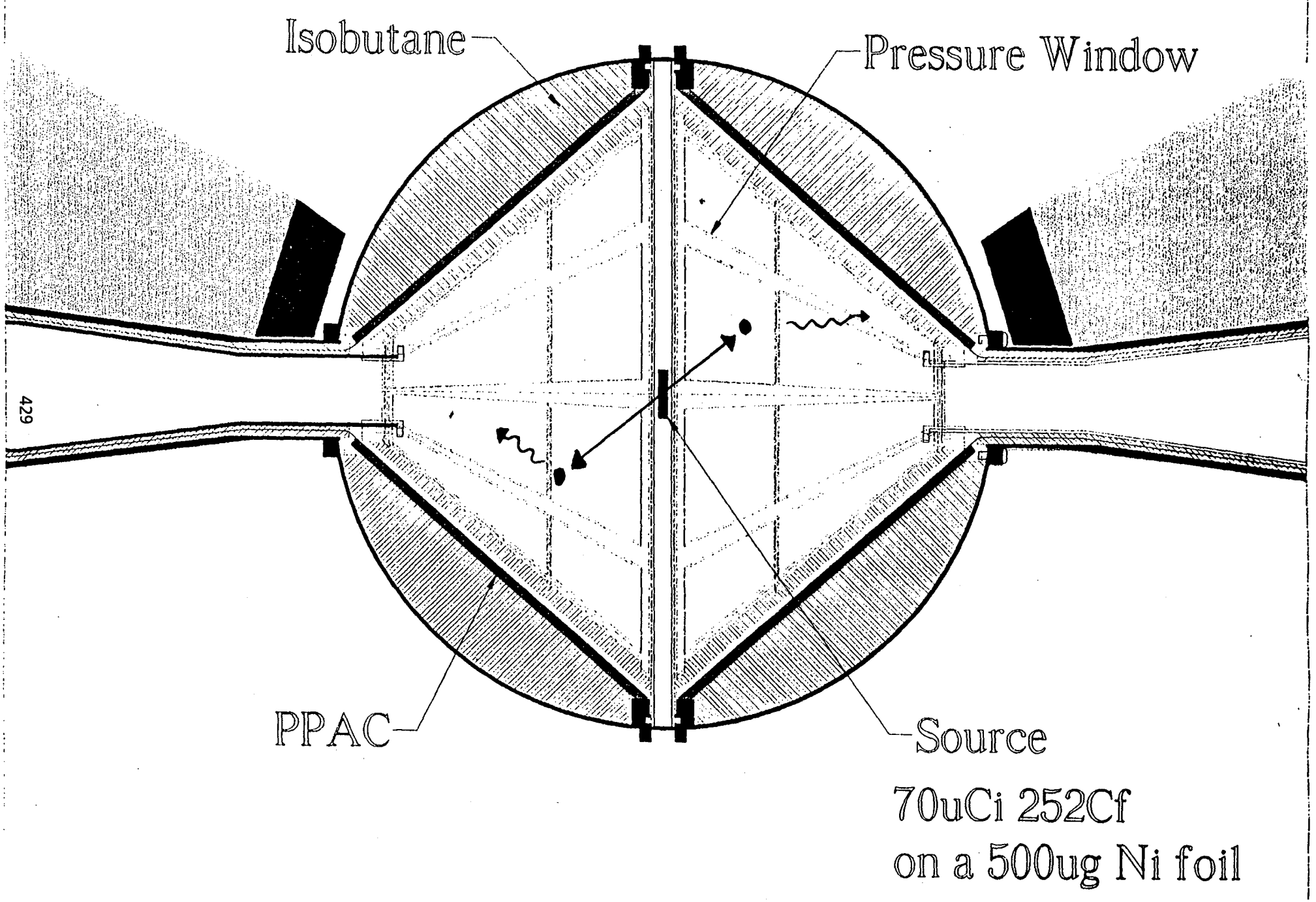
Isobutane
Pressure Window
PPAC
Source
70uCi 252Cf
on a 500ug Ni foil

# ADVANTAGES

## Mass:

- Gate on narrow mass regions

## Timing:

- Discriminate between prompt and delayed γ-ray emission
- Measure lifetimes of isomers
- Discriminate against β-decay events

## Identify γ-ray emitters:

- Doppler shift identifies γ-rays emitted by moving light, heavy and stopped fragments
- Can generate γ-rays cubes for light-light, heavy-heavy, and light-heavy transitions. Also can select γ-rays from moving versus stopped nuclei.

## High-spin spectroscopy:

- Eliminate thick-target Doppler broadened line shapes

## Angular distributions:

- Measure spins and multipolarities

## Lifetimes measurements:

- Isomer lifetimes
- Recoil distance lifetimes

# $^{252}$Cf SF Mass Spectrum

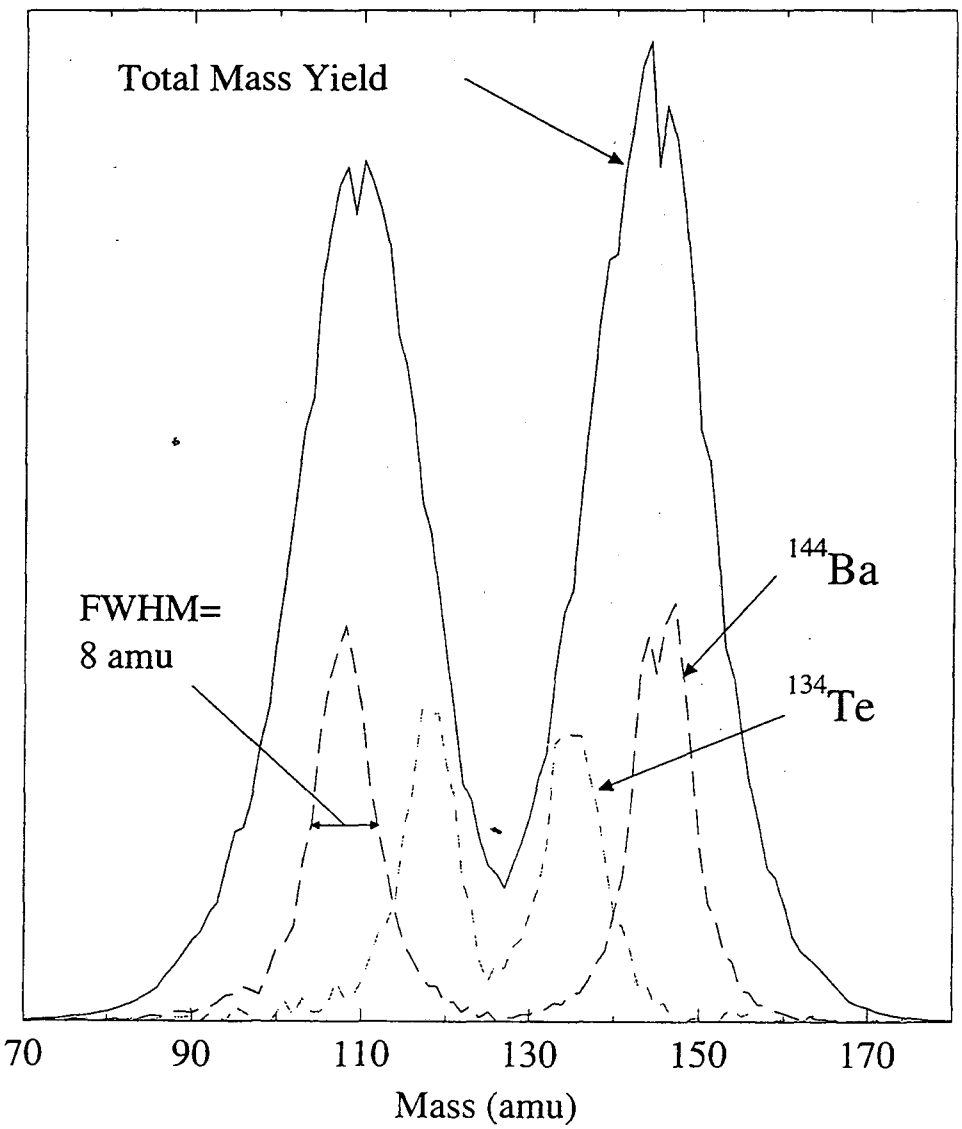

# Light fragment γ–ray

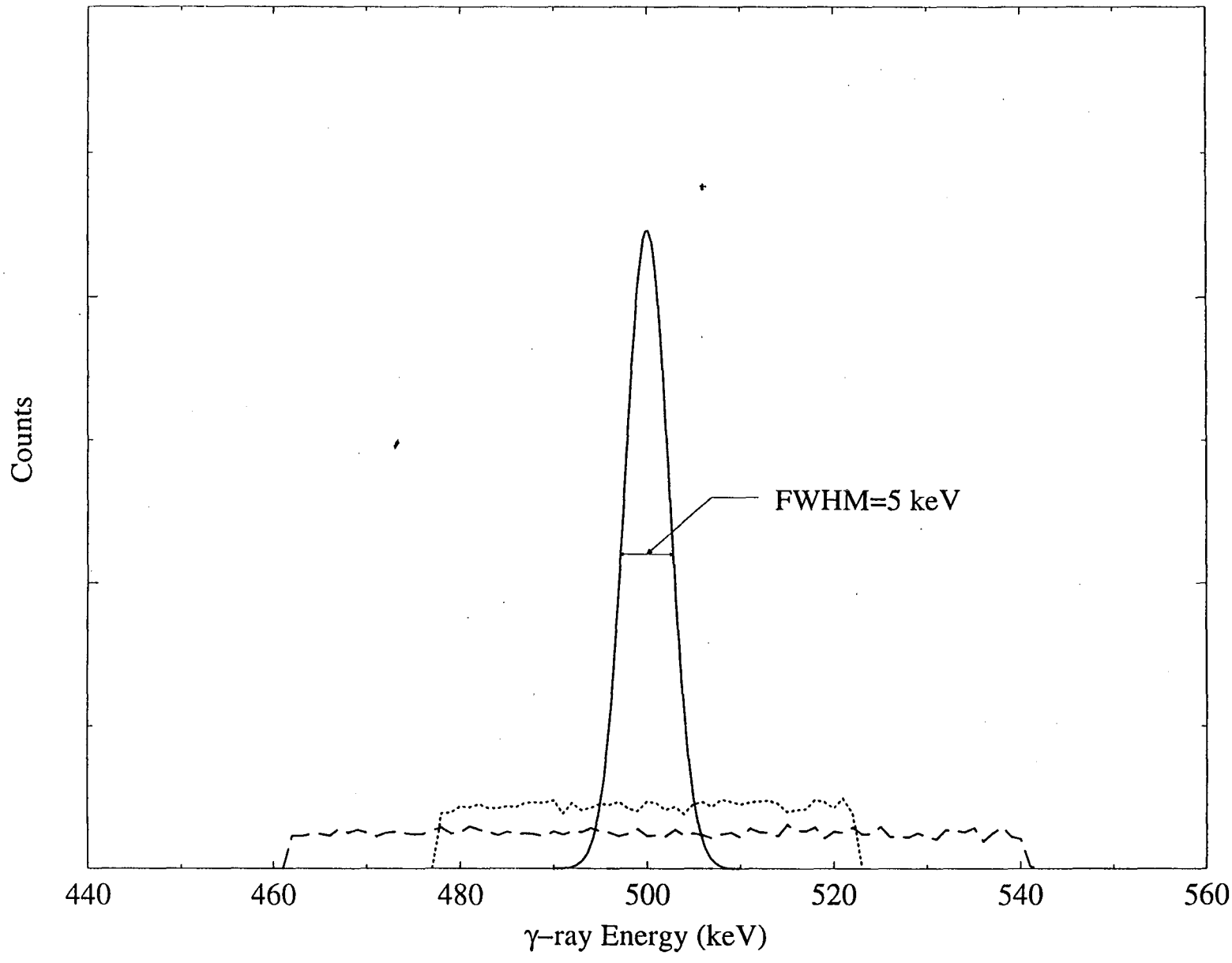

# $^{104}$Mo

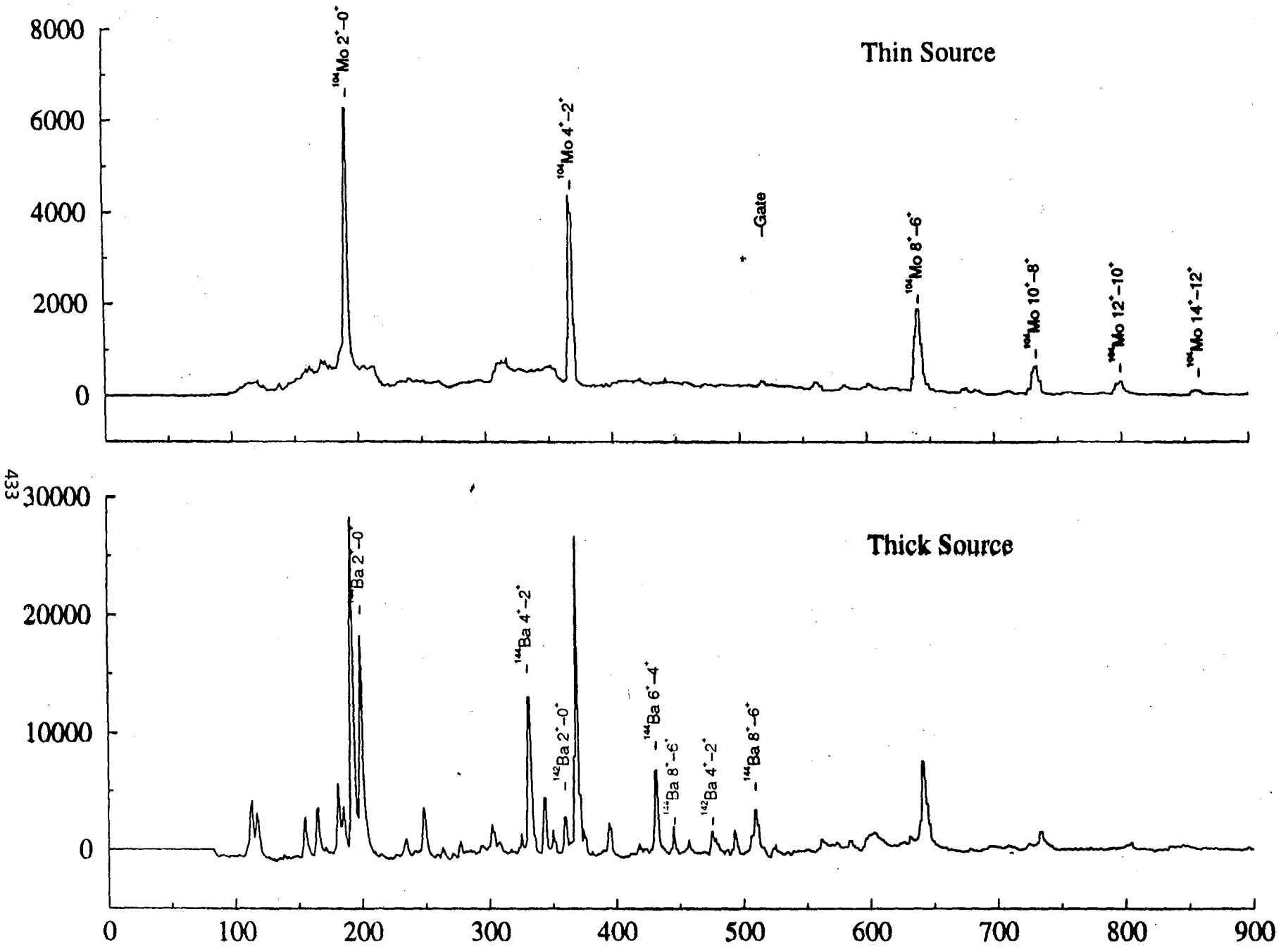
Thin Source
Thick Source
$^{104}$Mo 2$^+$–0$^+$
$^{104}$Mo 4$^+$–2$^+$
Gate
$^{104}$Mo 8$^+$–6$^+$
$^{104}$Mo 10$^+$–8$^+$
$^{104}$Mo 12$^+$–10$^+$
$^{104}$Mo 14$^+$–12$^+$
$^{144}$Ba 2$^+$–0$^+$
$^{144}$Ba 4$^+$–2$^+$
$^{142}$Ba 2$^+$–0$^+$
$^{144}$Ba 6$^+$–4$^+$
$^{142}$Ba 8$^+$–6$^+$
$^{142}$Ba 4$^+$–2$^+$
$^{144}$Ba 8$^+$–6$^+$
8000
6000
4000
2000
0
30000
20000
10000
0
0
100
200
300
400
500
600
700
800
900

# $^{104}$Mo

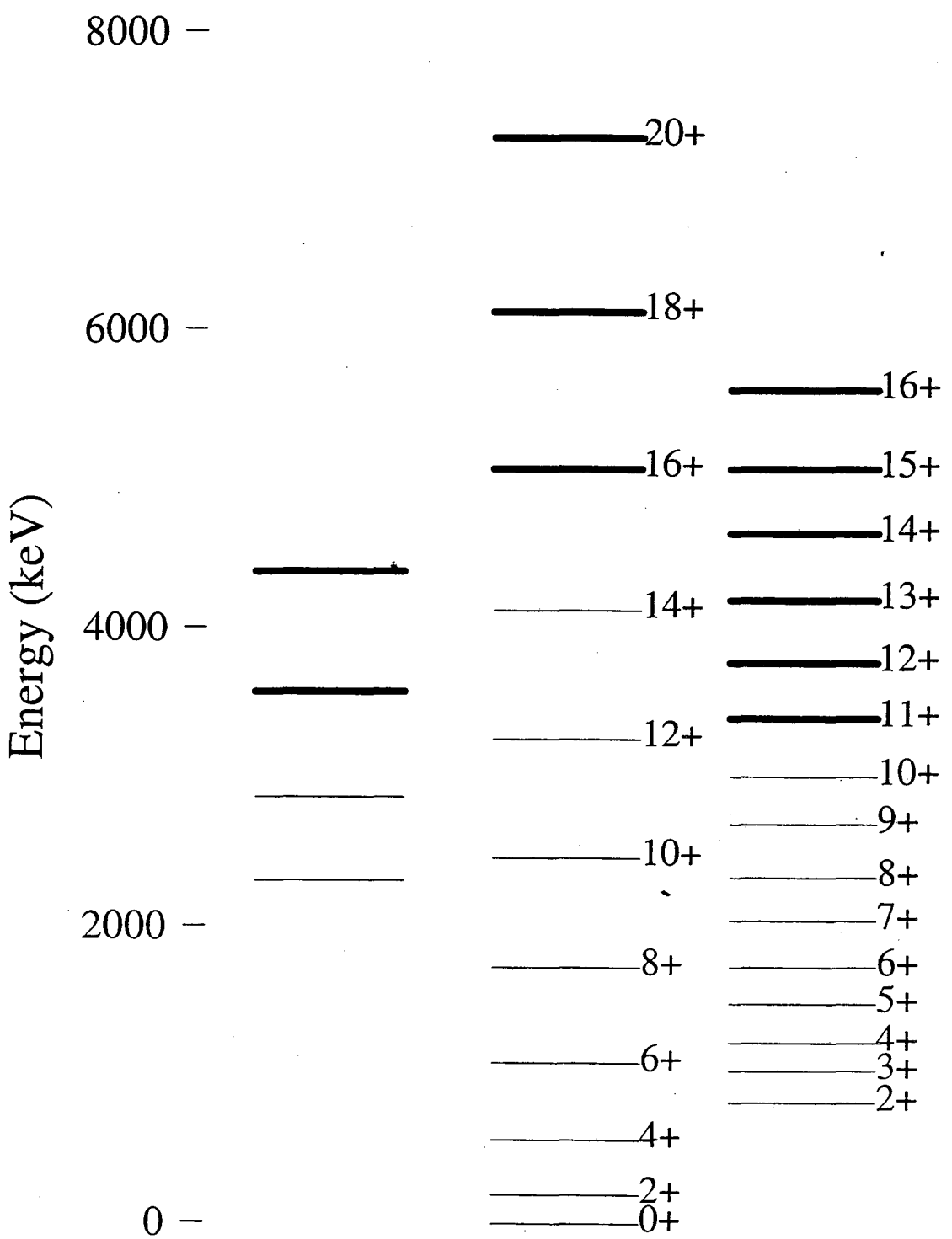
Energy (keV)
8000
6000
4000
2000
0
20+
18+
16+
14+
12+
10+
8+
6+
4+
2+
0+
16+
15+
14+
13+
12+
11+
10+
9+
8+
7+
6+
5+
4+
3+
2+

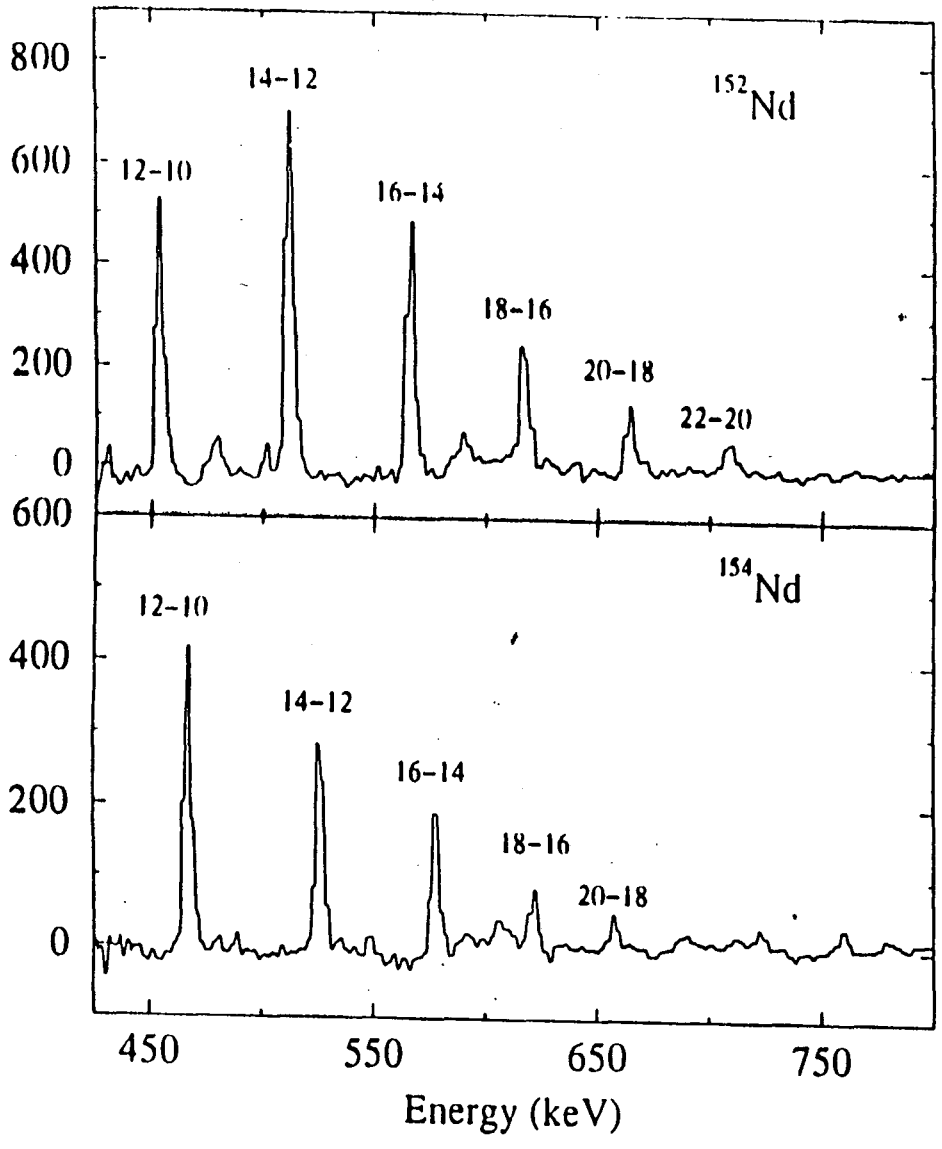


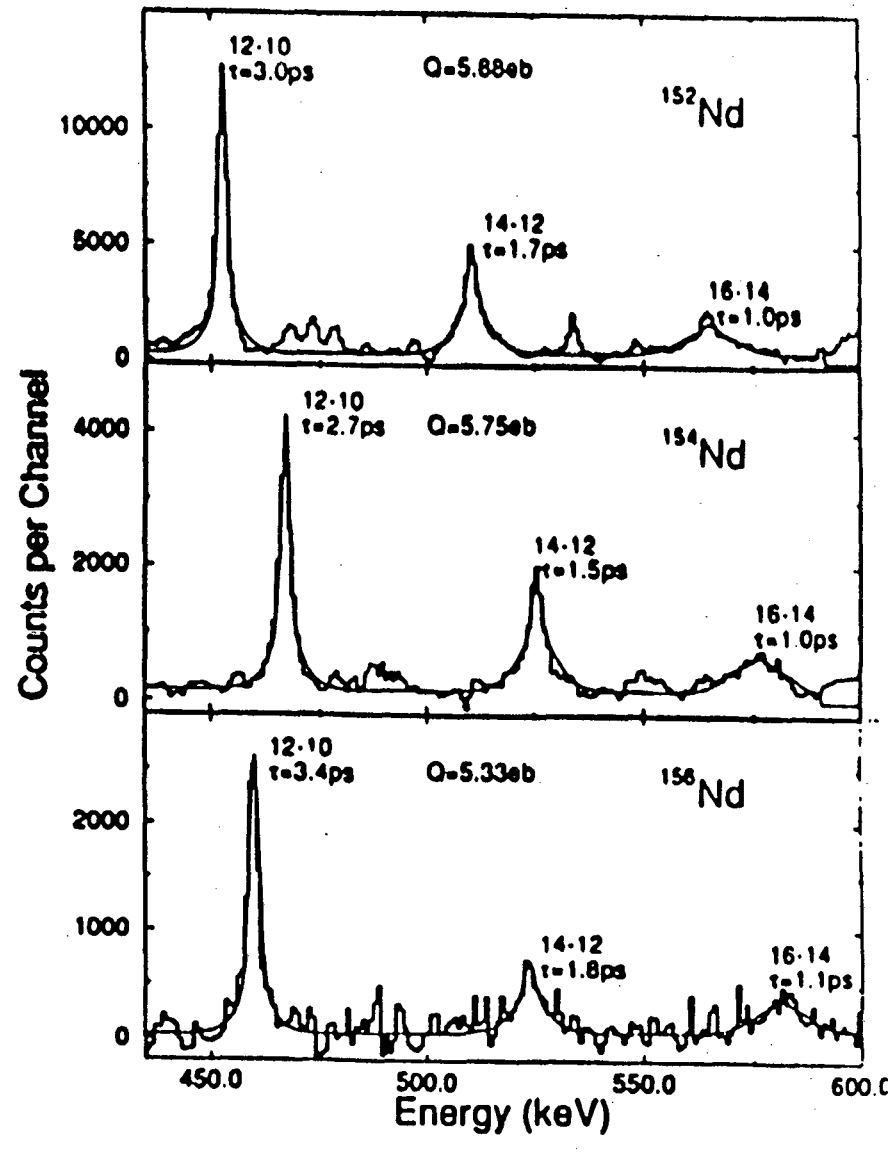


A.G.Smith et al. PRLv73 1994 p2540

# $^{112}$Ru

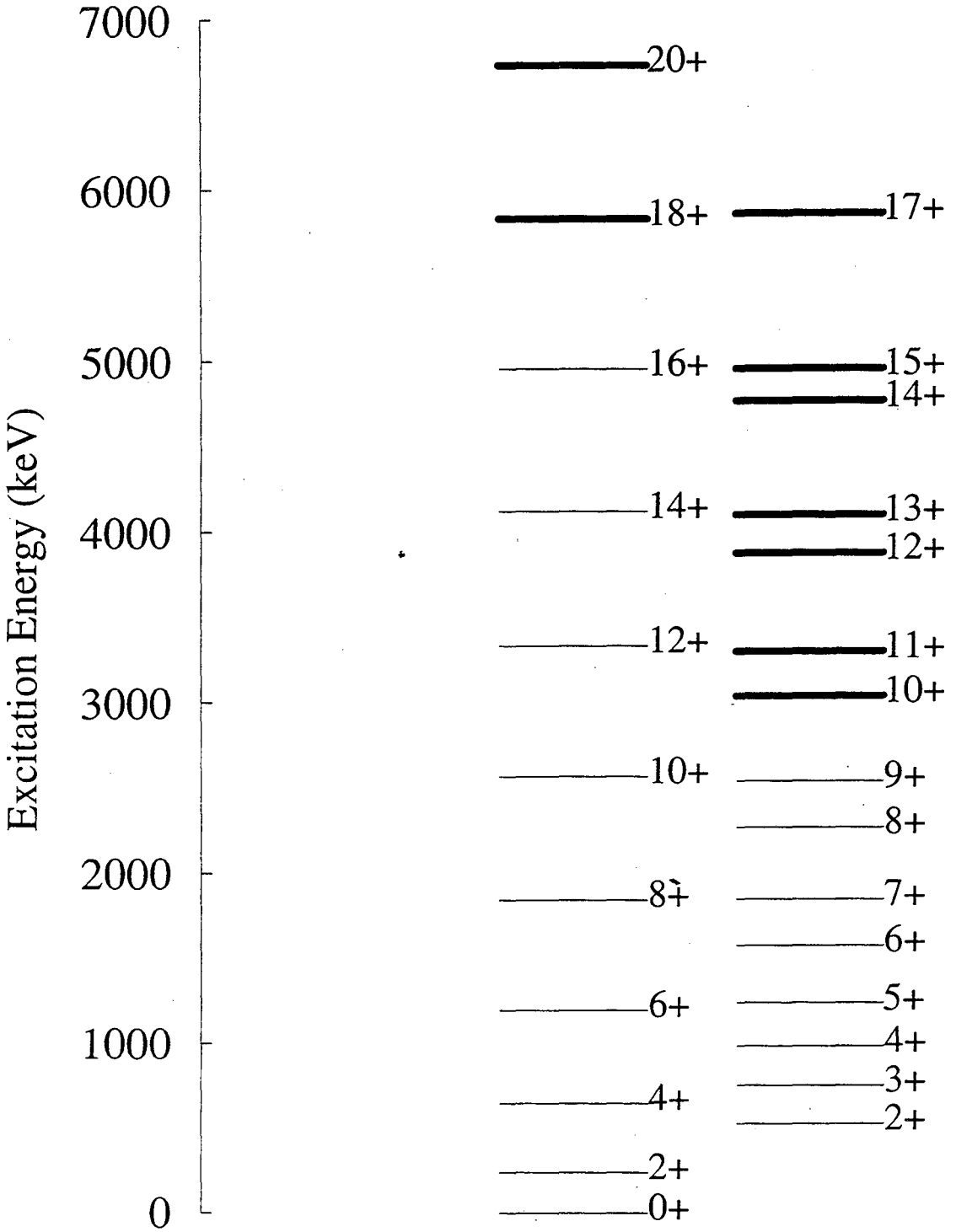
Excitation Energy (keV)
7000
6000
5000
4000
3000
2000
1000
0
20+
18+
16+
14+
12+
10+
8+
6+
4+
2+
0+
17+
15+
14+
13+
12+
11+
10+
9+
8+
7+
6+
5+
4+
3+
2+

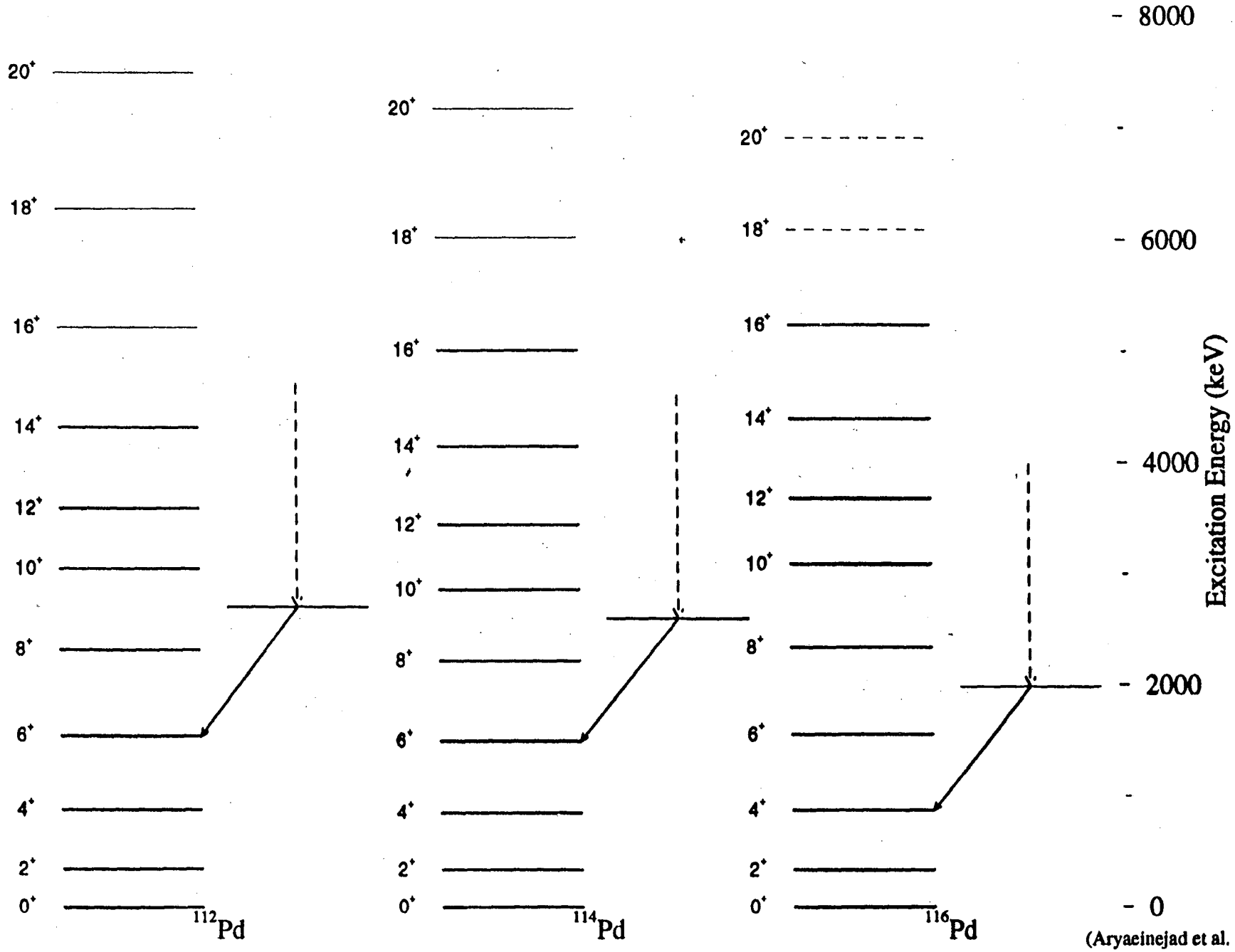


(Aryaeinejad et al.
PRC 48, p. 566)
(Zhu et al.) 1995

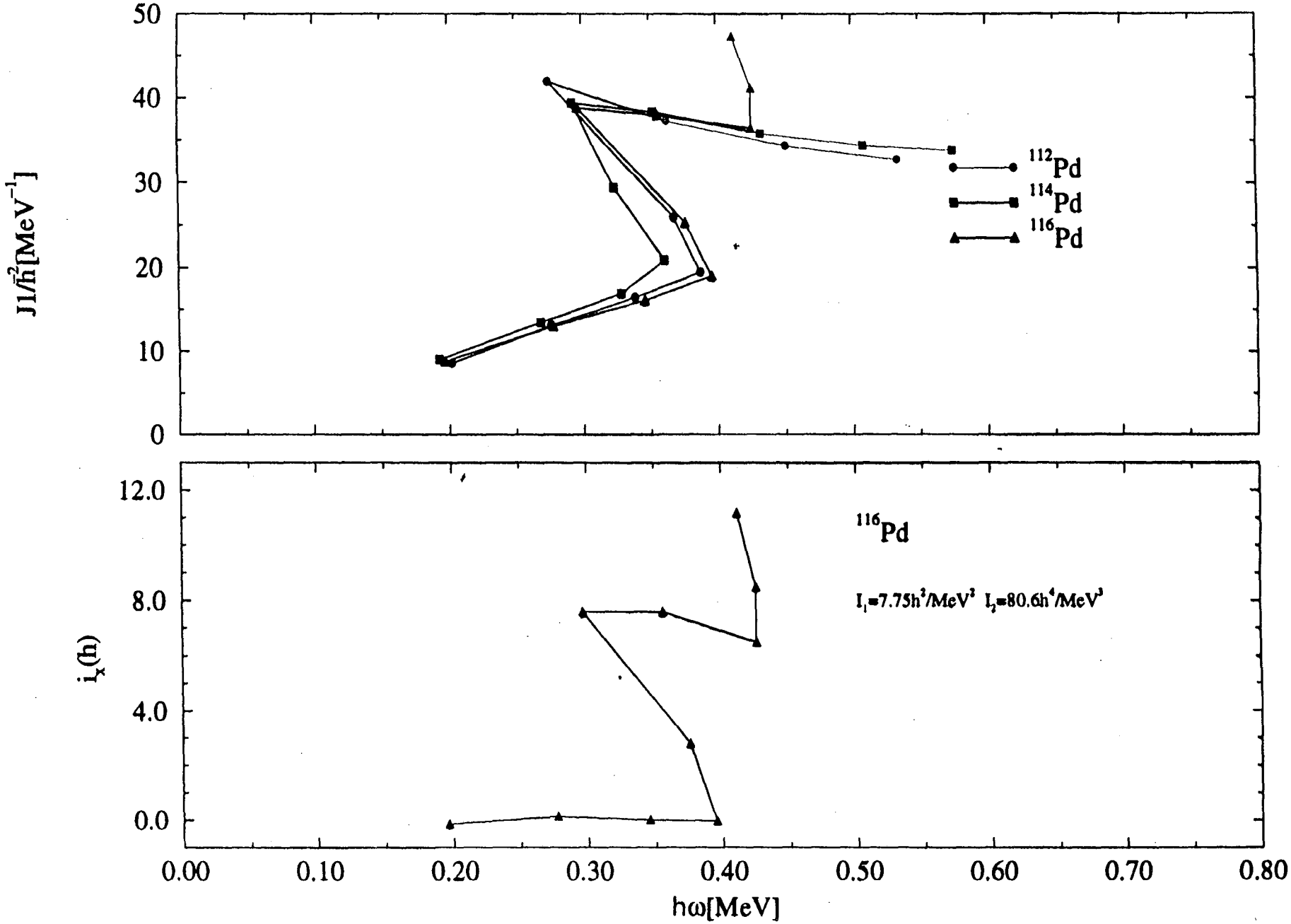
50
40
30
20
10
0
$J1/\hbar^2[MeV^{-1}]$
$^{112}Pd$
$^{114}Pd$
$^{116}Pd$
12.0
8.0
4.0
0.0
$i_x(\hbar)$
$^{116}Pd$
$I_1=7.75\hbar^2/MeV^2$ $I_2=80.6\hbar^4/MeV^3$
0.00
0.10
0.20
0.30
0.40
0.50
0.60
0.70
0.80
$\hbar\omega$[MeV]

# $^{144}$Ba

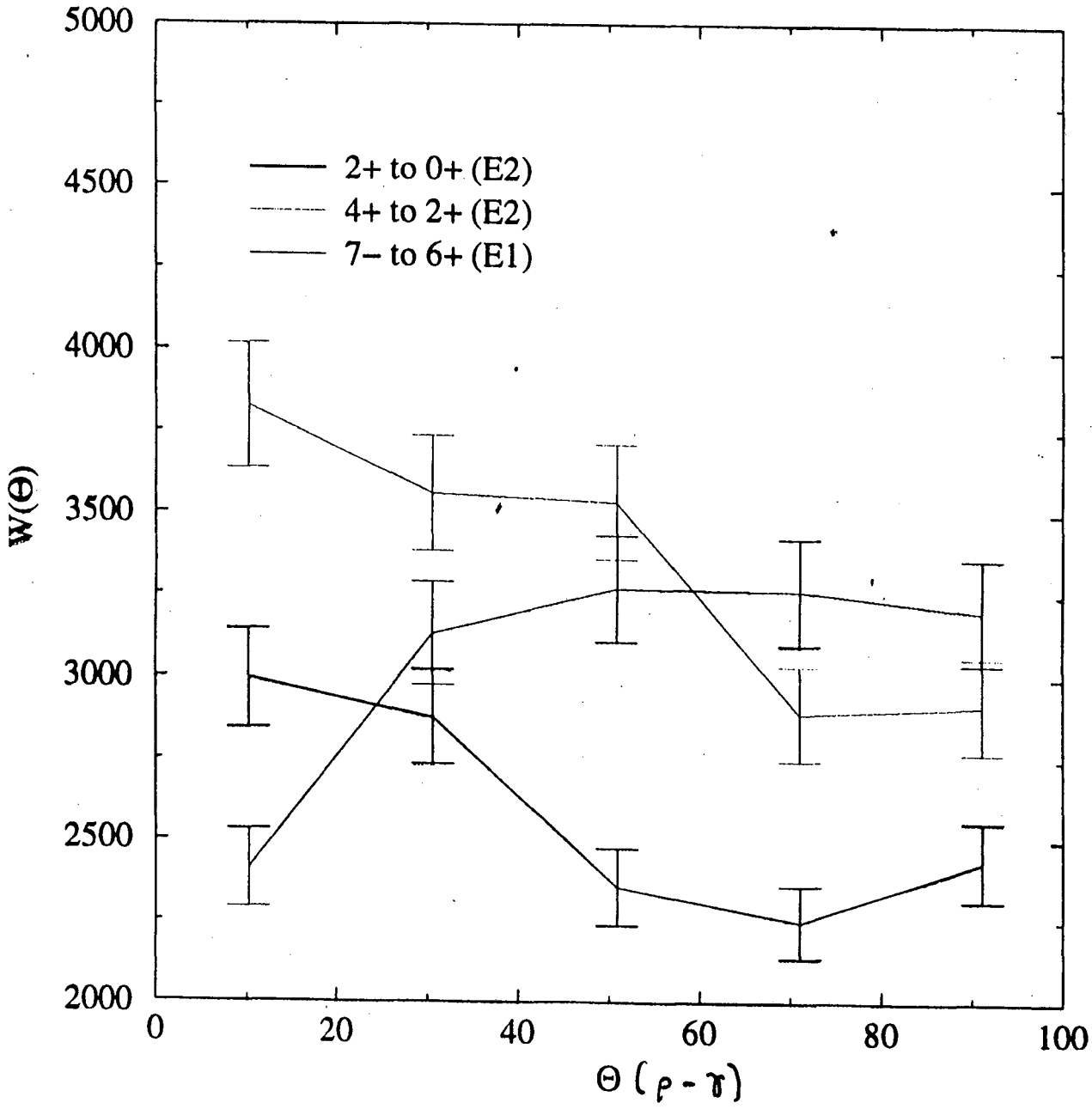
2+ to 0+ (E2)
4+ to 2+ (E2)
7− to 6+ (E1)
W(Θ)
Θ (ρ - γ)
5000
4500
4000
3500
3000
2500
2000
0
20
40
60
80
100

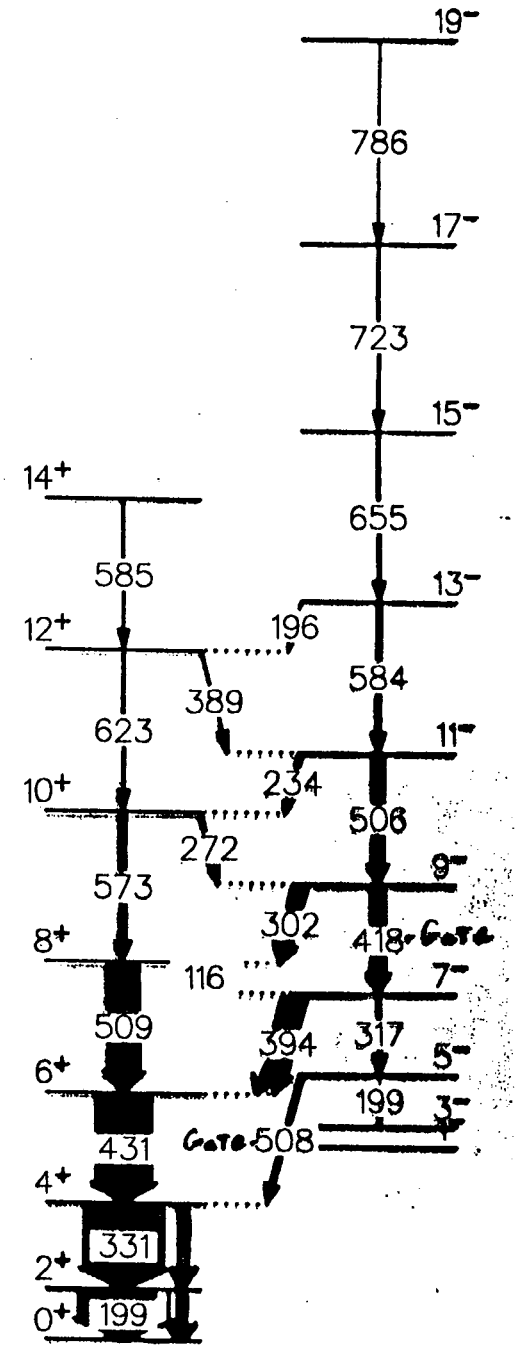
19−
786
17−
723
15−
655
13−
584
11−
506
9−
418
Gate
7−
317
5−
199
3−
Gate 508
14+
585
12+
623
10+
573
8+
509
6+
431
4+
331
2+
0+
199
196
389
234
272
302
116
394

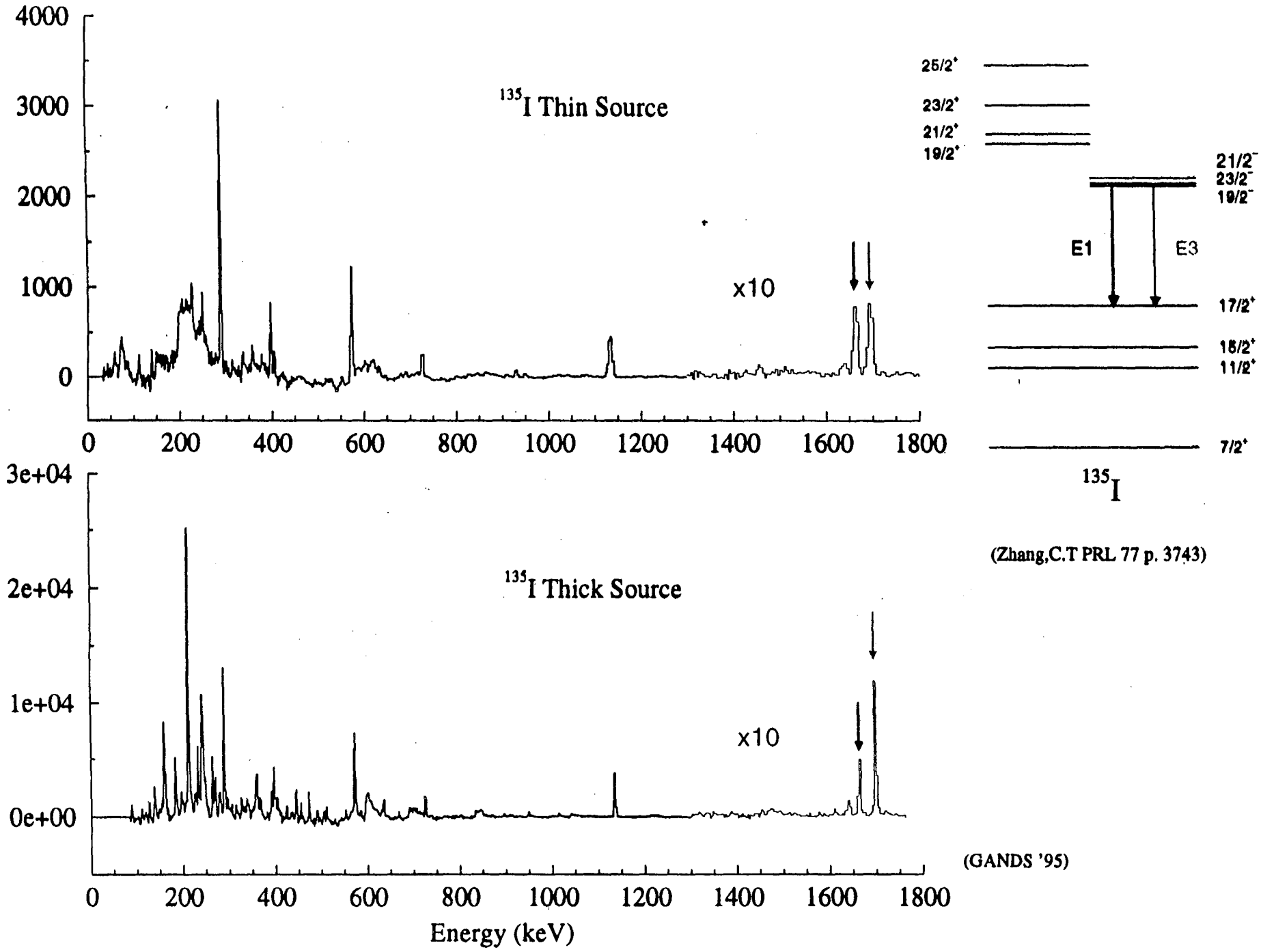
4000
3000
2000
1000
0
$^{135}$I Thin Source
x10
0
200
400
600
800
1000
1200
1400
1600
1800
3e+04
2e+04
1e+04
0e+00
$^{135}$I Thick Source
x10
Energy (keV)
25/2+
23/2+
21/2+
19/2+
21/2-
23/2-
19/2-
E1
E3
17/2+
15/2+
11/2+
7/2+
$^{135}$I
(Zhang,C.T PRL 77 p. 3743)
(GANDS '95)

# Fission fragment opportunities with GRETA

## Nuclear spectroscopy of neutron-rich nuclei

- Spectroscopy of neutron-rich nuclei up to 14 neutrons beyond stability.
- Nuclear spectroscopy above spin 20
- Study collective and single-particle structure
- Measure spins, multipolarities, polarization of $\gamma$ transitions
- RDM lifetime measurements
- Isomers

## Reaction induced fission:

- Can enhance mass region of interest,
  e.g. enhance $^{132}$Sn population ten fold
- Higher intrinsic excitation
- Allow use of less radioactive targets

## Fission dynamics

- Neutron emission, zero-neutron decay
- Mass and excitation energy distributions
- Ternary fission, exotic decay modes

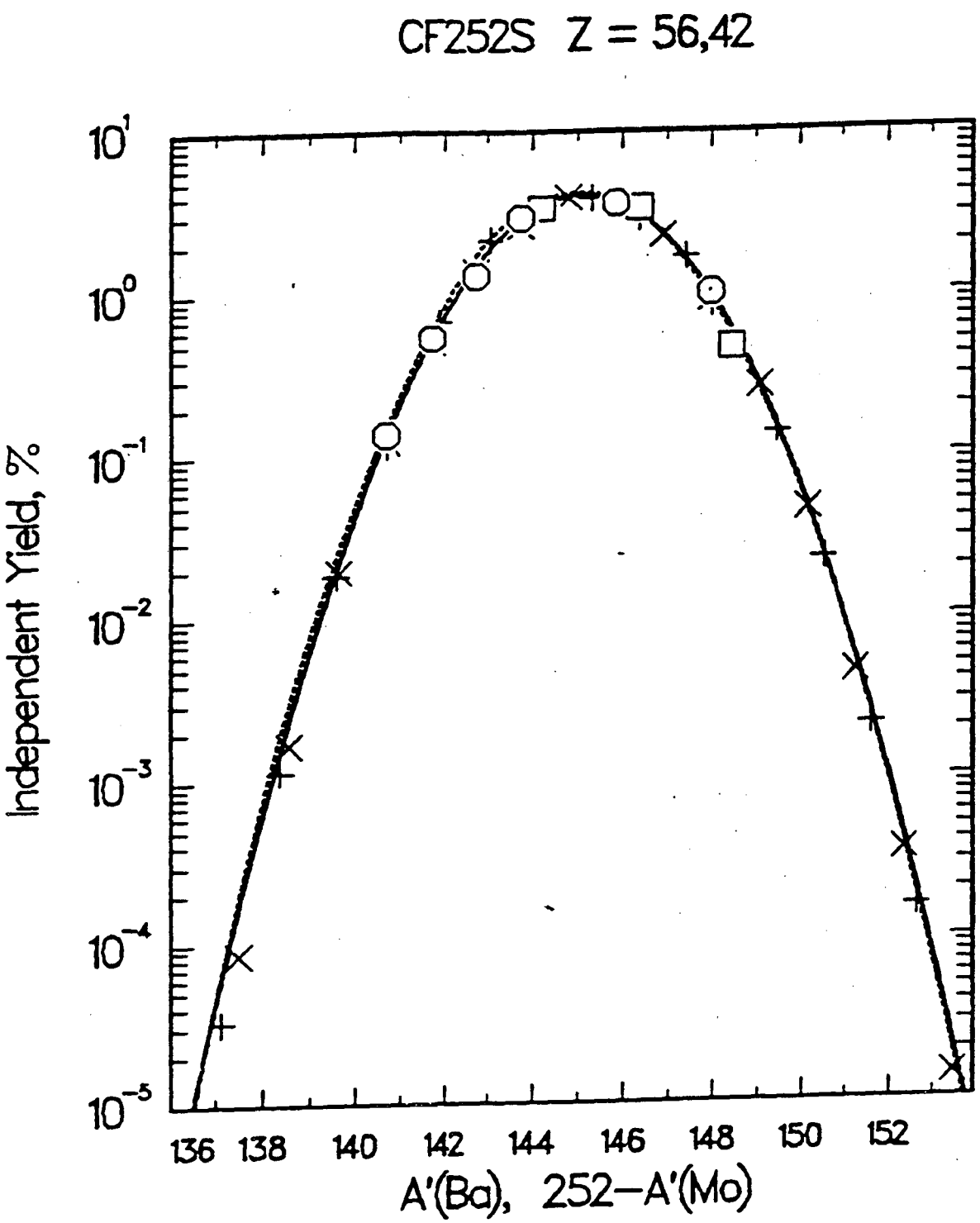
CF252S Z = 56,42
Independent Yield, %
$10^{1}$
$10^{0}$
$10^{-1}$
$10^{-2}$
$10^{-3}$
$10^{-4}$
$10^{-5}$
136 138 140 142 144 146 148 150 152
A'(Ba), 252−A'(Mo)

# CONCLUSIONS

## GRETA

- Will provide a considerable advance in sensitivity for study of neutron-rich nuclei.
    - Complete correction for Doppler effect.
    - Much better peak/Compton ratio
    - Much higher peak detection efficiency.
    - Better H and K resolution

## Heavy-ion transfer reactions:

- Possible to exploit heavy-ion induced transfer reactions to probe heavy neutron rich nuclei up to 6 neutrons beyond stability.
- Map single-particle, pairing and possible cluster modes in neutron-rich nuclei to beyond spin 20.
- Selective population of states as function of spin and temperature

## Fission fragmentation:

- Nuclear structure to beyond spin 20 in neutron-rich medium-mass nuclei with up to 14 neutrons beyond stability.
- Study fission dynamics, exotic decay modes

## Auxiliary detectors:

- Important component of the GRETA facility

S.Freedman
Weak interactions.

# WEAK INTERACTIONS

(~~Exploiting~~ Capitalizing on* GRETA)

## Outline:

§ Misuses of Gammasphere

- $^{10}C$ $\beta$-decay
- $^{22}Na$ $\beta$-$\gamma$ correlation
- Positronium decay

## Themes:

§ GRETA vs Gammasphere

§ New ideas and unique capabilities

* DOE official term.

ft values of $0^+ \to 0^+$ superallowed β-decays corrected for electromagnetic effects

$$\mathcal{F}t(0^+\to 0^+) = ft(1+\delta_R)(1-\delta_C) = \frac{2\pi^2 \log 2\ \hbar^7}{2G^2 g_V^2 \cos^2\theta_C\ m_e^5 c^4}$$

$$M_F^2 = 2(1-\delta_C)$$

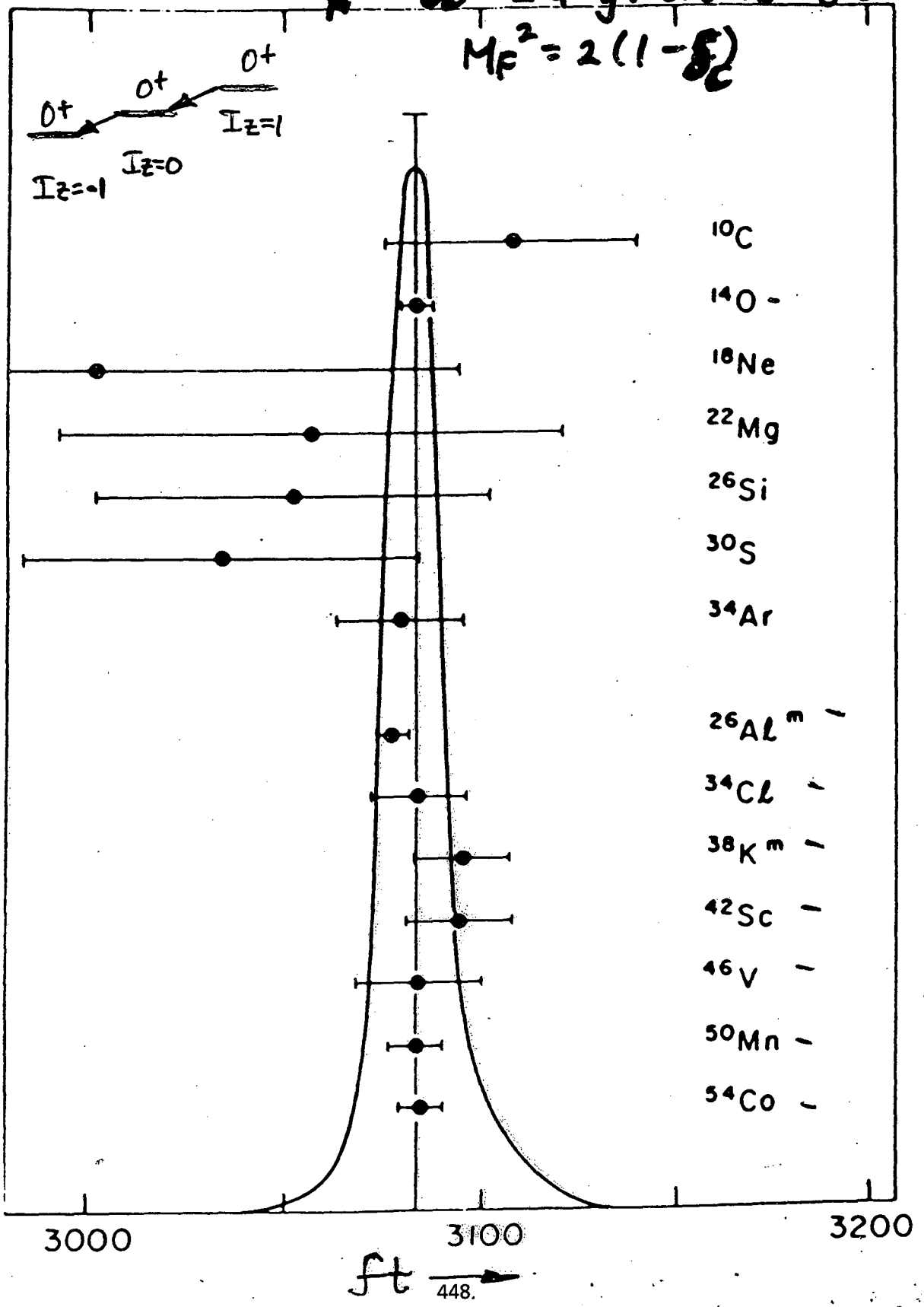

# CKM Matrix

## Weak Quark Mixing

$$\begin{pmatrix} u \\ d \end{pmatrix} \qquad \begin{pmatrix} c \\ s \end{pmatrix} \qquad \begin{pmatrix} t \\ b \end{pmatrix}$$

$$\begin{pmatrix} d' \\ s' \\ b' \end{pmatrix} = \begin{pmatrix} V_{ud} & V_{us} & V_{ub} \\ V_{cd} & V_{cs} & V_{cb} \\ V_{td} & V_{ts} & V_{tb} \end{pmatrix} \begin{pmatrix} d \\ s \\ b \end{pmatrix}$$

## Weak Lepton Mixing

$$\begin{pmatrix} e^- \\ \nu_e \end{pmatrix} \qquad \begin{pmatrix} \mu^- \\ \nu_\mu \end{pmatrix} \qquad \begin{pmatrix} \tau^- \\ \nu_\tau \end{pmatrix}$$

$$\begin{pmatrix} \nu_e \\ \nu_\mu \\ \nu_\tau \end{pmatrix} = \begin{pmatrix} U_{e1} & U_{e2} & U_{e3} \\ U_{\mu 1} & U_{\mu 2} & U_{\mu 3} \\ U_{\tau 1} & U_{\tau 2} & U_{\tau 3} \end{pmatrix} \begin{pmatrix} \nu_1 \\ \nu_2 \\ \nu_3 \end{pmatrix}$$

$$\mu^+ \to e^+ + \nu_e + \overline{\nu}_\mu$$

$$G_V = G_F \equiv G_\mu$$

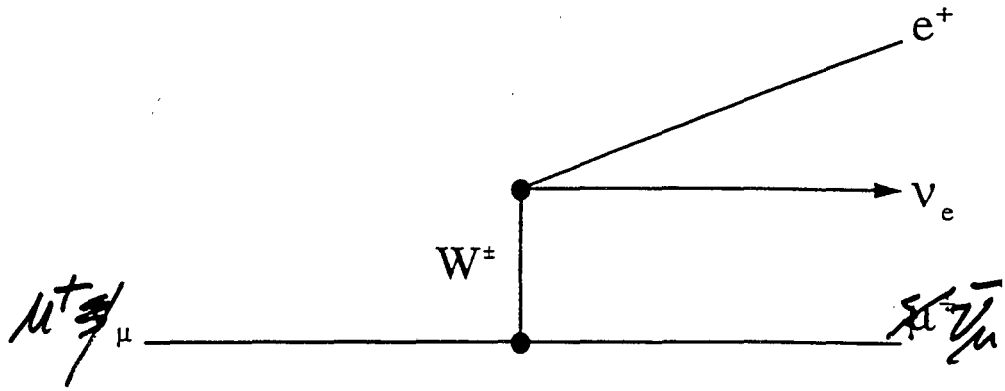


$$\Delta S = 0$$

$$\pi^+ \to \pi^0 + e^+ + \nu_e$$

$$G_V = G_F |V_{ud}| = G_F \cos\theta_C$$

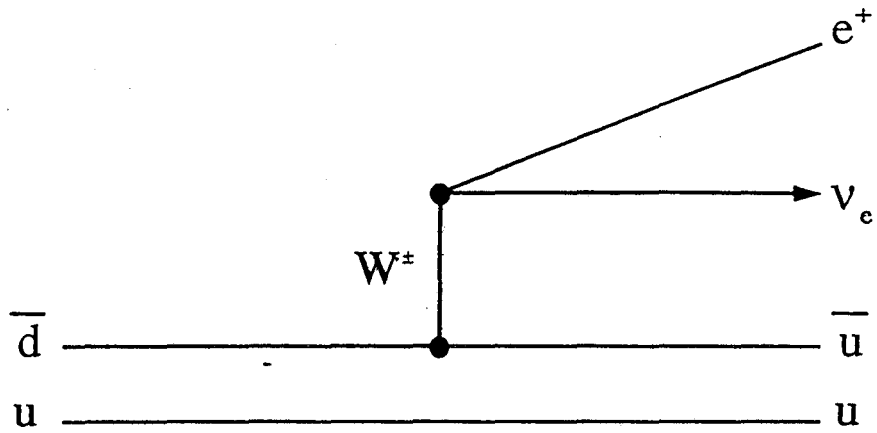


$$\Delta S = 1$$

$$K^+ \to \pi^0 + e^+ + \nu_e$$

$$G_V = G_F |V_{us}| = G_F \sin\theta_C$$

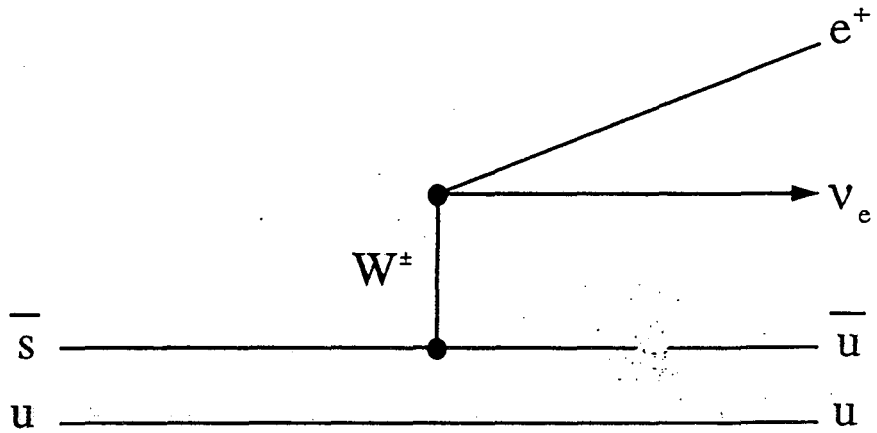


$$B^+ \to \pi^0 + e^+ + \nu_e$$

$$G_V = G_F |V_{ub}|$$

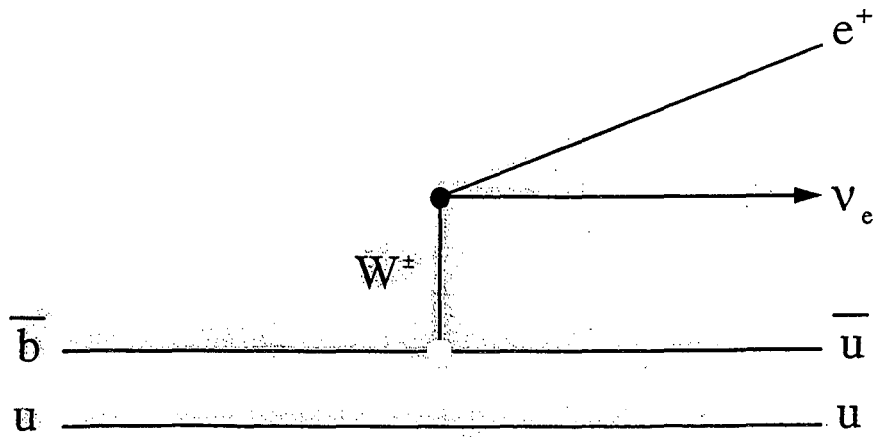

# $^{10}C$ Beta Decay

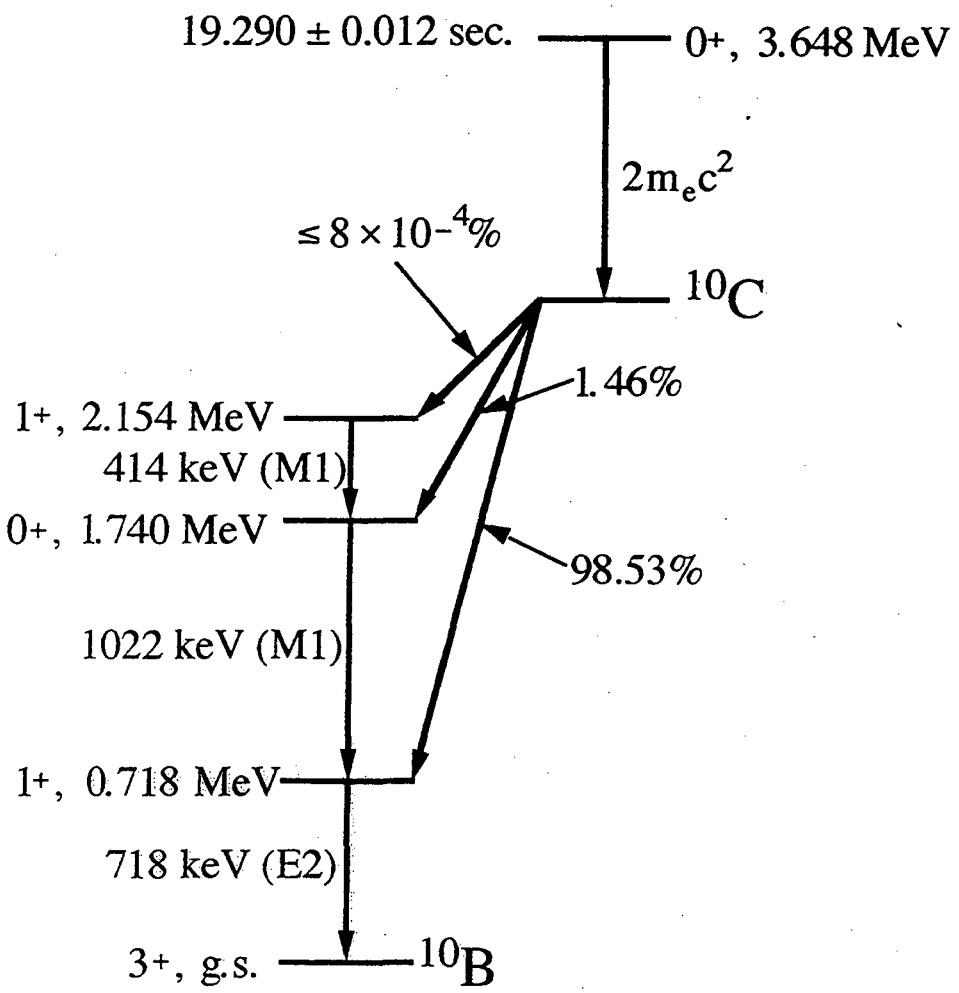

# Determination of the u-d CKM Matrix Element with Superallowed Fermi Decays

$$\begin{pmatrix} d' \\ s' \\ b' \end{pmatrix} = \begin{pmatrix} V_{ud} & V_{us} & V_{ub} \\ V_{cd} & V_{cs} & V_{cb} \\ V_{td} & V_{ts} & V_{tb} \end{pmatrix} \begin{pmatrix} d \\ s \\ b \end{pmatrix}$$

$$|V_{ud}|^2 = \frac{G_V^2\left(1-\Delta_R^V\right)}{G_F^2}$$

quark level correction $(2.40 \pm 0.08)\%$

$$G_V^2 = \frac{K}{2Ft}$$

$$Ft \equiv ft\left(1+\delta_R\right)\left(1-\delta_C\right)$$

Fermi function. Coulomb correction

nuclear charge dependent corrections

ordinary "radiative" corrections

$0^+$ $0^+$ $0^+$

$T=1$

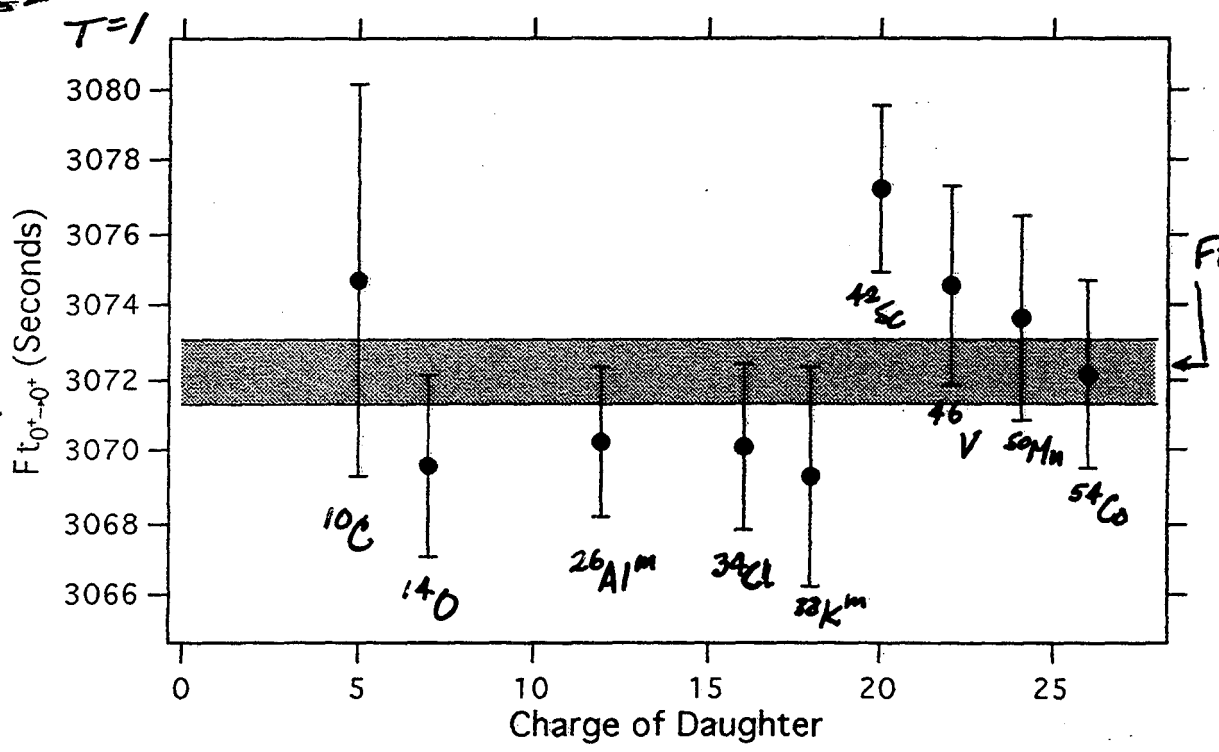


$Ft = 3072.3 \pm 1.05$

$V_{us} = 0.2205 \pm 0.0018$ $K_{e3}$, Hyperon decay

$V_{ub} = 0.0032 \pm 0.0009$ $\beta$-decay

$|V_{ud}|^2 + |V_{us}|^2 + |V_{ub}|^2 = 0.9972 \pm 0.0013$ (or worse)

# Radiative Corrections

$$1 + \Delta_R = \left(1 + \delta_R\right)\left(1 + \Delta_R^V\right)$$

$$1 + \Delta_R^V = \left\{1 + \frac{\alpha}{2\pi}\left[\ln\frac{m_p}{m_A} + 2C_{Born}\right] + \frac{\alpha(m_p)}{2\pi}\left[\bar{g}(E, E_0) + A_g\right]\right\} \times S(m_p, m_Z)\left\{1 - \frac{\alpha}{2\pi}\bar{g}(E, E_0)\right\}$$

$$\Delta_R^V = \left(2.40 \pm 0.08\right) \times 10^{-2}$$

$$1 + \delta_R = 1 + \frac{\alpha}{2\pi}\left[\bar{g}(E, E_0) + \delta_2 + \delta_3 + 2C_{NS}\right]$$

$$C = C_{Born} + C_{NS}$$

$C_{NS}$ Towner

Barker, Brown, Jaus, & Rasche

| Nuclei | Towner (no quenching) | Barker (no quenching) | Towner (quenching) | Barker (quenching) |
|---|---|---|---|---|
| $^{10}C$ | -1.67±0.20 | -1.72±0.22 | -1.35±0.16 | -1.43±0.18 |
| $^{14}O$ | -1.15±0.30 | -1.42±0.22 | -0.88±0.23 | -1.18±0.22 |
| $^{26}Al^m$ | 0.25±0.05 | 0.43±0.09 | 0.20±0.04 | 0.36±0.09 |
| $^{34}Cl$ | -0.17±0.06 | -0.13±0.09 | -0.13±0.05 | -0.11±0.09 |
| $^{38}K^m$ | -0.10±0.10 | -0.09±0.09 | -0.09±0.09 | -0.07±0.09 |
| $^{42}Sc$ | 0.50±0.10 | 0.60±0.04 | 0.40±0.07 | 0.50±0.04 |
| $^{46}V$ | 0.16±0.03 | 0.30±0.09 | 0.14±0.03 | 0.25±0.09 |
| $^{50}Mn$ | 0.16±0.03 | 0.30±0.09 | 0.14±0.03 | 0.25±0.09 |
| $^{54}Co$ | 0.20±0.03 | 0.34±0.09 | 0.17±0.03 | 0.29±0.09 |

THH : Towner, Hardy, & Harvey (WS + SM)
OB : Ormand & Brown (HF + SM)
SGII : Sagawa, Van Giai, & Suzuki (HF + RPA)

| Nuclei | $100\times\delta_c$(THH) | $100\times\delta_c$(OB) | $100\times\delta_c$(SGII) |
|---|---|---|---|
| $^{10}C$ | 0.18(10) | 0.15(9) | 0.00 |
| $^{14}O$ | 0.28(10) | 0.15(9) | 0.29 |
| $^{26}Al^m$ | 0.33(11) | 0.30(9) | 0.27 |
| $^{34}Cl$ | 0.64(12) | 0.57(9) | 0.33 |
| $^{38}K^m$ | 0.64(12) | 0.59(9) | 0.33 |
| $^{42}Sc$ | 0.39(12) | 0.42(9) | 0.44 |
| $^{46}V$ | 0.45(12) | 0.38(9) | na |
| $^{50}Mn$ | 0.47(13) | 0.35(9) | na |
| $^{54}Co$ | 0.61(12) | 0.44(9) | 0.49 |

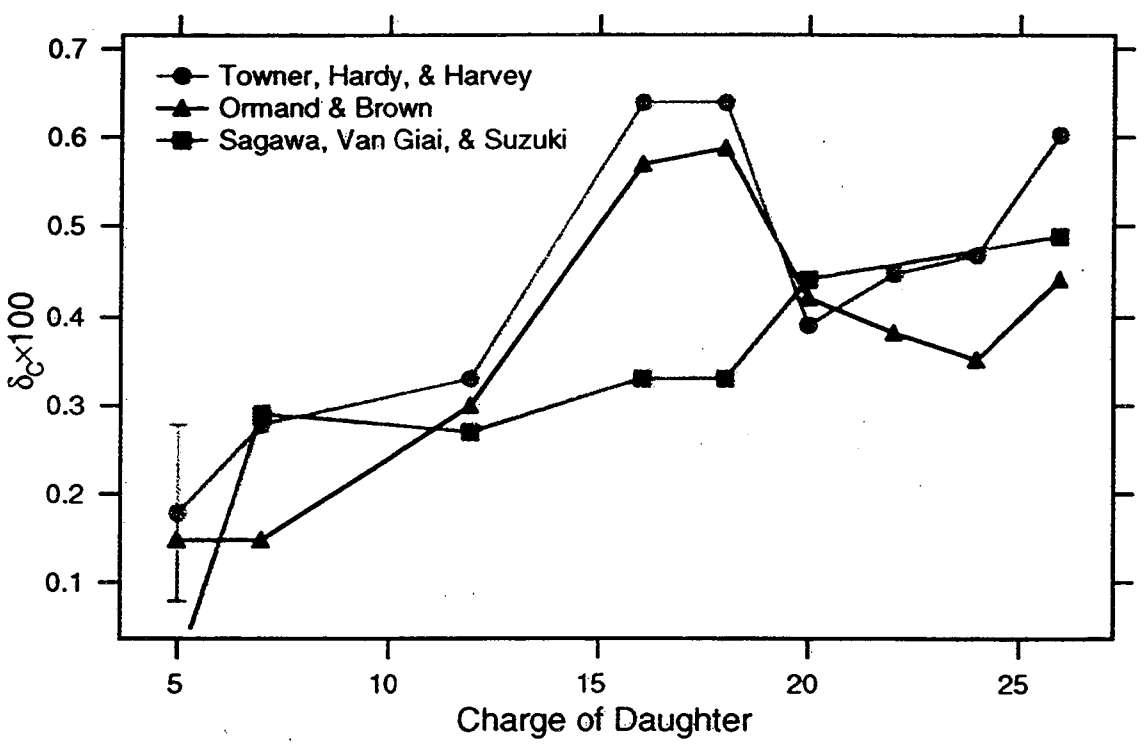

| Nuclei | Branching Ratio × 100 |
|---|---|
| $^{10}C$ | 1.4648±0.0019 |
| $^{14}O$ | 99.3355±0.0102 |
| $^{26}Al^{(m)}$ | >99.970 |
| $^{34}Cl$ | >99.988 |
| $^{38}K^{(m)}$ | >99.998 |
| $^{42}Sc$ | 99.9941±0.0014 |
| $^{46}V$ | 99.9848±0.0013 |
| $^{50}Mn$ | 99.9420±0.0030 |
| $^{54}Co$ | 99.9955±0.0006 |

## Vector Coupling Constant for $^{10}C(0^+ \longrightarrow 0^+)$

Kroupa et al.

Goal measure $G_V$

$$ft \propto \frac{1}{G_V^2}$$

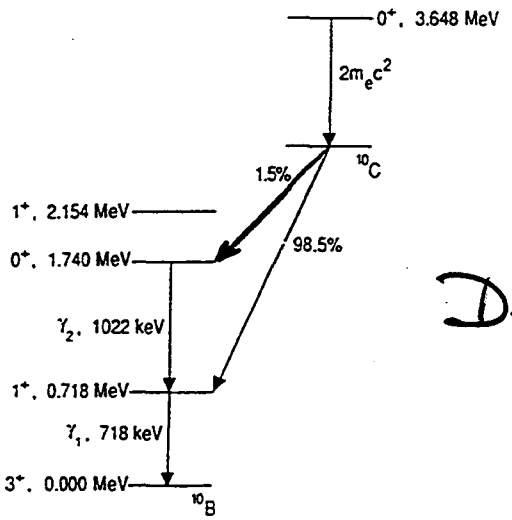


DECAY SCHEME OF $^{10}C$

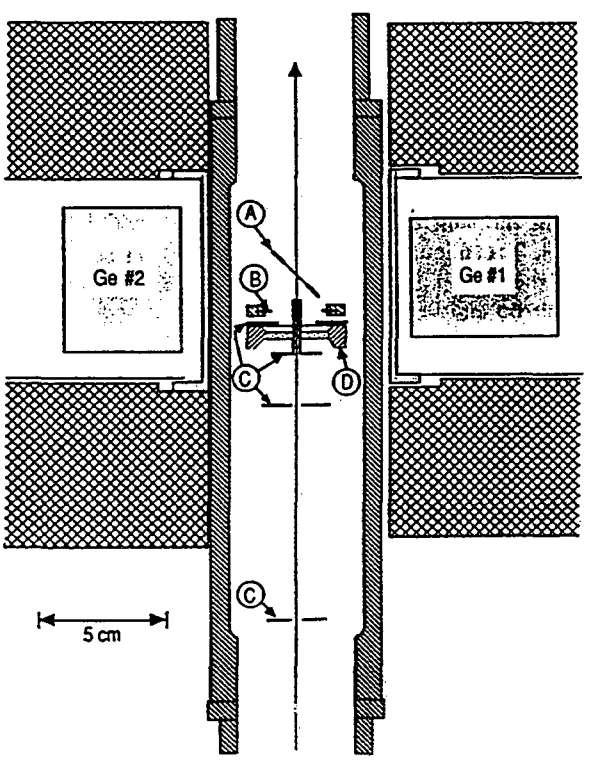


Experiment at Kalamazoo, MI

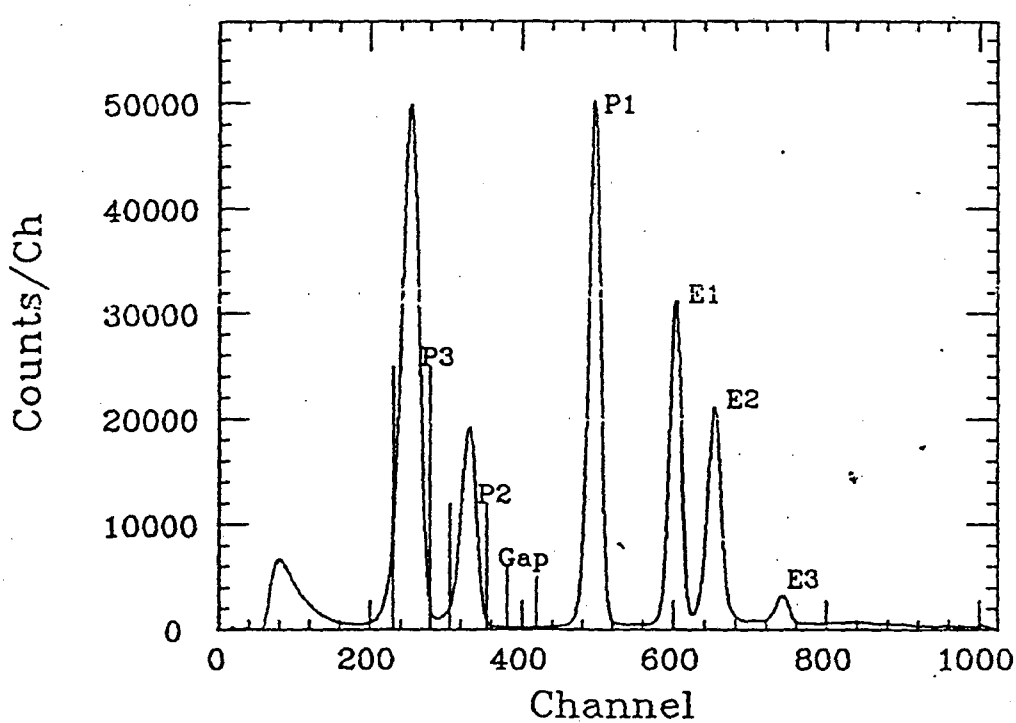


Figure 5.2 Coincident Silicon Energy Spectrum with Gates

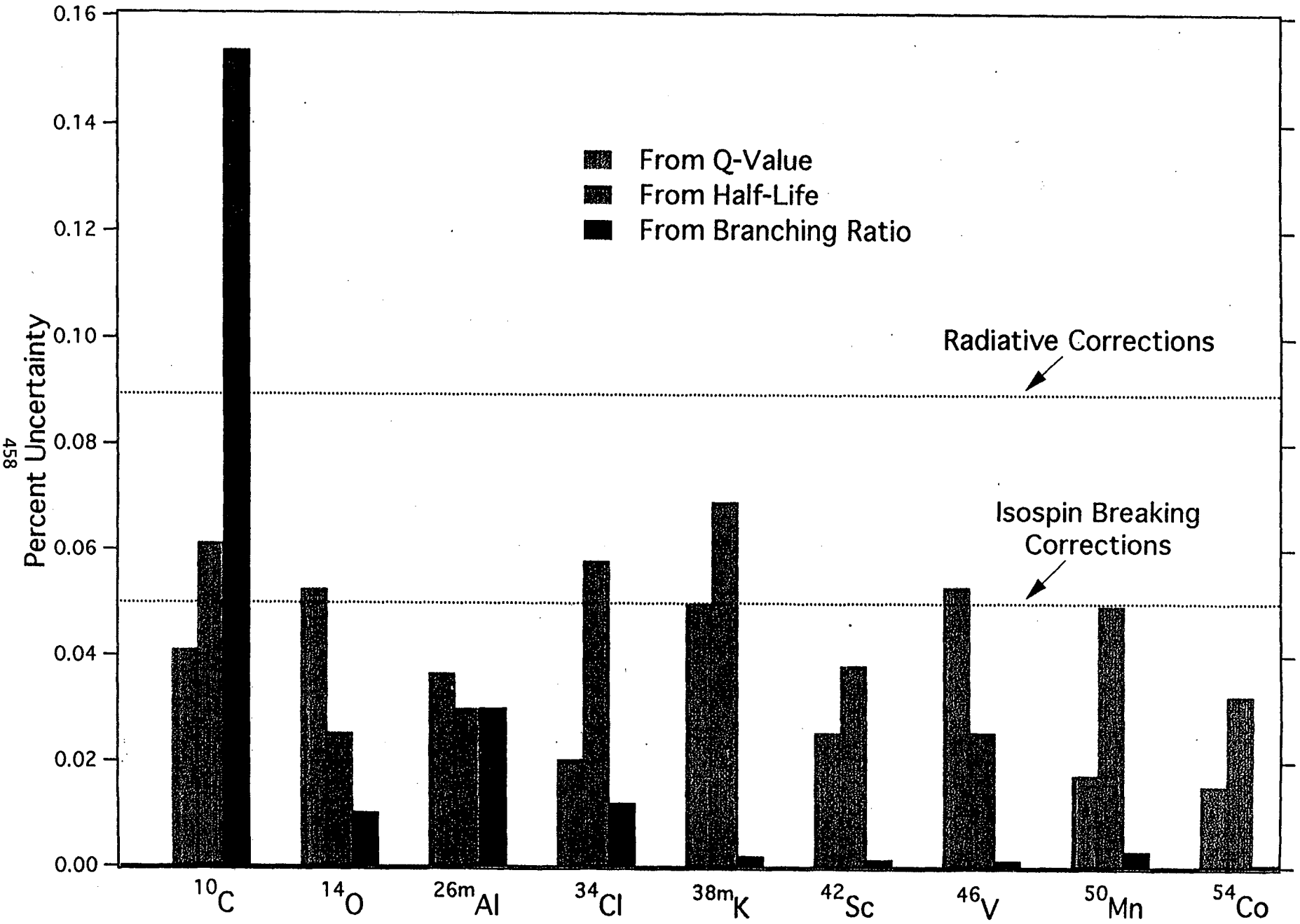
0.16
0.14
0.12
0.10
0.08
0.06
0.04
0.02
0.00
Percent Uncertainty
From Q-Value
From Half-Life
From Branching Ratio
Radiative Corrections
Isospin Breaking Corrections
10C
14O
26mAl
34Cl
38mK
42Sc
46V
50Mn
54Co

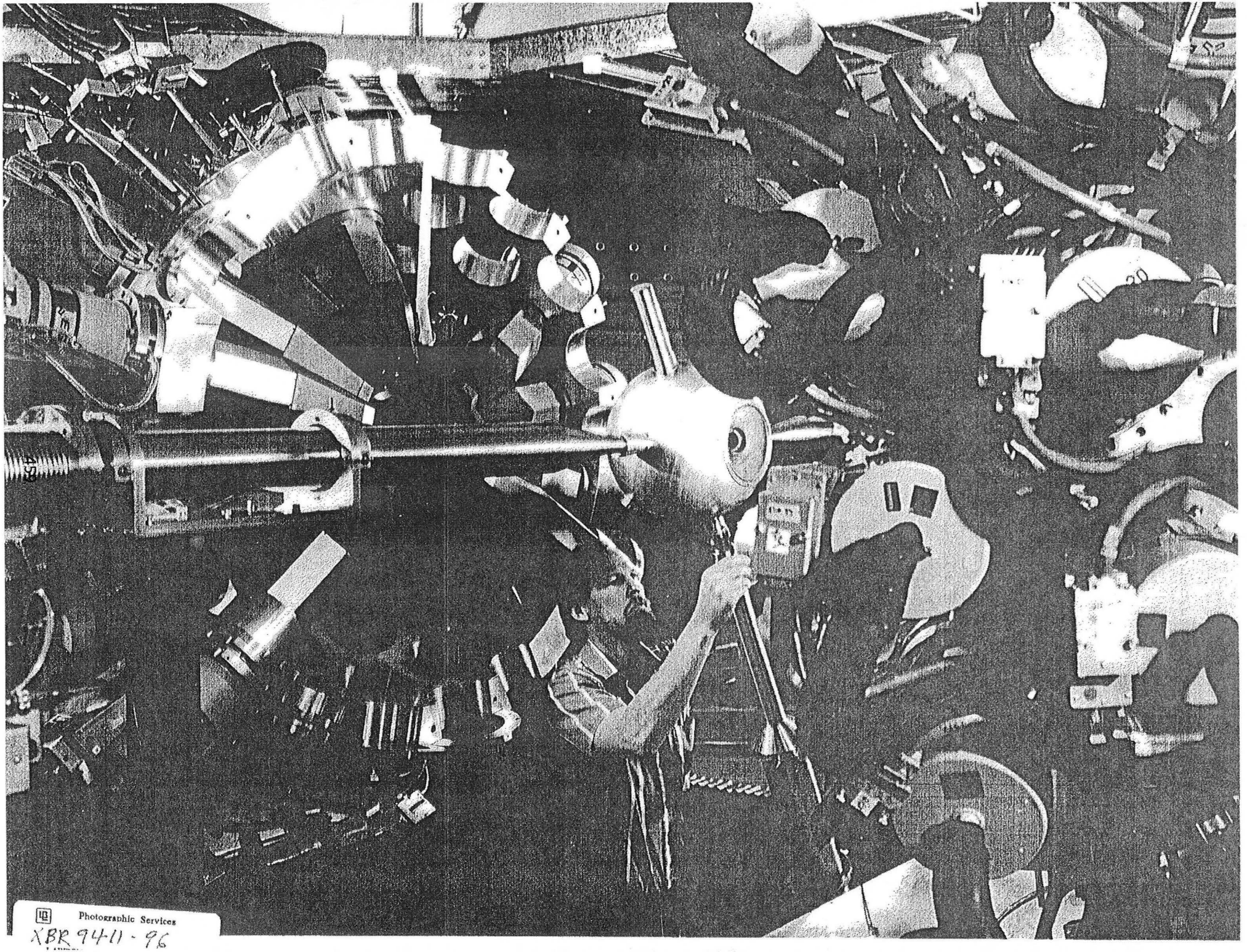

Photographic Services
XBR 9411-96

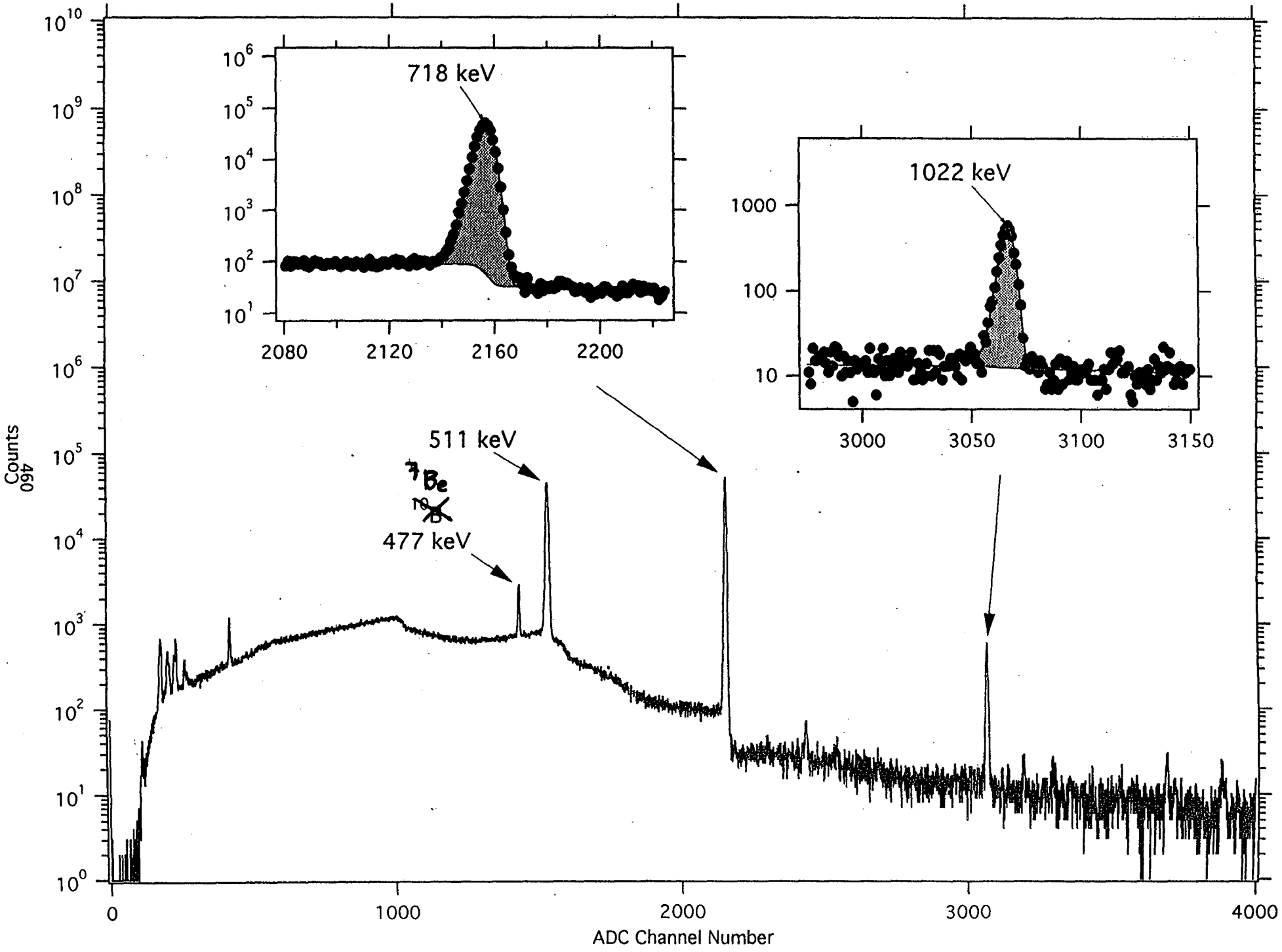
718 keV
1022 keV
511 keV
477 keV
Counts
ADC Channel Number
0
1000
2000
3000
4000
2080
2120
2160
2200
3000
3050
3100
3150
10
100
1000

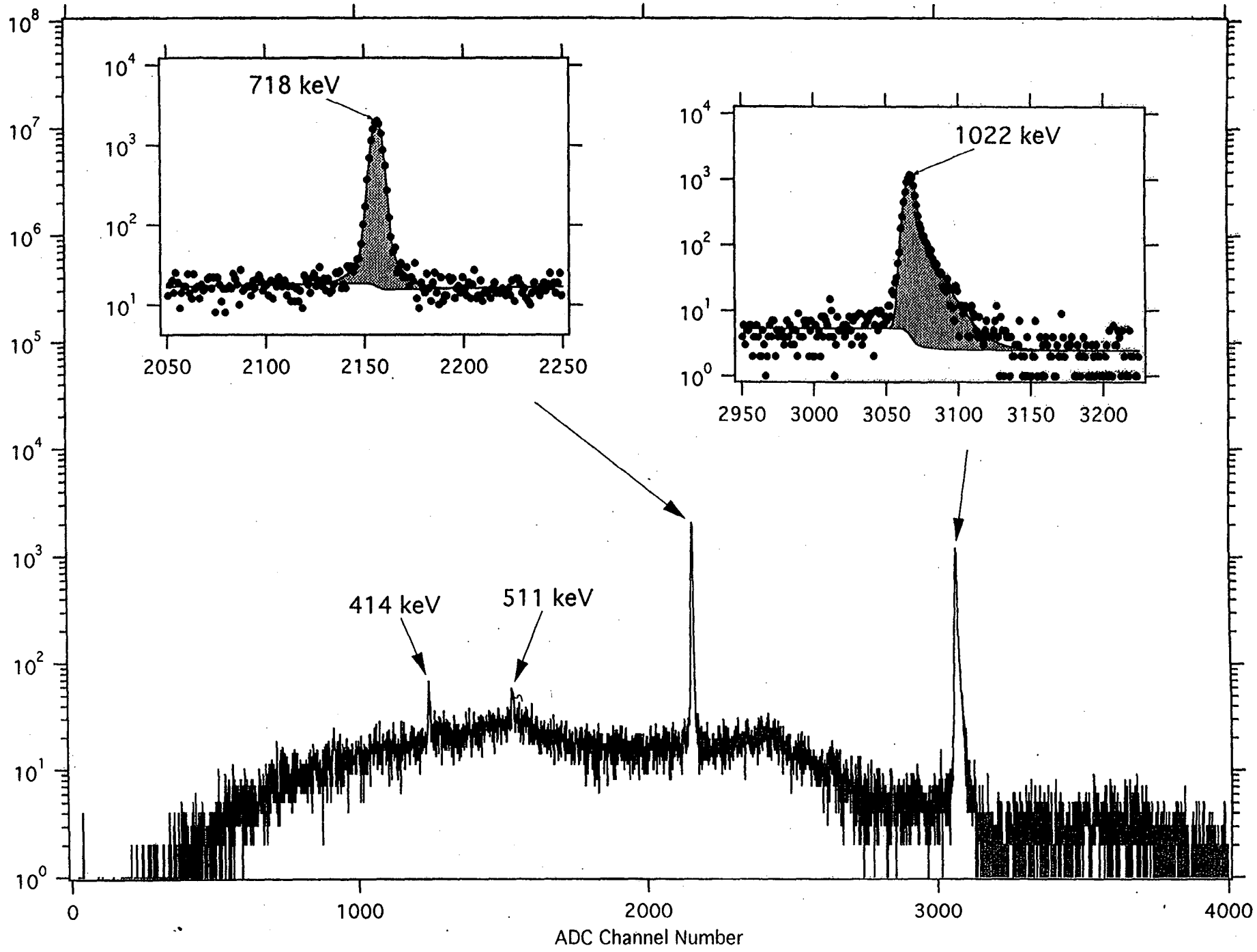
718 keV
1022 keV
414 keV
511 keV
Counts
ADC Channel Number
0
1000
2000
3000
4000
2050
2100
2150
2200
2250
2950
3000
3050
3100
3150
3200

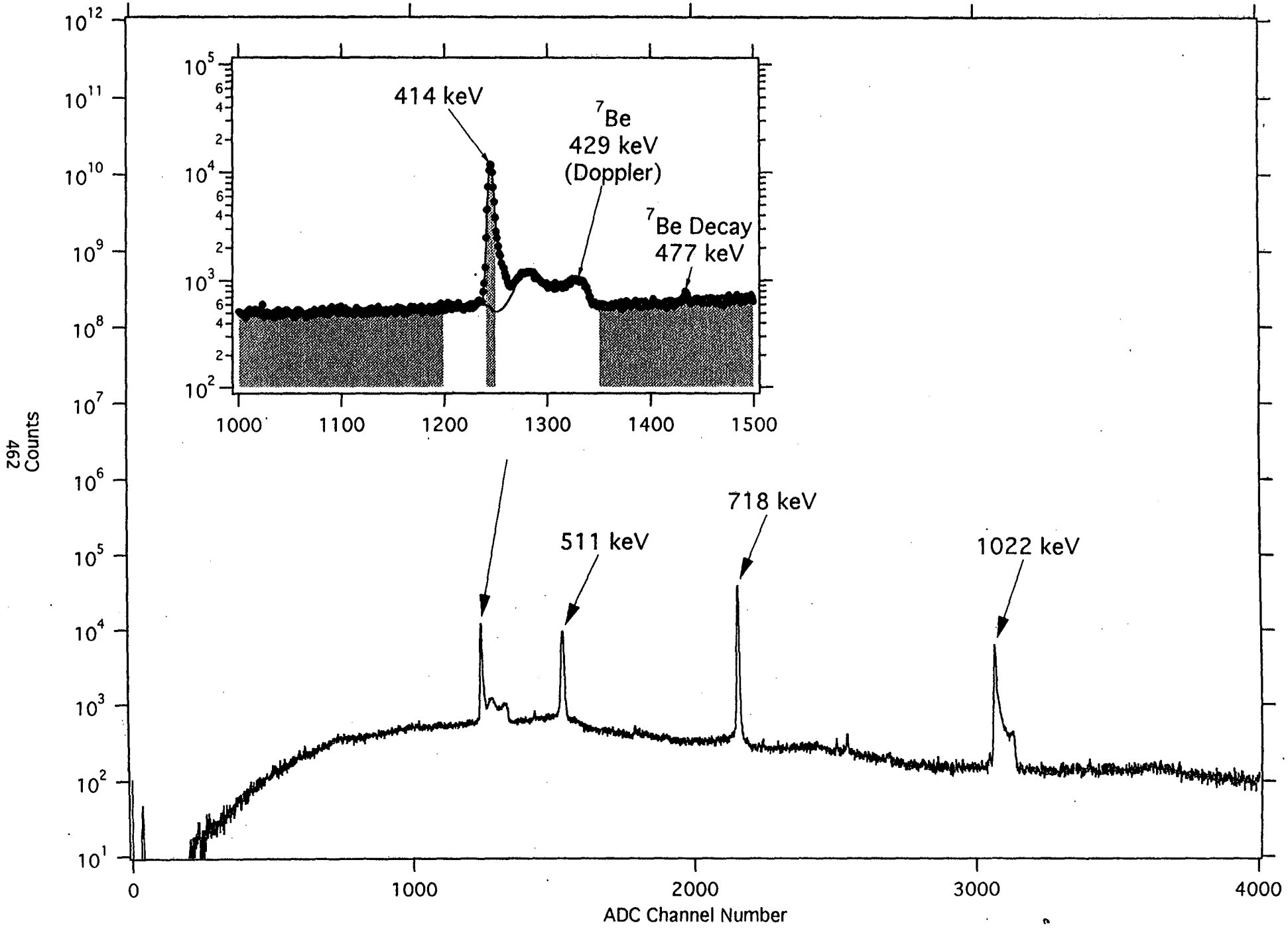
414 keV
$^7$Be
429 keV
(Doppler)
$^7$Be Decay
477 keV
511 keV
718 keV
1022 keV
Counts
ADC Channel Number

| | | |
|---|---|---|
| | Raw Ratio | $(1.5131\pm0.0016)\times10^{-2}$ |
| $^{10}B$ Analysis | Accidentals Coincidences | $-(1.944\pm0.017)\%$ |
| | Compton Background | $-(0.049\pm0.008)\%$ |
| $^{10}C$ Analysis | 2×511 Summing | $-(1.23\pm0.19)\%$ |
| | Prompt Summing | $+(0.441\pm0.010\pm0.044)\%$ |
| | Background ($^{120}Sb$) | $-(0.23\pm0.11)\%$ |
| | Branching Ratio | $(1.4679\pm0.0037\pm0.0006)\times10^{-2}$ |
| | BR(World Average) | $(1.4649\pm0.0019)\times10^{-2}$ |

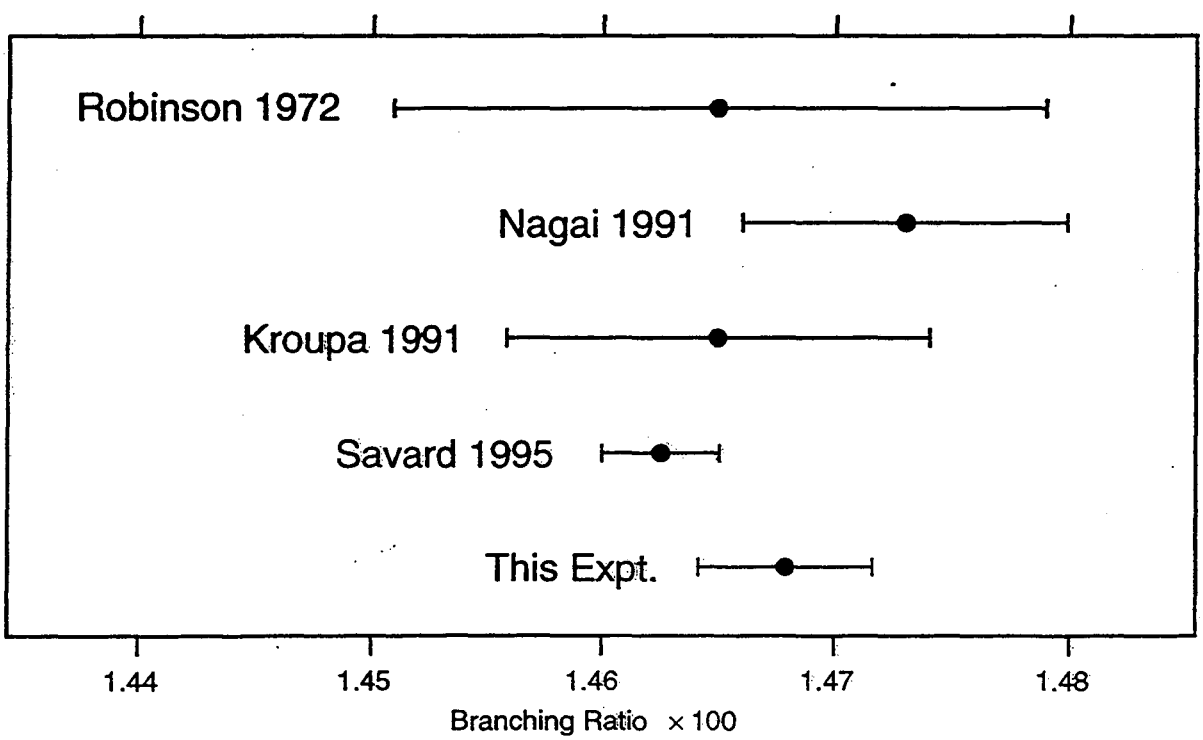

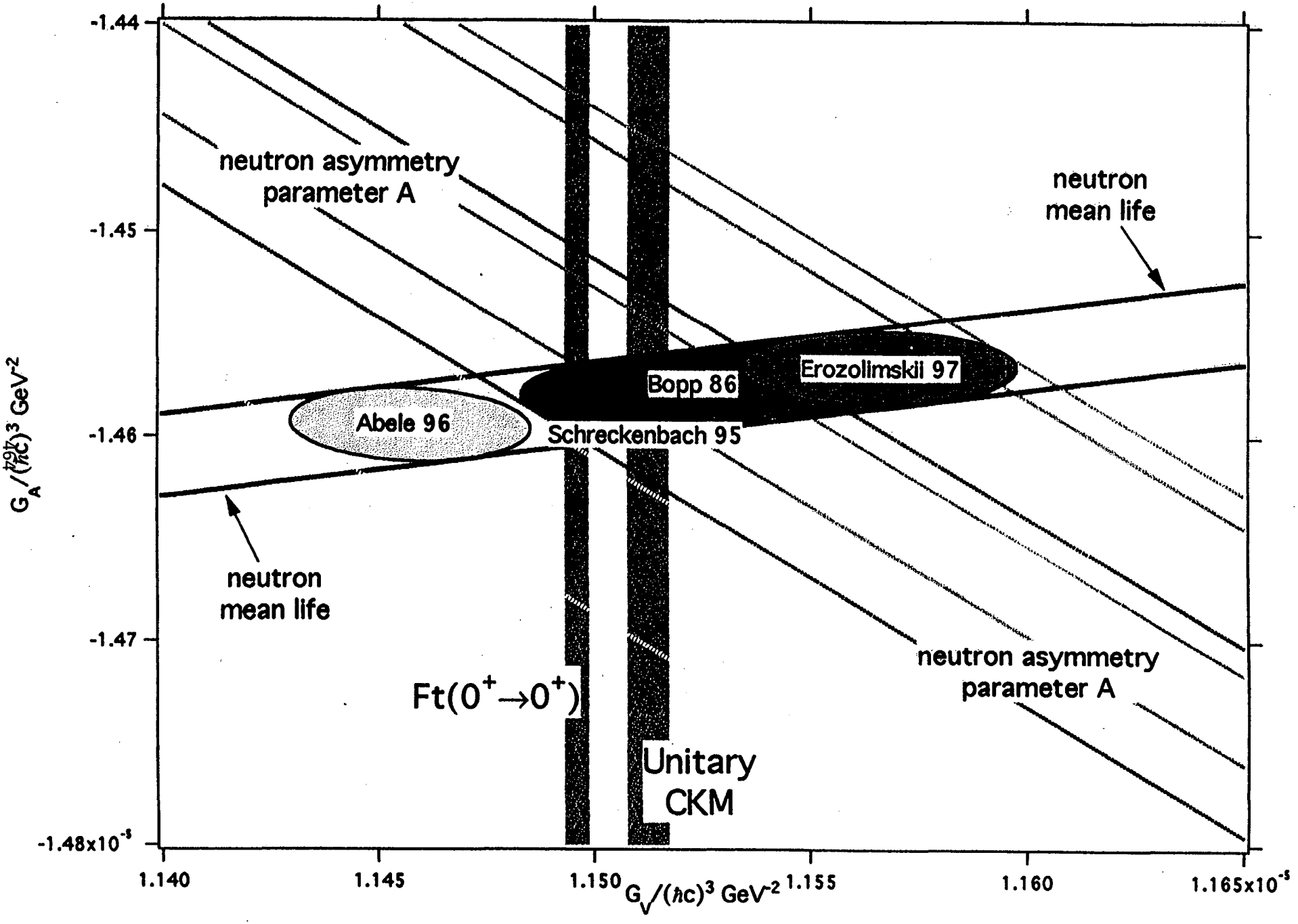
-1.44
-1.45
-1.46
-1.47
-1.48x10^-5
1.140
1.145
1.150
1.155
1.160
1.165x10^-5
G_V/(ħc)^3 GeV^-2
G_A/(ħc)^3 GeV^-2
neutron asymmetry parameter A
neutron mean life
Erozolimskii 97
Bopp 86
Abele 96
Schreckenbach 95
neutron mean life
neutron asymmetry parameter A
Ft(0+→0+)
Unitary CKM

# BaBar DETECTOR

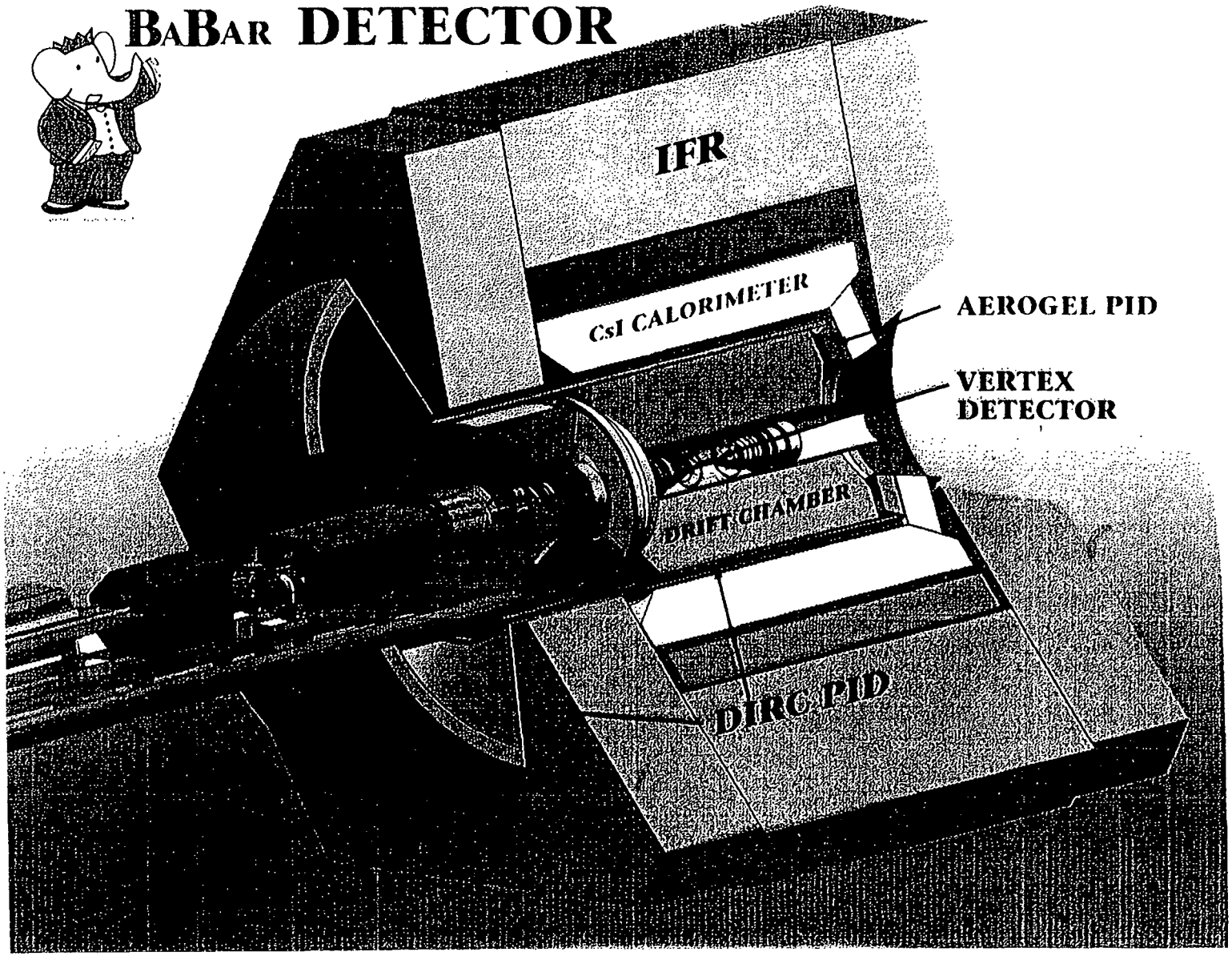

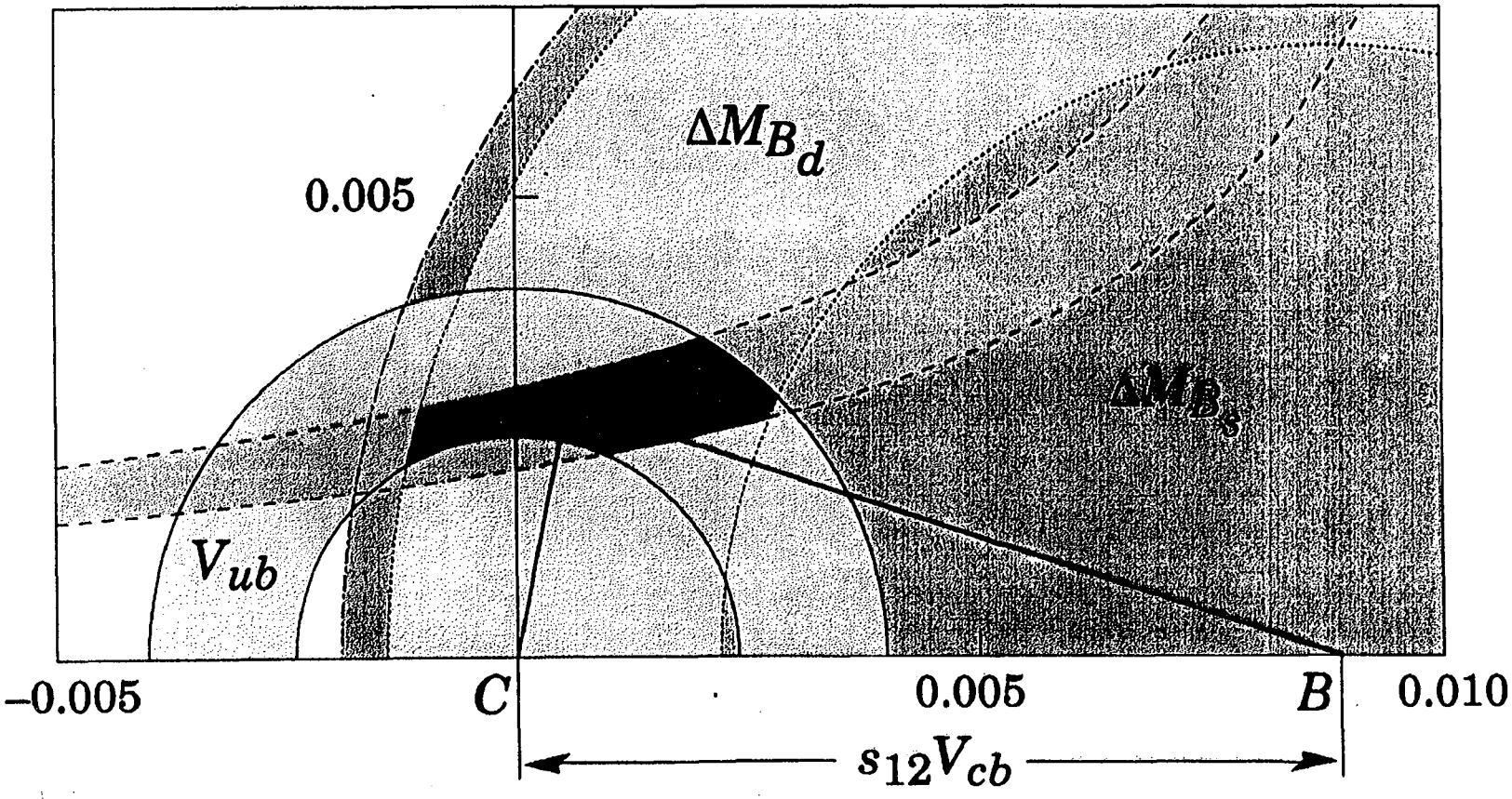
0.005
$\Delta M_{B_d}$
$\Delta M_{B_s}$
$V_{ub}$
–0.005
C
0.005
B
0.010
$s_{12}V_{cb}$

# *Table of Isotopes* (1994)

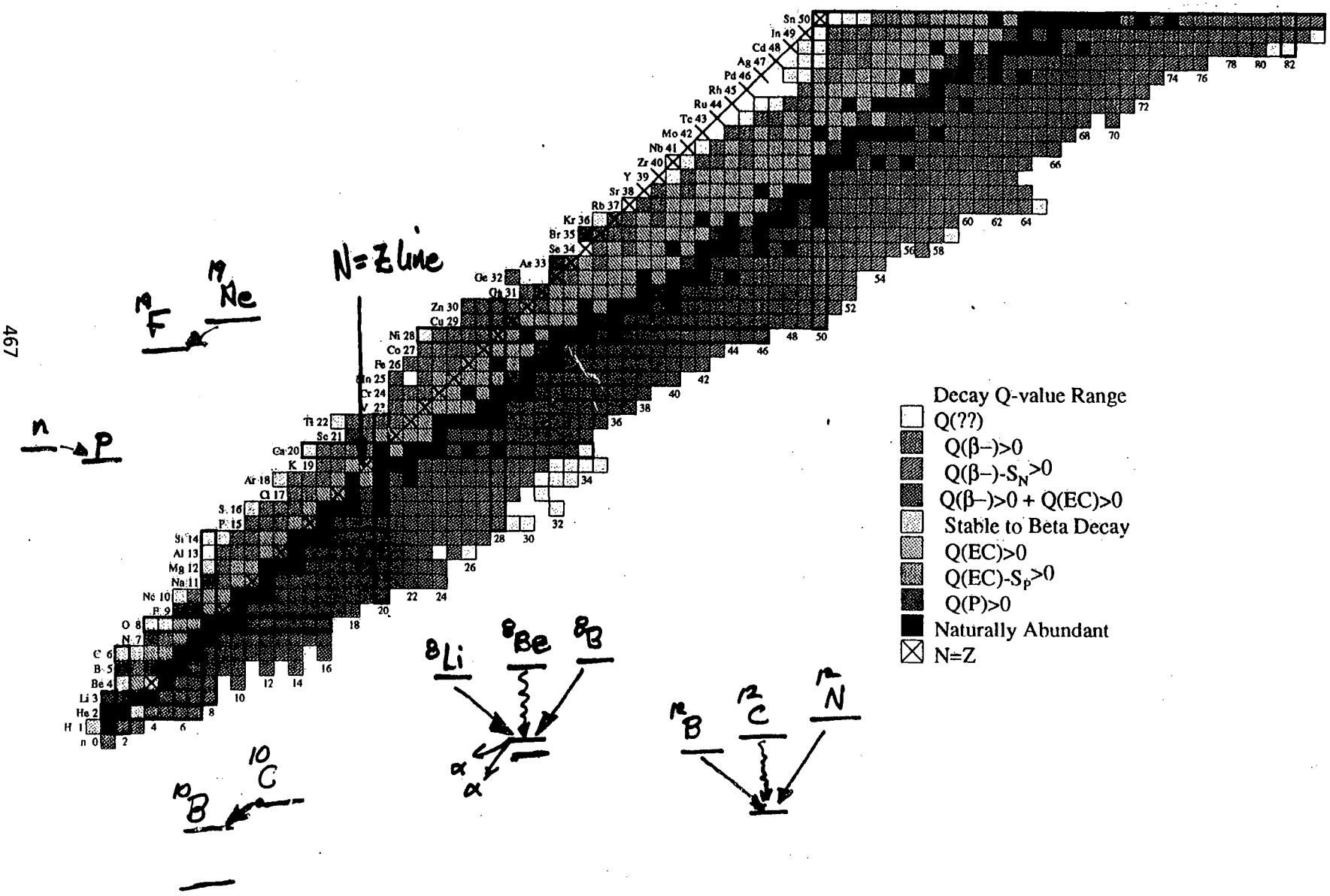

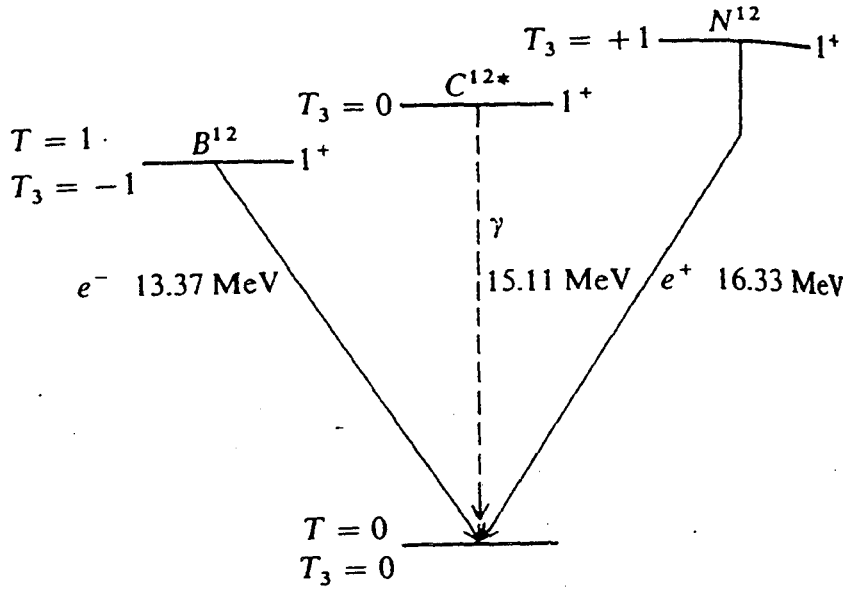


Wu et al. test of CVC

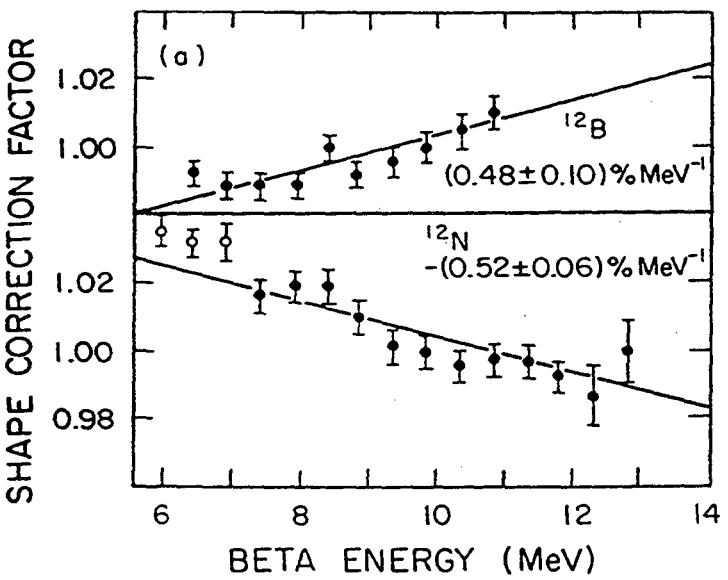


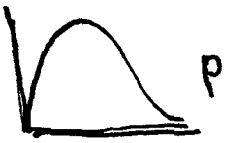

$pE(E_0-E)^2(1+\alpha E)$

shape correction

$\alpha \sim \sqrt{\Gamma_{FM}}$

But

Osaka search for SCC.

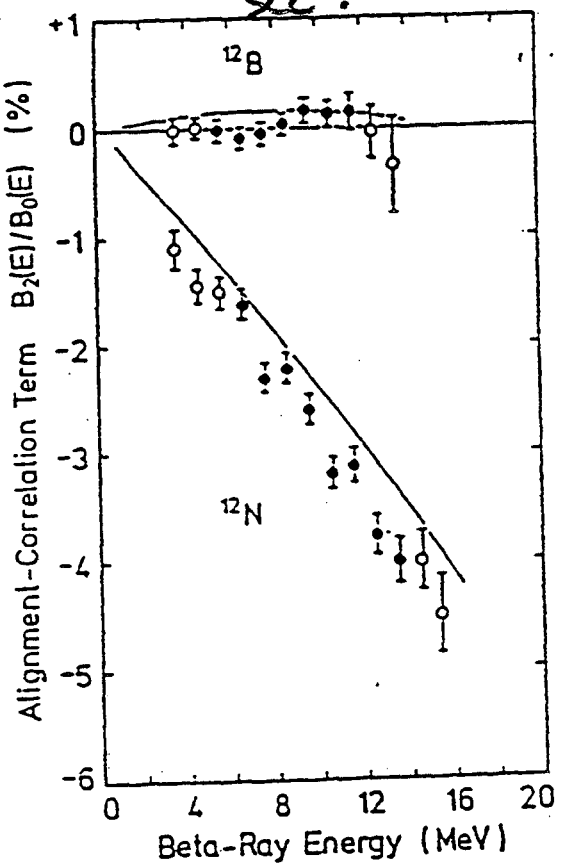


OSAKA measurement of electron anisotropy

$pE(E-E_0)^2[1+AP\cos\theta+\frac{B}{B_0}P\cos^2\theta]$

FROM: L. Grenacs "Induced Weak Currents in Nuclei"
Ann. Rev. Nucl. Part Sci. 35, 455 (1985)



**Table 6** Present status of experimentally determined induced weak form factors in nuclei[a]

| $A$ | Reaction | Weak magnetism $F_M/F_M$(CVC) | Induced pseudoscalar $f_P/f_P$(PCAC) | Induced tensor $F_E^{(2)}/F_A$ |
|---|---|---|---|---|
| 1 | $\mu$ capture | — | $1.04 \pm 0.23$ | — |
| 2 | $\nu$ scattering | — | — | $0.0 \pm 1.0$ |
| 6 | $\beta$ decay | — | — | $0.5 \pm 1.3$ |
| 8 | $\beta$ decay | $0.82 \pm 0.12$ | — | $0.0 \pm 0.6$ |
| 12 | $\beta$ decay | $1.00 \pm 0.11$ | — | $-0.2 \pm 0.5$ |
| 12 | $\mu$ capture | $1.10 \pm 0.15$ | $1.0 \pm 0.21$ | — |
| 19 | $\beta$ decay | $1.00 \pm 0.15$ | — | — |
| 20 | $\beta$ decay | $1.15 \pm 0.28$ | — | — |
| 40 | radiative $\mu$ capture | — | $0.95 \pm 0.23$ | — |

[a] In the case of first-class currents, the determination is compared with the corresponding theoretical prediction. The result for $A = 2$ is discussed in text.

$g_M = \mu_p - \mu_n - 1$ ($\pm 10-20\%$)

$|g_T| \lesssim 0.5 |g_A|$

$g_P \approx g_{P\,PCAC}$ ($\pm 20-30\%$)

$|g_S| \lesssim g_V$ from $0^+ \to 0^+$ systematics
Ormand, Brown, & Holstein PRC 40, 2914 (1989)

# $^{22}$Na Decay Scheme

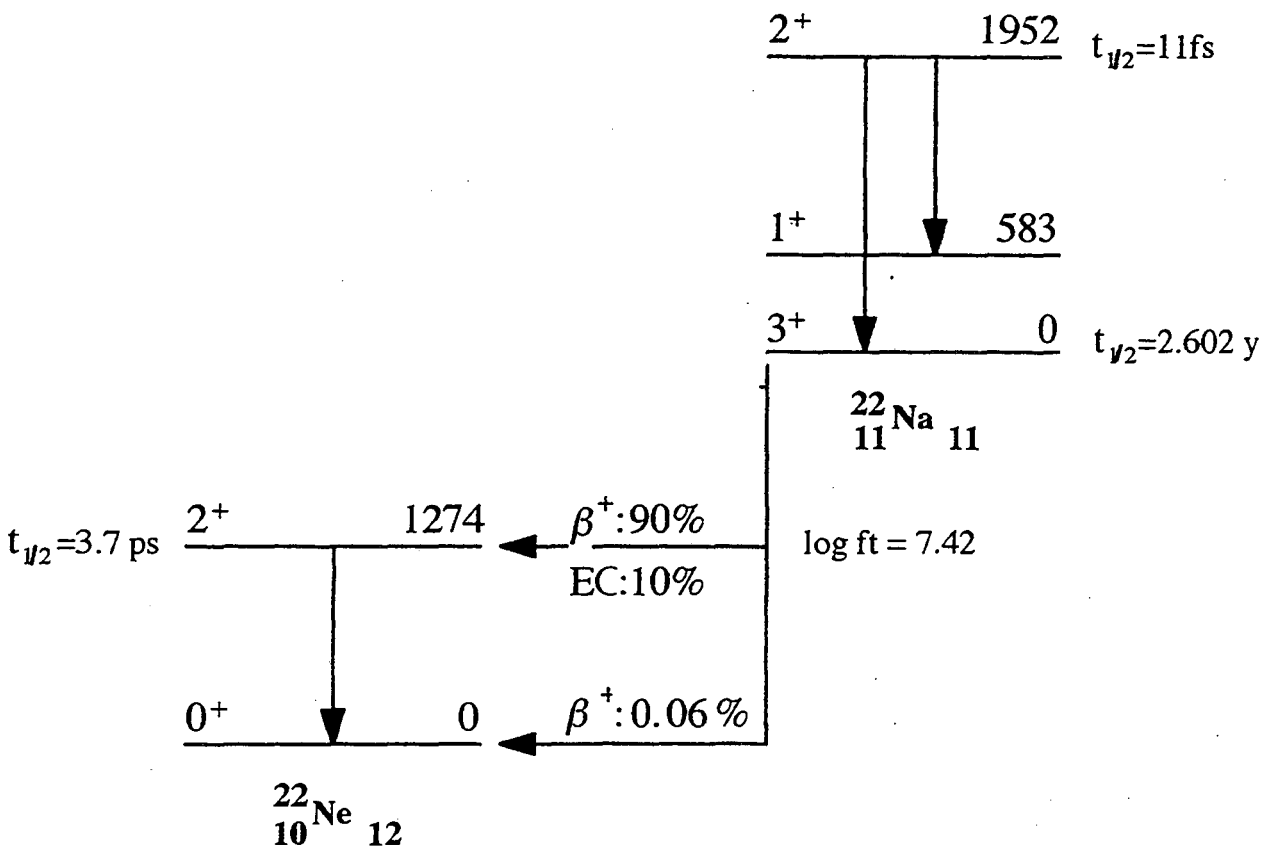

Mass 22 – Laboratory for fundamental interactions.

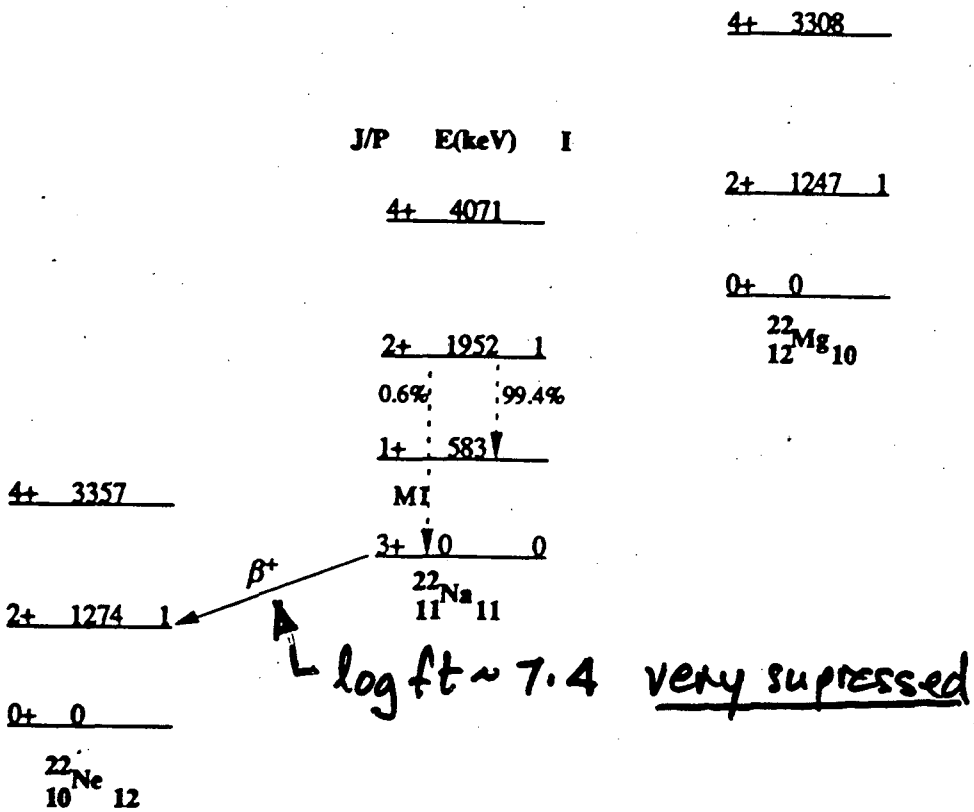


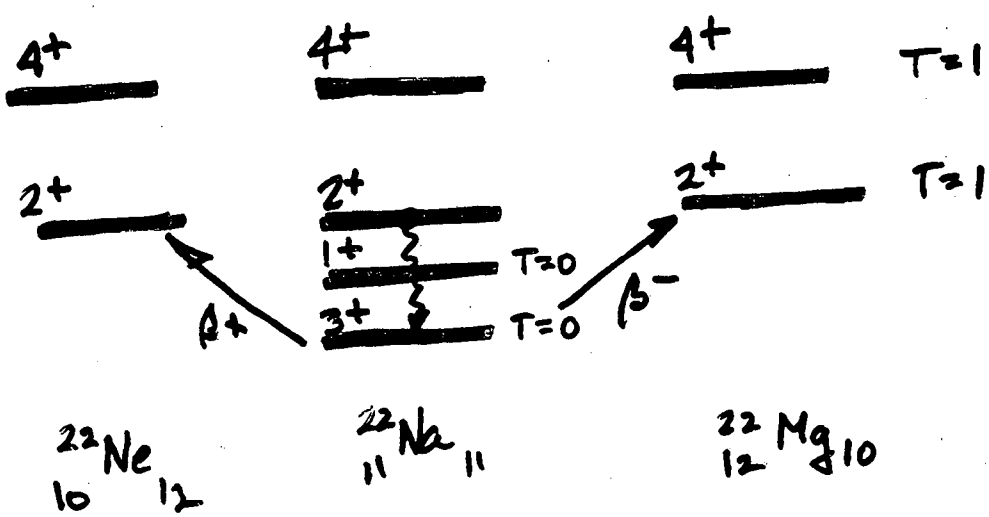


Treat the nuclei as if they were "elementary particles"

Mass 22 – Laboratory for fundamental interactions.

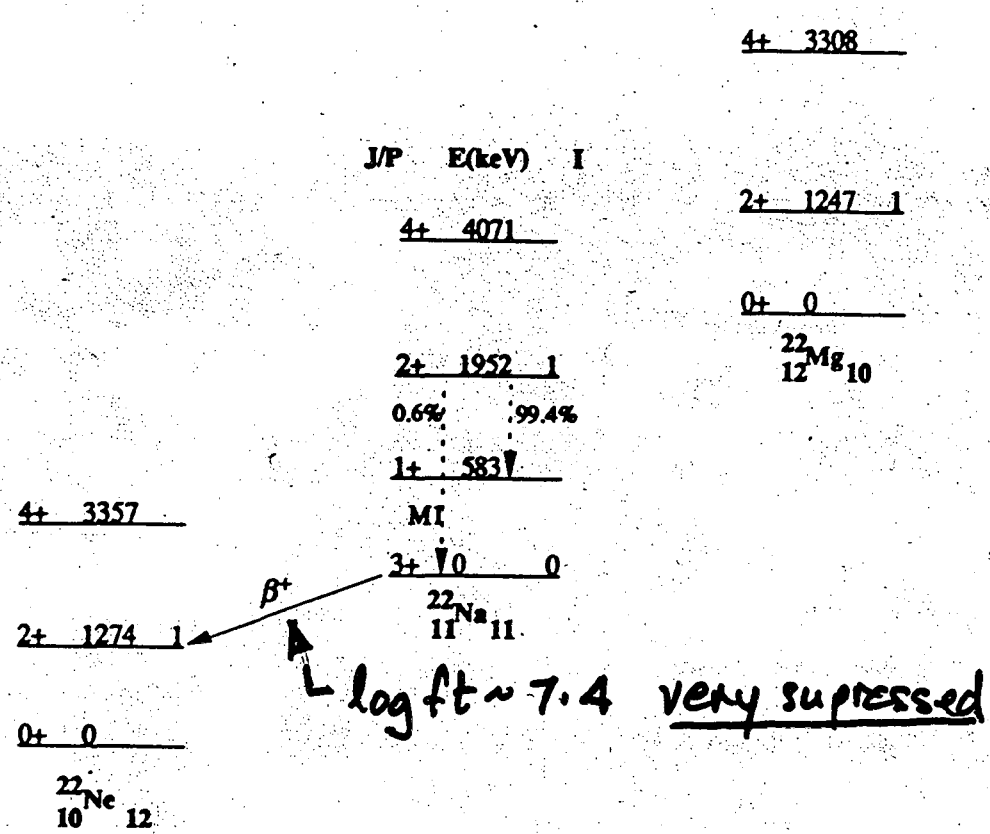


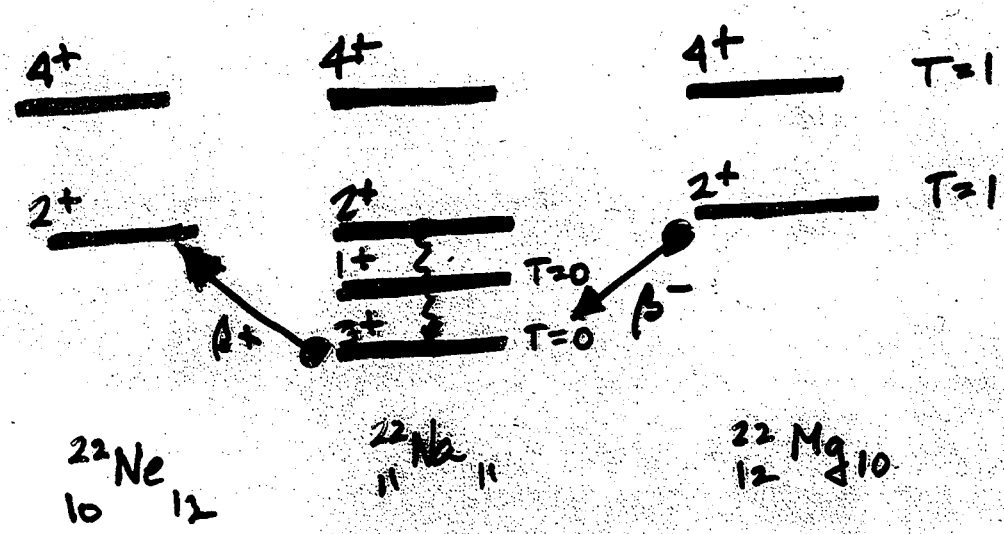


Treat the nuclei as if they were "elementary particles"

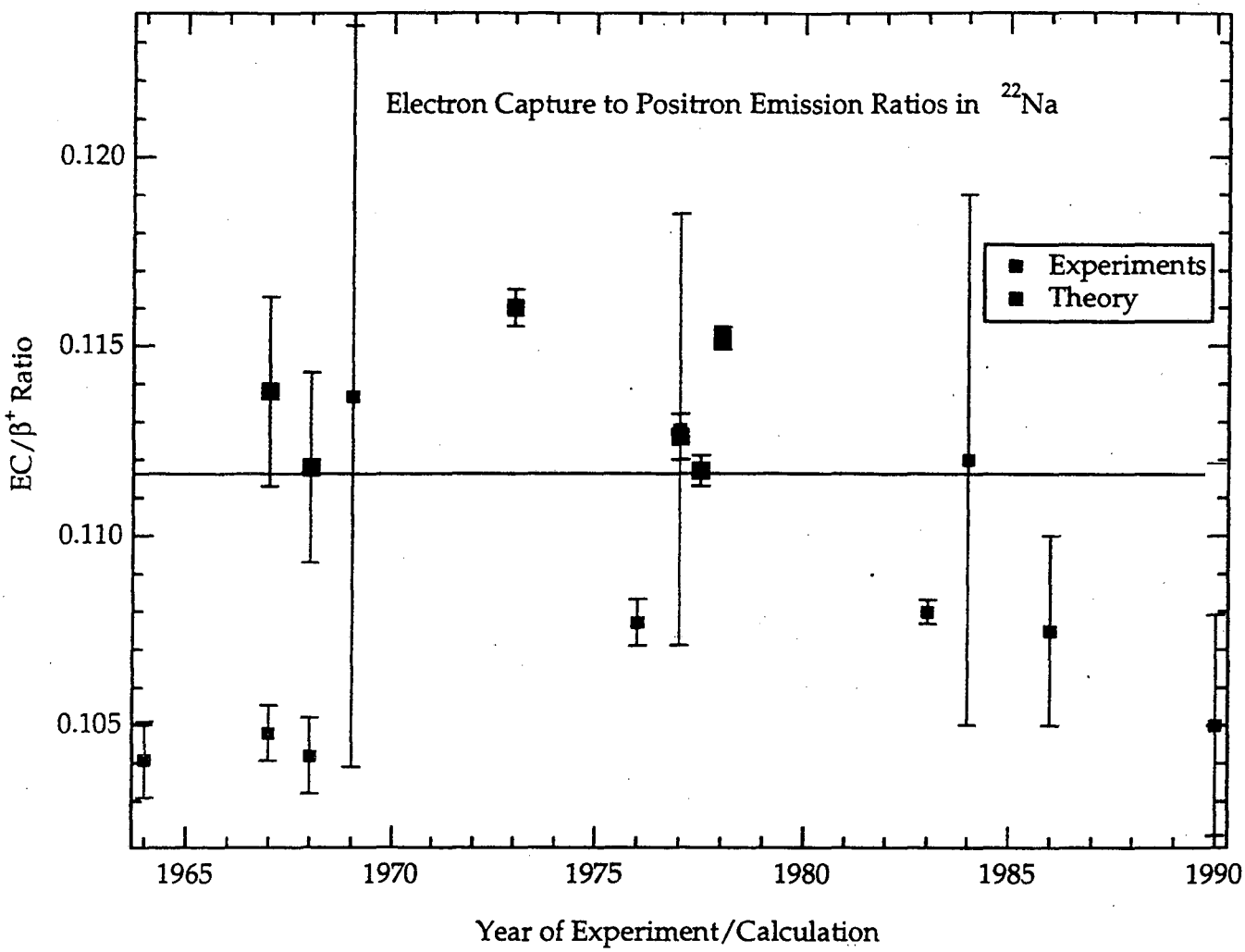


1990 REASSESSMENT CONCLUDED (5±2)%
EXPERIMENTAL DISCREPANCY
WITH ALLOWED ORDER THEORY

KUNZE, et al ZPHYS A 337 p169 (1990).

# Observables for $^{22}$Na

Beta-Gamma Angular Correlation

$$A_{22} = (4.4B + 4.4D - 0.6C_2) \times 10^{-5}$$

β+ Spectral Shape Factor

$$S \approx -(1.79\ B - 0.17\ D + 0.00074\ H - 7.78\ C_2) \times 10^{-3} / \text{MeV}$$

Electron Capture to β+ Emission Ratio

$$R \approx 1 - (-1.56\ B - 0.70\ D + 0.0013\ H + 18.0\ C_2) \times 10^{-3}$$

Longitudinal Polarization of β+

$$P_L / \beta \approx 1 - (2.16\ B + 1.08\ D + 0.0038\ H - 0.08\ C_2) \times 10^{-4}$$

Gamow-Teller Transition Strength

$$ft_{1/2} = \frac{2 ft_{1/2}(\text{Fermi})}{C_1}$$

Energy Width of Analog M1 Transition

$$\Gamma = \frac{22 e^2 \Delta^3}{24 \pi M^2}\ B^2\ C_1^{\ 2}$$

Form factors:

B = Weak Magnetism
$C_1$ = 1st order Gamow-Teller
D = Induced Tensor
H = Induced Pseudoscalar

MÜLLER 1965 – EXTRAPOLATE FROM 5 MM ABSORBER THICKNESS

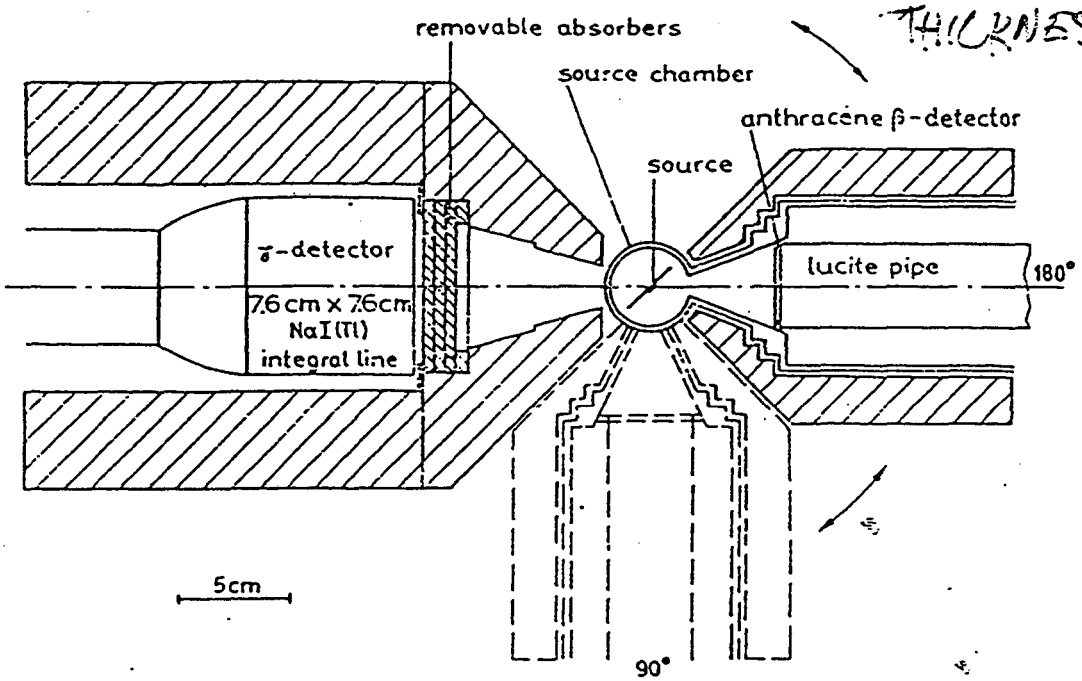


Fig. 1. Experimental arrangement for the measurement of the $\beta\gamma$ directional correlation. The removable lead absorbers allows variation of the contribution of the disturbing effects of annihilation quanta.



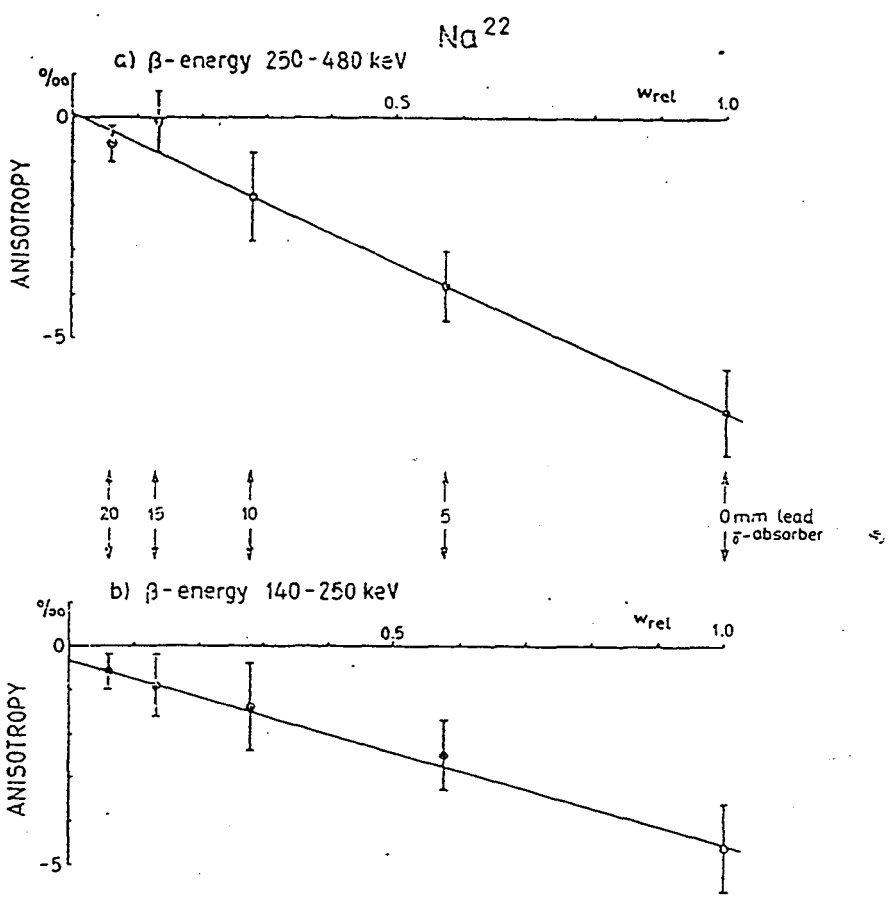


Fig. 2. Anisotropy for $^{22}$Na for the two $\beta$-energy intervals as as function of the relative detection probability $w_{rel}$ for annihilation quanta in the $\gamma$-detector. The corresponding thicknesses of the lead absorber are indicated. The straight lines represent the best fit to the data. Their intersections with the ordinate give the undisturbed anisotropies.

| | | | | |
|---|---|---|---|---|
| | | | | −0.03 ± 0.04 |
| | | | (a) | −0.27 ± 0.05 |
| | | | (b) | −0.25 ± 0.08 |
| | | | (c) | −0.30 ± 0.08 |
| 0008 | +0.013 | −0.02 | (d) | −0.18 ± 0.04 |
| 005) | | (−0.12) | Average | −0.27 ± 0.04 |

Steffen 1959

in columns
es in column
account the
ed on the basis
wed transition
rmi component
$Sc^{46}$ were taken

theory for the
nore difficult
/

ole other terms.

educed, the
ced and the
t. It is dif-
of this latter
le to do so.
$Na^{22}$ anisot-
heory arises
ontributions
one assumes
articular case,
parentheses.
directional
nuclides
amber and

the scintillation counter arrangement shown in Fig. 1. The concidence spectrometer was of the usual fast-slow type. The beta sources were less than 30 $\mu g/cm^2$ thick and were mounted on 0.9-mg/cm$^2$ Mylar films. The data were carefully corrected for the presence of gamma-gamma coincidences.

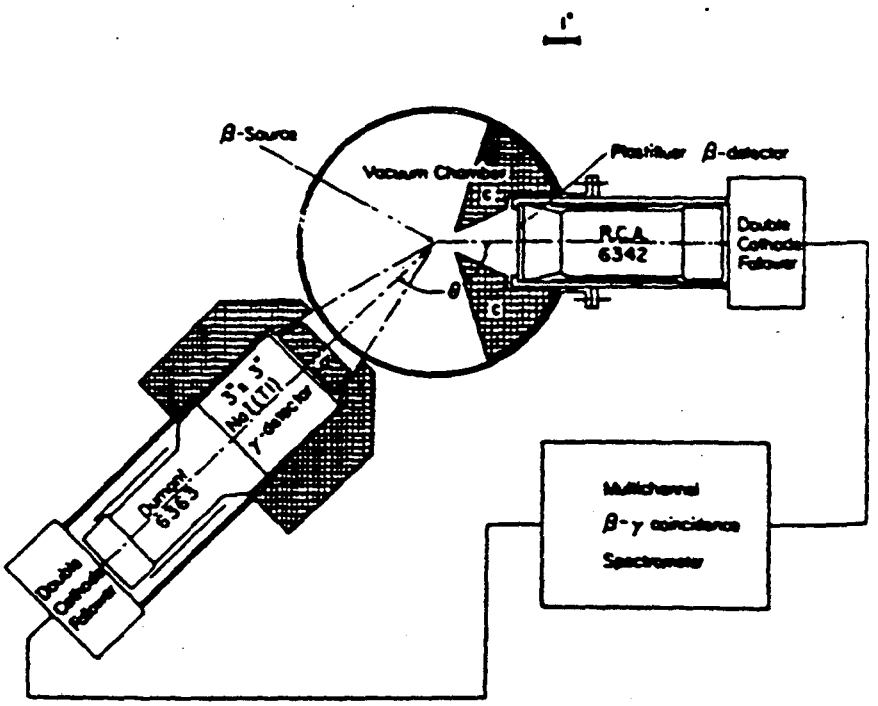


FIG. 1. Vacuum chamber and counter arrangement for beta-gamma directional correlation measurements. The lead shields (c) and the lead absorber (d) were only used in the $Na^{22}$ measurements (c) and (d), respectively.

tion phot
1.28-Mev
eral, mo
gamma c
detector
at 180°.
an appar
order of
tion effe
test for
beta-gan
under va
urement
ing the c
solid ang
the beta
270°) an
(d) were
ment an
ence of
in meas
effect w
wedges
a ½-inch
detector
The r

$^{60}$Co Angular Correlation

$\beta$-$\gamma$

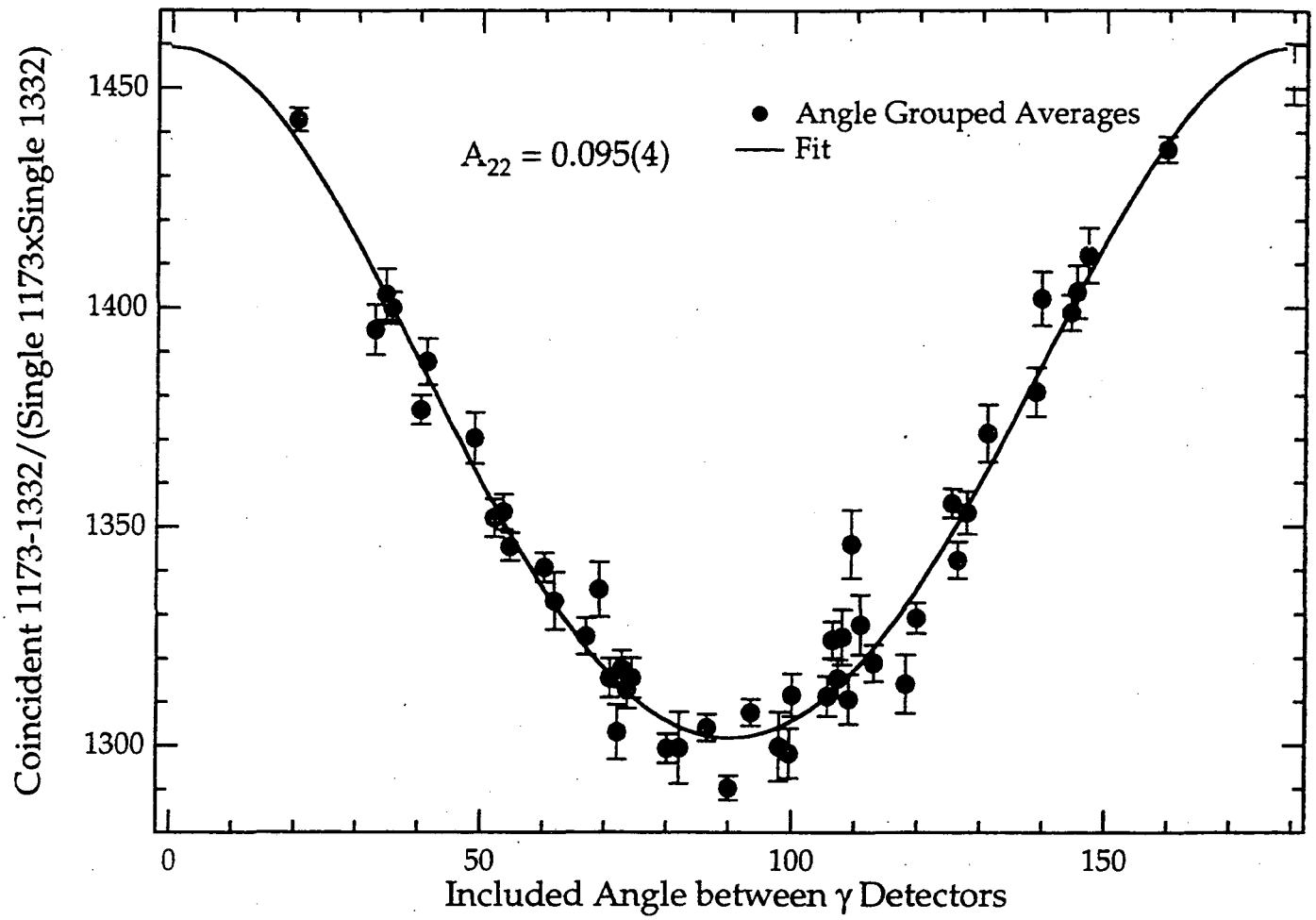


VS $A_{22} = .1021$ $\gamma\gamma$ CORRELATION

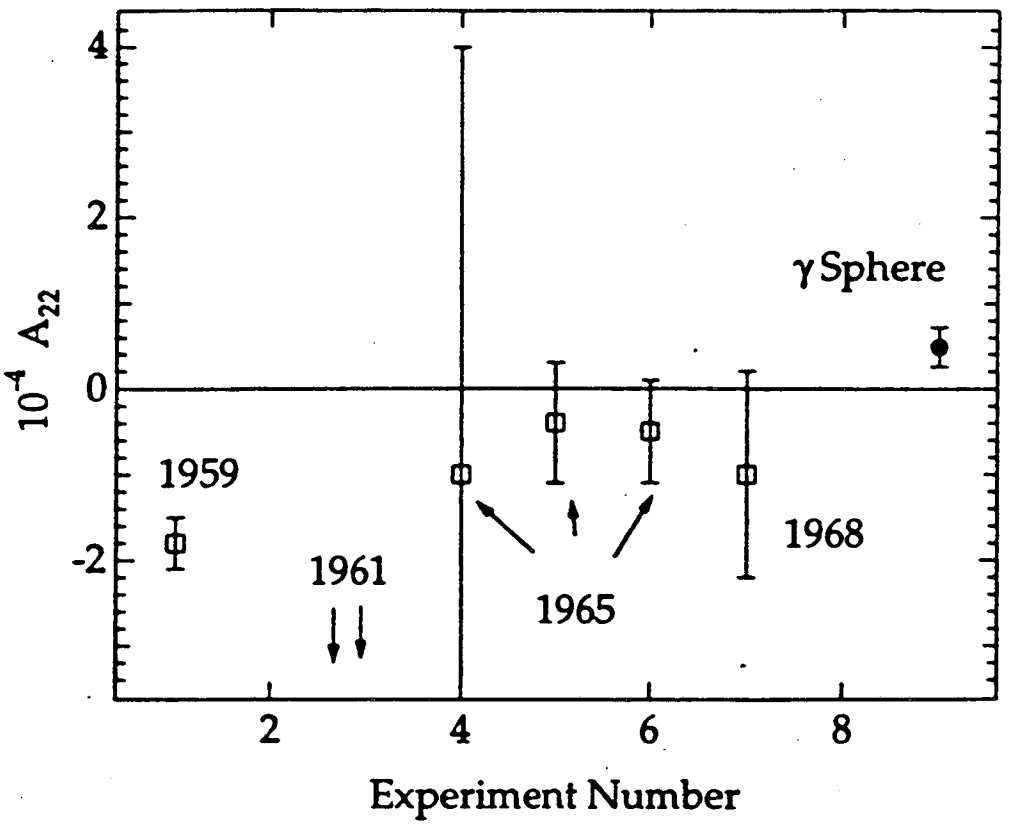


FIG. 7. Comparison of our experimental $A_{22}$ (circle) with earlier experiments (squares)

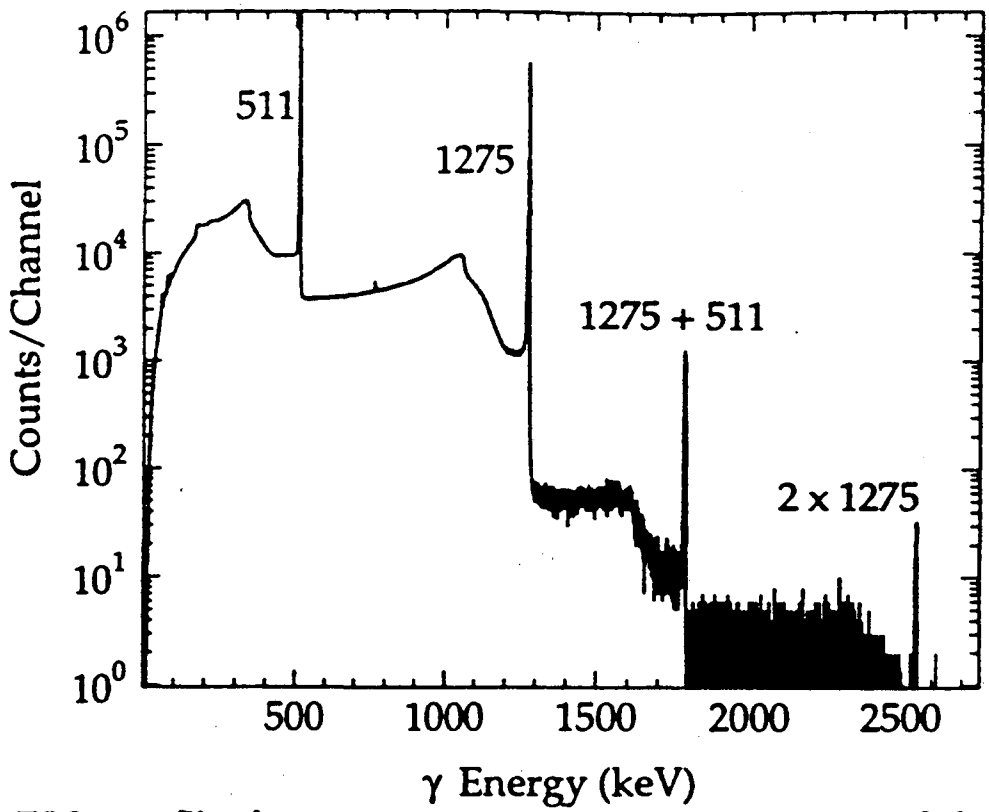


FIG. 2. Single $\gamma$ event energy spectrum summed for all Ge Gammasphere detectors

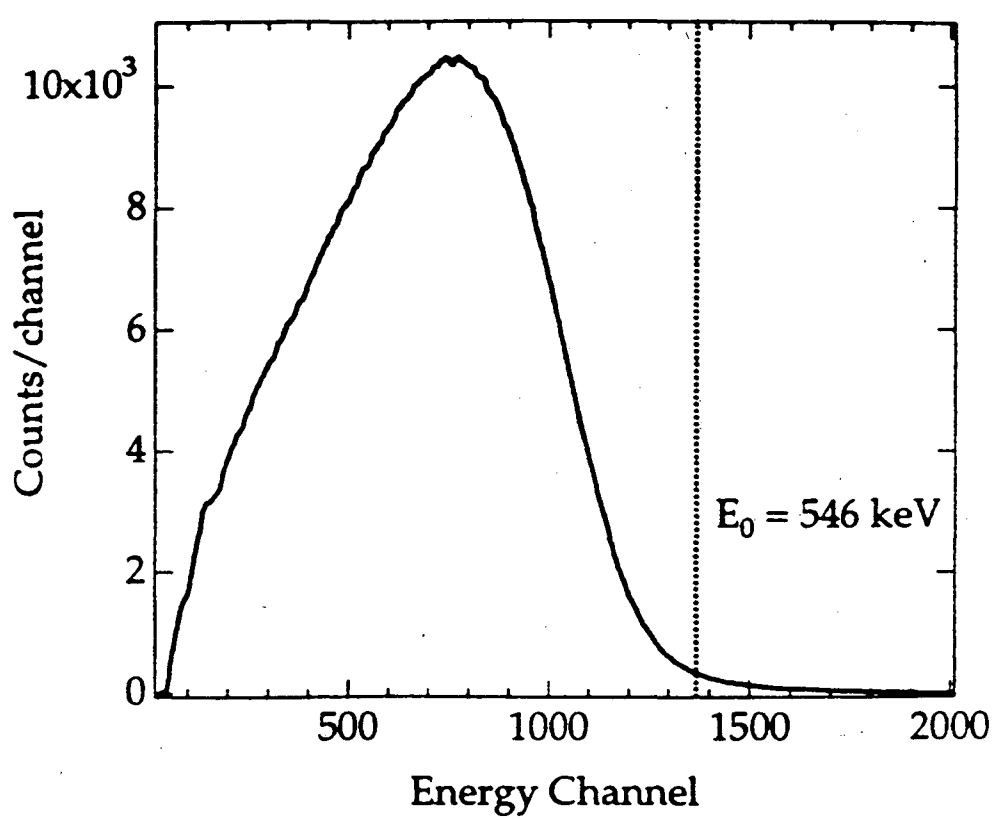


FIG. 5. $\beta^+$ Energy spectrum for events with a coinci 1275 kev $\gamma$. Energy uncertainty is about 8 keV.

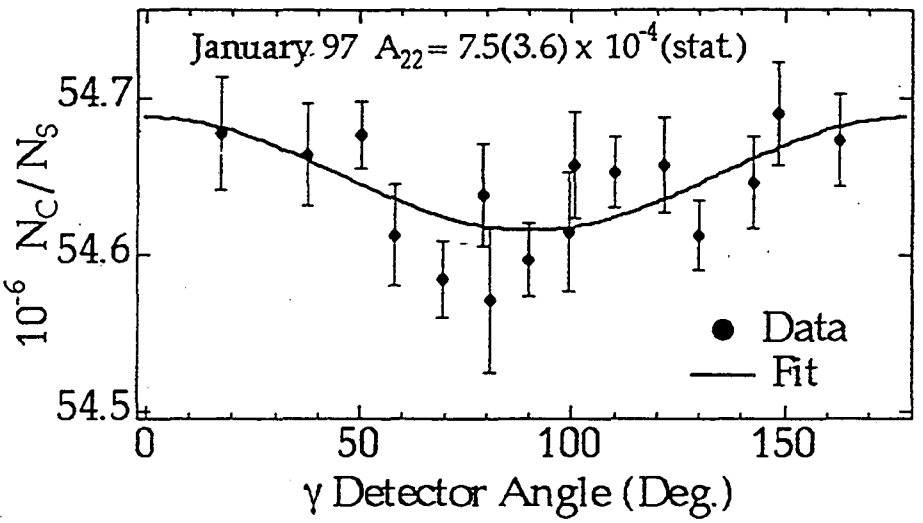
January 97 $A_{22}$= 7.5(3.6) x $10^{-4}$(stat.)
54.7
54.6
54.5
$10^{-6}$ $N_C/N_S$
0
50
100
150
γ Detector Angle (Deg.)
Data
Fit

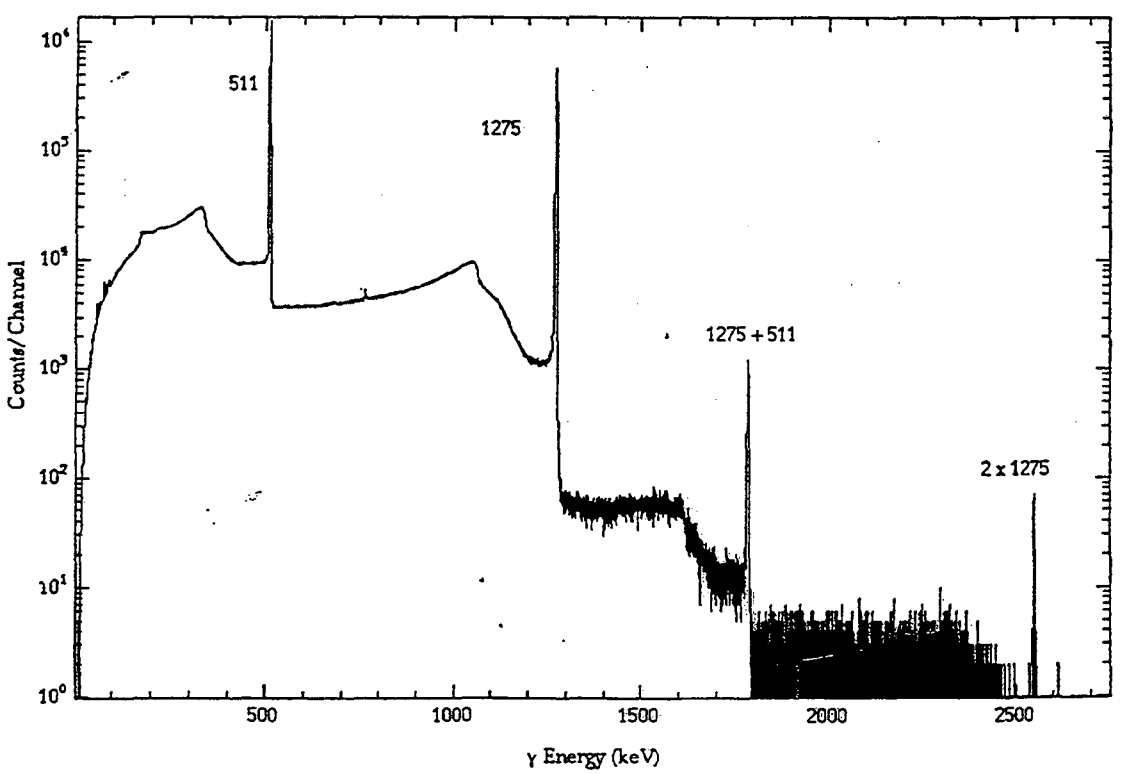
511
1275
1275 + 511
2 x 1275
Counts/Channel
500
1000
1500
2000
2500
γ Energy (keV)

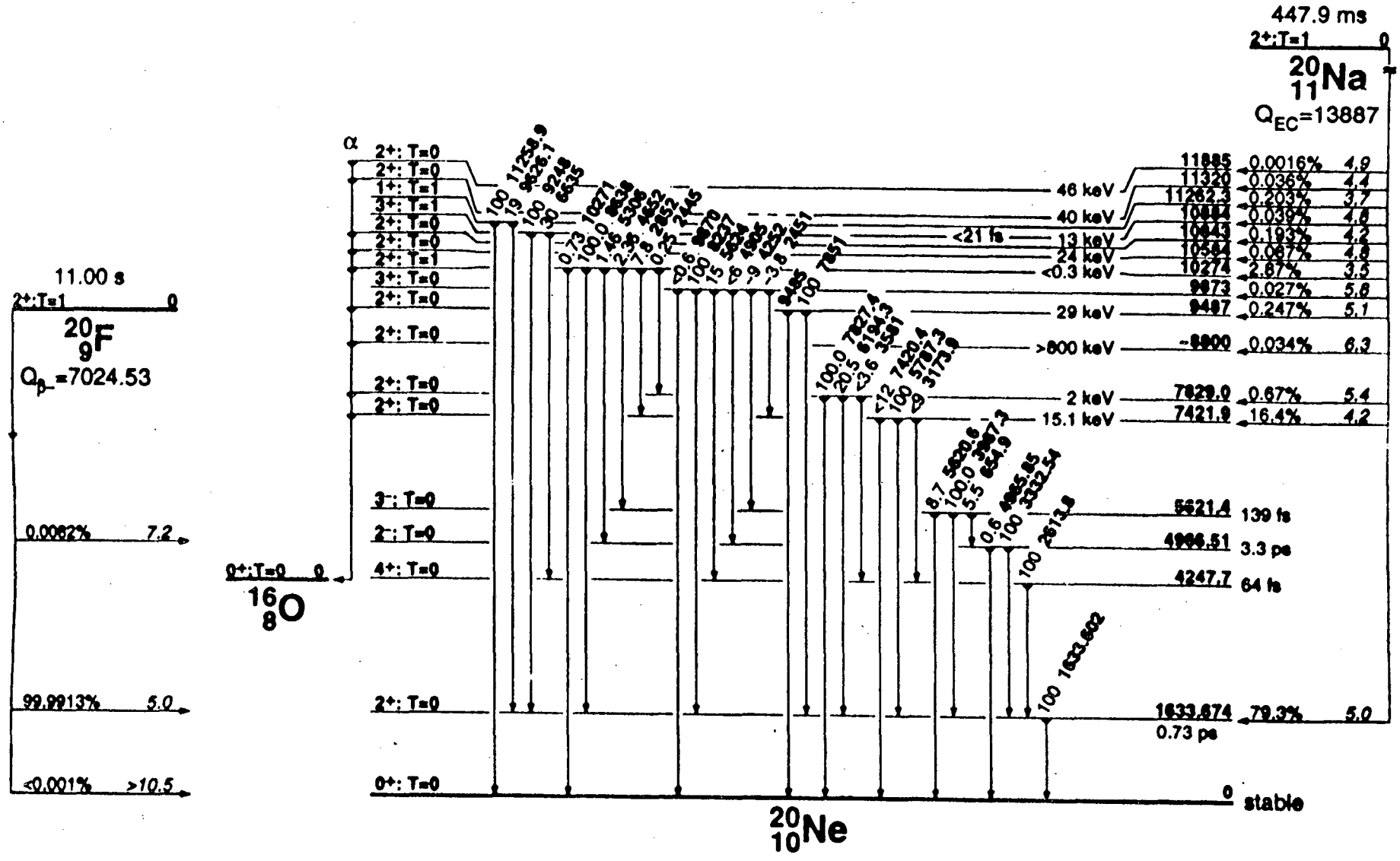
11.00 s
2+;T=1 0
20 9 F
Qβ-=7024.53
0.0082% 7.2
99.9913% 5.0
<0.001% >10.5
α
0+;T=0 0
16 8 O
2+: T=0
1+: T=1
3+: T=1
2+: T=1
3+: T=0
3-: T=0
2-: T=0
4+: T=0
0+: T=0
20 10 Ne
447.9 ms
2+;T=1 0
20 11 Na
QEC=13887
46 keV
40 keV
<21 fs
13 keV
24 keV
<0.3 keV
29 keV
>800 keV
2 keV
15.1 keV
11885 0.0016% 4.9
11320 0.036% 4.4
11262.3 0.203% 3.7
0.193%
0.067%
10274 2.67% 3.5
9873 0.027% 5.8
9487 0.247% 5.1
~8800 0.034% 6.3
7829.0 0.67% 5.4
7421.9 16.4% 4.2
5621.4 139 fs
4966.51 3.3 ps
4247.7 64 fs
1633.674 79.3% 5.0
0.73 ps
0 stable

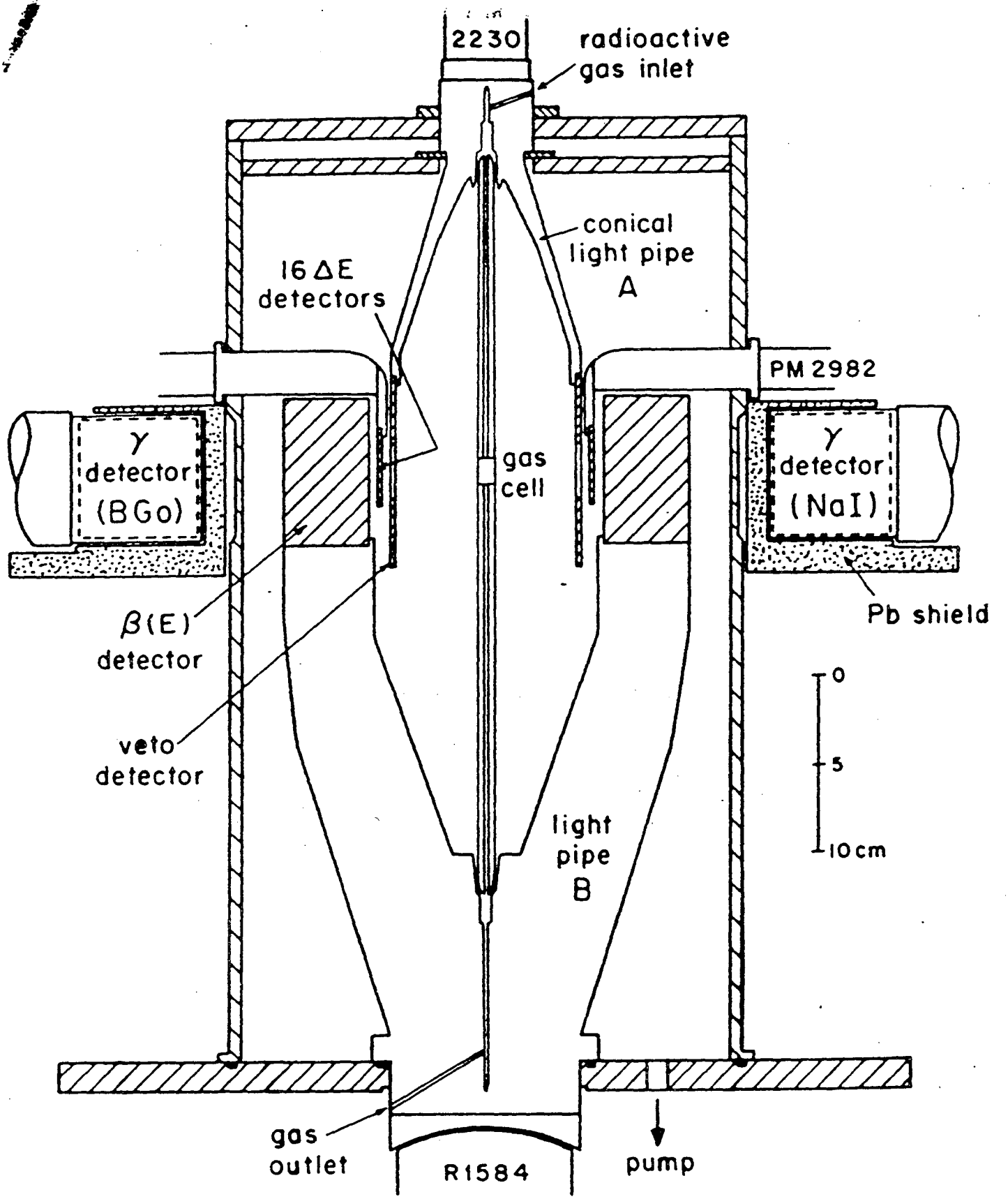
2230
radioactive
gas inlet
conical
light pipe
A
16 ΔE
detectors
PM 2982
γ
detector
(BGo)
gas
cell
γ
detector
(NaI)
Pb shield
β(E)
detector
veto
detector
0
5
10cm
light
pipe
B
gas
outlet
R1584
pump

Fig.2

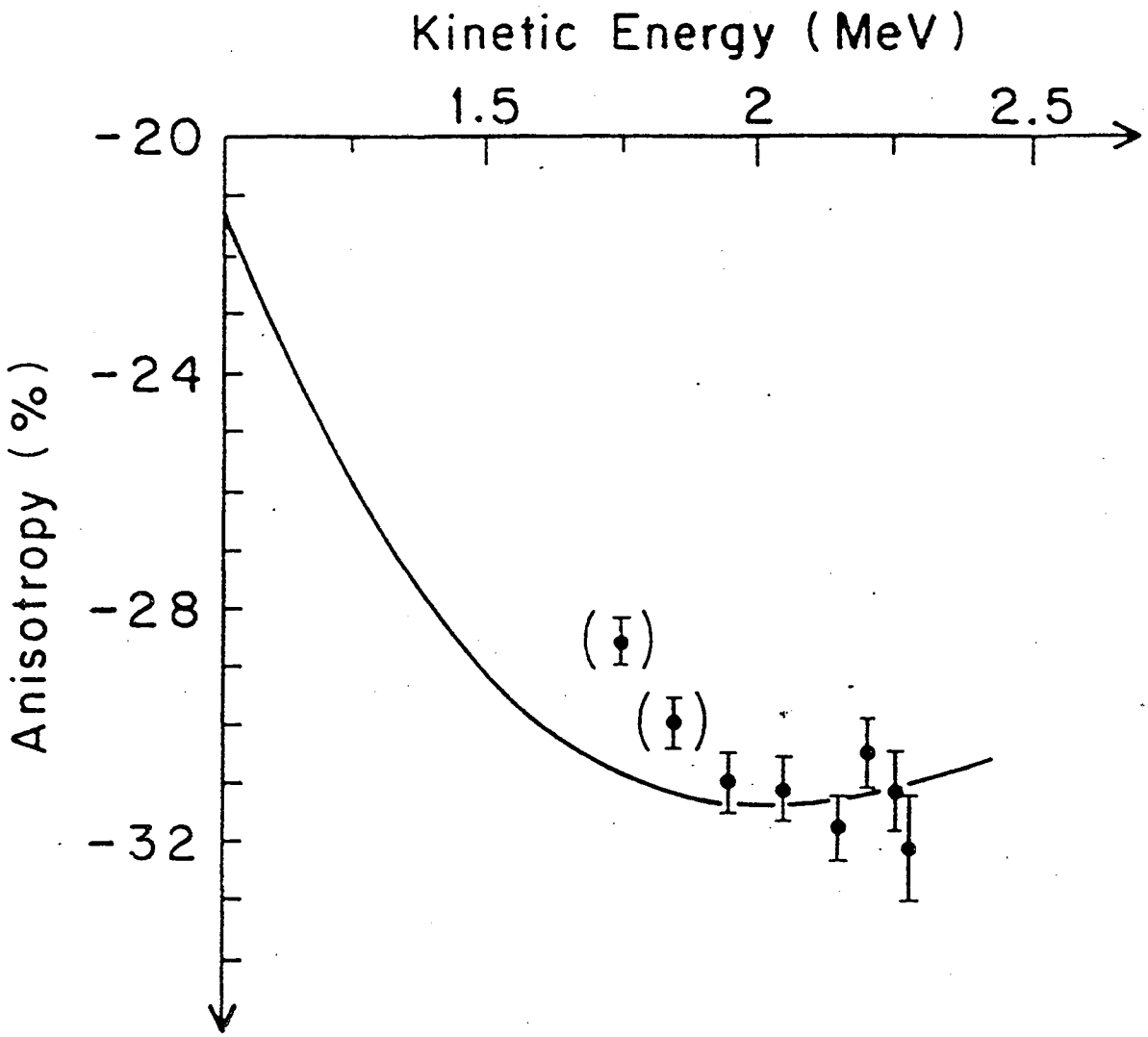


Fig 4.9 Energy dependence of the anisotropy $\{A_2(W)\times10^{-2}\}$ of the 2.301 MeV $\beta \rightarrow$ 0.603 MeV $\gamma$ directional correlation in $^{124}$Sb. The solid line represents the least squares fit performed to deduce the attenuation factor defined in the text.

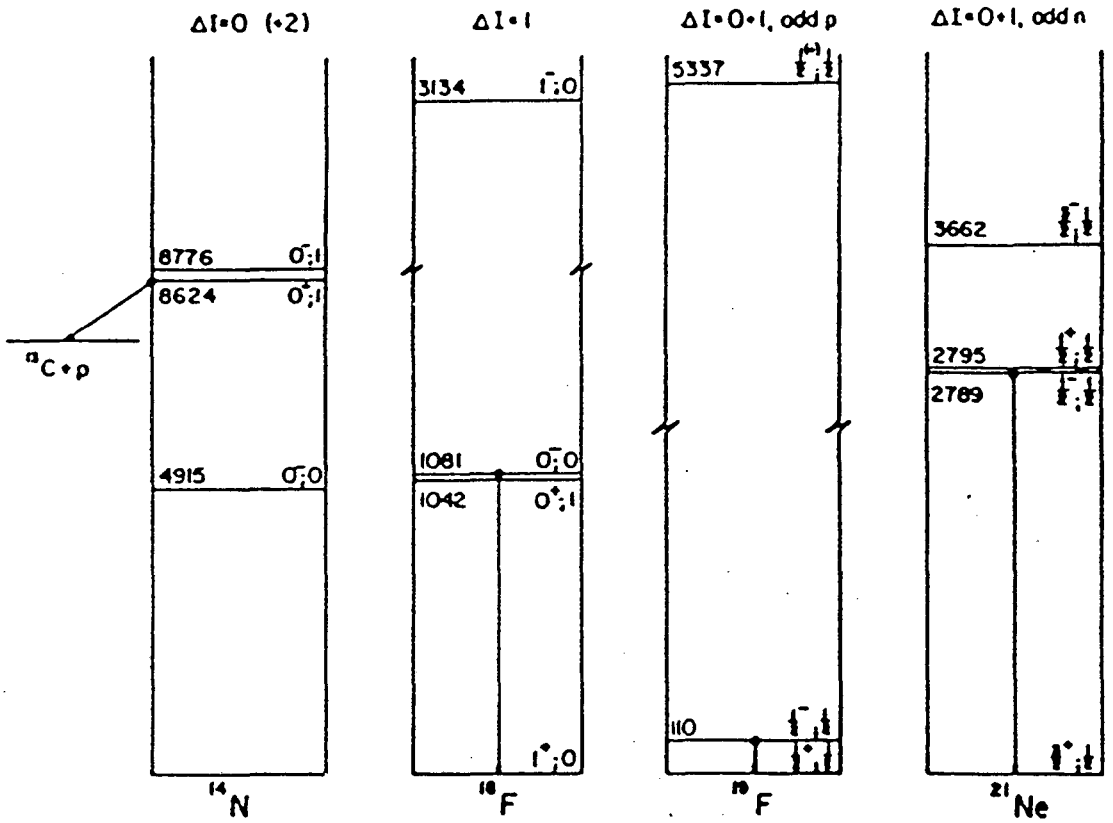


Systems where
two state mixing is fairly good

Strategy — (1) Find closely spaced levels $\frac{\langle V_{PNC}\rangle}{\Delta E}$ ← small

(2) Find a level with an inhibited transition that is enhanced by parity mixing to get an amplification factor.

Queens version of the measurement of $P_\gamma$(1081) line of $^{18}F$.

$^{16}O(^3He,p)^{18}F$ flowing water target

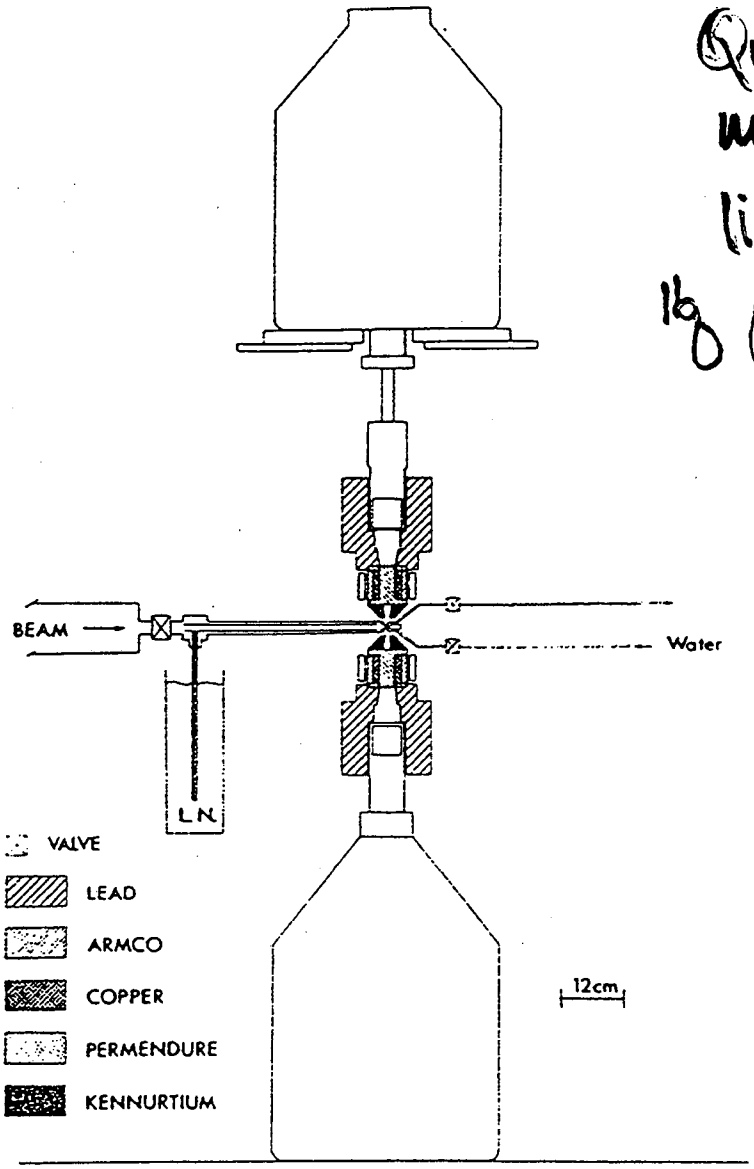


*Figure 10* Side view of the Queen's University $^{18}F$ PNC experiment. Only two of the four Ge(Li) detectors are shown.

$P_\gamma \sim 0$ in all experiments

this is a $\Delta I = 1$ example where neutral current effects are expected

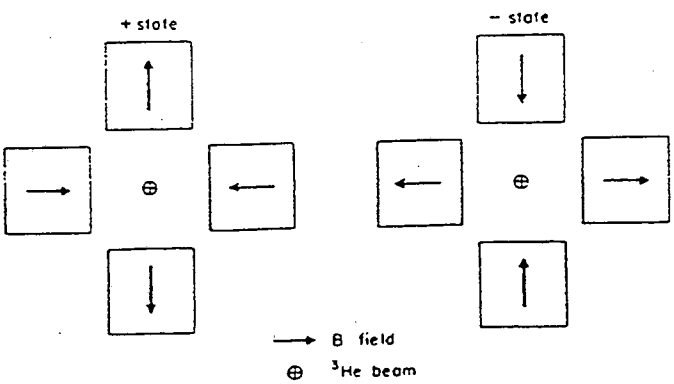


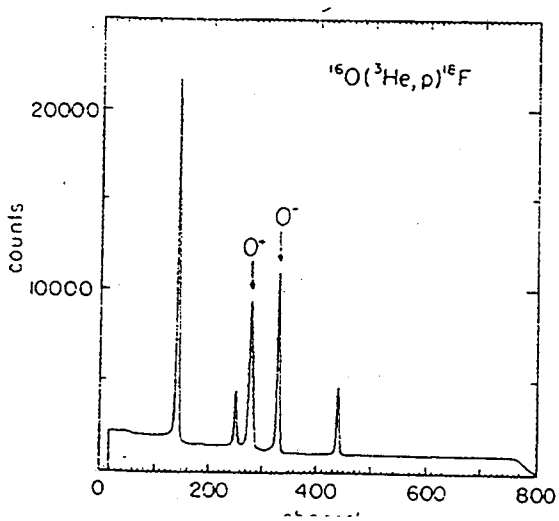

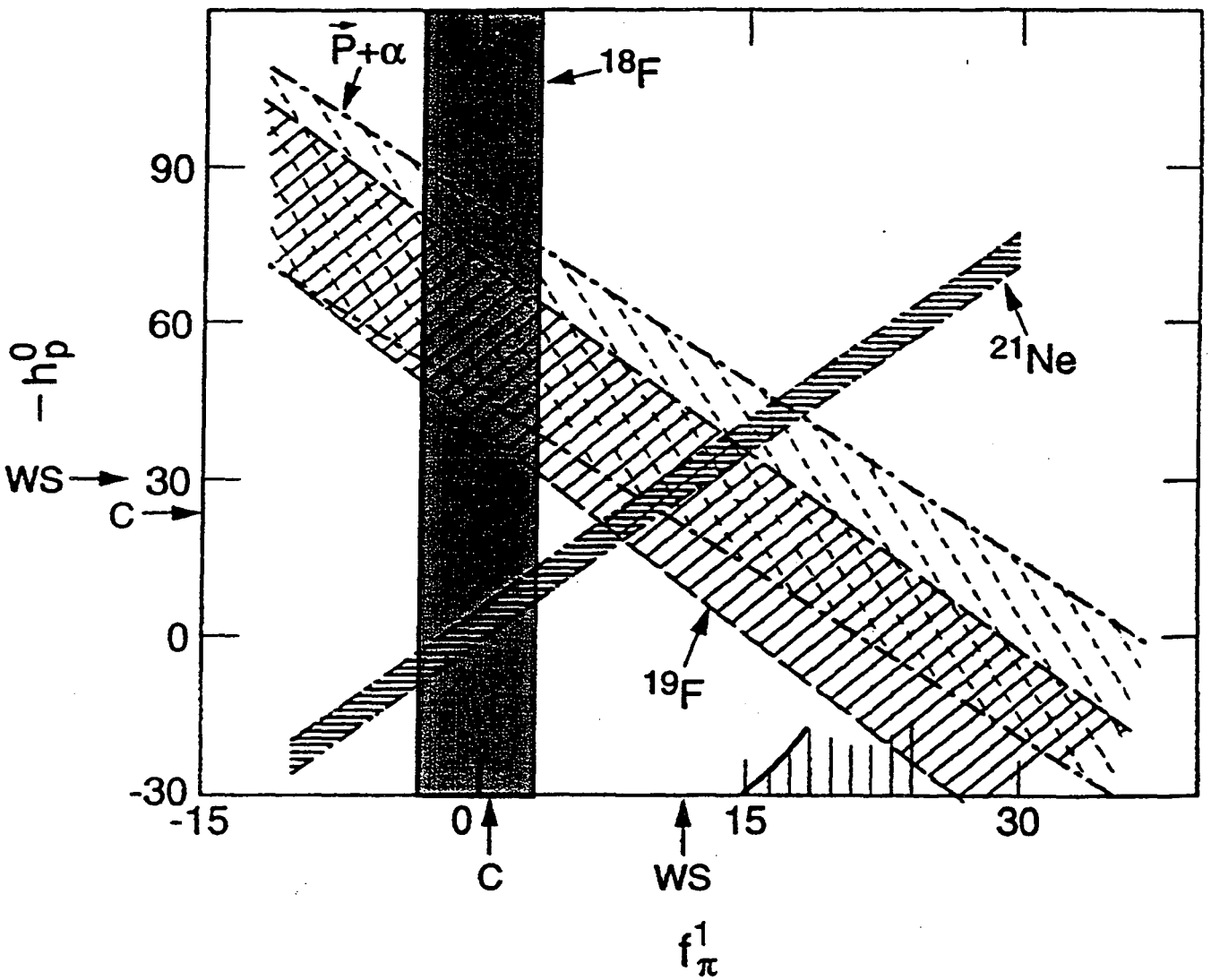
$\vec{P}+\alpha$
$^{18}F$
$^{21}Ne$
$^{19}F$
90
60
30
0
-30
WS
C
$-h_p^0$
-15
0
15
30
C
WS
$f_\pi^1$

REVIEW OF PARTICLE PROPERTIES, PRD 1992

## Tests of Conservation Laws: Discrete Space-Time Symmetries

| Quantity[a] | Value[b] | Symmetry tested or violated |
|---|---|---|
| $\pi^0 \to \gamma\gamma\gamma$/all | $< 3.1 \times 10^{-8}$ | $C$ |
| $(e^+e^-)_{J=0} \to 3\gamma/2\gamma$ | $< 1 \times 10^{-5}$[c] | $C$ |
| * $(e^+e^-)_{J=1} \to 4\gamma/3\gamma$ | $< 1 \times 10^{-5}$[c] | $C$ |
| $\eta \to \gamma\gamma\gamma$/all | $< 5 \times 10^{-4}$ | $C$ |
| $\eta \to \pi^0 e^+e^-$/all | $< 4 \times 10^{-5}$ | $C$ (single photon process) |
| $\eta \to \pi^0 \mu^+\mu^-$/all | $< 5 \times 10^{-6}$ | $C$ (single photon process) |
| $\eta \to \pi^+\pi^-\pi^0$ parameters : left-right asymmetry | $(0.9 \pm 1.7) \times 10^{-3}$ | $C$ |
| sextant asymmetry | $(1.8 \pm 1.6) \times 10^{-3}$ | $C$ |
| quadrant asymmetry | $(-1.7 \pm 1.7) \times 10^{-3}$ | $C$ |
| $\eta \to \pi^+\pi^-\gamma$ parameters: left-right asymmetry | $(9 \pm 4) \times 10^{-3}$ | $C$ |
| $\beta$ ($D$-wave) | $0.05 \pm 0.06$ | $C$ |
| $\eta \to \pi^+\pi^-$/all | $< 1.5 \times 10^{-3}$ | $P$ and $CP$ |
| $e$ electric dipole moment | $(-3 \pm 8) \times 10^{-27}$ $e$ cm | $T$ and $P$ |
| $\mu$ electric dipole moment | $(3.7 \pm 3.4) \times 10^{-19}$ $e$ cm | $T$ and $P$ |
| $p$ electric dipole moment | $(-4 \pm 6) \times 10^{-23}$ $e$ cm | $T$ and $P$ |
| $n$ electric dipole moment | $< 1.2 \times 10^{-25}$ $e$ cm | $T$ and $P$ |
| $\Lambda$ electric dipole moment | $< 1.5 \times 10^{-16}$ $e$ cm | $T$ and $P$ |
| $\alpha'/A$ from $\mu \to e\bar{\nu}\nu$ | $(0 \pm 4) \times 10^{-3}$ | $T$ |
| $\beta'/A$ from $\mu \to e\bar{\nu}\nu$ | $(2 \pm 6) \times 10^{-3}$ | $T$ |
| $e^+$ pol.$\perp$ $\mu$ spin and $e^+$ mom. from $\mu^+ \to e^+\bar{\nu}\nu$ | $0.007 \pm 0.023$ | $T$ |
| Im $\xi$ in $K^{\pm}_{\mu 3}$ decay (from transverse $\mu$ pol.) | $-0.017 \pm 0.025$ | $T$ |
| Im $\xi$ in $K^0_{\mu 3}$ decay (from transverse $\mu$ pol.) | $-0.007 \pm 0.026$ | $T$ |
| $\phi$, phase of $g_A/g_V$ for $n$ | $(180.07 \pm 0.18)°$ | $T$ (0° or 180°) |
| $n$ triple correlation coefficient | $(-5 \pm 14) \times 10^{-4}$ | $T$ |
| $\Sigma^- \to ne^-\bar{\nu}_e$ triple correlation coefficient | $0.11 \pm 0.10$ | $T$ |
| $K^{\pm} \to \pi^{\pm}\pi^+\pi^-$ rate difference/average | $(0.07 \pm 0.12)\%$ | $CP$ |
| $K^{\pm} \to \pi^{\pm}2\pi^0$ rate difference/average | $(0.0 \pm 0.6)\%$ | $CP$ |
| $K^{\pm} \to \pi^{\pm}\pi^0\gamma$ rate difference/average | $(0.9 \pm 3.3)\%$ | $CP$ |
| $K^{\pm} \to 3\pi^{\pm}$ slope $(g^+ - g^-)$/sum | $(-0.70 \pm 0.53)\%$ | $CP$ |
| $\lvert\eta_{+-0}\rvert^2 = \Gamma(K^0_S \to \pi^+\pi^-\pi^0,\ CP$ viol.$)/\Gamma(K^0_L \to \pi^+\pi^-\pi^0)$ | $< 0.12$ | $CP$ |
| $\lvert\eta_{000}\rvert^2 = \Gamma(K^0_S \to 3\pi^0)/\Gamma(K^0_L \to 3\pi^0)$ | $< 0.1$ | $CP$ |
| $K^0_L \to \pi^0\nu\bar{\nu}$/all | $< 7.6 \times 10^{-3}$ | $CP$[d] |
| $\to \pi^0\mu^+\mu^-$/all | $< 1.2 \times 10^{-6}$ | $CP$[e] |
| $\to \pi^0 e^+e^-$/all | $< 5.5 \times 10^{-9}$ | $CP$[e] |
| Charge asymmetry $j$ in $K^0_L \to \pi^+\pi^-\pi^0$ | $0.0011 \pm 0.0008$ | $CP$ |
| $K^0_L \to (\pi^-\mu^+\nu - \pi^+\mu^-\bar{\nu})$/sum | $(0.304 \pm 0.025)\%$ | $CP$ (violated) |
| $\to (\pi^-e^+\nu - \pi^+e^-\bar{\nu})$/sum | $(0.333 \pm 0.014)\%$ | $CP$ (violated) |
| $\lvert\eta_{00}\rvert = \lvert A(K^0_L \to \pi^0\pi^0)/A(K^0_S \to \pi^0\pi^0)\rvert$ | $(2.253 \pm 0.024) \times 10^{-3}$ | $CP$ (violated) |
| $\lvert\eta_{+-}\rvert = \lvert A(K^0_L \to \pi^+\pi^-)/A(K^0_S \to \pi^+\pi^-)\rvert$ | $(2.268 \pm 0.023) \times 10^{-3}$ | $CP$ (violated) |
| $\lvert\epsilon'/\epsilon\rvert = (1 - \lvert\eta_{00}/\eta_{+-}\rvert)/3$ | $(2.2 \pm 1.1) \times 10^{-3}$ | $CP$ (violated)[f] |
| $\phi_{+-}$ : phase of $\eta_{+-}$ | $(46.6 \pm 1.2)°$ | $CP$ (violated) |
| $\phi_{00}$ : phase of $\eta_{00}$ | $(46.6 \pm 2.0)°$ | $CP$ (violated) |
| $(D^0 - \bar{D}^0) \to K^+K^-$ rate difference/sum | $< 0.45$ | $CP$ |
| $[\alpha_-(\Lambda) + \alpha_+(\bar{\Lambda})]/[\alpha_-(\Lambda) - \alpha_+(\bar{\Lambda})]$ | $-0.03 \pm 0.06$ | $CP$ |
| $(g_{e^+} - g_{e^-})$/average | $(-0.5 \pm 2.1) \times 10^{-12}$ | $CPT$ |
| $(g_{\mu^+} - g_{\mu^-})$/average | $(-2.6 \pm 1.6) \times 10^{-8}$ | $CPT$ |
| $(\mu_p - \lvert\mu_{\bar{p}}\rvert)$/average | $(-2.6 \pm 2.9) \times 10^{-3}$ | $CPT$ |
| $e^+ - e^-$ mass difference/average | $< 4 \times 10^{-8}$ | $CPT$ |
| $\pi^+ - \pi^-$ mass difference/average | $(2 \pm 5) \times 10^{-4}$ | $CPT$ |
| $K^+ - K^-$ mass difference/average | $(-0.6 \pm 1.8) \times 10^{-4}$ | $CPT$ |
| $\lvert K^0 - \bar{K}^0\rvert$ mass difference/average | $< 4 \times 10^{-18}$ | $CPT$[g] |
| $\phi_{00} - \phi_{+-}$ | $(0.1 \pm 1.9)°$ | $CPT$ |
| $p - \bar{p}$ mass difference/average | $(2 \pm 4) \times 10^{-8}$ | $CPT$ |
| $n - \bar{n}$ mass difference/average | $(9 \pm 5) \times 10^{-5}$ | $CPT$ |
| $\Lambda - \bar{\Lambda}$ mass difference/average | $(0.0 \pm 1.1) \times 10^{-4}$ | $CPT$ |
| $\Xi^- - \bar{\Xi}^+$ mass difference/average | $(1.1 \pm 2.7) \times 10^{-4}$ | $CPT$ |
| $\Omega^- - \bar{\Omega}^+$ mass difference/average | $(-1 \pm 5) \times 10^{-4}$ | $CPT$ |
| $W^+ - W^-$ mass difference/average | $(-2 \pm 7) \times 10^{-3}$ | $CPT$ |
| $\mu^+ - \mu^-$ mean life difference/average | $(2 \pm 8) \times 10^{-5}$ | $CPT$ |
| $\pi^+ - \pi^-$ mean life difference/average | $(6 \pm 7) \times 10^{-4}$ | $CPT$ |
| $K^+ - K^-$ mean life difference/average | $(1.1 \pm 0.9) \times 10^{-3}$ | $CPT$ |
| $\Lambda - \bar{\Lambda}$ mean life difference/average | $(4 \pm 9) \times 10^{-2}$ | $CPT$ |
| $\Xi^- - \bar{\Xi}^+$ mean life difference/average | $(0.02 \pm 0.18)$ | $CPT$ |
| $K^{\pm} \to \mu^{\pm}\nu$ rate difference/average | $(-0.54 \pm 0.41)\%$ | $CPT$ |
| $K^{\pm} \to \pi^{\pm}\pi^0$ rate difference/average | $(0.8 \pm 1.2)\%$ | $CPT$[h] |

* $e^+e^-$ — MILLS + SERKO, PRL 18, 420 (1967).
MARKO + RICH, PRL 33, 980 (1974).

# Test of TRIV in isospin-hindered decay of $^{56}$Co

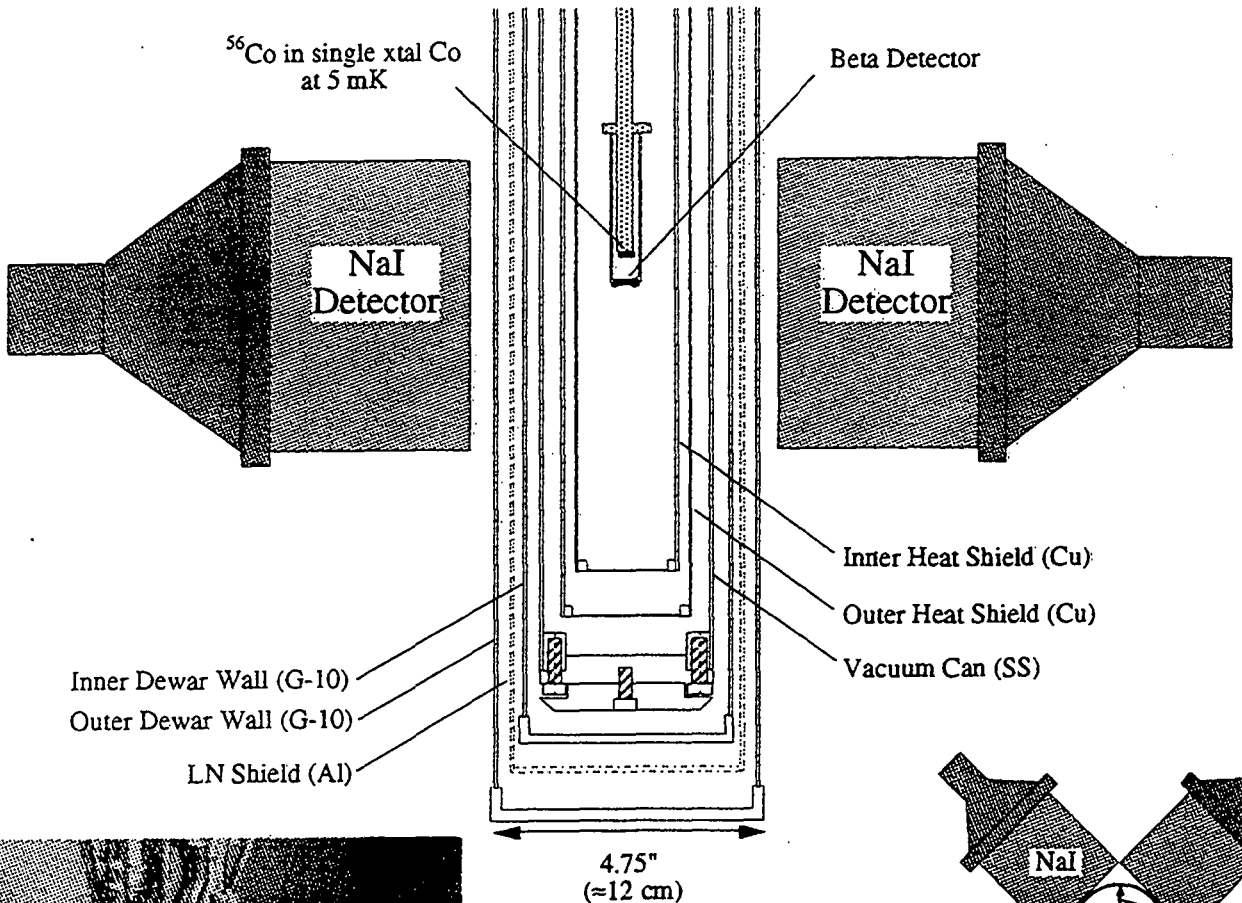


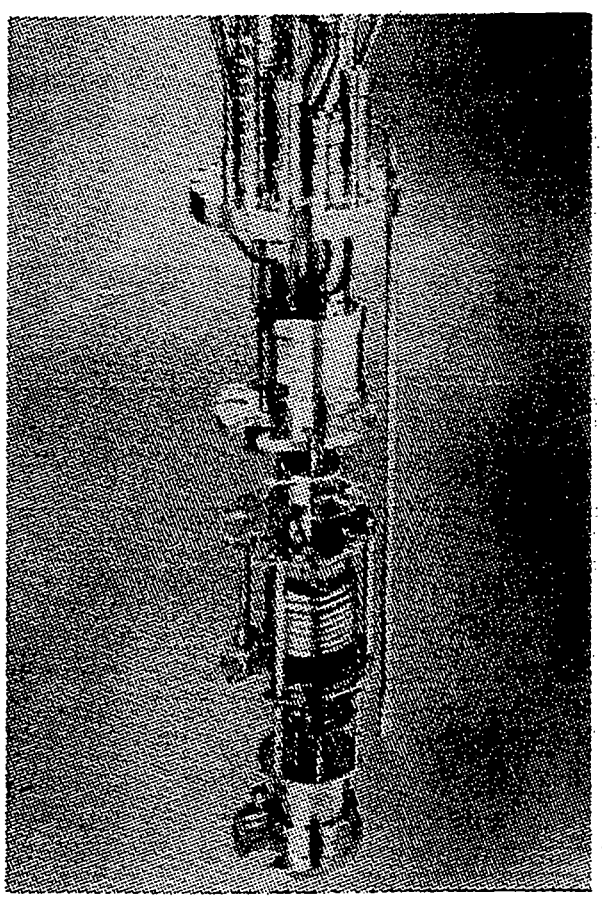

OXFORD Kelvinox 400

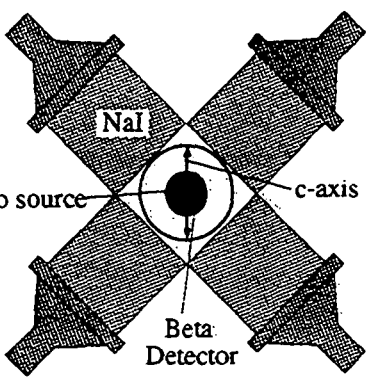


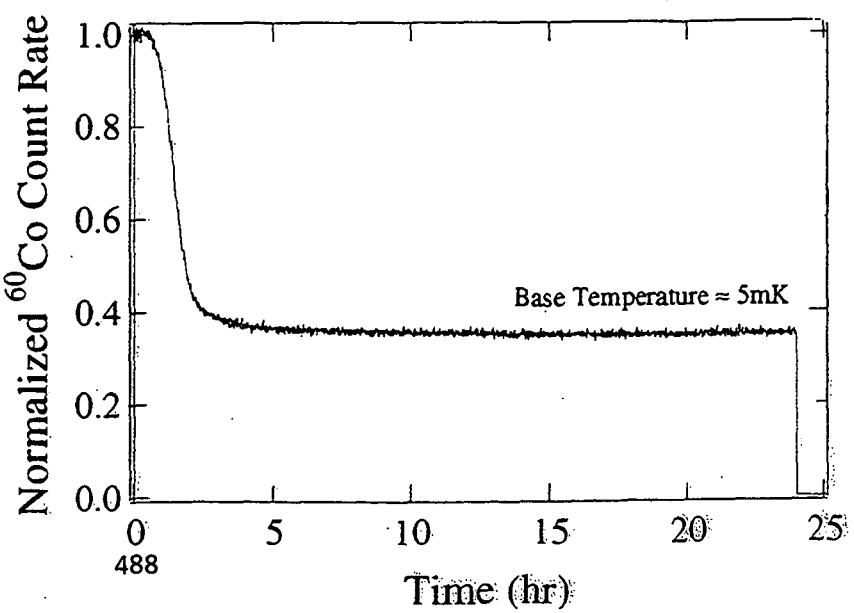

M.Smith

Nuclear astrophysics opportunities with GRETA.

# Nuclear Astrophysics Opportunities with GRETA

Michael Smith
Physics Division
Oak Ridge National Laboratory

## Contributors

| | |
|---|---|
| Jim Beene | ORNL |
| Jeff Blackmon | ORNL |
| Carl Brune | UNC Chapel Hill |
| Art Champagne | UNC Chapel Hill |
| Uwe Greife | Bochum |
| Gerry Hale | LANL |
| I Yang Lee | LBNL |
| Eric Norman | LBNL |
| Peter Parker | Yale |
| Claus Rolfs | Bochum |
| Michael Wiescher | Notre Dame |

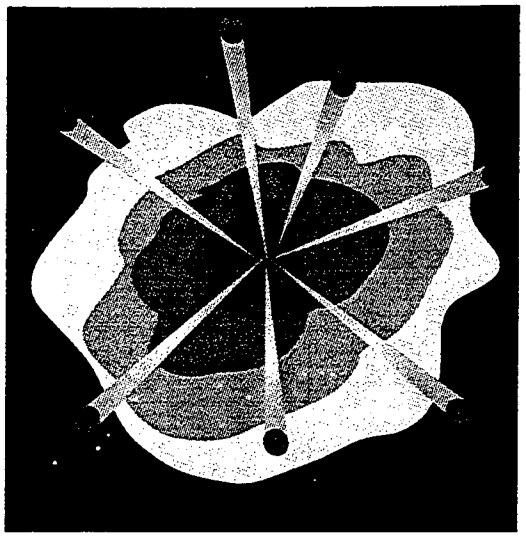

Big Bang

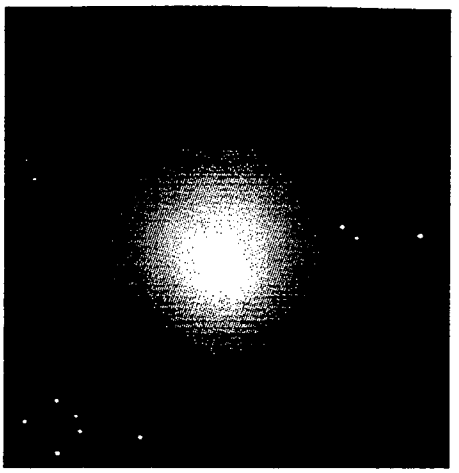

Red Giant
Betelgeuse

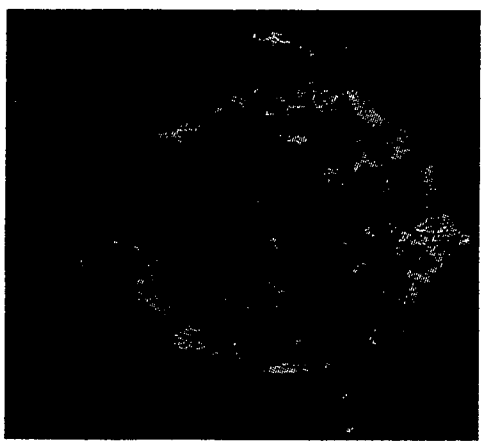

Cas A Supernova
Remnant

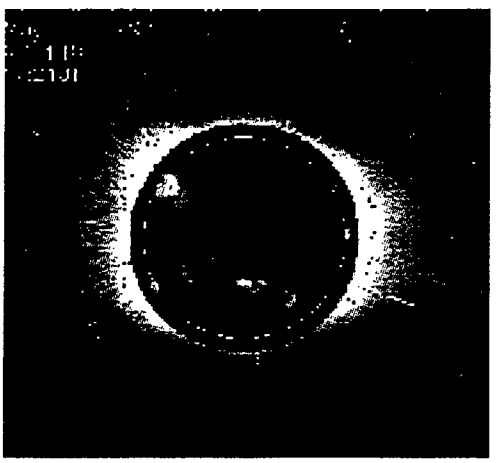

Solar Physics

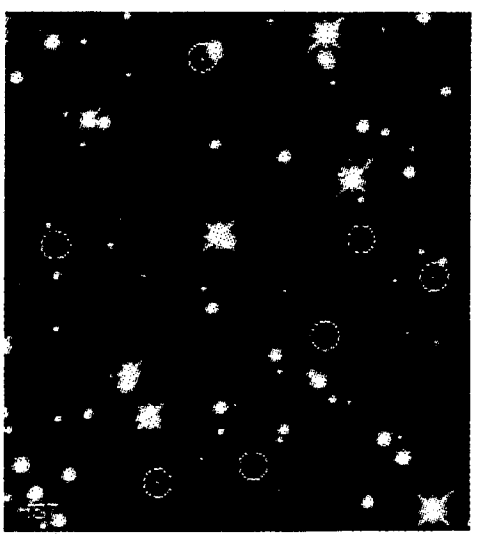

White Dwarfs

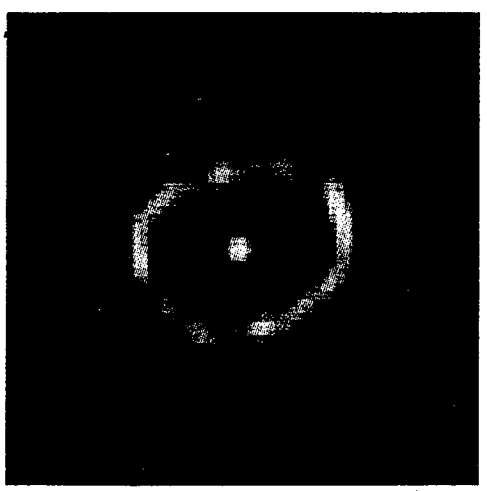

Nova Cygni 1992

# Nuclear Astrophysics Stud'es

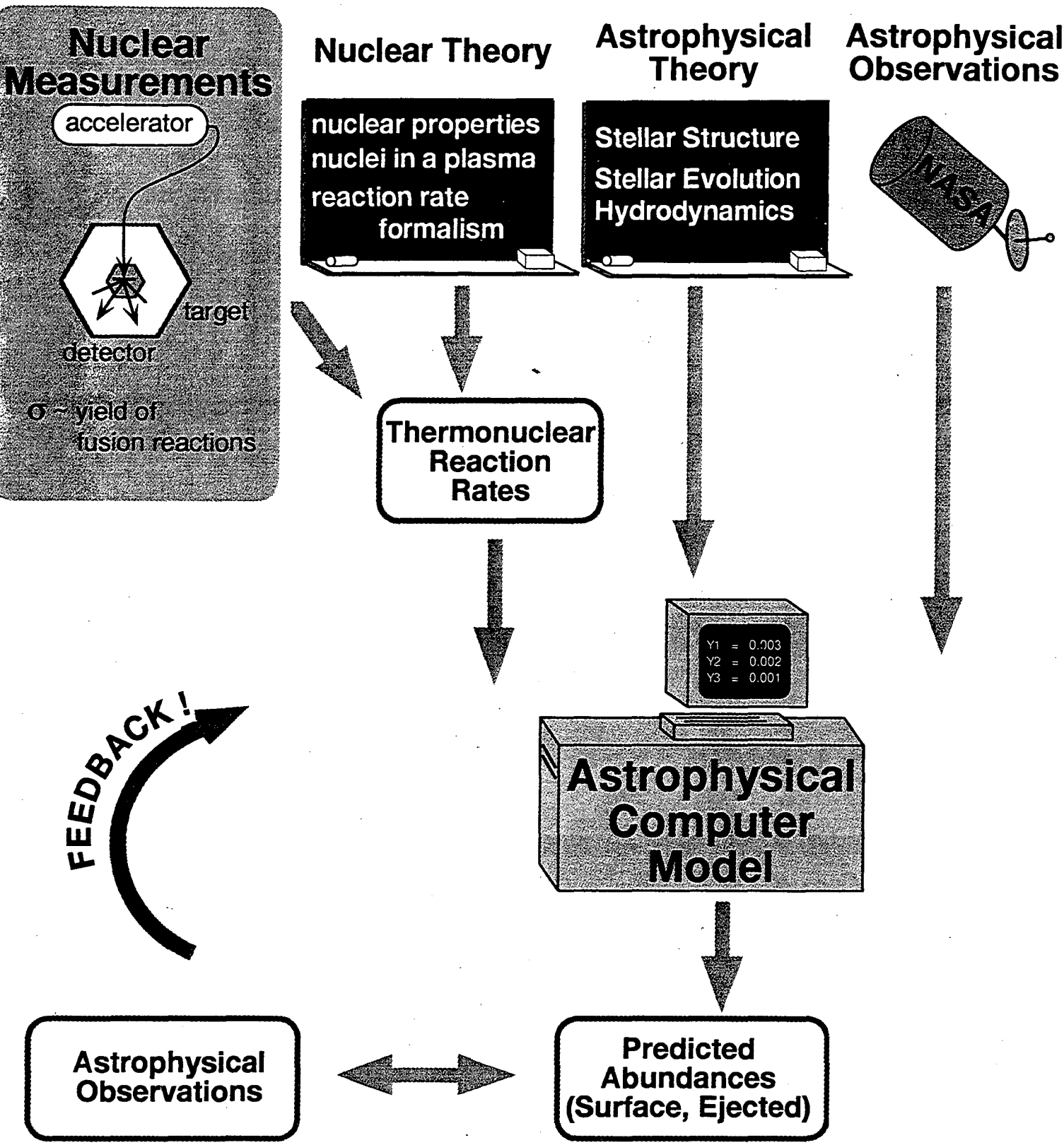

# Measurements w'th GRETA

## Capture Reactions

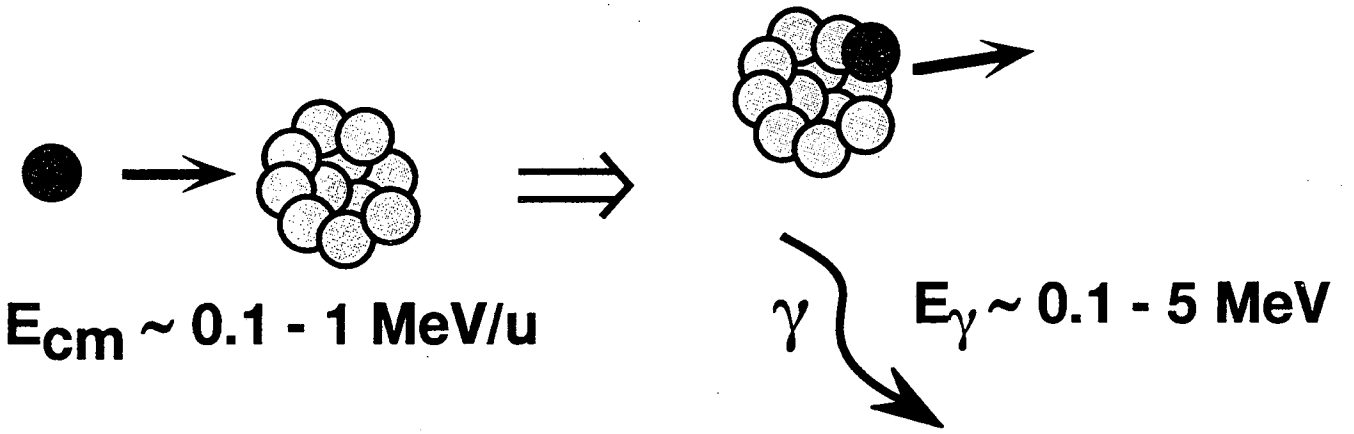


## Radioactive Beams

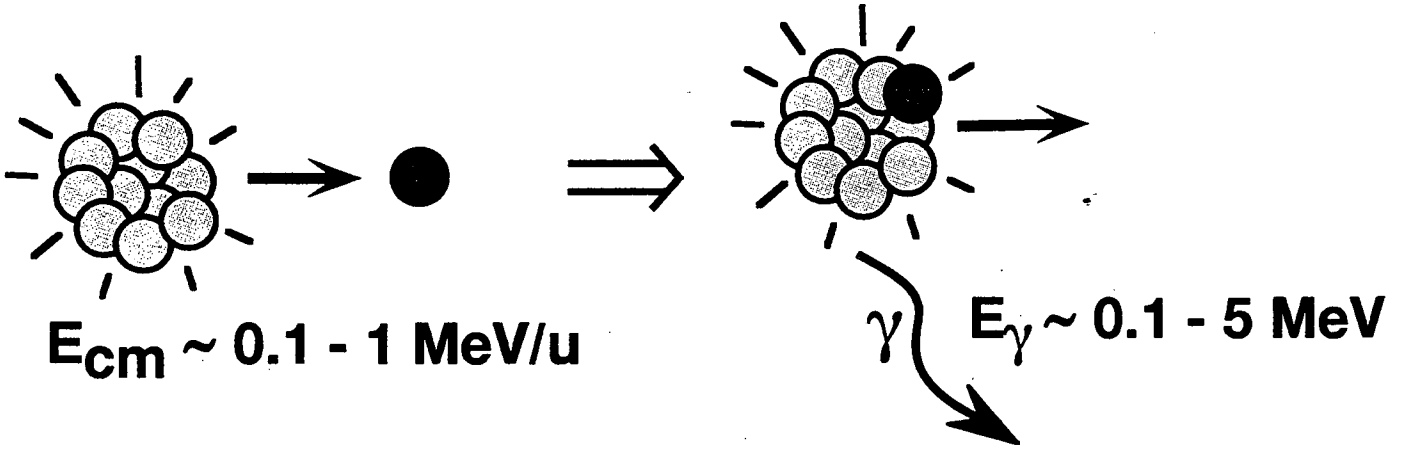


## Nuclear Structure

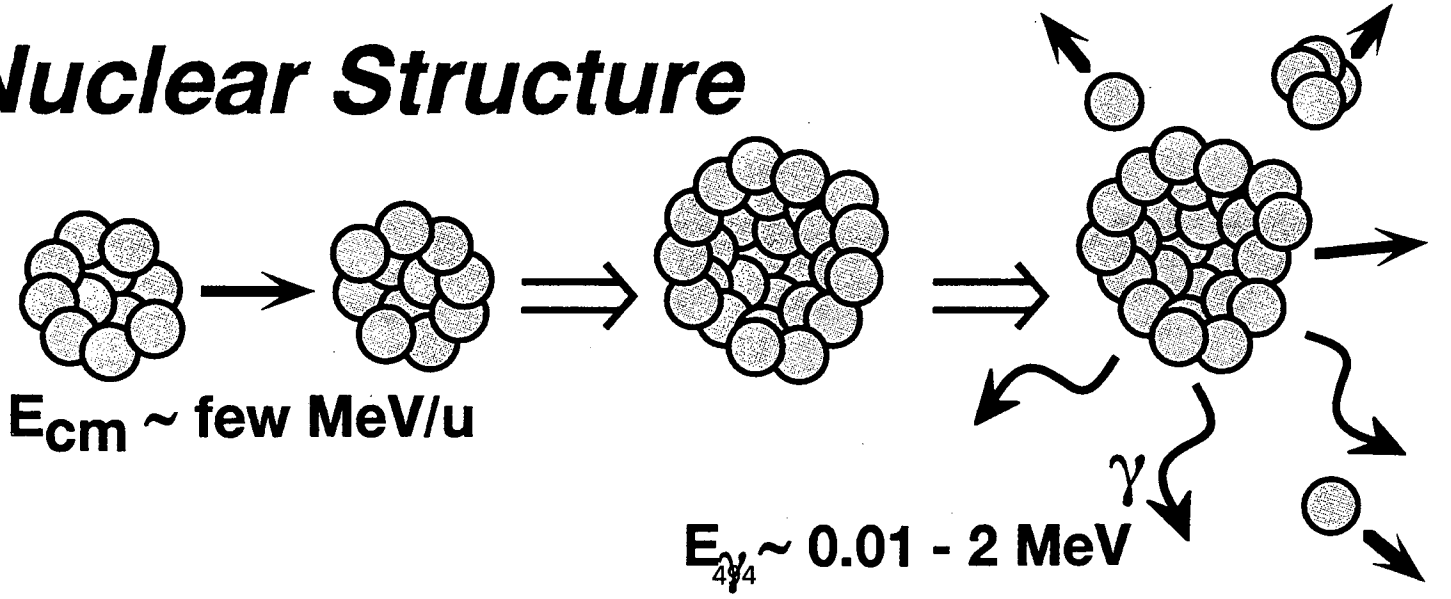

# Capture Reactions

**Directly measure Capture Reactions**

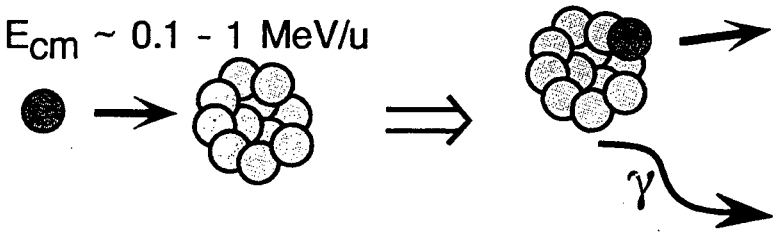


*A(p,γ)B occuring in stellar environments*

- **Fusion far below Coulomb barrier – very small $\sigma \lesssim$ pb**

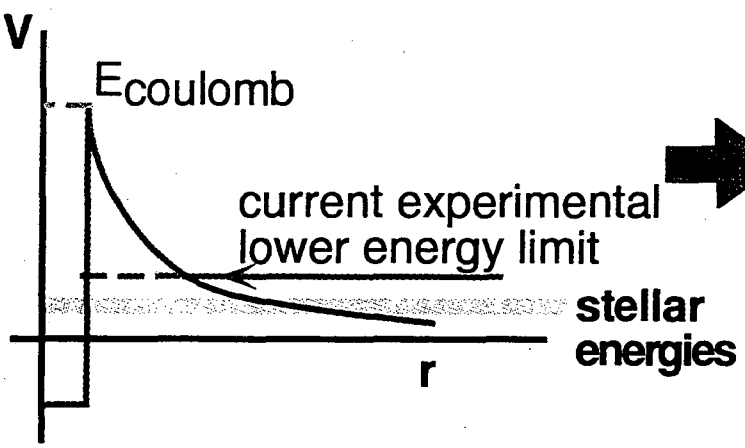


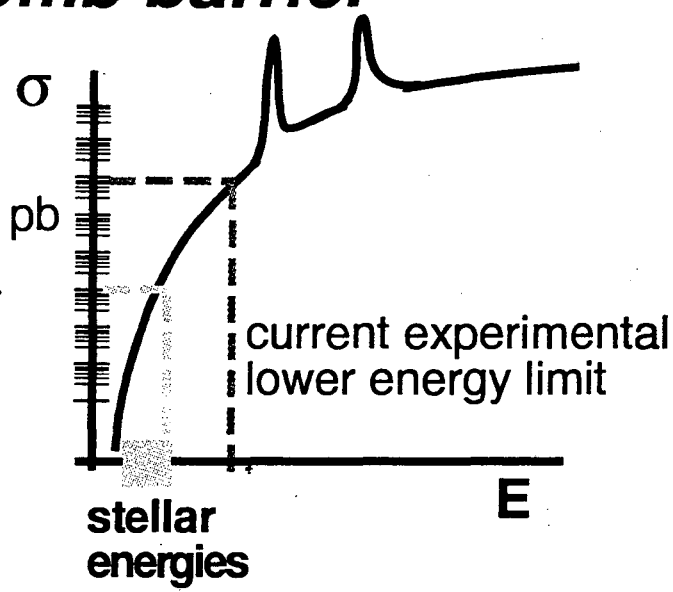


- **Cosmic Rays & Natural Radioactivity Limit Sensitivity**

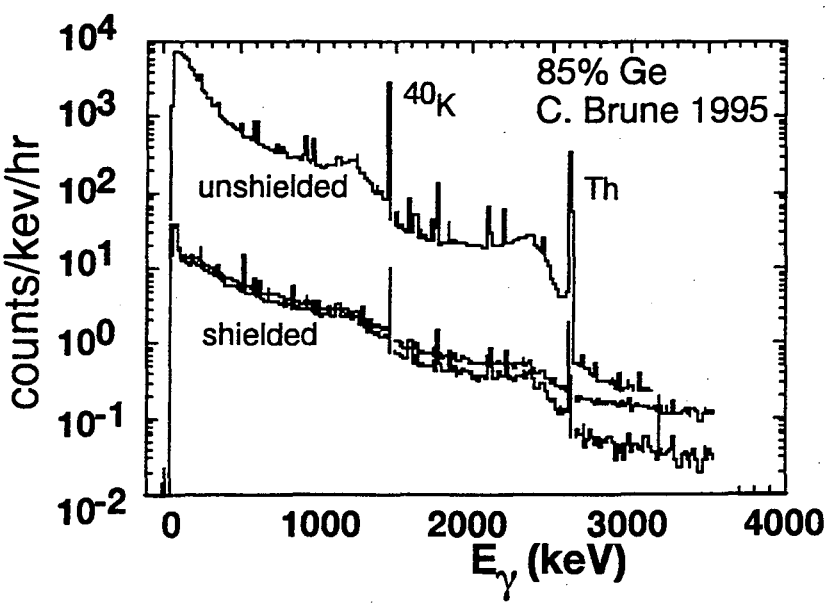


- **Cannot yet reach stellar energies**

# Capture Reactions

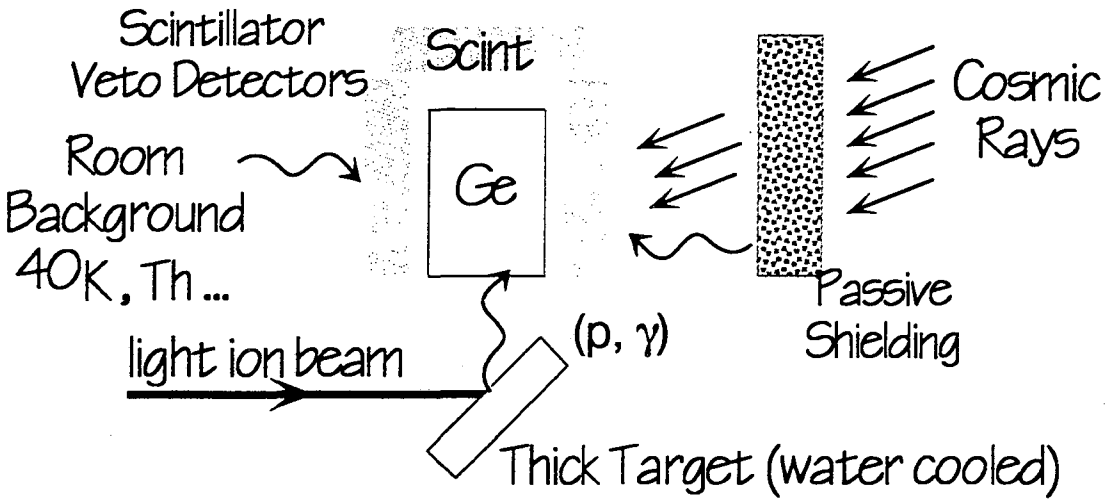


| | |
|---|---|
| ***Beam Current, Energy*** | *~ μA - mA (!), 0.01 - 2 MeV* |
| ***Typical Counting Rates*** | *~ 100 counts/hr σ ~ nb, I ~ μA* |
| | *~ few counts/day σ ~ pb, I ~ μA* |
| ***Typical Multiplicity*** | *~ 1 - 3* |
| ***Backgrounds*** | *Cosmic Rays* |
| | *Natural Radioactivity* |
| | *Beam-Induced Background* |
| | *Target Impurities* |
| ***Major Problems*** | *LOW Count Rates* |
| | *High Background Rates* |
| | *Long Running Times* |
| | *Target Damage & Impurities* |
| | *Passive Shielding Generates Backgrounds* |

# Capture Reactions

## Advantages of GRETA

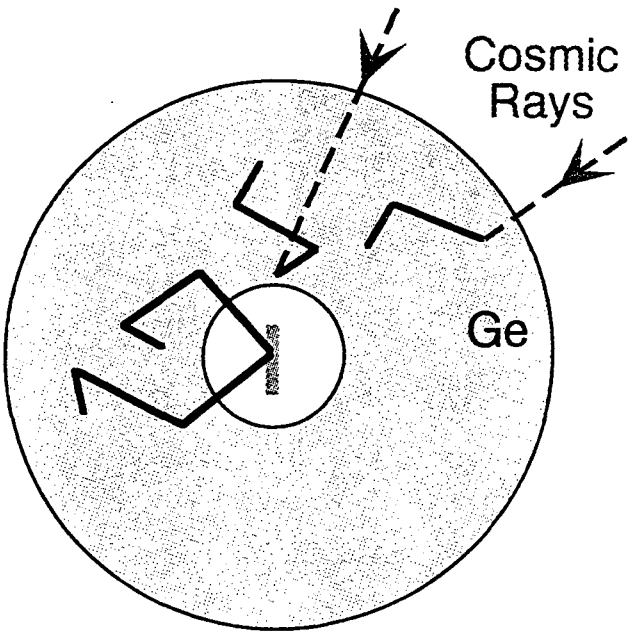


### Tracking

- *reject cosmic rays and room backgrounds from energy and angle info*
- *tracking plus energy resolution*
  *⇒ enhanced rejection*

- *rejection desired > 1 / 1000*

- *excellent angular distributions*

### High Efficiency

- *smaller cross sections*

*⇒ $\sigma$ at lower energy*

*⇒ closer to stellar energies*

*⇒ less extrapolation necessary to determine stellar reaction rates*

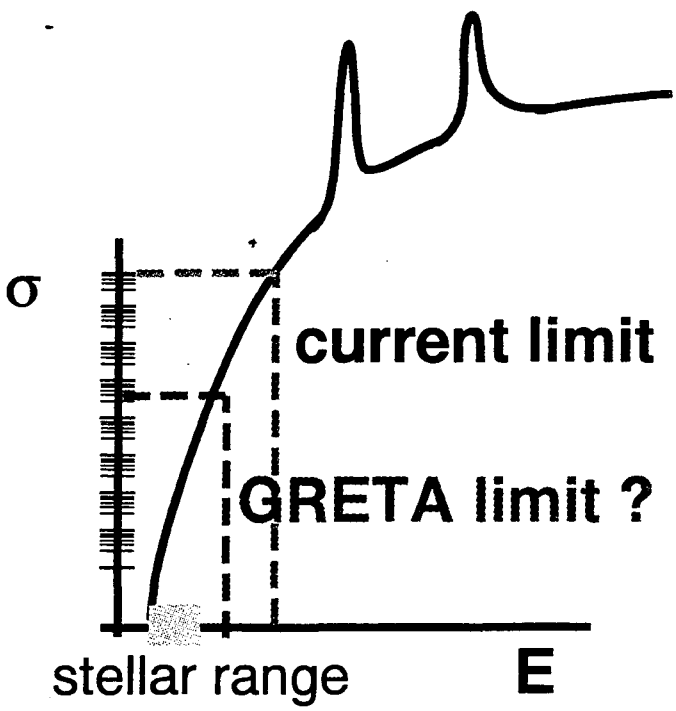


- *measure entire $\gamma$ yield (all multipolarities)*

## Goal: (p,$\gamma$) in the Stellar Energy Range

**Granularity** – *excellent angular distributions*

**Resolution** – *cascade $\gamma$'s for high level density nuclei*

# Capture Reaction Expts

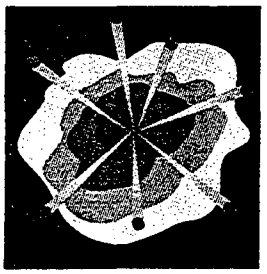

## Big Bang

$d(\alpha,\gamma)^6Li$

$d(p,\gamma)^3He$

$^3He(\alpha,\gamma)^7Be$

$^7Li(\alpha,\gamma)^{11}B$

$^7Be(\alpha,\gamma)^{11}C$

## Explosive Burning

$(p,\gamma)$ on

Ne Na

Mg Al

Si P ...

for the NeNa cycle,

MgAl cycle, SiP cycle ...

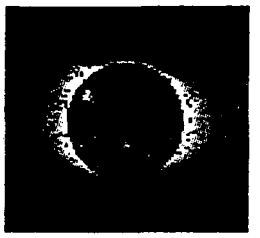

## Solar Neutrino Problem

$^3He(\alpha,\gamma)^7Be$

$^7Be(p,\gamma)^8B$

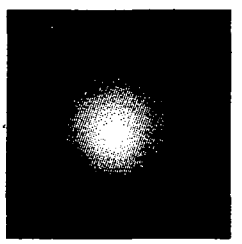

## Hydrostatic Burning

$^{14}N(p,\gamma)^{15}O$

$^{17}O(p,\gamma)^{18}F$

$^{12}C(\alpha,\gamma)^{16}O$

$^{14}N(\alpha,\gamma)^{18}F$

$^{16}O(\alpha,\gamma)^{20}Ne$

$^{18}O(\alpha,\gamma)^{22}Ne$

$^{20}Ne(\alpha,\gamma)^{24}Mg$

$^{12}C + {}^{12}C$

# $^{12}C(\alpha,\gamma)^{16}O$ Capture Reaction

- *Determines Carbon / Oxygen Ratio in Red Giant stars*
- *Helps Determine subsequent evolution into White Dwarfs or Supernovae*
- *Helps Determine abundances of heavier elements formed in later life of star*
- *Important Energy Range $E_{cm}$ = 0.3 MeV*

  *Current Experimental Limit: $E_{cm} \gtrsim 1.0$ MeV*

  *(25 years of Measurements !)*
- *NEED*

  *Total Cross Section to low energies*

  *Angular Distributions for extrapolation*

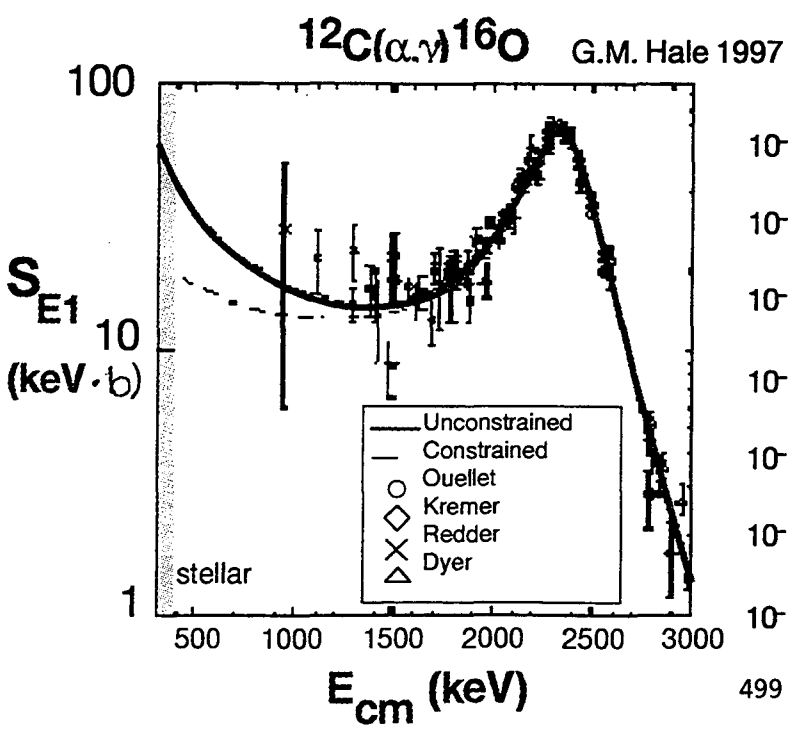


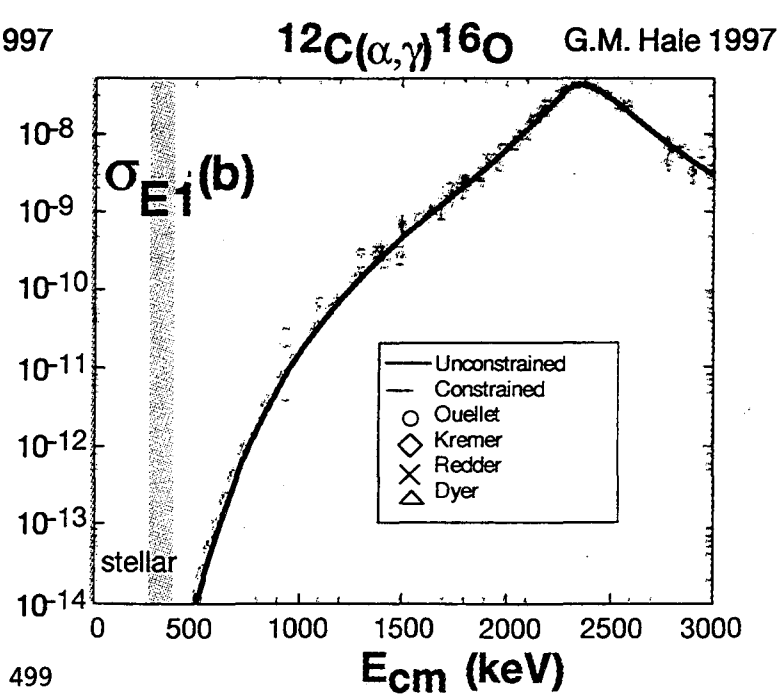

# Rad'oactive Beam Expts

Nova Cygni 1992

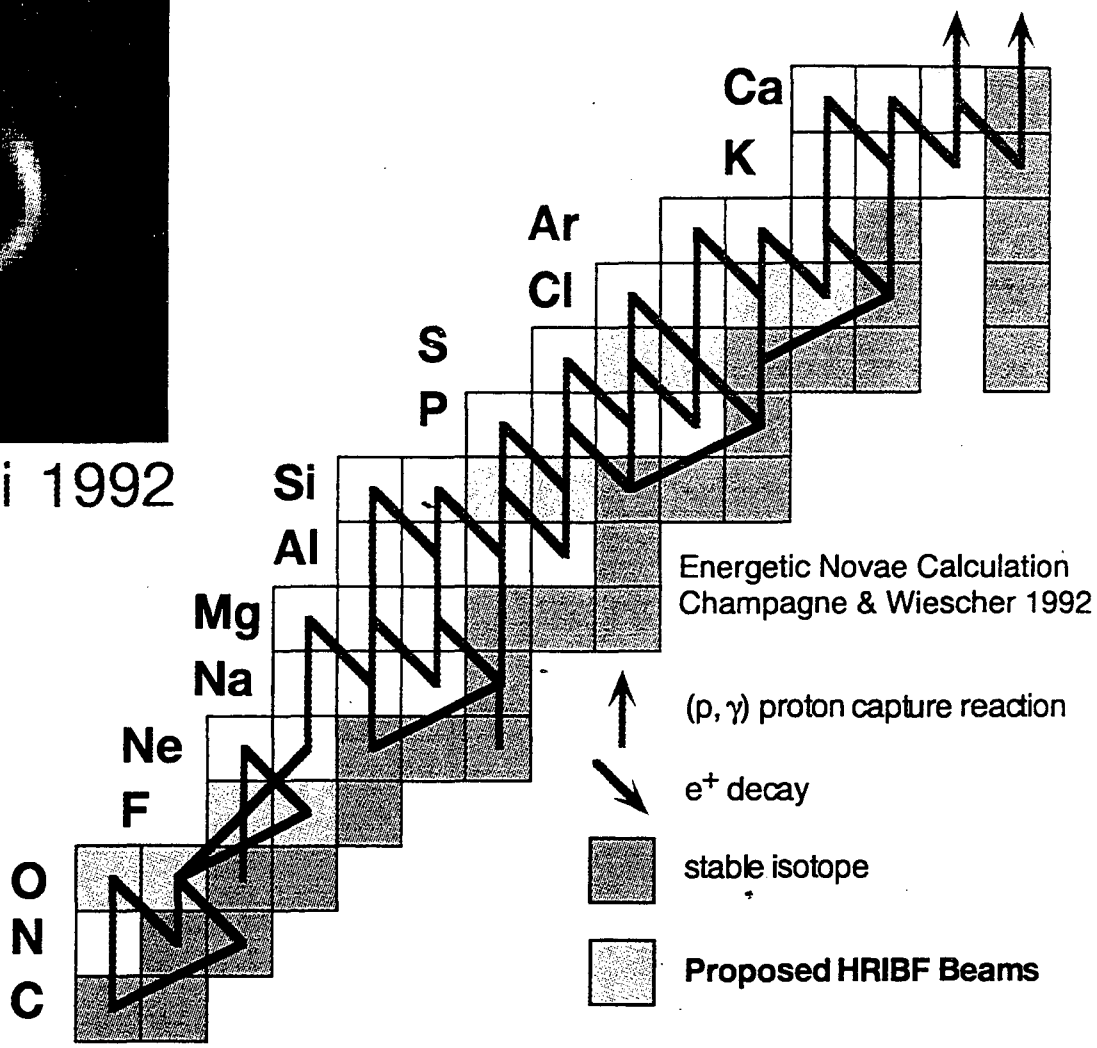


**rp-process: C, N, O...(SEED) + protons (FUEL)**

**⇒ Synthesize Elements up to Iron (and beyond)**

---

*Use Radioactive Ion Beams to **Directly** measure reactions occurring in stellar explosions*

***GRETA** offers required background rejection & energy resolution for these measurements*

# Radioactive Beam Expts

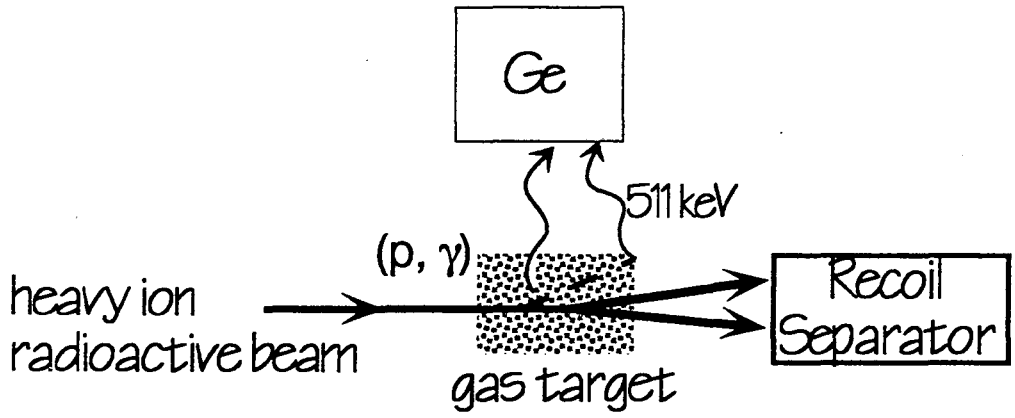


## Major Problems

*LOW radioactive beam currents*

*LOW cross sections ( ~ μb or less)*

*⇒ LOW count rates*

*INTENSE Backgrounds:*

*$10^{4-5}$ Hz 511-keV γ from scattered beam particles in target chamber*

## Advantages of GRETA

*Granularity – reduce pileup from 511 keV background*

*Efficiency – can measure with LOW RIB currents*

*Tracking – reject cosmic rays and room backgrounds*
*– better angular distributions*

*Resolution – cascade γ's for high level density nuclei*

# Radioactive Beam Expts

## Possible Experiments

- *Inverse-Kinematics Capture Reactions for Explosive Burning*

| | |
|---|---|
| $^{15}O(\alpha,\gamma)^{19}Ne$ | *Hot CNO Breakout* |
| $^{14}O(\alpha,p)^{17}F$ | *Hot CNO; rp transition* |
| $^{19}Ne(p,\gamma)^{20}Na$ | *rp - transition* |
| $^{23}Mg(p,\gamma)^{24}Al$ | *rp bottleneck* |
| $^{26}Al(p,\gamma)^{27}Si$ | *$^{26}Al$ Abundance* |
| $^{27}Si(p,\gamma)^{28}P$ | *rp bottleneck* |
| $^{31}S(p,\gamma)^{32}Cl$ | *rp bottleneck* |
| $^{35}Ar(p,\gamma)^{36}K$ | *rp bottleneck* |
| $^{39}Ca(p,\gamma)^{40}Sc$ | *rp bottleneck* |

# Nuclear Structure Expts

**Fusion Evaporation Reactions**

*A(B,xpyn)C used to populate nuclei important to astrophysical processes*

**Indirectly Determine Reaction Rates**

*Measure Level Structure*
*Branching Ratios*
*Decay Properties*
*Masses*
*Lifetimes*

**GRETA High Efficiency**

*⇒ possible / practical to study weaker channels in A(B,xpyn)C reactions*

- *~ 6 mass units closer to drip line important for r-, p-, rp-processes*
- *new nuclear structure info not possible/practical with current arrays*

# Nuclei of Interest

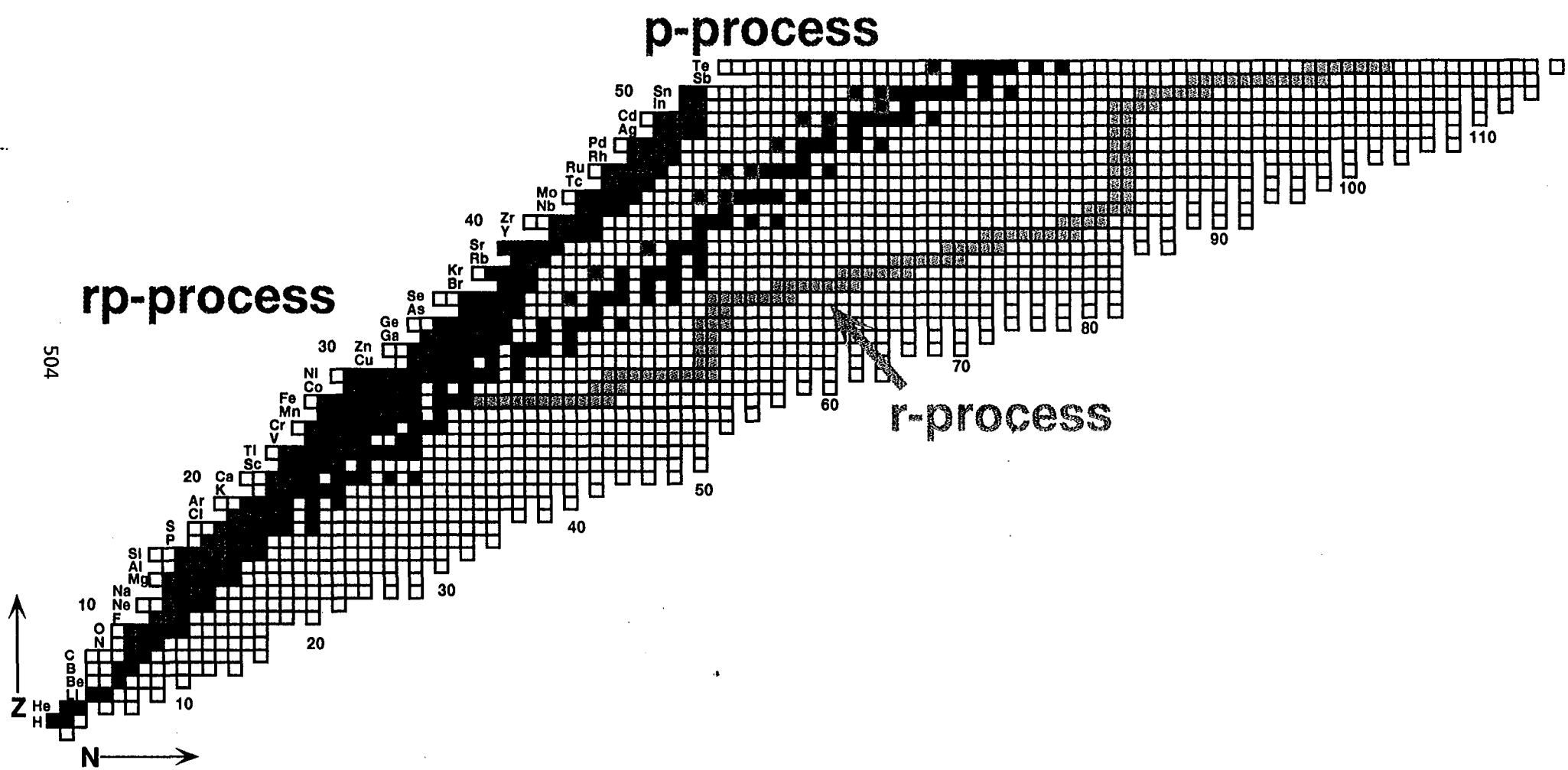

# Nuclear Structure Expts

- ***high-temperature rp-process waiting points: Beta-Decay, Beta-Delayed Decay Measurements, Decay Schemes***

  $^{66}Se$, $^{70}Kr$, $^{74}Sr$, $^{78}Zr$, $^{84}Mo$, $^{88}Ru$, $^{92}Pd$, $^{96}Cd$ (all N=Z nuclei)

- ***r-process: Beta-Decay, Beta-Delayed Decay Measurements, Decay Schemes***

$^{81-82}Ga$, $^{82-83}Ge$, $^{84-85}As$, $^{85-91}Se$, $^{91-97}Br$, $^{98-103}Kr$, $^{102-107}Rb$, $^{134-139}Sn$, $^{139-149}Sb$, $^{149-155}Te$, $^{155-160}I$, $^{160-165}Xe$, $^{165-170}Cs$

- ***Level Structure Measurements***
  - $^{46}Cr$ for supernovae
  - $^{12}C$ 7.65 MeV level $\Gamma_\gamma$ for $3\alpha$ process

- ***Rare Decay Measurements***
  - $^{54}Mn$, $^{144}Pm$ galactic chronometers

- ***Many Measurements may require RIBs***

# $^{46}$Cr Level Structure

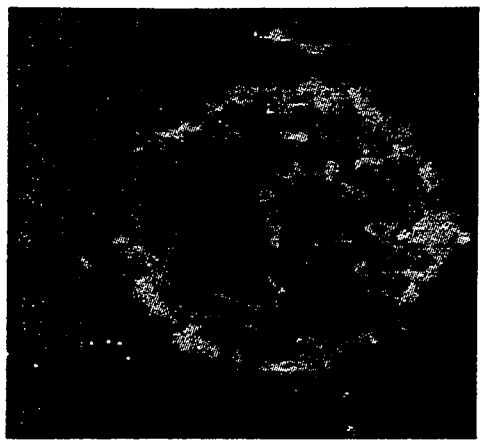

**Cas A Supernova Remnant**

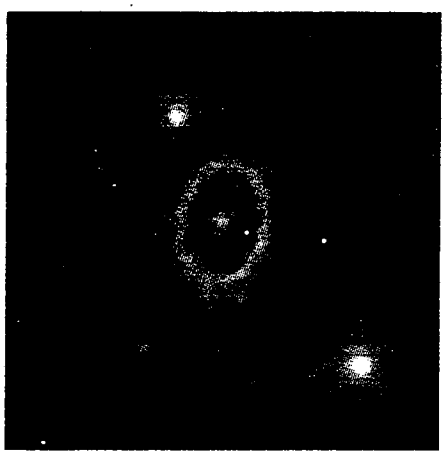

**Supernova 1987a**

- *$^{44}$Ti observed in ejecta of Supernovae*
- *$^{44}$Ti decay powers long-term ( $\tau \sim 60$ years )*

  *light output of supernova*
- *Predicted abundances incorrect*
- *Predicted abundances depend on*

  *$^{44}$Ti lifetime $\Rightarrow$ numerous recent measurements*

  *$^{45}$V(p,$\gamma$)$^{46}$Cr reaction rate (Meyer et al. 1997)*
- *No information on Level Structure of $^{46}_{24}Cr_{22}$ : $N = Z - 2$ !*
- *Very Difficult to get information from current $\gamma$ arrays*
- *Measurements with GRETA may be possible:*

  *$^{24}$Mg($^{28}$Si, $\alpha$ 2n)$^{46}$Cr:*

# Implementation

## GRETA Design

*Interface with*

*Recoil Separator*

*Charged-Particle Detectors*

*Gas targets*

## GRETA Siting

*At Facility with Capabilities of*

*Low Energy Beams*

*Radioactive Beams*

# Summary

## Many Astrophysics Measurements are possible with GRETA

*Capture Reactions*

*Radioactive Beams*

*Nuclear Structure*

## Numerous Advantages of GRETA for Astrophysics Measurements

*Tracking*

*Efficiency*

*Granularity*

*Resolution*

## Some Experiments Require Planning at the Design Phase of GRETA

W. Swiatecki

Jacobi shapes, fission barriers, surface diffuseness.

1. JACOBI SUPERDEFORMATION

2. THE EGG-CRATE TOPOGRAPHIC THEOREM CONCERNING FISSION BARRIERS

3. THE SNAKE PHENOMENON OF MISALIGNED FISSION-FUSION VALLEYS

4. SURFACE DIFFUSENESS AS A DEGREE OF FREEDOM

5. ONE-BODY DISSIPATION

# ① JACOBIS
## SPONTANEOUS BREAKING OF AXIAL SYMMETRY

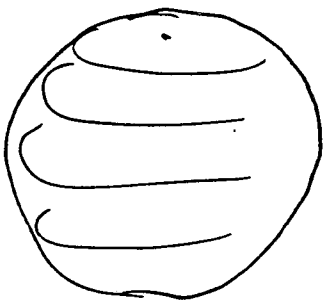

$L = 0$

SPHERE

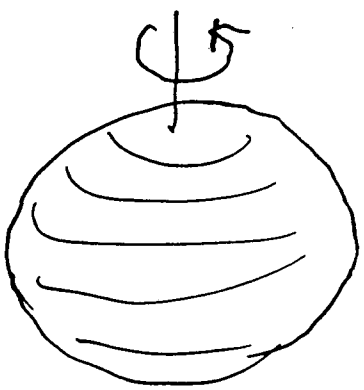

$L < L_{crit}$

OBLATE

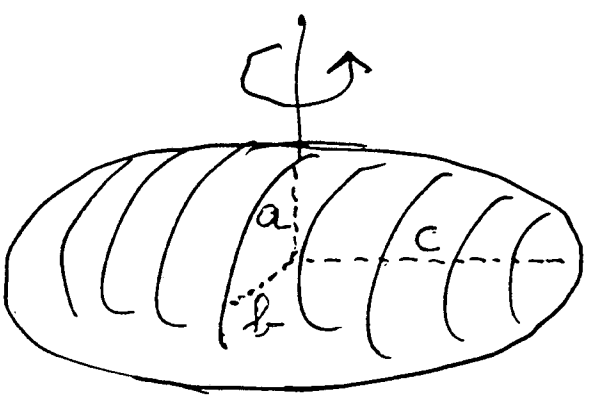


$L > L_{crit}$

TRIAXIAL

(JACOBI)

$c > b > a$

# $^{74}_{34}Se$ WITH $L = 53\hbar$

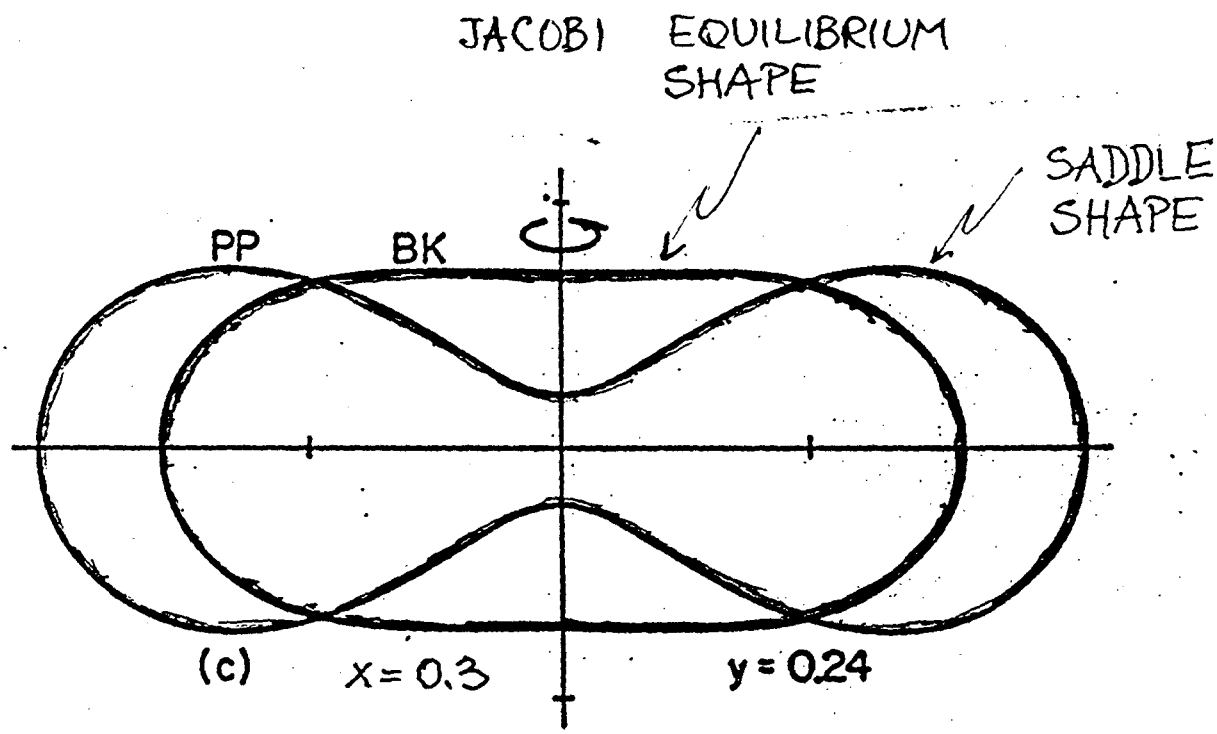


$c : \bar{a} \approx 2.3 : 1$ $\qquad$ $\mathcal{J}/\mathcal{J}_{SPHERE} \approx 1.8$

$(c = 1.58$
$b = 0.80$
$a = 0.68)$

# TWO STRIKING CHARACTERISTICS OF THE PREDICTED JACOBI CONFIGURATIONS:

1. HUGE QUADRUPOLE MOMENTS

   $c:a \gtrsim 2$ $\qquad \mathcal{J}/\mathcal{J}_{sphere} \approx 1.8$

   (1.58 FOR 2:1 SPHEROID)

2. EXTREME SOFTNESS AGAINST FURTHER STRETCHING (IN THE ABSENCE OF SHELL EFFECTS).

   → GAMMA TRANSITION ENERGIES DECREASING FUNCTIONS OF $L$ (SUPER BACKBENDING).

QUESTION:

WHERE TO LOOK FOR SUPERDEFORMED JACOBI NUCLEI?

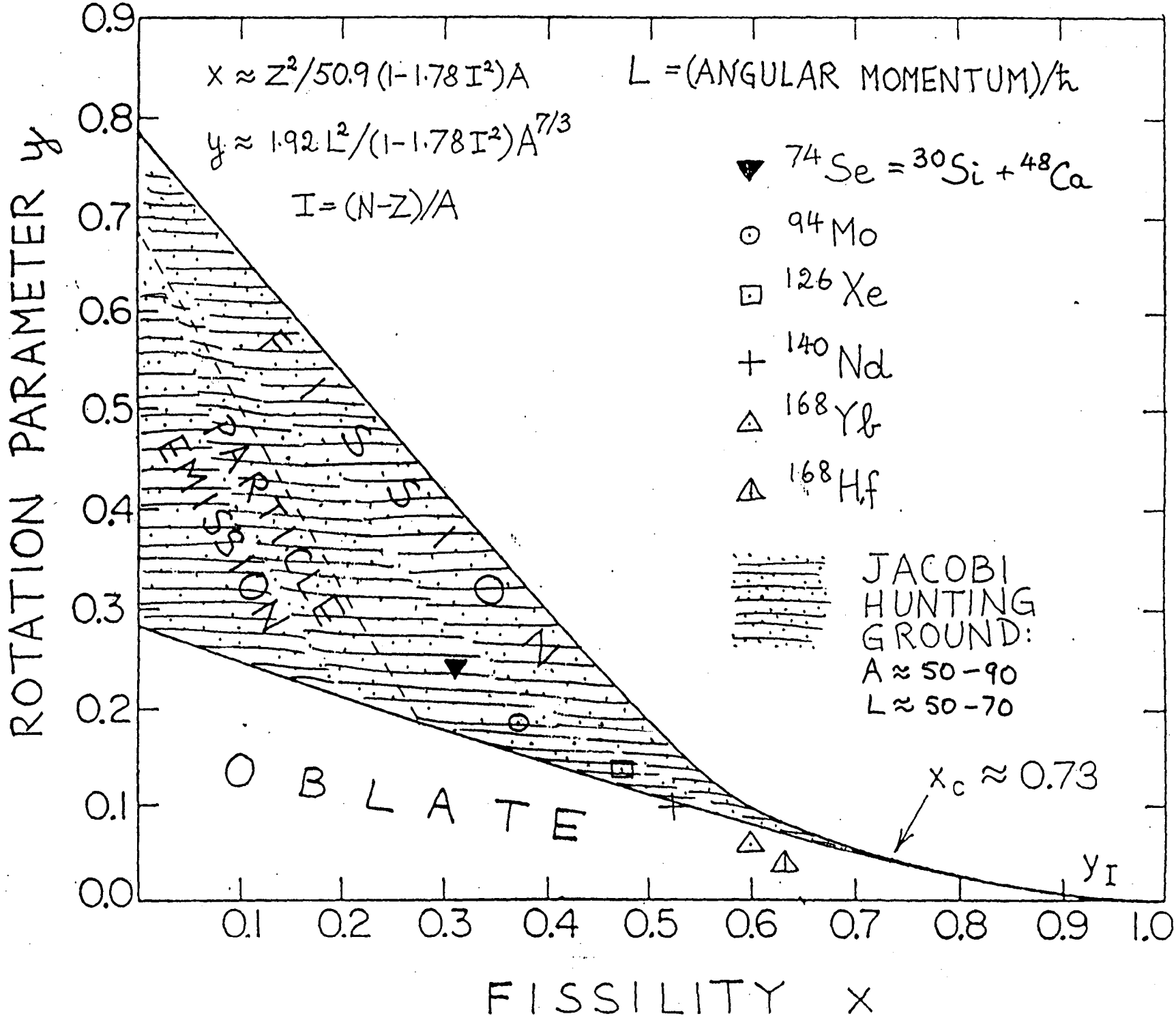
$x \approx Z^2/50.9(1-1.78I^2)A$
$y \approx 1.92L^2/(1-1.78I^2)A^{7/3}$
$I = (N-Z)/A$
$L = (\text{ANGULAR MOMENTUM})/\hbar$
$^{74}Se = {}^{30}Si + {}^{48}Ca$
$^{94}Mo$
$^{126}Xe$
$^{140}Nd$
$^{168}Yb$
$^{168}Hf$
JACOBI HUNTING GROUND:
$A \approx 50-90$
$L \approx 50-70$
FISSION
OBLATE
$x_c \approx 0.73$
$y_I$
ROTATION PARAMETER $y$
FISSILITY $x$
0.0
0.1
0.2
0.3
0.4
0.5
0.6
0.7
0.8
0.9
1.0

# SUMMARY

1. THE HUNTING GROUND FOR JACOBIS IS $A \approx 50-90$

2. FISSION BARRIERS FOR JACOBIS ARE COMPARABLE TO NEUTRON/PROTON SEPARATION ENERGIES; LOSS OF CROSS-SECTION AND OF ENTRANCE-CHANNEL ANGULAR MOMENTUM MAKES LIFE DIFFICULT

3. IDENTIFICATION OF JACOBIS MIGHT BE BY CHARACTERISTICS OF PARTICLES EMITTED (FROM TIPS) OR, WITH LUCK AND HELP FROM GRETA, BY GAMMAS

4. IF SHELL EFFECTS SMALL, THE SIGNATURE WOULD BE A PILE-UP OF CONTINUUM GAMMAS NEAR A CHARACTERISTIC CUT-OFF ENERGY

5. IF A SHELL EFFECT HAPPENS TO ADD STABILITY, A HYPERDEFORMED NUCLEUS WITH A DISCRETE ROTATIONAL BAND MIGHT SHOW UP IN THIS RANGE OF A.

# SIX 4n REACTIONS WITH $^{48}_{20}Ca$ BEAMS

| | TARGET | SPINNING NUCLEUS | CALCULATED CUT-OFF L/ħ (50% SURVIVAL) | CALCULATED MAXIMUM γ-ENERGY | MEASURED MAXIMUM γ-ENERGY |
|---|---|---|---|---|---|
| 1. | $^{30}_{14}Si$ (3.1%) | $^{74}_{34}Se$ | 53 ✓✓✓ | ~3.6 MeV | — |
| 2. | $^{50}_{22}Ti$ (5.4%) | $^{94}_{42}Mo$ | 65 ✓✓ | ~3 MeV | — |
| 3. | $^{82}_{34}Se$ (8.7%) | $^{126}_{54}Xe$ | 73 ✓ | ~2.3 MeV | — |
| 4. | $^{96}_{40}Zr$ (2.8%) | $^{140}_{60}Nd$ | 70 × | ~2.1 MeV | — |
| 5. | $^{124}_{50}Sn$ (5.8%) | $^{168}_{70}Yb$ | 64 ×× | ~1.5 MeV | ~1.45 |
| 6. | $^{124}_{52}Te$ (4.8%) | $^{168}_{72}Hf$ | 52 ××× | ~1.3 MeV ↑ (SUPER BACK-BEND) | ~1.15 |

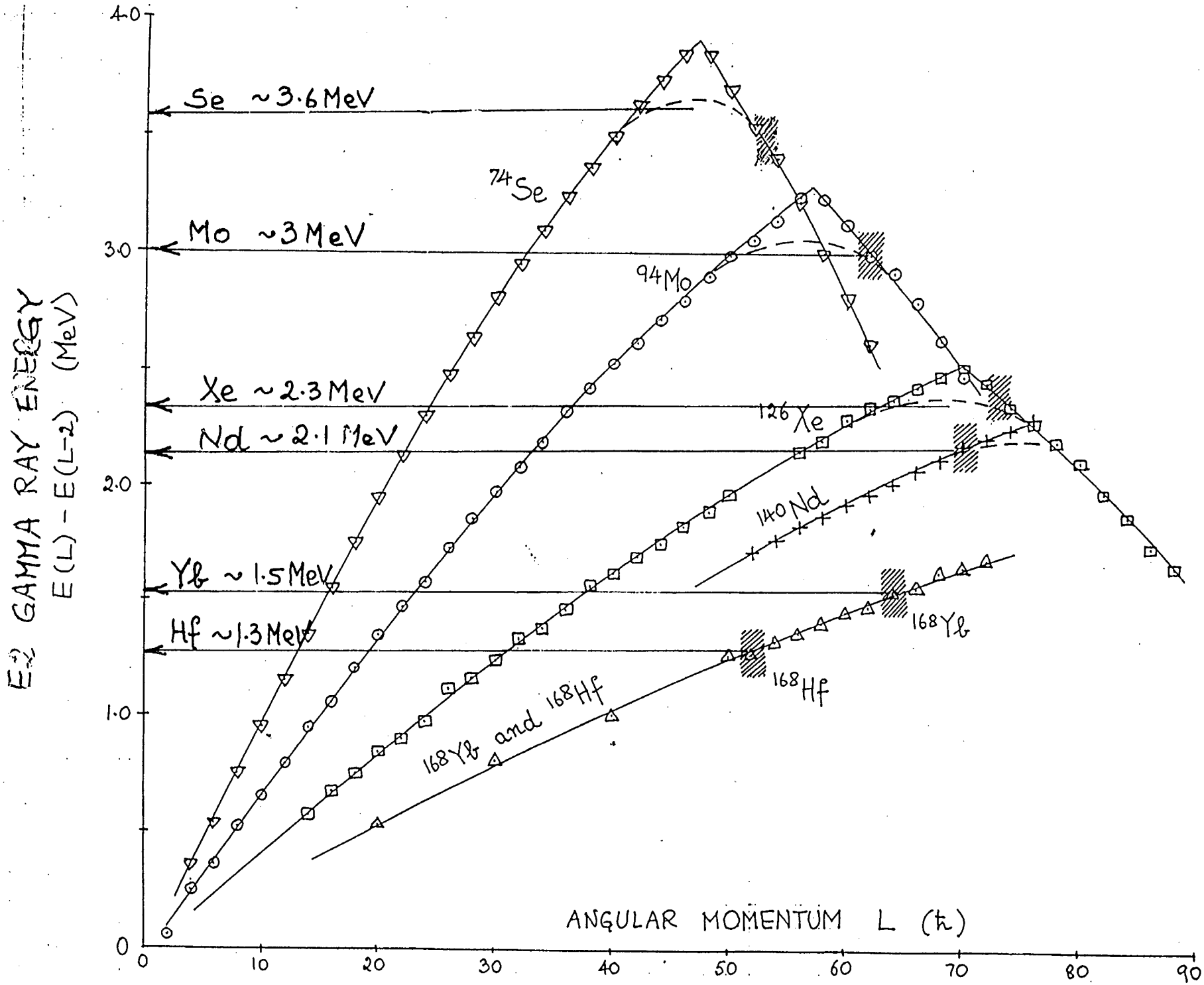
E2 GAMMA RAY ENERGY
E(L) - E(L-2) (MeV)
ANGULAR MOMENTUM L (ħ)
Se ~3.6 MeV
Mo ~3 MeV
Xe ~2.3 MeV
Nd ~2.1 MeV
Yb ~1.5 MeV
Hf ~1.3 MeV
74Se
94Mo
126Xe
140Nd
168Yb
168Hf
168Yb and 168Hf
0
1.0
2.0
3.0
4.0
0
10
20
30
40
50
60
70
80
90

## (2) THE EGG-CRATE THEOREM:

"SADDLE MASSES ARE INSENSITIVE TO SHELL EFFECTS".

OR

"FISSION BARRIERS ARE INSENSITIVE TO SHELL EFFECTS NEAR SADDLE"

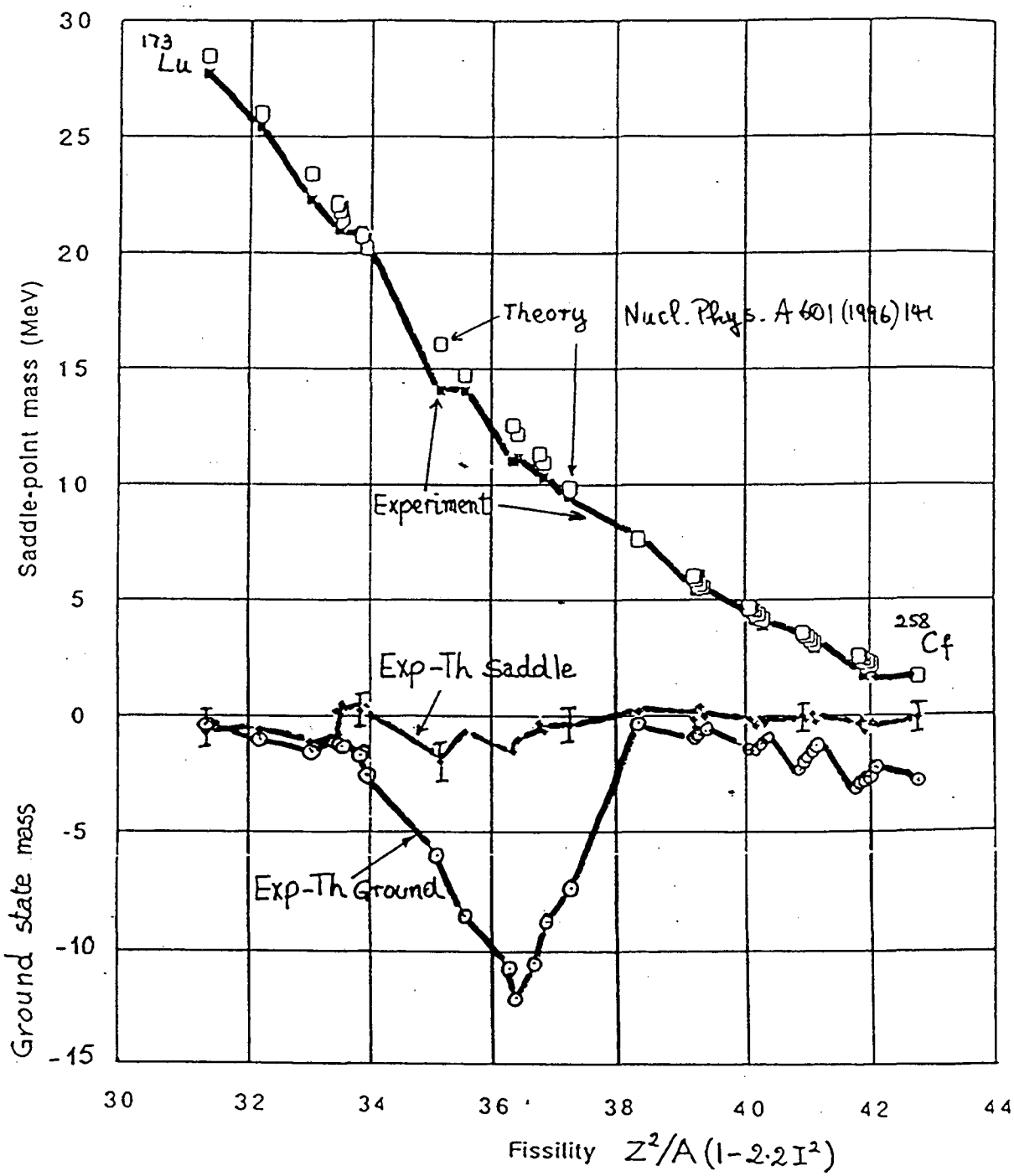


THE EGG-CRATE THEOREM CONFIRMED:

"SADDLE MASSES ARE INSENSITIVE TO SHELL EFFECTS"

# 3 THE SNAKE PHENOMENON

(MISALIGNED FISSION-FUSION VALLEYS)

# SINGLE-VALLEY TOPOGRAPHY

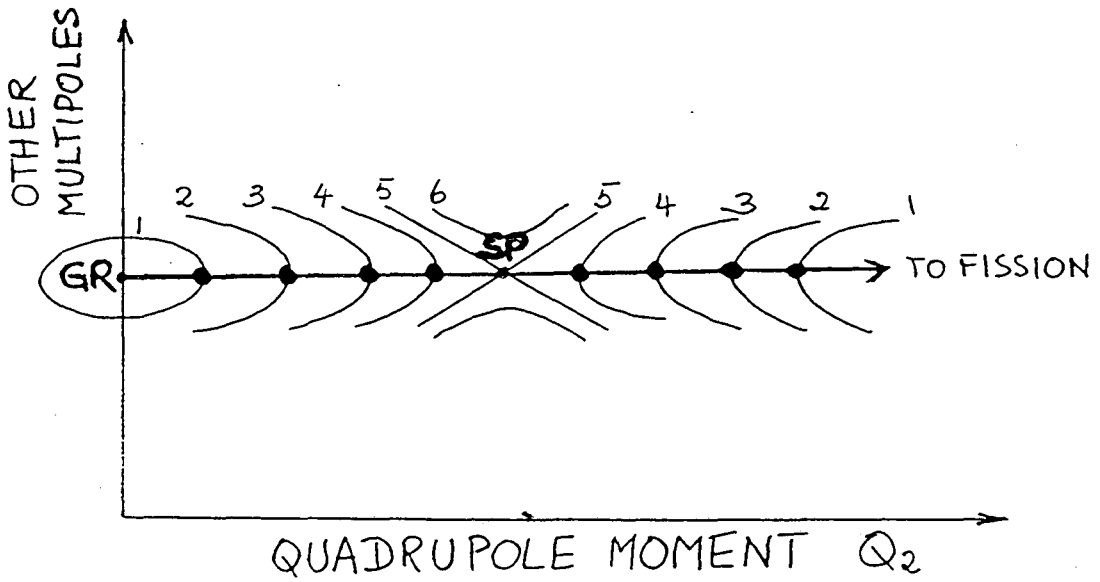


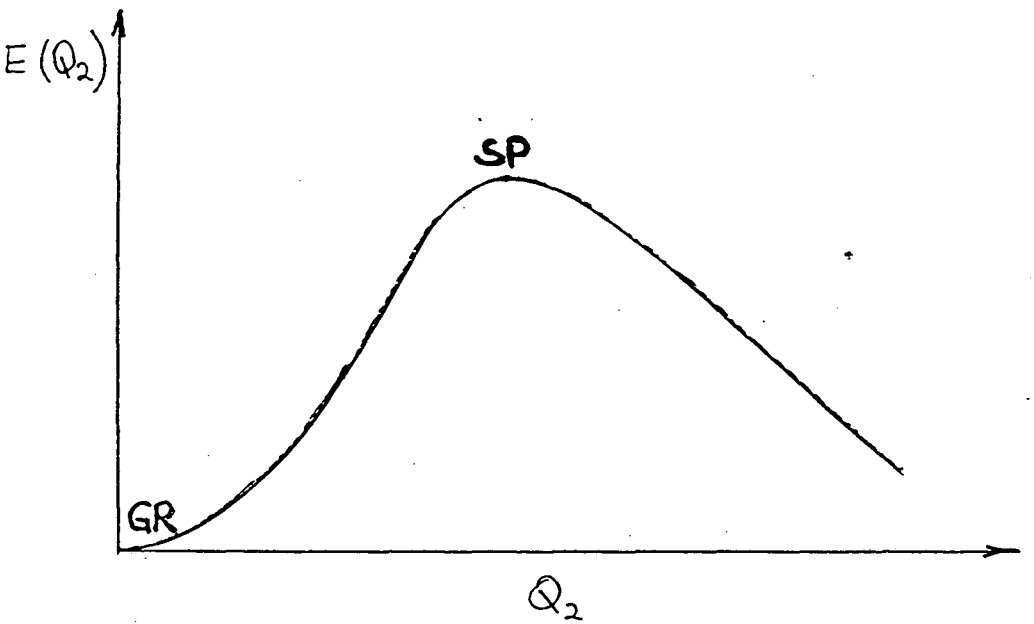

# MISALIGNED-VALLEYS TOPOGRAPHY

(THE SNAKE!)

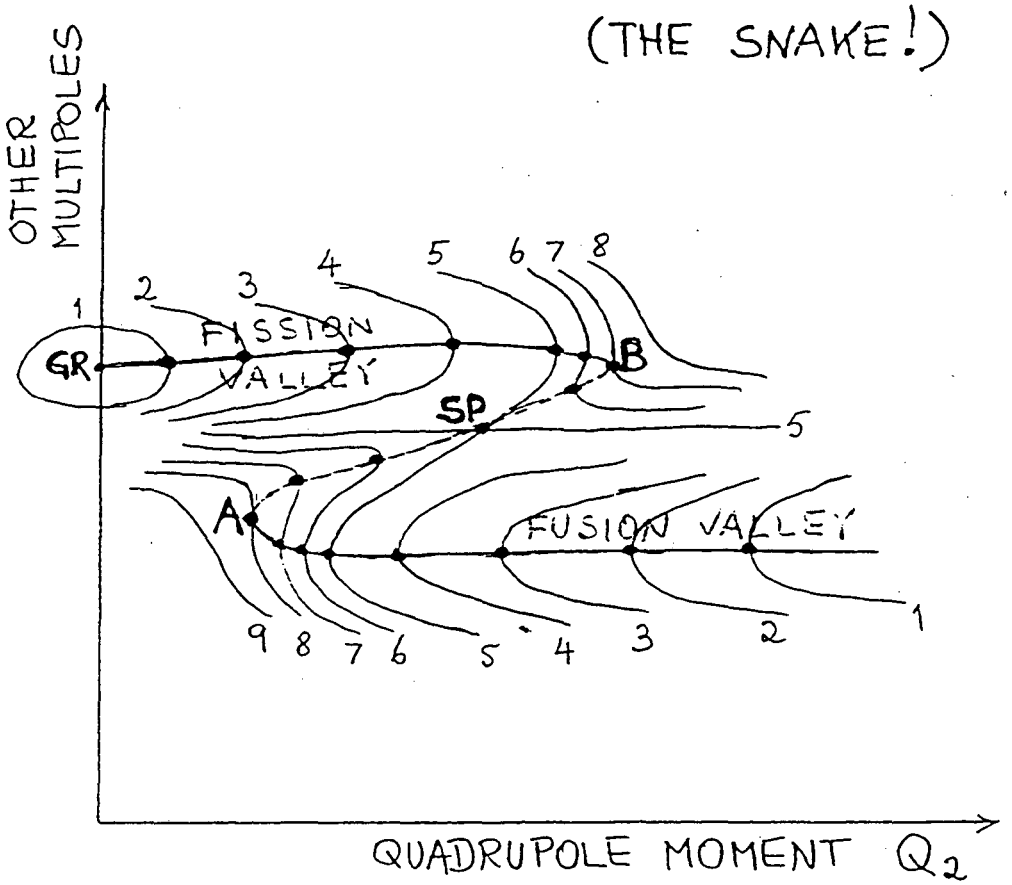


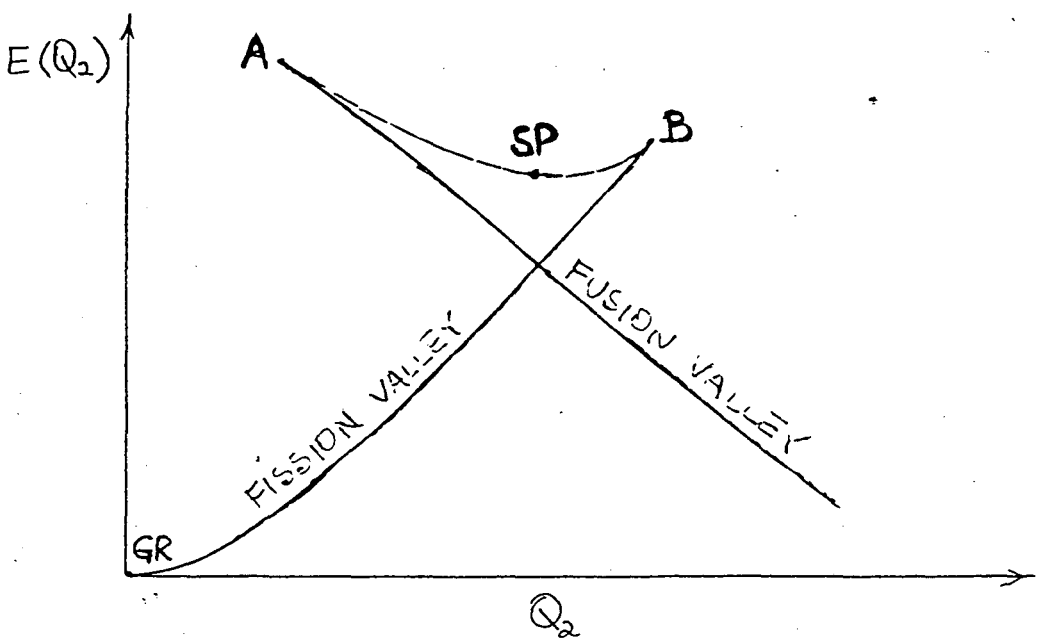

# How close are hyperdeformed states to the scission point?

Proc. Conf. Argonne July 1996

L.M. Robledo[†], R.R. Chasman[††] and J.L. Egido [†]
[†] Departamento de Física Teórica C-XI
Universidad Autónoma de Madrid, 28049 Madrid, Spain
[††] Physics Division, Argonne National Laboratory
Argonne, IL 60439, USA

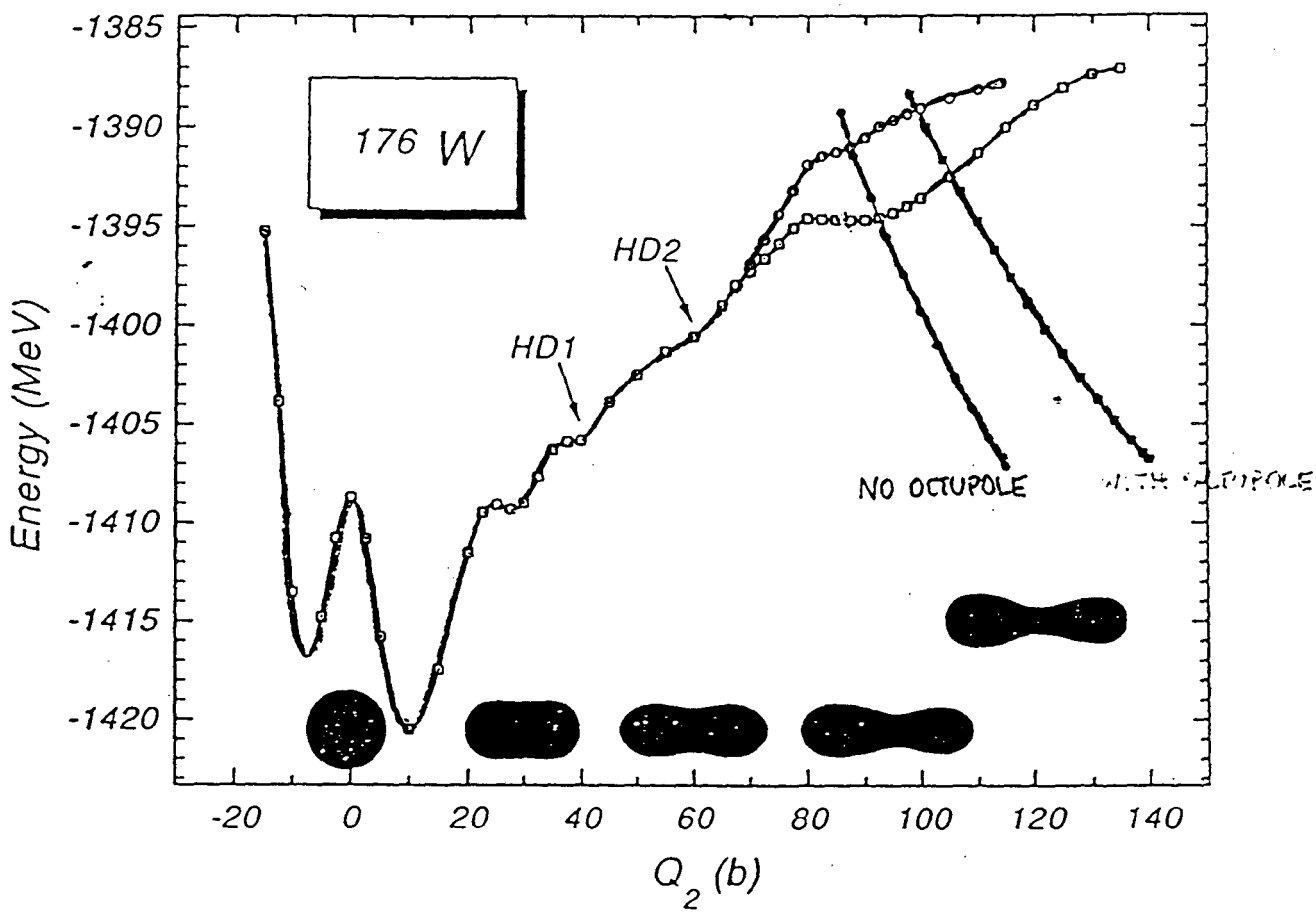


Figure 1: The HFB energy in MeV versus the mass quadrupole moment $Q_2$ given in barns.

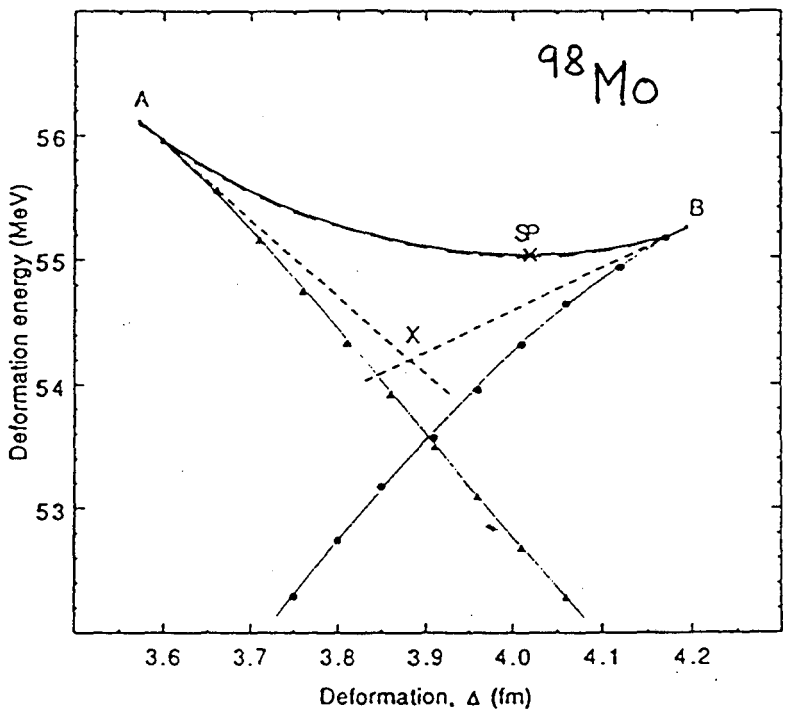


Fig. B.1. The equilibrium deformation energy for a reflection and axially symmetric $^{98}$Mo nucleus, constrained to have the centers of mass of its two halves at a separation exceeding by $2\Delta$ the separation for the spherical ground-state configuration. The circles follow the fission valley up to the limiting point B. The triangles follow the fusion valley down to the limiting point A. The tangents at A and B cross at X, and Eq. (B.2) in the text gives the saddle-point energy $V_{SP}$ in terms of the energies at A, B, and X.

NOTE A SHOCKING CONSEQUENCE:

THE TURNING POINTS A, B GIVE UPPER NOT LOWER LIMITS ON THE FISSION BARRIER!

# Selfconsistent Calculations for Hyperdeformed Nuclei

H. Molique, J. Dobaczewski *, J. Dudek and W.D. Luo

Argonne 1996

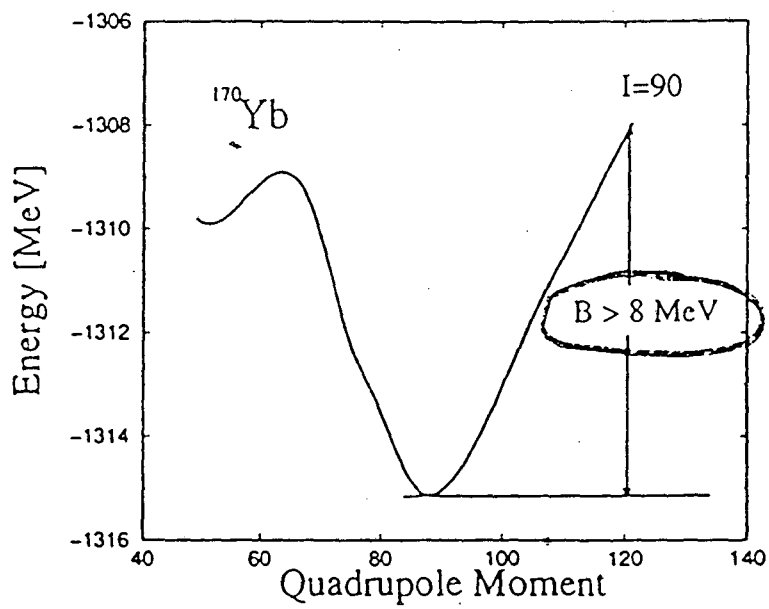


?

B<8MeV

Figure 4: *Preliminary results of the HF calculations for the hyperdeformed* $^{170}$Yb

BEWARE OF SNAKE BITE!

4

# RESPONSE OF SURFACE ENERGY TO SURFACE DIFFUSENESS

(THOMAS-FERMI MODEL, W.D. MYERS & WJS NUCL. PHYS. A601 (1996) 141)
AND WORK IN PROGRESS

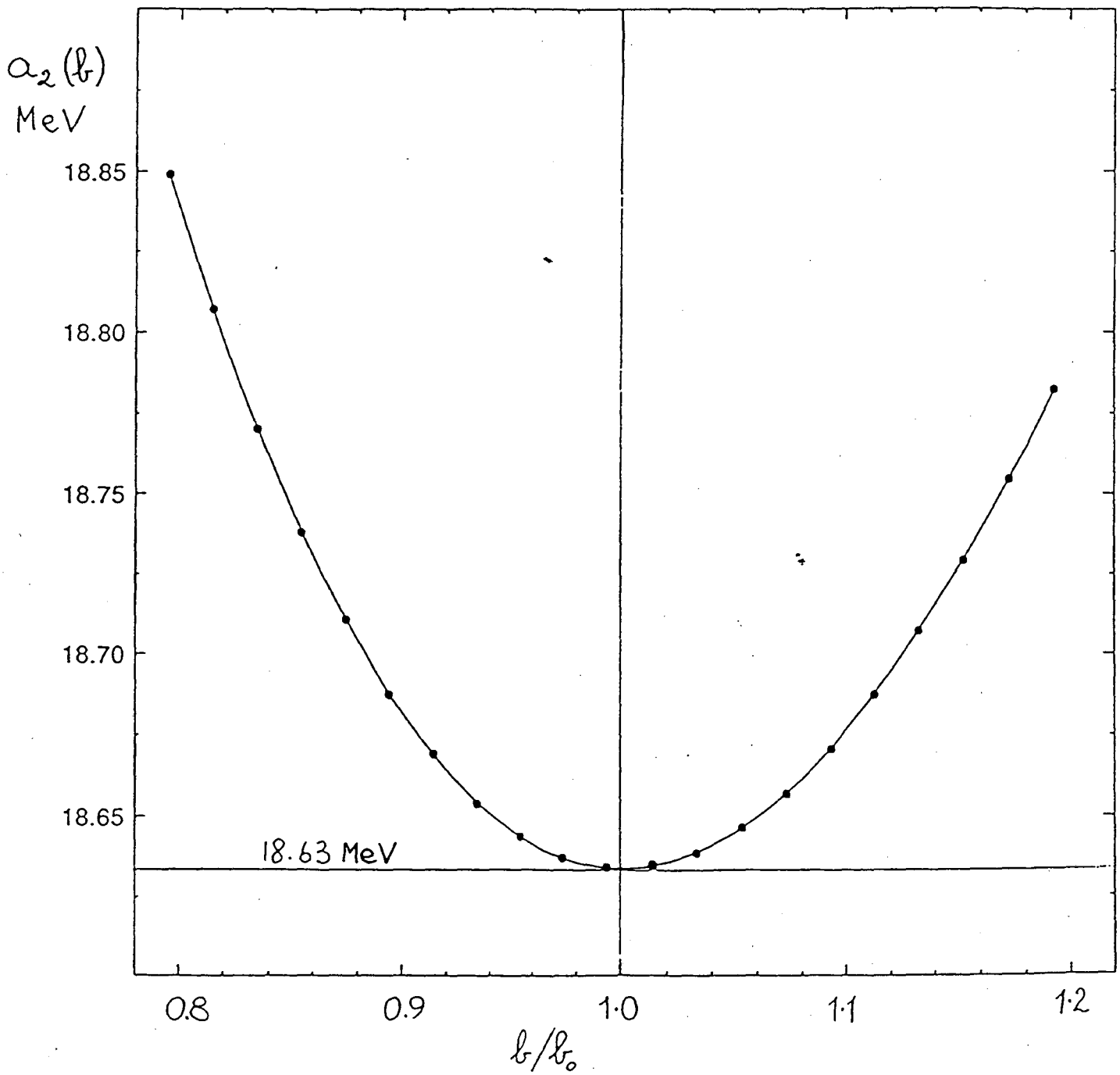


$b$ = "SÜSSMANN WIDTH" (DIFFUSENESS)

$b_0 = 1.0$ fm

# RESPONSE OF SURFACE ENERGY TO CHANGES IN NEUTRON & PROTON DIFFUSENESS

RECALL:

$$\frac{E_{VOL}}{A} = -a_1(\rho_0) + \frac{1}{2}K_0\left(\frac{1}{3}\frac{\rho-\rho_0}{\rho_0}\right)^2 + J_0\left(\frac{\rho_n-\rho_p}{\rho_0}\right)^2$$

COMPRESSIBILITY COEFF. SYMMETRY ENERGY COEFF.

SIMILARLY:

$$\frac{E_{SURF}}{A^{2/3}} = a_2(b_0) + \frac{1}{2}k_0\left(\frac{b-b_0}{b_0}\right)^2 + j_0\left(\frac{b_n-b_p}{b_0}\right)^2 ; \quad b = \frac{1}{2}(b_n+b_p)$$

DIFFUSENESS COMPRESSIBILITY COEFFICIENT

DIFFUSENESS SYMMETRY ENERGY COEFFICIENT

THOMAS-FERMI MODEL (W.D.MYERS & WJS, Nucl.Phys.A601 (1996) 141

| | NUCLEAR MATTER (∞ OR SEMI-∞) | | | | |
|---|---|---|---|---|---|
| | EQUILIBRIUM | | COMPRESSIBILITY | SYMMETRY | |
| VOLUME | $a_1(\rho_0) = -16.24$ MeV | $r_0 = 1.14$ fm | $K_0 = 234$ MeV | $J_0 = 32.65$ MeV | |
| SURFACE | $a_2(b_0) = 18.36$ MeV | $b_0 = 1.0$ fm | $k_0 = 9.51$ MeV | $j_0 = 5.19$ MeV | NEW |

A-DEPENDENCES:

$$K(A) \approx K_0 \frac{E(A)}{E_0}$$

W.D.Myers & WJS, Nucl. Phys. A587 (1995) 92

$$J(A) = \frac{J_0}{1+\frac{9}{4}\frac{J_0}{Q}A^{-1/3}}$$

DROPLET MODEL; $Q = 35.4$ MeV

NEW:

$$\boxed{\begin{aligned} k(A) &= k_0(1 + 3.0A^{-1/3} + 29A^{-2/3} + \cdots) \\ j(A) &= j_0(1 + 1.3A^{-1/3} + 15A^{-2/3} + \cdots) \end{aligned}}$$

GSI-Preprint-97- 40
August 1997

# MASSES AND RADII OF SPHERICAL NUCLEI CALCULATED IN VARIOUS MICROSCOPIC APPROACHES

Z. Patyk. A. Baran, J. F. Berger, J. Dechargé, J. Dobaczewski, P. Ring, A. Sobiczewski

(Submitted to Phys. Rev. C)

## 3 Results and discussion

### 3.1 Masses

Table IV gives the rms values of the difference between the calculated and experimental masses. The differences are calculated for 116 even-even spherical nuclei, from $^{16}$O to $^{220}$Th, for which the experimental masses are known. The table is very similar to that given by us earlier [9]. Only in the RMF case, the NLSH variant [40] of the parameters has been presently replaced by the more recent variant NL3 [36]. All HFB and RMF masses are calculated by us, the ETFSI results are taken from [28] and the MM masses are taken from [37] in their FRDM and FRLDM variants, and from [38] in their TF variant of the smooth part of the mass. As the experimental values, the masses evaluated by Audi and Wapstra [41] are used.

Table IV. Mass rms deviations in MeV

| | | | | | | |
|---|---|---|---|---|---|---|
| SIII: | 4.74 | SkP: | 2.37 | SkM*: | 6.32 | HFB |
| SIII$^{\delta}$: | 3.07 | SkP$^{\delta}$: | 2.53 | SkM*$^{\delta}$: | 5.36 | |
| SIII$^{\delta\rho}$: | 2.26 | SkP$^{\delta\rho}$: | 2.32 | SkM*$^{\delta\rho}$: | 4.74 | |
| Gogny: | 2.07 | | | | | |
| RMF(NL1): | 3.94 | RMF(NL2): | 11.24 | RMF(NL3): | 2.48 | |
| ETFSI: | 0.80 | | | | | MICRO-MACRO |
| MM(FRDM): | 0.65 | MM(FRLDM): | 0.76 | MM(TF): | 0.57 | THOMAS-FERMI |

PEARSON et al.

One can see in Table IV that the smallest deviations from experimental masses are obtained in the MM approach. Within the HFB approximation, the best results

(SIX MASS CALCULATIONS) – (THOMAS-FERMI-STRUTINSKY)

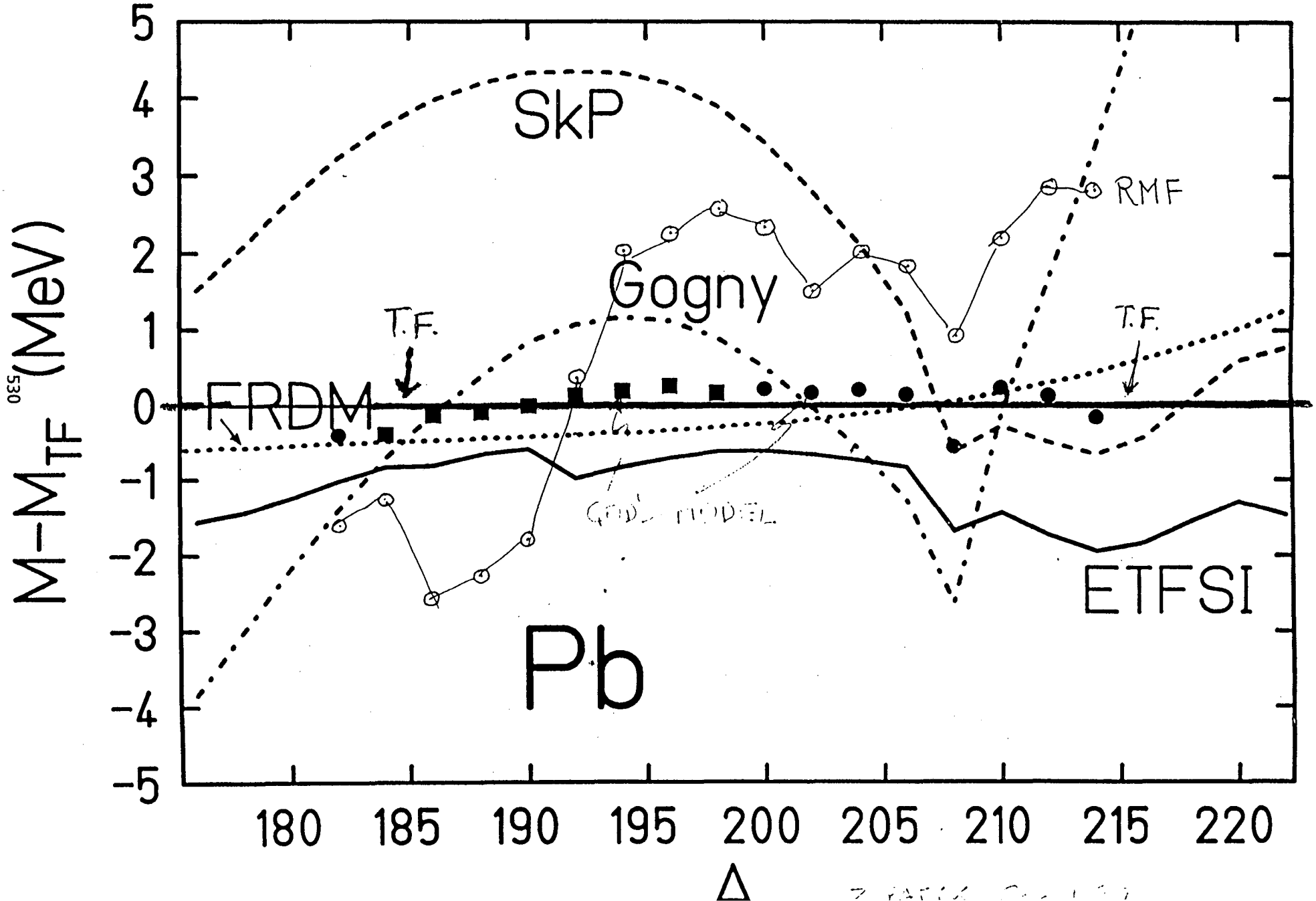

5

# TESTS OF WALL FORMULA FOR ONE-BODY DISSIPATION

DOTS: COMPUTER SIMULATIONS, CLASSICAL OR QUANTAL

------ WALL FORMULA; ——— WALL FORMULA + CORRECTIONS

curves to Eq. (6).

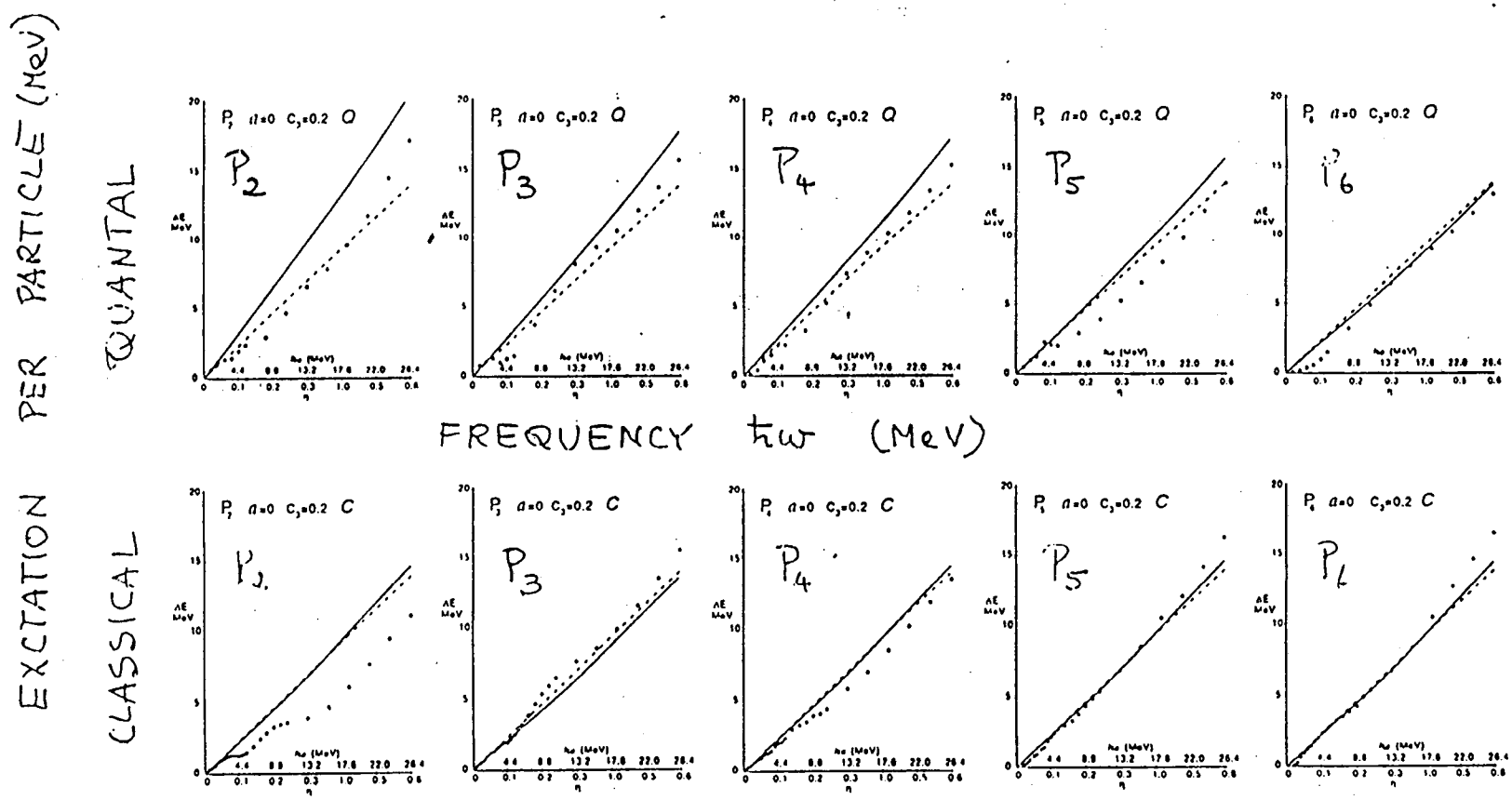


Fig. 5. As Fig. 4, but the oscillation is around a sphere deformed by $0.2\sqrt{7/5}\,P_3$.

5

# ONE-BODY DISSIPATION DYNAMICS

## MACROSCOPIC PART:

PROTOTYPE EQUATION OF MOTION:

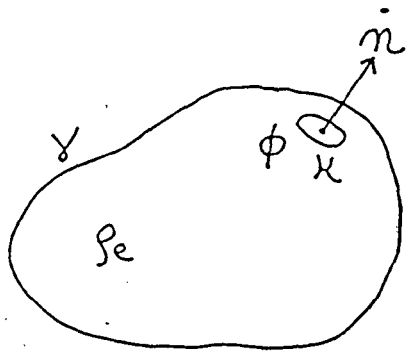


$$\frac{dn}{dt} = \frac{P}{\rho v}$$

$P$ = EXCESS PRESSURE

$$= \rho_e(\bar{\phi} - \phi) + \gamma(\bar{\kappa} - \kappa)$$

$$\rho v = 1.0 \times 10^{-22}\ \mathrm{MeV\,sec\,fm^{-4}}$$

## RECENT PROGRESS:

a) INCLUSION OF SHELL EFFECTS IN POTENTIAL ENERGY

b) INCLUSION OF FLUCTUATIONS AROUND MEAN DYNAMICAL TRAJECTORY (C. JARZYNSKI, O. MAZONKA, J. BLOCKI)

B.Herskind
Limit to completeness.

Bent

# Where Are We Heading
## in the Study of the Quasi-Continuum

### What Do We Know at Present especially from the Nuclei: ($^{143}$Eu, $^{163}$Er, $^{168}$Yb,)

- *The Fluctuation Analysis* shows that rotational damping sets in at: $U_o \approx 800keV. \Rightarrow$ (10 Bands of each $(\pi, \alpha)$)
- *Cranking + band mixing calculations* shows that **residual interaction** of ($V = 10 - 20keV \Rightarrow$ is responsible for the rotational damping.)
- *2 Different Components* are identified in the calculations:
  $\Gamma_{narrow} \approx 50keV$ from a rotational correlated structure
  $\Gamma_{damp} \approx 250keV$ which seems completely uncorrelated
  *Microscopic Simulations* based on this reproduce the spectra quite well.

### Problems yet to be solved:

- **Evidence for Motional Narrowing** has not been given yet.
- **Predicted Compound Bands** has not been observed yet.
- **A systematic study of residual interactions** as function of excitation energy and spin. → GO TO THE LIMIT OF COMPLETENESS.
- **Damping for other mass regions not known. (A ≠ 150-170)**
- **Damping in connection with:**
  **High-K bands.**
  **Super- and hyperdeformed Bands.**
  **Vibrational structures.** are not known.
- **Feeding and decay-out** of super- and hyperdeformed bands?
  Lifetimes and interaction through the barrier.
  GDR built on superdeformed bands
- **Development of new analysis methods:**
  Configuration dependent fluctuations (variance and co-variance.)
  High-Fold Mapping, Auto-Correlations ...

PHYSICAL REVIEW LETTERS
Vol 18 (1993) 2694

M. Matsuo,[1] T. Døssing,[2] E. Vigezzi,[3] and R. A. Broglia[2],[3],[4]
[1]*Yukawa Institute for Theoretical Physics, Kyoto University, Kyoto, Japan*
[2]*The Niels Bohr Institute, University of Copenhagen, Copenhagen, Denmark*
[3]*Istituto Nazionale di Fisica Nucleare, Sezione di Milano, Milano, Italy*
[4]*Dipartimento di Fisica dell'Università di Milano, Milano, Italy*

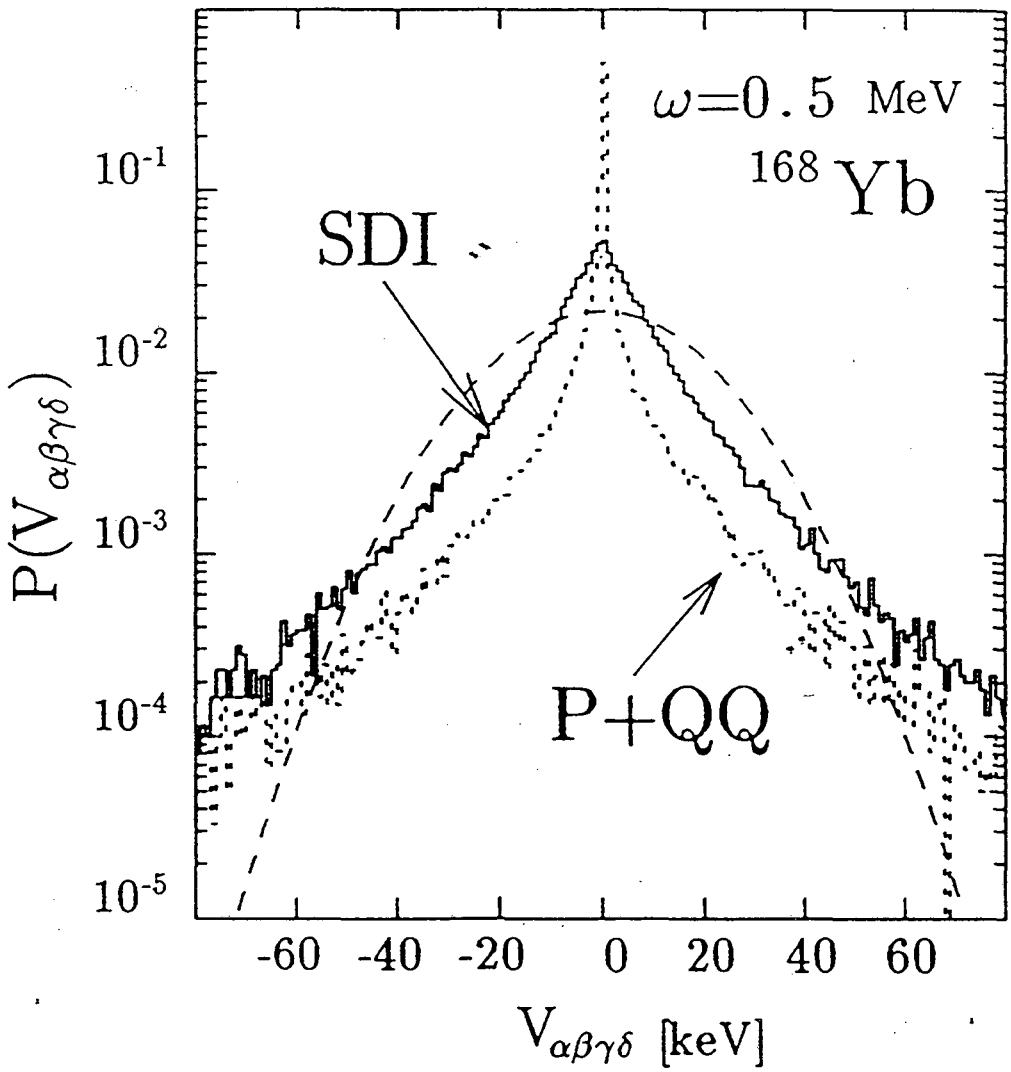


FIG. 1. Distributions of the off-diagonal two-body matrix elements of the pairing plus quadrupole (P+QQ) force and the surface delta interaction (SDI). The figure includes the two-body matrix elements $V_{\alpha\beta\gamma\delta}$, where $\alpha,\beta,\gamma,\delta$ denote the cranked shell model single-particle orbits lying near the Fermi surface within 3 MeV, defined at $\omega=0.5$ MeV in $^{168}$Yb. The strength of SDI is taken from Ref. [9] ($F=27.5/A$ MeV) while those of P+QQ are given by the self-consistent values with polarization

(a)

G.B. Hagemann et al. Nucl. Phys. A 618 (1997)

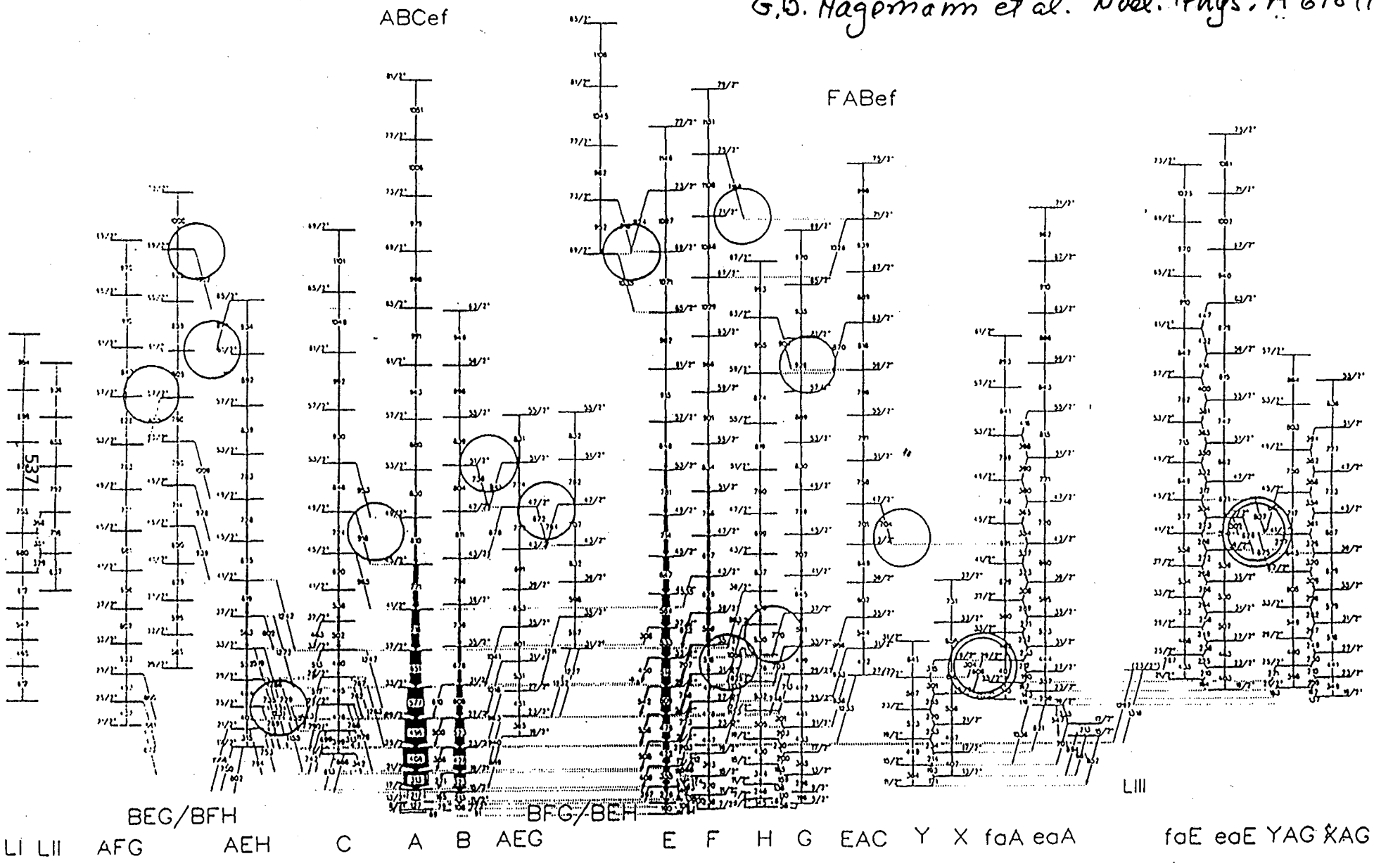


Fig. 1. (a) The full level scheme of $^{163}$Er. Circles mark crossings of bands where E2 cross-band transitions are observed.

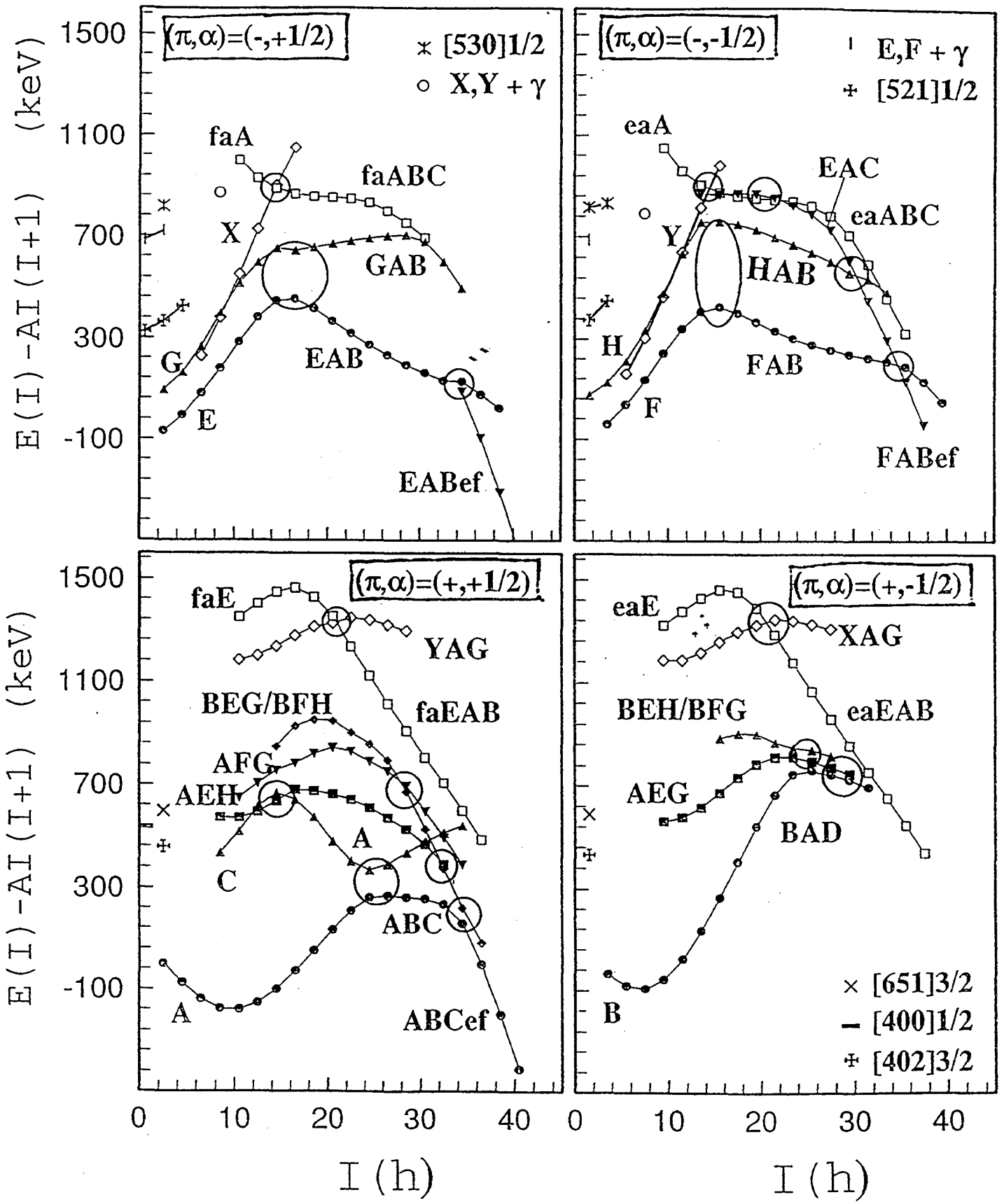
(π,α)=(-,+1/2)
[530]1/2
X,Y + γ
faA
faABC
X
GAB
G
EAB
E
EABef
(π,α)=(-,-1/2)
E,F + γ
[521]1/2
eaA
EAC
eaABC
Y
HAB
H
FAB
F
FABef
(π,α)=(+,+1/2)
faE
YAG
BEG/BFH
faEAB
AFG
AEH
A
C
ABC
A
ABCef
(π,α)=(+,-1/2)
eaE
XAG
BEH/BFG
eaEAB
AEG
BAD
B
[651]3/2
[400]1/2
[402]3/2
E(I)-AI(I+1) (keV)
1500
1100
700
300
-100
0
10
20
30
40
I (h)

$^{162}$Tm : JM. Espino, GB. Hagemann et. al. NP, Jan 98
$^{163}$Er : G.B. Hagemann, H. Ryde, P. Bosetti et.al. NP. 618 (1997) 199
$^{163}$Tm : H.J. Jensen, GB. Hagemann et al., Z Phys. A 340 (1991)

Table 3. Interactions between rotational bands in $^{162,163}$Tm and $^{163}$Er. Cases where both bands are known below and above the crossing are included. For the classification of assignments see table 1. Orbitals changed in the interaction are underlined. Partly aligned pairs of $i_{13/2}$ quasineutrons are given in parenthesis.

| Nucleus | Interacting bands | | | | | Strength V | ~ ΔK | ~Spin | ~ Δi |
|---|---|---|---|---|---|---|---|---|---|
| | $K_1$ | $Label_1$ | ⟺ | $Label_2$ | $K_2$ | keV | ħ | ħ | ħ |
| $^{162}$Tm | 6 | bA(BC) | ⟺ | dA(BC)[a] | 2 | < 1.5 | 4 | 20 | 0.6 |
| | 5 | fG(AB) | ⟺ | dA | 2 | 5(1) | 3 | 18 | 2.0 |
| | 5 | fH(AB) | ⟺ | cA | 2 | 5(1) | 3 | 17 | 1.9 |
| | 5 | fFAB | ⟺ | aA(BC) | 6 | 11(1) | 1 | 21 | 2.8 |
| | 6 | fEAB | ⟺ | dABC | 2 | 7(1) | 3 | 26 | 0.5 |
| $^{163}$Er | 11/2 | X | ⟺ | G[a] | 3/2 | < 2 | 4 | 11 | 0 |
| | 11/2 | Y | ⟺ | H[a] | 3/2 | < 2 | 4 | 11 | 0 |
| | 5/2 | EAB | ⟺ | GAB | 3/2 | 50-80 | 1 | 16 | 0 |
| | 5/2 | FAB | ⟺ | HAB | 3/2 | < 150 | 1 | 16 | 0 |
| | 7/2[b] | C(γ) | ⟺ | AEH | 9/2[b] | < 11 | 1 | 13 | 0 |
| | 5/2 | BAD | ⟺ | AEGBC | 9/2[b] | (~13) | 2 | 29 | 0 |
| | 9/2[b] | BEHAD | ⟺ | AEGBC | 9/2[b] | (~14) | 0 | 23 | 0 |
| | 9/2[b] | AEHBC | ⟺ | ABCef | 5/2 | ~6 | 2 | 32 | 5 |
| | 9/2[b] | AFGBC | ⟺ | ABCef | 5/2 | ~11 | 2 | 28 | 4 |
| | 3/2 | HAB | ⟺ | FABef | 5/2 | ~10 | 1 | 29 | 4 |
| | 13/2[b] | EAC | ⟺ | eaA | 19/2 | 1-2 | 3 | 21 | 0 |
| | 11/2 | X | ⟺ | faA | 19/2 | 1.4 | 3 | 15 | 3.5 |
| | 11/2 | Y | ⟺ | eaA | 19/2 | 1.3 | 3 | 15 | 3.5 |
| | 19/2 | XAG | ⟺ | eaEAB | 19/2 | 16 | 0 | 21 | 3.5 |
| | 19/2 | YAG | ⟺ | faEAB | 19/2 | 14 | 0 | 21 | 3.5 |
| $^{163}$Tm | 7/2 | aAB | ⟺ | cAB | 1/2 | <5 | 3 | 43/2 | 0 |
| | 7/2 | aAB | ⟺ | fAE | 17/2 | ~ 6.6 | 5 | 39/2 | 0.5 |
| | 1/2 | d(AB) | ⟺ | eAE | 17/2 | ~ 1-2.5 | 8 | 31/2 | 1 |

[a] No cross band transitions are observed in this case
[b] Estimated K-values

→ different Nilsson configurations: (simple crossings)
→ Beyond Mean field treatment.

Table 3. Interactions between rotational bands in $^{162}$Tm. Cases where both bands are known below and above the crossing are included. For the classification of assignments see table 1. Orbitals changed in the interaction are underlined. Partly aligned pairs of $i_{13/2}$ quasineutrons are given in parenthesis.

| Interacting bands | | | | | Strength V | $\sim \Delta K$ | $\sim$Spin | $\sim \Delta i$ |
|---|---|---|---|---|---|---|---|---|
| $K_1$ | $Label_1$ | $\Longleftrightarrow$ | $Label_2$ | $K_2$ | keV | $\hbar$ | $\hbar$ | $\hbar$ |
| 6 | $\underline{b}$A(BC) | $\Longleftrightarrow$ | $\underline{d}$A(BC)[a] | 2 | < 1.5 | 4 | 20 | 0.6 |
| 5 | f$\underline{G}$(A$\underline{B}$) | $\Longleftrightarrow$ | $\underline{d}$A | 2 | 5(1) | 3 | 18 | 2.0 |
| 5 | f$\underline{H}$(A$\underline{B}$) | $\Longleftrightarrow$ | $\underline{c}$A | 2 | 5(1) | 3 | 17 | 1.9 |
| 5 | f$\underline{F}$AB | $\Longleftrightarrow$ | $\underline{a}$A(B$\underline{C}$) | 6 | 11(1) | 1 | 21 | 2.8 |
| 6 | f$\underline{E}$AB | $\Longleftrightarrow$ | $\underline{d}$AB$\underline{C}$ | 2 | 7(1) | 3 | 26 | 0.5 |

[a] No cross band transitions are observed in this case

Table 4. Possible crossings between quasiparticle bands, schematically. (In reality, the excitation energies have to be comparable, and aligning quasiparticles will in many cases also be present)

| Nucleus | Interacting bands | | | $\Delta$ K |
|---|---|---|---|---|
| Even-even | AF,AE | $\Longleftrightarrow$ | af,ae | 2 |
| Odd-Z | a,b | $\Longleftrightarrow$ | fAE,eAE | 5 |
| Odd-Z | e,f | $\Longleftrightarrow$ | bAE,aAE | 5 |
| Odd-N | A,B | $\Longleftrightarrow$ | Fae,Eae | 7 |
| Odd-N | E,F | $\Longleftrightarrow$ | Aaf,Aae | 7 |
| Odd-odd | aF,aE | $\Longleftrightarrow$ | Af,Ae | 0 |

Table 0. Single quasiparticles and labels (not to be used in the paper)

| Neutrons | | | Protons | | |
|---|---|---|---|---|---|
| Configuration | $\alpha = +1/2$ | $\alpha = -1/2$ | Configuration | $\alpha = +1/2$ | $\alpha = -1/2$ |
| $i_{13/2}[642]5/2^+$ | A | B | $g_{7/2}[404]7/2^+$ | a | b |
| $i_{13/2}[651]3/2^+$ | C | D | $d_{3/2}[411]1/2^+$ | c | d |
| $h_{9/2}[523]5/2^-$ | E | F | $d_{5/2}[402]5/2^+$ | k | l |
| $f_{7/2}[521]3/2^-$ | G | H | $h_{11/2}[523]7/2^-$ | e | f |
| $h_{11/2}[505]11/2^-$ | X | Y | $h_{9/2}[541]1/2^-$ | g | h |

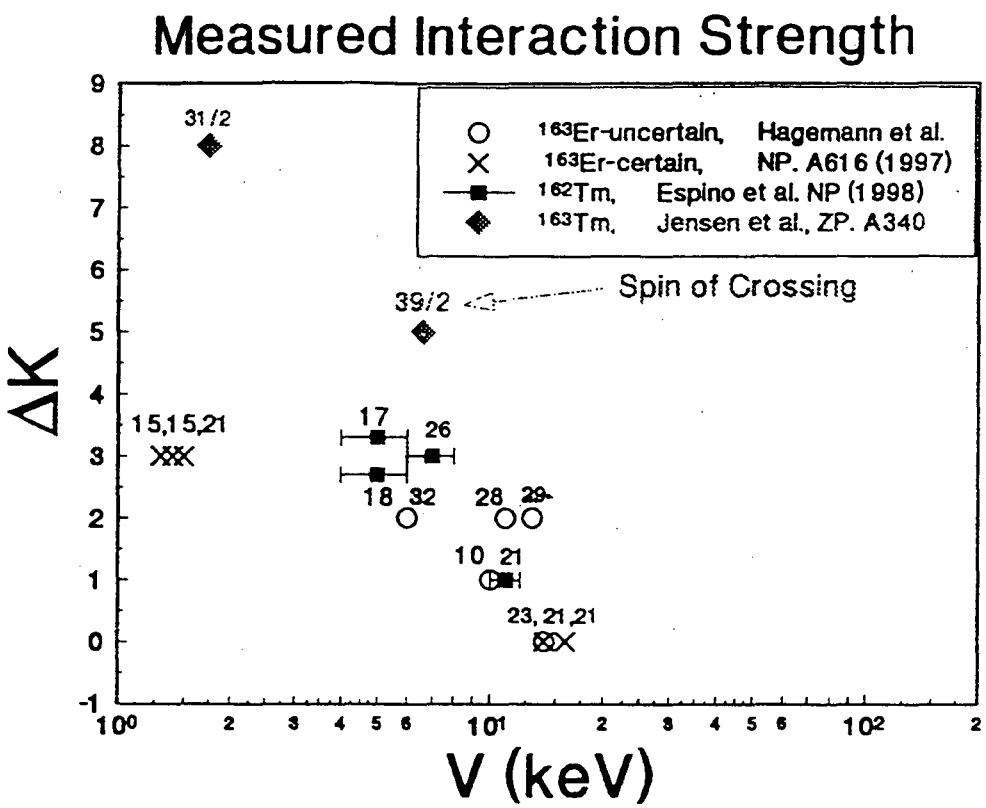
Measured Interaction Strength
163Er-uncertain, Hagemann et al.
163Er-certain, NP. A616 (1997)
162Tm, Espino et al. NP (1998)
163Tm, Jensen et al., ZP. A340
Spin of Crossing
31/2
39/2
15,15,21
17
26
18
32
28
29
10
21
23,21,21
ΔK
V (keV)

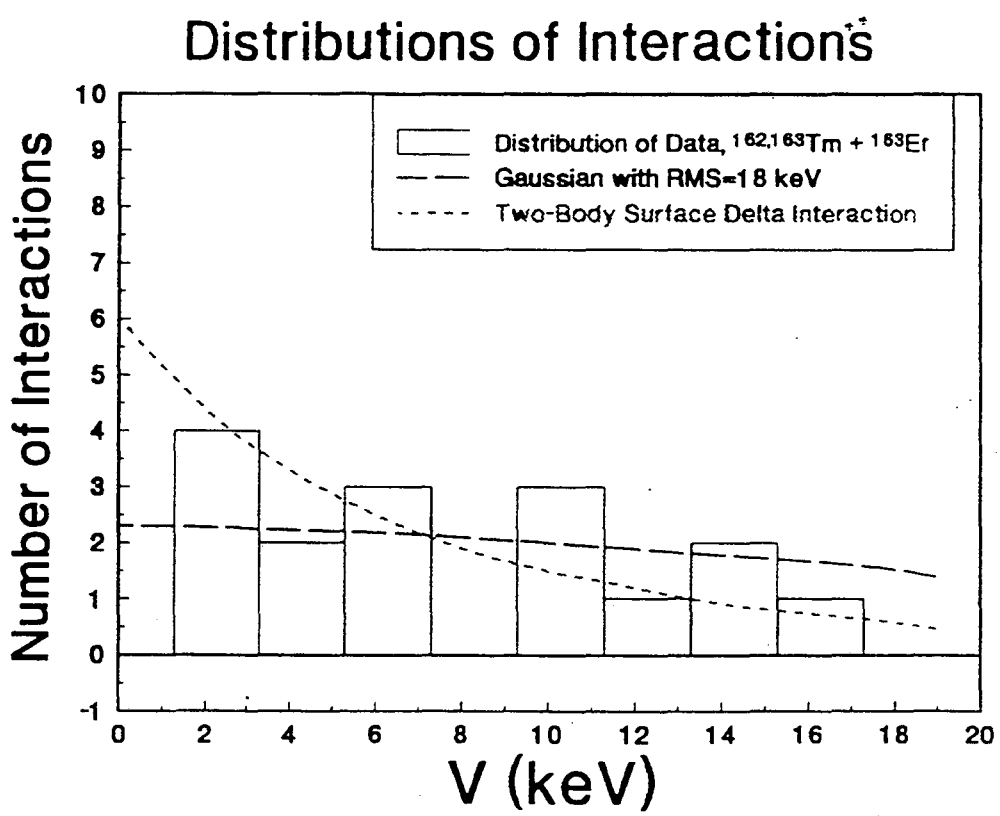
Distributions of Interactions
Distribution of Data, 162,163Tm + 163Er
Gaussian with RMS=18 keV
Two-Body Surface Delta Interaction
Number of Interactions
V (keV)

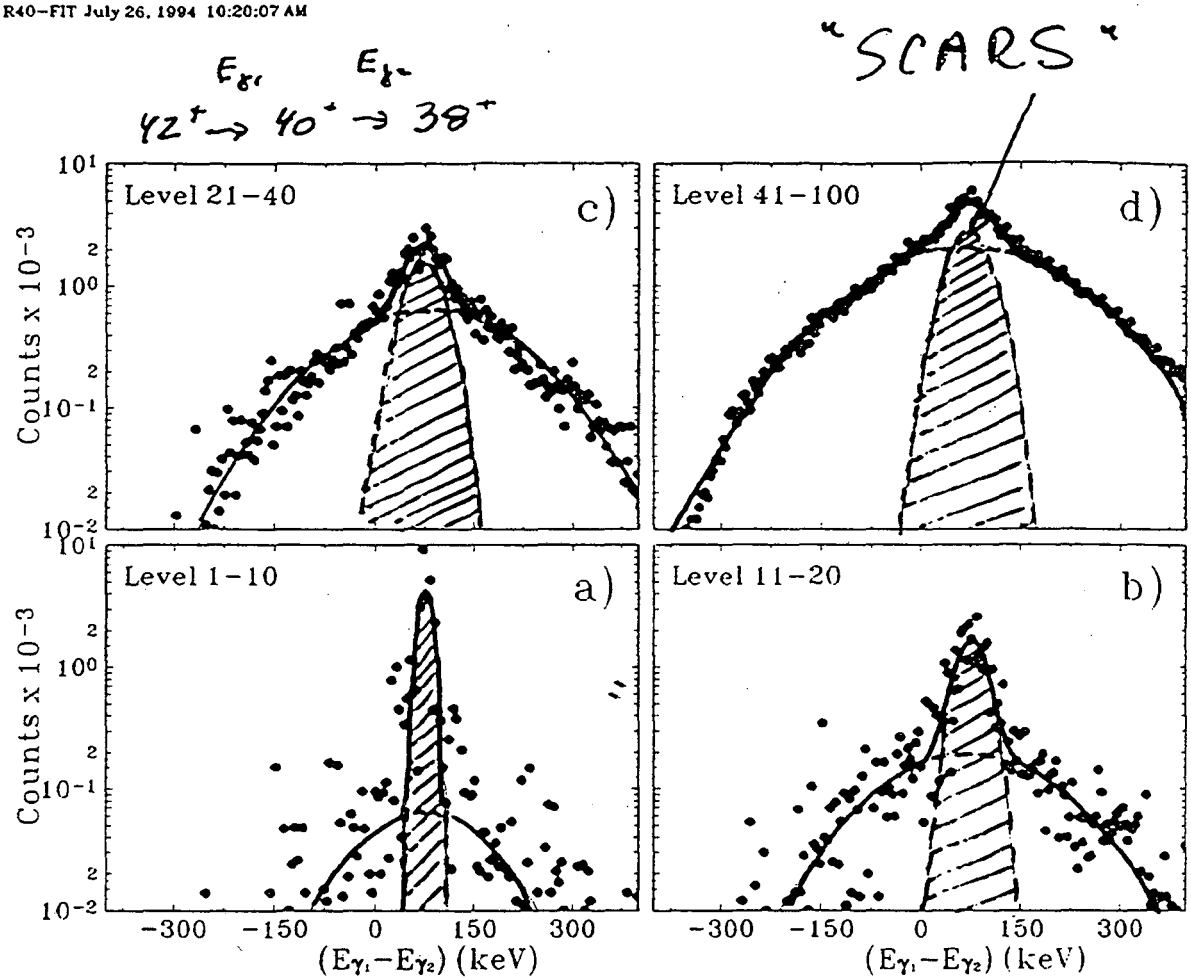
"SCARS"
$E_{\gamma_1}$ $E_{\gamma_2}$
$42^+ \rightarrow 40^+ \rightarrow 38^+$
Level 21-40
c)
Level 41-100
d)
Level 1-10
a)
Level 11-20
b)
Counts x 10-3
$(E_{\gamma_1}-E_{\gamma_2})$ (keV)

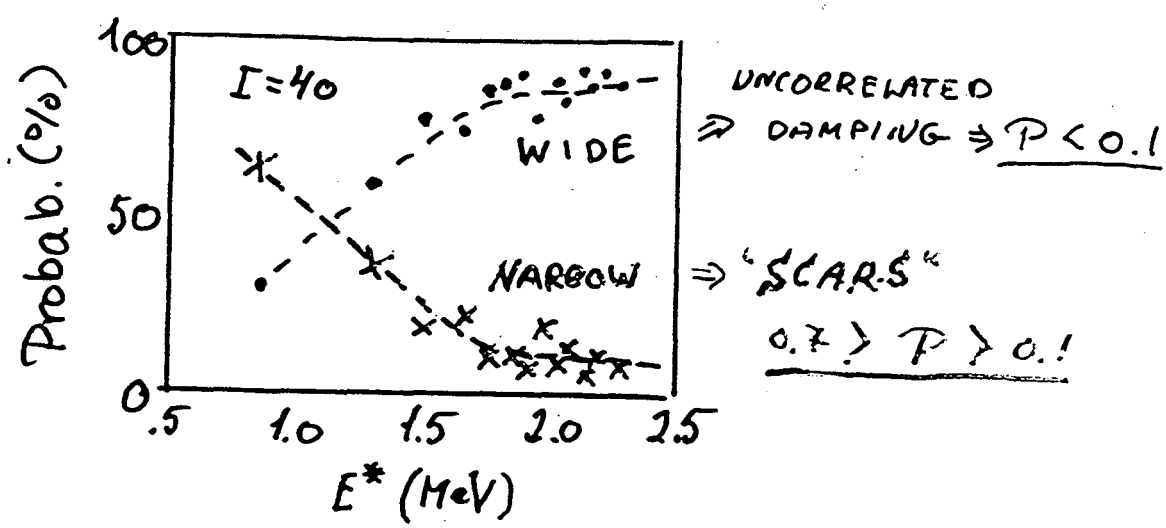
I=40
WIDE
NARROW
Probab. (%)
E* (MeV)
UNCORRELATED
⇒ DAMPING ⇒ P < 0.1
⇒ "SCARS"
0.7 > P > 0.1

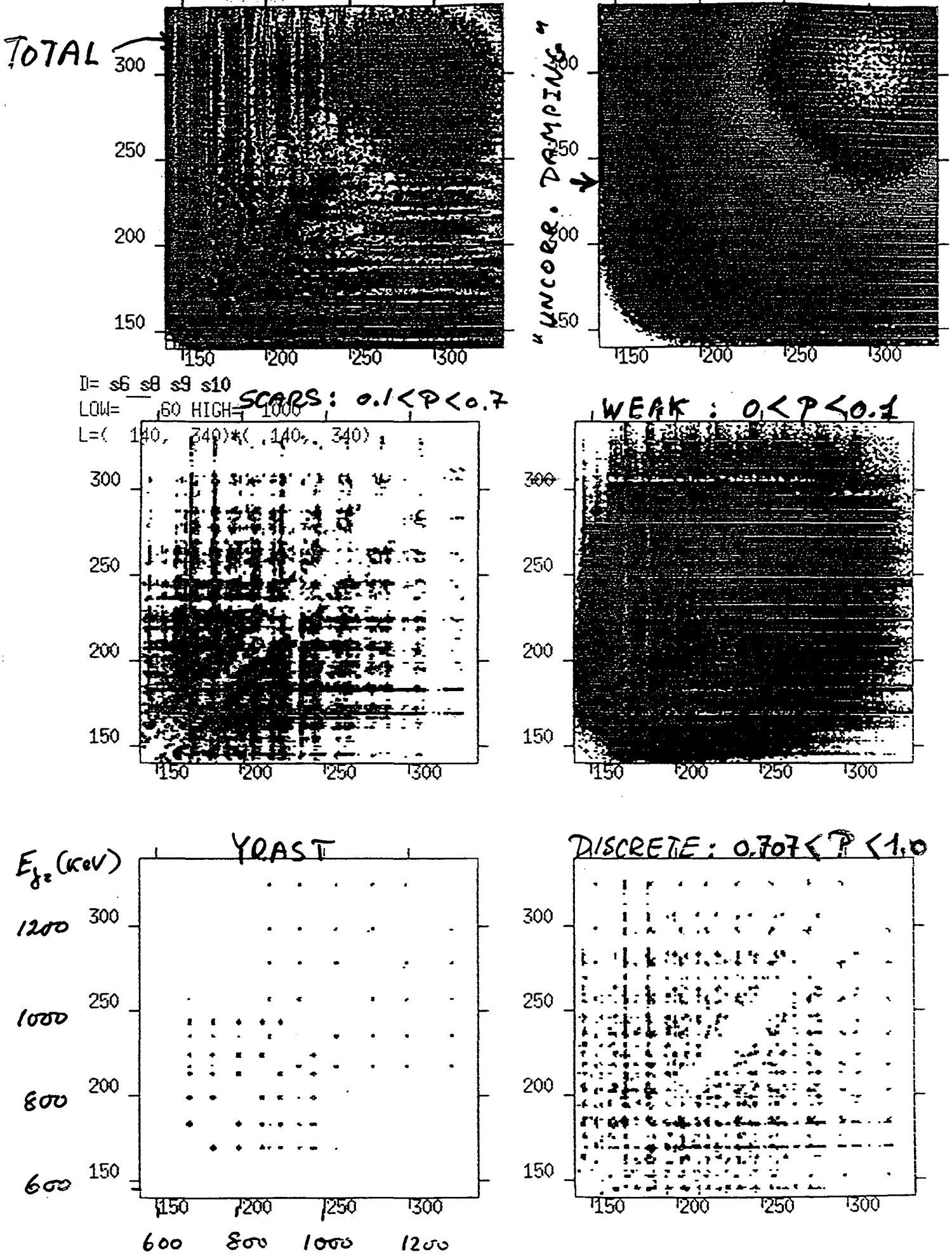
TOTAL
"UNCOR. DAMPING"
D= s6 s8 s9 s10
LOW= 60 HIGH= 1000
L=( 140, 340)*( 140, 340)
SCARS: 0.1<P<0.7
WEAK: 0<P<0.1
YEAST
DISCRETE: 0.707<P<1.0
$E_{\gamma_2}$ (KeV)
1200
1000
800
600
$E_{\gamma_1}$ (KeV
TITLE :
s6 :
543
ca/i/di/u/du/u0/be/ec= 300000/55./10./5.5/2.0/ 400/ 400./0.0

PLOT started : 16-FEB-95 12:17:13
DUMP created : 4-FEB-95 09:48:01 BH

D= s28 s25 s22 s19 s13 PERPENDICULAR CUTS
F = 8192.
L= 150 H= 650 $(E_{\gamma_1} + E_{\gamma_2})/2 = 1100$ KeV

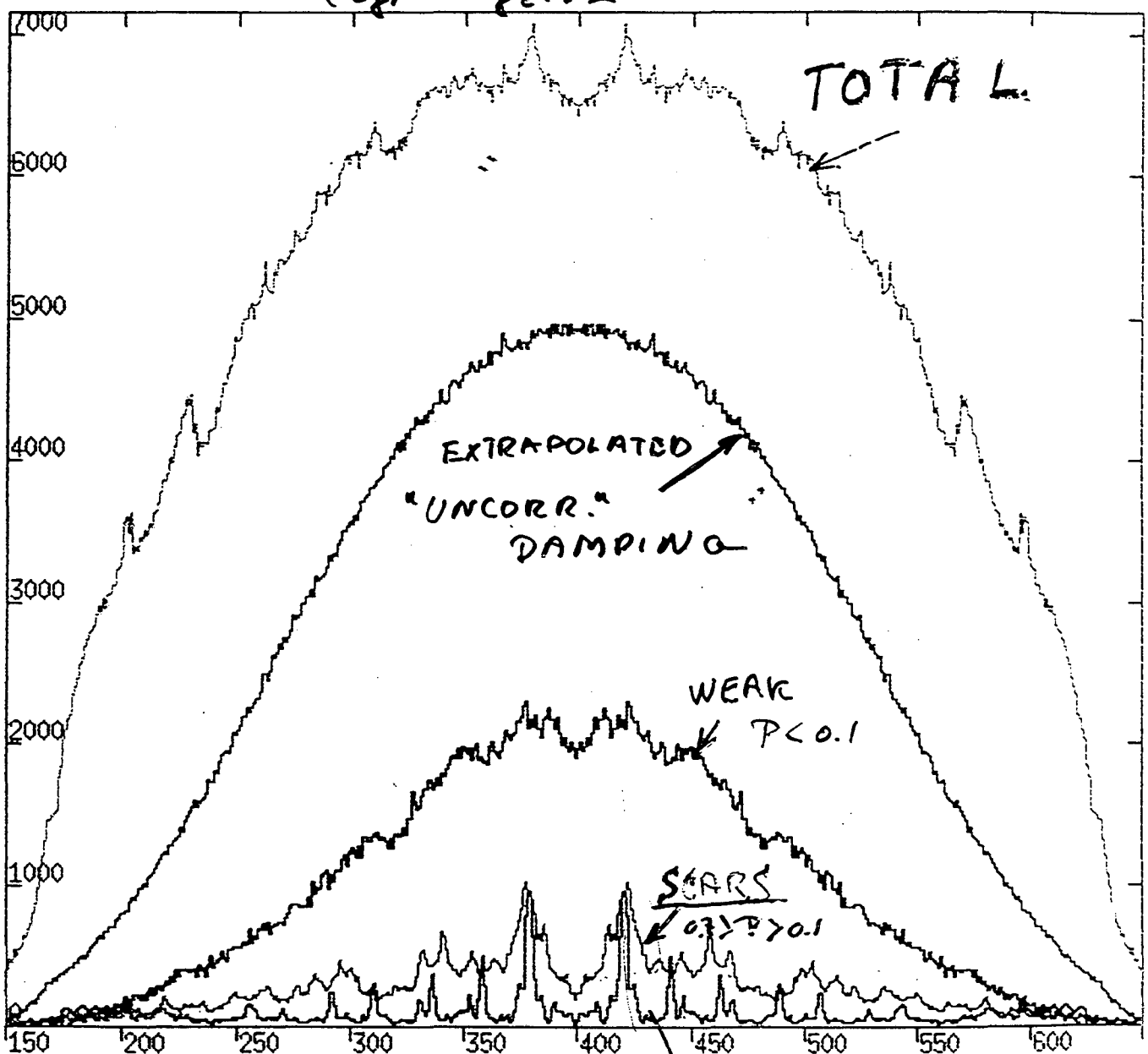


TITLE :
s28 : Peak Comp, P > 0.70700
cut at chanel 275 width= 15
s25 : Narrow Comp, P_min<P<P_max 0.7,1.0
cut at chanel 275 width= 15
s22 : bands P<0.1
cut at chanel 275 width= 15
s19 :
cut at chanel 275 width= 15

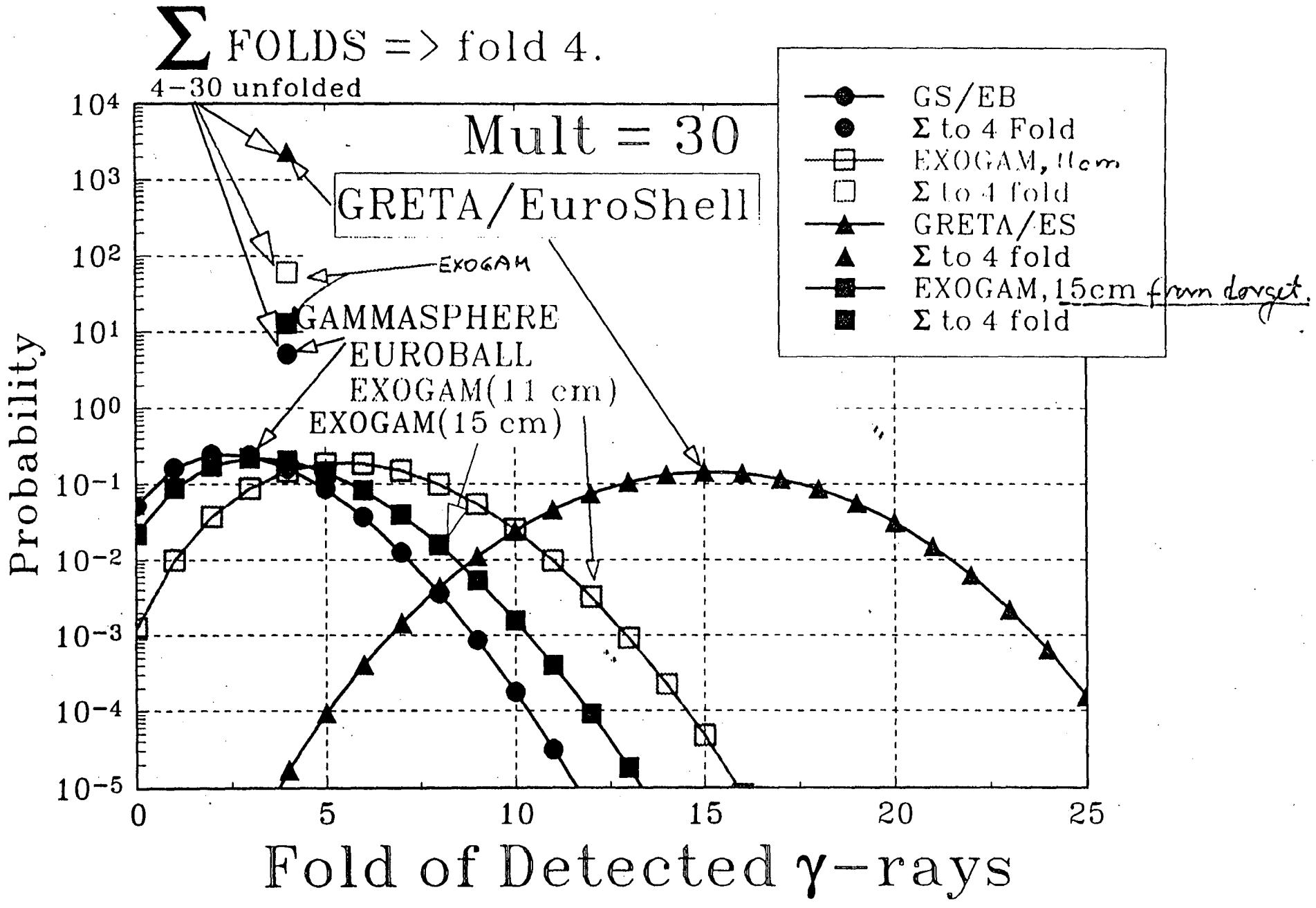
Σ FOLDS => fold 4.
4−30 unfolded
Mult = 30
GRETA/EuroShell
EXOGAM
GAMMASPHERE
EUROBALL
EXOGAM(11 cm)
EXOGAM(15 cm)
GS/EB
Σ to 4 Fold
EXOGAM, 11cm
Σ to 4 fold
GRETA/ES
Σ to 4 fold
EXOGAM, 15cm from target.
Σ to 4 fold
Probability
Fold of Detected γ−rays

# INTERACTIVE SCANNER FOR HIGH FOLDS

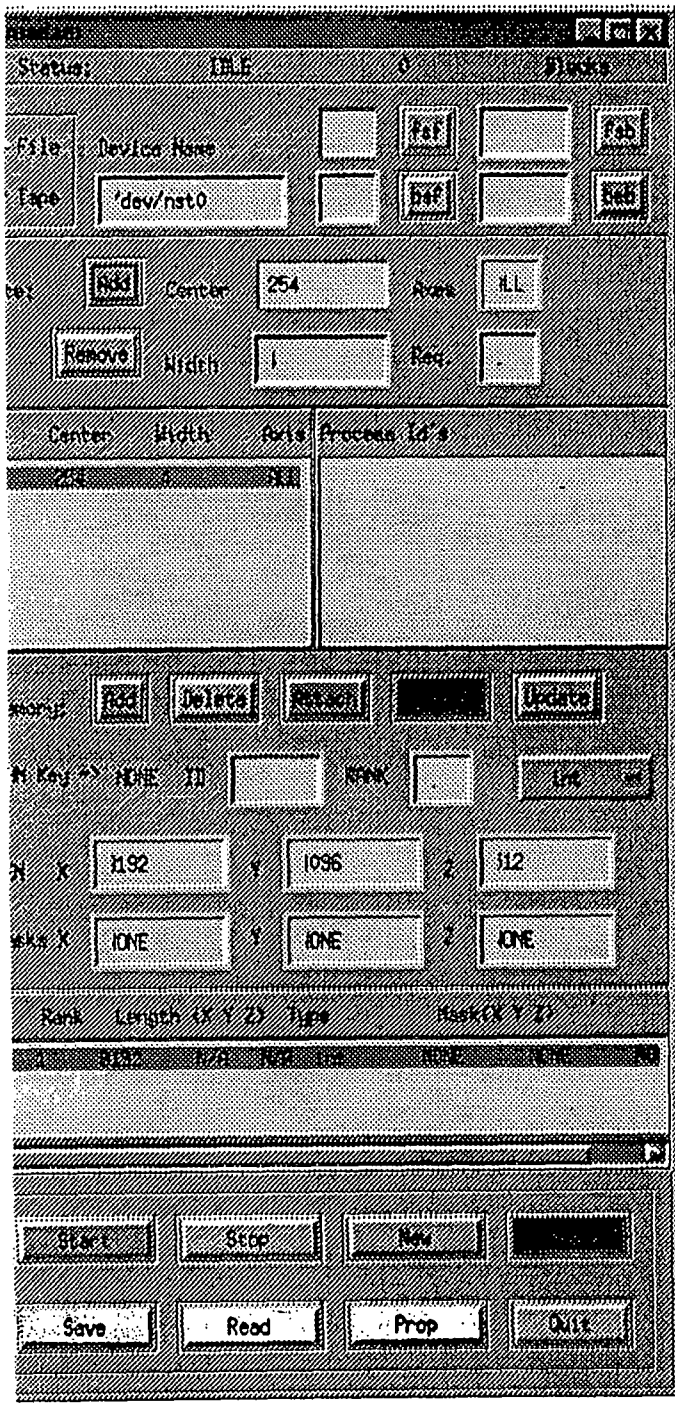


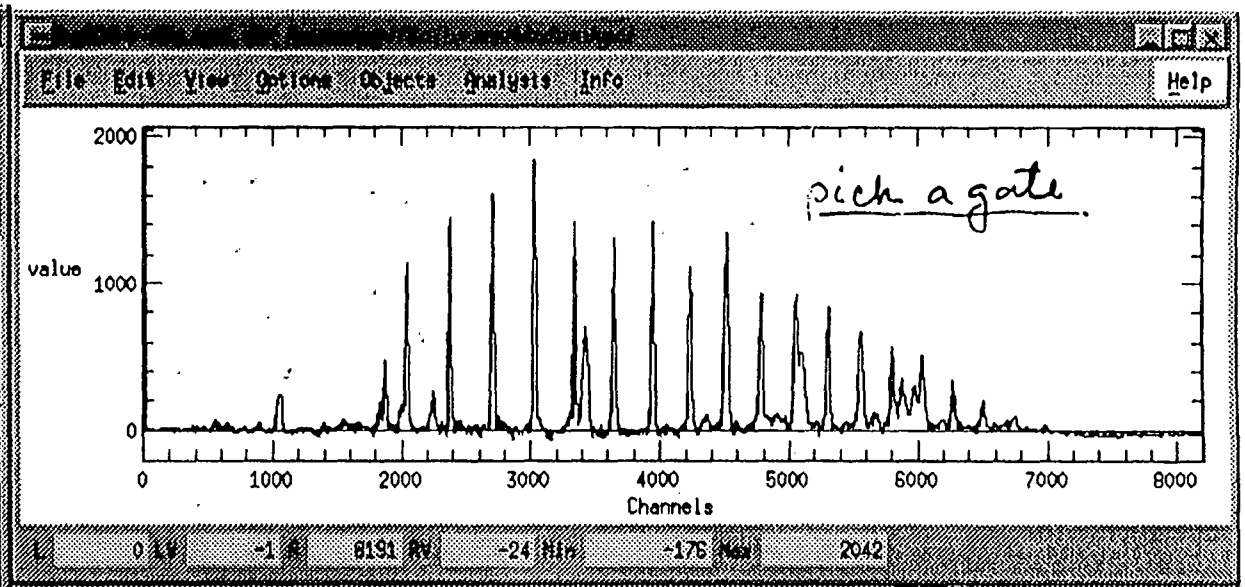


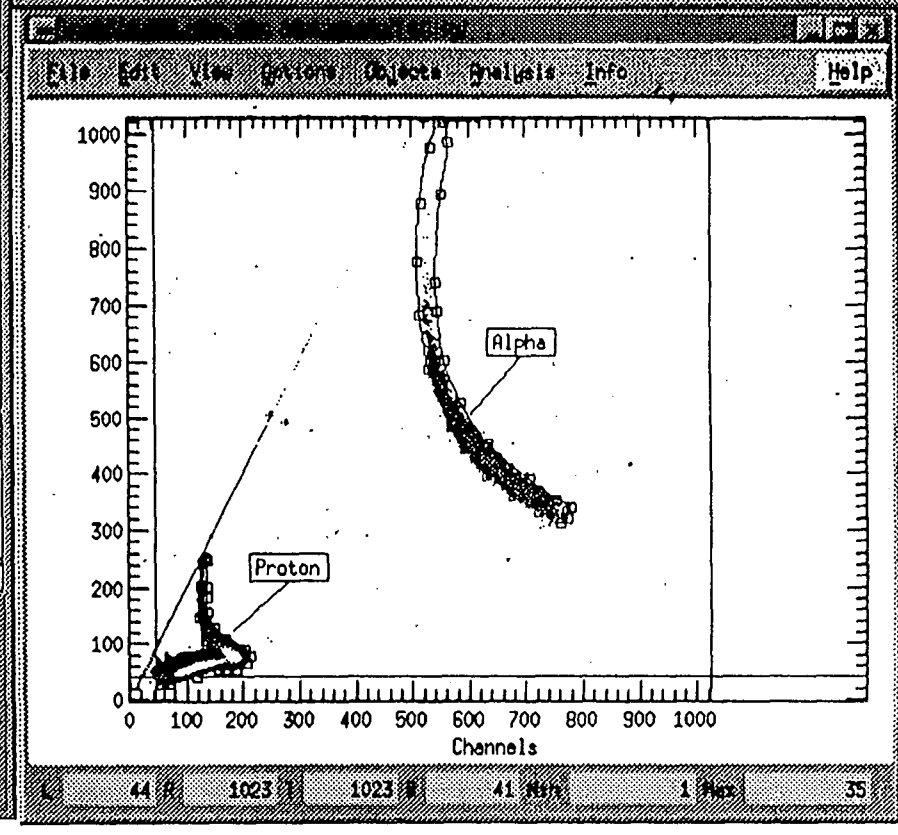

Madam:
by Peter G. Varmette

Interactive Scanner and 2D Plot. The 1D hist is from 194Hg and the 2D hist is from 90Zr + 90 Zr.

FROM FLUTUATION ANALYSIS

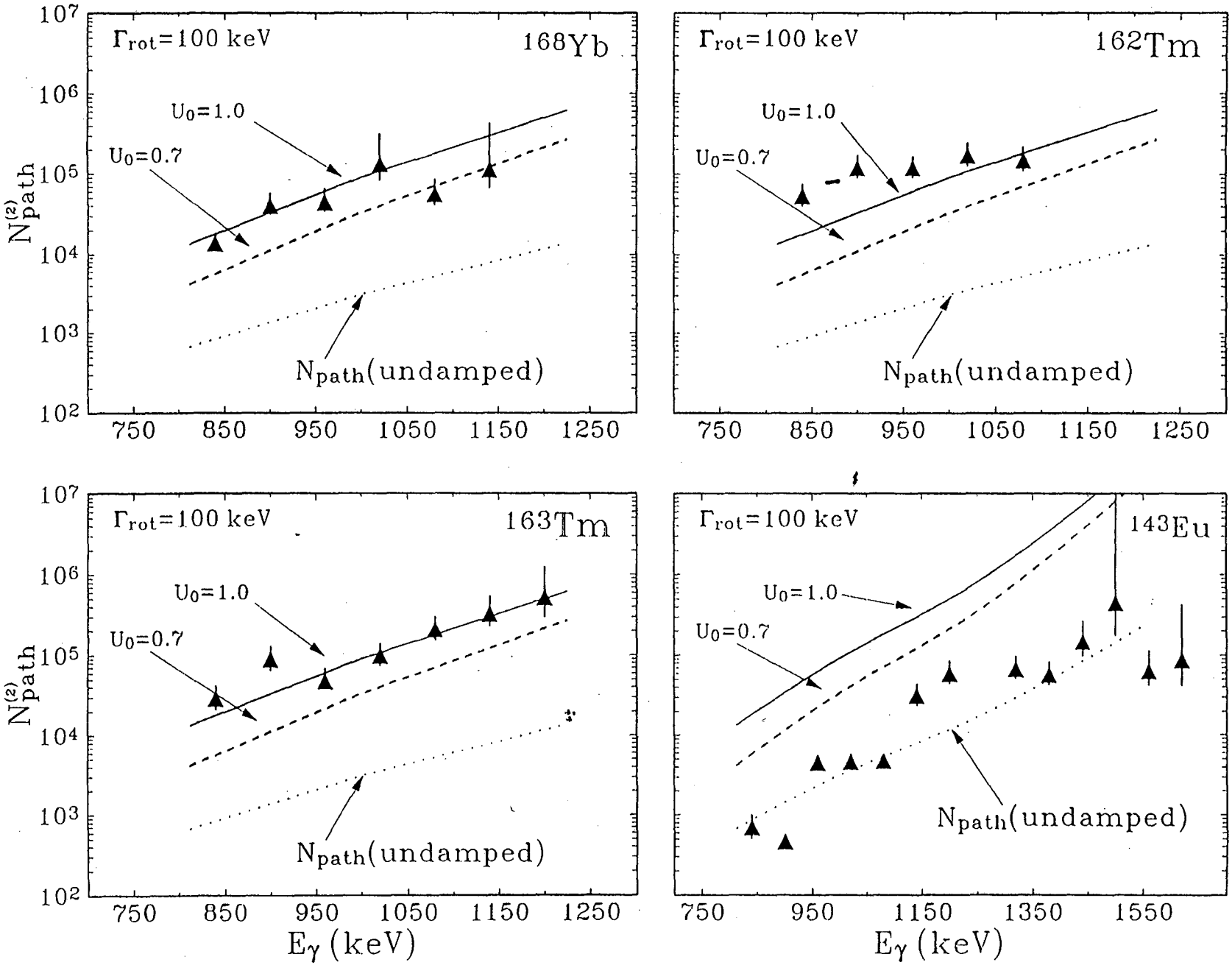

USE OF PATTERN RECOGNITION TECHNIQUES TO SORT IDENTICAL event into ~ $10^5$ PATHWAYS

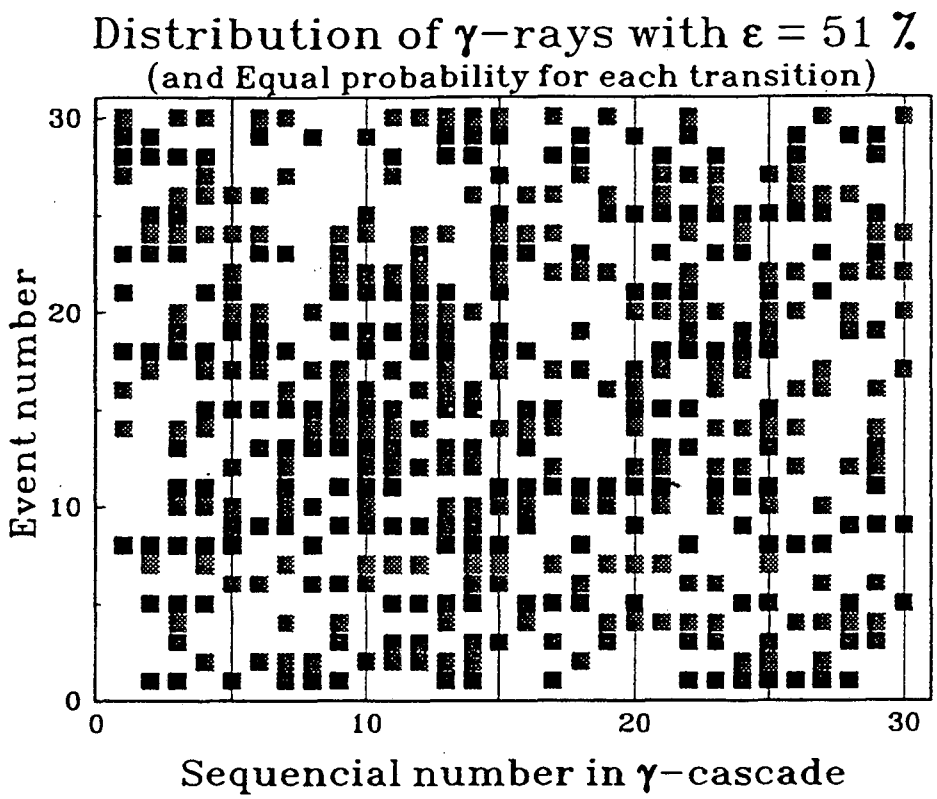


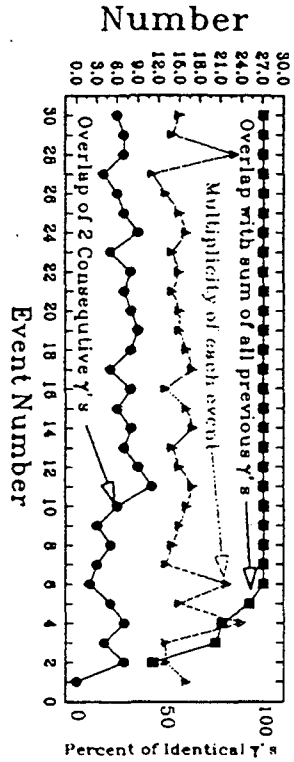


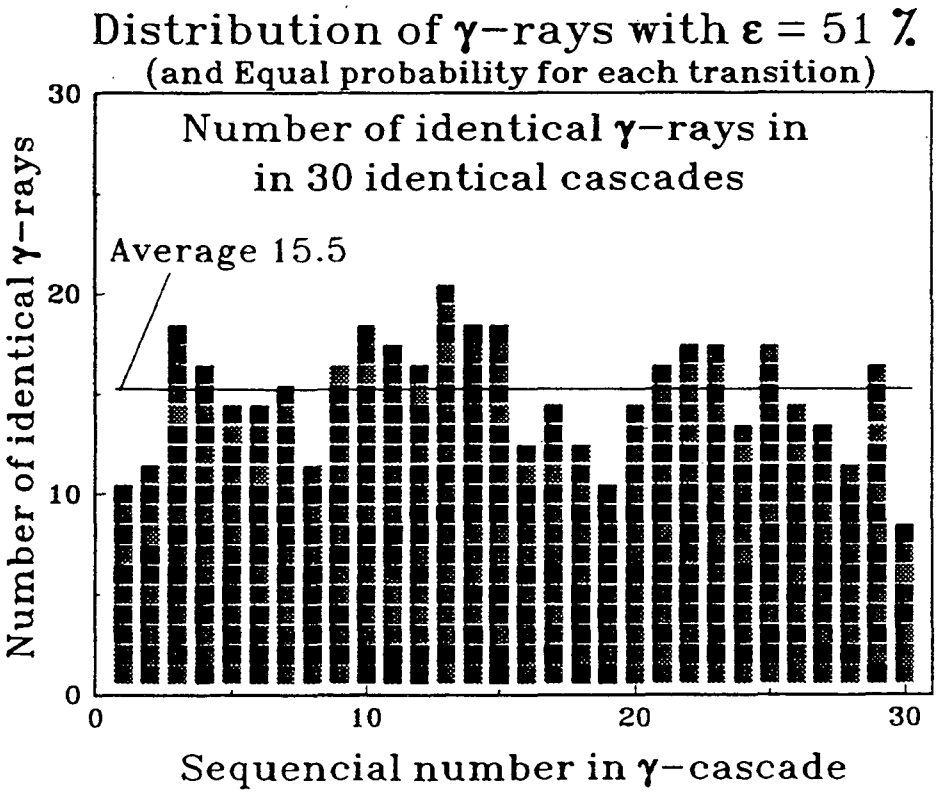


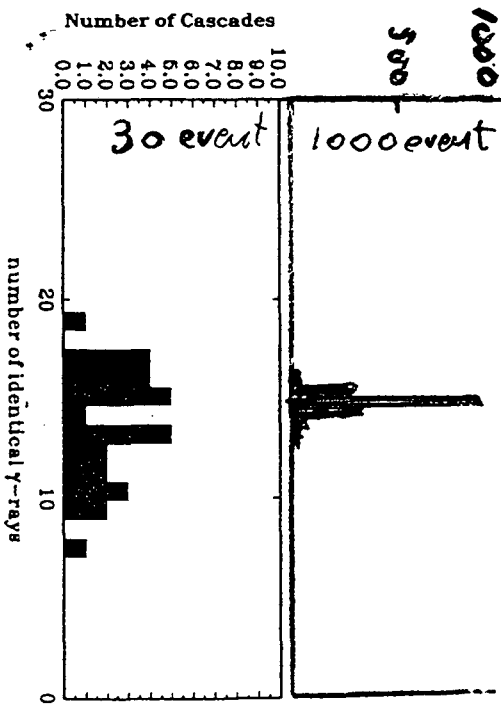

## Typical Matrix Sorted after a GRETA Experiment into 99003 Pathways of ~30 Transitions

| | | | | | | | | | | | |
|---|---|---|---|---|---|---|---|---|---|---|---|
| Path 99003 | Y40,1 | Y60,2 | Y105,3 | Y307,4 | Y1017,5 | Y2009,6 | Y3031,7 | Y3790,8 | Y4200,9 | Y91234,29 | Y98000,30 |
| | E40,1 | E60,2 | E105,3 | E307,4 | E1017,5 | E2009,6 | E3031,7 | E3790,8 | E4200,9 | E91234,29 | E98000,30 |
| Path 99002 | Y40,1 | Y60,2 | Y105,3 | Y307,4 | Y1017,5 | Y2009,6 | Y3030,7 | Y3789,8 | Y3999,9 | Y91233,29 | Y97999,30 |
| | E40,1 | E60,2 | E105,3 | E307,4 | E1017,5 | E2009,6 | E3030,7 | E3789,8 | E3999,9 | E91233,29 | E97999,30 |
| Path 99001 | Y40,1 | Y60,2 | Y105,3 | Y307,4 | Y1016,5 | Y2008,6 | Y3029,7 | Y3788,8 | Y3998,9 | Y91232,29 | Y97998,30 |
| | E40,1 | E60,2 | E105,3 | E307,4 | E1016,5 | E2008,6 | E3029,7 | E3788,8 | E3998,9 | E91232,29 | E97998,30 |
| | | | | | | | | | | | |
| Path 1004 | Y3,1 | Y9,2 | Y14,4 | Y27,4 | Y38,5 | Y59,6 | Y79,7 | Y83,8 | Y90,8 | Y706,29 | Y804,30 |
| | E3,1 < | E9,2 < | E14,4 < | E27,4 < | E38,5 < | E59,6 < | E79,7 < | E83,8 < | E90,8 < | E706,29 | E804,30 |
| Path 1003 | Y3,1 | Y9,2 | Y13,3 | E26,4 | Y37,5 | Y58,6 | Y78,7 | Y82,8 | Y89,9 | Y705,29 | Y803,30 |
| | E3,1 < | E9,2 < | E13,3 < | E26,4 < | E37,5 < | E58,6 < | E78,7 < | E82,8 < | E89,9 < | E705,29 | E803,30 |
| Path 1002 | Y3,1 | Y9,2 | Y13,3 | E26,4 | Y37,5 | Y58,6 | Y78,7 | Y82,8 | Y89,9 | Y704,29 | Y802,30 |
| | E3,1 < | E9,2 < | E13,3 < | E26,4 < | E37,5 < | E58,6 < | E78,7 < | E82,8 < | E89,9 < | E704,29 | E802,30 |
| Path 1001 | Y3,1 | Y9,2 | Y13,3 | E26,4 | Y37,5 | Y58,6 | Y78,7 | Y82,8 | Y89,9 | Y703,29 | Y801,30 |
| | E3,1 < | E9,2 < | E13,3 < | E26,4 < | E37,5 < | E58,6 < | E78,7 < | E82,8 < | E89,9 < | E703,29 | E801,30 |
| Path 1000 | Y2,1 | Y8,2 | Y12,3 | Y25,4 | Y36,5 | Y57,6 | Y77,7 | Y81,8 | Y88,9 | Y702,29 | Y800,30 |
| | E2,1 | E8,2 < | E12,3 < | E25,4 < | E36,5 < | E57,6 < | E77,7 < | E81,8 < | E88,9 < | E702,29 | E800,30 < |
| | | | | | | | | | | | |
| Path 9 | Y1,1 | Y2,2 | Y2,3 | Y3,4 | Y3,5 | Y3,6 | Y3,7 | Y4,8 | Y7,9 | Y9,10 | Y9,30 |
| | E1,1 < | E2,2 < | E2,3 < | E3,4 < | E3,5 < | E3,6 < | E3,7 < | E4,8 < | E7,9 | E9,29 < | E9,30 < |
| Path 8 | Y1,1 | Y2,2 | Y2,3 | Y3,4 | Y3,5 | Y3,6 | Y3,7 | Y4,8 | Y6,9 | Y8,29 | Y8,30 |
| | E1,1 < | E2,2 < | E2,3 < | E3,4 < | E3,5 < | E3,6 < | E3,7 < | E4,8 < | E6,9 | E8,28 < | E8,30 < |
| Path 7 | Y1,1 | Y1,2 | Y1,3 | Y2,4 | Y2,5 | Y2,6 | Y3,7 | Y4,8 | Y5,9 | Y7,29 | Y7,30 |
| | E1,1 < | E1,2 < | E1,3 < | E2,4 < | E2,5 < | E2,6 < | E3,7 < | E4,8 < | E5,9 < | E7,29 < | E7,30 |
| Path 6 | Y1,1 | Y1,2 | Y1,3 | Y2,4 | Y2,5 | Y2,6 | Y3,7 | Y4,8 | Y4,9 | Y6,29 | Y6,30 |
| | E1,1 < | E1,2 < | E1,3 < | E2,4 < | E2,5 < | E2,6 < | E3,7 < | E4,8 < | E4,9 | E6,29 < | E6,30 < |
| Path 5 | Y1,1 | Y1,2 | Y1,3 | Y1,4 | Y1,5 | Y1,6 | Y2,7 | Y2,8 | Y3,9 | Y5,29 | Y5,30 |
| | E1,1 < | E1,2 < | E1,3 < | E1,4 < | E1,5 < | E1,6 < | E2,7 < | E2,8 < | E3,9 < | E5,29 < | E5,30 < |
| Path 4 | Y1,1 | Y1,2 | Y1,3 | Y1,4 | Y1,5 | Y1,6 | Y2,7 | Y2,8 | Y3,9 | Y4,29 | Y4,30 |
| | E1,1 < | E1,2 < | E1,3 < | E1,4 < | E1,5 < | E1,6 < | E2,7 < | E2,8 < | E3,9 < | E4,29 < | E4,30 |
| Path 3 | Y1,1 | Y1,2 | Y1,3 | Y1,4 | Y1,5 | Y1,6 | Y1,7 | Y1,8 | Y2,9 | Y3,29 | Y3,30 |
| | E1,1 < | E1,2 < | E1,3 < | E1,4 < | E1,5 < | E1,6 < | E1,7 < | E1,8 < | E2,9 < | E3,29 < | E3,30 < |
| Path 2 | Y1,1 | Y1,2 | Y1,3 | Y1,4 | Y1,5 | Y1,6 | Y1,7 | Y1,8 | Y1,9 | Y2,29 | Y2,30 |
| | E1,1 < | E1,2 < | E1,3 < | E1,4 < | E1,5 < | E1,6 < | E1,7 < | E1,8 < | E1,9 < | E2,29 < | E2,30 < |
| Path 1 | Y1,1 | Y1,2 | Y1,3 | Y1,4 | Y1,5 | Y1,6 | Y1,7 | Y1,8 | Y1,9 | Y1,10 | Y1,30 |
| | E1,1 < | E1,2 < | E1,3 < | E1,4 < | E1,5 < | E1,6 < | E1,7 < | E1,8 < | E1,9 < | E1,10< | E1,30 |

| | | | | | | | | | | | |
|---|---|---|---|---|---|---|---|---|---|---|---|
| **Typical Path** | Y1 > | Y2 > | Y3 > | Y4 > | Y5 > | Y7 > | Y8 > | Y6 > | Y9 > | Y29 > | Y30 |
| | E1 < | E2 < | E3 < | E4 < | E5 < | E6 < | E7 < | E8 < | E9 < | E29 < | E30 |
| **Spin** | 2=>0 | 4=> 6 | 6=> 8 | 8=>10 | 10=>8 | 14=> 12 | 16=> 14 | 12=> 10 | 18=>16 | 58 => 56 | 60 => 58 |

$^{177}$Ho

D.C. Radford et al. / Multiple band structure, NP A545 (1992)

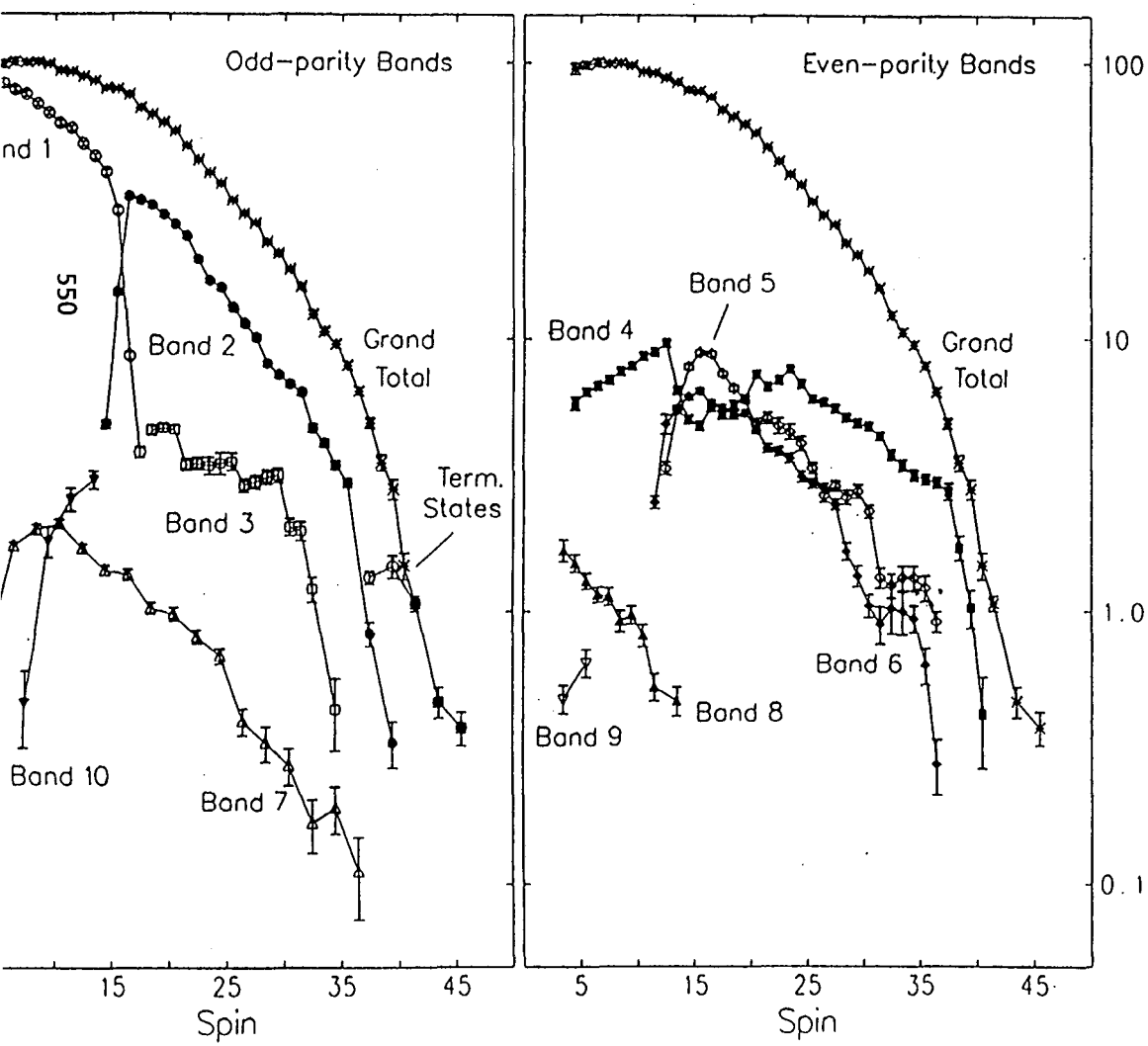


R.A. Bark et al. / Nuclear Physics A 591 (1995) 265–322

$^{177}$Re

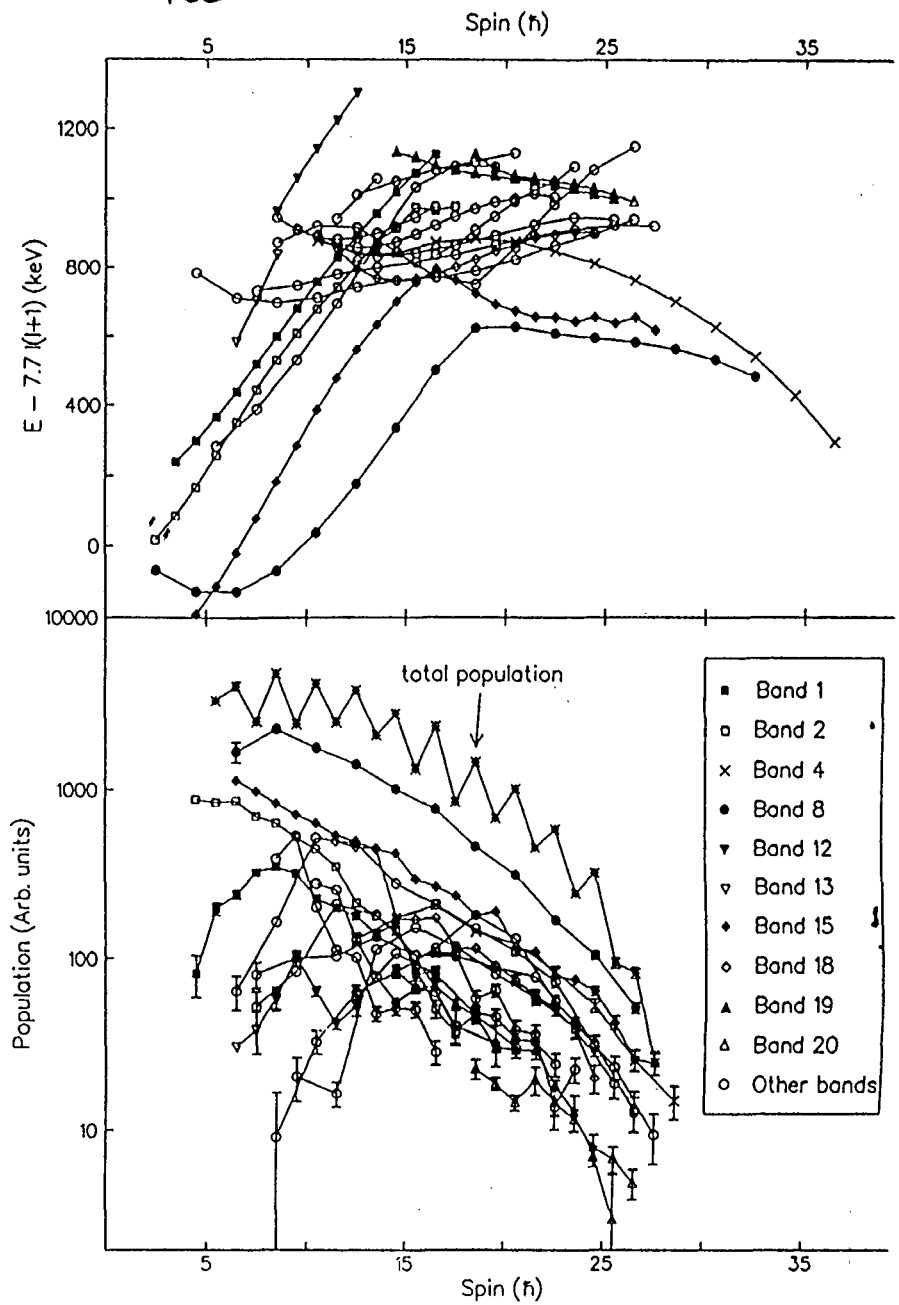

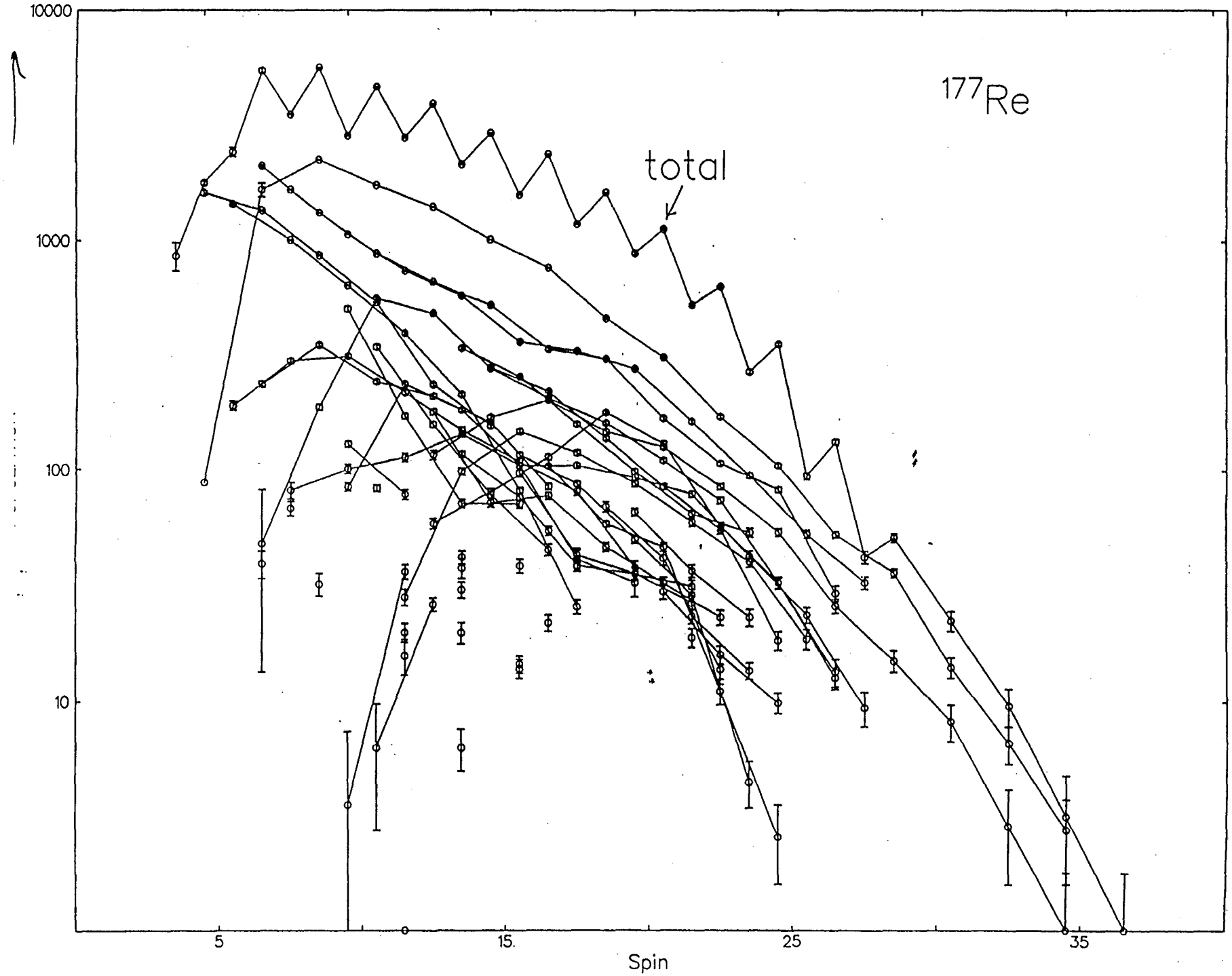
10000
1000
100
10
5
15.
25
35
Spin
total
177Re

CUT_2D1D Jan. 30, 1998 11:00:51 PM

a)

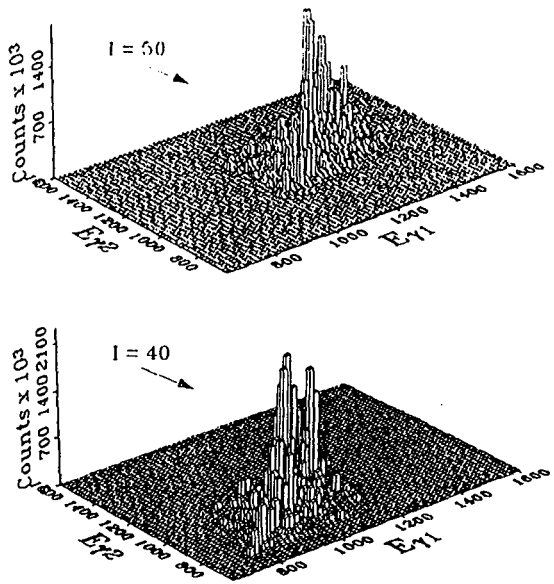


c)

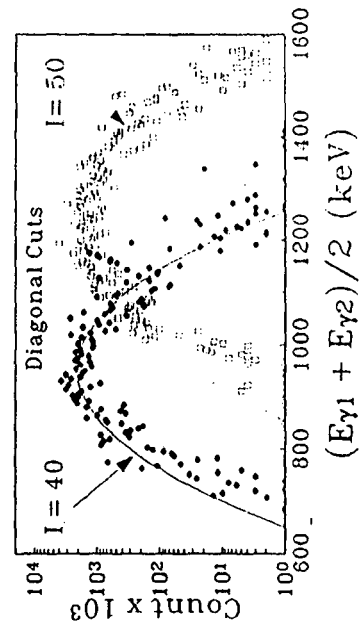


b)

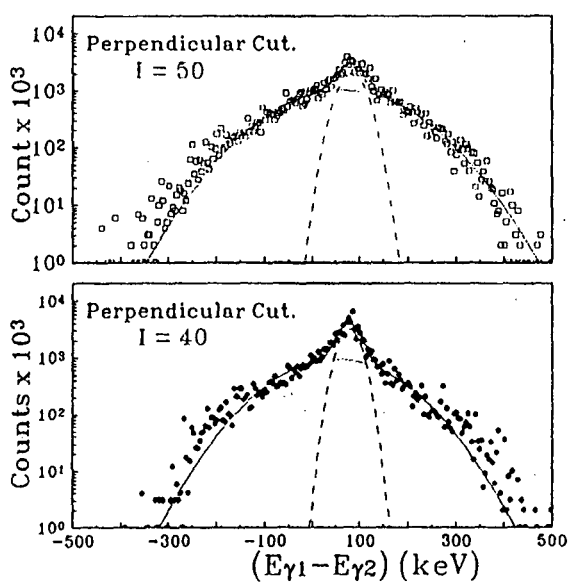


# Band−Mixing Calculations

Level 11−40

Both Parities

Both Signatures

γ-γ-coincidence for the first 40 levels of each (π,0
for I's 42 → 40 → 38 or 41 → 39 → 37

REDUCED
SURFACE-DELTA INT.

(SDI) × 2

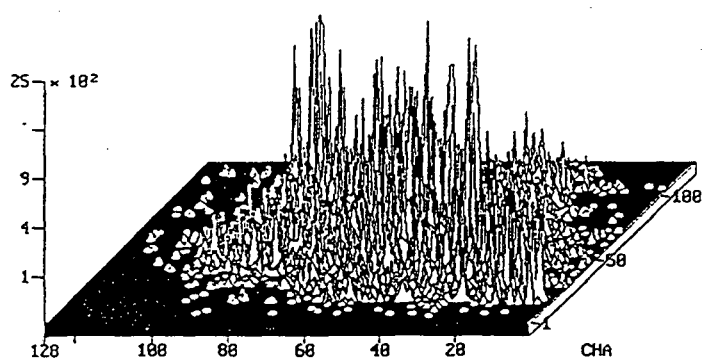


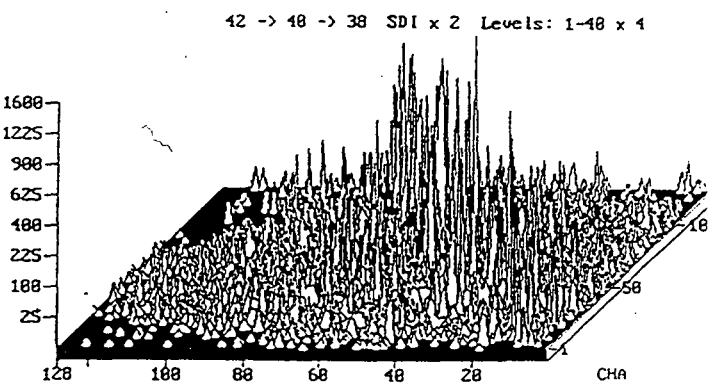


42 -> 40 -> 38 No Interaction Levels: 1-40 x 4

NO-INTERACTION

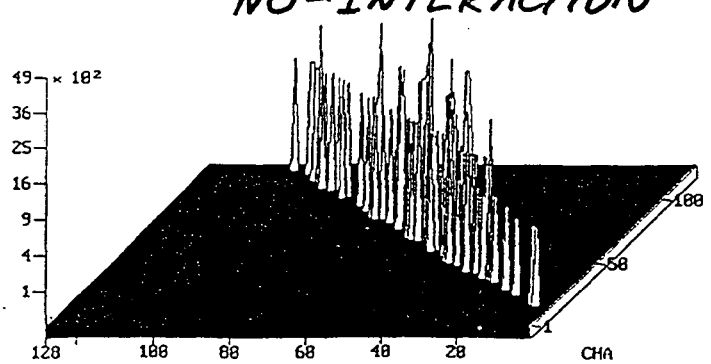


SDI:

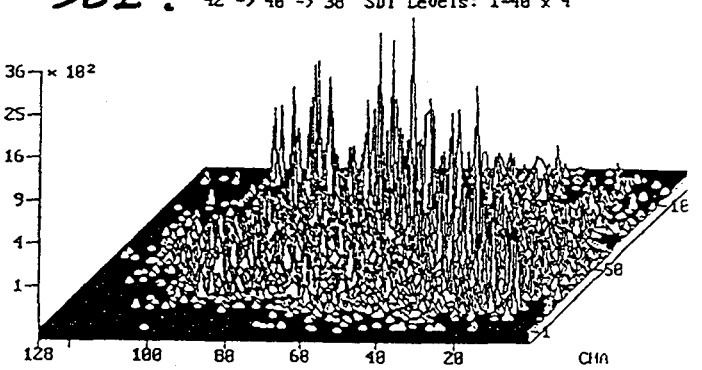

# Conclusions:

There are good reasons to believe that:
**The Limit to Completeness, today with** *Gammasphere* **and EUROBALL** at hand will be close to $U_0$, the borderline between discrete and damped rotational motion. It will allow for a detailed study of

**The Residual Two Body Interactions** in the discrete region.

but

**The Limit to Completeness after GRÈTA and EUROSHELL** are realized, will be pushed through the damped region into the chaotic regime towards the **Real Continuum**, and we may then get:

**A Complete Picture of the Nuclear Many Body Quantal System.**

T-L.Khoo
Structure of hot nuclei.

# Structure of hot nuclei

($U \lesssim 8$ MeV)

1. Physics motivation

2. 3 examples

a) phase transitions in a mesoscopic system

b) excited states in a false vacuum (superdef.)

c) order to chaos transition

(signatures, quantification)

# Physics of excited states above yrast line

a) Nuclear structure as function of

$\underbrace{N, Z, I}_{\text{abundant data}}$, $U$ & $T$

$U$: virtually unexploned (esp. with GS, EG, EB)

$T$: radioactive beams

b) What is the physics

(i) Nuclear structure

→ Melting of shell structure
Loss/gain of collectivity with increasing $U$
Quenching of pairing — " —

(ii) The nucleus as a lab for general phys

a) mesoscopic system
phase transition — collective to oblate
— superfluid to normal

b) excited states in a false (superdef.) vacuum

coupling of states in false & true vacua

→ c) order to chaos transition

c) order to chaos transition

loss or remnance of selection rules

clisbn. in transition strengths

$\frac{\Gamma_{g^{no}}}{D}$ – spreading width at g.no.

<u>Intellectual motivation</u>

Need to devise:

a) what to measure

b) how to extract physics from what is measured.

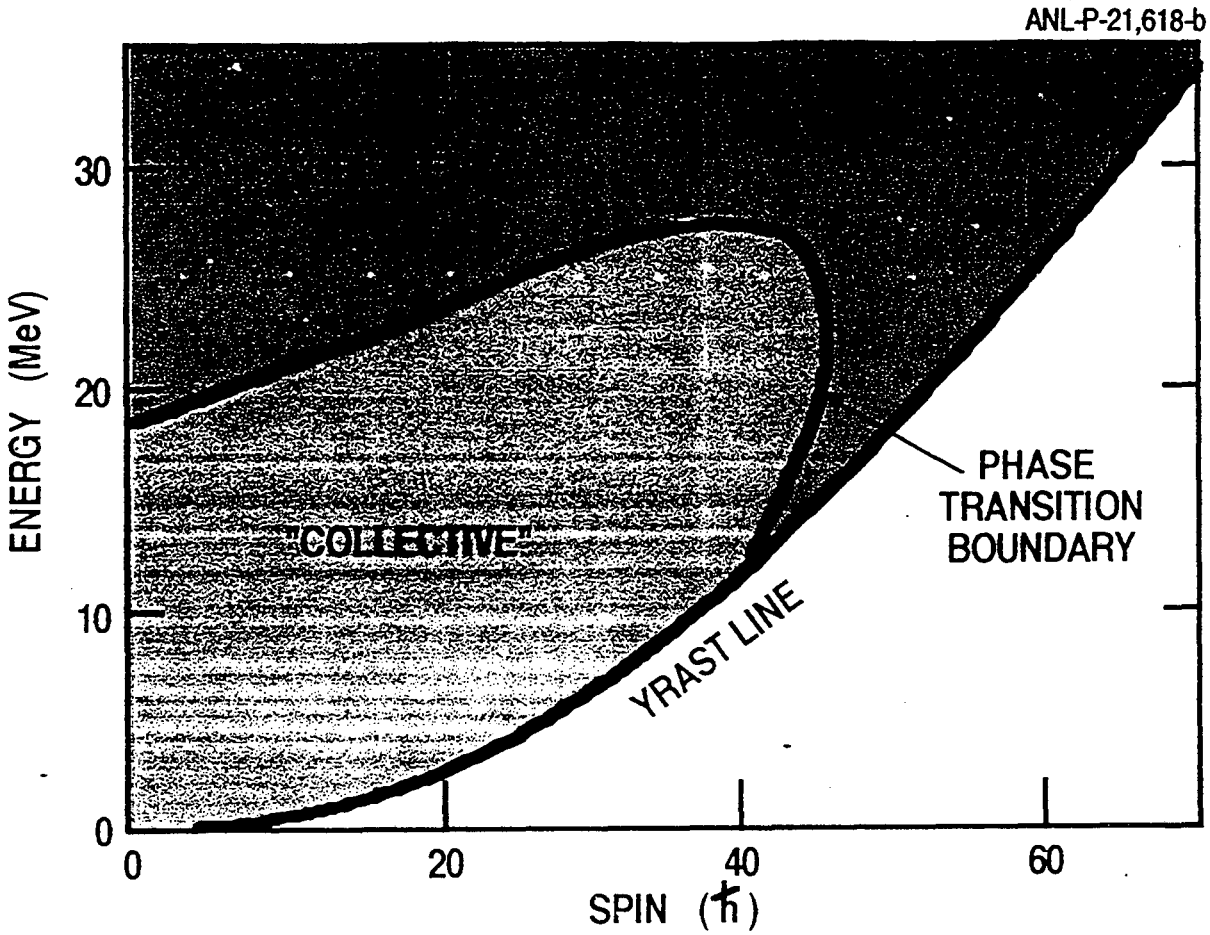


*In a mesoscopic system, fluctuations smear phase transition. Can a remnant signature be observed?*

*The nucleus is a laboratory for mesoscopic phenomena of general interest*
*Cf. quantum dots, metal clusters*

## Task

Study nuclear structure as function of U,
& for varying I,

i.e. in different (I,U) regions

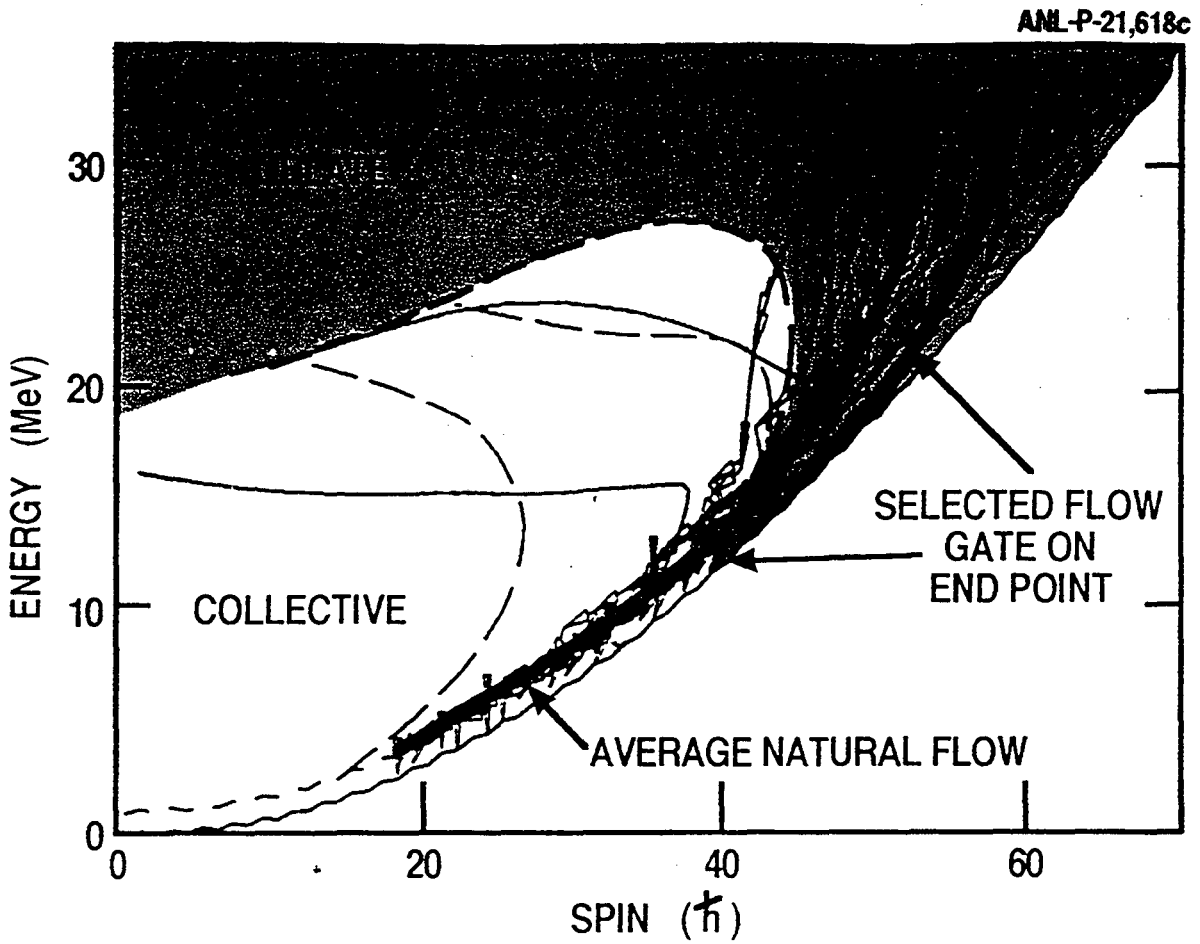


# How to define regions in (I,U)?

nuclear structure
rotational damping
fluctuations

Gate on selected yrast region to define end-point of cascade

(Also maps out selected near-yrast region)

Initial region may be *enhanced using (fold, sum-energy)*
or, in reactions with no neutron emission (possible for A<100),
better defined by *measuring energies of all charged particles,*
e.g. ~~with μ-ball~~

Initial region defined by $M_\gamma$, $E_\gamma^{sum}$
GRETA should provide significantly better resolution than μ-ball

MARTIN et al. MADRID / ANL

Temperature - Dependent Hartree Fock

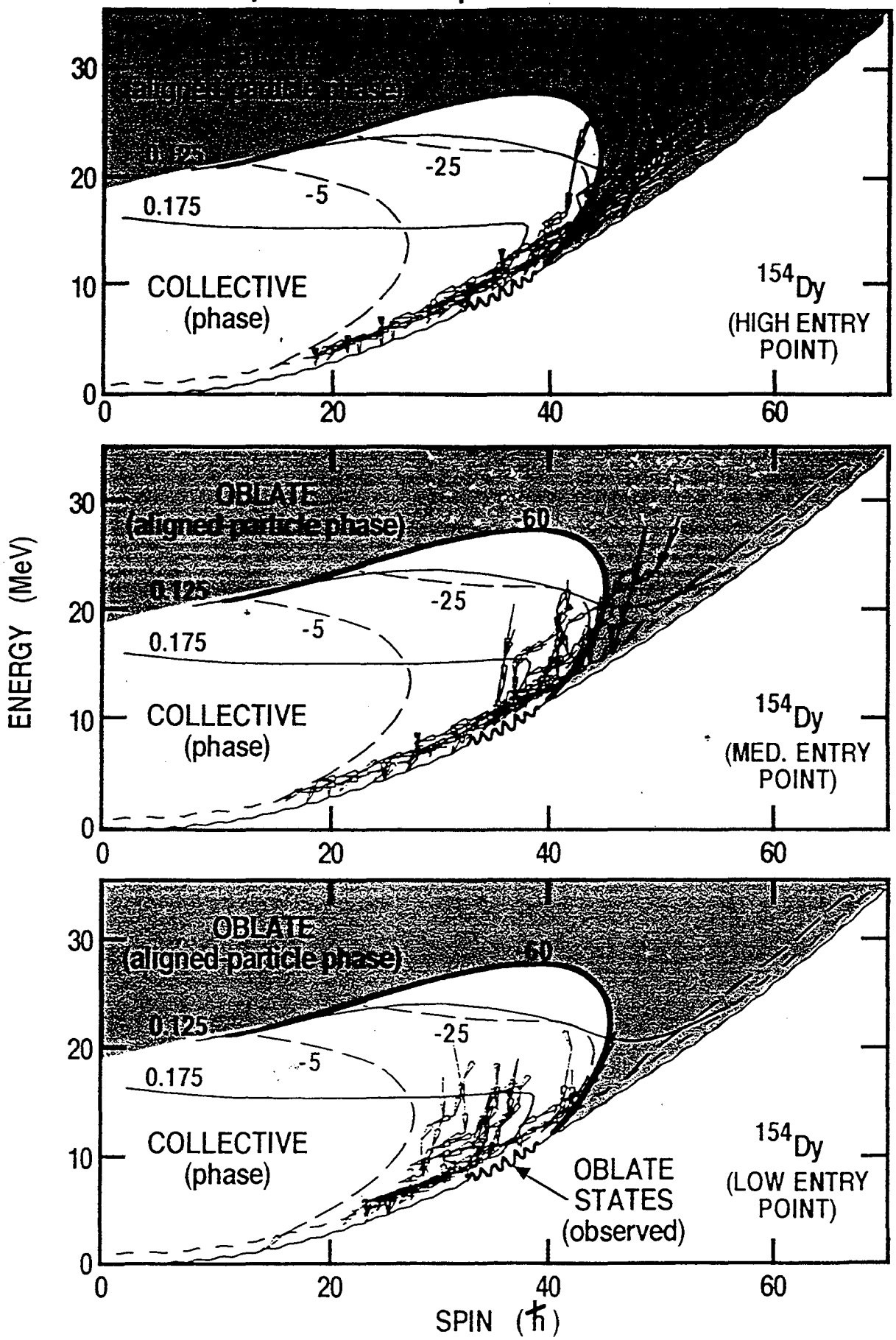

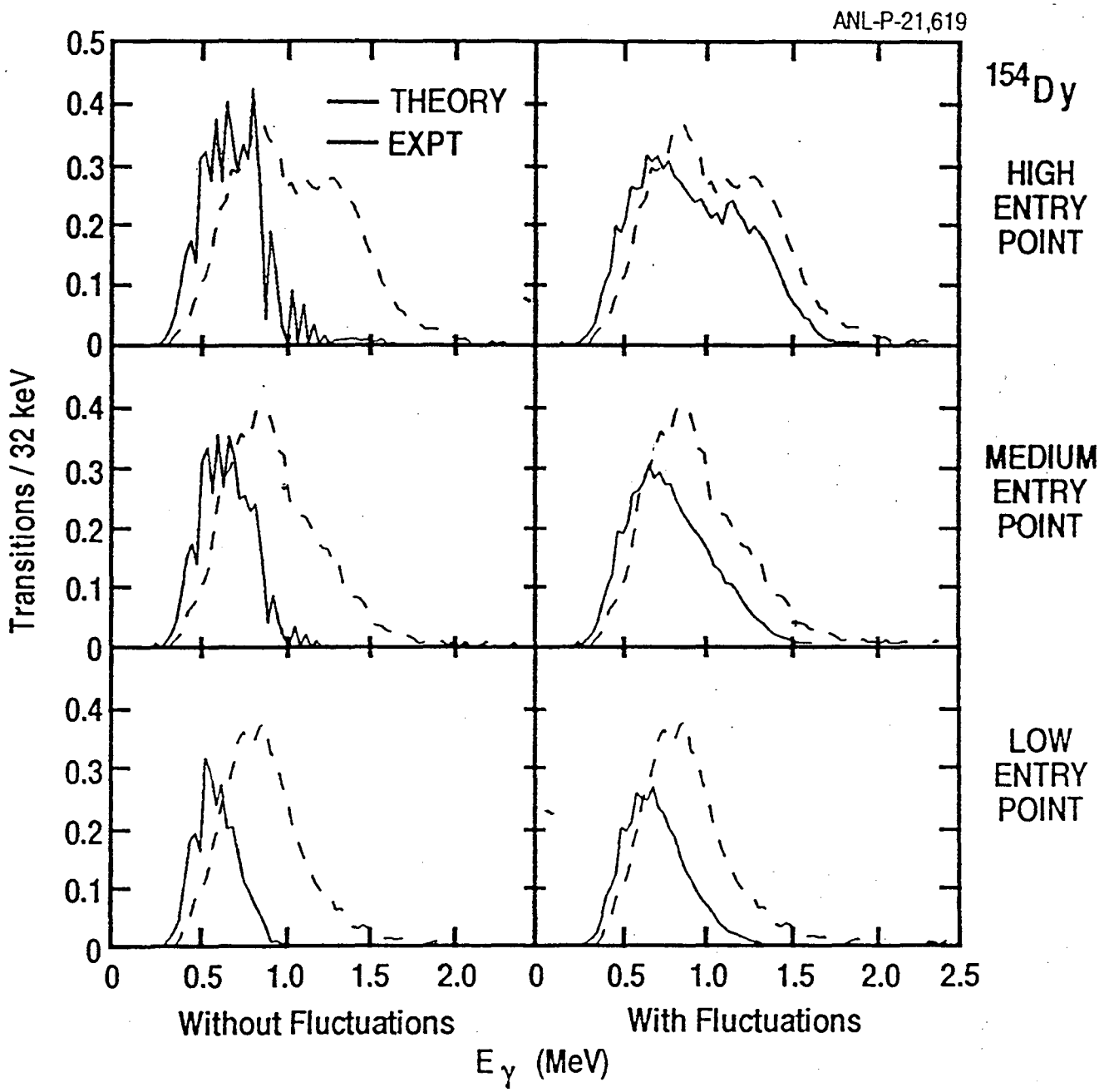
ANL-P-21,619
154Dy
THEORY
EXPT
HIGH ENTRY POINT
MEDIUM ENTRY POINT
LOW ENTRY POINT
Transitions / 32 keV
0.5
0.4
0.3
0.2
0.1
0
0.5
1.0
1.5
2.0
2.5
Without Fluctuations
With Fluctuations
Eγ (MeV)

Ma, Martin et al

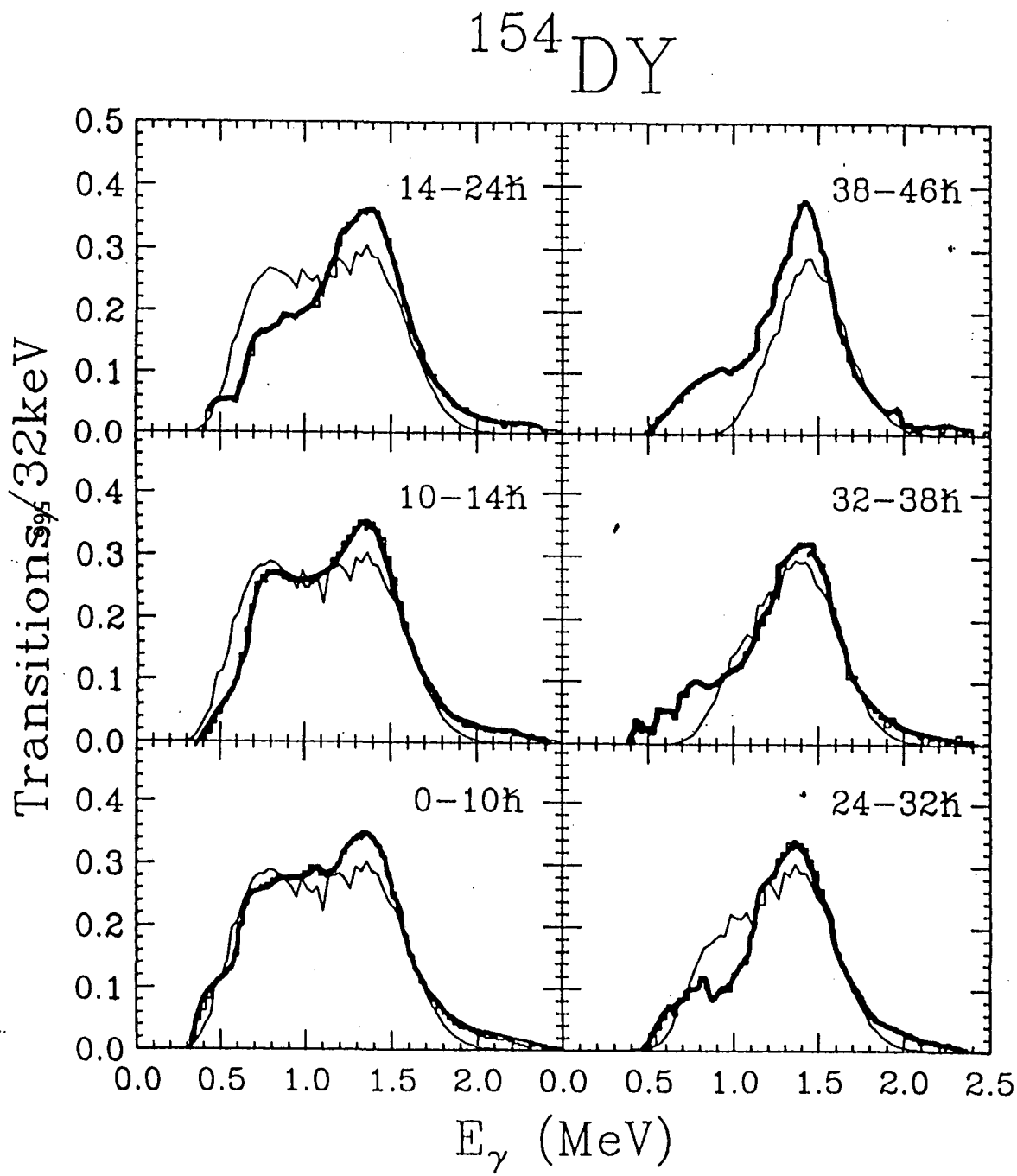


— exp (GS)

— theory

Monte Carlo simln. based on H-F + fluctuations

Theor. yrast, BS=0.0, QC Cut=0.4 at I=30

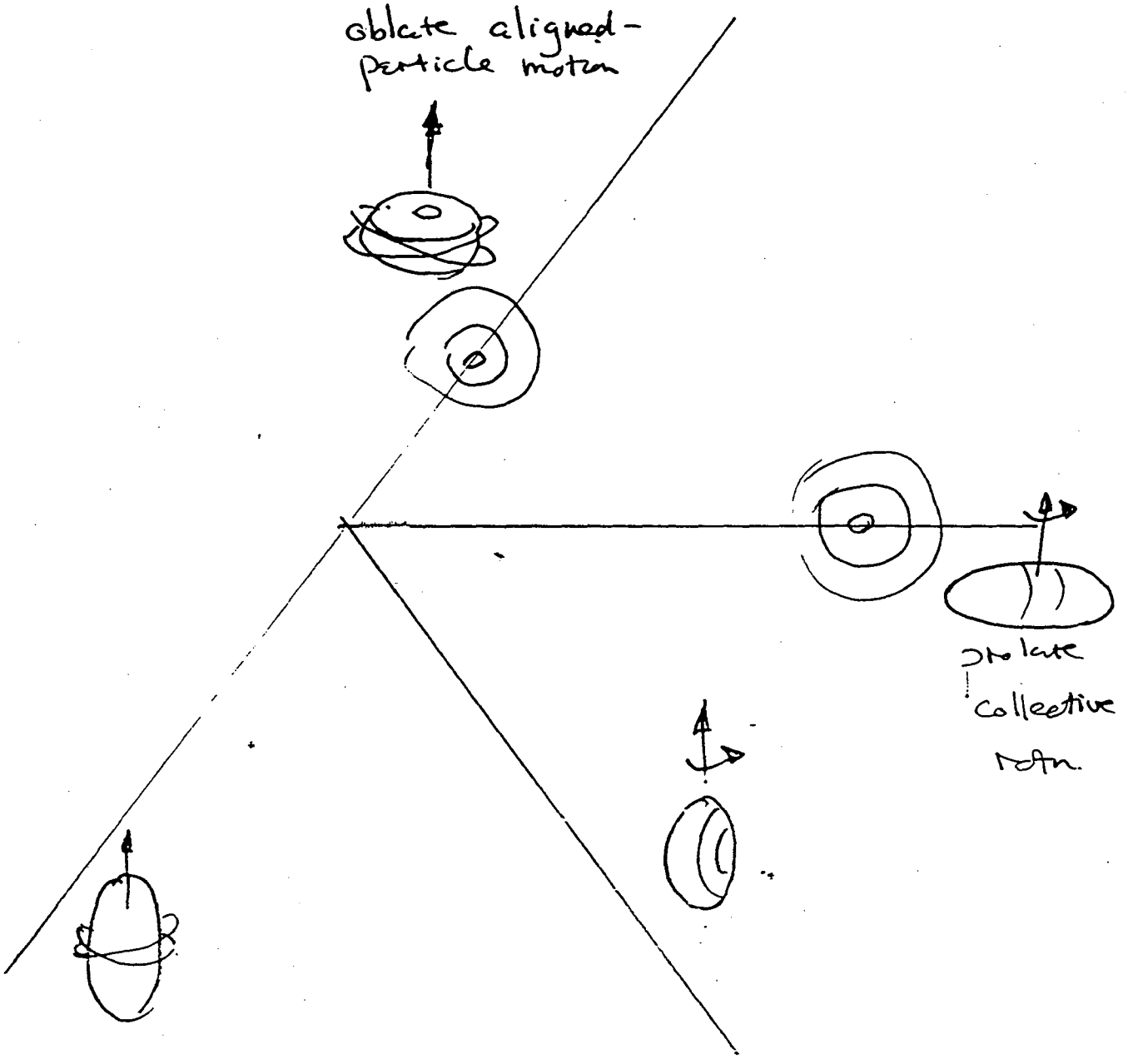
oblate aligned-
particle motion
prolate
collective
rotn.

Fig. 1 (part)

QC. cutoff = 0.4

Yrast Theor.
$\bar{U}$ = 7.1 ± 2.4
$\bar{I}$ = 57 ± 6
} Entry pop.

$^{154}$Dy, $\langle I_{entry} \rangle$ = ii.ii, $\langle E_{entry} \rangle$ = ee.ee

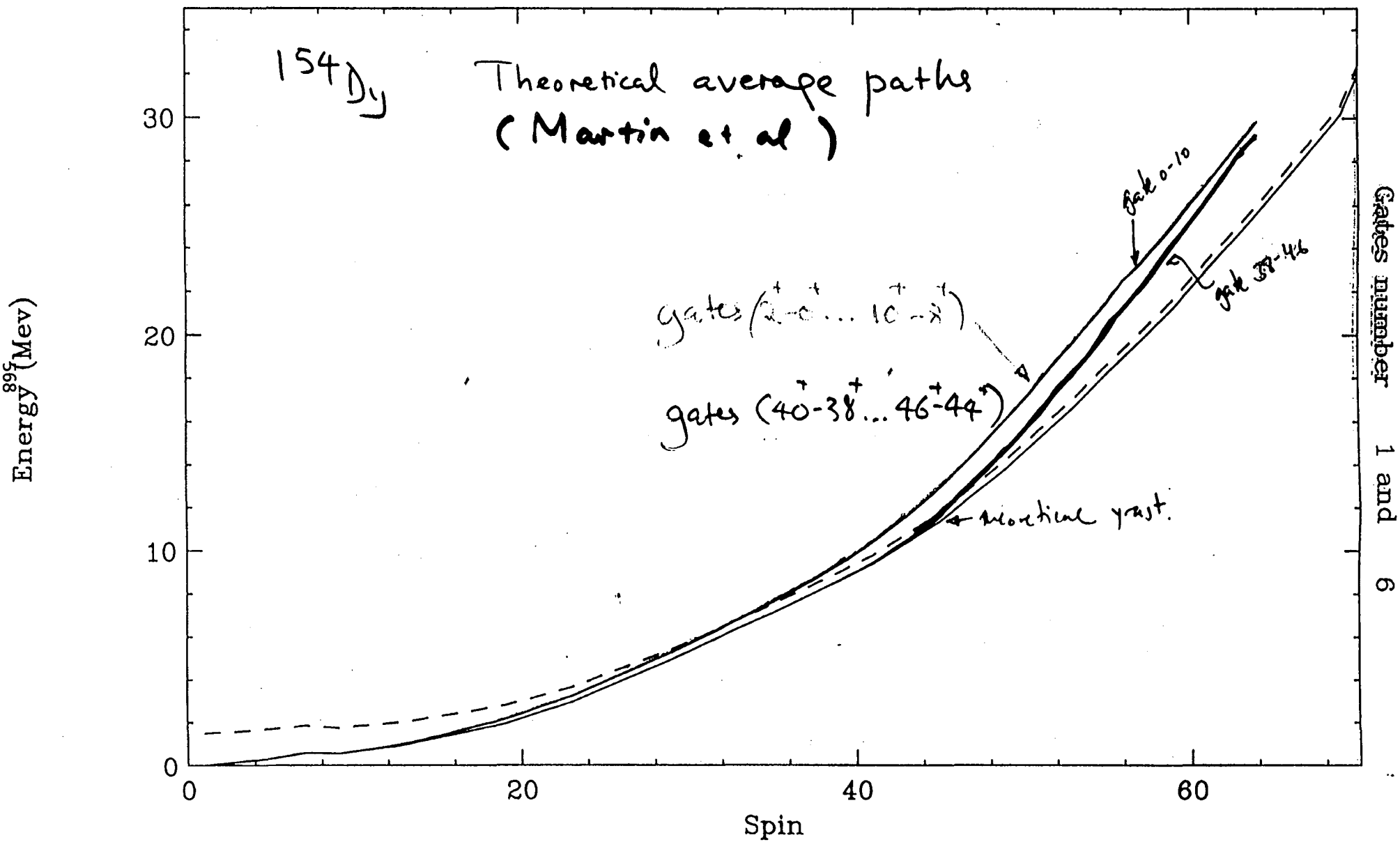

$^{154}$Dy quasicontinuum analysis (~~12/12/1999~~ 1/23/98)

| | 10 − 0 | | 14 − 10 | | 24 − 14 | | 32 − 24 | | 38 − 32 | | 46 − 38 | |
|---|---|---|---|---|---|---|---|---|---|---|---|---|
| | M | $\bar{E}$ | M | $\bar{E}$ | M | $\bar{E}$ | M | $\bar{E}$ | M | $\bar{E}$ | M | $\bar{E}$ |
| E2 | 10.7 | 1.143 | 10.0 | 1.188 | 9.0 | 1.250 | 7.3 | 1.306 | 7.1 | 1.308 | 6.9 | 1.339 |
| E1/M1 | 1.9 | 0.554 | 1.2 | 0.563 | 1.9 | 0.666 | 1.6 | 0.630 | 1.4 | 0.562 | 2.2 | 0.651 |
| stat. | 3.4 | 2.138 | 3.5 | 2.126 | 3.5 | 2.116 | 3.5 | 2.116 | 3.5 | 2.096 | 3.5 | 2.111 |
| discrete | 15.5 | 0.655 | 16.8 | 0.674 | 17.3 | 0.682 | 18.6 | 0.696 | 19.5 | 0.693 | 19.1 | 0.704 |
| total | 31.5 | | 31.5 | | 31.7 | | 31.0 | | 31.3 | | 31.7 | |
| I entry | 56.0 | | 56.6 | | 56.3 | | 55.2 | | 56.2 | | 56.0 | |
| $E_{entry}$ | | 30.7 | | 31.3 | | 31.7 | | 30.9 | | 31.0 | | 31.5 |

# Decay from Super- to Normal-Deformed States

Nuclei can have an excited minimum (or false vacuum) in the potential energy at large deformation.

Superdeformed (SD) states in the excited minima decay by tunneling through a barrier, a process possible only in very small objects governed by quantum mechanics, but not in everyday classical objects.

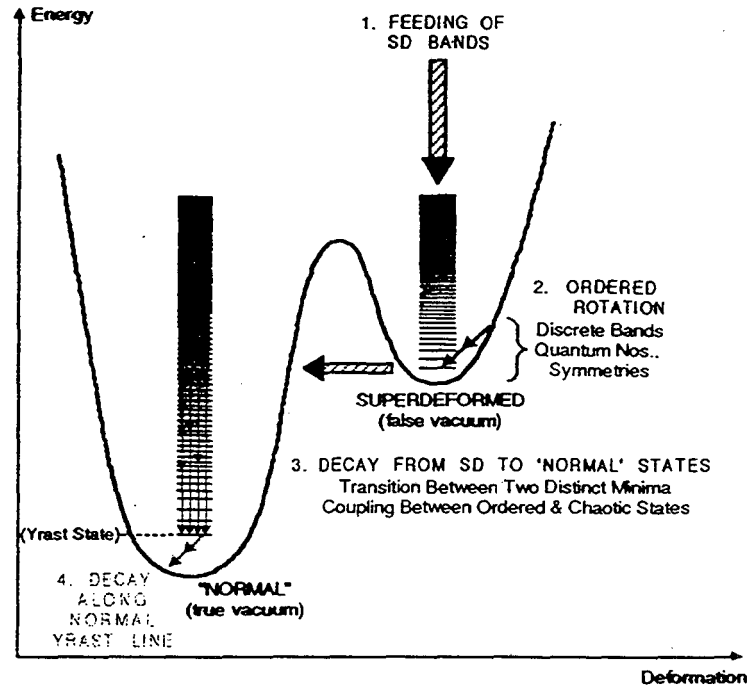


The spectra emitted in the feeding and decay of a SD band show a unique *double cycle of chaos-to-order transition.*

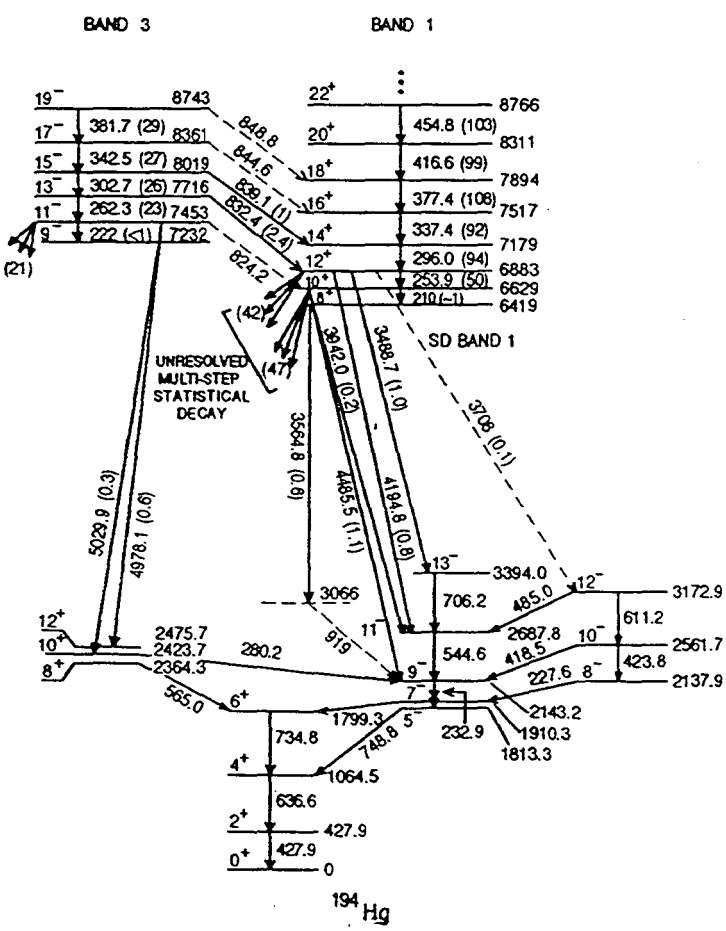


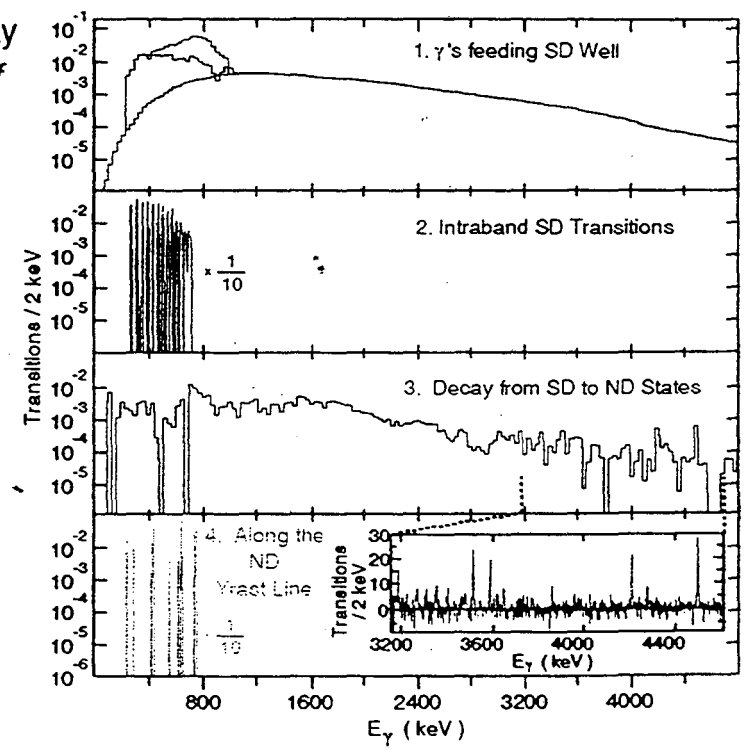


Very high-energy transitions, observed from SD bands in $^{194}$Hg and $^{194}$Pb, provide information on the fundamental properties *(energies, spins, parities)* of SD states.

# Feeding of SD Bands

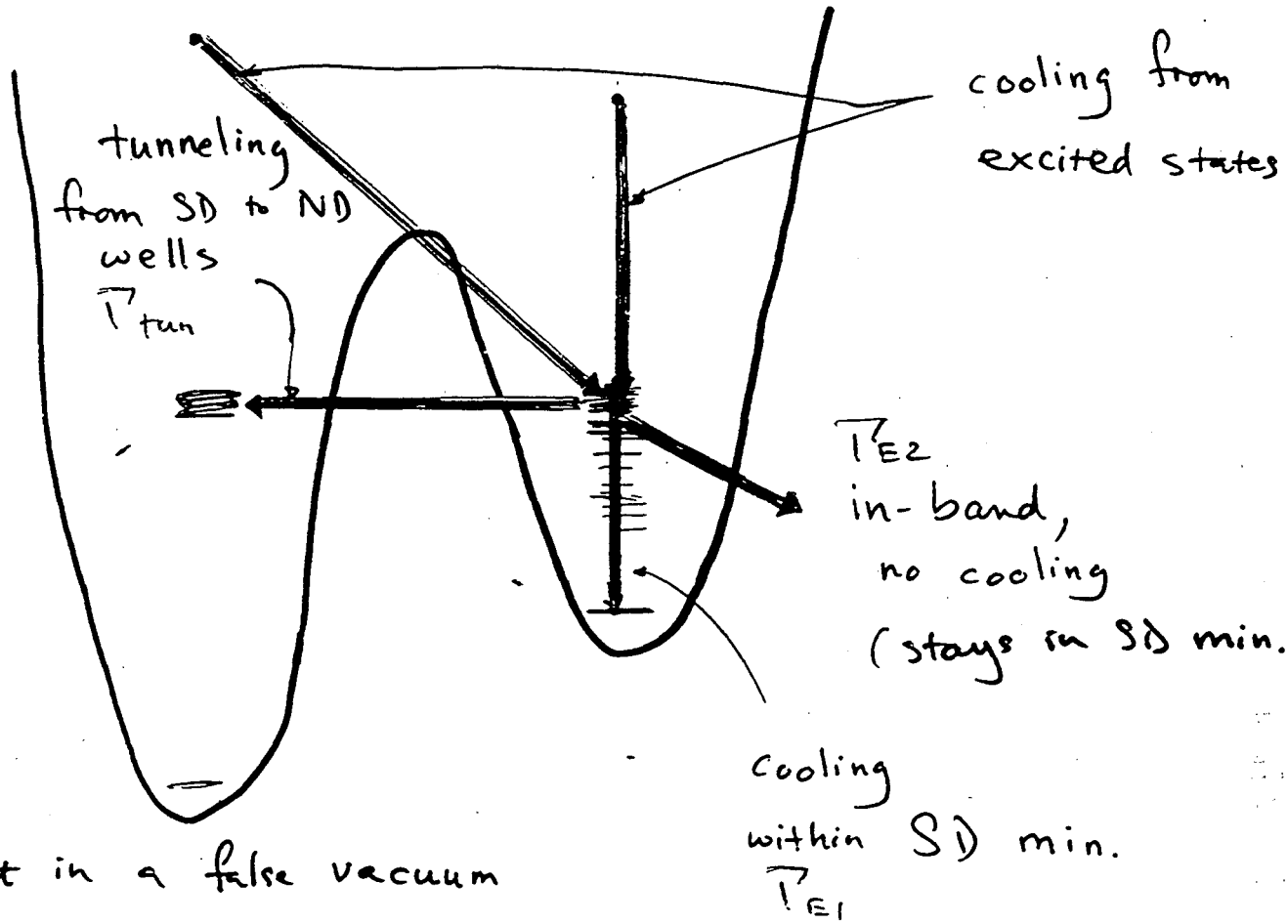


Caught in a false vacuum

Feeding of "ground state" in SD minimum

is understood by:

Statistical process

+ Tunneling between hot SD & ND states

Monte Carlo simulations reproduce all observables

Intensity, Intensity vs spin, Entry distribution, Spec. of feeding $\gamma$,

1-2% of $\sigma_{channel}$

Lauritsen et al
$^{194}$Hg band 1

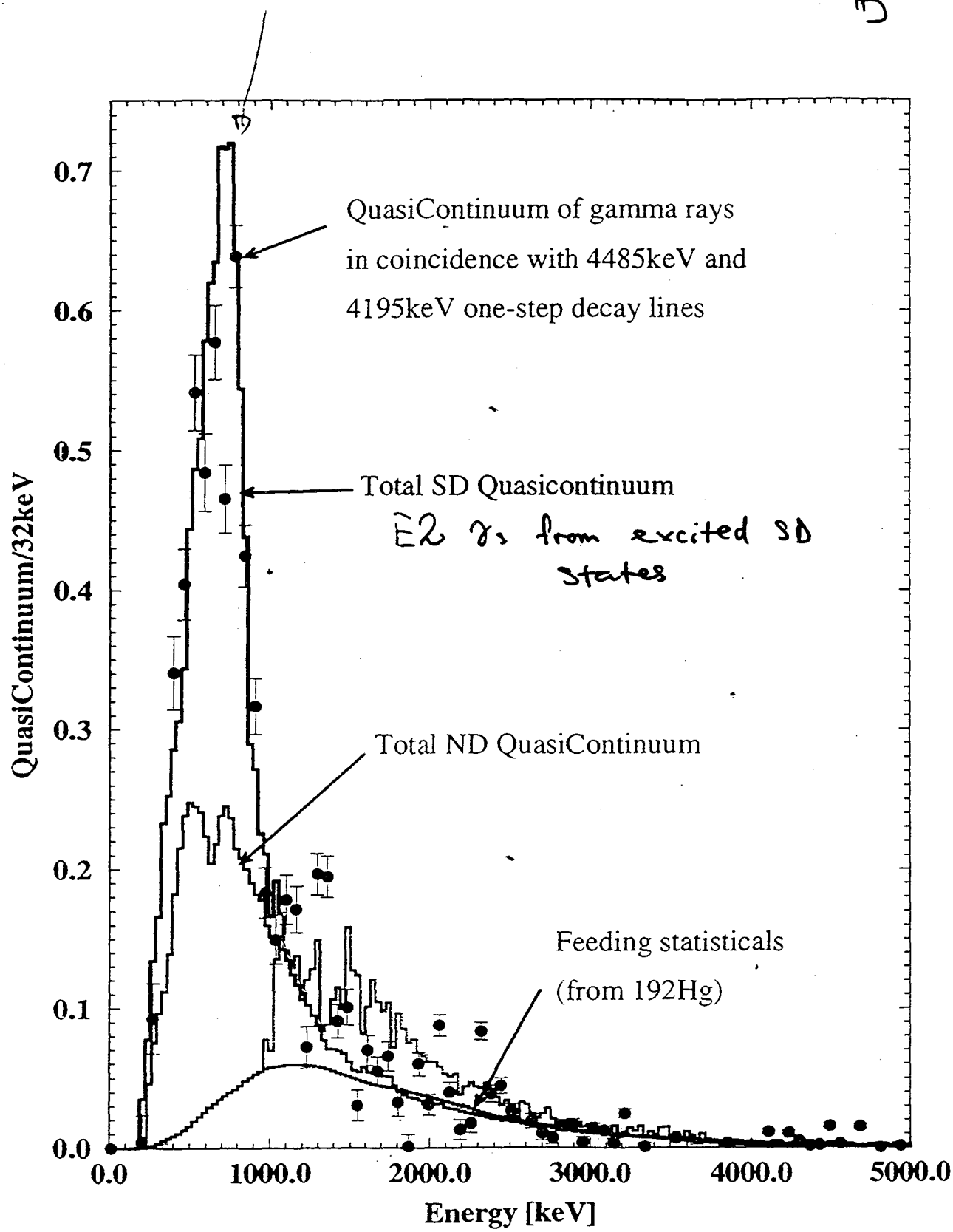

Why is the power of GRETA needed?

Quasicontinuous spectra

Need to be sure of the source

a) nucleus

b) I, U region

5- or 6- fold coincidences

$E_\gamma E_\gamma$ . } correlations selected by

$E_\gamma E_\gamma E_\gamma$ } $\gamma\gamma\gamma$ coincidence gates

with $I^{ND}_{yrast}$ or $I^{SD}_{yrast}$ selection

$I_{yrast}$ → end point of cascade

$M_\gamma$, $E^\gamma_{sum}$ → initial region of cascade

⇓

Definition of I, U region

Properties as function of I, U

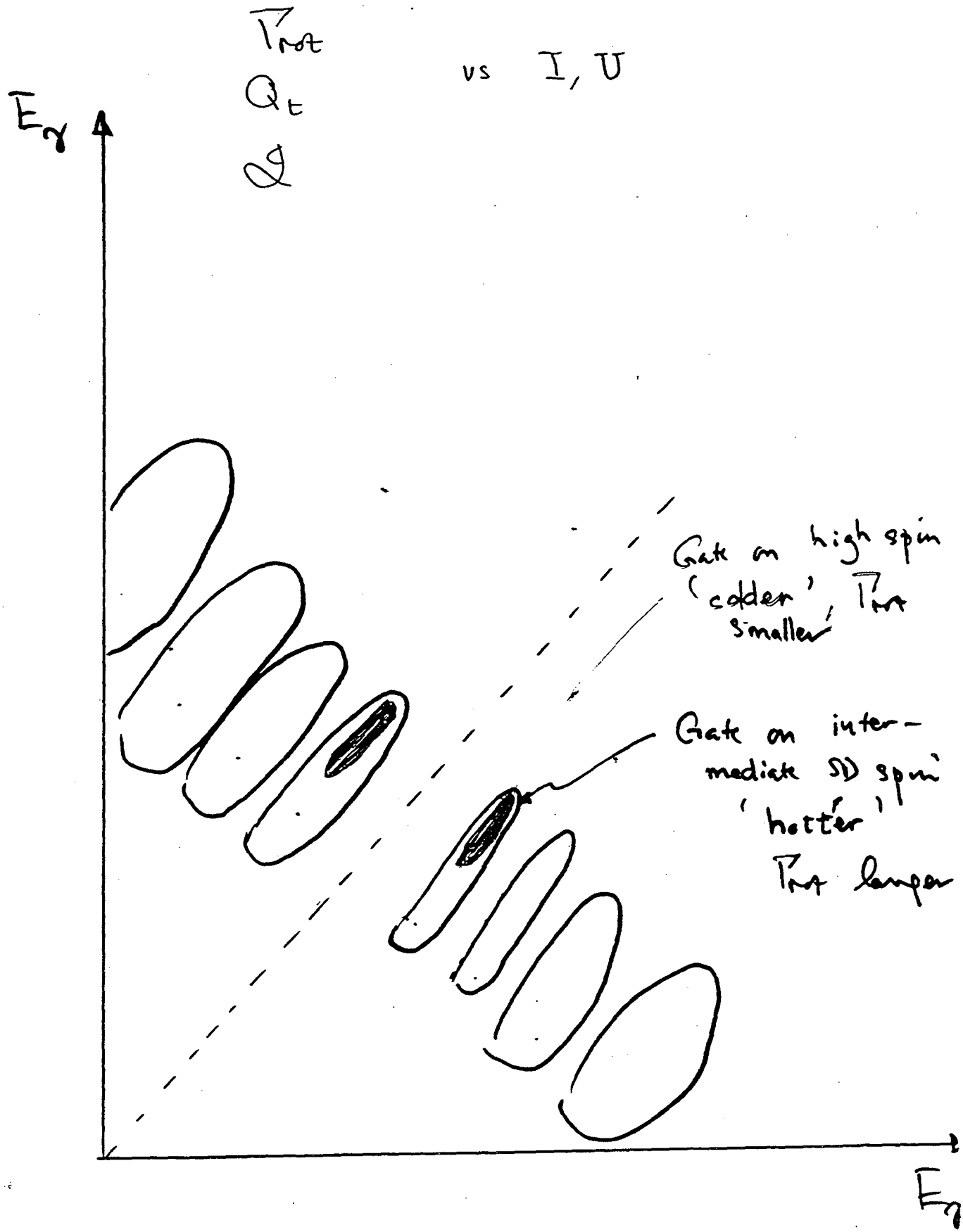
$\Gamma_{rot}$
$Q_t$
$\mathcal{J}$
vs I, U
$E_\gamma$
Gate on high spin
'colder', $\Gamma_{rot}$
smaller
Gate on inter-
mediate SD spin
'hotter'
$\Gamma_{rot}$ larger
$E_\gamma$

# Order to chaos transition

Physics often attempts to distill simplicity (order)

Nature is not ordered
cf. brain, heart

Order
Classical — characterized by constants of motion
Quantal — " " conserved quantum numbers

Chaos
Loss of above

Signatures
a) nearest neighbor spacings
— difficult due to completeness req.
— does not provide measure of complexity of w.f.
b) loss of selection rules (which result from conserved q. nos.)
→ Porter-Thomas distbn. in transition strong
c) spreading widths of q. nos., $P_{gne}$ / D

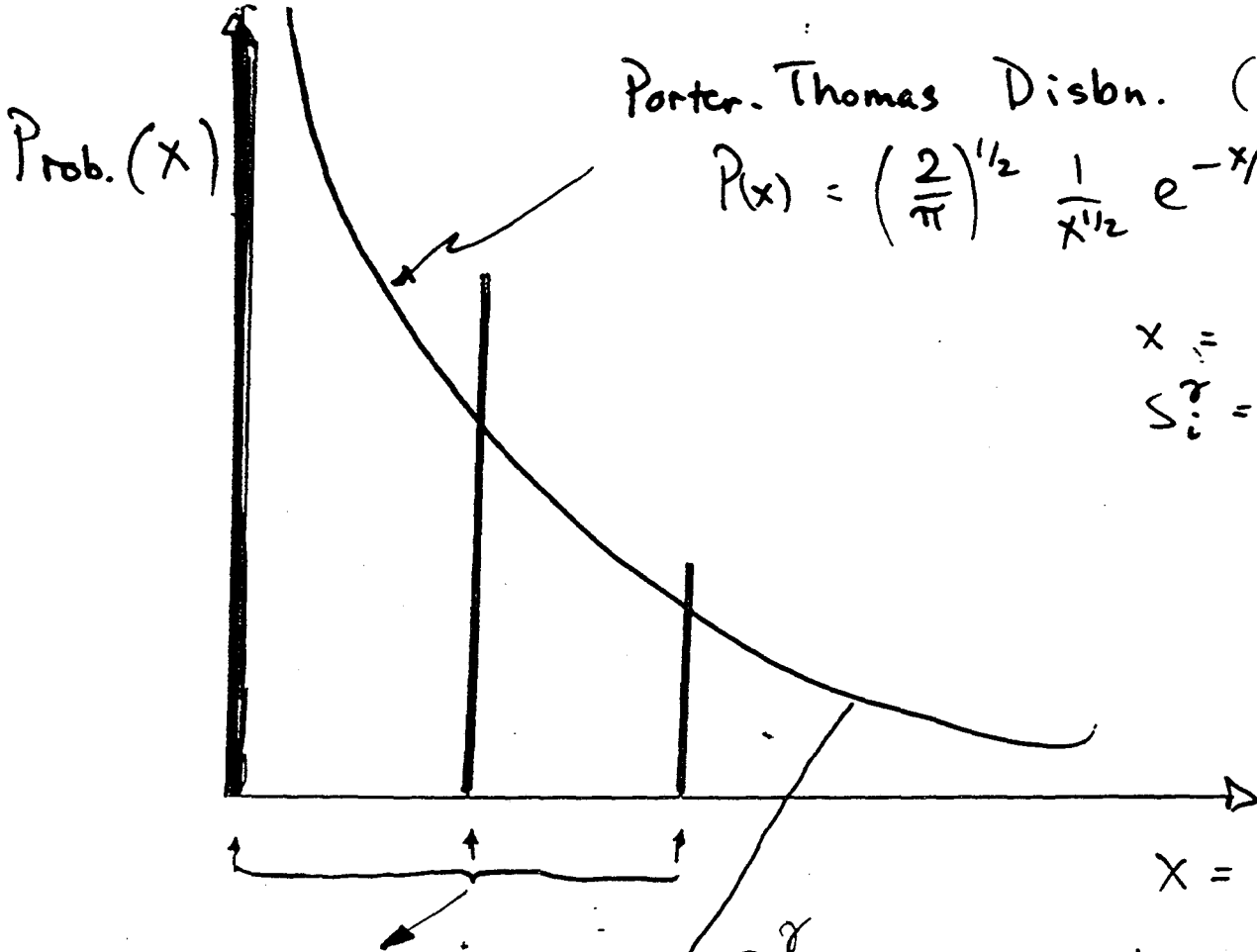


Porter-Thomas Distbn. (hand-sketcha

$$P(x) = \left(\frac{2}{\pi}\right)^{1/2} \frac{1}{x^{1/2}} e^{-x/2}.$$

$x = S_i^\gamma / \bar{S}^\gamma$

$S_i^\gamma$ = $\gamma$ strength

$$X = \frac{S_i^\gamma}{\bar{S}^\gamma}$$

$S_i^\gamma$ governed by selection rules (imposed by quantum numbers)

$S_i^\gamma$ $\delta$-functions

i.e. typically 1-3 states populated

Chaos

Distribution of $S_i^\gamma$

Fluctuations in $S_i^\gamma$

Specific $S_i^\gamma$ cannot be predic

but Distribution can - has Porter-Thomas form

2- step $\gamma$s

1 - step $\gamma$s ?? in $^{192}$Hg

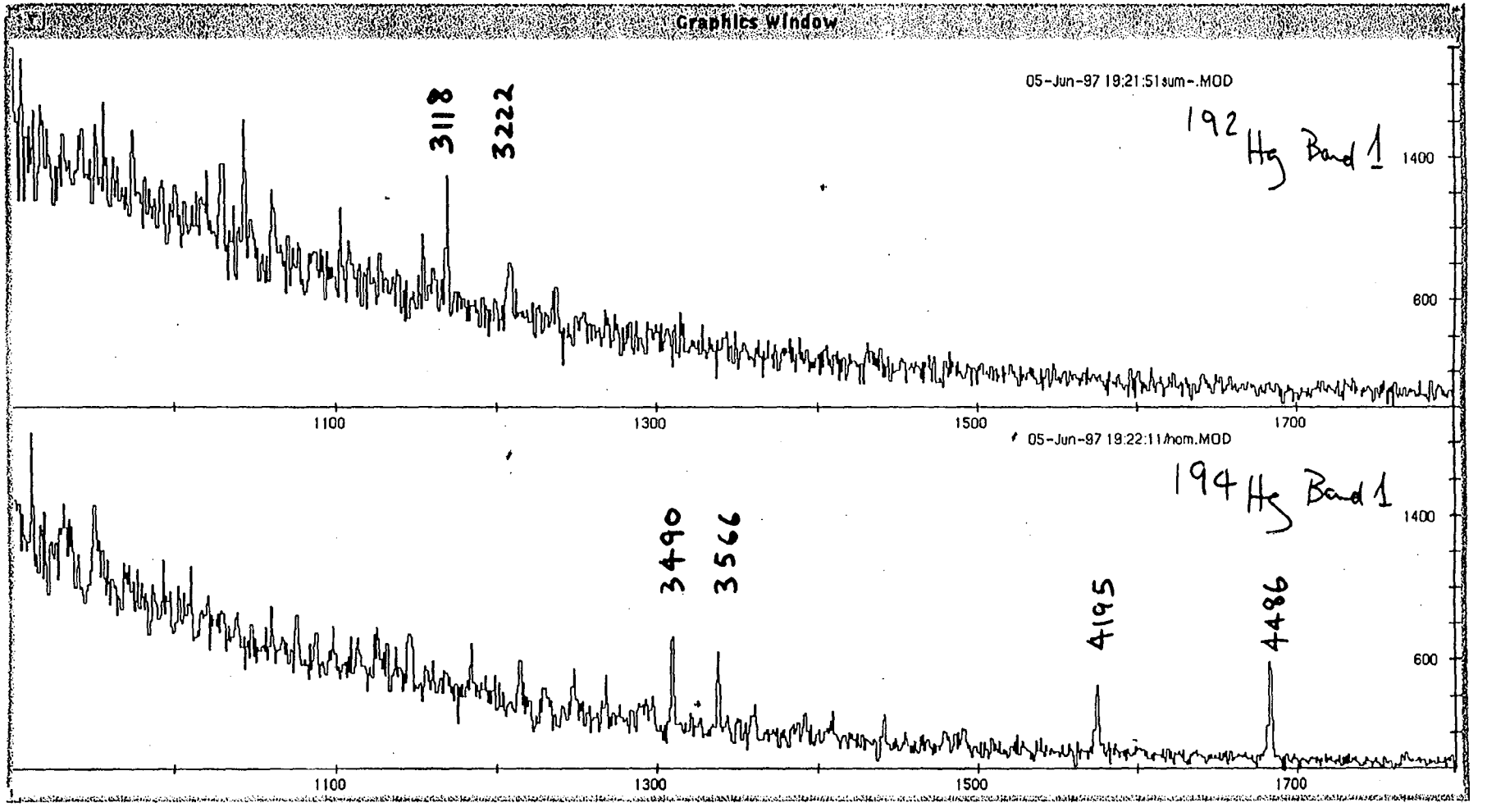


1 - step $\gamma$s from SD to ND yrast line

Lopez-Martens, Døssing et al
GS data on $^{194}$Hg SD decay

Primary (first-step) $\gamma$s from SD decay

1. Fluctuations observed
2. Decay has statistical origin (cf. n-capture $\gamma$ spec.)
   ∴ largely chaotic
   quantum numbers virtually lost

BUT

3. Very strong 1-step $\gamma$s — prob. ~ $10^{-4}$
   Decay to all <u>odd</u> spin, negative $\pi$ states
   (from $K^{\pi} = 0^+$ band)

4. Also 1-step $\gamma$s from excited band observed.

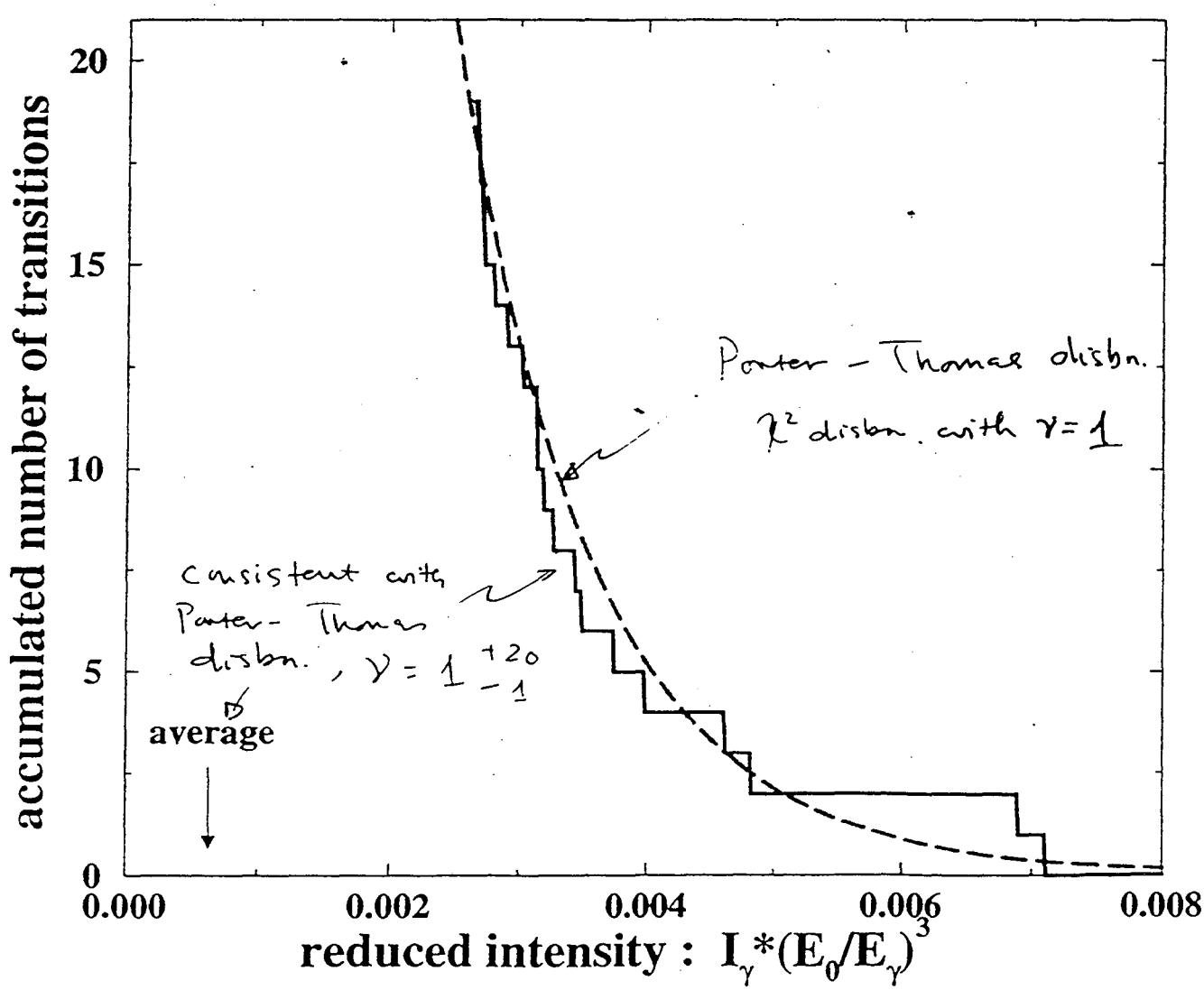

Ernest Orlando Lawrence Berkeley National Laboratory
One Cyclotron Road | Berkeley, California 94720

Prepared for the U.S. Department of Energy under Contract No. DE-AC03-76SF00098